Universidad de Valladolid

Escuela de Doctorado Universidad de Valladolid

PROGRAMA DE DOCTORADO EN FÍSICA

TESIS DOCTORAL

THERMOPHYSICAL PROPERTIES, INTERACTIONS AND STRUCTURE IN ORGANIC LIQUID MIXTURES INCLUDING POLAR AND/OR ASSOCIATED COMPOUNDS: *N,N*-DIALKYLAMIDES, AMINES, 1-ALKANOLS, KETONES AND ORGANIC CARBONATES

Presentada por Luis Fernando Hevia de los Mozos
para optar al grado de Doctor por la Universidad de Valladolid

Dirigida por:

José Carlos Cobos Hernández

Juan Antonio González López

Isaías García de la Fuente

A Marta.

A mis padres, Luis y María del Mar.

A mi padrino, Fernando.

Table of contents

Agradecimientos/acknowledgements

Es imposible dar una cuenta exhaustiva de todas las personas que, de una forma o de otra, han contribuido a que esta Tesis Doctoral haya salido adelante. Para bien o para mal, todo aquel con el que nos cruzamos en la vida aporta su granito de arena en la construcción de quienes llegamos a ser (aunque no sabemos la manera exacta en que esos granitos de arena interaccionan entre sí, dando lugar a resultados inesperados; en otras palabras, no son entidades elementales independientes y nosotros somos propiedades emergentes). Incluso resulta difícil mencionar a todos los que han intervenido en mi vida durante estos cuatro años de doctorado.

En primer lugar, tengo que agradecer al Ministerio de Educación, Cultura y Deporte el haber financiado mi contrato predoctoral y dos estancias breves de investigación a través de dos ayudas complementarias (actualmente, la financiación está a cargo del Ministerio de Educación y Formación Profesional). También a la Universidad de Valladolid, por haberme concedido las dos ayudas por asistencia a cursos, congresos y jornadas relevantes para el desarrollo de tesis doctorales que he solicitado para financiar parte de los gastos generados por dichas actividades, de interés para mi formación doctoral.

I switch to English to acknowledge Jean-Yves Coxam and Karine Ballerat-Busserolles for the opportunity to stay six months at their laboratory in Clermont-Ferrand. I also thank Yohann Coulier for his supervision and useful help. It has been a great experience, both proffessionally and personally, and it has given be me the chance to learn other expermental techniques and subjects of theoretical study.

I also want to thank Olympe, Shyam, Emilie, Laura, Sven, Antoine..., because I come back home with a new group of friends who took me as one of them.

Es imposible pasar por alto que no estaría escribiendo esta Tesis de no ser por José Carlos Cobos. Casi diez años hace ya que nos conocemos y, desde entonces, ha sabido alimentar mi interés natural por la Física y mi especial gusto por la Termodinámica y la Física Estadística. No puedo ver ya la Física, ni tampoco la ciencia en general, sino con los ojos, y el espíritu, de alguien que ha sido su alumno. Por otro lado, este trabajo no habría sido posible sin la inestimable dirección de Juan Antonio González e Isaías García, cuya concienzuda supervisión ha sido constante. Por ello, agradezco a mis directores su esfuerzo, dedicación y paciencia durante todo este periodo, y la oportunidad de especializarme en un campo tan universal como es la Termodinámica.

También quiero dar las gracias a mis compañeros y amigos del grupo de investigación. A Cristina y Felipe, por ayudarme siempre que lo he necesitado. A Ana, con quien he compartido las horas de iniciación en este campo de investigación y también otras muchas experiencias y viajes. Querría hacer un agradecimiento especial a Víctor por haber dedicado, desinteresada y

vocacionalmente, tanto tiempo a Ana y a mí para ayudarnos, enseñarnos y compartir con nosotros gran parte de lo que ha aprendido con su experiencia en el laboratorio.

No puedo olvidarme tampoco de mi compañera de pasillo, Bea, a veces también guía de viajes.

Si bien trabajar en Física me resultaba muy interesante, no pensaba que también fuera a dedicarle una parte tan grande de mi tiempo libre cuando decidí unirme a Physics League en 2015. Involucrarme en la asociación y en su directiva ha sido una de las grandes experiencias de la Tesis. Hemos vivido situaciones bastante variopintas en las que nunca me habría imaginado metido. He conocido a personas con una gran vocación por transmitir la pasión por la ciencia, y en particular por la Física, de una forma divertida para nuestro público, pero más aún para nosotros. Ha sido un honor unirme, junto con mi amigo Luis (Teje), a David (Bro), Vero (B) y Bea en el proyecto que pusieron en marcha con tanto esfuerzo e ilusión, seguramente sin pensar que crecería tanto hasta convertirse en lo que es hoy. Y llevarme, de paso, unos buenos amigos.

Quiero y debo dedicar un párrafo aparte a Luis, un gran científico y mejor amigo, junto al que estudiar y aprender Física ha sido siempre un privilegio. Con un espíritu crítico ante la vida y una mente siempre alerta, no me deja dormirme en los laureles hasta que hemos llegado al fondo de cualquier cuestión. Espero que sigamos compartiendo buenos momentos y, si hace falta, afrontaremos los malos también.

Andrés ($\mathbb{Z}$), Marta (MG^2), Cristina ($\mathbb{C}$) y María (mmorped), el resto de mis grandes amigos de la carrera, merecen también un hueco en estas páginas. Espero que tras el caos que nos dispersa siempre tengamos esos momentos de reencuentro.

Otro que me ha hecho compañía durante todos mis años universitarios ha sido el hermano pequeño gordo de la familia, Pepo. Supongo que se habrá preguntado por qué pasaba tantas horas fuera o "sin hacer nada" (trabajando) en lugar de haciéndole caso.

Por supuesto, quiero dar las gracias a mis padres (María del Mar y Luis) por ser los mejores que podría tener. Gracias por enseñarme que madurar como persona no significa no poder pedir ayuda cuando la necesitas. Y por animarme siempre a hacer lo que realmente me gusta y apoyarme para ello, pues esto es, sin duda alguna, un factor muy importante para ser feliz en la vida.

Una felicidad que es completa gracias a Marta. Por ser mi compañera de vida, por aguantar la incertidumbre que supone mi decisión de dedicarme al mundo de la ciencia, y porque errar es de humanos y herrar es de herreros. Hemos recorrido mucho camino juntos, y por ello mi crecimiento como persona, si es que ha habido alguno, es mayoritariamente gracias a ti.

Por último, quiero escribir unas líneas para aquellos que nos han dejado durante estos duros años. Vosotros también habéis sido, y seguís siendo, referentes en mi vida. Mere, que nos contagiabas a todos con tu optimismo y alegría. José, grande, generoso y honrado: ya puedes decir por ahí que tu sobrino es por fin Doctor en Física. Padrino, siempre dispuesto a ayudar a todos, un segundo padre para mí. Todos estáis hoy conmigo, en mi corazón y en el de toda la familia, y sois parte indiscutible de esta Tesis.

En Valladolid, a 3 de julio de 2019

The structure of this Thesis

This Thesis is written as a "PhD Thesis with publications". In order to unify the different works carried out, we proceed now to describe briefly the structure of the Thesis and the relations among its parts.

Part I aims to give a global vision of the work performed in this Thesis, describing the **pursued objectives** (Chapter 1) and the **selected experimental and theoretical methodology** to accomplish them (Chapters 2 to 4).

- Chapter 1 describes all the work performed during these four years and the main goals of the Thesis.
- Chapter 2 summarizes the studied thermodynamic properties and notation, assuming that the reader has some previous knowledge about the subject.
- In Chapter 3, the experimental equipment and methodology are described in detail, since much of the information about calibration and test of the techniques is not provided in the publications included in this Thesis. This is the only part of the manuscript that is written in **spanish**, so that future students in the University of Valladolid find easier to start working in our laboratory.
- The theoretical models used are described in Chapter 4. It includes information not given in the publications, and also some original contributions.

The results in complete form are given in **Part II** as copies of the corresponding publications or the corresponding manuscripts. They are completed with appendices, included in **Part IV**. The **publications** included in the present manuscript have been ordered by subjects, rather than chronologically.

- Experimental determination of volumetric, dielectric and refractive properties of amide + amine liquid mixtures (**Articles 1 to 4**).
- Experimental determination of dielectric and refractive properties of 1-alkanol + amine liquid mixtures (**Articles 5 to 6**).
- Study of orientational (i.e. non-random) effects in liquid mixtures by means of thermophysical properties, the Flory model and the concentration-concentration structure factor formalism (**Articles 7 to 8**).

The **summary of the discussion of the results** and the **conclusions** extracted from their analysis are included in **Part III** (Chapters 5 and 6).

- Chapter 5 is a summary of the main points of discussion of the results. It includes only the discussion of the experimental data from liquid mixtures and of the results of

the application of the theoretical models to these data. It does *not* include the theoretical studies based on data from other sources or the solution enthalpies of gases in water; these other parts of the Thesis are included in the form of appendices or copies of the corresponding publications, as they are somewhat independent.

- Chapter 6 includes the conclusions from all the work performed, both experimental and theoretical.

The **bibliography** is given chapter by chapter instead of at the end of the manuscript.

Part I

Objectives and methodology

Chapter 1.

Introduction

1.1. About this research group

The Applied Physics Department of the Faculty of Science of the University of Valladolid (in Spanish, Departamento de Física Aplicada de la Facultad de Ciencias de la Universidad de Valladolid) has a remarkably wide experience in the study of thermodynamic properties of non-electrolyte liquid mixtures. These studies started in the 1970s with works by M.A. Villamañán [1] and J.C. Cobos [2, 3], supervised by C. Casanova –members then of the so-called Fundamental Physics Department– and collaborations with the Santiago de Compostela (Spain), Marseille and Clermont-Ferrand (France) Universities.

In the mid-1980s, I. García de la Fuente [4] and J.A. González [5] began here as PhD students and, since then, never took their research activity apart from J.C. Cobos. They founded in 1994 the research group GETEF ('Grupo Especializado en Termodinámica de los Equilibrios entre Fases', which can be translated as 'Group Specialized in Thermodynamics of Phase Equilibria'). The work in this PhD Thesis has been developed within the framework of this research group.

1.1.1. Members of GETEF

Since the creation of the group, many researchers have been part of it:

- The Professors:
  - D. José Carlos Cobos Hernández.
  - D. Isaías García de la Fuente.
  - D. Juan Antonio González López.
  - D. José Ricardo Páramo Vela.
  - Dña. Cristina Alonso Tristán (University of Burgos).

- The PhD:
  - D. Juan María Fernández Martínez.
  - D. Francisco Javier Carmona del Río.
  - D. Nicolás Riesco Fernández.
  - Dña. Susana Villa Vallejo.
  - D. Ismael Mozo Ruiz.
  - D. Iván Alonso Miguel.

  - D. Víctor Alonso Gómez.
  - D. Luis Felipe Sanz del Soto.

- The PhD students:
  - D. Francisco Javier Arroyo Maestu.
  - D. Rubén Martínez Díez.
  - Dña. Marta Fernández Régulez.
  - D. Juan Lobos Martín.
  - Dña. Ángela Mediavilla Trabada.
  - Dña. Ana Cobos Huerga.
  - D. Luis Fernando Hevia de los Mozos.

- The Bachelors:
  - Juan Francisco Rodríguez Cogollos.
  - Dña. María Aboy Cebrián.
  - D. Tomás Romero Albillos.
  - D. Miguel Ángel Rubio Hernández.
  - D. Andrés Serna Gutiérrez.

1.1.2. Lines of research

The research activity of the group is defined by a general line, which gives the group its name, and seven specific lines according to it.

1.1.2.1 General line of research

The general line can be summarized as **thermodynamic study of phase equilibria in gaseous, liquid and solid mixtures**. The main experimental projects performed according to this line include the assembly and commissioning of experimental equipment:

- A *Tian-Calvet* microcalorimeter.
- A densimeter *Anton Paar DMA 602*.
- A densimeter and sound analyzer *Anton Paar DSA 5000*.
- A self-constructed experimental device for the determination of liquid-liquid and solid-liquid equilibria by the observation of the phenomenon of critical opalescence.
- A refractometer *Bellingam + Stanley RFM970*.
- An experimental setup for the determination of relative permittivity including an *Agilent 4294A High Precision Impedance Analyzer, 40 Hz to 110 MHz* and an *Agilent 16452 Liquid Test Fixture*.
- A differential scanning calorimeter *TA Instruments DSC Q2000*.

Among the theoretical works carried out, the following must be highlighted:

- Application of the DISQUAC (DISpersive-QUAsiChemical) model to liquid mixtures.
- Application of the UNIFAC (UNIQUAC Functional-group Activity Coefficients) model, in its different versions, to liquid mixtures.
- Application of the Flory model to liquid mixtures.
- Application of the ERAS (Extended Real Associated Solution) model to liquid mixtures.
- Application of the Kirkwood-Buff formalism for concentration fluctuations to liquid mixtures.

- Application of the Bhatia-Thornton formalism for concentration fluctuations to liquid mixtures.
- Application of the Kirkwood-Fröhlich model for dielectrics to liquid mixtures.

1.1.2.2 Specific lines of research

1. Experimental study of associated mixtures.
    - Alcohol + hydrocarbon.
    - Alcohol + ether.
    - Hydroxy ether + hydrocarbon.
    - Hydroxy ether + ether.
    - Hydroxy ether + alcohol.
    - Hydroxy ether + hydroxy ether.
    - Primary or secondary amine + hydrocarbon.
    - Primary or secondary amine + ketone.
    - Amine + alcohol.
    - Amide + primary or secondary amine.
2. Experimental study of mixtures with purely dipolar interactions.
    - Ether + alkane.
    - Ketone + alkane.
    - Ketone + ether.
    - Organic carbonate + organic solvents.
    - Alkyl anhydride + organic solvents.
    - *N,N,N*-trialkylamine + alkane.
    - Amide + alkane.
    - *N,N*-dialkylamide + ketone.
3. Investigation of the behavior of the excess heat capacity for several fundamental theories of mixtures.
    - Experimental study of mixtures whose excess molar isobaric heat capacity shows a W-shaped dependence (double minimum) with concentration.
    - Theoretical study of W-shaped concentration dependence in excess heat capacities. First step: Strictly Regular Solution Theory. Second step: Flory Theory.
4. Application of theories based on group-contribution methods to characterize the thermodynamic properties of mixtures.
    - Systematic application of the DISQUAC model (purely physical theory with no association or solvation parameters) to justify the properties of all types of mixtures and phase equilibria.
    - Application of group-contribution models to predict vapor-liquid equilibrium and excess functions in multicomponent liquid mixtures.
5. Study of models based on the random mixing hypothesis.
    - Application of the Flory model to characterize orientational effects in mixtures of polar compounds with hydrocarbons or other polar compounds.
    - Analysis of the limitations of the Flory model with the purpose to improve the ERAS model.
6. Application of association models to explain the thermodynamic properties and phase equilibria in associated mixtures.

- Systematic application of the ERAS model.
- Comparison of the results from the ERAS model with those from group-contribution models.

7. Application of theories of fluctuations of concentration to study orientational and structural effects in mixtures. In particular:
    - The Kirkwood-Buff formalism, following Ben Naim's method.
    - The Bhatia-Thornton formalism.

1.1.2.3 Other lines of research

- An *a priori* mathematical analysis of the Wilson equation.
- Determination of solid-liquid equilibria of mixtures that can form complexes in condensed phase with a *Setaram DSC 111* calorimeter.
- Calibration of a vibrating-tube densimeter R.-K.-Wood-type and density measurement of pure liquids and mixtures at high temperature and pressure.
- Development of a latent-heat cover for greenhouses in Castilla y León.
- Thermodynamic study of basic structural units in polymers (oligomers) in solution.
- Determination of critical exponents from liquid-liquid equilibrium coexistence curves.
- Study of the influence of the combinatory term on the prediction of thermodynamic properties of mixtures containing long-chain molecules.
- Experimental study and modeling of solid-solid first-order phase transitions in mixtures of alcohols with different organic solvents.
- Study of biologically interesting liquid mixtures.

1.1.3. Collaboration with other research groups

GETEF has been continuously collaborating with many universities and research centers, such as:

1.1.3.1 National centers

- Dr. M.A. Villamañán and collaborators (co.). Laboratorio de Termodinámica. Departamento de Ingeniería Energética y Fluidomécanica. E.T.S. de Ingenieros Industriales. Universidad de Valladolid.
- Dra. M.J. Cocero and co., Dr. A. Cartón and co. Departamento de Ingeniería Química. Universidad de Valladolid.
- Dr. R. Bravo and co. Departamento de Física Aplicada. Universidad de Santiago de Compostela.
- Dr. A. Lainez, Dr. J.A.R. Renuncio and co. Departamento de Química-Física I. Universidad Complutense de Madrid.
- Dr. S. Otín and co., Dr. P. Pérez and co., and Dr. C. Lafuente and co. Departamento de Química-Física y Química Orgánica. Universidad de Zaragoza.
- Dra. C. Alonso Tristán. Departamento de Ingeniería Electromecánica. Escuela Politécnica Superior. Universidad de Burgos.
- Dra. M^{a} Purificación Cuadrado Curto. Departamento de Química Orgánica. Universidad de Valladolid.

1.1.3.2 Foreign centers

- Prof. J.-P.E. Grolier, A.H. Roux, G. Roux-Desgranges, Prof. J.R. Quint, Prof. J.-Y. Coxam, K. Ballerat-Busserolles and co. Université Blaise-Pascal. Clermont-Ferrand (France).
- Prof. E. Wilhelm. Institut für Physikalische Chemie. Universität Wien. Vienna (Austria).
- Prof. U. Domanska and Prof. T. Hofman. Department of Chemistry. Physical Chemistry Division. Faculty of Chemistry. Warsaw University of Technology. Warsaw (Poland).
- Prof. S.W. Campbell. Department of Chemical Engineering. University of South Florida. Tampa, Florida (USA).
- Prof. J.P. M. Trusler y Dr. A. Fenghour. Chemical Engineering and Chemical Technology Department. Imperial College. London (UK).
- Dr. N. Riesco. Department of Earth Science and Engineering. Imperial College. London (UK).
- Prof. J. Gmehling. Technische Chemie Department. Carl von Ossietzky Universität. Oldenburg (Germany).
- Dr. I. Mozo. Universidad de Yachay. Imbabura (Ecuador).

In addition, more sporadic collaborations have existed, as those with Dra. Magda Sampaio (Universidade de Lisboa, Portugal) or with Dr. A. Ait-Kaci (Université des sciences et de la technologie Houari-Boumediene, Dar el Beïda, Algeria).

1.2. About this PhD Thesis

This PhD Thesis continues the exhaustive scientific work carried out by GETEF, not only following their general research lines but also the specific ones.

This PhD Thesis began in October 2015 as a continuation of a Master Thesis [6] developed in the same research group in 2014-2015. It started as the **first systematic investigation of thermophysical properties of amide + amine liquid mixtures**, but soon its scope became wider. Not only it reached other kinds of experimental and theoretical lines of research, but it also was enriched with two international research stays at the 'Institut de Chimie de Clermont-Ferrand' (ICCF), in 'Université Clermont Auvergne', with the group MAG ('Mécanismes d'Absorption des Gaz'), directed by Jean-Yves Coxam.

1.2.1. Experimental objectives

The experimental contribution consists essentially of the measurement of thermophysical properties of binary liquid mixtures of biologically interesting molecules. Particularly:

- **Measurement of thermophysical properties of amide + amine mixtures** (**Articles 1 to 4, Appendix A**). These include calorimetric, volumetric, dielectric and refractive properties.
- **Measurement of dielectric and refractive properties of 1-alkanol + isomeric amine mixtures** (**Articles 5 to 6, Appendix B**). The considered amines are hexan-1-amine (HxA), *N*-propylpropan-1-amine (DPA) and *N,N,N*-triethylamine (TEA). The work continues the investigation carried out by S. Villa in her PhD Thesis [7] and is complementary to L.F. Sanz and V. Alonso's PhD Theses [8, 9]. It allows to study the effect of the replacement of a strongly polar compound (amide) by an associated liquid (1-alkanol).

Complementarily, other experimental works were performed during the first of the stays in Clermont-Ferrand (**Appendix C**, [10]). More precisely:

- Measurement of the enthalpy of solution of sulfur dioxide in water and in electrolyte aqueous solutions of sodium chloride and sodium sulfate.
- Measurement of the enthalpy of solution of nitric oxide in water.

The details of the measurements performed can be seen in Table 1.1. It must be noted that the isobaric heat capacity measurements have not been included in this Thesis, as their analysis is not yet finished.

Table 1.1: Experimental work performed in this PhD Thesis.

The properties determined are (see Chapter 2): density (ρ), speed of sound (c), isentropic compressibility (κ_S), isobaric thermal expansion coefficient (α_p), excess molar volume ($V_{\mathrm{m}}^{\mathrm{E}}$), excess isentropic compressibility (κ_S^{E}), excess speed of sound (c^{E}), excess isobaric thermal expansion coefficient (α_p^{E}), refractive index at the sodium D-line (n_{D}), excess refractive index at the sodium D-line ($n_{\mathrm{D}}^{\mathrm{E}}$), relative permittivity at 1 MHz (ε_{r}), excess relative permittivity at 1 MHz ($\varepsilon_{\mathrm{r}}^{\mathrm{E}}$), excess molar enthalpy ($H_{\mathrm{m}}^{\mathrm{E}}$), volumetric heat capacity ($\rho c_p = C_{p,\mathrm{m}}/V_{\mathrm{m}}$), molar isobaric heat capacity ($C_{p,\mathrm{m}}$), excess molar isobaric heat capacity ($C_{p,\mathrm{m}}^{\mathrm{E}}$), enthalpy of solution ($\Delta_{\mathrm{sol}}H$).

Device	Location	Measured properties	Derived properties	Mixtures
Anton Paar DSA5000	GETEF	ρ , c	κ_S , α_p , $V_{\mathrm{m}}^{\mathrm{E}}$, κ_S^{E} , c^{E} , α_p^{E}	DMF + BA, HxA, DPA or DBA DMA + BA, HxA, DPA or DBA
Bellingham + Stanley RFM970	GETEF	n_{D}	$n_{\mathrm{D}}^{\mathrm{E}}$	DMF + BA, HxA, DPA or DBA DMA + BA, HxA, DPA or DBA HxA + 1OH, 3OH, 4OH, 5OH or 7OH DPA + 1OH, 3OH, 4OH, 5OH or 7OH TEA + 1OH, 3OH, 4OH, 5OH or 7OH
Agilent 4294A and 16452A	GETEF	ε_{r}	$\varepsilon_{\mathrm{r}}^{\mathrm{E}}$	DMF + BA, HxA, DPA, DBA or aniline DMA + BA, HxA, DPA or DBA HxA + 1OH, 3OH, 4OH, 5OH or 7OH DPA + 1OH, 3OH, 4OH, 5OH or 7OH TEA + 1OH, 3OH, 4OH, 5OH or 7OH
Setaram BT2.15	MAG	$H_{\mathrm{m}}^{\mathrm{E}}$		DMF + BA, HxA, DPA or DBA DMA + BA, HxA, DPA or DBA
Setaram Micro DSC III and Micro SC	MAG	ρc_p	$C_{p,\mathrm{m}}$, $C_{p,\mathrm{m}}^{\mathrm{E}}$	DMF + BA, HxA, DPA or DBA DMA + BA, HxA, DPA or DBA

The organic liquids used are:
N,N-dimethylformamide (DMF), *N,N*-dimethylacetamide (DMA), butan-1-amine (BA), hexan-1-amine (HxA), *N*-propylpropan-1-amine (DPA), *N*-butylbutan-1-amine (DBA), *N,N,N*-triethylamine (TEA), aniline, methanol (1OH), 1-propanol (3OH), 1-butanol (4OH), 1-pentanol (5OH) and 1-heptanol (7OH).

Device	Location	Measured properties	Derived properties	Solutions
Setaram C80	MAG	$\Delta_{sol}H$		SO_2 + H_2O, NaCl(aq) or Na_2SO_4(aq) NO + H_2O

The salts dissolved in water (H_2O) are: sodium chloride (NaCl) and sodium sulfate (Na_2SO_4). The gases dissolved in water and electrolyte aqueous solutions are: sulfur dioxide (SO_2) and nitric oxide (NO).

1.2.2. Theoretical objectives

In addition to the exhaustive experimental work of this Thesis, a significant amount of theoretical investigations has been conducted. Some of them are related to the knowledge and interpretation of properties of amide or 1-alkanol + amine liquid mixtures:

- Application of DISQUAC to justify excess molar enthalpies and heat capacities of amide + amine liquid mixtures (in progress).
- Application of the ERAS model to reproduce excess molar volumes and enthalpies of amide + amine liquid mixtures (**Appendix A**).
- Application of the Prigogine-Flory-Patterson model to describe excess molar volumes of amide + amine liquid mixtures (**Article 2**).
- Application of the Kirkwood-Fröhlich model to interpret the permittivity for the liquid mixtures studied experimentally (amide + amine and 1-alkanol + amine, see Table 1.1; **Articles 1 to 6, Appendix B**).

Nevertheless, other works were thought to open the scope of the Thesis:

- Investigation of orientational (i.e. non-random) effects in alkanone, alkanal or dialkyl carbonate + alkane mixtures and in alkanone + alkanone or + dialkyl carbonate liquid mixtures by means of experimental data (excess molar enthalpies, volumes or isobaric heat capacities, and liquid-liquid equilibria) and the application of the Prigogine-Flory-Patterson model to describe excess molar enthalpies and volumes (**Article 7**).
- Investigation of orientational effects in mixtures of organic carbonates with alkanes or 1-alkanols by means of experimental data (excess molar enthalpies, volumes, isobaric heat capacities, entropies or permittivities, internal pressures and liquid-liquid equilibria) and several theoretical approaches: the Prigogine-Flory-Patterson model to describe excess molar enthalpies and volumes, the Bhatia-Thornton concentration-concentration structure factor formalism, and the Kirkwood-Fröhlich model (**Article 8**).
- Study of the dielectric behavior of binary liquid mixtures involving 1–alkanols and strongly polar compounds (benzonitrile, nitrobenzene, ethanenitrile, nitromethane, sulfolane or dimethyl sulfoxide), using experimental data available in the literature. Application of the Kirkwood–Fröhlich model to these mixtures (**Chapter 5**, [11]).
- Review of the Thermodynamics and Statistical Physics of homogeneous dielectric media. Clarification of the macroscopic and microscopic hypothesis characterizing existing theories. Proposal of a consistent classification of microscopic models of dielectrics within the general modern scheme of Equilibrium Thermodynamics and Statistical Physics. In particular, careful study of the implicit macroscopic and microscopic assumptions in the Kirkwood-Fröhlich model and clear derivation of its equations as a fluctuation theory at zero electric field (**Chapter 4**).

Finally, it must be mentioned that some theoretical work was done to complement the experimental work carried out in Clermont-Ferrand, namely:

- Study, programming and modeling to predict the enthalpy of solution of sulfur dioxide in water and comparison of the calculations with measured and literature data (**Appendix C**).

1.2.3. Scientific activities related to the PhD Thesis

Conference attendance:

- **14th Joint European Thermodynamics Conference (JETC)**. Budapest University of Technology and Economics, Department of Energy Engineering (BME, DEE). 21/05/2017 – 25/05/2017, Budapest, Hungary.
- **Cutting-Edge Technology for Carbon Capture, Utilization and Storage (CETCCUS)**. Institut de Chimie de Clermont-Ferrand, France; Sphere Technology Connection, Calgary, Canada; CALNESIS, Riom, France. 24/09/2017 – 27/09/2017, Clermont-Ferrand, France.
- **Thermodynamique des Équilibres Entre Phases (TEEP)**. Institut de Chimie de Clermont-Ferrand; Laboratoire des Multimatériaux et Interfaces, Lyon; CALNESIS, Clermont-Ferrand. 07/12/2017 – 08/12/2017, Clermont-Ferrand, France.
- **23rd International Congress of Chemical and Process Engineering (CHISA 2018 Prague)**. Czech Society of Chemical Engineering. 25/08/2018 – 29/08-2018, Prague, Czech Republic.

International courses:

- **Summer School and Workshop in Calorimetry 2017: Calorimetry and thermal methods in material science**. Institut de Recherches sur la Catalyse et l'Environnement de Lyon (IRCELYON); Association de Calorimétrie et Effets Thermiques en Catalyse (ACETC); Societé Chimique de France; CNRS.

1.2.4. Scientific production of the author

Scientific articles:

1. J.A. González, F. Hevia, A. Cobos, I.G.d.l. Fuente, C. Alonso-Tristán, *Thermodynamics of mixtures containing a very strongly polar compound. 11. 1-Alkanol + alkanenitrile systems.* Thermochim. Acta **605** (2015) 121-129.
   https://doi.org/10.1016/j.tca.2015.02.021

2. A. Cobos, F. Hevia, J.A. González, I. García De La Fuente, C. Alonso Tristán, *Thermodynamics of amide + ketone mixtures. 1. Volumetric, speed of sound and refractive index data for N,N-dimethylformamide + 2-alkanone systems at several temperatures.* J. Chem. Thermodyn. **98** (2016) 21-32.
   https://doi.org/10.1016/j.jct.2016.02.016

3. F. Hevia, A. Cobos, J.A. González, I. García de la Fuente, L.F. Sanz, *Thermodynamics of Amide + Amine Mixtures. 1. Volumetric, Speed of Sound, and Refractive Index Data for N,N-Dimethylformamide + N-Propylpropan-1-amine, + N-Butylbutan-1-amine, + Butan-1-amine, or + Hexan-1-amine Systems at Several Temperatures.* J. Chem. Eng. Data **61** (2016) 1468-1478.
   https://doi.org/10.1021/acs.jced.5b00802

4. F. Hevia, A. Cobos, J.A. González, I.G. de la Fuente, V. Alonso, *Thermodynamics of Amide + Amine Mixtures. 2. Volumetric, Speed of Sound and Refractive Index Data for N,N-Dimethylacetamide + N-Propylpropan-1-Amine, + N-Butylbutan-1-Amine, + Butan-1-Amine, or + Hexan-1-Amine Systems at Several Temperatures.* J. Solution Chem. **46** (2017) 150-174.
https://doi.org/10.1007/s10953-016-0560-0

5. C. Alonso Tristán, J.A. González, F. Hevia, I. García de la Fuente, J.C. Cobos, *Liquid–Liquid Equilibria for Systems Containing 4-Phenylbutan-2-one or Benzyl Ethanoate and Selected Alkanes.* J. Chem. Eng. Data **62** (2017) 988-994.
https://doi.org/10.1021/acs.jced.6b00803

6. F. Hevia, J.A. González, C. Alonso-Tristán, I. García de la Fuente, L.F. Sanz, *Orientational effects in alkanone, alkanal or dialkyl carbonate + alkane mixtures and in alkanone + alkanone or + dialkyl carbonate systems.* J. Mol. Liq. **233** (2017) 517-527.
https://doi.org/10.1016/j.molliq.2017.03.014

7. F. Hevia, J.A. González, I. García de la Fuente, L.F. Sanz, J.C. Cobos, *Thermodynamics of amide + amine mixtures. 3. Relative permittivities of N,N-dimethylformamide + N-propylpropan-1-amine, + N-butylbutan-1-amine, + butan-1-amine, or + hexan-1-amine systems at several temperatures.* J. Mol. Liq. **238** (2017) 440-446.
https://doi.org/10.1016/j.molliq.2017.05.025

8. J.A. González, F. Hevia, C. Alonso-Tristán, I. García de la Fuente, J.C. Cobos, *Orientational effects in mixtures of organic carbonates with alkanes or 1-alkanols.* Fluid Phase Equilib. **449** (2017) 91-103.
https://doi.org/10.1016/j.fluid.2017.06.012

9. J.A. González, C.A. Tristán, F. Hevia, I.G. De La Fuente, L.F. Sanz, *Thermodynamics of mixtures containing aromatic nitriles.* J. Chem. Thermodyn. **116** (2018) 259-272.
https://doi.org/10.1016/j.jct.2017.09.027

10. A. Cobos, J.A. González, F. Hevia, I.G.D. La Fuente, C.A. Tristán, *Thermodynamics of amide+ketone mixtures. 2. Volumetric, speed of sound and refractive index data for N,N-dimethylacetamide+2-alkanone systems at several temperatures. Application of Flory's model to tertiary amide+n-alkanone systems.* J. Mol. Liq. **248** (2017) 286-301.
https://doi.org/10.1016/j.molliq.2017.10.007

11. F. Hevia, J.A. González, A. Cobos, I. García de la Fuente, L.F. Sanz, *Thermodynamics of amide + amine mixtures. 4. Relative permittivities of N,N-dimethylacetamide + N-propylpropan-1-amine, + N-butylbutan-1-amine, + butan-1-amine, or + hexan-1-amine systems and of N,N-dimethylformamide + aniline mixture at several temperatures. Characterization of amine + amide systems using ERAS.* J. Chem. Thermodyn. **118** (2018) 175-187.
https://doi.org/10.1016/j.jct.2017.11.011

12. J.A. Gonzalez, F. Hevia, L.F. Sanz, I. García de la Fuente, C. Alonso-Tristán, *Thermodynamics of mixtures containing a very strongly polar compound. 12. Systems with nitrobenzene or 1-nitroalkane and hydrocarbons or 1-alkanols.* Fluid Phase Equilib. **471** (2018) 24-39.
https://doi.org/10.1016/j.fluid.2018.04.022

13. F. Hevia, J.A. González, A. Cobos, I. García de la Fuente, C. Alonso-Tristán, *Thermodynamics of mixtures with strongly negative deviations from Raoult's law. XV. Permittivities and refractive indices for 1-alkanol + n-hexylamine systems at (293.15–303.15) K. Application of the Kirkwood-Fröhlich model.* Fluid Phase Equilib. **468** (2018) 18-28.
https://doi.org/10.1016/j.fluid.2018.04.007

14. F. Hevia, A. Cobos, J.A. González, I. García de la Fuente, L.F. Sanz, *Thermodynamics of mixtures with strongly negative deviations from Raoult's law. XVI. Permittivities and refractive indices for 1-alkanol + di-n-propylamine systems at (293.15–303.15) K. Application of the Kirkwood-Fröhlich model.* J. Mol. Liq. **271** (2018) 704-714.
https://doi.org/10.1016/j.molliq.2018.09.040

15. J.A. González, F. Hevia, L.F. Sanz, I.G. De La Fuente, J.C. Cobos, *Characterization of 1-alkanol + strongly polar compound mixtures from thermophysical data and the application of the Kirkwood-Buff integrals and Kirkwood-Fröhlich formalisms.* Fluid Phase Equilib. **492** (2019) 41-54.
https://doi.org/10.1016/j.fluid.2019.03.012

16. J.A. González, C. Alonso-Tristán, F. Hevia, L.F. Sanz, I. García de la Fuente, *Liquid-liquid equilibria for (2-hydroxy benzaldehyde + n-alkane) mixtures. Intermolecular and proximity effects in systems containing hydroxyl and aldehyde groups.* J. Chem. Thermodyn. **135** (2019) 359-368.
https://doi.org/10.1016/j.jct.2019.04.002

Presentations at conferences:

1. F. Hevia, J.A. González, I. García de la Fuente, L.F. Sanz, J.C. Cobos. *Relative permittivities of N,N-dimethylformamide + N-propylpropan-1-amine, + N-butylbutan-1-amine, + butan-1-amine, or + hexan-1-amine systems at several temperatures.* **Poster** presented at: **14th Joint European Thermodynamics Conference (JETC)**. Budapest University of Technology and Economics, Department of Energy Engineering (BME, DEE). 21/05/2017 – 25/05/2017, Budapest, Hungary.
https://www.researchgate.net/publication/318041239

2. F. Hevia, A. Cobos, J.A. González, I. García de la Fuente, C. Alonso Tristán. *Relative permittivities of N,N-dimethylacetamide + N-propylpropan-1-amine, + N-butylbutan-1-amine, + butan-1-amine, or + hexan-1-amine systems at several temperatures.* **Poster** presented at: **14th Joint European Thermodynamics Conference (JETC)**. Budapest University of Technology and Economics, Department of Energy Engineering (BME, DEE). 21/05/2017 – 25/05/2017, Budapest, Hungary.
https://doi.org/10.13140/RG.2.2.10576.51209

3. F. Hevia, J.A. González, C. Alonso Tristán, I. García de la Fuente, J.C. Cobos. *Orientational effects in mixtures of organic carbonates with alkanes or 1-alkanols.* **Poster** presented at: **14th Joint European Thermodynamics Conference (JETC)**. Budapest University of Technology and Economics, Department of Energy Engineering (BME, DEE). 21/05/2017 – 25/05/2017, Budapest, Hungary.
https://www.researchgate.net/publication/318041013

4. F. Hevia, J.A. González, C. Alonso Tristán, I. García de la Fuente, L.F. Sanz. *Orientational effects in alkanone, alkanal or dialkyl carbonate + alkane mixtures and in alkanone + alkanone or + dialkyl carbonate systems.* **Poster** presented at: **14th Joint European Thermodynamics Conference (JETC)**. Budapest University of Technology and Economics, Department of Energy Engineering (BME, DEE). 21/05/2017 – 25/05/2017, Budapest, Hungary.
https://www.researchgate.net/publication/318041103

5. F. Hevia, A. Cobos, J.A. González, I. García de la Fuente, C. Alonso Tristán. *Dielectric and refractive index measurements of 1-alkanol + N-propylpropan-1-amine systems at several temperatures.* **Poster** presented at: **14th Joint European Thermodynamics Conference (JETC)**. Budapest University of Technology and Economics, Department of Energy Engineering (BME, DEE). 21/05/2017 – 25/05/2017, Budapest, Hungary.
https://doi.org/10.13140/RG.2.2.35742.33603

6. A. Cobos, F. Hevia, J.A. González, I. García de la Fuente, L.F. Sanz. *Volumetric, speed of sound, refractive index and permittivity data for N,N-dimethylformamide, N,N-dimethylacetamide + acetophenone systems at several temperatures.* **Poster** presented at: **14th Joint European Thermodynamics Conference (JETC)**. Budapest University of Technology and Economics, Department of Energy Engineering (BME, DEE). 21/05/2017 – 25/05/2017, Budapest, Hungary.
https://doi.org/10.13140/RG.2.2.15609.67688

7. A. Cobos, F. Hevia, J.A. González, I. García de la Fuente, C. Alonso Tristán. *Volumetric, speed of sound and refractive index data for N,N-dimethylacetamide + 2-alkanone systems at several temperatures.* **Poster** presented at: **14th Joint European Thermodynamics Conference (JETC)**. Budapest University of Technology and Economics, Department of Energy Engineering (BME, DEE). 21/05/2017 – 25/05/2017, Budapest, Hungary.
https://doi.org/10.13140/RG.2.2.29031.44968

8. C. Alonso Tristán, I. García de la Fuente, J.A. González, J.C. Cobos, F. Hevia, A. Cobos, L.F. Sanz. *LLE of mixtures of phenyl acetonitrile + n-alkanes.* **Poster** presented at: **10º Congreso Nacional de Ingeniería Termodinámica (10CNIT)**. GREA Innovació Concurrent; Tecnio Catalonia, Acció, Generalitat de Catalunya; Institut Politècnic d'Innovació i Recerca en Sostenibilitat, Universitat de Lleida. 28/06/2017 – 30/06/2017, Lérida, Spain.
https://www.researchgate.net/publication/321184598

9. C. Alonso Tristán, F. Hevia, A. Cobos, I. García de la Fuente; J.A. González, J.C. Cobos. *Dielectric and refractive index measurements of 1-alkanol + hexan-1-amine systems at several temperatures.* **Poster** presented at: **10º Congreso Nacional de Ingeniería Termodinámica (10CNIT)**. GREA Innovació Concurrent; Tecnio Catalonia, Acció, Generalitat de Catalunya; Institut Politècnic d'Innovació i Recerca en Sostenibilitat, Universitat de Lleida. 28/06/2017 – 30/06/2017, Lérida, Spain.
https://www.researchgate.net/publication/318041499

10. F. Hevia, A. Cobos, J.A. González, I. García de la Fuente, J.C. Cobos, V. Alonso, C. Alonso Tristán, L.F. Sanz. *Dielectric and refractive index measurements of 1-alkanol + triethylamine systems. Application of the Kirkwood-Fröhlich model.* **Poster** presented at: **Thermodynamique des Équilibres Entre Phases (TEEP)**. Institut de Chimie de

Clermont-Ferrand; Laboratoire des Multimatériaux et Interfaces, Lyon; CALNESIS, Clermont-Ferrand. 07/12/2017 – 08/12/2017, Clermont-Ferrand, France.
https://doi.org/10.13140/RG.2.2.12354.07365

11. F. Hevia de los Mozos, K. Ballerat-Buserolles, B. Liborio, Y. Coulier; J.-Y. Coxam. *Calorimetric and Densimetric Data to Help the Simulation of the Impact of Annex Gases Co-injected with CO_2 During its Geological Storage.* **Oral presentation** at: **7th International Acid Gas Injection Symposium (AGIS VII)**. Sphere Technology Connection. 22/05/2018 – 25/05/2018, Calgary, Canadá.

12. F. Hevia, V. Alonso, A. Cobos, L. F. Sanz, J. A. González, I. García de la Fuente, J. C. Cobos, C. Alonso Tristán. *Excess molar volumes, isentropic compressibilities and refractive indices of 1-alkanol + aniline liquid mixtures.* **Poster** presented at: **23rd International Congress of Chemical and Process Engineering (CHISA 2018 Prague)**. Czech Society of Chemical Engineering. 25/08/2018 – 29/08-2018, Prague, Czech Republic.
https://doi.org/10.13140/RG.2.2.30745.47204

13. F. Hevia, A. Cobos, V. Alonso, L. F. Sanz, J. A. González, I. García de la Fuente, J. C. Cobos, C. Alonso Tristán. *Dielectric properties and Kirkwood correlation factors of liquid mixtures of 1-alkanols and strongly polar compounds.* **Poster** presented at: **23rd International Congress of Chemical and Process Engineering (CHISA 2018 Prague)**. Czech Society of Chemical Engineering. 25/08/2018 – 29/08-2018, Prague, Czech Republic.
https://doi.org/10.13140/RG.2.2.34100.91521

14. A. Cobos, V. Alonso, F. Hevia, L. F. Sanz, J. A. González, I. García de la Fuente, J. C. Cobos. *Excess molar volumes, isentropic compressibilities and refractive indices of 1-alkanol+benzylamine systems.* **Poster** presented at: **12th European Symposium on Thermal Analysis and Calorimetry (ESTAC12)**. CEEC-TAC, UniTBv, INFLPR, ICF, CATCAR. 27/08/2018 – 30/08-2018, Brasov, Romania.
https://doi.org/10.13140/RG.2.2.10021.35040

15. A. Cobos, P. Sikorski, T. Hofman, F. Hevia, J. A. González, I. García de la Fuente. *Determination of SLE and LLE equilibria in binary systems with complex carbonyl compounds.* **Poster** presented at: **12th European Symposium on Thermal Analysis and Calorimetry (ESTAC12)**. CEEC-TAC, UniTBv, INFLPR, ICF, CATCAR. 27/08/2018 – 30/08-2018, Brasov, Romania.
https://doi.org/10.13140/RG.2.2.16732.23688

Book chapters:

1. F. De los Mozos, K. Ballerat-Busserolles, B. Liborio, N. Nénot, J.-Y. Coxam, Y. Coulier, *Calorimetric and Densimetric Data to Help the Simulation of the Impact of Annex Gases Co-Injected with CO_2 During Its Geological Storage.* In: Ying (Alice) Wu, John J. Carroll, and Yongle Hu (eds.), *The Three Sisters: Acid Gas Injection, Carbon Capture and Sequestration, and Enhanced Oil Recovery*, Advances in Natural Gas Engineering, Vol. 7, Ch. 4, pp. 39-54, Scrivener Publishing and John Wiley & Sons, 2019.
https://doi.org/10.1002/9781119510079.ch4

1.2.5. Funding

This PhD Thesis is funded by public grants from 'Ministerio de Educación, Cultura y Deporte' and the University of Valladolid:

- 'Ayuda para la Formación del Profesorado Universitario' (FPU) (reference FPU14/04104). A four-year contract funded by 'Ministerio de Educación, Cultura y Deporte' for the entire PhD studentship period.
- 'Ayuda a la movilidad para estancias breves y traslados temporales' (reference: EST16/00824). Complementary grant from 'Ministerio de Educación, Cultura y Deporte' destined to fund the first of the two stays at ICCF (20/09/2017 – 19/12/2017).
- 'Ayuda a la movilidad para estancias breves y traslados temporales' (reference: EST17/00292). Complementary grant from 'Ministerio de Educación, Cultura y Deporte' destined to fund the second of the two stays at ICCF (18/09/2018 – 17/12/2018).
- 'Ayuda por asistencia a cursos, congresos y jornadas relevantes para el desarrollo de tesis doctorales, convocatoria 2017'. Given by University of Valladolid to attend the international course 'Summer School and Workshop in Calorimetry 2017: Calorimetry and thermal methods in material science'.
- 'Ayuda por asistencia a cursos, congresos y jornadas relevantes para el desarrollo de tesis doctorales, convocatoria 2018'. Given by University of Valladolid to attend the international conference '23rd International Conference of Chemical and Process Engineering (CHISA 2018 Prague)'.

1.3. Detail of the work at ICCF

The two stays in Clermont-Ferrand were completely covered by complementary grants from 'Ministerio of Educación, Cultura y Deporte' (see above). The researcher responsible for the project at ICCF was Dr. J.-Y. Coxam. The daily work at the laboratory was also supervised by Dr. K. Ballerat-Busserolles and with useful help from Dr. Y. Coulier.

One of the objectives of the stays was to learn and apply techniques which were not available in the laboratory of GETEF. That is why some scientific activity is not directly related to the subject of this Thesis.

1.3.1. September 2017 – December 2017

1.3.1.1 Experimental part

The experimental part of the first stay at ICCF involved the familiarization with techniques based on **flow calorimetry** that would be used to determine excess and solution enthalpies. With this aim, two devices were employed:

- *Setaram C80* calorimeter, adapted to flow calorimetry, high pressures and high temperatures.
- *Setaram BT 2.15* calorimeter, adapted to flow calorimetry, high pressures and low temperatures.

The training included, specifically:

- Safety training to work with dangerous gases at high pressure.
- Configuration of the different preheaters and precoolers to perform measurements at a desired temperature.
- Characteristics of the calorimeters and different fluid pumps to work with liquids and gases.
- Calibration of the calorimeters using the excess molar enthalpy of the ethanol + water mixture as a reference system.
- Maintenance and cleaning, with special emphasis on avoiding corrosion by acid gases.

Using this equipment, the following research works were completed:

- Measurement of the enthalpy of solution of sulfur dioxide (SO_2) in water and in aqueous solutions of sodium chloride and sodium sulfate at 323.15 K and 0.3 MPa (*Setaram C80*).
- Measurement of the enthalpy of solution of nitric oxide (NO) in water at 323.15 K and at 2.27, 2.50 and 2.80 MPa (*Setaram C80*).
- It must be mentioned that some measurements of the enthalpy of solution of NO in water at 373.15 K were also carried out but, due to the smallness of the solubility of NO in water at this temperature, no conclusive results could be obtained. This motivates some future modifications of the technique to measure very low heat effects.

Between December 2017 and September 2018, the results obtained for sulfur dioxide were prepared for publication as a book chapter [10] (see above). Also, the MAG researchers at ICCF continued the work trying to measure the enthalpy of solution of sulfur dioxide in water and in aqueous solutions of sodium chloride and sodium sulfate at 373.15 K. They found important corrosion problems inside the calorimetric cell at this temperature, which made them stop the measurements for some months. The measurements involving pure water and sulfur dioxide at 373.15 K were repeated between September 2018 and December 2018 (during the second stay), yielding results which were consistent with those obtained before, but the experiments corroded the system once more.

- Measurement of the molar excess enthalpy of the liquid mixture *N,N*-dimethylformamide + butan-1-amine at 298.15 K and 0.3 MPa (*Setaram BT 2.15*).

The last of these works was performed as a first attempt to measure the excess molar enthalpies of the amide + amine mixtures studied in this PhD Thesis, which would be the subject of the second stay at ICCF. The results were quite satisfactory, although the job was to be repeated using new liquids.

1.3.1.2 Theoretical part

The objective of the theoretical part of the first stay has been basically the modeling of the enthalpy of solution experimentally determined in the laboratory. In systems including SO_2, there are chemical reactions alongside the physical process of dissolution, and the equations become somewhat complex. An attempt was made to calculate the enthalpy of solution of NO in water, but the lack of extensive reliable experimental data on the solubility prevented from a reasonable application of the model.

More precisely, the stages of the development of this theoretical task were the following:

- Application of the thermodynamic formalism to vapor-liquid equilibria (VLE) of aqueous solutions of molecular compounds and electrolytes among which simultaneous chemical reactions can take place.
- Selection of a microscopic model for the liquid phase of these systems. With the help of the formalism of Statistical Physics, it is possible to obtain an expression of the natural thermodynamic potential for the appropriate state variables (temperature, pressure and composition). The selected theory was the Pitzer model as modified by Edwards *et al.*, which had already been used by MAG researchers to describe satisfactorily the dissolution process of other gases of environmental interest (CO_2, CO, etc.) in different kinds of aqueous mixtures and solutions.
- Combination of the thermodynamic formalism and the model to describe the VLE of the studied systems. It is assumed that only molecules of the molecular gas and of water are present in the vapor phase or, in other words, that the ions are non-volatile. This allows to obtain, after an iterative process, the adjustable parameters of the model (suitably chosen), Henry's law constant and the compositions of the liquid and the vapor from experimental measurements of solubility (as a function of pressure and temperature) of the gas in the mentioned solutions.
- Calculation of the enthalpy of solution at laboratory conditions using the adjusted parameters, and taking into account the physical part of the process and the chemical reactions. Programming of the calculations.

1.3.2. September 2018 – December 2018

In Valladolid, after moving the laboratory to the building of the new Faculty of Science, the available Tian-Calvet microcalorimeter was not ready to do the measurements of the excess molar enthalpies of amide + amide mixtures. The success of the measurements of the excess molar enthalpy of the mixture *N,N*-dimethylformamide + butan-1-amine in 2017 at ICCF motivated a second stay for 2018 in order to determine them using the calorimeter *Setaram BT 2.15*. In addition, DSC-type calorimeters were available for the simultaneous determination of the volumetric heat capacity of these mixtures. Therefore, the experimental part of the stay can be summarized as:

- Measurement of excess molar enthalpy and volumetric heat capacity of amide + amine liquid mixtures at 298.15 K and 0.1 MPa (see Table 1.1 for details).

The heat capacity measurements were initially going to be performed using a fixed cell, power compensation, differential scanning calorimeter *CSC 6100 NanoDSC II* from Calorimetry Sciences Corporation. However, technical problems giving incorrect signals from the thermopile led to the decision of using another calorimeter for this task: a *Setaram MicroDSC III*. The measurements with this calorimeter started normally, but after two weeks of measurements some serious problems of thermal stability appeared, and could not be solved. The values obtained during this period needed to be checked again, so K. Ballerat-Busserolles decided to repeat the measurements by herself using a *Setaram MicroSC* differential scanning calorimeter. The measurements are not ready to analyze but are being processed at the moment of writing this Thesis.

1.3.3. Publication of the results

The results obtained in both periods are being prepared for publication at the time of writing this manuscript, and they are shown in the appendices.

1.4. References

[1] M.Á. Villamañán, *Estudio termodinámico de mezclas líquidas alcohol + éter*. Tesis Doctoral, 1979. Departamento de Física Fundamental, Facultad de Ciencias, Universidad de Valladolid.

[2] J.C. Cobos, *Montaje y puesta a punto de un microcalorímetro Tian-Calvet*. Trabajo de Licenciatura, 1979. Departamento de Física Fundamental, Facultad de Ciencias, Universidad de Valladolid.

[3] J.C. Cobos, *Estudio termodinámico de mezclas líquidas de alcoxietanoles con disolventes orgánicos*. Tesis Doctoral, 1987. Departamento de Física Aplicada II, Facultad de Ciencias, Universidad de Valladolid.

[4] I. García de la Fuente, *Estudio termodinámico de mezclas líquidas de carbonatos con disolventes orgánicos*. Tesis Doctoral, 1987. Departamento de Física Aplicada II, Facultad de Ciencias, Universidad de Valladolid.

[5] J.A. González, *Estudio termodinámico de las mezclas líquidas de cetonas con alcanos mediante el modelo DISQUAC. Comparación de las predicciones del modelo UNIFAC.* Tesis Doctoral, 1987. Departamento de Física Aplicada II, Facultad de Ciencias, Universidad de Valladolid.

[6] F. Hevia, *Estudio experimental y teórico de mezclas binarias de amidas y aminas*. Trabajo Fin de Máster, 2015. Departamento de Física Aplicada, Facultad de Ciencias, Universidad de Valladolid.

[7] S. Villa, *Contribución experimental y teórica al estudio de las propiedades termodinámicas de mezclas líquidas formdas por aminas y alcanos o 1-alcoholes*. Tesis Doctoral, 2003. Departamento de Física Aplicada, Facultad de Ciencias, Universidad de Valladolid.

[8] L.F. Sanz, *Estudio experimental y teórico de mezclas líquidas binarias formadas por 1-alcoholes y ciclohexilamina*. Tesis Doctoral, 2016. Departamento de Física Aplicada, Facultad de Ciencias, Universidad de Valladolid.

[9] V. Alonso, *Estudio experimental de propiedades termofísicas de mezclas binarias formadas por 1-alcohol + alcano, + éter lineal o + amina aromática primaria*. Tesis Doctoral, 2016. Departamento de Física Aplicada, Facultad de Ciencias, Universidad de Valladolid.

[10] F. De Los Mozos, K. Ballerat-Busserolles, B. Liborio, N. Nénot, J.-Y. Coxam, Y. Coulier, *Calorimetric and Densimetric Data to Help the Simulation of the Impact of Annex Gases Co-Injected with CO2 During Its Geological Storage*, in *The Three Sisters: Acid Gas Injection, Carbon Capture and Sequestration, and Enhanced Oil Recovery*, Y. Wu, J.J. Carroll, and Y. Hu, Editors. 2019, Scrivener Publishing and John Wiley & Sons: USA. p. 39-54.

[11] J.A. González, F. Hevia, L.F. Sanz, I.G. De La Fuente, J.C. Cobos, *Characterization of 1-alkanol + strongly polar compound mixtures from thermophysical data and the application of the Kirkwood-Buff integrals and Kirkwood-Fröhlich formalisms.* Fluid Phase Equilib. **492** (2019) 41-54. https://doi.org/10.1016/j.fluid.2019.03.012

Chapter 2.

Mixing and excess functions

Thermodynamics of heterogeneous and multicomponent systems is of the greatest importance. Not only is it of great theoretical significance, but it also has many scientific and industrial applications. As a consequence, it is used every day by physicists, chemists and engineers. It covers a very wide range of subjects, and therefore an extensive treatment is beyond the scope of this chapter. Thus, it is intended to briefly summarize most of the topics used along this Thesis. In addition, the basic concepts are assumed known by the reader. In Table 2.1 we give the notation used for some thermodynamic properties used in the text, and also their expressions for an ideal mixture in the sense explained below.

2.1. Mixing functions

A **mixing process at constant pressure (and temperature)** is understood as a thermodynamic process in which certain amounts of several pure substances (homogeneous and monocomponent systems), which at a given pressure and temperature are **in the same state of aggregation**, transform into an only homogeneous and multicomponent system (called a **mixture**) at the same pressure and temperature.

As a result of intermolecular forces existing among the different structural units (atoms, molecules...) of the substances involved, the properties of the mixture cannot be obtained as a simple consequence of the properties of the pure substances separately: they are **emergent properties**. Thus, the extensive properties of the mixture will not be, in general, the sum of the extensive properties of the separate components. This leads to the concepts of molar property of the mixture, partial molar properties and molar mixing properties.

Let X denote an extensive property of the mixture, T the temperature, p the pressure, n_i the amount of substance of component i, $n = \sum_i n_i$ the total amount of substance of the mixture and $x_i = n_i/n$ the mole fraction of component i. The **molar property of the mixture**, X_m, and the **partial molar property of component *i***, $\bar{X}_{\mathrm{m},i}$, are defined by:

$$X_\mathrm{m} = \frac{X}{n} \tag{2.1}$$

$$\bar{X}_{\mathrm{m},i} = \left(\frac{\partial X}{\partial n_i}\right)_{T,p,n_{j\neq i}} \tag{2.2}$$

Table 2.1: Notation and ideal thermodynamic functions (see sections 2.2 to 2.4). Meaning of symbols: T, temperature; R, universal gas constant; x_i, mole fraction of component i, $\phi_i = x_i V_{\mathrm{m},i} / V_{\mathrm{m}}^{\mathrm{id}}$, volume fraction of component i; M_i, molar mass of pure component i; subscript "m", molar quantity.

Extensive property	Symbol (X)	$\Delta X_{\mathrm{m}}^{\mathrm{id}}$	$X_{\mathrm{m}}^{\mathrm{id}}$
Volume	V	0	$\sum x_i V_{\mathrm{m},i}$
Entropy	S	$-R\sum x_i \ln x_i$	$\sum x_i S_{\mathrm{m},i} - R\sum x_i \ln x_i$
Gibbs function	G	$RT\sum x_i \ln x_i$	$\sum x_i G_{\mathrm{m},i} + RT\sum x_i \ln x_i$
Helmholtz function	F	$RT\sum x_i \ln x_i$	$\sum x_i F_{\mathrm{m},i} + RT\sum x_i \ln x_i$
Internal energy	U	0	$\sum x_i U_{\mathrm{m},i}$
Enthalpy	H	0	$\sum x_i H_{\mathrm{m},i}$
Isobaric heat capacity	C_p	0	$\sum x_i C_{p\mathrm{m},i}$
Isochoric heat capacity	C_V	$T\left[\sum\left(x_i \frac{V_{\mathrm{m},i}\alpha_{p,i}^2}{\kappa_{T,i}}\right) - \frac{V_{\mathrm{m}}^{\mathrm{id}}\left(\alpha_p^{\mathrm{id}}\right)^2}{\kappa_T^{\mathrm{id}}}\right]$	$C_{p,\mathrm{m}}^{\mathrm{id}} - \frac{TV_{\mathrm{m}}^{\mathrm{id}}\left(\alpha_p^{\mathrm{id}}\right)^2}{\kappa_T^{\mathrm{id}}} = \frac{C_{p,\mathrm{m}}^{\mathrm{id}}\kappa_S^{\mathrm{id}}}{\kappa_T^{\mathrm{id}}}$

Intensive property	Symbol (X)	X^{id}
Isobaric thermal expansion coefficient	α_p	$\sum \phi_i \alpha_{p,i}$
Isothermal compressibility coefficient	κ_T	$\sum \phi_i \kappa_{T,i}$
Isentropic compressibility coefficient	κ_S	$\kappa_T^{\mathrm{id}} - \frac{TV_{\mathrm{m}}^{\mathrm{id}}\left(\alpha_p^{\mathrm{id}}\right)^2}{C_{p,\mathrm{m}}^{\mathrm{id}}}$
Density	ρ	$\frac{\sum x_i M_i}{V_{\mathrm{m}}^{\mathrm{id}}}$
Speed of sound	c	$\left(\rho^{\mathrm{id}}\kappa_S^{\mathrm{id}}\right)^{-1/2}$
Relative permittivity	ε_{r}	$\sum \phi_i \varepsilon_{\mathrm{r},i}$
Refractive index (at the sodium D-line)	n_{D}	$\left(\sum \phi_i n_{\mathrm{D},i}^2\right)^{1/2}$

Due to extensivity (homogeneity of degree one of the extensive state variables):

$$X_{\mathrm{m}} = \sum_i x_i \bar{X}_{\mathrm{m},i} \tag{2.3}$$

The **molar mixing property or function (at constant pressure)** is defined as:

$$\Delta X_{\mathrm{m}}(T,p,x) = X_{\mathrm{m}}(T,p,x) - \sum_i x_i X_{\mathrm{m},i}(T,p) \tag{2.4}$$

where x denotes the set of mole fractions needed to specify the composition and $X_{\mathrm{m},i}(T,p)$ is the molar property of the pure compound i.

Particularly important is the well-known fact that the mixing molar volume, $\Delta V_{\mathrm{m}}(T,p,x)$, is not zero. Therefore, there exists a contribution to all mixing properties at constant pressure that arises from the **volume variation** of the system. It depends on several factors, such as the nature and strength of intermolecular forces, the size and shape of the molecules and the supramolecular structural units, and their reorganization to form the mixture. This contribution can be quantified rigorously by means of the variation of pressure $\Delta p(T,p,x)$ that the system should experience in order to keep the volume constant:

$$V_{\mathrm{m}}\left(T,p+\Delta p(T,p,x),x\right)=\sum_i x_i V_{\mathrm{m},i}(T,p)=V_{\mathrm{m}}(T,p,x)-\Delta V_{\mathrm{m}}(T,p,x) \tag{2.5}$$

It is useful to define a **mixing process at constant volume (and temperature)**, which is different from the constant pressure mixing only because the **final state** is not defined by the same pressure as before mixing, but by a **volume equal to the sum of the volumes of the pure substances (at the initial pressure) separately**. The **molar mixing properties at constant volume** are defined by:

$$\Delta X_{\mathrm{m},V}(T,p,x)=X_{\mathrm{m}}\left(T,p+\Delta p(T,p,x),x\right)-\sum_i x_i X_{\mathrm{m},i}(T,p) \tag{2.6}$$

The volume variation contribution:

$$\begin{aligned}\Delta X_{\mathrm{m}}^{\Delta V}(T,p,x)&=\Delta X_{\mathrm{m}}(T,p,x)-\Delta X_{\mathrm{m},V}(T,p,x)\\&=X_{\mathrm{m}}(T,p,x)-X_{\mathrm{m}}\left(T,p+\Delta p(T,p,x),x\right)\\&=X_{\mathrm{m}}(T,V_{\mathrm{m}},x)-X_{\mathrm{m}}(T,V_{\mathrm{m}}-\Delta V_{\mathrm{m}},x)\end{aligned} \tag{2.7}$$

can be calculated with a very good degree of approximation by expanding $X_{\mathrm{m}}(T,V_{\mathrm{m}}-\Delta V_{\mathrm{m}},x)$ in powers of ΔV_{m}. To second order, it is:

$$\Delta X_{\mathrm{m}}^{\Delta V}\approx\left(\frac{\partial X_{\mathrm{m}}}{\partial V_{\mathrm{m}}}\right)_{T,x}\Delta V_{\mathrm{m}}-\frac{1}{2}\left(\frac{\partial^2 X_{\mathrm{m}}}{\partial V_{\mathrm{m}}^2}\right)_{T,x}(\Delta V_{\mathrm{m}})^2 \tag{2.8}$$

In the majority of cases, it is easier to evaluate the derivatives in equation (2.8) in terms of derivatives with respect to p. The following expressions are useful for that purpose:

$$\left(\frac{\partial X_{\mathrm{m}}}{\partial V_{\mathrm{m}}}\right)_{T,x}=-\frac{1}{V_{\mathrm{m}}\kappa_T}\left(\frac{\partial X_{\mathrm{m}}}{\partial p}\right)_{T,x} \tag{2.9}$$

$$\left(\frac{\partial^2 X_{\mathrm{m}}}{\partial V_{\mathrm{m}}^2}\right)_{T,x}=\frac{1}{(V_{\mathrm{m}}\kappa_T)^2}\left[\left(\frac{\partial^2 X_{\mathrm{m}}}{\partial p^2}\right)_{T,x}-\frac{1}{V_{\mathrm{m}}\kappa_T}\left(\frac{\partial\{V_{\mathrm{m}}\kappa_T\}}{\partial p}\right)_{T,x}\left(\frac{\partial X_{\mathrm{m}}}{\partial p}\right)_{T,x}\right] \tag{2.10}$$

We give below the most used mixing functions at constant volume up to the first nonzero term of the series expansion:

$$\Delta F_{\mathrm{m},V}\approx\Delta G_{\mathrm{m}}+\frac{1}{2V_{\mathrm{m}}\kappa_T}(\Delta V_{\mathrm{m}})^2 \tag{2.11}$$

$$\Delta S_{\mathrm{m},V}\approx\Delta S_{\mathrm{m}}-\frac{\alpha_p}{\kappa_T}\Delta V_{\mathrm{m}} \tag{2.12}$$

$$\Delta U_{\mathrm{m},V}\approx\Delta H_{\mathrm{m}}-T\frac{\alpha_p}{\kappa_T}\Delta V_{\mathrm{m}} \tag{2.13}$$

2.2. Excess functions

In many situations it is useful to compare the mixing functions with those of a very simple mixture model that is well known and understood. Such a model is termed **ideal mixture**. We will use the Lewis-Randall model, defined by a mixing molar Gibbs function $\Delta G_{\mathrm{m}}^{\mathrm{id}}$ given by:

$$\Delta G_{\mathrm{m}}^{\mathrm{id}} = RT\sum_i x_i \ln x_i \tag{2.14}$$

which is the mixing molar Gibbs function of a mixture of ideal gases (R is the universal gas constant). More details about ideal states can be found in the usual literature of the subject (e.g. [1-3]); here we are only interested in a summary of the properties used throughout this Thesis. The rest of the mixing properties of the ideal mixture can be calculated from $\Delta G_{\mathrm{m}}^{\mathrm{id}}$. They are tabulated in Table 2.1. Since $\Delta V_{\mathrm{m}}^{\mathrm{id}} = 0$, **ideal mixing properties at constant volume are the same as those at constant pressure**.

To perform the mentioned comparison of real and ideal quantities, we define the **excess molar functions at constant pressure**:

$$X_{\mathrm{m}}^{\mathrm{E}} = \Delta X_{\mathrm{m}} - \Delta X_{\mathrm{m}}^{\mathrm{id}} = X_{\mathrm{m}} - X_{\mathrm{m}}^{\mathrm{id}} \tag{2.15}$$

and the corresponding **excess molar functions at constant volume**:

$$X_{\mathrm{m},V}^{\mathrm{E}} = \Delta X_{\mathrm{m},V} - \Delta X_{\mathrm{m}}^{\mathrm{id}} \tag{2.16}$$

Between these two classes of functions there is a relationship:

$$X_{\mathrm{m}}^{\mathrm{E}} - X_{\mathrm{m},V}^{\mathrm{E}} = \Delta X_{\mathrm{m}} - \Delta X_{\mathrm{m},V} = \Delta X_{\mathrm{m}}^{\Delta V} \tag{2.17}$$

which allows to use the results for the molar mixing functions already obtained to calculate the excess molar functions at constant volume. Particularly, and since $V_{\mathrm{m}}^{\mathrm{E}} = \Delta V_{\mathrm{m}}$:

$$F_{\mathrm{m},V}^{\mathrm{E}} \approx G_{\mathrm{m}}^{\mathrm{E}} + \frac{1}{2V_{\mathrm{m}}\kappa_T}\left(V_{\mathrm{m}}^{\mathrm{E}}\right)^2 \tag{2.18}$$

$$S_{\mathrm{m},V}^{\mathrm{E}} \approx S_{\mathrm{m}}^{\mathrm{E}} - \frac{\alpha_p}{\kappa_T} V_{\mathrm{m}}^{\mathrm{E}} \tag{2.19}$$

$$U_{\mathrm{m},V}^{\mathrm{E}} \approx H_{\mathrm{m}}^{\mathrm{E}} - T\frac{\alpha_p}{\kappa_T} V_{\mathrm{m}}^{\mathrm{E}} \tag{2.20}$$

Although it does *not* make sense to define an intensive property of mixing, it does to talk about the **deviation from ideality of an intensive property**. By extension of equation (2.15), they are also called excess functions. The **excess of an intensive property $\boldsymbol{X}$** is therefore defined by:

$$X^{\mathrm{E}} = X - X^{\mathrm{id}} \tag{2.21}$$

where X^{id} is the value of the property in an ideal mixture.

There has been considerable confusion about the ideal value of some thermodynamic properties, but the procedure to obtain them is actually very simple: one only has to use general thermodynamic relations starting from the definition of ideal mixture.

2.3. Speed of sound

The propagation of sound waves in a fluid is, strictly speaking, a non-equilibrium phenomenon. There is, however, a sufficiently approximated method to analyze the situation in the framework of near-equilibrium Thermodynamics. When the speed of the fluid particles (macroscopic portions of fluid treatable as mechanical points) is sufficiently small, the local equilibrium hypothesis can be applied. More precisely, the speed of the fluid particles has to be smaller than $\sqrt{\delta p/\delta\rho}$, where δp is the amplitude of the pressure oscillation and $\delta\rho$ is the amplitude of the associated density oscillation. Both oscillations are assumed very small compared to their equilibrium values.

Wave equations are characterized by the presence of a quantity having the dimensions of velocity. This quantity will be called **wave velocity**. The wave velocity represents the speed at which the wave would propagate with the same properties in a medium if there were no absorption or dispersion. It must be noted that, in the general case, wave velocity does not represent a phase velocity or a group velocity. In fact, in the presence of absorption or dispersion a wave packet does not preserve its shape as it moves forward, which makes it difficult to give a precise meaning to the group velocity. When there are no dispersion or absorption, both the phase velocity of a monochromatic wave and the group velocity of a wave packet are equal to the wave velocity.

It is well-known that the sound in a fluid has a wave velocity, c, given by the Newton-Laplace equation [4]:

$$\kappa_S = \frac{1}{\rho c^2} \tag{2.22}$$

Consequently, the measurement of ρ and c allows to obtain the value of κ_S. In order to consider the speed of a pulse through the fluid (see section 3.1) as the wave velocity, the effect of absorption and dispersion must be negligible. This is the case when the length traveled by the pulse is sufficiently small, provided there are no important resonance processes at the range of frequencies covered by the pulse.

2.4. Dielectric and refractive properties

2.4.1. Static relative permittivity

For a dielectric to be considered in thermodynamic equilibrium, it has to be linear and homogeneous, and the true electric field[1] ($\vec{E}$) has to be static and uniform everywhere outside the conductors responsible of the presence of the field.

Thermodynamics of systems under the action of an electric field can be made on the basis of different kinds of thermodynamic potentials. In other words, one can use different "energies" to derive the rest of the thermodynamic potentials by Legendre transformation [5]. Caution must always be exercised, since not all of them are adaptable to different situations and, more importantly, they are not necessarily consistent with the general formalism of Statistical Physics. Particularly popular is the function $\tilde{G}$ whose differential is given by:

[1] For more details about dielectric behavior and all the physical quantities used along section 2.4, see section 4.3.

$$d\tilde{G} = -SdT + Vdp - \vec{M}\cdot d\vec{E} + \sum_i \mu_i dn_i \tag{2.23}$$

where $\vec{M}$ is the macroscopic dipole moment of the dielectric and μ_i is the chemical potential of species i. Actually, this should be a natural choice if we want to work with a **mixing process at constant T, p and $\vec{E}$**. Nevertheless, there are sound reasons to be careful with the function $\tilde{G}$, since it is obtained by Legendre transformation of an "energy" which does not have a clear physical meaning. The reasons are the following:

- The use of $\vec{E}\cdot d\vec{M}$ as the electric work term, in which $\vec{E}$ is the field already modified by the polarization of the dielectric (see section 4.3), does not define an internal energy. To clarify its meaning, we exclude at first expansion work. The term $\vec{E}\cdot d\vec{M}$ can be obtained from the following steps: (i) treat the volume of the dielectric as a constant, rather than a thermodynamic variable; (ii) consider the total work on the system (including the conductors) needed to modify the field produced by the conductors, $V\vec{E}\cdot d(\varepsilon_0\vec{E}+\vec{P})$ [5], where $\vec{P}$ is the polarization (macroscopic density of dipole moment); (iii) subtract the exact differential $V\vec{E}\cdot d(\varepsilon_0\vec{E}) = d\left(\varepsilon_0 VE^2/2\right)$, obtaining the desired result. $\vec{E}\cdot d\vec{M}$ defines de adiabatic variation of an "energy" (let us call it $\tilde{U}$), which is the difference between two contributions: (i) an energy including the internal energy of the dielectric and all the electrostatic energy of the system and conductors; and (ii) a quantity $\varepsilon_0 VE^2/2$ having the dimensions of energy but, as argued by Landau and Lifshitz [5], not representing the energy of any of the parts of the system (including the conductors). In the mentioned conditions, $\tilde{U}$ has an exact differential:

$$d\tilde{U} = TdS + \vec{E}\cdot d\vec{M} + \sum_i \mu_i dn_i \tag{2.24}$$

  from which equations of state can be derived consistently.
- The addition of the expansion work term to different electric work approaches can lead to different expressions of the entropy variation with a change of the electric field at constant temperature and pressure. In fact, this simple addition is an approximation, as the forces on a dielectric inside the influence of an electric field do not simply reduce to the external uniform pressure exerted by a non-dielectric medium [5]. One must proceed with caution after including expansion work, because some approximations are not fully consistent and may lead to contradictions if their consequences are led sufficiently far.

Being warned of this, we will follow the usual treatments of the subject and define the **ideal mixture (at constant T, p and $\vec{E}$)** by an extension of equation (2.14):

$$\Delta\tilde{G}_{\mathrm{m}}^{\mathrm{id}} = RT\sum_i x_i \ln x_i \tag{2.25}$$

This gives $\Delta\vec{M}_{\mathrm{m}}^{\mathrm{id}} = \vec{0}$. Using the relationship between $\vec{M}$ and the relative permittivity, ε_{r}, one obtains $\varepsilon_{\mathrm{r}}^{\mathrm{id}}$ as given in Table 2.1. An equivalent definition has been given by Reis *et al.* [6].

2.4.2. Refractive index

The refractive index is related to the propagation of electromagnetic waves in the system. Non-static electromagnetic fields make the system undergo a non-equilibrium process. Electric

and magnetic losses always exist, to some extent, in variable electromagnetic fields; in other words, the imaginary parts of the dielectric permittivity and magnetic permeability do not vanish, strictly speaking, for any value of the frequency different from zero. However, there exist regions of frequencies where the imaginary parts are very small compared to the real parts, called **transparency ranges** [5]. For sufficiently weak fields, in these regions it is possible to neglect the absorption and, in a similar way to the case of sound waves, apply the local equilibrium hypothesis. The weakness of the field guarantees that the local thermodynamic properties remain practically uniform and at their equilibrium values. Then the static result can be extrapolated to some extent to define the ideal value of the refractive index for a mixture at constant T, p, and $\vec{E}$ (Table 2.1). This definition relies on the fact that for non-magnetic fluids the refractive index at a certain frequency is given by the square root of the relative permittivity at that frequency.

2.5. Redlich-Kister equation

In the present section we assume that the system is a binary mixture, like the liquid mixtures studied in this Thesis. The Redlich-Kister (RK) equation is a polynomic equation proposed by O. Redlich and A.T. Kister [7] to adjust the experimental data of an excess function (X^{E}) as a function of the composition. A RK equation with m terms is of the form:

$$\left(X^{\mathrm{E}}\right)^{\mathrm{RK}} = x_1 x_2 \sum_{i=0}^{m-1} A_i \left(x_1 - x_2\right)^i = x_1 \left(1 - x_1\right) \sum_{i=0}^{m-1} A_i \left(2x_1 - 1\right)^i \tag{2.26}$$

Each term of the sum includes the factor $x_1 x_2$, and therefore the sum vanishes for the pure compounds. Moreover, it is expressed in terms of powers of $x_1 - x_2$ so that, if the order of the components is exchanged, the only change in the coefficients is the sign of those corresponding to odd powers.

The coefficients are determined by an unweighted linear least-squares regression. The number of necessary coefficients has been decided by applying an F-test of additional term [8] at a 99.5% confidence level. The standard deviation of the fit is calculated from the equation:

$$\sigma\left(X^{\mathrm{E}}\right) = \left[\frac{1}{N-m} \sum_{j=1}^{N} \left(X^{\mathrm{E}}_{\mathrm{cal},j} - X^{\mathrm{E}}_{\mathrm{exp},j}\right)^2\right]^{1/2} \tag{2.27}$$

where the index j takes one value for each of the N experimental data $X^{\mathrm{E}}_{\mathrm{exp},j}$, and $X^{\mathrm{E}}_{\mathrm{cal},j}$ is the corresponding value of the excess property calculated from equation (2.26).

2.6. References

[1] W.E. Acree, *Thermodynamic Properties of Nonelectrolyte Solutions*. Academic Press, Orlando, Florida, USA, 1984.

[2] J.M. Prausnitz, R.N. Lichtenthaler, E. Gomes de Azevedo, *Termodinámica Molecular de los Equilibrios de Fases*. 3ª ed. Prentice-Hall, Madrid, España, 2000.

[3] J.M. Smith, H.C. Van Ness, M.M. Abott, *Introducción a la Termodinámica en Ingeniería Química*. 5ª ed. Mc-Graw Hill/Interamericana, México, 1997.

[4] O. Kiyohara, C.J. Halpin, G.C. Benson, *Ultrasonic velocities, compressibilities, and heat capacities for binary mixtures of benzene, cyclohexane, and tetrachloromethane at 298.15 K.* J. Chem. Thermodyn. **10** (1978) 721-730. https://doi.org/10.1016/0021-9614(78)90130-1

[5] L.D. Landau, E.M. Lifshitz, *Electrodinámica de los Medios Continuos.* Curso de Física Teórica. Vol. 8. Reverté, 1981.

[6] J.C.R. Reis, T.P. Iglesias, G. Douhéret, M.I. Davis, *The permittivity of thermodynamically ideal liquid mixtures and the excess relative permittivity of binary dielectrics.* Phys. Chem. Chem. Phys. **11** (2009) 3977-3986. https://doi.org/10.1039/B820613A

[7] O. Redlich, A.T. Kister, *Algebraic Representation of Thermodynamic Properties and the Classification of Solutions.* Ind. & Eng. Chem. **40** (1948) 345-348. https://doi.org/10.1021/ie50458a036

[8] P.R. Bevington, D.K. Robinson, *Data Reduction and Error Analysis for the Physical Sciences.* McGraw-Hill, New York, 2000.

Chapter 3.

Experimental equipment

In this chapter we describe the experimental devices used to perform the measurements, the working principles on which they are based, the calibration methods and, if convenient, the work done to check their proper functioning.

3.1. Densidad y velocidad del sonido. *Anton Paar DSA 5000*

El instrumento utilizado para la medida de la densidad y de la velocidad del sonido es el densímetro y analizador del sonido *Anton Paar DSA 5000* (Figura 3.1). Este dispositivo contiene dos celdas de medida conectadas en serie (Figura 3.2), que permiten determinar simultáneamente estas dos propiedades para una misma muestra líquida. En una celda se mide la densidad mediante el **método del tubo vibrante**, mientras en la otra se determina la velocidad del sonido mediante el **método del pulso**.

Figura 3.1: *Anton Paar DSA 5000.*

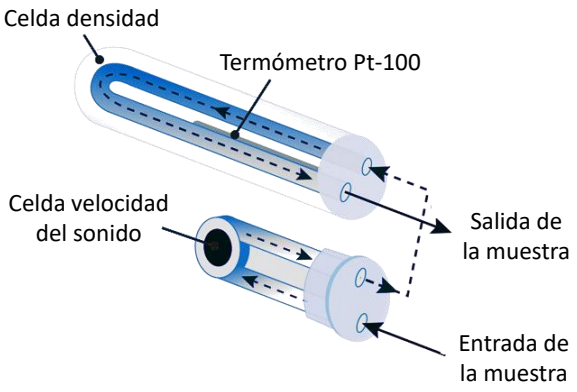

Figura 3.2: Esquema de la celda de medida del *Anton Paar DSA 5000.*

3.1.1. El método del tubo vibrante

El *Anton Paar DSA 5000* es un densímetro de tubo vibrante [1, 2]. Existen muchas variantes de este tipo de densímetros, que difieren en diversos aspectos como la forma de excitación del tubo, la forma de detección de la frecuencia y amplitud de resonancia, métodos correctivos, etc.

No obstante, su principio general de funcionamiento es, esencialmente, el mismo. Simplificando mucho, se puede esbozar como sigue. Un tubo (en este caso de vidrio borosilicatado y en forma de U) relleno del líquido de interés se hace vibrar. Mediante la medida de la amplitud del movimiento a diferentes frecuencias de excitación, se determina su frecuencia de resonancia. La situación es análoga (siempre hablando de forma simplificada) a la de un oscilador armónico simple forzado y amortiguado. En la frecuencia de resonancia, el sistema entra en estado estacionario y el período de resonancia, τ, está dado por la ecuación:

$$\frac{4\pi^2}{\tau^2} = \frac{K}{m_0 + \rho V} \tag{3.1}$$

donde K es la constante elástica del oscilador (que puede considerarse igual a la del tubo, ya que la influencia del líquido es de varios órdenes de magnitud menor), m_0 es la masa del tubo vacío y de las cargas unidas a él, y V es el volumen del líquido en el interior del tubo. La densidad del líquido, ρ, puede despejarse quedando:

$$\rho = A' + B'\tau^2 \tag{3.2}$$

siendo A' y B' constantes, que dependen de la presión y de la temperatura de trabajo (aunque son prácticamente insensibles a las variaciones de la presión atmosférica [3]), y se ven afectados por la fatiga de los materiales por el uso continuado.

El problema general del densímetro de tubo vibrante es, evidentemente, mucho más complejo. Pero se ha comprobado empíricamente que estos densímetros se rigen por la ecuación (3.2), aunque el significado físico de las constantes de la ecuación no sea tan inmediato. Sin embargo, el *DSA 5000* incluye ciertos añadidos que han de ser tenidos en cuenta. V. Alonso, en su Tesis Doctoral [4], incluye una revisión de artículos y patentes relacionados con estas mejoras (aclarando ciertas imprecisiones de trabajos anteriores, como las Tesis Doctorales de I. Mozo [5] e I. Alonso [6]) de la cual a continuación se expone un breve resumen. El lector interesado puede consultar allí más detalles y comentarios.

- Se introduce un tubo de referencia adicional con el objeto de reducir el efecto del envejecimiento en las constantes del aparato y de compensar ciertos efectos térmicos [7]. Es idéntico en sus propiedades físicas (composición, espesor, etc.) al tubo en el que se introduce la muestra, pero un 40% más corto (con ello se busca que la frecuencia de oscilación del de referencia sea al menos el doble que la del de la muestra, para evitar acoplamientos en sus oscilaciones). La ecuación característica del densímetro, con estas modificaciones, se convierte en:

  $$\rho = A + BQ^2 \tag{3.3}$$

  donde A y B incluyen parámetros característicos del tubo de referencia y del de la muestra, y Q es el cociente entre el período de resonancia del tubo de medida y el del tubo de referencia. Tanto A como B tienen dimensiones de densidad, y dependen de factores similares a los que se han comentado sobre A' y B' más arriba.
- Se implementa un método para tratar de corregir el efecto de la viscosidad en la determinación de la densidad. Consiste en medir la frecuencia de resonancia del modo fundamental de vibración y aplicar una fuerza de dicha frecuencia pero desfasada. Ello produce una ligera modificación de la frecuencia de resonancia debida al amortiguamiento producido por la viscosidad de la muestra. Con estos datos es posible

determinar este amortiguamiento y relacionarlo con su efecto en la densidad. Este efecto es mayor en el primer armónico y, por ello, si el procedimiento anterior se lleva a cabo con el primer armónico en lugar de con el modo fundamental, se puede hacer la corrección con más precisión y en un rango de viscosidades más amplio.

Es posible obtener el valor de Q de una medida directamente del equipo. Por tanto, A y B pueden hallarse con distintos líquidos de densidad conocida y realizando un ajuste a una recta de los valores de ρ (tomados de la bibliografía) en función de los datos experimentales de Q^2.

La corrección de viscosidad es realizada automáticamente por el *DSA 5000* al mostrar la densidad en su pantalla. No obstante, la densidad se ha determinado a partir de la ecuación (3.3), con las constantes que resultan de una calibración personalizada del equipo, de modo que esta corrección no se ha tenido en cuenta. Esto no supone problema, pues las viscosidades de los líquidos empleados son muy pequeñas, aunque sí que habría que considerarlo si en un futuro se investiga con líquidos de mayor viscosidad.

3.1.2. El método del pulso

El *Anton Paar DSA 5000* mide la velocidad del sonido mediante una de las posibles variantes del método del pulso [7-9]. Un transmisor piezoeléctrico de cuarzo emite, a intervalos regulares, pulsos de una duración de unos pocos microsegundos a través de una celda (de acero inoxidable) llena del líquido cuya velocidad del sonido se desea medir. Los pulsos tienen una frecuencia central de unos 3 MHz [7, 9]. La celda consiste en una cavidad cilíndrica de aproximadamente 8 mm de diámetro y 5 mm de longitud [7]. En el extremo opuesto de la cavidad se encuentra otro receptor piezoeléctrico que transforma los pulsos sonoros en señales eléctricas. Determinando el tiempo de llegada de los pulsos se puede hallar la velocidad del sonido, c, en el líquido.

La técnica de medida de estos tiempos no es inmediata, ya que son del orden de microsegundos, a los que hay que añadir un tiempo adicional, t_{retrasos}, debido a que el pulso tiene que recorrer el metal del tubo y a la electrónica. Sin entrar en detalles (para los cuales se remite al lector al artículo de Schneditz y Kenner [9]), la medida se realiza sintonizando un VCO (Oscilador Controlado por Voltaje) de modo que el período de n ciclos del VCO se corresponda con el tiempo de propagación del pulso por la muestra más los retrasos. Para poder sintonizar de forma precisa el VCO, es necesario realizar medidas consecutivas y, para asegurar que las señales parásitas han desaparecido entre medida y medida, se introduce un tiempo de espera de $512n$ veces el período del VCO. Este período se mide mediante un cristal que hace de base de tiempos. Según el análisis realizado por V. Alonso en su Tesis Doctoral [4], el tiempo que el *DSA 5000* proporciona como medida en bruto para la determinación de la velocidad del sonido es precisamente este tiempo de espera, que es lo que el fabricante llama **período de la velocidad del sonido** y que denominaremos t. Así, teniendo en cuenta que $t/512 = L/c + t_{\text{retrasos}}$ (siendo L la longitud exacta de la cavidad), se obtiene una relación de la forma:

$$c^{-1} = a + bt \tag{3.4}$$

En esta ecuación, a y b son dos constantes que dependen, al igual que las de la densidad, de la presión y temperatura de trabajo y del envejecimiento del aparato. La calibración del equipo consiste en este caso en ajustar a una recta los valores de c^{-1} (tomados de la bibliografía) en función de los resultados experimentales de t para una serie de líquidos bien caracterizados.

Para que el método del pulso proporcione resultados correctos, el espectro del pulso no debe contener demasiadas frecuencias. Además, la longitud de la cavidad debe ser suficientemente grande como para evitar que se formen ondas estacionarias en su interior, pero suficientemente pequeña como para que el pulso no se atenúe demasiado antes de llegar al receptor. A este respecto, conviene recordar que la velocidad del sonido en la ecuación de Newton-Laplace es la *velocidad de onda*, es decir, la constante con dimensiones de velocidad que aparece en la ecuación diferencial de la onda sonora (véase sección 2.3).

3.1.3. Características del *Anton Paar DSA 5000*

El volumen total de las celdas de medida es de unos 2 cm^3. Ambas celdas se encuentran en el interior de un tubo cilíndrico de doble pared recubierto de cobre. El espacio comprendido entre el oscilador, la celda de sonido y la pared interna del cilindro está lleno de un gas de elevada conductividad térmica, cuya misión es facilitar un rápido equilibrio térmico entre la muestra inyectada y un líquido termostático que circula por la doble pared del cilindro. La temperatura se controla con unos módulos Peltier y un termómetro de resistencia de platino Pt-100, con una precisión de 0.001 K y una exactitud de 0.01 K [5].

El equipo es capaz de medir densidades entre 0 y 3 $g \cdot cm^{-3}$ y velocidades del sonido entre 1000 y 2000 $m \cdot s^{-1}$ en el intervalo de temperaturas desde 273.15 K hasta 343.15 K y a presión atmosférica. De acuerdo con el protocolo puesto a punto por I. Mozo [5], está conectado a un ordenador mediante puerto serie y con el entorno de programación *VEE*, de manera que se pueden tomar los datos del cociente de períodos, Q, y del tiempo de espera entre pulsos sonoros, t, cuyos errores de escala son respectivamente de 10^{-7} y de 10^{-3} μs. A la hora de garantizar la precisión en las medidas y una suficiente estabilidad térmica, se estableció como criterio de repetitividad que, en las últimas 20 medidas de las magnitudes anteriores, sus desviaciones estándar fuesen menores que 10^{-6} y de 0.02 μs respectivamente. Los valores que se toman de los tiempos son los valores medios de esas 20 últimas medidas. A partir de la calibración (véase más adelante), la incertidumbre estándar relativa en la medida de la densidad se estima (teniendo en cuenta la pureza de los compuestos utilizados) en 0.12%, y la incertidumbre estándar en la velocidad del sonido, en 0.4 $m \cdot s^{-1}$.

La inyección de la mezcla en las celdas se realiza con jeringuillas de plástico de 2 cm^3 de capacidad. El tiempo en que la mezcla y el plástico están en contacto debe ser el menor posible para evitar reacciones con el plástico y contaminación de las muestras. Tras la medida, las celdas deben lavarse con un disolvente apropiado según los líquidos utilizados (para las medidas realizadas en esta Tesis, se ha utilizado primero etanol y después acetona), y secarse mediante un pequeño flujo de aire. El dispositivo cuenta con una bomba que proporciona dicho chorro, que se aplica durante 5 minutos.

3.1.4. Uso de un líquido de referencia

Como ya se ha comentado, la evolución de las constantes de calibración del equipo es de sobra conocida, dada la dilatada experiencia del grupo en determinación de este tipo de propiedades. Si bien que lo ideal sería trabajar con las ecuaciones (3.3) y (3.4) realizando calibraciones muy frecuentes, el tiempo necesario para las calibraciones entorpecería bastante el trabajo experimental. Por ello, se trabaja con una modificación de estas ecuaciones basada en la utilización de un **líquido de referencia** estable y cuya densidad es perfectamente conocida: el **isoctano**.

El GETEF ha demostrado que la evolución de la constante A es más rápida que la de la

constante B. Este hecho es analizado ampliamente en la Tesis Doctoral de V. Alonso [4] utilizando las constantes de calibración de distintos miembros del grupo a lo largo de los años, demostrando que la variación temporal de la constante A es en torno a un orden de magnitud más grande que la de la constante B. Parece conveniente entonces tratar de eliminar la influencia de las ordenadas en el origen de las ecuaciones de calibración en los cálculos. Para ello, a las ecuaciones (3.3) y (3.4) se les resta la particularización de ellas mismas para el líquido de referencia, obteniendo:

$$\rho = \rho_{\text{ref}} + B\left(Q^2 - Q_{\text{ref}}^2\right) \tag{3.5}$$

$$c^{-1} = c_{\text{ref}}^{-1} + b\left(t - t_{\text{ref}}\right) \tag{3.6}$$

donde ρ_{ref} y c_{ref} son la densidad y la velocidad del sonido de la referencia tomadas de la bibliografía, y Q_{ref} y t_{ref} son los valores de Q y t medidos experimentalmente para la referencia. De este modo, midiendo cada día estos dos últimos valores y utilizando las ecuaciones (3.5) y (3.6), es posible omitir las ordenadas en el origen en los cálculos y así evitar tener que calibrar tan a menudo.

3.1.5. Calibración

La calibración se ha llevado a cabo con una serie de líquidos puros de acuerdo al procedimiento descrito anteriormente. La Tabla 3.1 recoge la información sobre el origen y pureza de los líquidos utilizados.

Tabla 3.1: Origen y pureza de los líquidos utilizados para la calibración del *Anton Paar DSA 5000.*

Compuesto	CAS	Origen	Pureza inicial (fracción molar)
Heptano	142-82-5	Fluka	≥ 0.995 GC [a]
Isoctano	540-84-1	Fluka	≥ 0.995 GC
Octano	111-65-9	Sigma-Aldrich	≥ 0.995
Ciclohexano	110-82-7	Fluka	≥ 0.995 GC
Tolueno	108-88-3	Fluka	≥ 0.997 GC
Benceno	71-43-2	Sigma-Aldrich	≥ 0.995
Agua	7732-18-5	Bidestilada, desionizada y degasificada	

[a]Gas chromatography.

En la Tabla 3.2 se muestran los valores tomados de la literatura de la densidad y velocidad del sonido de estos líquidos a diferentes temperaturas, así como los resultados obtenidos por nosotros para Q y t. Puede apreciarse que hay resultados de dos calibraciones diferentes. Una fue realizada en septiembre de 2014 y con ella se han medido las densidades y velocidades del sonido de los sistemas *N*,*N*-dimetilformamida + amina lineal primaria o secundaria. La segunda calibración fue llevada a cabo en septiembre de 2015, y con ella se han estudiado los sistemas *N*,*N*-dimetilacetamida + amina lineal primaria o secundaria, además de haberse determinado la densidad de la anilina y de los 1-alcoholes empleados en las respectivas medidas de permitividad e índice de refracción de los sistemas *N*,*N*-dimetilformamida + anilina y 1-alcanol + amina. Los resultados de ambas calibraciones pueden consultarse en la Tabla 3.3 y en la Tabla 3.4.

Tabla 3.2: Medidas efectuadas para calibrar el *Anton Paar DSA 5000* a temperatura T y presión $p = 0.1$ MPa. Valores tomados de la bibliografía: ρ , densidad; c, velocidad del sonido. Resultados experimentales: Q, cociente de períodos de resonancia; t, período de la velocidad del sonido.

T/K	Compuesto	ρ /g·cm^{-3}	Q		c/m·s^{-1}	t/μs	
			Sep. 2014	Sep. 2015		Sep. 2014	Sep. 2015
293.15	Heptano	0.68375 [10]	2.6850045	2.6851655	1152.20 [11]	2489.800	2489.93
	Isoctano	0.691959 [12]	2.6911505	2.6913110	1102.2 [13]	2588.466	2588.291
	Octano	0.70267 [10]	2.6995546	2.6997249	1193 [14]	2413.071	2413.516
	Ciclohexano	0.778583 [12]	2.7569543	2.7571047	1279.32 [15]	2269.624	2269.311
	Tolueno	0.86683 [10]		2.8224925	1326.9 [7]		2197.242
	Benceno	0.87900 [10]	2.8311997	2.8313659	1322.95 [16]	2202.654	2203.043
	Agua	0.9982058 [10]	2.9169572	2.9171441	1482.32 [17]	1993.869	1993.405
298.15	Heptano	0.67946 [10]	2.6817884	2.6819880	1129.92 [18]	2532.614	2532.792
	Isoctano	0.687849 [12]	2.6880285	2.6882353	1081.28 [19]	2634.450	2634.285
	Octano	0.69862 [10]	2.6965075	2.6967167	1171.768 [10]	2451.472	2451.571
	Ciclohexano	0.773896 [12]	2.7534700	2.7536656	1253.79 [12]	2309.552	2309.473
	Tolueno	0.86219 [10]		2.8191709	1305.1 [7]		2230.165
	Benceno	0.87360 [10]	2.8273440	2.8275406	1299.11 [10]	2238.346	2238.807
	Agua	0.9970474 [10]	2.9161843	2.9163698	1496.69 [17]	1977.796	1977.558
303.15	Heptano	0.67519 [10]	2.6785394	2.6786866	1108.99 [11]	2576.980	2577.042
	Isoctano	0.683711 [12]	2.6848848	2.6850423	1061.6 [20]	2681.751	2681.602
	Octano	0.69445 [20]	2.6934413	2.6936087	1151.6 [21]	2491.101	2491.654
	Ciclohexano	0.769172 [12]	2.7499621	2.7501049	1230.00 [15]	2350.646	2351.118
	Tolueno	0.85754 [10]		2.8157548	1283.6 [7]		2263.327
	Benceno	0.86829 [10]	2.8234752	2.8236423	1275.70 [16]	2275.040	2275.019
	Agua	0.9956504 [10]	2.9152424	2.9154284	1509.12 [19]	1964.120	1963.646

Tabla 3.3: Valores de las constantes de calibración de la densidad del *Anton Paar DSA 5000* a temperatura T y presión $p = 0.1$ MPa. A, ordenada en el origen; B, pendiente; r, coeficiente de correlación lineal. Los valores tras el ± se corresponden con la desviación estándar muestral del ajuste, esto es, con la desviación estándar del ajuste dividida por la raíz cuadrada del número de puntos.

T/K	Septiembre 2014			Septiembre 2015		
	A/g·cm^{-3}	B/g·cm^{-3}	r^2	A/g·cm^{-3}	B/g·cm^{-3}	r^2
293.15	−1.0606 ± 3·10^{-4}	0.24197 ± 4·10^{-5}	0.9999995	−1.0606 ± 2·10^{-4}	0.24194 ± 3·10^{-5}	0.9999995
298.15	−1.0606 ± 4·10^{-4}	0.24197 ± 5·10^{-5}	0.9999993	−1.0610 ± 3·10^{-4}	0.24197 ± 3·10^{-5}	0.9999994
303.15	−1.0609 ± 5·10^{-4}	0.24200 ± 6·10^{-5}	0.9999988	−1.0609 ± 3·10^{-4}	0.24196 ± 5·10^{-5}	0.9999988

Tabla 3.4: Valores de las constantes de calibración de la velocidad del sonido del *Anton Paar DSA 5000* a temperatura T y presión $p = 0.1$ MPa. a, ordenada en el origen; b, pendiente; r, coeficiente de correlación lineal. Los valores tras el ± se corresponden con la desviación estándar muestral del ajuste (véase la aclaración en la Tabla 3.3).

T/K	Septiembre 2014			Septiembre 2015		
	a/m^{-1}·s	b/ m^{-1}·s·μs^{-1}	r^2	a/m^{-1}·s	b/ m^{-1}·s·μs^{-1}	r^2
293.15	$-1.053\cdot10^{-4}$ ± $3\cdot10^{-7}$	$3.9103\cdot10^{-7}$ ± $1.4\cdot10^{-10}$	0.9999978	$-1.053\cdot10^{-4}$ ± $7\cdot10^{-7}$	$3.910\cdot10^{-7}$ ± $3\cdot10^{-10}$	0.9999764
298.15	$-1.055\cdot10^{-4}$ ± $3\cdot10^{-7}$	$3.9108\cdot10^{-7}$ ± $1.4\cdot10^{-10}$	0.9999978	$-1.055\cdot10^{-4}$ ± $5\cdot10^{-7}$	$3.9121\cdot10^{-7}$ ± $1.9\cdot10^{-10}$	0.9999915
303.15	$-1.027\cdot10^{-4}$ ± $5\cdot10^{-4}$	$3.897\cdot10^{-7}$ ± $2\cdot10^{-10}$	0.9999926	$-1.027\cdot10^{-4}$ ± $4\cdot10^{-4}$	$3.8948\cdot10^{-7}$ ± $1.8\cdot10^{-10}$	0.9999925

Tabla 3.5: Propiedades de los líquidos puros utilizados en el sistema test a temperatura T y presión $p = 0.1$ MPa: ρ, densidad; c, velocidad del sonido; α_p, coeficiente de dilatación térmica isóbaro; κ_S, coeficiente de compresibilidad isoentrópico; κ_T, coeficiente de compresibilidad isotermo; C_{pm}, capacidad calorífica isobárica molar.

Propiedad	T/K	Ciclohexano		Benceno	
		Este trabajo	Literatura	Este trabajo	Literatura
ρ /g·cm^{-3}	293.15	0.778694	0.778583 [12]	0.879125	0.87900 [10]
	298.15	0.773998	0.773896 [12]	0.873802	0.87360 [10]
	303.15	0.769285	0.769172 [12]	0.868486	0.86829 [10]
c/m·s^{-1}	293.15	1277.8	1279.32 [15]	1321.9	1322.95 [16]
	298.15	1253.2	1253.789 [12]	1298.5	1299.109 [10]
	303.15	1229.8	1230.00 [15]	1276.3	1275.70 [16]
α_p /10^{-3}K^{-1}	298.15	1.216	1.220 [10]	1.218	1.213 [10]
κ_S /TPa^{-1}	293.15	786.46	785.00 [5]	650.93	650.25 [5]
	298.15	822.69	822.79 [22]	678.77	678.51 [5]
	303.15	859.50	860.26 [5]	706.85	707.87 [5]
κ_T /TPa^{-1}	298.15	1129.80	1129.4 [16]	969.94	969.6 [16]
C_{pm} /J·mol^{-1}·K^{-1}	298.15		156.00 [23]		135.69 [24]

Incertidumbres estándar: $u(T) = 0.01$ K; $u(p) = 1$ kPa; $u(c) = 0.4$ m·s^{-1}. Incertidumbres estándar relativas: $u_r(\rho) = 0.0012$; $u_r(\alpha_p) = 0.015$; $u_r(\kappa_S) = 0.002$; $u_r(\kappa_T) = 0.012$.

3.1.6. Sistema test de volúmenes de exceso y compresibilidades isoentrópicas

Con el objetivo de comprobar la fiabilidad de la calibración del *Anton Paar DSA 5000*, se procedió a medir el sistema ciclohexano (1) + benceno (2) como sistema test ampliamente recomendado en la bibliografía.

Tabla 3.6: Datos experimentales de la densidad, ρ, velocidad del sonido, c, volumen molar de exceso, $V_{\mathrm{m}}^{\mathrm{E}}$, y compresibilidad isoentrópica de exceso, κ_S^{E}, del sistema ciclohexano (1) + benceno (2) en función de la fracción molar de ciclohexano, x_1, a temperatura $T = 298.15$ K y presión $p = 0.1$ MPa.

x_1	ρ /g·cm^{-3}	c/m·s^{-1}	$V_{\mathrm{m}}^{\mathrm{E}}$ /cm^3·mol^{-1}	κ_S^{E} /TPa^{-1}
0.0519	0.866375	1291.3	0.1248	4.5
0.1033	0.859227	1284.2	0.2456	9.2
0.1512	0.853003	1279.1	0.3274	12.1
0.1999	0.846823	1273.9	0.4094	15.2
0.2463	0.841175	1269.4	0.4746	17.9
0.3141	0.833238	1263.8	0.5568	21.0
0.3487	0.829321	1261.2	0.5935	22.4
0.4012	0.823670	1257.6	0.6272	24.1
0.4539	0.818274	1254.9	0.6423	24.7
0.4977	0.813844	1252.8	0.6585	25.3
0.5558	0.808373	1250.8	0.6441	24.9
0.6204	0.802460	1249.3	0.6242	23.7
0.6598	0.799064	1248.4	0.5939	23.0
0.7045	0.795342	1247.9	0.5502	21.4
0.7519	0.791510	1247.8	0.4970	19.3
0.8097	0.787078	1248.2	0.4113	16.0
0.8433	0.784533	1248.2	0.3626	14.4
0.8960	0.780821	1249.4	0.2558	10.2
0.9475	0.777363	1251.0	0.1363	5.5

Incertidumbres estándar: $u(T) = 0.01$ K; $u(p) = 1$ kPa; $u(x_1) = 0.0010$; $u(c) = 0.4$ m·s^{-1}; $u\left(V_{\mathrm{m}}^{\mathrm{E}}\right) = (0.010\left|V_{\mathrm{m,max}}^{\mathrm{E}}\right| + 0.005$ cm^3·mol^{-1}). Incertidumbres estándar relativas: $u_{\mathrm{r}}(\rho) = 0.0012$; $u_{\mathrm{r}}\left(\kappa_S^{\mathrm{E}}\right) = 0.015$.

Los valores de su volumen molar de exceso, $V_{\mathrm{m}}^{\mathrm{E}}$, se han obtenido con diferentes técnicas de medida, dando resultados consistentes entre sí. Handa y Benson [2] realizaron el ajuste de 164 puntos experimentales a la temperatura de 298.15 K y presión atmosférica, correspondientes a las determinaciones dilatométricas de Stokes *et al.* [25], de Tanaka *et al.* [26] y de Kumaran y McGlashan [27]. Asimismo, establecieron los valores de este $V_{\mathrm{m}}^{\mathrm{E}}$ que se aceptan como patrón. Por otro lado, también existe para este sistema una variedad de medidas de la compresibilidad isoentrópica de exceso, κ_S^{E}.

Los líquidos puros utilizados son los mismos que los del calibrado, y por tanto su origen y pureza pueden consultarse en la Tabla 3.1. En la Tabla 3.5 se muestran las propiedades físicas de los compuestos puros obtenidas en este trabajo y se comparan con los valores existentes en la literatura. En la Tabla 3.6 se recogen los datos experimentales correspondientes al sistema ciclohexano (1) + benceno (2). En la Tabla 3.7 pueden verse los resultados del ajuste de los

datos de $V_{\mathrm{m}}^{\mathrm{E}}$ y κ_S^{E} a una ecuación de Redlich-Kister. En la Figura 3.3 se representan los resultados del $V_{\mathrm{m}}^{\mathrm{E}}$ junto con los de otros trabajos anteriores, y en la Figura 3.4 se comparan todos ellos con el ajuste patrón de Handa y Benson. Los resultados de κ_S^{E} se comparan con los de otros trabajos en la Figura 3.5.

También se midieron las propiedades de este sistema a las temperaturas de 293.15 K y 303.15 K. Estas propiedades, junto con el cálculo de la velocidad del sonido de exceso y el coeficiente de dilatación térmica de exceso, pueden consultarse en un trabajo anterior [28] y no se documentarán aquí.

Tabla 3.7: Coeficientes de ajuste de los datos experimentales de la propiedad F^{E} a una ecuación de Redlich-Kister (ecuación (2.26)), y desviación estándar del ajuste, $\sigma(F^{\mathrm{E}})$ (ecuación (2.27)), a temperatura $T = 298.15$ K y presión $p = 0.1$ MPa.

Propiedad F^{E}	T/K	A_0	A_1	$\sigma(F^{\mathrm{E}})$
$V_{\mathrm{m}}^{\mathrm{E}}$ /cm^3·mol^{-1}	298.15	2.621	0.09	0.004
κ_S^{E} /TPa^{-1}	298.15	100.4	7.2	0.2

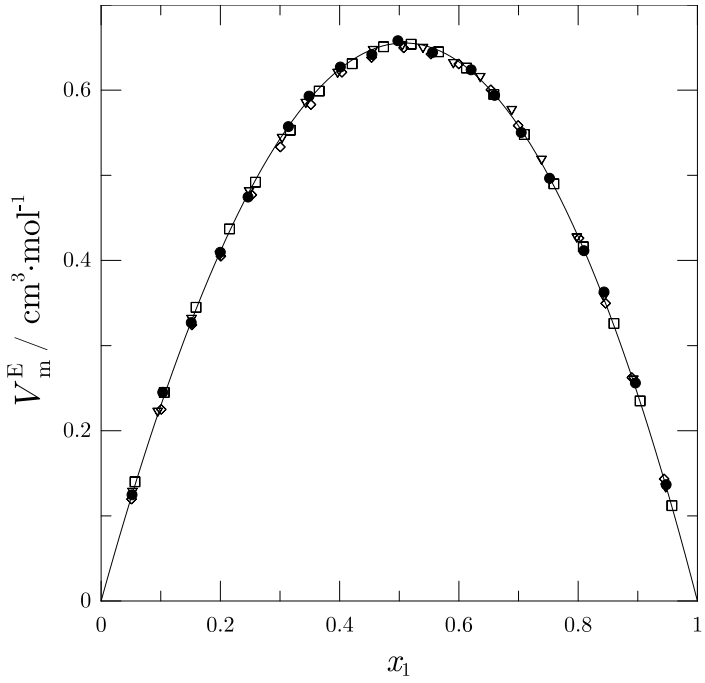

Figura 3.3: Volumen molar de exceso, $V_{\mathrm{m}}^{\mathrm{E}}$, del sistema ciclohexano (1) + benceno (2) en función de la fracción molar de ciclohexano, x_1. Símbolos, resultados experimentales: este trabajo (●), V. Alonso (◊) [4], I. Alonso (▽) [6], Mozo (□) [5]. Línea sólida, ajuste de Redlich-Kister de los puntos de este trabajo.

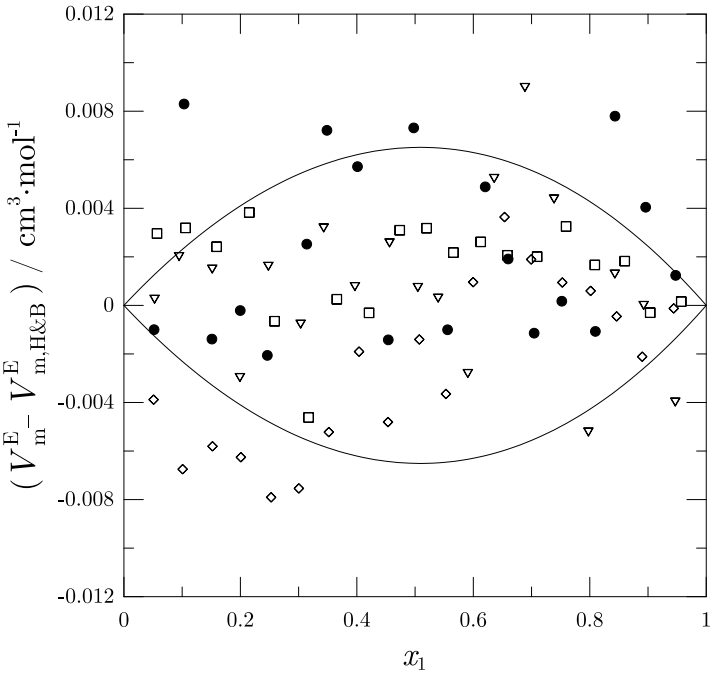

Figura 3.4: Diferencias entre los datos experimentales del volumen molar de exceso, $V^{\mathrm{E}}_{\mathrm{m}}$, y el ajuste patrón de Handa y Benson [2], $V^{\mathrm{E}}_{\mathrm{m,H\&B}}$, del sistema ciclohexano (1) + benceno (2) en función de la fracción molar de ciclohexano, x_1. Símbolos, resultados experimentales: este trabajo (●), V. Alonso (◊) [4], I. Alonso (▽) [6], Mozo (□) [5]. Líneas sólidas, diferencias de ±1%.

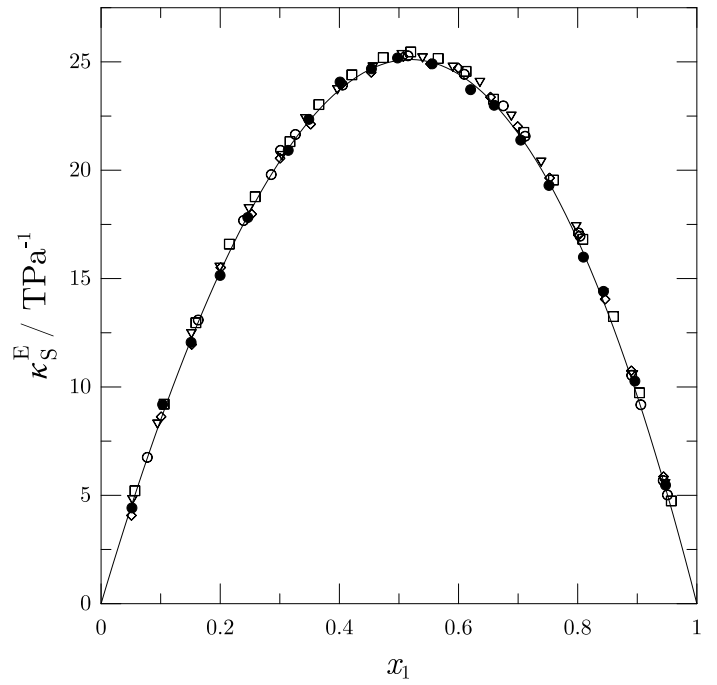

Figura 3.5: κ^{E}_S del sistema ciclohexano (1) + benceno (2) en función de la fracción molar de ciclohexano, x_1. Símbolos, resultados experimentales: este trabajo (●), V. Alonso (◊) [4], I. Alonso (▽) [6], Mozo (□) [5], Tamura *et al.* (○) [29]. Línea sólida, ajuste de Redlich-Kister de los puntos de este trabajo.

3.2. Índice de refracción. *Bellingham + Stanley RFM970*

El dispositivo utilizado para la medida del índice de refracción es el refractómetro *Bellingham + Stanley RFM970* (Figura 3.6 y Figura 3.7).

Figura 3.6: *Bellingham + Stanley RFM970.*

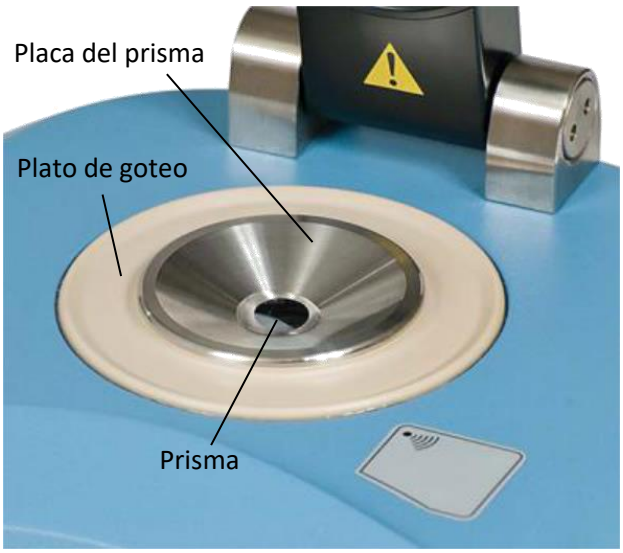

Figura 3.7: Detalle de la zona de medición del *Bellingham + Stanley RFM970.*

Las muestras de líquido, de 10 µL, se toman con una micropipeta y se vierten sobre el prisma de medición de zafiro artificial, que tiene un índice de refracción de 1.7681 para la longitud de onda de medida (véase más abajo). La placa del prisma es de acero inoxidable y está rodeada por un plato de goteo de plástico PEEK, que tiene una buena resistencia química y ofrece aislamiento térmico. La temperatura es controlada por módulos Peltier con una precisión de 0.03 K y una estabilidad de 0.05 K, entre 273.15 K y 353.15 K. La prensa (tapa del prisma) minimiza las variaciones de temperatura, y evita la entrada de luz ambiental durante la medida. El conjunto se encuentra insertado en un armazón de espuma de poliuretano expandido de baja densidad, que aporta una buena resistencia y estabilidad mecánicas.

El instrumento mide el índice de refracción a la longitud de onda de la línea D del sodio ($\approx$589 nm), n_D, entre los valores 1.30 y 1.70, con una precisión de $8{\cdot}10^{-5}$, mediante un método basado en la detección del **ángulo límite** (Figura 3.8). La fuente de luz, que no es más que un diodo LED de la longitud de onda deseada, emite luz hacia la muestra. Debido a los diferentes ángulos de incidencia en la interfaz prisma-muestra, algunos rayos se refractan hacia la muestra y otros sufren reflexión total en la cara interior del prisma. Estos últimos salen a través de otra cara del prisma y, mediante un objetivo, son enfocados hacia un circuito integrado sensible a la luz (una matriz de fotodiodos). Cierta región queda iluminada por estos rayos, mientras que la correspondiente a los rayos que no han sufrido reflexión total (por haberse refractado a través de la muestra) queda oscura. En otras palabras, idealmente existe una línea correspondiente al ángulo límite que separa la zona oscura de la zona iluminada en la matriz de fotodiodos. Es posible por tanto determinar este ángulo y, conociendo el índice de refracción del prisma, hallar el índice de refracción de la muestra. En realidad, esta línea en muchas ocasiones no está perfectamente definida, pero el fabricante indica [30] que el equipo incorpora un software que determina de forma razonablemente objetiva la posición de esa hipotética línea.

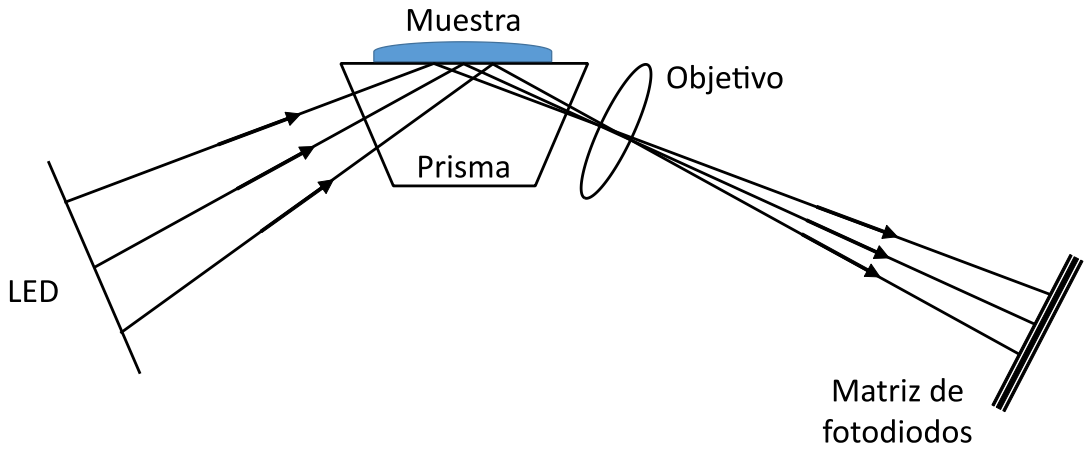

Figura 3.8: Esquema del método de medida utilizado por los refractómetros automáticos digitales *Bellingham + Stanley* como el *RFM970*.

Incluso bajando la prensa del refractómetro, la evaporación de parte de la muestra durante la medida causa que no sea lo suficientemente estable. Esto, que ya se aprecia en la medida de compuestos puros, resulta decisivo cuando se trata de mezclas. La diferencia en las presiones de vapor de los componentes se traduce en una variación de la composición durante el proceso, lo que resulta en errores sistemáticos de magnitud importante. Por ello, **se ha incorporado a la prensa un tapón de teflón** que, sin entrar en contacto con la muestra líquida, minimiza el volumen de aire con el que está en contacto y evita en lo posible su evaporación. Las medidas realizadas con este tapón han demostrado alcanzar la estabilidad requerida [4].

Tras la medida, se retira la muestra del prisma con un trozo de papel. Para limpiar el prisma, primero se aplica con la pipeta una cantidad aproximada de 20 µL de metanol[2]. Después, con papel secante, se frota suavemente tanto el prisma como la placa de acero inoxidable. Seguidamente, con un paño limpiador de lentes, se frota para eliminar restos adheridos a la superficie del prisma y en los bordes de la placa del prisma. Por último, se utiliza aire comprimido para terminar de secar y eliminar restos de papel que hayan podido quedar en el prisma. Antes de pasar a la siguiente medida, hay que asegurarse de que tanto el prisma como la placa de acero están completamente limpios y secos y de que no hay sobre ellos ningún resto sólido. Si el tapón o la prensa han tocado la muestra, o han acumulado parte de la condensación del vapor formado durante la medida, hay que limpiarlos de forma similar.

La calibración del refractómetro se realiza cada vez que se enciende el instrumento o se cambia la temperatura de medida[3], y se lleva a cabo mediante dos líquidos patrón, identificados por el aparato como muestra "cero" (para la cual se ha usado isoctano) y muestra "intervalo" (tolueno) [12]. La calibración con la muestra "intervalo" es recomendable y el valor de su índice de refracción ha de ser superior al del de la muestra "cero", además de asegurar un buen intervalo índices de refracción.

[2] Si la muestra no se mezcla bien con el metanol, es posible que haga falta realizar antes con otro disolvente el proceso descrito en este párrafo. Sin ir más lejos, para las medidas con 1-heptanol realizadas en esta tesis fue necesario limpiar con 1-propanol antes de proceder con el metanol.
[3] Es posible saltar este paso si se desea conservar el valor de calibración anterior.

Tabla 3.8: Índice de refracción, n_D, de los líquidos puros utilizados en el sistema test a temperatura T y presión $p = 0.1$ MPa.

Propiedad	T/K	Ciclohexano		Benceno	
		Este trabajo	Literatura	Este trabajo	Literatura
n_D	293.15	1.42638	1.42638 [14]	1.50117	1.50112 [10]
	298.15	1.42367	1.42363 [14] 1.42360 [31]	1.49797	1.49792 [10]
	303.15	1.42080	1.4210 [32]	1.49471	1.4949 [33]

Incertidumbres estándar: $u(T) = 0.01$ K; $u(p) = 1$ kPa; $u(n_D) = 0.00008$.

Tabla 3.9: Índice de refracción, n_D, y la correspondiente función de exceso, n_D^E, del sistema ciclohexano (1) + benceno (2) en función de la concentración de ciclohexano (x_1, fracción molar; ϕ_1; fracción de volumen) a temperatura $T = 298.15$ K y presión $p = 0.1$ MPa.

x_1	ϕ_1	n_D	$10^5 n_D^E$	x_1	ϕ_1	n_D	$10^5 n_D^E$
0.0519	0.0624	1.49251	–93	0.5590	0.6066	1.44916	–419
0.1048	0.1246	1.48717	–174	0.6204	0.6653	1.44501	–395
0.1512	0.1781	1.48281	–220	0.6598	0.7023	1.44237	–382
0.1999	0.2331	1.47819	–279	0.7045	0.7436	1.43956	–353
0.2463	0.2844	1.47405	–317	0.7519	0.7866	1.43673	–312
0.3141	0.3577	1.46818	–364	0.8097	0.8381	1.43341	–255
0.3487	0.3944	1.46507	–404	0.8481	0.8717	1.43127	–215
0.4058	0.4538	1.46040	–432	0.8960	0.9129	1.42879	–150
0.4539	0.5027	1.45676	–433	0.9475	0.9564	1.42617	–82
0.4977	0.5465	1.45348	–435				

Incertidumbres estándar: $u(T) = 0.01$ K; $u(p) = 1$ kPa; $u(x_1) = 0.0010$; $u(\phi_1) = 0.004$; $u(n_D) = 0.00008$. Incertidumbre expandida (nivel de confianza 0.95): $U_c\left(n_D^E\right) = 0.0002$.

Tabla 3.10: Coeficientes de ajuste de los datos experimentales del índice de refracción de exceso $F^E = 10^5 n_D^E$ a una ecuación de Redlich-Kister (ecuación (2.26)), y desviación estándar del ajuste, $\sigma(F^E)$ (ecuación (2.27)), a temperatura $T = 298.15$ K y presión $p = 0.1$ MPa.

Propiedad F^E	T/K	A_0	A_1	$\sigma(F^E)$
$10^5 n_D^E$	298.15	–1720	77	7

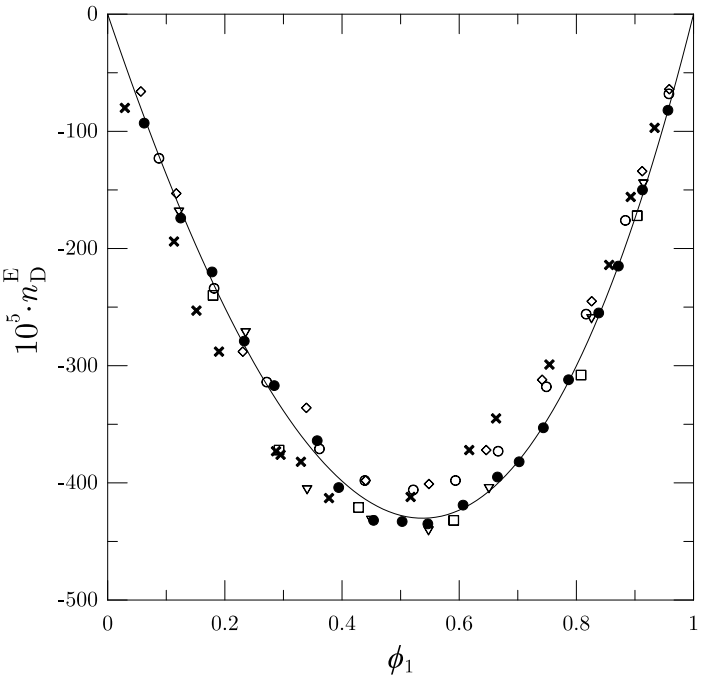

Figura 3.9: Índice de refracción de exceso, n_D^E, del sistema ciclohexano (1) + benceno (2) en función de la fracción de volumen de ciclohexano, ϕ_1 . Símbolos, resultados experimentales: este trabajo (•), González *et al.* (◊) [31], Tasic *et al.* (▽) [34], Ridgway y Butler (□) [35], Iglesias *et al.* (x) [36], Piñeiro *et al.* (○) [37]. Línea sólida, ajuste de Redlich-Kister de los puntos de este trabajo.

La comprobación del calibrado puede hacerse con agua destilada, pues la experiencia ha demostrado su gran reproducibilidad. Si bien hay que tener cuidado ya que, debido a su elevada tensión superficial, la gota puede adoptar formas variopintas para las cuales se producen reflexiones parásitas que hacen que el resultado de la medida sea absurdo. A este respecto, es conveniente indicar que el indicador de calidad de la medida, que se puede leer en la pantalla, debe ser lo más próximo a 100 posible. Según el fabricante, la calidad es un valor arbitrario que se utiliza para describir el valor de una lectura. El valor de la calidad se deriva del patrón óptico producido al colocar una muestra en el prisma. Un valor alto indica un patrón óptico bien definido, lo que facilita la resolución de la señal; un valor bajo indica un patrón menos bien definido y por lo tanto una lectura menos fiable. El valor de la calidad de la muestra "cero" del calibrado se fija automáticamente a 100, lo cual se puede utilizar como una referencia con la que comparar otras muestras medidas.

3.2.1. Sistema test de índices de refracción

Aunque menos documentado que el V_m^E, existen diversas fuentes bibliográficas que aportan el n_D del sistema ciclohexano (1) + benceno (2) a la temperatura de 298.15 K y presión atmosférica. Al no existir ningún patrón aceptado de forma general, se ha escogido este sistema para comprobar la viabilidad de la determinación de n_D y su propiedad de exceso, n_D^E, con este refractómetro. De igual manera que con el V_m^E, también se midió este sistema a las temperaturas de 293.15 K y 303.15 K [28], pero aquí solo se mostrarán las medidas a 298.15 K.

De nuevo, el origen y pureza de los líquidos utilizados se encuentra en la Tabla 3.1. La Tabla 3.8 muestra el índice de refracción de estos líquidos puros, mientras que los datos experimentales de n_D y n_D^E pueden consultarse en la Tabla 3.9. Los resultados del ajuste de Redlich-Kister de los datos de n_D^E se muestran en la Tabla 3.10. En la Figura 3.9 se representan estos resultados de n_D^E y se comparan con los de otros autores.

3.3. Permitividad dieléctrica

El método de medida de la permitividad que se ha empleado se basa en la determinación de la impedancia de una muestra de líquido en un condensador de placas plano-paralelas mediante el **método del puente autoequilibrado**. Para ello se dispone de un baño termostático *Lauda RE 304*, en el cual se sumerge una celda de medida de permitividades *Agilent 16452A Liquid Test Fixture*. La celda se conecta a un analizador de impedancias *Agilent 4294A Precision Impedance Analyzer, 40 Hz to 110 MHz* a través de unos cables coaxiales denominados *Agilent 16048G Test Lead*. El esquema del montaje experimental puede verse en la Figura 3.10. Ahora se procede a explicar el principio de medida y cada uno de los elementos del montaje.

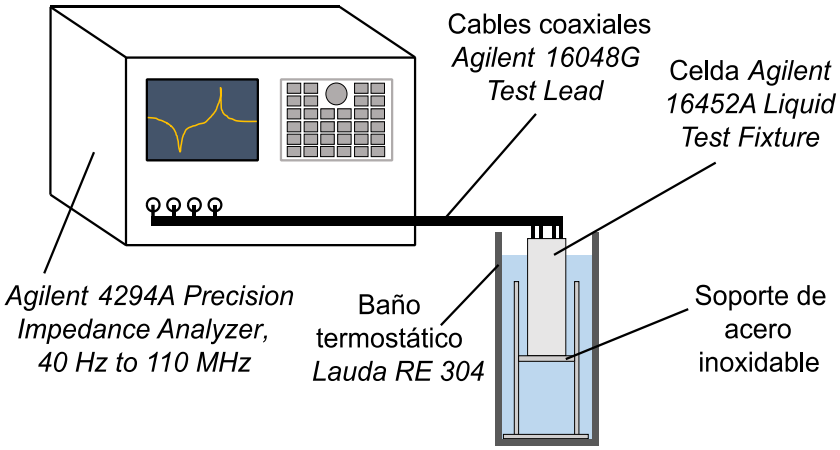

Figura 3.10: Esquema del montaje experimental.

3.3.1. El método del puente autoequilibrado en configuración 4TP

El método del puente autoequilibrado es uno de los métodos más utilizados para medir impedancia. Tiene la ventaja de cubrir con mucha precisión y exactitud un intervalo de frecuencias bastante amplio (desde 20 Hz hasta 120 MHz) y también un intervalo de impedancias muy grande (incluso para valores muy pequeños). Aunque para ello no sirve cualquier configuración de medida. Al elevar la frecuencia, aparecen impedancias residuales y parásitas que afectan al resultado. Si, además, la frecuencia es suficientemente elevada, la teoría de circuitos de baja frecuencia deja de ser aplicable y hay que tener en cuenta la distribución de los parámetros eléctricos a lo largo de la línea. Para minimizar todos estos efectos, puede usarse la denominada **configuración 4TP** (*Four-terminal pair configuration*), que se caracteriza por las siguientes peculiaridades:

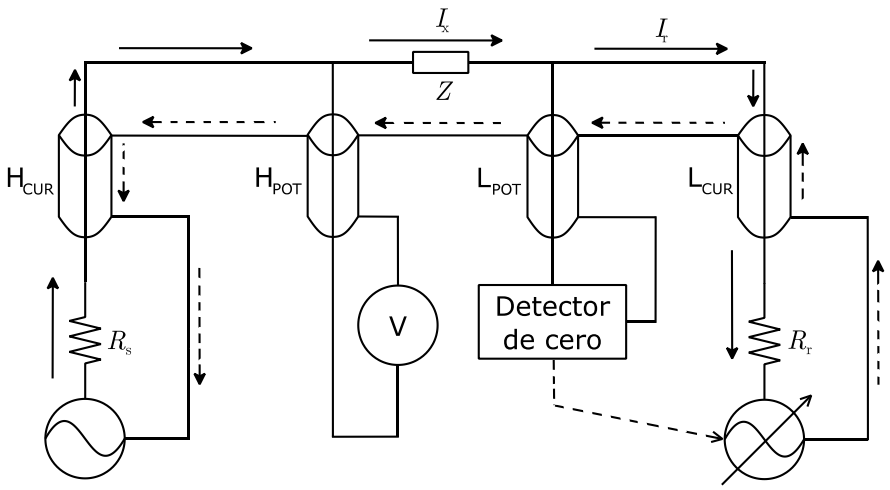

Figura 3.11: Vista esquemática del método del puente autoequilibrado en configuración 4TP. Los conductores exteriores de los cables coaxiales se encuentran conectados por la parte más cercana a la impedancia problema. Las flechas con línea continua paralelas a los hilos representan la "corriente de la señal de test", mientras que las de línea discontinua representan la "corriente de retorno" (aunque no debe olvidarse que es una corriente alterna). El detector de cero actúa sobre el generador de la parte derecha de la figura, que produce la corriente de realimentación.

- *Four-terminal*: Utiliza cables diferentes para llevar la corriente de la señal de test (denominados H_{CUR} y L_{CUR}) que para la determinación del voltaje (H_{POT} y L_{POT}). Esto permite eliminar las resistencias de contacto y otras impedancias parásitas. Los terminales denominados con una H se conectan al punto de potencial "alto" del circuito, mientras que los designados con una L miden en el punto de potencial "bajo".
- *Pair*: Los cables son coaxiales y por sus conductores exteriores circula la "corriente de retorno"; no están conectados a tierra, aunque lo están entre sí por su parte final (la que va conectada a la impedancia problema). El campo magnético en el exterior del cable se anula, minimizando así el efecto de la inducción mutua entre cables CUR y POT. Mediante un voltímetro vectorial se determina la diferencia de potencial entre los conductores interiores y exteriores; este método diferencial también ayuda a eliminar el efecto de la inducción mutua.

Teniendo las anteriores particularidades en mente, pasamos a describir esquemáticamente (y omitiendo muchos detalles, para los que el lector es referido a la literatura del fabricante [38-40]) el método de medida (Figura 3.11). El objetivo del puente autoequilibrado es igualar la corriente I_r que circula por la resistencia R_r con la corriente I_x que circula por la impedancia problema, Z. Para ello, cuando por el detector de cero pasa una corriente, se genera[4] una señal que se retroalimenta hacia R_r para compensar esa corriente no equilibrada. El proceso debe converger

[4] Para generar esta señal se utilizan componentes electrónicos de gran precisión. A grandes rasgos, dos detectores de fase separan la corriente (compleja) que sale del detector de cero en componentes perpendiculares. Las señales de salida de los detectores de fase pasan por un integrador (filtro pasa-baja) y se envían a un modulador vectorial que crea las componentes de la señal que se va a retroalimentar. Aunque el bucle tenga errores de fase, la componente de la corriente no equilibrada debida a estos errores es también detectada y compensada para anular el error en la corriente de la resistencia.

hasta que la corriente por el detector de cero es exactamente nula. Cuando el puente se ha equilibrado, el voltaje en la resistencia vale $V_r = I_r R_r = I_x R_r$ y la impedancia problema puede calcularse como:

$$Z = \frac{V_x}{I_x} = \frac{V_x}{V_r} R_r \tag{3.7}$$

donde V_x es el voltaje en la impedancia problema. Los voltajes complejos V_x y V_r se determinan con un voltímetro vectorial. La resistencia R_r recibe el nombre de "resistencia de intervalo" (*range resistor*) y es un elemento clave del circuito, pues determina el intervalo de impedancias que se puede medir. Se selecciona de entre varias en función del orden de magnitud de la impedancia problema.

3.3.2. Relación de la impedancia medida con la permitividad

La impedancia problema es un condensador de placas plano-paralelas. Teóricamente, la impedancia de un condensador ideal con placas de área A separadas una distancia d (muy pequeña en relación su tamaño) y relleno de un dieléctrico de permitividad relativa compleja $\tilde{\varepsilon}_r$ cuando está sometido a una tensión alterna de frecuencia angular ω es:

$$Z_{\text{condensador ideal}} = \frac{d}{j\omega A \varepsilon_0 \tilde{\varepsilon}_r} \tag{3.8}$$

La impedancia del mismo condensador vacío es:

$$Z_{\text{condensador ideal,0}} = \frac{d}{j\omega A \varepsilon_0} \tag{3.9}$$

Y en consecuencia $\tilde{\varepsilon}_r$ puede obtenerse como:

$$\tilde{\varepsilon}_r = \frac{Z_{\text{condensador ideal,0}}}{Z_{\text{condensador ideal}}} \tag{3.10}$$

Sin embargo, existen capacidades parásitas debido, entre otras cosas, a que el tamaño de las placas no es infinito. Por ello, si en la ecuación (3.10) se sustituyen las impedancias reales, Z_0 (en vacío) y Z (con muestra), en lugar de las respectivas ideales, se obtendrá un valor $\tilde{\varepsilon}_{rm}$ que diferirá del valor real $\tilde{\varepsilon}_r$:

$$\tilde{\varepsilon}_{rm} = \frac{Z_0}{Z} < \tilde{\varepsilon}_r \tag{3.11}$$

Para eliminar el efecto de la capacidad parásita, *Agilent* propone en el manual de uso de la celda un factor de corrección que varía entre 1 (para el vacío) y ≈ 1.030 (para valores altos de $|\tilde{\varepsilon}_{rm}|$):

$$\tilde{\varepsilon}_r = \frac{100|\tilde{\varepsilon}_{rm}|}{97.0442|\tilde{\varepsilon}_{rm}| + 2.9558} \tilde{\varepsilon}_{rm} \tag{3.12}$$

Se puede modelar esta impedancia como una resistencia y una capacidad en paralelo. Así, puede escribirse:

$$\frac{1}{Z} = \frac{1}{R_p} + j\omega C_p \tag{3.13}$$

$$\frac{1}{Z_0} = j\omega C_0 \tag{3.14}$$

Para el caso del condensador vacío el valor de la resistencia sería infinito. En la práctica, el condensador no se mide vacío sino lleno de aire, que tiene una permitividad prácticamente igual a la del vacío para la precisión de las medidas. De hecho, la resistencia que se mide experimentalmente es del orden de los GΩ. El valor que se obtiene para $\tilde{\varepsilon}_{\mathrm{rm}}$ en términos de estos parámetros es:

$$\tilde{\varepsilon}_{\mathrm{rm}} = \frac{C_{\mathrm{p}}}{C_0} - j\frac{1}{\omega C_0 R_{\mathrm{p}}} \tag{3.15}$$

$$|\tilde{\varepsilon}_{\mathrm{rm}}| = \sqrt{\left(\frac{C_{\mathrm{p}}}{C_0}\right)^2 + \left(\frac{1}{\omega C_0 R_{\mathrm{p}}}\right)^2} \tag{3.16}$$

3.3.3. Montaje experimental

Todos los elementos necesarios para el método del puente autoequilibrado distintos de los cables y de la impedancia problema se encuentran implementados en el analizador de impedancias de alta precisión *Agilent 4294A* (Figura 3.12). Sus características técnicas detalladas pueden consultarse en la documentación aportada por el fabricante (ahora *Keysight Technologies*). Los cables coaxiales (*Agilent 16048G Test Lead*), de 1 m de longitud, van conectados a su parte frontal mediante conectores BNC. Los extremos contrarios van conectados también con conectores BNC a la impedancia problema, que es la celda *Agilent 16452A Liquid Test Fixture*, o bien vacía (llena de aire) o llena del líquido cuya permitividad desea medirse. La celda se introduce en el baño colocada verticalmente sobre un soporte de acero inoxidable fabricado a tal efecto.

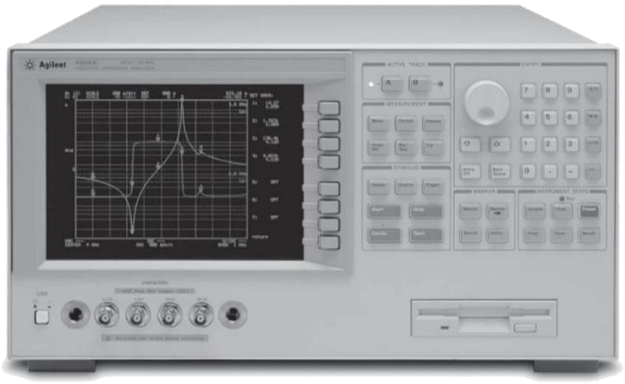

Figura 3.12: El analizador de impedancias *Agilent 4294A*. Imagen tomada de documentación original de Agilent [41].

Agilent 16452A Liquid Test Fixture

La celda *Agilent 16452A* es un condensador de placas plano-paralelas diseñado para medir permitividades de líquidos. Puede realizar medidas desde 20 Hz hasta 30 MHz de frecuencia de señal, en el intervalo de temperaturas entre 253.15 K y 398.15 K.

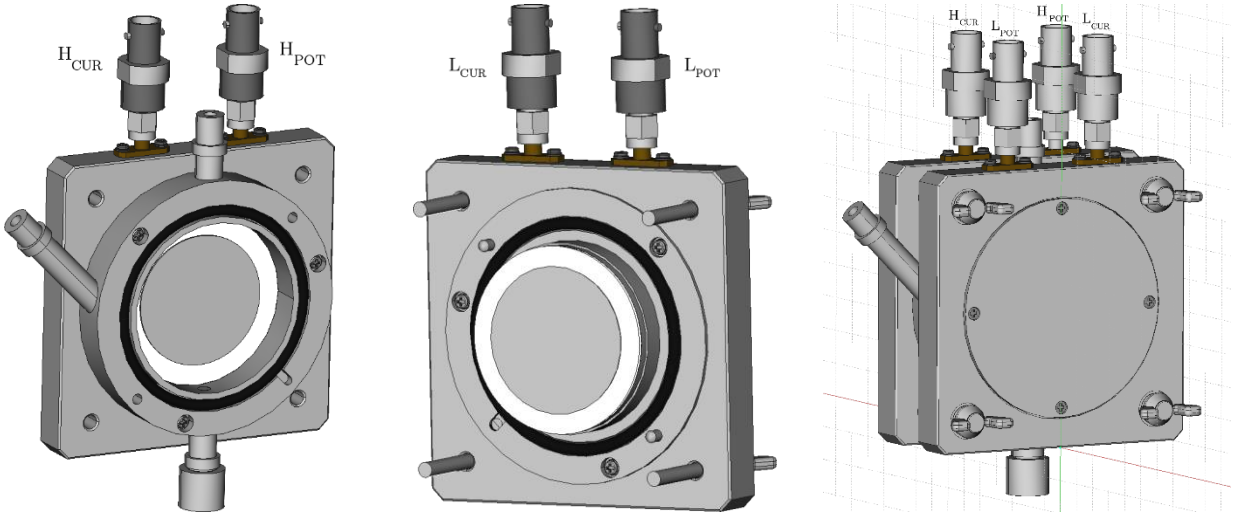

a) Mitad H. b) Mitad L. c) Celda ensamblada.

Figura 3.13: Recreación de la celda de medida de permitividades de líquidos *Agilent 16452A Liquid Test Fixture* realizada por V. Alonso [4].

Un detalle de la celda puede verse en la Figura 3.13. Está formada por dos mitades (mitad H y mitad L, en referencia al tipo de electrodos al que van conectadas) que se ensamblan mediante cuatro tornillos. Entre ellas se puede intercalar un disco espaciador, a elegir entre varios de distinto espesor proporcionados por el fabricante (1.3 mm, 1.5 mm, 2 mm, y 3 mm), con el objetivo de aumentar o disminuir la distancia entre las placas y con ello el volumen de líquido necesario. Para las medidas realizadas en esta Tesis se ha utilizado el espaciador de 2 mm, que requiere un volumen de líquido de aproximadamente 4.8 mL. Además, cada mitad dispone de un orificio para alojar una junta tórica, lo que asegura que no hay pérdida de líquido durante la medida.

La celda consta de tres orificios: el superior, el inferior y el lateral. Por el lateral se vierte la muestra, por el inferior se vacía la celda y el superior sirve para evitar sobrepresiones. El fabricante provee con la celda un tapón metálico para el orificio inferior, pero no para el superior (que es liso) ni el lateral (que tiene el mismo tipo de rosca que el inferior). Sin embargo, tapar el orificio inferior no es suficiente para realizar medidas con la suficiente exactitud [4], dado que existen problemas de evaporación. Cuando el equipo se puso a punto, se fabricaron dos tapones de nylon para los otros dos orificios [4]. No obstante, desde entonces se ha adquirido otra celda del mismo modelo, de modo que para esta Tesis se ha dispuesto de otro tapón de metal roscado, que se ha utilizado para tapar el orificio lateral. Para asegurar la hermeticidad se colocan dos pequeñas juntas tóricas en los tapones metálicos lateral e inferior. El tapón superior cumple la función de evitar la evaporación, pero no está anclado de ningún modo y en caso de una sobrepresión excesiva en el interior de la celda puede moverse y permitir su salida al exterior.

Ciertos líquidos, como las aminas utilizadas en esta Tesis (especialmente las lineales primarias), deterioran bastante las juntas tóricas (hechas de vitón), lo que obliga a reemplazarlas tras unas cuantas medidas para evitar fugas de líquido y entrada de agua del baño o de restos de las propias juntas en el espacio reservado al líquido, lo que puede falsear la medida. Otro efecto conocido de algunos líquidos sobre las juntas es su dilatación, que cuando es suficientemente notoria también hace necesaria su sustitución.

Baño termostático *Lauda RE 304*

Para controlar la temperatura durante el experimento se dispone de este baño termostático (Figura 3.14), que puede programarse desde 253.15 K hasta 473.15 K con una precisión de 0.01 K y una estabilidad de 0.02 K. Dispone de una bomba de circulación que ayuda a mantener una temperatura homogénea en el baño, con 5 niveles de potencia (de los cuales se ha usado el nivel 3 por ser suficiente y emitir menos ruido que los niveles superiores).

La exactitud de la temperatura de la celda en relación a la programada en el baño se comprobó colocando un termómetro de resistencia de platino Pt100 (calibrado conforme a la norma ITS90 con el punto triple del agua y el de fusión del galio) en una posición cercana a la celda [4]. Se comprobó que ambas temperaturas diferían en un valor constante, pero que el baño controlaba la temperatura con la precisión arriba mencionada. Por lo tanto se procedió a modificar el *offset* en el baño para que la temperatura programada se correspondiese con la de la sonda calibrada, y así poder usar la temperatura medida por el baño para controlar la temperatura de la celda.

Estudios de la variación de la capacidad del condensador con el tiempo y de simulación térmica de la celda [4] indican que el tiempo necesario para garantizar el equilibrio térmico de la muestra con el baño está entre 10 y 15 minutos.

Figura 3.14: Baño termostático *Lauda RE 304*.

3.3.4. Compensación

Al utilizar los cables coaxiales y la celda de medida para la determinación de la impedancia, aparecen unas impedancias residuales entre la impedancia problema y el plano de calibración [40] del instrumento (situado en los conectores BNC en su frontal). Para reducir los errores derivados de ellas se utiliza un conjunto de técnicas denominado **compensación**. En este caso se realizan dos tipos de compensación:

- **Compensación de fase y carga para la longitud de los cables**. Se realiza conectando una resistencia patrón de 100 Ω.
- **Compensación de cortocircuito de la celda**. Se lleva a cabo conectando las dos mitades de la celda con una pequeña chapa metálica en la zona de medida. La impedancia residual se modela como una autoinducción y una resistencia en serie.

Para realizar estas tareas hay que conectar los elementos de una cierta forma y programar el analizador de impedancias para que haga las medidas necesarias. Las indicaciones a tal efecto están implementadas como mensajes al usuario en el programa de control (véase 3.3.5).

Idealmente, la compensación de la celda debería realizarse en tres situaciones: cortocircuito, circuito abierto y carga [39, 40]. Por la estructura de la celda, no se puede hacer la compensación de carga, y la situación de circuito abierto se utiliza para medir la impedancia de la celda con aire.

Cabe añadir que, en este analizador, debido a que los extremos del camino de medida están terminados con una impedancia característica de 50 Ω, las medidas realizadas con los cables de 1 m presentan un salto a una frecuencia aproximada de 5 MHz. Dicho gap podría evitarse con la compensación de carga de la celda [39], que como se acaba de mencionar no se puede realizar. Por lo tanto, por encima de dicha frecuencia las medidas están afectadas de un error adicional.

3.3.5. Procedimiento de medida y limpieza. Programas de control

Las medidas fueron automatizadas por V. Alonso [4], quien desarrolló un programa de control en el lenguaje *VEE* que controla simultáneamente el analizador de impedancias y el baño termostático, se encarga de tomar y exportar los datos automáticamente y además guía al usuario para realizar las tareas de compensación. Posteriormente, L.F. Sanz [42] realizó ciertas modificaciones sobre dicho programa. Para las medidas de esta Tesis, ambas versiones han sido utilizadas. No se describirán aquí dichos programas dado el exhaustivo detalle con el que se describen ambos en sus respectivas Tesis Doctorales. Conviene señalar, sin embargo, que aseguran la estabilidad térmica de la muestra y, una vez alcanzada ésta, se toma el promedio de 200 medidas de la impedancia, que tienen una precisión muy elevada[5].

El procedimiento de medida se puede resumir en los siguientes pasos (para los pasos 2-6, 8-10, 14 y 18 se siguen las indicaciones dadas por el programa de control):

1. **Comprobación de que la bomba de circulación del baño está encendida**. El programa de control apaga la bomba después de cada medida, pero no lo enciende al arrancar de nuevo, por lo que hay que encenderla manualmente.
2. **Conexión de los cables a la resistencia patrón para la compensación de fase**.
3. **Realización de la compensación de fase**.
4. **Conexión de los cables a la resistencia patrón para la compensación de carga**.
5. **Realización de la compensación de carga**.
6. **Comprobación de la compensación de la longitud de los cables**.
7. **Ensamblado de la celda para cortocircuito**. Se colocan las juntas tóricas y la pieza de cortocircuito, que debe ponerse lo más centrada posible en el interior de la mitad H, evitando ensuciarla agarrándola con unas pinzas o unos guantes. Debe encajarse el espaciador de 1.3 mm (que tiene 3 agujeros, en lugar de 2 como el resto) en la mitad L. Al llevar la mitad L sobre la mitad H, hay que moverla con mucho cuidado para no golpear la cerámica. Después se cierra la celda y se atornilla, tratando de ejercer la misma presión con cada uno de los cuatro tornillos; para ello, es útil apretar a la vez las

[5] La repetitividad típica de estas medidas es muy buena. Sirvan de ejemplo las desviaciones estándar muestrales de las partes real e imaginaria de la permitividad relativa de una medida de *N,N*-dimetilformamida a temperatura de 298.15 K y frecuencia de 1 MHz, iguales ambas a $5 \cdot 10^{-5}$. Para decano y dietil carbonato, líquidos con una permitividad relativa un orden de magnitud menor, los valores son incluso más pequeños ($3 \cdot 10^{-6}$ y $5 \cdot 10^{-6}$ respectivamente)

esquinas opuestas en diagonal. Después se ponen las juntas tóricas en los tapones metálicos y se ponen éstos en la celda junto con el tapón superior de nylon.

8. **Conexión de los cables para cortocircuito**.
9. **Realización de la compensación de cortocircuito**.
10. **Comprobación de la compensación de cortocircuito**.
11. **Ensamblado de la celda para medida**. En este caso hay que desatornillar la celda (sin quitar los tapones), retirar la pieza de corto, cambiar el espaciador por el que se vaya a usar en la medida (para las medidas de esta Tesis, el de 2 mm) y volver a atornillarla.
12. **Introducción en el baño.** Al introducir la celda en el baño termostático, ha de asegurarse que hay suficiente agua como para que toda la cavidad del condensador (marcada con un círculo línea discontinua sobre el lateral de la celda) esté totalmente sumergida, para conseguir el equilibrio térmico. Pero también conviene que el agua no supere el orificio lateral ni, en ningún caso, llegue a tocar el tapón superior (ya que es el menos hermético y podría entrar agua en la celda).
13. **Conexión de los cables para medida**. Se conectan igual que en la compensación de cortocircuito.
14. **Medida con la celda vacía**.
15. **Desconexión de los cables y extracción de la celda del baño**. La celda debe estar colocada verticalmente sobre el soporte del que se dispone para sujetarla.
16. **Introducción de la muestra en la celda**. Para llenar la celda, el orificio inferior debe estar cerrado y los otros dos abiertos. Es conveniente tapar los electrodos de la celda para evitar que caiga polvo o alguna gota de líquido en ellos durante el proceso de llenado. El líquido se vierte en su interior mediante una jeringuilla a través del orificio lateral, lentamente y deslizando por la pared del orificio para evitar la formación de burbujas. Una vez se vea el líquido llegar hasta el orificio lateral, se procede a tapar en primer lugar este orificio, y una vez que está bien cerrado se pone el tapón de nylon en el orificio superior. Es posible que al cerrar el orificio lateral el líquido rebose por el superior, para lo cual puede ser práctico tener algo de papel preparado para absorberlo antes de que se deslice hacia abajo.
17. **Reintroducción de la celda en el baño y conexión de los cables**.
18. **Medida con la celda llena** (si se mide con el programa de V. Alonso, hay que reiniciar el programa y saltar todas las comprobaciones y compensaciones y programar las mismas condiciones que se establecieron para la celda vacía).
19. **Desconexión de los cables y extracción de la celda del baño**.
20. **Cubrimiento de los electrodos de la celda con sus tapones de plástico**.
21. **Vaciado de la celda**. Se retira primero el tapón inferior, tras lo cual el líquido solamente gotea un poco debido al equilibrio de presiones. Después, se retira el tapón superior para que caiga todo el líquido de una vez.
22. **Desensamblado y limpieza de la celda y de sus elementos**. La rutina de limpieza podría ser la siguiente:
    - Antes de abrirla, puede ser aconsejable pasar etanol para evitar excesivos vapores del líquido que se ha medido, en el caso de que éste sea muy tóxico. Para este paso no se debe usar acetona, pues corroe el vitón de las juntas.
    - Se limpian los tapones metálicos por dentro, aún con sus juntas, con etanol (por la misma razón que en el paso anterior). Con unos golpecitos suele ser suficiente para que las juntas caigan de los tapones. No obstante, si se han deshecho o

dilatado demasiado puede ser necesario usar una aguja para romperlas, teniendo que reemplazarlas para la medida siguiente. Después se frotan las juntas con agua y etanol.

- Se limpian los tres tapones con etanol y acetona.
- Se desatornilla la celda y se extraen las juntas con una pequeña espátula (que no tenga punta para no rayar la celda) para limpiarlas con agua y etanol.
- Se limpian las dos mitades de la celda con etanol y acetona.
- Se pone todo a secar durante unos 10 minutos en la estufa. No se debería dejar la celda un tiempo excesivo en el horno, ya que cuando está muy caliente tarda mucho en volver a la temperatura ambiente y eso podría interrumpir el ritmo de las medidas.

3.3.6. Resultados de la técnica

El método descrito permite medir la permitividad relativa en forma compleja en un amplio intervalo de frecuencia. Podría complementarse esta técnica con otras de más alta frecuencia para la obtención del espectro dieléctrico de líquidos y mezclas líquidas. La caracterización de las relajaciones y resonancias podría aportar mucha información sobre sus interacciones y estructura a nivel microscópico.

Ocurre sin embargo que esta técnica no llega a las frecuencias a las que ocurren las relajaciones dieléctricas correspondientes al desacople de la contribución orientacional de la permitividad, comenzando típicamente a partir de dos órdenes de magnitud por encima del MHz [43-45]. En consecuencia, la parte imaginaria medida es muy próxima a cero y la parte real prácticamente igual a la permitividad relativa estática. Es por ello que en este trabajo solo se hará referencia a la **parte real de la permitividad relativa a 1 MHz** y a la hora de analizar sus valores **se considerará que representa la permitividad relativa estática**. **Esta parte real será llamada simplemente permitividad relativa y se representará por** ε_{r}**.**

Ya se ha comentado más arriba la elevada precisión de estas medidas. En cuanto al valor relativo de la exactitud, de acuerdo con el fabricante de la celda oscila entre un 0.3% y un 1% (nótese, sin embargo, que los fabricantes suelen especificar los errores con tolerancias muy altas).

Tabla 3.11: Origen y pureza de los compuestos puros utilizados para el sistema test de permitividad relativa.

Compuesto	CAS	Origen	Pureza inicial (fracción molar)
Dietil carbonato	105-58-8	Fluka	≥0.99 GC
Decano	124-18-5	Fluka	≥0.98 GC

3.3.7. Sistema test de permitividad relativa

Tras poner a punto el equipo experimental, V. Alonso realizó un gran número de medidas de la permitividad de compuestos puros en un amplio intervalo de temperaturas [4], concluyendo que la técnica proporcionaba valores suficientemente buenos. Complementariamente, estudió el sistema test dietil carbonato (1) + decano (2) a las temperaturas de 288.15 K, 298.15 K y 308.15 K, comparando sus resultados con los de Mosteiro *et al.* [46], que disponían de la misma celda de medida. En esta Tesis se han realizado las mismas medidas de comprobación.

Tabla 3.12: Permitividad relativa, ε_r, a temperatura T y presión $p = 0.1$ MPa de los compuestos puros utilizados en el sistema test.

Propiedad	T/K	Dietil carbonato		Decano	
		Este trabajo	Literatura [46]	Este trabajo	Literatura [46]
ε_r	288.15	2.835	2.83	2.011	2.01
	298.15	2.835	2.83	1.997	2.00
	308.15	2.839	2.83	1.987	1.98

Incertidumbres estándar: $u(T) = 0.01$ K; $u(p) = 1$ kPa; $u_r(\varepsilon_r) = 0.003$.

Tabla 3.13: Permitividad relativa, ε_r, y la correspondiente función de exceso, ε_r^E, del sistema dietil carbonato (1) + decano (2) en función de la concentración de dietil carbonato (x_1, fracción molar; ϕ_1; fracción de volumen) a temperatura T y presión $p = 0.1$ MPa.

x_1	ϕ_1	ε_r	ε_r^E	x_1	ϕ_1	ε_r	ε_r^E
			T/K = 288.15				
0.1089	0.0706	2.052	–0.017	0.6008	0.4832	2.353	–0.056
0.2090	0.1410	2.101	–0.026	0.7047	0.5972	2.448	–0.055
0.3115	0.2194	2.153	–0.039	0.8027	0.7165	2.555	–0.046
0.4079	0.2997	2.211	–0.047	0.8976	0.8449	2.676	–0.031
0.5058	0.3887	2.276	–0.055				
			T/K = 298.15				
0.1089	0.0706	2.037	–0.019	0.6008	0.4835	2.347	–0.055
0.2090	0.1412	2.090	–0.025	0.7047	0.5975	2.444	–0.054
0.3115	0.2196	2.144	–0.037	0.8027	0.7168	2.554	–0.044
0.4079	0.3000	2.202	–0.046	0.8976	0.8450	2.672	–0.033
0.5058	0.3890	2.269	–0.054				
			T/K = 308.15				
0.1089	0.0707	2.027	–0.020	0.6008	0.4838	2.335	–0.064
0.2090	0.1413	2.073	–0.034	0.7047	0.5978	2.434	–0.062
0.3115	0.2198	2.129	–0.045	0.8027	0.7170	2.546	–0.052
0.4079	0.3002	2.188	–0.055	0.8976	0.8452	2.672	–0.035
0.5058	0.3893	2.257	–0.062				

Incertidumbres estándar: $u(T) = 0.01$ K; $u(p) = 1$ kPa; $u(x_1) = 0.0010$; $u(\phi_1) = 0.004$. Incertidumbre estándar relativa: $u_r(\varepsilon_r) = 0.003$. Incertidumbre combinada relativa (nivel de confianza 0.95): $U_{rc}(\varepsilon_r^E) = 0.02$.

Tabla 3.14: Coeficientes de ajuste de los datos experimentales de la permitividad relativa de exceso $F^{\mathrm{E}} = \varepsilon_{\mathrm{r}}^{\mathrm{E}}$ a una ecuación de Redlich-Kister (ecuación (2.26)), y desviación estándar del ajuste, $\sigma(F^{\mathrm{E}})$ (ecuación (2.27)), a temperatura T y presión $p = 0.1$ MPa.

Propiedad F^{E}	T/K	A_0	A_1	A_2	$\sigma(F^{\mathrm{E}})$
$\varepsilon_{\mathrm{r}}^{\mathrm{E}}$	288.15	–0.213	–0.107	–0.05	0.0012
	298.15	–0.206	–0.10	–0.07	0.002
	308.15	–0.242	–0.106	–0.073	0.0006

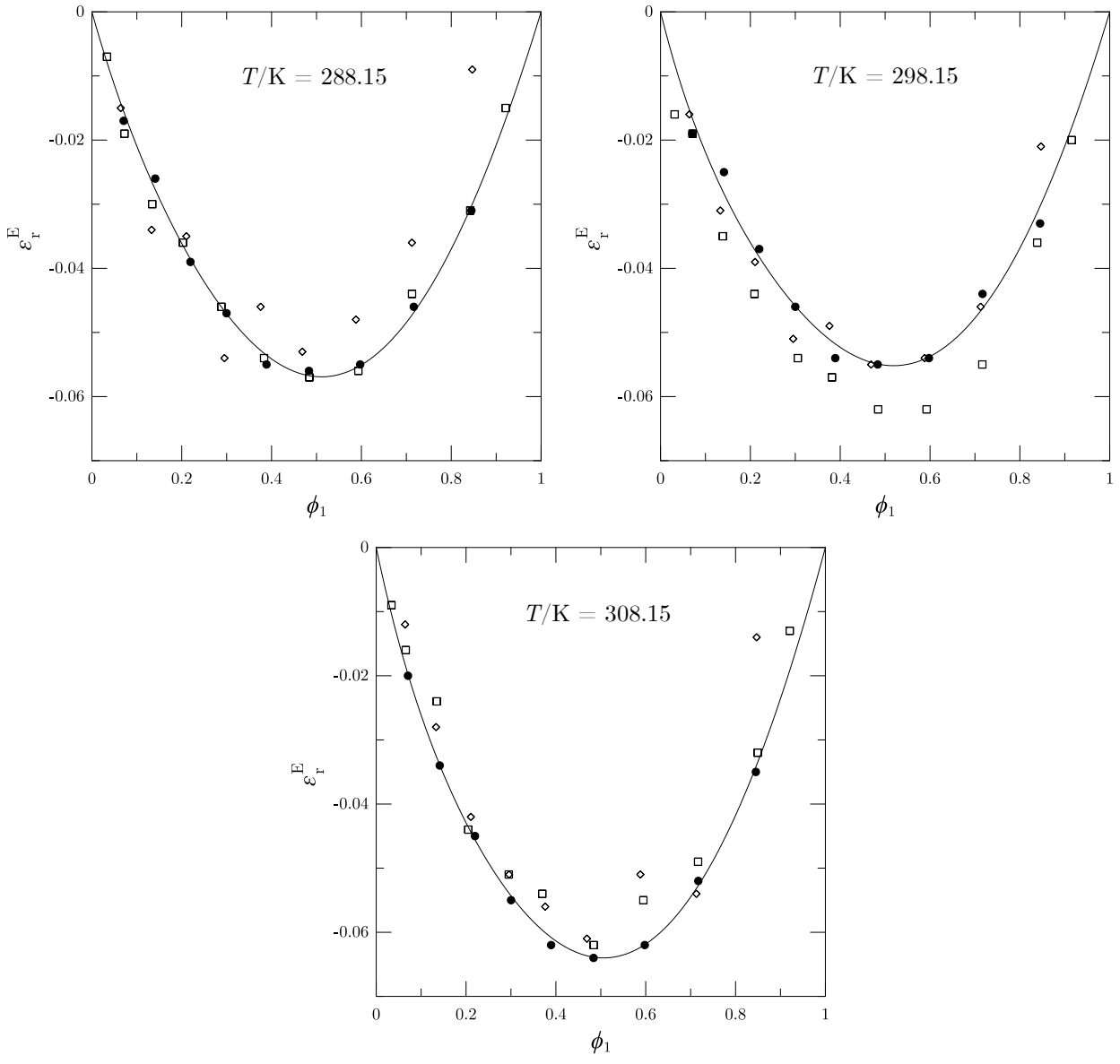

Figura 3.15: Permitividad relativa de exceso, $\varepsilon_{\mathrm{r}}^{\mathrm{E}}$, del sistema dietil carbonato (1) + decano (2) en función de la fracción de volumen de dietil carbonato, ϕ_1, a temperatura T y presión $p = 0.1$ MPa. Símbolos, resultados experimentales: este trabajo (•), V. Alonso (◊) [4], Mosteiro *et al.* (□) [46]. Línea sólida, ajuste de Redlich-Kister de los puntos de este trabajo.

En la Tabla 3.11 puede consultarse el origen y pureza de los compuestos puros usados. Su permitividad relativa, ε_r, puede verse en la Tabla 3.12. Los datos experimentales de ε_r de las mezclas y su correspondiente magnitud de exceso, ε_r^E, se encuentran en la Tabla 3.13. Los datos de ε_r^E se han ajustado a una ecuación de Redlich-Kister, y la Tabla 3.14 recoge los coeficientes y desviación estándar de los ajustes. Estos resultados se representan en la Figura 3.15 junto con los resultados de V. Alonso y de Mosteiro *et al.* para su comparación.

3.4. Entalpía molar de exceso

Las entalpías molares exceso (o de mezcla) se han medido mediante un calorímetro *Setaram BT2.15* adaptado a una celda para calorimetría de flujo. Estas medidas se llevaron a cabo durante la estancia de realizada en 2018 en el Institut de Chimie de Clermont-Ferrand.

3.4.1. Montaje experimental

El esquema del montaje experimental puede verse en la Figura 3.16.

El calorímetro *Setaram BT2.15* consta de un gran bloque calorimétrico y dos orificios, en los que se pueden alojar dos celdas, una de medida y una de referencia. Los orificios están rodeados de sendas termopilas (termopares conectados en serie) que detectan el flujo de calor entre las celdas y el bloque calorimétrico. Este último se aloja en una camisa interna que puede rellenarse con un líquido refrigerante, como por ejemplo nitrógeno líquido.

Los fluidos circulan por tubos de acero inoxidable de 1.6 mm de diámetro exterior y 1.0 mm de diámetro interior, y son inyectados en el sistema mediante sendas bombas de jeringuilla modelo *Teledyne ISCO 260 D Syringe Pump*, que están conectadas a su vez a un controlador *Teledyne ISCO D-Series Pump Controller*. Las diferentes concentraciones se obtienen variando los flujos proporcionados por las bombas. El flujo en volumen puede variarse desde 1 $\mu L \cdot min^{-1}$ hasta 25 $mL \cdot min^{-1}$, con una incertidumbre estándar relativa del 0.5%. La capacidad de las bombas es de 266.05 mL, y pueden regularse hasta una presión de 52 MPa con una incertidumbre estándar relativa del 2%. Para asegurar la estabilidad del flujo molar y con ello la fracción molar, los fluidos en las bombas se mantienen a una temperatura constante de 298.15 K mediante un baño termostático *Fisher Scientific Polystat 36*, con una estabilidad de 0.03 K.

La presión en el sistema se mantiene constante mediante un regulador de presión colocado a la salida del recorrido del flujo. La presión relativa a la presión atmosférica se mide junto con la temperatura ambiente por medio de un transductor Keller conectado al ordenador. Este sensor puede medir hasta 40 MPa con una incertidumbre estándar relativa del 0.25%.

Para controlar la temperatura del bloque calorimétrico, se enfría inicialmente haciendo circular un fluido termostatado a 10 K por debajo de la temperatura del experimento, usando un baño ultra-criostático *Julabo FL1201*. Después se regula la temperatura calentando el bloque mediante una unidad *Setaram G11 Universal Controller* con una estabilidad de 0.01 K

La temperatura de los fluidos inyectados se ajusta a la temperatura de trabajo del calorímetro mediante un prerrefrigerador externo y un precalentador interno. El prerrefrigerador externo se encuentra encima del bloque calorimétrico y está conectado en serie al compartimento por donde circula el fluido que enfría el bloque calorimétrico y al baño *Julabo FL1201*. El precalentador interno se encuentra dentro del bloque calorimétrico; suministra la potencia necesaria para alcanzar la temperatura exacta del experimento por medio de cartuchos

calefactores, y su temperatura se controla mediante una resistencia de platino conectada a un controlador PID *Fluke Hart Scientific 2200* con una estabilidad de 0.01 K.

Se ha trabajado con una única celda, prescindiendo del montaje diferencial. La celda está diseñada de modo que los fluidos se comienzan a mezclar en un punto en la parte inferior, y después hacen un largo recorrido en espiral hasta que llegan de nuevo a la parte superior. Con esto se busca que todo el proceso de mezcla se produzca en la celda y pueda ser detectado completamente por la termopila. La señal (fuerza electromotriz) de la termopila correspondiente se mide con un multímetro digital de 6 ½ dígitos *Keysight 34401A*. Éste está conectado a un ordenador a través de un puerto GPIB y, con ayuda de un programa en lenguaje *VEE*, se representa en tiempo real la señal en función del tiempo y se guarda en archivos de texto.

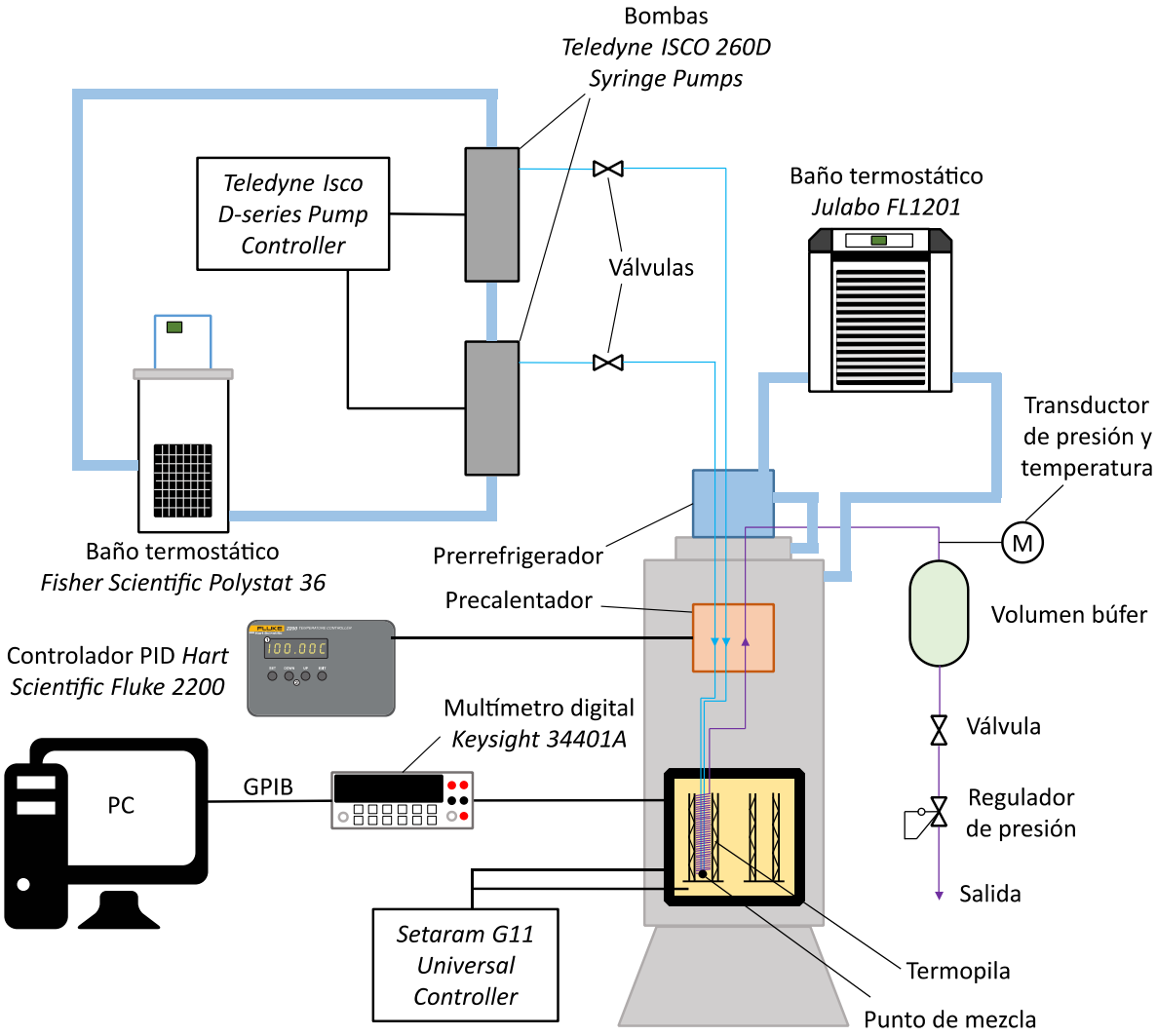

Figura 3.16: Esquema del montaje experimental utilizado para la medida de la entalpía de mezcla.

3.4.2. Principio de medida del calorímetro

La calorimetría de flujo se basa en la medida del flujo de calor que se produce en la celda de medida cuando se introducen a través de ella unos flujos de materia constantes en el tiempo y se espera hasta alcanzar el estado estacionario. El efecto térmico a medir se produce en una zona del bloque calorimétrico que puede dividirse en tres partes:

- La parte exterior, que se mantiene a una temperatura regulada constante.
- La parte interior, donde se encuentra la celda de medida y de donde procede el flujo de calor que se desea medir.
- La parte intermedia, donde se encuentra la termopila.

Se admitirán como válidas las siguientes hipótesis en el estado estacionario:

- Las temperaturas de la parte exterior y la parte interior son uniformes a lo largo de toda su longitud. En consecuencia, en el estado estacionario se produce una diferencia de temperatura entre ambas partes que es constante y uniforme.
- A una temperatura exterior fija, el flujo de calor total entre la parte interior y la exterior es proporcional a la diferencia de temperaturas entre ellas. Esta proporcionalidad puede entenderse de forma similar a la ley de Fourier de conducción del calor.
- A una temperatura exterior fija, la fuerza electromotriz producida en la termopila por efecto Seebeck es proporcional a la diferencia de temperatura entre la parte interior y la parte exterior.

En virtud de estas relaciones de proporcionalidad, es evidente que la fuerza electromotriz (señal de la termopila), S, deberá ser proporcional al flujo de calor, P:

$$S = kP \tag{3.17}$$

donde la **sensibilidad**, k, será una función de la temperatura de la parte exterior, es decir, de la temperatura a la que se regule el calorímetro. Esta constante se determina con una calibración adecuada. Básicamente, la calibración puede realizarse o bien de forma puramente eléctrica, suministrando una potencia eléctrica con un elemento calefactor (típicamente una resistencia de platino), o bien mediante un ajuste de los datos de la medida de un sistema patrón cuya entalpía molar de exceso sea conocida.

La entalpía de exceso, $H_{\mathrm{m}}^{\mathrm{E}}$, cuando se introduce un flujo molar $\dot{n}_1$ del líquido (1) y uno $\dot{n}_2$ del líquido (2) a través de la celda se determina como sigue. Si los líquidos no se mezclaran al pasar por la celda, se produciría un flujo de calor P_{LB} y una correspondiente señal en la termopila S_{LB} que serían próximos a cero. Esta señal se denomina **línea de base**, y corresponde a la señal que se produce al entrar los líquidos sin mezclarse con esos flujos molares. Al producirse la mezcla, el flujo de calor tomará un valor P, correspondiente a una señal S generada en la termopila, y se tendrá:

$$H_{\mathrm{m}}^{\mathrm{E}} = \frac{P - P_{\mathrm{LB}}}{\dot{n}_1 + \dot{n}_2} = \frac{S - S_{\mathrm{LB}}}{k\left(\dot{n}_1 + \dot{n}_2\right)} \tag{3.18}$$

La fracción molar del componente i, x_i, se calcula como:

$$x_i = \frac{\dot{n}_i}{\dot{n}_1 + \dot{n}_2} \tag{3.19}$$

Y los flujos molares $\dot{n}_i$ se relacionan con los flujos volumétricos programables en las bombas, $\dot{V}_i$, a través de la masa molar M_i y de la densidad del compuesto, ρ_i, a la presión de trabajo y a la temperatura a la que se encuentran en las bombas (regulada por el baño termostático):

$$\dot{n}_i = \frac{\rho_i \dot{V}_i}{M_i} \tag{3.20}$$

3.4.3. Procedimiento de medida y calibración

Tanto para la calibración como para las medidas el procedimiento a seguir es similar. Antes de introducir nuevos líquidos en las bombas, éstas se limpian llenándolas con etanol y haciéndolo fluir hacia el sistema. Una vez hecho esto, se procede a secar cada una de las bombas (primero una y después la otra). Para ello, se conecta nitrógeno seco a presión a la entrada de bomba y se deja fluir por el sistema durante un tiempo prudencial (20 minutos suele ser suficiente). Durante ese tiempo, conviene crear "pulsos" de sobrepresiones cerrando y abriendo la válvula de salida de la bomba, ya que esto ayuda a secar gotas que se hayan quedado adheridas. Después se procede a llenar las bombas con los líquidos. Antes de empezar a medir, se debe hacer fluir cada uno de los líquidos hasta que la línea hasta la celda esté llena con ellos. Para realizar una medida (o tomar la línea de base), se ajustan los flujos de las bombas a los valores deseados y se espera hasta el estado estacionario, es decir, a que el promedio de la señal de la termopila sea constante en el tiempo.

En esta Tesis se han determinado las entalpías de exceso de mezclas binarias amida + amina a presión de 0.1 MPa y temperatura de 298.15 K. La sensibilidad del calorímetro a esta temperatura se ha determinado tomando como patrón los datos de Ott *et al.* [47, 48] de la entalpía de exceso del sistema etanol + agua. La calibración arrojó un resultado para la sensibilidad de $k = 32.0$ mV·mW^{-1}, estimándose una incertidumbre estándar relativa del 2%. Teniendo en cuenta la incertidumbre de los flujos, de la densidad, de la sensibilidad y de la señal de la termopila, se estima que la incertidumbre estándar relativa de la entalpía de exceso es, a lo sumo, del 5%. Valores del 5% se han alcanzado solamente en el caso de señales muy pequeñas correspondientes a los extremos de concentración, mientras que típicamente suelen presentarse valores del 3%. La incertidumbre estándar relativa de la fracción molar se estima en un 0.4%.

3.5. Referencias

[1] O. Kratky, H. Leopold, H. Stabinger, *Determination of density of liquids and gases to an accuracy of 10^{-6} g/cm^3, with a sample volume of only 0.6 cm^3.* H. Z. Angew. Phys. **27** (1969) 273-277.

[2] Y.P. Handa, G.C. Benson, *Volume changes on mixing two liquids: A review of the experimental techniques and the literature data.* Fluid Phase Equilib. **3** (1979) 185-249. https://doi.org/10.1016/0378-3812(79)85010-4

[3] O. Kiyohara, G.C. Benson, *Determination of Excess Volumes of Cyclohexane + Benzene Mixtures with a Mechanical Oscillator Densimeter.* Can. J. Chem. **51** (1973) 2489-2491. https://doi.org/10.1139/v73-373

[4] V. Alonso, *Estudio experimental de propiedades termofísicas de mezclas binarias formadas por 1-alcohol + alcano, + éter lineal o + amina aromática primaria.* Tesis Doctoral, 2016. Departamento de Física Aplicada, Facultad de Ciencias, Universidad de Valladolid.

[5] I. Mozo, *Estudio experimental y teórico de mezclas binarias de n-butan-1-ol, di-n-butiléter y celosolvas*. Tesis Doctoral, 2010. Departamento de Física Aplicada, Facultad de Ciencias, Universidad de Valladolid.

[6] I. Alonso, *Estudio experimental y teórico de mezclas binarias de aminas y cetonas*. Tesis Doctoral, 2014. Departamento de Física Aplicada, Facultad de Ciencias, Universidad de Valladolid.

[7] T.J. Fortin, A. Laesecke, M. Freund, S. Outcalt, *Advanced calibration, adjustment, and operation of a density and sound speed analyzer*. J. Chem. Thermodyn. **57** (2013) 276-285. https://doi.org/10.1016/j.jct.2012.09.009

[8] U. Kaatze, E. Frieder, L. Karl, *Ultrasonic velocity measurements in liquids with high resolution—techniques, selected applications and perspectives*. Meas. Sci. Technol. **19** (2008) 062001. https://doi.org/10.1088/0957-0233/19/6/062001

[9] D. Schneditz, T. Kenner, H. Heimel, H. Stabinger, *A sound - speed sensor for the measurement of total protein concentration in disposable, blood - perfused tubes*. J. Acoust. Soc. Am. **86** (1989) 2073-2080. https://doi.org/10.1121/1.398466

[10] J.A. Riddick, W.B. Bunger, T.K. Sakano, *Organic solvents: physical properties and methods of purification*. Wiley, New York, 1986.

[11] K. Tamura, K. Ohomuro, S. Murakami, *Speeds of sound, densities, and isentropic compressibilities of {xC7H16 + (1 − x)C6H6} at 293.15 and 303.15 K*. J. Chem. Thermodyn. **16** (1984) 121-125. https://doi.org/10.1016/0021-9614(84)90143-5

[12] K.N. Marsh, *Recommended reference materials for the realization of physicochemical properties*. Blackwell Scientific Publications, Oxford, UK, 1987.

[13] J. Nath, *Speeds of sound in and isentropic compressibilities of (n-butanol+n-pentane, or n-hexane, or n-heptane, or n-octane, or 2,2,4-trimethylpentane, or carbon tetrachloride) at T=293.15 K*. J. Chem. Thermodyn. **29** (1997) 853-863. https://doi.org/10.1006/jcht.1997.0200

[14] A. Rodríguez, J. Canosa, J. Tojo, *Physical properties of the binary mixtures (diethyl carbonate + hexane, heptane, octane and cyclohexane) from T=293.15 K to T=313.15 K*. J. Chem. Thermodyn. **35** (2003) 1321-1333. https://doi.org/10.1016/S0021-9614(03)00096-X

[15] M. Nishimoto, S. Tabata, K. Tamura, S. Murakami, *Thermodynamic properties of the mixture of methoxyethanol and cyclohexane: Measurements at the temperatures 293.15, 298.15 and 303.15 K above and below UCST*. Fluid Phase Equilib. **136** (1997) 235-247. https://doi.org/10.1016/S0378-3812(97)00128-3

[16] K. Tamura, S. Murakami, *Speeds of sound, isentropic and isothermal compressibilities, and isochoric heat capacities of {xc-C6H12 + (1 − x)C6H6} from 293.15 to 303.15 K*. J. Chem. Thermodyn. **16** (1984) 33-38. https://doi.org/10.1016/0021-9614(84)90072-7

[17] H. Doi, K. Tamura, S. Murakami, *Thermodynamic properties of aqueous solution of 2-isobutoxyethanol at T = (293.15, 298.15, and 303.15) K, below and above LCST*. J. Chem. Thermodyn. **32** (2000) 729-741. https://doi.org/10.1006/jcht.1999.0645

[18] M. Dzida, S. Ernst, *Speed of Sound in Propan-1-ol + Heptane Mixtures under Elevated Pressures*. J. Chem. Eng. Data **48** (2003) 1453-1457. https://doi.org/10.1021/je030136n

[19] A.J. Treszczanowicz, Y.P. Handa, G.C. Benson, *Excess volumes and isentropic compressibilities of decan-1-ol + 2,2-dimethylbutane and + 2,2,4-trimethylpentane*. J. Chem. Thermodyn. **14** (1982) 871-881. https://doi.org/10.1016/0021-9614(82)90161-6

[20] J. Nath, *Speeds of sound in and isentropic compressibilities of (n-butanol + n-pentane) at T=298.15 K, and (n-butanol + n-hexane, or n-heptane, or n-octane, or 2,2,4-*

trimethylpentane) at T=303.15 K. J. Chem. Thermodyn. **30** (1998) 885-895. https://doi.org/10.1006/jcht.1998.0358

[21] B. Orge, A. Rodríguez, J.M. Canosa, G. Marino, M. Iglesias, J. Tojo, *Variation of Densities, Refractive Indices, and Speeds of Sound with Temperature of Methanol or Ethanol with Hexane, Heptane, and Octane.* J. Chem. Eng. Data **44** (1999) 1041-1047. https://doi.org/10.1021/je9900676

[22] E. Junquera, G. Tardajos, E. Aicart, *Speeds of sound and isentropic compressibilities of (cyclohexane + benzene and (1-chlorobutane + n-hexane or n-heptane or n-octane or n-decane) at 298.15 K.* J. Chem. Thermodyn. **20** (1988) 1461-1467. https://doi.org/10.1016/0021-9614(88)90041-9

[23] L.M. Trejo, M. Costas, D. Patterson, *Effect of molecular size on the W-shaped excess heat capacities: oxaalkane-alkane systems.* J. Chem. Soc. Faraday. Trans **87** (1991) 3001-3008. https://doi.org/10.1039/FT9918703001

[24] J.P.E. Grolier, G. Roux-Desgranges, M. Berkane, E. Jiménez, E. Wilhelm, *Heat capacities and densities of mixtures of very polar substances 2. Mixtures containing N, N-dimethylformamide.* J. Chem. Thermodyn. **25** (1993) 41-50. https://doi.org/10.1006/jcht.1993.1005

[25] R.H. Stokes, B.J. Levien, K.N. Marsh, *A continuous dilution dilatometer the excess volume for the system cyclohexane + benzene.* J. Chem. Thermodyn. **2** (1970) 43-52. https://doi.org/10.1016/0021-9614(70)90062-5

[26] R. Tanaka, O. Kiyohara, P.J. D'Arcy, G.C. Benson, *A Micrometer Syringe Dilatometer: Application to the Measurement of the Excess Volumes of some Ethylbenzene Systems at 298.15K.* Can. J. Chem. **53** (1975) 2262-2267. https://doi.org/10.1139/v75-317

[27] M.K. Kumaran, M.L. McGlashan, *An improved dilution dilatometer for measurements of excess volumes.* J. Chem. Thermodyn. **9** (1977) 259-267. https://doi.org/10.1016/0021-9614(77)90045-3

[28] F. Hevia, *Estudio experimental y teórico de mezclas binarias de amidas y aminas.* Trabajo Fin de Máster, 2015. Departamento de Física Aplicada, Facultad de Ciencias, Universidad de Valladolid.

[29] K. Tamura, K. Ohomuro, S. Murakami, *Speeds of sound, isentropic and isothermal compressibilities, and isochoric heat capacities of {xc-C6H12+(1−x)C6H6}, x{CCl4+(1−x)C6H6}, and x{C7H16+(1−x)C6H6} at 298.15 K.* J. Chem. Thermodyn. **15** (1983) 859-868. https://doi.org/10.1016/0021-9614(83)90092-7

[30] Bellingham+Stanley, *Technical Bulletin R001: Principles of Refractometry.*

[31] B. González, I. Domínguez, E.J. González, Á. Domínguez, *Density, Speed of Sound, and Refractive Index of the Binary Systems Cyclohexane (1) or Methylcyclohexane (1) or Cyclo-octane (1) with Benzene (2), Toluene (2), and Ethylbenzene (2) at Two Temperatures.* J. Chem. Eng. Data **55** (2010) 1003-1011. https://doi.org/10.1021/je900468u

[32] D. Gómez-Díaz, J.C. Mejuto, J.M. Navaza, *Physicochemical Properties of Liquid Mixtures. 1. Viscosity, Density, Surface Tension and Refractive Index of Cyclohexane + 2,2,4-Trimethylpentane Binary Liquid Systems from 25 °C to 50 °C.* J. Chem. Eng. Data **46** (2001) 720-724. https://doi.org/10.1021/je000310x

[33] A.K. Nain, *Refractive Indices of Binary Mixtures of Tetrahydrofuran with Aromatic Hydrocarbon at Temperatures from (288.15 to 318.15) K.* J. Chem. Eng. Data **53** (2008) 850-853. https://doi.org/10.1021/je700564c

[34] A.Z. Tasic, B.D. Djordjevic, D.K. Grozdanic, N. Radojkovic, *Use of mixing rules in predicting refractive indexes and specific refractivities for some binary liquid mixtures.* J. Chem. Eng. Data **37** (1992) 310-313. https://doi.org/10.1021/je00007a009

[35] K. Ridgway, P.A. Butler, *Physical properties of the ternary system benzene-cyclohexane-hexane.* J. Chem. Eng. Data **12** (1967) 509-515. https://doi.org/10.1021/je60035a012

[36] M. Iglesias, B. Orge, J. Tojo, *Speeds of sound, densities, refractive indices, and isentropic compressibilities of {x1C6H6 + x2c-C6H12 + (1 - x1 - x2)C6H5Cl} at the temperature 298.15 K.* J. Chem. Thermodyn. **26** (1994) 1179-1185. https://doi.org/10.1006/jcht.1994.1137

[37] Á. Piñeiro, P. Brocos, A. Amigo, M. Pintos, R. Bravo, *Prediction of Excess Volumes and Excess Surface Tensions from Experimental Refractive Indices.* Phys. Chem. Liq. **38** (2000) 251-260. https://doi.org/10.1080/00319100008030275

[38] Agilent-Technologies, *Agilent 4294A Precision Impedance Analyzer Service Manual, Third Edition.* 2009.

[39] Agilent-Technologies, *Agilent 4294A Precision Impedance Analyzer Operation Manual, Seventh Edition.* 2003.

[40] Keysight-Technologies, *Impedance Measurement Handbook, Sixth Edition.* 2016.

[41] Agilent-Technologies, *Agilent 4294A Precision Impedance Analyzer - Technical overview.*

[42] L.F. Sanz, *Estudio experimental y teórico de mezclas líquidas binarias formadas por 1-alcoholes y ciclohexilamina.* Tesis Doctoral, 2016. Departamento de Física Aplicada, Facultad de Ciencias, Universidad de Valladolid.

[43] G.-Z. Jia, K.-M. Huang, L.-J. Yang, X.-Q. Yang, *Composition-Dependent Dielectric Properties of DMF-Water Mixtures by Molecular Dynamics Simulations.* Int. J. Mol. Sci. **10** (2009) 1590-1600. https://doi.org/10.3390/ijms10041590

[44] G.-Z. Jia, Q. Jie, W. Feng, *Hydrogen bond analysis in alcohol (1-Propanol, 2-Propanol and Glycerol)-DMF mixtures based on dielectric spectroscopy.* J. Mol. Struct. **1100** (2015) 354-358. https://doi.org/10.1016/j.molstruc.2015.07.065

[45] G.-Z. Jia, J.-C. Liu, *The hydrogen bonding dynamics and cooperative interactions of DMAC–water mixture studied by dielectric relaxation spectroscopy.* Phys. Chem. Liq. **52** (2014) 608-617. https://doi.org/10.1080/00319104.2014.890896

[46] L. Mosteiro, E. Mascato, B.E. de Cominges, T.P. Iglesias, J.L. Legido, *Density, speed of sound, refractive index and dielectric permittivity of (diethyl carbonate + n -decane) at several temperatures.* J. Chem. Thermodyn. **33** (2001) 787-801. https://doi.org/10.1006/jcht.2000.0779

[47] J.B. Ott, C.E. Stouffer, G.V. Cornett, B.F. Woodfield, R.C. Wirthlin, J.J. Christensen, U.K. Deiters, *Excess enthalpies for (ethanol + water) at 298.15 K and pressures of 0.4, 5, 10, and 15 MPa.* J. Chem. Thermodyn. **18** (1986) 1-12. https://doi.org/10.1016/0021-9614(86)90036-4

[48] J.B. Ott, G.V. Cornett, C.E. Stouffer, B.F. Woodfield, C. Guanquan, J.J. Christensen, *Excess enthalpies of (ethanol+water) at 323.15, 333.15, 348.15, and 373.15 K and from 0.4 to 15 MPa.* J. Chem. Thermodyn. **18** (1986) 867-875. https://doi.org/10.1016/0021-9614(86)90121-7

Chapter 4.

Theoretical models

The theoretical models used to analyze and interpret experimental data of liquids and liquid mixtures are briefly presented. The physical hypotheses and the final equations are stated. References to the original works are given for the interested reader. Special emphasis is put on the concepts behind the Kirkwood-Fröhlich model for dielectrics. Some equations of the model are derived using a new approach, clearer than the original and subsequent works.

4.1. Prigogine-Flory-Patterson model

The Flory model [1-5] is a purely physical theory. It is essentially a theory of the Van der Waals type, taking into account free volume and also attractive intermolecular interactions. The main feature of the Flory model is the random mixing hypothesis, and serves as a tool to evaluate if orientational (i.e., non-random) effects are relevant in the mixtures.

4.1.1. Hypotheses for pure liquids

In the Flory model, a liquid, occupying the volume V, is formed by N molecules (of mean volume $v_{\mathrm{m}} = V / N$), each of which is divided into r **segments**. The mean volume of a segment is denoted $v_{\mathrm{s}} = V / rN = v_{\mathrm{m}} / r$. A segment is an arbitrarily chosen isomeric portion of the molecule; its precise definition is left open and may be adapted to circumstances. The **core volume** of a molecule is defined as $v_{\mathrm{m}}^{*} = rv_{\mathrm{s}}^{*}$, where v_{s}^{*} is the **core volume of a segment**. Each segment is endowed with s **contacts**. The interactions considered are: (i) An **attractive intermolecular interaction between pairs of contacts**, with a mean potential energy per pair of the form $-\eta / v_{\mathrm{s}}$, where η is a positive constant of the liquid considered. (ii) A **repulsive interaction**, leading to a **free volume term** in the partition function [6]. (iii) The effect of the rest of the intramolecular interactions is treated assuming [7] that the $3r$ degrees of freedom of a molecule can be divided into two uncoupled categories, i.e., **internal** (not appreciably affected by neighbors in the liquid, and therefore dependent only on temperature) and **external** (dependent on molar volume as well as on temperature). For fluids with densities of liquids, the intramolecular potentials associated with the latter degrees of freedom are supposed to merely restrict the degrees of freedom per molecule from $3r$ to an effective number of $3rc$. The constant $c \leq 1$ would take into account the restrictions on the precise location of a segment by its neighbors in the same chain. Some parameters of the model are better replaced by the **reduction parameters** p^{*} and T^{*}, defined together with the **reduced parameters** of

the liquid, namely, $\bar{T} = T / T^*$, $\bar{p} = p / p^*$ (where p is the pressure and T is the temperature) and $\bar{V} = v_\mathrm{m} / v_\mathrm{m}^* = v_\mathrm{s} / v_\mathrm{s}^* = V_\mathrm{m} / V_\mathrm{m}^*$. In these relations, $V_\mathrm{m} = N_\mathrm{A} v_\mathrm{m}$ denotes the **molar volume** of the liquid and $V_\mathrm{m}^* = N_\mathrm{A} v_\mathrm{m}^*$ the **core molar volume** (N_A stands for Avogadro's constant).

4.1.2. Hypotheses for binary mixtures

The components of a binary mixture will be indexed by subscripts $i = 1,2$. Because the definition of segment is arbitrary, it is convenient to impose that the **segments of both components have the same core volume**. It is supposed that the **number of contacts per molecule of a given component is proportional to the core surface area of the corresponding molecule**, assumed spherical. The total number of molecules in the mixture is $N = N_1 + N_2$. The total **numbers of segments, contacts and effective number of degrees of freedom** (rN, srN and $3rcN$) **are taken as additive**. It is convenient to define the **segment and contact fractions**, respectively, by $\varphi_i = r_i N_i / rN$ and $\theta_i = s_i r_i N_i / srN = \varphi_i s_i / s$. Of course, $\sum_i \varphi_i = \sum_i \theta_i = 1$. It is also assumed that **the mean intensity of the interaction between segments of molecules of the same component is the same in the mixture as in the pure species**; the total intermolecular energy of the binary mixtures can be written in the same form as for pure compounds, by defining $v_\mathrm{s} = V / rN$, and the η parameter of the mixture by $\eta = \theta_1\eta_1 + \theta_2\eta_2 - A_{12}\Delta\eta / (srN)$. Here, A_{ii} and A_{12} are the numbers of pairs of contacts between equal and different molecules respectively, $\Delta\eta = \eta_1 + \eta_2 - 2\eta_{12}$ and η_{12} characterizes the mean intensity of the interaction between segments of different molecules. Moreover, **random mixing** is assumed. This hypothesis states that, given a contact, the remaining contacts in the mixture have the same probability of forming an interacting pair with it. It is expressed by the equations $A_{12,\mathrm{random}} = srN\theta_1\theta_2$ and $\eta_\mathrm{random} = \theta_1\eta_1 + \theta_2\eta_2 - \theta_1\theta_2\Delta\eta$.

4.1.3. Equations

For both pure compounds and binary mixtures, the molar intermolecular energy, E_m, and the thermal equation of state (in reduced form) are:

$$E_\mathrm{m} = -\frac{p^* V_\mathrm{m}^*}{\bar{V}} = -T V_\mathrm{m}^* \frac{p^*}{T^*} \frac{1}{\bar{V}\bar{T}} \tag{4.1}$$

$$\frac{\bar{p}\bar{V}}{\bar{T}} = \frac{\bar{V}^{1/3}}{\bar{V}^{1/3} - 1} - \frac{1}{\bar{V}\bar{T}} \tag{4.2}$$

(the last equality of equation (2.4) is useful when treating mixtures; see below). The so-called geometrical parameter of the mixture, $S_{12} = s_1 / s_2$, is

$$S_{12} = \left(\frac{V_\mathrm{m1}^*}{V_\mathrm{m2}^*} \right)^{-1/3} \tag{4.3}$$

The relation of the parameters of the mixture and of the pure compounds is

$$V_\mathrm{m}^* = x_1 V_\mathrm{m1}^* + x_2 V_\mathrm{m2}^* \tag{4.4}$$

$$\varphi_i = \frac{x_i V^*_{\mathrm{m}i}}{V^*_{\mathrm{m}}} \tag{4.5}$$

$$\theta_2 = 1 - \theta_1 = \frac{\varphi_2}{\varphi_2 + S_{12}\varphi_1} \tag{4.6}$$

$$p^* = \varphi_1 p_1^* + \varphi_2 p_2^* - \varphi_1 \theta_2 X_{12} \tag{4.7}$$

$$\frac{p^*}{T^*} = \varphi_1 \frac{p_1^*}{T_1^*} + \varphi_2 \frac{p_2^*}{T_2^*} \tag{4.8}$$

where x_i is the mole fraction of component i and, in equation (4.7), the parameter $\Delta\eta$ has been replaced by the so-called energetic parameter $X_{12} = s_1 \Delta\eta / 2(v_{\mathrm{s}}^*)^2$. Also, using equations (2.4) and (4.2) one can derive [1] simple expressions to obtain $V^*_{\mathrm{m},i}$ and p_i^* of the pure compounds in terms of experimental molar volumes and coefficients of isobaric thermal expansion, $\alpha_{p,i}$, and isothermal compressibility, $\kappa_{T,i}$:

$$V^*_{\mathrm{m},i} = V_{\mathrm{m},i} \left[\frac{3T\alpha_{p,i} + 3\left(1 - 2p\kappa_{T,i}\right)}{4T\alpha_{p,i} + 3\left(1 - 2p\kappa_{T,i}\right)} \right]^3 \tag{4.9}$$

$$p_i^* = \left(\frac{T\alpha_{p,i}}{\kappa_{T,i}} - p \right) \bar{V}_i^2 \tag{4.10}$$

Ignoring the difference between internal energy and enthalpy in condensed systems at low pressure, the molar excess enthalpy, $H^{\mathrm{E}}_{\mathrm{m}}$, can be calculated from the molar intermolecular energies of the mixture and of the pure compounds, $H^{\mathrm{E}}_{\mathrm{m}} = E_{\mathrm{m}} - x_1 E_{\mathrm{m}1} - x_2 E_{\mathrm{m}2}$, or:

$$H^{\mathrm{E}}_{\mathrm{m}} = x_1 p_1^* V^*_{\mathrm{m}1} \left(\frac{1}{\bar{V}_1} - \frac{1}{\bar{V}} \right) + x_2 p_2^* V^*_{\mathrm{m}2} \left(\frac{1}{\bar{V}_2} - \frac{1}{\bar{V}} \right) + \frac{x_1 V^*_{\mathrm{m}1} \theta_2 X_{12}}{\bar{V}} \tag{4.11}$$

The part in equation (4.11) containing X_{12} is named the interactional term. The rest of the contributions are called the equation of state term. These names are not truly appropriate, since none of these terms in equation (4.11) isolates interactional or structural effects.

The molar volume $V_{\mathrm{m}} = \bar{V} V^*_{\mathrm{m}}$ of the mixture is known from the equation of state, which permits to calculate as well the molar excess volume $V^{\mathrm{E}}_{\mathrm{m}} = V_{\mathrm{m}} - x_1 V_{\mathrm{m}1} - x_2 V_{\mathrm{m}2}$.

4.1.4. Estimation of the Flory energetic parameter

From the composition, pressure, temperature and the reduction parameters of the pure liquids, there are several quantities that can be directly calculated: $S_{12}, V^*_{\mathrm{m}}, \varphi_i, \theta_i$ and the ratios p^* / T^* and $\bar{p} / \bar{T}$ (see equations (4.3) to (4.6) and (4.8)). A procedure to obtain the energetic parameter X_{12} from $H^{\mathrm{E}}_{\mathrm{m}}$ at a given composition without approximations will be now exposed. From $H^{\mathrm{E}}_{\mathrm{m}}$, the value of E_{m} follows. Next, use the second equality of equation (2.4) to obtain $(1 / \bar{V}\bar{T})$. Then, solve the equation of state for $\bar{V}^{1/3}$ (for example, obtaining it by the Newton-

Raphson method with initial estimate of the unknown equal to 1), and use the first equality of equation (2.4) to determine p^*. Finally, X_{12} can be calculated from equation (4.7).

X_{12} can also be estimated from V_m^E at a given composition. From V_m^E, one can obtain V_m, and then $\bar{V}$. Use the thermal equation of state to calculate $\bar{V}\bar{T}$. Then, $\bar{T} = \bar{V}\bar{T} / \bar{V}$ and $T^* = T / \bar{T}$. Finally, $p^* = T^*(p^* / T^*)$ and X_{12} is obtained from equation (4.7).

When X_{12} for a given composition is known, the calculation of $\bar{V}$ from the equation of state is somewhat different. First, obtain p^* from equation (4.7), together with $\bar{p}$. From the value of $\bar{p} / \bar{T}$, obtain $1 / \bar{T}$. Then, rewrite the equation of state in the form $[(\bar{p} / \bar{T})\bar{V}^2 + (1 / \bar{T})](\bar{V}^{1/3} - 1) - \bar{V}^{4/3} = 0$ and solve it for $\bar{V}^{1/3}$, a task for which the Newton-Raphson method is also easy to use.

4.1.5. Study of the random mixing hypothesis

If random mixing is not considered but the definition of X_{12} is used, then one can write

$$\eta = \theta_1\eta_1 + \theta_2\eta_2 - X_{12}\frac{A_{12}}{srN}\frac{2(v_s^*)^2}{s_1} = \theta_1\eta_1 + \theta_2\eta_2 - \theta_1\theta_2 X'_{12}(x_1)\frac{2(v_s^*)^2}{s_1} \tag{4.12}$$

where the composition-dependent function $X'_{12}(x_1)$ has been defined by

$$X'_{12}(x_1) = X_{12}\frac{A_{12}}{A_{12,\text{random}}} \tag{4.13}$$

When the random mixing hypothesis is excluded, the equations of the model for binary mixtures have the same form as when including it, by replacing X_{12} by $X'_{12}(x_1)$. Therefore, one can obtain $X'_{12}(x_1)$ from H_m^E at different compositions by exactly the same procedure considered before for X_{12} (see 4.1.4). Furthermore, if X_{12} (the Flory energetic parameter of the mixture) is considered as known, it is possible to study the deviations from the random mixing hypothesis as a function of composition, by means of the quantity $X'_{12}(x_1) / X_{12} = A_{12} / A_{12,\text{random}}$. In this procedure, the selection of a criterion for the value of X_{12} is implicit. Note that if X_{12} is estimated from H_m^E for some x_1 value, then the value obtained for $X'_{12}(x_1) / X_{12}$ at that composition will be 1, because, in the estimation of X_{12}, random mixing is assumed.

4.1.6. Patterson's series expansions

In order to gain some insight into the interpretation of the results of the Flory model, Patterson and collaborators [8] developed approximate expressions for the main quantities calculated by the model. This approximation has the advantage of splitting them into the terms depending on X_{12} (which he calls "interactional") and the ones independent of it ("free volume" terms). The literature refers to it as the Prigogine-Flory-Patterson model.

Let us summarize the foundations of the method, skipping the intermediate calculations. A detailed derivation is given in section 4.4. They define, for pure liquids and for mixtures, the **energy reduction parameter** as:

$$E_m^* = p^* V_m^* \tag{4.14}$$

If A_{m} is a molar quantity with energy dimensions, then the **reduced** A_{m}, denoted $\bar{A}$, can be defined as $\bar{A} = A_{\mathrm{m}} / E^*_{\mathrm{m}}$. Other convenient definitions are the parameter X:

$$X = \frac{\psi_1 \theta_2 X_{12}}{p^*_1} \tag{4.15}$$

and the **contact energy fraction** of component i, ψ_i:

$$\psi_i = \frac{x_i E^*_{\mathrm{m}i}}{x_1 E^*_{\mathrm{m}1} + x_2 E^*_{\mathrm{m}2}} \tag{4.16}$$

Naturally, $\psi_1 + \psi_2 = 1$. Note here that $E^*_{\mathrm{m}} \neq x_1 E^*_{\mathrm{m}1} + x_2 E^*_{\mathrm{m}2}$ and $\psi_i \neq x_i E^*_{\mathrm{m}i} / E^*_{\mathrm{m}}$. In the **low pressure approximation** ($\bar{p} \approx 0$), which we will use through the rest of the exposition, the mixing molar enthalpy $\Delta H_{\mathrm{m}} = H^{\mathrm{E}}_{\mathrm{m}}$ is identical to the mixing molar intermolecular energy ($A_{\mathrm{m}} = E_{\mathrm{m}}$), and the following relation holds:

$$\frac{H^{\mathrm{E}}_{\mathrm{m}}}{x_1 E^*_{\mathrm{m}1} + x_2 E^*_{\mathrm{m}2}} = (1 - X)\,\bar{E} - \left(\psi_1 \bar{E}_1 + \psi_2 \bar{E}_2\right) \tag{4.17}$$

where $\bar{E} = E_{\mathrm{m}} \big/ E^*_{\mathrm{m}} = -1 \big/ \bar{V}$ defines (for pure compounds and for mixtures) the **reduced intermolecular energy**. The mixing molar volume $\Delta V_{\mathrm{m}} = V^{\mathrm{E}}_{\mathrm{m}}$ can be treated in a similar manner by putting

$$\frac{V^{\mathrm{E}}_{\mathrm{m}}}{x_1 V^*_{\mathrm{m}1} + x_2 V^*_{\mathrm{m}2}} = \bar{V} - \left(\varphi_1 \bar{V}_1 + \varphi_2 \bar{V}_2\right) \tag{4.18}$$

Now more sophisticated manipulations are performed:

1. **Series expansion of the mixing functions**. Inspired by equations (4.17) and (4.18), one considers the reduced quantities $\bar{E}\left(\bar{T}\right)$ and $\bar{V}\left(\bar{T}\right)$ as functions of the reduced temperature $\bar{T}$, and defines two characteristic reduced temperatures $\bar{T}_E$ and $\bar{T}_V$ such that:

$$\bar{E}\left(\bar{T}_E\right) = \psi_1 \bar{E}_1 + \psi_2 \bar{E}_2 \tag{4.19}$$

$$\bar{V}\left(\bar{T}_V\right) = \varphi_1 \bar{V}_1 + \varphi_2 \bar{V}_2 \tag{4.20}$$

   Then, series expansions of $H^{\mathrm{E}}_{\mathrm{m}}$ and $V^{\mathrm{E}}_{\mathrm{m}}$ are performed around the corresponding characteristic reduced temperatures up to first-order terms (and approximating $1/(1 - X) \approx 1 + X$). The result is the expression of these quantities as a sum of two terms: one "interactional" (subscript "int") dependent on X_{12}, and a "free volume" term (subscript "fv") independent of X_{12}. According to Patterson and Delmas, these expansions correspond to an error in the calculated functions of 1% at worst (for high polymer solutions) and usually much less. The results are:

$$\frac{H^{\mathrm{E}}_{\mathrm{m,int}}}{x_1 E^*_{\mathrm{m}1} + x_2 E^*_{\mathrm{m}2}} = -\frac{\bar{E}\left(\bar{T}_E\right)}{4 + 3\bar{E}\left(\bar{T}_E\right)^{-1/3}} \frac{\psi_1 \theta_2 X_{12}}{p^*_1} \tag{4.21}$$

$$\frac{H^{\mathrm{E}}_{\mathrm{m,fv}}}{x_1 E^*_{\mathrm{m1}} + x_2 E^*_{\mathrm{m2}}} = -\frac{\left(\psi_1\bar{T}_1 + \psi_2\bar{T}_2\right) + \bar{E}\left(\bar{T}_E\right)\left[\bar{E}\left(\bar{T}_E\right)^{1/3} + 1\right]}{\frac{4}{3}\bar{E}\left(\bar{T}_E\right)^{1/3} + 1} \tag{4.22}$$

$$\frac{V^{\mathrm{E}}_{\mathrm{m,int}}}{x_1 V^*_{\mathrm{m1}} + x_2 V^*_{\mathrm{m2}}} = \frac{\left(\psi_1\bar{T}_1 + \psi_2\bar{T}_2\right)\bar{V}\left(\bar{T}_V\right)^2}{\frac{4}{3}\bar{V}\left(\bar{T}_V\right)^{-1/3} - 1}\frac{\psi_1\theta_2 X_{12}}{p^*_1} \tag{4.23}$$

$$\frac{V^{\mathrm{E}}_{\mathrm{m,fv}}}{x_1 V^*_{\mathrm{m1}} + x_2 V^*_{\mathrm{m2}}} = \frac{\bar{V}\left(\bar{T}_V\right)^2\left(\psi_1\bar{T}_1 + \psi_2\bar{T}_2\right) + \bar{V}\left(\bar{T}_V\right)\left[\bar{V}\left(\bar{T}_V\right)^{-1/3} - 1\right]}{\frac{4}{3}\bar{V}\left(\bar{T}_V\right)^{-1/3} - 1} \tag{4.24}$$

Equation (4.23) is not the same as the one given in the original works but, as it is shown in section 4.4, it is a correct result. The equation normally given for $V^{\mathrm{E}}_{\mathrm{m,int}}$ can be obtained from equation (4.23) by replacing the quantity $\psi_1\bar{T}_1 + \psi_2\bar{T}_2$ by $\bar{T}_V$. Perhaps this way of proceeding has the objective of obtaining expressions for $H^{\mathrm{E}}_{\mathrm{m,int}}$ and $V^{\mathrm{E}}_{\mathrm{m,int}}$ that have the same mathematical structure (see section 4.4).

2. **Series expansion of the free volume terms**. The nature of the free-volume terms may be seen through an expansion of $\bar{T}_i$ around $\bar{E}\left(\bar{T}_E\right)$ or $\bar{V}\left(\bar{T}_V\right)$, neglecting terms of order greater than two. The result is given in powers of $\bar{E}_1 - \bar{E}_2$ or $\bar{V}_1 - \bar{V}_2$. The approximation is, according to Patterson and Delmas, good to $\approx 4\%$ in the worst cases and usually much better. For $H^{\mathrm{E}}_{\mathrm{m}}$, one simply obtains another approximate expression of $H^{\mathrm{E}}_{\mathrm{m,fv}}$. However, the results are more interesting for $V^{\mathrm{E}}_{\mathrm{m}}$, as $V^{\mathrm{E}}_{\mathrm{m,fv}}$ splits into two terms: a "p^* effect" term ($V^{\mathrm{E}}_{\mathrm{m},p^*\mathrm{eff}}$, which depends on the difference $p^*_1 - p^*_2$) and a "curvature" term ($V^{\mathrm{E}}_{\mathrm{m,curv}}$, the name is related to the presence of a second derivative). The following formulas are obtained:

$$\frac{H^{\mathrm{E}}_{\mathrm{m,fv}}}{x_1 E^*_{\mathrm{m1}} + x_2 E^*_{\mathrm{m2}}} = \frac{2\left(\bar{E}_1 - \bar{E}_2\right)^2\psi_1\psi_2}{3\bar{E}\left(\bar{T}_E\right)\left[4 + 3\bar{E}\left(\bar{T}_E\right)^{-1/3}\right]} \tag{4.25}$$

$$\frac{V^{\mathrm{E}}_{\mathrm{m},p^*\mathrm{eff}}}{x_1 V^*_{\mathrm{m1}} + x_2 V^*_{\mathrm{m2}}} = \left(\psi_1 - \varphi_1\right)\left(\bar{V}_1 - \bar{V}_2\right) = \frac{\psi_1\psi_2\left(p^*_1 - p^*_2\right)\left(\bar{V}_1 - \bar{V}_2\right)}{\psi_1 p^*_2 + \psi_2 p^*_1} \tag{4.26}$$

$$\frac{V^{\mathrm{E}}_{\mathrm{m,curv}}}{x_1 V^*_{\mathrm{m1}} + x_2 V^*_{\mathrm{m2}}} = -\frac{\left[\frac{14}{9}\bar{V}\left(\bar{T}_V\right)^{-1/3} - 1\right]\left(\bar{V}_1 - \bar{V}_2\right)^2}{\left[\frac{4}{3}\bar{V}\left(\bar{T}_V\right)^{-1/3} - 1\right]\bar{V}\left(\bar{T}_V\right)}\left[\psi_1\psi_2 + \left(\psi_1 - \varphi_1\right)^2\right] \tag{4.27}$$

The term $\left(\psi_1 - \varphi_1\right)^2$ in equation (4.27) is generally omitted.

4.2. The ERAS model

The Extended Real Associated Solution (ERAS) model [9, 10] combines the Real Association Solution Model [11-14] with Flory's thermal equation of state. Nowadays, it is applied to mixtures where self-association effects, solvation effects between a self-associated compound and a polar one, or solvation effects between two self-associated compounds are expected.

4.2.1. Hypotheses

We will not present a detailed derivation of the equations. The model assumes the partition function of the mixture as a product of a combinatorial part, a chemical part (which includes the hydrogen-bonding contribution, inspired in the Real Association Solution Model), and a physical part (imitating that of the Flory model). As a result, the thermodynamic functions are sums of contributions of different nature. In addition, the thermal equation of state and the intermolecular energy are formally identical to Flory's, but with one fundamental difference: the reduction parameters V_{m}^{*}, p^{*} and T^{*} are defined differently (see below). This is due to the interplay between the physical and the chemical contributions.

Let us summarize the main hypotheses of the chemical part. For a self-associated compound A, there is a chemical equilibrium involving only linear consecutive multimers:

$$\mathrm{A}_n + \mathrm{A} \overset{K_{\mathrm{A}}}{\rightleftharpoons} \mathrm{A}_{n+1} \tag{4.28}$$

where the degree of association, n, ranges from 1 to ∞. When there exists cross-association between two components A and B in a mixture, if A is self-associated but not B, then the cross-association chemical equilibrium is described by:

$$\mathrm{A}_n + \mathrm{B} \overset{K_{\mathrm{AB}}}{\rightleftharpoons} \mathrm{A}_n\mathrm{B} \tag{4.29}$$

In the case of the cross-association of two self-associated compounds:

$$\mathrm{A}_n + \mathrm{B}_\ell \overset{K_{\mathrm{AB}}}{\rightleftharpoons} \mathrm{A}_n\mathrm{B}_\ell \tag{4.30}$$

It is assumed that the equilibrium constants governing the above equilibria (K_{A} and K_{AB}) are independent of the chain length of the polymeric species. The explicit form of K_{A} and K_{AB} is also assumed. The **molar enthalpies of intermolecular hydrogen bonding** for these two kinds of reactions, $\Delta h_{\mathrm{A}}^{*}$ and $\Delta h_{\mathrm{AB}}^{*}$, are introduced, and the corresponding equilibrium constants depend on temperature according to them following the Van't Hoff equation. Moreover, negative **molar hydrogen-bonding volumes**, $\Delta v_{\mathrm{A}}^{*}$ and $\Delta v_{\mathrm{AB}}^{*}$, are defined in order to take into account the decrease of the core volume of the molecules upon multimer formation.

4.2.2. Equations

In this section, we will denote the different compounds by subscripts i = A or B.

The model has been worked out fundamentally under the $\overline{p} \approx 0$ approximation (see above). The reduction parameters of pure species are defined by:

$$V^*_{\mathrm{m},i} = V_{\mathrm{m},i}\left[\frac{3T\left(\alpha_{p,i}-\alpha^*_{p,i}\right)+3}{4T\left(\alpha_{p,i}-\alpha^*_{p,i}\right)+3}\right]^3 \tag{4.31}$$

$$\alpha^*_{p,i} = \Delta v^*_i \Delta h^*_i \frac{\left(4K_i+1\right)^{1/2} - 2K_i\left(4K_i+1\right)^{-1/2} - 1}{2K_i V^*_{\mathrm{m},i} R T^2} \tag{4.32}$$

$$p^*_i = \left(\alpha_{p,i}-\alpha^*_{p,i}\right) T \bar{V}_i^2 \left(\kappa_{T,i} - \alpha^*_{p,i} T \frac{\Delta v^*_i}{\Delta h^*_i}\right)^{-1} \tag{4.33}$$

$$T^*_i = \frac{\bar{V}_i^{4/3}}{\bar{V}_i^{1/3}-1} T \tag{4.34}$$

If the pure compound is not self-associated, then Δv^*_i, Δh^*_i, K_i are zero. Note that in such a case the above relations reduce to those of the Flory model with $\overline{p} \approx 0$.

The mixing rules for the reduction parameters are the same as in the Flory model (equations (4.4) to (4.8)). In the context of this model, s_i is the so-called **surface-to-volume ratio** of molecule i, and φ_i and θ_i are the **reduction volume fraction** and the **surface fraction** respectively. The total relative molecular volumes and surfaces of the compounds were calculated additively on the basis of the group volumes and surfaces recommended by Bondi [15]. Using s_i calculated in this way, S_{AB} is automatically determined. We must remark that φ_i and θ_i are different quantities from the homologous ones in the Flory model because, although they are obtained using the same equations, the reduction volumes are defined differently (as has been previously mentioned). The thermal equation of state (4.2) from the Flory model holds for both the pure compounds and the mixture, provided the reduction parameters are obtained from equations (4.31) to (4.34).

Another important quantity in the model is the **volume fraction of monomeric species of *i*** in the mixture, φ_{1i}. They can be calculated numerically from the following system of two equations:

$$\varphi_{\mathrm{A}} = \frac{\varphi_{1\mathrm{A}}}{\left(1-K_{\mathrm{A}}\varphi_{1\mathrm{A}}\right)^2}\left(1+\frac{V_{\mathrm{m,A}}K_{\mathrm{AB}}\varphi_{1\mathrm{B}}}{V_{\mathrm{m,B}}\left(1-K_{\mathrm{B}}\varphi_{1\mathrm{B}}\right)}\right) \tag{4.35}$$

$$\varphi_{\mathrm{B}} = \frac{\varphi_{1\mathrm{B}}}{\left(1-K_{\mathrm{B}}\varphi_{1\mathrm{B}}\right)^2}\left(1+\frac{K_{\mathrm{AB}}\varphi_{1\mathrm{A}}}{1-K_{\mathrm{A}}\varphi_{1\mathrm{A}}}\right) \tag{4.36}$$

The **volume fractions of monomeric species in the pure compounds**, φ^0_{1i}, are:

$$\varphi^0_{1i} = \frac{2K_i+1-\sqrt{4K_i+1}}{2K_i^2} \tag{4.37}$$

We will focus only on the equations to calculate $H^{\mathrm{E}}_{\mathrm{m}}$ and $V^{\mathrm{E}}_{\mathrm{m}}$. These are obtained from:

$$F^{\mathrm{E}}_{\mathrm{m}} = F^{\mathrm{E}}_{\mathrm{m,phys}} + F^{\mathrm{E}}_{\mathrm{m,chem}} \qquad \left(F = H, V\right) \tag{4.38}$$

The physical contributions, $F^{\mathrm{E}}_{\mathrm{m,phys}}$, are obtained in the same way as in the Flory model but with the variables defined in this section. The chemical contributions, $F^{\mathrm{E}}_{\mathrm{m,chem}}$, are calculated from:

$$V^{\mathrm{E}}_{\mathrm{m,chem}} = \bar{V}\Big[x_{\mathrm{A}}\Delta v^{*}_{\mathrm{A}} K_{\mathrm{A}}\left(\varphi_{1\mathrm{A}} - \varphi^{0}_{1\mathrm{A}}\right) + x_{\mathrm{B}}\Delta v^{*}_{\mathrm{B}} K_{\mathrm{B}}\left(\varphi_{1\mathrm{B}} - \varphi^{0}_{1\mathrm{B}}\right) + x_{\mathrm{A}}\Delta v^{*}_{\mathrm{AB}} K_{\mathrm{AB}} \frac{\varphi_{1\mathrm{B}}\left(1 - K_{\mathrm{A}}\varphi_{1\mathrm{A}}\right)}{\left(V_{\mathrm{m,B}}/V_{\mathrm{m,A}}\right)\left(1 - K_{\mathrm{B}}\varphi_{1\mathrm{B}}\right) + K_{\mathrm{AB}}\varphi_{1\mathrm{B}}} \Big] \tag{4.39}$$

$$H^{\mathrm{E}}_{\mathrm{m,chem}} = x_{\mathrm{A}}\Delta h^{*}_{\mathrm{A}} K_{\mathrm{A}}\left(\varphi_{1\mathrm{A}} - \varphi^{0}_{1\mathrm{A}}\right) + x_{\mathrm{B}}\Delta h^{*}_{\mathrm{B}} K_{\mathrm{B}}\left(\varphi_{1\mathrm{B}} - \varphi^{0}_{1\mathrm{B}}\right)\bar{V} + x_{\mathrm{A}}\Delta h^{*}_{\mathrm{AB}} K_{\mathrm{AB}} \frac{\varphi_{1\mathrm{B}}\left(1 - K_{\mathrm{A}}\varphi_{1\mathrm{A}}\right)}{\left(V_{\mathrm{m,B}}/V_{\mathrm{m,A}}\right)\left(1 - K_{\mathrm{B}}\varphi_{1\mathrm{B}}\right) + K_{\mathrm{AB}}\varphi_{1\mathrm{B}}} - \frac{p^{*}V^{\mathrm{E}}_{\mathrm{m,chem}}}{\bar{V}^{2}} \tag{4.40}$$

Parameters adjustable to excess properties are: K_i, K_{AB}, Δh^{*}_i, $\Delta h^{*}_{\mathrm{AB}}$, Δv^{*}_i, $\Delta v^{*}_{\mathrm{AB}}$ and X_{AB}. The number of adjustable parameters can be reduced by fitting the parameters K_i, Δh^{*}_i and Δv^{*}_i of a self-associated compound to $H^{\mathrm{E}}_{\mathrm{m}}$ and $V^{\mathrm{E}}_{\mathrm{m}}$ data of its mixture with an appropriate inert compound, or to enthalpy of vaporization data. The molar enthalpy of vaporization, $\Delta H^{\mathrm{v}}_{\mathrm{m},i}$, of a pure compound in the ERAS model is calculated as:

$$\Delta H^{\mathrm{v}}_{\mathrm{m},i} = \frac{p^{*}_i V^{*}_{\mathrm{m},i}}{\bar{V}_i} - \Delta h^{*}_i \frac{2K_i + 1 - \sqrt{4K_i + 1}}{2K_i} + RT \tag{4.41}$$

4.3. Kirkwood-Fröhlich model

4.3.1. Dielectric behavior

In the presence of an external electric field, a dielectric gives rise to a macroscopic dipole moment, due to some well-defined physical processes:

- **Induced polarization**, which includes the polarization mechanisms due to the elastic displacement of charges under the field. There are two classes of induced polarization: **electronic polarization**, in which the electron cloud surrounding atomic nuclei moves in the opposite sense to the field, and **atomic (or ionic) polarization**, by which ions of different charge sign in a molecule or crystal are displaced in opposite senses from their equilibrium positions.
- **Orientational polarization**, due to the partial orientation of the permanent dipole moments in the presence of a field. It is not present in nonpolar substances.
- **Interfacial polarization**, present in many non-homogeneous (multiphasic, porous, polycrystalline, with crystal defects...) materials, arises because of the motion of free charge across the interphases subject to the action of the field.

It is possible to decompose the high complexity of the dielectric response of a system in such a way because the characteristic time of each of the polarization mechanisms described above is different. For a static field, all of them work at the same time and it is not possible to physically distinguish among them. In contrast, harmonic fields excite only some of these contributions depending on the value of their frequency.

More precisely, in the case of time-varying fields, the fact that matter shows a nonzero response time implies the existence of a delay of the polarization with respect to the electric field. The weak-field linear relationship between polarization and field must then account for the value of the field in all the earlier instants of time, therefore taking an integral form. The linear relation is simplified to a simple proportionality after a Fourier expansion, thus defining the **complex relative permittivity**. This is a very well-known fact from electromagnetic theory. But it is worthwhile to summarize the main properties of this frequency-dependent function.

The **imaginary part** is related to energy dissipation and remains close to zero except for some absorption peaks in regions where notable phenomena occur. The first group of them are **relaxation processes**, in which interfacial or orientational polarization stop contributing. In contrast, in **resonance processes** ions or electrons absorb energy when their vibration enters into resonance under the action of the field at a critical frequency. For frequencies higher than the resonances, the induced polarization mechanisms associated to these charges stop contributing. These absorption peaks of the imaginary part as a function of frequency are significantly wider in relaxation than in resonance, since the latter are due to electronic or ionic transitions between discrete energy levels.

The **real part** is approximately constant in certain frequency ranges, in which well-defined polarization mechanisms are in operation, and varies in the regions in which the aforementioned absorption peaks appear. It is at frequencies immediately higher than these peaks where the polarization mechanisms related to them are uncoupled from the excitation caused by the field. Thus, interfacial polarization has a very high response time, as the distances that the free charge has to cover are large compared to atomic and molecular lengths; therefore, it only contributes at very low frequencies (and in non-homogeneous materials). Orientational polarization usually ceases to contribute in the microwave region, since at higher frequencies the dipoles cannot rotate at the speed imposed by the external field. Atomic polarization typically has peaks in the infrared, and electronic polarization in near-infrared, visible and ultraviolet. Electrons in internal shells have characteristic frequencies of the order of 10^{19} Hz (X-ray) and, for this reason, any electromagnetic wave having a frequency above it does not cause any absorption or polarization effects.

4.3.2. Long-range interactions and the local field hypothesis

From now on, we will restrict ourselves to **homogeneous** materials, where only orientational and induced polarization need be considered. Also, thermodynamic equilibrium requires that the electric field be **static and uniform** in all the space outside the conductors that cause it. Furthermore, we will consider the dielectric to be **isotropic**. The considerations from now on will then apply for homogeneous and isotropic fluids (liquids, vapors and gases) under static and uniform fields.

The action of a static electric field on a dielectric produces the emergence of a macroscopic polarization. The **polarization** or density of macroscopic dipole moment, $\vec{P}$, is related to the true field $\vec{E}$ inside the dielectric by:

$$\vec{P} = \varepsilon_0 \left(\varepsilon_\mathrm{r} - 1\right) \vec{E} \tag{4.42}$$

where ε_r is the relative permittivity of the dielectric and ε_0 the vacuum permittivity.

Each portion of the dielectric shows a macroscopic dipole moment having its own field acting on the surroundings. This is of major importance, as **long-range interactions** between

different parts of the dielectric cannot be neglected and need be considered even at macroscopic distances. As Fröhlich explains [16], this can be seen explicitly in the fact that dielectric thermodynamic properties (in a somewhat extended sense) depend on the shape of the dielectric [17]. The development of a rigorous microscopic model, solvable from the point of view of Statistical Physics, is then a hardly viable task.

This fact led to the development of **local field models**. According to the local field hypothesis, we take a portion of an infinitely large dielectric in a cavity of a given volume V, assuming that:

- The existence of long-range interactions can be ignored if in the thermodynamic relations the external field is replaced by an effective external field $\vec{E}_G$ (the **local field**, also called cavity field).
- The outside of the cavity is treated as a dielectric continuum with the same dielectric properties as the complete system. The field $\vec{E}_G$ is the result of the superposition of: (i) the external field, and (ii) the field produced by this dielectric continuum in the cavity, assuming that the cavity is empty[6].

Typically, a **spherical cavity** is considered for these models. It has the great advantage of having a scalar polarizability (i.e., the polarizability tensor[7] of the cavity is proportional to the identity tensor), and thus the local field is parallel to the polarization. Standard electrostatic calculations [16, 18] lead to:

$$\vec{E}_G = g\vec{E} \quad , \quad g = \frac{3\varepsilon_\mathrm{r}}{2\varepsilon_\mathrm{r}+1} \tag{4.43}$$

4.3.3. Fröhlich's fluctuation theory of dielectrics at zero field

Let $\vec{M}$ denote the macroscopic dipole moment of the cavity, and M_E its component in the direction of the field. Starting from the local field hypothesis applied to a spherical cavity, Fröhlich [16] evaluates the **mean value of M^2 at zero field**. We propose here a direct form to obtain it, more consistent with the usual formalism of Statistical Mechanics. Taking into account the isotropy of the dielectric (at zero field), and that $\left\langle M_E \right\rangle_0 = 0$ (the brackets $\langle\ \rangle_0$ denote averaging at zero field), general fluctuation equations[8] lead to:

$$\left\langle M^2 \right\rangle_0 = 3\left\langle M_E^2 \right\rangle_0 = 3k_\mathrm{B}T\left[\left(\frac{\partial M_E}{\partial E_G}\right)_T\right]_0 = k_\mathrm{B}T\varepsilon_0 V\,\frac{(\varepsilon_\mathrm{r}-1)(2\varepsilon_\mathrm{r}+1)}{\varepsilon_\mathrm{r}} \tag{4.44}$$

Equation (4.44) is called the **Fröhlich equation** (k_B denotes Boltzmann's constant). It is exact in the framework of the hypothesis given above. To further develop it, he generalizes the procedure employed by Kirkwood for systems composed of rigid dipoles [19]. Let us assume that

[6] The emptiness of the cavity for the evaluation of this field is essential for the next steps to be correct. We give below more details about this (see section 4.3.4).

[7] The polarizability tensor relates the total macroscopic dipole moment of a dielectric with the applied external field. The external field is *not* the same as the true field ($\vec{E}$), the latter resulting from the superposition of this external field and the field due to the polarization of the dielectric.

[8] For these fluctuation equations to hold, the energy appearing in the thermodynamic relations needs to be the internal energy. Therefore, it is essential to this treatment that the thermodynamic force conjugated to the macroscopic dipole moment be the external field, and *not* the true field.

the cavity is composed of N "units" (molecules, or other groups of atoms) such that each unit makes the same average contribution to the polarization in an external field. After some calculations, the following formula is obtained:

$$\left\langle M^2 \right\rangle_0 = N \left\langle \vec{m} \cdot \vec{m}^* \right\rangle_0^1 \tag{4.45}$$

In equation (4.45), $\vec{m}$ denotes the dipole moment of a unit, $\vec{m}^*$ is the dipole moment of the whole cavity when it is polarized by one of its units kept at a constant configuration with dipole moment of value $\vec{m}$, and $\langle\ \rangle_0^1$ denotes averaging over the configurations of a single unit at zero field. The meaning of $\vec{m}^*$ is subtle. It can be shown [16] that: (i) $\vec{m}^*$ is affected by short-range interactions and it is independent of the position of the unit with dipole moment $\vec{m}$ inside the sphere, provided its distance from the surface is large enough to allow its interaction with the outside to be treated on a macroscopic basis (the number of units for which this is not valid can be made very small compared with N as long as the cavity is sufficiently large); (ii) the result is the same either if $\vec{m}$ is treated as a point dipole or as a uniformly polarized sphere. From these considerations, it follows that a region makes a contribution to $\vec{m}^*$ only if the average dipole moment induced in it by $\vec{m}$ cannot be obtained by treating $\vec{m}$ as a point dipole or a uniformly polarized sphere. Therefore, **the deviations of $\vec{m}^*$ from $\vec{m}$ are due, essentially, to short-range forces and the deviation of the shape of the molecules from a sphere.**

For mixtures containing different kinds of units, the treatment is the same as above taking into account the additivity of the dipole moments of the units. If the mixture contains N_i units of kind i, equation (4.45) must be replaced by:

$$\left\langle M^2 \right\rangle_0 = \sum_i N_i \left\langle \vec{m}_i \cdot \vec{m}_i^* \right\rangle_0^1 \tag{4.46}$$

where, obviously, $\vec{m}_i$ denotes the dipole moment of a unit of type i, and $\vec{m}_i^*$ is the dipole moment of the whole cavity when it is polarized by one of the i-type units kept at a constant configuration with dipole moment of value $\vec{m}_i$.

4.3.4. Macroscopic separation of induced and orientational contributions

In order to further simplify the task of obtaining a formula for the relative permittivity, it is possible to perform a macroscopic approximation to separate the induced and orientational contributions to the polarization. To do it, the induced contribution is treated macroscopically assuming a relation with the **high-frequency relative permittivity,** ε_r^∞, which is the relative permittivity at a frequency at which only the induced polarizability contributes. For nonpolar fluids $\varepsilon_r^\infty = \varepsilon_r$, while for polar fluids it is frequently estimated from the refractive index at optical wavelengths, n, using the formula $\varepsilon_r^\infty = 1.1n^2$ [20]. There are two methods to do this macroscopic separation. One of them is described in Fröhlich's book [16] and also by Chelkowski [18], and it is widely used in the literature on dielectrics[9]. A second and more consistent treatment, also due to Fröhlich [21], is the one to be described here (but presented in a different way from the original reference), and from it we will derive all the possible variations of the model.

[9] In fact, it was used to discuss some results obtained in this Thesis regarding amide + amine mixtures.

It must be noted, however, that the first approach (not described here) leads to the same results in the context of pure fluids and one-fluid or *c*-fluid models (see sections 4.3.5 and 4.3.6.1) for mixtures of polar compounds. However, if we try to derive a model like the one described in section 4.3.6.2 (which is obtained there using the second approach), it does not reduce to the equations from Onsager's model [16, 18] (and it should) when spherical molecules and negligible short-range interactions are assumed (see below).

In this second method, the induced polarizability (α^{ind}) of the sphere is defined from the same relation as the total polarizability of the sphere [16] (α):

$$\alpha = 3\varepsilon_0 V \frac{\varepsilon_r - 1}{\varepsilon_r + 2} \tag{4.47}$$

(which is called **macroscopic Clausius-Mossoti relation**[10]) but replacing ε_r by ε_r^∞:

$$\alpha^{\text{ind}} = 3\varepsilon_0 V \frac{\varepsilon_r^\infty - 1}{\varepsilon_r^\infty + 2} \tag{4.48}$$

Then, the orientational polarizability (α^{or}) is assumed additive with α_{ind} and defined by $\alpha^{\text{or}} = \alpha - \alpha^{\text{ind}}$. To understand the subsequent definition of the orientational ($\vec{M}^{\text{or}}$) and induced ($\vec{M}^{\text{ind}}$) contributions to $\vec{M}$, we must first make some clarifications regarding the correct use of the polarizability for the case of our cavity, which is immersed in the dielectric continuum. If the cavity were in vacuum, it would possess a dipole moment $\vec{M}_{\text{vac}} = \alpha\vec{E}_e$, where $\vec{E}_e$ is the external field. However, if the cavity is inside the dielectric, its dipole moment is not[11] $\alpha\vec{E}_G$, but $\vec{M} = \alpha\left(\vec{E}_G + \vec{E}_R\right)$. The **reaction field**, $\vec{E}_R$, added is the field in the cavity due to the fact that the presence of the dipole moment of the dielectric *inside* the sphere modifies the polarization of the surrounding medium. It can be calculated from electrostatics [16, 18], giving:

$$\vec{E}_R = f\vec{M}, \quad , \quad f = \frac{2(\varepsilon_r - 1)}{2\varepsilon_r + 1}\frac{1}{3\varepsilon_0 V} \tag{4.49}$$

Now we can proceed to the definition of $\vec{M}^{\text{or}}$ as the sum of two contributions: (i) the orientational contribution due to the total field inside the sphere, $\alpha^{\text{or}}\left(\vec{E}_G + \vec{E}_R\right)$; (ii) the induced contribution due to the reaction field $f\vec{M}^{\text{or}}$ of this orientational contribution, $\alpha^{\text{ind}} f\vec{M}^{\text{or}}$. We see that in this way $\vec{M}^{\text{or}}$ includes *all* the effects derived from the orientational contribution to the polarization. This definition of the orientational contribution differs from that given in the first of the mentioned two methods. Now, since by definition $\vec{M} = \vec{M}^{\text{ind}} + \vec{M}^{\text{or}}$, we have:

$$\vec{M}^{\text{ind}} = \alpha^{\text{ind}}\left(\vec{E}_G + f\vec{M}\right) - \alpha^{\text{ind}} f\vec{M}^{\text{or}} = \alpha^{\text{ind}}\left(\vec{E}_G + f\vec{M}^{\text{ind}}\right) \tag{4.50}$$

$$\vec{M}^{\text{or}} = \alpha^{\text{or}}\left(\vec{E}_G + f\vec{M}\right) + \alpha^{\text{ind}} f\vec{M}^{\text{or}} \tag{4.51}$$

[10] An analogous relation (the "microscopic" Clausius-Mossoti relation) is obtained in a simple model due to Lorentz for the polarizability of spherical nonpolar molecules with no short-range forces. In contrast, equation (4.47) is macroscopic and exact.

[11] Here, the local field $\vec{E}_G$ plays the role of the "external" field, not caused by the portion of dielectric inside the cavity, because it is calculated assuming that the cavity is empty.

Or, solving the equations:

$$\vec{M}^{\text{ind}} = \frac{\alpha^{\text{ind}}}{1-\alpha^{\text{ind}} f}\vec{E}_G = \varepsilon_0 V \frac{\left(\varepsilon_{\text{r}}^{\infty}-1\right)\left(2\varepsilon_{\text{r}}+1\right)}{2\varepsilon_{\text{r}}+\varepsilon_{\text{r}}^{\infty}}\vec{E}_G \tag{4.52}$$

$$\vec{M}^{\text{or}} = \frac{\alpha^{\text{or}}}{\left(1-\alpha f\right)\left(1-\alpha^{\text{ind}} f\right)}\vec{E}_G = \varepsilon_0 V \frac{\left(\varepsilon_{\text{r}}-\varepsilon_{\text{r}}^{\infty}\right)\left(2\varepsilon_{\text{r}}+1\right)^2}{3\varepsilon_{\text{r}}\left(2\varepsilon_{\text{r}}+\varepsilon_{\text{r}}^{\infty}\right)}\vec{E}_G \tag{4.53}$$

Finally, following an analogous procedure to the one used to calculate $\left\langle M^2\right\rangle_0$, we obtain straightforwardly the orientational ($\left\langle M^2\right\rangle_0^{\text{or}}$) and induced ($\left\langle M^2\right\rangle_0^{\text{ind}}$) contributions:

$$\left\langle M^2\right\rangle_0^{\text{ind}} = 3k_{\text{B}}T\varepsilon_0 V \frac{\left(\varepsilon_{\text{r}}^{\infty}-1\right)\left(2\varepsilon_{\text{r}}+1\right)}{2\varepsilon_{\text{r}}+\varepsilon_{\text{r}}^{\infty}} \tag{4.54}$$

$$\left\langle M^2\right\rangle_0^{\text{or}} = k_{\text{B}}T\varepsilon_0 V \frac{\left(\varepsilon_{\text{r}}-\varepsilon_{\text{r}}^{\infty}\right)\left(2\varepsilon_{\text{r}}+1\right)^2}{\varepsilon_{\text{r}}\left(2\varepsilon_{\text{r}}+\varepsilon_{\text{r}}^{\infty}\right)} \tag{4.55}$$

These equations were obtained by Fröhlich [21] using another formalism. Perhaps this development can help to clarify the concepts behind his work.

4.3.5. The Kirkwood-Fröhlich equation for pure polar fluids

If the fluid is made of polar molecules, we can develop $\left\langle M^2\right\rangle_0^{\text{or}}$ assuming that there is only one type of unit and:

$$\left\langle M^2\right\rangle_0^{\text{or}} = N\left\langle \vec{\mu}_{\text{int}} \cdot \vec{\mu}_{\text{int}}^{*}\right\rangle_0^1 \tag{4.56}$$

Equation (4.56) is analogous to (4.45), but instead of $\vec{m}$ and $\vec{m}^*$ we use their orientational contributions $\vec{\mu}_{\text{int}}$ and $\vec{\mu}_{\text{int}}^{*}$. In order to be consistent with the above definition of $\vec{M}^{\text{or}}$, $\vec{\mu}_{\text{int}}$ must include not only the value of the permanent dipole moment of the unit inside the dielectric, but also an induced contribution due to the reaction field from the surroundings of the unit caused by its presence in the cavity. The quantity $\vec{\mu}_{\text{int}}$ is normally called **internal dipole moment** of the unit immerse in its own medium. If the short-range interactions reach z neighbors from $\vec{\mu}_{\text{int}}$, then;

$$\vec{\mu}_{\text{int}}^{*} = \vec{\mu}_{\text{int}} + \sum_{k=1}^{z}\vec{\mu}_{\text{int},k} \tag{4.57}$$

where $\vec{\mu}_{\text{int},k}$ is the internal dipole moment of the kth neighbor. Substituting in (4.56) and taking into account the isotropy of the dielectric, one reaches the result:

$$\left\langle M^2\right\rangle_0^{\text{or}} = Ng_{\text{K}}\mu_{\text{int}}^2 \tag{4.58}$$

where

$$g_K = 1 + z\langle \cos\theta \rangle_0^1 \tag{4.59}$$

is the so-called **Kirkwood correlation factor**. θ is the relative angle between the dipole $\vec{\mu}_{int}$ and its neighbors. Consequently, the value of g_K allows to distinguish among three kinds of behavior:

- If $g_K = 1$, then short-range interactions and the non-spherical shape of the units have no effect on the average relative orientation of neighboring permanent dipoles.
- If $g_K > 1$, there is a trend to parallel orientation of neighboring dipoles.
- If $g_K < 1$, the trend is to antiparallel orientation.

Since in practical situations $\vec{\mu}_{int}$ is not known, it should be calculated in relation to the permanent dipole moment in vacuum, $\vec{\mu}$. To do this, we should subtract the influence of all the surroundings, inside and outside the cavity, which is not an easy task. To make an estimation, it is assumed that the reaction is mostly due to the outside of the cavity. Therefore, $\vec{\mu}$ will be estimated by simply subtracting from $\vec{\mu}_{int}$ the induced contribution due to the reaction field from the outside of the cavity caused by its presence in the cavity. In other words, we approximate $\vec{\mu}_{int} = \vec{\mu} + \alpha^{ind} f \vec{\mu}_{int}$. This gives:

$$\vec{\mu}_{int} = \frac{\varepsilon_r^\infty + 2}{3} \frac{2\varepsilon_r + 1}{2\varepsilon_r + \varepsilon_r^\infty} \vec{\mu} \tag{4.60}$$

After combining equations (4.55), (4.58) and (4.60), we finally obtain:

$$g_K = \frac{9 k_B T \varepsilon_0 V_m}{N_A \mu^2} \frac{\left(\varepsilon_r - \varepsilon_r^\infty\right)\left(2\varepsilon_r + \varepsilon_r^\infty\right)}{\varepsilon_r \left(\varepsilon_r^\infty + 2\right)^2} \tag{4.61}$$

(N_A is Avogadro's constant). Equation (4.61) is called the **Kirkwood-Fröhlich equation**. Using experimental data, it is straightforward to evaluate g_K of pure fluids. Neglecting short-range interactions and assuming the molecules spherical, g_K must be equal to 1 and one obtains the **Onsager equation**.

4.3.6. The adaptation of Kirkwood-Fröhlich model to mixtures

4.3.6.1 Models with global separation of the orientational contribution

The first family of models generalizing equation (4.61) to mixtures separate the induced and orientational contributions to the polarization of the mixture globally (i.e., all the components "together"). In other words, they start from equation (4.55), with different variations. Therefore, they will only make sense if there is **at least one polar component**, as otherwise there would be no orientational contribution.

The first and most direct possibility is to interpret the quantities of the right-hand side of equation (4.55) as referring to the mixture. It is the natural and least artificial extension of equation (4.55) to mixtures. An analogous development to the one performed to get to equation (4.61) leads to:

$$\sum_i x_i \left\{ g_{\mathrm{K},ii}\mu_i^2 + \sum_{j\neq i}\left(g_{\mathrm{K},ij}-1\right)\mu_i\mu_j \right\} = \frac{9k_{\mathrm{B}}T\varepsilon_0 V_{\mathrm{m}}}{N_{\mathrm{A}}} \frac{\left(\varepsilon_{\mathrm{r}}-\varepsilon_{\mathrm{r}}^{\infty}\right)\left(2\varepsilon_{\mathrm{r}}+\varepsilon_{\mathrm{r}}^{\infty}\right)}{\varepsilon_{\mathrm{r}}\left(\varepsilon_{\mathrm{r}}^{\infty}+2\right)^2} \tag{4.62}$$

where μ_i is the dipole moment of species i under vacuum, and $g_{\mathrm{K},ij} = 1 + z_j \left\langle \cos\theta_{ij} \right\rangle_0^1$ is the Kirkwood correlation factor for an i-type central molecule interacting with z_j j-type neighbors and whose dipole moments are oriented relatively to the central molecule with an angle θ_{ij}. The application of equation (4.62) is not easy, as it contains a whole set of unknown composition-dependent parameters $g_{\mathrm{K},ij}$. However, particularly for an **ideal mixture of ideal gases** (point-like and non-interacting molecules), all the $g_{\mathrm{K},ij}$ must be equal to 1 and the system behaves as if it were a pure ideal gas with a dipole moment μ given by:

$$\mu^2 = \sum_i x_i \mu_i^2 \tag{4.63}$$

For a mixture including only one polar compound (1), the left-hand side of equation (4.62) reduces to $x_1 g_{\mathrm{K},11}\mu_1^2$ and it is possible to obtain $g_{\mathrm{K},11}$ from experimental data. It can also be used to determine experimentally μ_1 by measuring volumetric, dielectric and refractive properties of the mixture at high dilution ($x_1 \approx 0$), where $g_{\mathrm{K},1} \approx 1$ can be assumed[12].

The second possibility, called **one-fluid approach** [22], assumes that the mixture is composed of a hypothetic fluid behaving as a Kirkwood-Fröhlich pure compound, whose units are located in spherical cavities of molar volume V_{m} (= molar volume of the mixture) and embedded in a continuum with the properties of the mixture at the same composition. The equation defining this model is, therefore, the same as that for the pure fluids but with an "effective" dipole moment dependent on the composition. The dipole moment under vacuum of these units, μ, is taken as that of a Kirkwood-Fröhlich ideal mixture of ideal gases, and then it is obtained from equation (4.63). The justification of this choice is quite convincing from equations (4.62) and (4.63). Reis and Iglesias argue other reasons [22], but they might add more confusion to the subject. This model has been used in this Thesis to gain insight into the experimental results of mixtures of two polar liquids. The g_{K} obtained in this way can be interpreted as an averaged measure of the dipole relative orientation.

A third possibility, proposed by Reis and Iglesias [22], is the so-called ***c*-fluid approach** (where c is the number of *polar* components of the mixture), in which c hypothetical fluids are assumed to behave as Kirkwood-Fröhlich pure compounds. The hypothetical fluid i is defined as made by molecules of component i located in spherical cavities of molar volume $\bar{V}_{\mathrm{m},i}$ (= partial molar volume of component i) and embedded in a continuum with the properties of the mixture at the same composition[13]. The Kirkwood correlation factor of fluid i ($g_{\mathrm{K},i}$) is, therefore:

[12] We must remark here that $\vec{\mu}_{\mathrm{int}}$ must be affected by the environment of the unit inside the cavity, and that equation (4.60) does not include this contribution. Therefore, it should not be surprising to obtain slightly different results for μ_1 depending on the nonpolar solvent used.

[13] Formally, this means that in the definition of α_{ind} (equation (4.48)) we must replace $\varepsilon_{\mathrm{r}}^{\infty}$ by the high-frequency relative permittivity of pure component i, $\varepsilon_{\mathrm{r},i}^{\infty}$.

$$g_{\mathrm{K},i} = \frac{9k_{\mathrm{B}}T\varepsilon_0\bar{V}_{\mathrm{m},i}}{N_{\mathrm{A}}\mu_i^2}\frac{\left(\varepsilon_{\mathrm{r}}-\varepsilon_{\mathrm{r},i}^{\infty}\right)\left(2\varepsilon_{\mathrm{r}}+\varepsilon_{\mathrm{r},i}^{\infty}\right)}{\varepsilon_{\mathrm{r}}\left(\varepsilon_{\mathrm{r},i}^{\infty}+2\right)^2} \tag{4.64}$$

4.3.6.2 Models treating additively orientational and induced contributions

Instead of taking the separation of the global orientational contribution as the starting point, another of the possible generalizations of the Kirkwood-Fröhlich equation for mixtures is to assume that the value of $\left\langle M^2\right\rangle_0$ given by equation (4.44) can be obtained additively from the induced and orientational contributions of hypothetical fluids in the mixture, in a number equal to the number of components. The hypothetical fluid i is defined in the same way as in the c-fluid model described just above. This kind of model has been particularly popular for the description of binary mixtures of a polar compound (1) and a nonpolar compound (2), for which the final result is:

$$\frac{V_{\mathrm{m}}\left(\varepsilon_{\mathrm{r}}-1\right)}{\varepsilon_{\mathrm{r}}} - x_1\frac{3\bar{V}_{\mathrm{m},1}\left(\varepsilon_{\mathrm{r},1}^{\infty}-1\right)}{2\varepsilon_{\mathrm{r}}+\varepsilon_{\mathrm{r},1}^{\infty}} - x_2\frac{3\bar{V}_{\mathrm{m},2}\left(\varepsilon_{\mathrm{r},2}-1\right)}{2\varepsilon_{\mathrm{r}}+\varepsilon_{\mathrm{r},2}} = \frac{N_{\mathrm{A}}x_1\mu_1^2 g_{\mathrm{K},1}}{9k_{\mathrm{B}}T\varepsilon_0}\frac{\left(2\varepsilon_{\mathrm{r}}+1\right)\left(\varepsilon_{\mathrm{r},1}+2\right)^2}{\left(2\varepsilon_{\mathrm{r}}+\varepsilon_{\mathrm{r},1}^{\infty}\right)^2} \tag{4.65}$$

Equation (4.65) reduces to Onsager's equation for such mixtures [16] in the limit of spherical molecules and absence of short-range interactions (see above). It has been used to determine experimentally μ_1 from high dilution measurements ($x_1 \approx 0$, $g_{\mathrm{K},1} \approx 1$) [23], proceeding as already described in section 4.3.6.1. It is also the formula normally taken to define the Kirkwood correlation factor in such (polar + nonpolar) mixtures[14].

4.3.7. Molar refraction and dispersive interactions

In section 4.3.4 we defined an induced polarizability α^{ind} for the macroscopic sphere. Analogously, we can define its **electronic polarizability**, α^{e}, by:

$$\alpha^{\mathrm{e}} = 3\varepsilon_0 V\frac{n^2-1}{n^2+2} \tag{4.66}$$

Here, the squared refractive index at optical frequencies, n^2, plays the role of the permittivity at such frequencies (for non-magnetic substances). A widely used related quantity is the so-called **molar refraction** (or **molar refractivity**), R_{m}, defined by:

$$R_{\mathrm{m}} = \frac{n^2-1}{n^2+2}V_{\mathrm{m}} = \frac{N_{\mathrm{A}}\alpha_1^{\mathrm{e}}}{3\varepsilon_0} \tag{4.67}$$

Since $\alpha_1^{\mathrm{e}} = \alpha^{\mathrm{e}}/N$ is the molecule-averaged electronic contribution to the polarizability of the macroscopic sphere, R_{m} can be interpreted as a **measure of the dispersion forces** present in the fluid.

[14] We note here that a procedure based on equation (4.62) might be more appropriate, as fewer approximations are involved in its derivation. In order to apply (4.62), a reasonable estimation of $\varepsilon_{\mathrm{r}}^{\infty}$ of such polar + nonpolar mixtures needs to be proposed.

4.4. Appendix: derivation of Prigogine-Flory-Patterson equations

A detailed derivation of the equations resulting from Patterson's approximations of the Flory (or Prigogine-Flory) model is lacking in the literature. Moreover, it is typical to find errors in the equations in many publications. The aim of this appendix is to provide the necessary details in order to help the reader to understand the model itself and the interpretation of its results, and justify properly which of these equations are correct.

4.4.1. Reduced and mixing functions

Recalling definitions given in section 4.1.6, we can write E_{m}^{*} for binary mixtures ($i = 1,2$) as:

$$E_{\mathrm{m}}^{*} = \sum_i x_i E_{\mathrm{m}i}^{*} - x_1 E_{\mathrm{m}1}^{*} \theta_2 \frac{X_{12}}{p_1^{*}} = (1 - X) \sum_i x_i E_{\mathrm{m}i}^{*} \tag{4.68}$$

The A_{m} of mixing, ΔA_{m}, can then be written as $\Delta A_{\mathrm{m}} = E_{\mathrm{m}}^{*} \overline{A} - \sum_i x_i E_{\mathrm{m}i}^{*} \overline{A}_i$ or, rearranging:

$$\frac{\Delta A_{\mathrm{m}}}{\sum_i x_i E_{\mathrm{m}i}^{*}} = (1 - X) \overline{A} - \sum_i \psi_i \overline{A}_i \tag{4.69}$$

The equation for the mixing volume $\Delta V_{\mathrm{m}} = V_{\mathrm{m}}^{\mathrm{E}}$ has already been given in section 4.1.6:

$$\frac{\Delta V_{\mathrm{m}}}{\sum_i x_i V_{\mathrm{m}i}^{*}} = \overline{V} - \sum_i \varphi_i \overline{V}_i \tag{4.70}$$

4.4.2. Series expansion of the mixing functions

Let us consider from now on the reduced quantity $\overline{A}$ as a function of $\overline{T}$, $\overline{A}(\overline{T})$, keeping constant the other variables, and define a characteristic reduced temperature for $\overline{A}$, $\overline{T}_A$, such that

$$\overline{A}(\overline{T}_A) = \sum_i \psi_i \overline{A}_i \tag{4.71}$$

Patterson then performs a series expansion of $\overline{A}$ around $\overline{T}_A$ up to first-order terms:

$$\overline{A} \approx \overline{A}(\overline{T}_A) + \overline{A}'(\overline{T}_A)(\overline{T} - \overline{T}_A) \tag{4.72}$$

where the prime denotes derivative. From equations (4.8), (4.14), (4.16) and (4.68), $\overline{T}$ can be written

$$\overline{T} = \frac{\sum_i \varphi_i p_i^{*} \overline{T}_i}{p^{*}} = \frac{\sum_i x_i E_{\mathrm{m}i}^{*} \overline{T}_i}{E_{\mathrm{m}}^{*}} = \frac{\sum_i \psi_i \overline{T}_i}{1 - X} \tag{4.73}$$

Substituting equations (4.72) and (4.73) into equation (4.69), one obtains $\Delta A_{\mathrm{m}} = \Delta A_{\mathrm{m,int}} + \Delta A_{\mathrm{m,fv}}$, where the interactional term, $\Delta A_{\mathrm{m,int}}$, and the free volume term, $\Delta A_{\mathrm{m,fv}}$, are given respectively by

$$\frac{\Delta A_{\mathrm{m,int}}}{\sum_i x_i E^*_{\mathrm{m}i}} = \left[-\bar{A}\left(\bar{T}_A\right) + \bar{T}_A \bar{A}'\left(\bar{T}_A\right)\right] X \tag{4.74}$$

$$\frac{\Delta A_{\mathrm{m,fv}}}{\sum_i x_i E^*_{\mathrm{m}i}} = \bar{A}'\left(\bar{T}_A\right)\left(\sum_i \psi_i \bar{T}_i - \bar{T}_A\right) \tag{4.75}$$

Analogously, consider the reduced volume as a function $\bar{V}\left(\bar{T}\right)$ and define a characteristic reduced temperature for $\bar{V}$, $\bar{T}_V$, such that

$$\bar{V}\left(\bar{T}_V\right) = \sum_i \varphi_i \bar{V}_i \tag{4.76}$$

Now, an expansion of $\bar{V}$ around $\bar{T}_V$ up to first-order terms must be performed:

$$\bar{V} \approx \bar{V}\left(\bar{T}_V\right) + \bar{V}'\left(\bar{T}_V\right)\left(\bar{T} - \bar{T}_V\right) \tag{4.77}$$

Patterson also neglects terms of order higher than one in X, so that $1/(1-X) \approx 1 + X$ and

$$\bar{T} \approx (1 + X)\sum_i \psi_i \bar{T}_i \tag{4.78}$$

Substituting equations (4.77) and (4.78) into (4.70) gives $\Delta V_{\mathrm{m}} = \Delta V_{\mathrm{m,int}} + \Delta V_{\mathrm{m,fv}}$, where

$$\frac{\Delta V_{\mathrm{m,int}}}{\sum_i x_i V^*_{\mathrm{m}i}} = \left(\sum_i \psi_i \bar{T}_i\right) \bar{V}'\left(\bar{T}_V\right) X \tag{4.79}$$

$$\frac{\Delta V_{\mathrm{m,fv}}}{\sum_i x_i V^*_{\mathrm{m}i}} = \bar{V}'\left(\bar{T}_V\right)\left(\sum_i \psi_i \bar{T}_i - \bar{T}_V\right) \tag{4.80}$$

Finally, note that in the Flory model it is much easier to work with the inverse functions $\bar{T}\left(\bar{A}\right)$ and $\bar{T}\left(\bar{V}\right)$, rather than $\bar{A}\left(\bar{T}\right)$ and $\bar{V}\left(\bar{T}\right)$. For that reason, it is convenient to replace the original equations (4.74), (4.75), (4.79) and (4.80), given by Patterson, by the following ones. For ΔA_{m}:

$$\frac{\Delta A_{\mathrm{m,int}}}{\sum_i x_i E^*_{\mathrm{m}i}} = \left[-\bar{A}\left(\bar{T}_A\right) + \frac{\bar{T}_A}{\bar{T}'\left[\bar{A}\left(\bar{T}_A\right)\right]}\right] X \tag{4.81}$$

$$\frac{\Delta A_{\mathrm{m,fv}}}{\sum_i x_i E^*_{\mathrm{m}i}} = \frac{\sum_i \psi_i \bar{T}_i - \bar{T}_A}{\bar{T}'\left[\bar{A}\left(\bar{T}_A\right)\right]} \tag{4.82}$$

And for ΔV_{m}:

$$\frac{\Delta V_{\mathrm{m,int}}}{\sum_i x_i V^*_{\mathrm{m}i}} = \frac{\sum_i \psi_i \bar{T}_i}{\bar{T}'\left[\bar{V}\left(\bar{T}_V\right)\right]} X \tag{4.83}$$

$$\frac{\Delta V_{\mathrm{m,fv}}}{\sum_i x_i V^*_{\mathrm{m}i}} = \frac{\sum_i \psi_i \bar{T}_i - \bar{T}_V}{\bar{T}'\left[\bar{V}\left(\bar{T}_V\right)\right]} \tag{4.84}$$

4.4.3. Series expansion of the free volume terms

The nature of the free-volume terms may be seen through an expansion of $\bar{T}_i$ around $\bar{A}\left(\bar{T}_A\right)$ or $\bar{V}\left(\bar{T}_V\right)$ up to second-order terms.

In the case of $\bar{A}$, the expansion has the form:

$$\bar{T}_i \approx \bar{T}_A + \bar{T}'\left[\bar{A}\left(\bar{T}_A\right)\right]\left[\bar{A}_i - \bar{A}\left(\bar{T}_A\right)\right] + \frac{1}{2}\bar{T}''\left[\bar{A}\left(\bar{T}_A\right)\right]\left[\bar{A}_i - \bar{A}\left(\bar{T}_A\right)\right]^2 \tag{4.85}$$

If k denotes an index different from i, using equation (4.71):

$$\bar{A}_i - \bar{A}\left(\bar{T}_A\right) = \psi_k\left(\bar{A}_i - \bar{A}_k\right) \tag{4.86}$$

So that:

$$\begin{aligned}\sum_i \psi_i \bar{T}_i = &\left(\sum_i \psi_i\right)\bar{T}_A + \bar{T}'\left[\bar{A}\left(\bar{T}_A\right)\right]\sum_i \psi_i\psi_k\left(\bar{A}_i - \bar{A}_k\right) \\ &+ \frac{1}{2}\bar{T}''\left[\bar{A}\left(\bar{T}_A\right)\right]\sum_i \psi_i{\psi_k}^2\left(\bar{A}_i - \bar{A}_k\right)^2\end{aligned} \tag{4.87}$$

But the sums are

$$\sum_i \psi_i\psi_k\left(\bar{A}_i - \bar{A}_k\right) = \left(\bar{A}_1 - \bar{A}_2\right)\left(\psi_1\psi_2 - \psi_2\psi_1\right) = 0 \tag{4.88}$$

$$\sum_i \psi_i{\psi_k}^2\left(\bar{A}_i - \bar{A}_k\right)^2 = \left(\bar{A}_1 - \bar{A}_2\right)^2\left(\psi_1{\psi_2}^2 + \psi_2{\psi_1}^2\right) = \left(\bar{A}_1 - \bar{A}_2\right)^2\psi_1\psi_2 \tag{4.89}$$

and thus:

$$\sum_i \psi_i\bar{T}_i - \bar{T}_A = \frac{1}{2}\bar{T}''\left[\bar{A}\left(\bar{T}_A\right)\right]\left(\bar{A}_1 - \bar{A}_2\right)^2\psi_1\psi_2 \tag{4.90}$$

The corresponding free volume term becomes

$$\frac{\Delta A_{\mathrm{m,fv}}}{\sum_i x_i E^*_{\mathrm{m}i}} = \frac{1}{2}\frac{\bar{T}''\left[\bar{A}\left(\bar{T}_A\right)\right]}{\bar{T}'\left[\bar{A}\left(\bar{T}_A\right)\right]}\left(\bar{A}_1 - \bar{A}_2\right)^2\psi_1\psi_2 \tag{4.91}$$

More interesting are the results for the volume of mixing. In this case, the free volume term splits into two. The expansion of $\bar{T}_i$ is:

$$\bar{T}_i \approx \bar{T}_V + \bar{T}'\left[\bar{V}\left(\bar{T}_V\right)\right]\left[\bar{V}_i - \bar{V}\left(\bar{T}_V\right)\right] + \frac{1}{2}\bar{T}''\left[\bar{V}\left(\bar{T}_V\right)\right]\left[\bar{V}_i - \bar{V}\left(\bar{T}_V\right)\right]^2 \tag{4.92}$$

Using equation (4.76):

$$\bar{V}_i - \bar{V}\left(\bar{T}_V\right) = \varphi_k\left(\bar{V}_i - \bar{V}_k\right) \tag{4.93}$$

Therefore:

$$\begin{aligned}\sum_i \psi_i \bar{T}_i = &\left(\sum_i \psi_i\right)\bar{T}_V + \bar{T}'\left[\bar{V}\left(\bar{T}_V\right)\right]\sum_i \psi_i\varphi_k\left(\bar{V}_i - \bar{V}_k\right) \\ &+\frac{1}{2}\bar{T}''\left[\bar{V}\left(\bar{T}_V\right)\right]\sum_i \psi_i{\varphi_k}^2\left(\bar{V}_i - \bar{V}_k\right)^2\end{aligned} \tag{4.94}$$

In this case, the calculation of the sums is as follows:

$$\sum_i \psi_i\varphi_k\left(\bar{V}_i - \bar{V}_k\right) = \left(\bar{V}_1 - \bar{V}_2\right)\left(\psi_1\varphi_2 - \psi_2\varphi_1\right) = \left(\bar{V}_1 - \bar{V}_2\right)\left(\psi_1 - \varphi_1\right) \tag{4.95}$$

$$\begin{aligned}\sum_i \psi_i{\varphi_k}^2\left(\bar{V}_i - \bar{V}_k\right)^2 &= \left(\bar{V}_1 - \bar{V}_2\right)^2\left(\psi_1{\varphi_2}^2 + \psi_2{\varphi_1}^2\right) \\ &= \left(\bar{V}_1 - \bar{V}_2\right)^2\left[\psi_1\psi_2 + \left(\psi_1 - \varphi_1\right)^2\right]\end{aligned} \tag{4.96}$$

Which leads to:

$$\begin{aligned}\sum_i \psi_i\bar{T}_i - \bar{T}_V = &\bar{T}'\left[\bar{V}\left(\bar{T}_V\right)\right]\left(\bar{V}_1 - \bar{V}_2\right)\left(\psi_1 - \varphi_1\right) + \\ &+\frac{1}{2}\bar{T}''\left[\bar{V}\left(\bar{T}_V\right)\right]\left(\bar{V}_1 - \bar{V}_2\right)^2\left[\psi_1\psi_2 + \left(\psi_1 - \varphi_1\right)^2\right]\end{aligned} \tag{4.97}$$

Accordingly, the free volume term is $\Delta V_{\mathrm{m,fv}} = \Delta V_{\mathrm{m},p^*\mathrm{eff}} + \Delta V_{\mathrm{m,curv}}$, where the p^* effect term and the curvature term are given respectively by:

$$\frac{\Delta V_{\mathrm{m},p^*\mathrm{eff}}}{\sum_i x_i V^*_{\mathrm{m}i}} = \left(\bar{V}_1 - \bar{V}_2\right)\left(\psi_1 - \varphi_1\right) \tag{4.98}$$

$$\frac{\Delta V_{\mathrm{m,curv}}}{\sum_i x_i V^*_{\mathrm{m}i}} = \frac{1}{2}\frac{\bar{T}''\left[\bar{V}\left(\bar{T}_V\right)\right]}{\bar{T}'\left[\bar{V}\left(\bar{T}_V\right)\right]}\left(\bar{V}_1 - \bar{V}_2\right)^2\left[\psi_1\psi_2 + \left(\psi_1 - \varphi_1\right)^2\right] \tag{4.99}$$

Also, one can eliminate $\varphi_1 = \psi_1 p_2^* / (\psi_1 p_2^* + \psi_2 p_1^*)$ to obtain:

$$\psi_1 - \varphi_1 = \frac{\psi_1\psi_2(p_1^* - p_2^*)}{\psi_1 p_2^* + \psi_2 p_1^*} \tag{4.100}$$

$$\psi_1\psi_2 + \left(\psi_1 - \varphi_1\right)^2 = \frac{\psi_1\psi_2\left[\psi_1(p_2^*)^2 + \psi_2(p_1^*)^2\right]}{\left(\psi_1 p_2^* + \psi_2 p_1^*\right)^2} \tag{4.101}$$

The name "curvature term" is related to the presence of a second derivative. According to equation (4.100), the "p^* effect term" would be zero if $p_1^* = p_2^*$.

4.4.4. Derivatives of the reduced temperature

The only task left for the application of the above formulas for the mixing functions is the calculation of the derivatives involved. Here, it will be done for the case of $\Delta H_{\mathrm{m}} = H_{\mathrm{m}}^{\mathrm{E}}$ and $\Delta V_{\mathrm{m}} = V_{\mathrm{m}}^{\mathrm{E}}$.

As already mentioned, at low pressure $H_{\mathrm{m}}^{\mathrm{E}} = E_{\mathrm{m}}^{\mathrm{E}} + pV_{\mathrm{m}}^{\mathrm{E}} \approx E_{\mathrm{m}}^{\mathrm{E}} = \Delta E_{\mathrm{m}}$ ($\bar{p} \approx 0$ approximation). Therefore, the reduced quantity with energy dimensions that must be considered is the reduced intermolecular energy $\bar{E}$:

$$\bar{E} = \frac{E_{\mathrm{m}}}{E_{\mathrm{m}}^{*}} = -\frac{1}{\bar{V}} \tag{4.102}$$

The substitution of equation (4.102) into the thermal equation of state gives the function $\bar{T}\left(\bar{E}\right)$, and the function $\bar{T}\left(\bar{V}\right)$ is the thermal equation of state itself.

$$\bar{T}\left(\bar{E}\right) = -\bar{E}\left(\bar{E}^{1/3} + 1\right) - \bar{p}\bar{E}^{-1}\left(\bar{E}^{1/3} + 1\right) \tag{4.103}$$

$$\bar{T}\left(\bar{V}\right) = \bar{V}^{-1}\left(1 - \bar{V}^{-1/3}\right) + \bar{p}\,\bar{V}\left(1 - \bar{V}^{-1/3}\right) \tag{4.104}$$

(the terms including $\bar{p}$ have been separated from the others). These equations can be used to obtain $\bar{T}_E$ and $\bar{T}_V$.The first derivatives of these functions are then:

$$\bar{T}'\left(\bar{E}\right) = -\frac{4}{3}\bar{E}^{1/3} - 1 + \bar{p}\bar{E}^{-2}\left(\frac{2}{3}\bar{E}^{1/3} + 1\right) \tag{4.105}$$

$$\bar{T}'\left(\bar{V}\right) = \bar{V}^{-2}\left(\frac{4}{3}\bar{V}^{-1/3} - 1\right) + \bar{p}\left(1 - \frac{2}{3}\bar{V}^{-1/3}\right) \tag{4.106}$$

And, finally, the second derivatives:

$$\bar{T}''\left(\bar{E}\right) = -\frac{4}{9}\bar{E}^{-2/3} - 2\bar{p}\bar{E}^{-3}\left(\frac{5}{9}\bar{E}^{1/3} + 1\right) \tag{4.107}$$

$$\bar{T}''\left(\bar{V}\right) = 2\bar{V}^{-3}\left(1 - \frac{14}{9}\bar{V}^{-1/3}\right) + \bar{p}\,\bar{V}^{-1}\left(\frac{2}{9}\bar{V}^{-1/3}\right) \tag{4.108}$$

Taking the $\bar{p} \approx 0$ approximation and replacing $\bar{E}$ by $\bar{E}\left(T_E\right)$ and $\bar{V}$ by $\bar{V}\left(\bar{T}_V\right)$ in the above formulas, we get:

$$\bar{T}_E = \bar{T}\left[\bar{E}\left(T_E\right)\right] = -\bar{E}\left(T_E\right)\left[\bar{E}\left(T_E\right)^{1/3} + 1\right] \tag{4.109}$$

$$\bar{T}_V = \bar{T}\left[\bar{V}\left(\bar{T}_V\right)\right] = \bar{V}\left(\bar{T}_V\right)^{-1}\left[1 - \bar{V}\left(\bar{T}_V\right)^{-1/3}\right] \tag{4.110}$$

$$\bar{T}'\left[\bar{E}\left(T_E\right)\right] = -\frac{4}{3}\bar{E}\left(T_E\right)^{1/3} - 1 \tag{4.111}$$

$$\bar{T}'\left[\bar{V}\left(\bar{T}_V\right)\right] = \bar{V}\left(\bar{T}_V\right)^{-2}\left[\frac{4}{3}\bar{V}\left(\bar{T}_V\right)^{-1/3} - 1\right] \tag{4.112}$$

$$\bar{T}''\left[\bar{E}\left(T_E\right)\right] = -\frac{4}{9}\bar{E}\left(T_E\right)^{-2/3} \tag{4.113}$$

$$\bar{T}''\left[\bar{V}\left(\bar{T}_V\right)\right] = 2\bar{V}\left(\bar{T}_V\right)^{-3}\left[1 - \frac{14}{9}\bar{V}\left(\bar{T}_V\right)^{-1/3}\right] \tag{4.114}$$

Substituting these values in the equations obtained along sections 4.4.2 and 4.4.3, we obtain the desired results (equations (4.21)-(4.27)).

4.5. References

[1] P.J. Flory, R.A. Orwoll, A. Vrij, *Statistical Thermodynamics of Chain Molecule Liquids. I. An Equation of State for Normal Paraffin Hydrocarbons.* J. Am. Chem. Soc. **86** (1964) 3507-3514. https://doi.org/10.1021/ja01071a023

[2] P.J. Flory, R.A. Orwoll, A. Vrij, *Statistical Thermodynamics of Chain Molecule Liquids. II. Liquid Mixtures of Normal Paraffin Hydrocarbons.* J. Am. Chem. Soc. **86** (1964) 3515-3520. https://doi.org/10.1021/ja01071a024

[3] P.J. Flory, *Statistical Thermodynamics of Liquid Mixtures.* J. Am. Chem. Soc. **87** (1965) 1833-1838. https://doi.org/10.1021/ja01087a002

[4] A. Abe, P.J. Flory, *The Thermodynamic Properties of Mixtures of Small, Nonpolar Molecules.* J. Am. Chem. Soc. **87** (1965) 1838-1846. https://doi.org/10.1021/ja01087a003

[5] R.A. Orwoll, P.J. Flory, *Thermodynamic properties of binary mixtures of n-alkanes.* J. Am. Chem. Soc. **89** (1967) 6822-6829. https://doi.org/10.1021/ja01002a003

[6] L. Tonks, *The Complete Equation of State of One, Two and Three-Dimensional Gases of Hard Elastic Spheres.* Phys. Rev. **50** (1936) 955-963.

[7] I. Prigogine, *The Molecular Theory of Solutions.* North-Holland Publishing Company, Amsterdam, 1957.

[8] D. Patterson, G. Delmas, *Corresponding states theories and liquid models.* Discuss. Faraday Soc. **49** (1970) 98-105. https://doi.org/10.1039/DF9704900098

[9] A. Heintz, *A New Theoretical Approach for Predicting Excess Properties of Alkanol/Alkane Mixtures.* Ber. Bunsenges. Phys. Chem. **89** (1985) 172-181. https://doi.org/10.1002/bbpc.19850890217

[10] H. Funke, M. Wetzel, A. Heintz, *New applications of the ERAS model. Thermodynamics of amine + alkane and alcohol + amine mixtures.* Pure Appl. Chem. **61** (1989) 1429-1439. https://doi.org/10.1351/pac198961081429

[11] C.B. Kretschmer, R. Wiebe, *Thermodynamics of Alcohol - Hydrocarbon Mixtures.* J. Chem. Phys. **22** (1954) 1697-1701. https://doi.org/10.1063/1.1739878

[12] H. Renon, J.M. Prausnitz, *On the thermodynamics of alcohol-hydrocarbon solutions.* Chem. Eng. Sci. **22** (1967) 299-307. https://doi.org/10.1016/0009-2509(67)80116-7

[13] H.V. Kehiaian, Bull. Acad. Pol. Sci. **16** (1968) 165.

[14] H.V. Kehiaian, A. Treszczanowicz, Bull. Acad. Pol. Sci. **16** (1968) 171.

[15] A. Bondi, *Physical Properties of Molecular Crystals, Liquids and Glasses.* Wiley, New York, 1968.

[16] H. Fröhlich, *Theory of Dielectrics.* Clarendon Press, Oxford, 1958.

[17] L.D. Landau, E.M. Lifshitz, *Electrodinámica de los Medios Continuos.* Curso de Física Teórica. Vol. 8. Reverté, 1981.

[18] A. Chelkowski, *Dielectric Physics.* Elsevier, Amsterdam, 1980.

[19] J.G. Kirkwood, *The Dielectric Polarization of Polar Liquids.* **7** (1939) 911-919. https://doi.org/10.1063/1.1750343

[20] Y. Marcus, *The structuredness of solvents.* J. Solution Chem. **21** (1992) 1217-1230. https://doi.org/10.1007/bf00667218

[21] H. Fröhlich, *Remark on the calculation of the static dielectric constant.* Physica **22** (1956) 898-904. https://doi.org/10.1016/S0031-8914(56)90044-1

[22] J.C.R. Reis, T.P. Iglesias, *Kirkwood correlation factors in liquid mixtures from an extended Onsager-Kirkwood-Frohlich equation.* Phys. Chem. Chem. Phys. **13** (2011) 10670-10680. https://doi.org/10.1039/C1CP20142E

[23] M. El-Hefnawy, K. Sameshima, T. Matsushita, R. Tanaka, *Apparent Dipole Moments of 1-Alkanols in Cyclohexane and n-Heptane, and Excess Molar Volumes of (1-Alkanol + Cyclohexane or n-Heptane) at 298.15 K.* J. Solution Chem. **34** (2005) 43-69. https://doi.org/10.1007/s10953-005-2072-1

Part II

Copies of the published works

Thermodynamics of amide + amine mixtures. 1. Volumetric, speed of sound and refractive index data for *N,N*-dimethylformamide + *N*-propylpropan-1-amine, + *N*-butylbutan-1-amine, + butan-1-amine, or + hexan-1-amine systems at several temperatures

Fernando Hevia, Ana Cobos, Juan Antonio González*, Isaías García de la Fuente, Luis Felipe Sanz

G.E.T.E.F., Departamento de Física Aplicada, Facultad de Ciencias, Universidad de Valladolid, Paseo de Belén, 7, 47011 Valladolid, Spain

*e-mail: jagl@termo.uva.es; Tel: +34 983 423757

Abstract

Values of density (ρ), speed of sound (c) and refractive index (n_{D}) for *N,N*-dimethylformamide (DMF) + *N*-propylpropan-1-amine (DPA) or + butan-1-amine (BA) mixtures at (293.15-303.15) K, and for DMF + *N*-butylbutan-1-amine (DBA) or hexan-1-amine (HxA) mixtures at 298.15 K are reported. Density and speed of sound measurements were conducted using a vibrating-tube densimeter and sound analyzer, Anton Paar model DSA5000; refractive index, n_{D}, values were obtained by means of a RFM970 refractometer from Bellingham+Stanley. The experimental ρ, c and n_{D} values have been used to determine excess molar volumes, $V_{\mathrm{m}}^{\mathrm{E}}$, excess adiabatic compressibilities, κ_S^{E}, excess speeds of sound, c^{E}, excess thermal expansion coefficients, α_p^{E}, and excess refractive indices, $n_{\mathrm{D}}^{\mathrm{E}}$. This set of data show the existence of interactions between unlike molecules and of structural effects in the mixtures under study. $V_{\mathrm{m}}^{\mathrm{E}}$ values of solutions including linear secondary amines are lower than those of mixtures with linear primary amines. In fact, the contribution to $V_{\mathrm{m}}^{\mathrm{E}}$ from the breaking of amine-amine interactions is larger for the latter systems. Calculations on Rao's constant point out that there is no complex formation between the mixture components. Dispersive interactions have been analyzed by means of the molar refraction. It is shown that solutions with DPA or HxA are characterized by similar dispersive interactions and that they mainly differ in dipolar interactions.

Adapted with permission from F. Hevia, A. Cobos, J.A. González, I. García de la Fuente, L.F. Sanz, *Thermodynamics of amide + amine mixtures. 1. Volumetric, speed of sound and refractive index data for N,N-dimethylformamide + N-propylpropan-1-amine, + N-butylbutan-1-amine, + butan-1-amine, or + hexan-1-amine systems at several temperatures,* J. Chem. Eng. Data **61** (2016) 1468-1478. https://doi.org/10.1021/acs.jced.5b00802.

1. Introduction

N,N-dimethylformamide (DMF) is a very polar liquid (3.7 D [1]) which is able to dissolve many organic substances, as it is an aprotic protophilic compound with excellent donor-acceptor properties. Consequently, this amide has many technical applications. For example, it is used for the production of acrylic fibers, plastics, pesticides or surface coatings [2]. In the oil industry, due to its good properties as selective extractant, it is used for the extraction of aromatic and saturated hydrocarbons and of compounds containing nitrogen [3, 4]. In addition, it results very effective in nanotechnology [5-7]. Interestingly, the detailed knowledge of liquid mixtures containing the amide functional group is essential for the understanding of complex molecules of biological interest [8]. In this context, DMF is useful as a model compound for peptides. The aqueous solution of DMF is a simple biochemical model of biological aqueous solutions [9, 10]. On the other hand, the significant local order characteristic of pure DMF and of other *N,N*-dialkylamides, related to the existence of strong dipole-dipole interactions [11], makes their theoretical study of high interest [12].

Primary and secondary amines are polar molecules (see below) which can also form hydrogen bonds giving self-associated complexes or, with the appropriate group, heterocomplexes [13-15]. Amines are also very common in Biology. In fact, the breaking of amino acids releases amines; neurotransmitters as dopamine or histamine are amines [16, 17], and the polymer DNA is usually bound to proteins which contain several amine groups [18]. In addition, many of the cations and anions of the technically important ionic liquids are related to amine groups [19].

We start this series of articles reporting density, ρ, data, speeds of sound, c, and refractive indices, n_D, at (293.15 K-303.15) K for DMF mixtures with *N*-propylpropan-1-amine (DPA) or butan-1-amine (BA), and at 298.15 K for DMF systems with *N*-butylbutan-1-amine (DBA) or hexan-1-amine (HxA). A literature survey shows that there are no such data for the systems under study. In contrast, volumetric [4, 20], n_D [4], vapor-liquid equilibrium [21] or excess molar enthalpy [22] (H_m^E) measurements are available for the DMF + aniline mixture. Data on H_m^E are also available for the *N*-methylethanamide + HxA system at 363.15 K [23]. The large and negative H_m^E value at equimolar composition for this mixture (–1005 J·mol^{-1}) [23], and for the DMF + aniline system at 298.15 K (–2946 J·mol^{-1}) [22] reveal the existence of strong interactions between unlike molecules in amide + amine mixtures.

2. Experimental section

Materials. All the compounds were used without further purification. Table 1 contains information regarding their source and purity, and Table 2 shows their physical properties, ρ, c, n_D, thermal expansion coefficient, α_p, adiabatic compressibility, κ_S, and isothermal compressibility, κ_T. The values listed in Table 2 are in good agreement with the data available in the literature.

Apparatus and procedure. Binary mixtures were prepared by mass in small vessels of about 10 cm^3, using an analytical balance HR-202 (weighing accuracy 0.01 mg), with all weighings corrected for buoyancy effects. The standard uncertainty in the final mole fraction is estimated to be 0.0008. Molar quantities were calculated on the basis of the relative atomic mass table of 2015 issued by the Commission on Isotopic Abundances and Atomic Weights (IUPAC) [24].

Table 1. Sample description.

Chemical name	CAS number	Source	Purification method	Mole fraction purity	Analysis method
N,N-dimethylformamide (DMF)	68-12-2	Fluka	none	≥ 0.995	GC[a]
N-propylpropan-1-amine (DPA)	142-84-7	Fluka	none	≥ 0.99	GC[a]
N-butylbutan-1-amine (DBA)	111-92-2	Aldrich	none	≥ 0.995	GC[a]
butan-1-amine (BA)	109-73-9	Sigma--Aldrich	none	≥ 0.99	GC[a]
hexan-1-amine (HxA)	111-26-2	Aldrich	none	≥ 0.995	GC[a]

[a] Gas-liquid chromatography.

Temperatures were measured using Pt-100 resistances, calibrated according to the ITS-90 scale of temperature, against the triple point of water and the melting point of Ga. The repeatability of the equilibrium temperature measurements is 0.01 K. The standard uncertainties for this quantity are 0.02 K and 0.03 K for ρ and n_D measurements, respectively (see below).

Densities and speeds of sound of both pure liquids and of the mixtures were measured by means of a vibrating-tube densimeter and sound analyzer, Anton Paar model DSA 5000, automatically thermostated within 0.01 K. A detailed description of the calibration of the apparatus has been given in an earlier work [25]. The repeatability of the ρ measurements is $5 \cdot 10^{-3}$ kg·m^{-3}, while the relative standard uncertainty of the measurements is estimated to be 0.12%. The determination of the speed of sound is based on the measurement of the propagation time of short acoustic pulses (3 MHz center frequency [26]), which are repeatedly transmitted to the sample. The repeatability and standard uncertainty of the c measurements are, respectively, 0.1 and 0.4 m·s^{-1}. The experimental technique was checked through the determination of V_m^E and c^E of the (cyclohexane + benzene) mixture at (293.15-303.15) K. Our results and published values [27-29] are in good agreement. The standard uncertainty in V_m^E is $(0.012\left|V_{m,max}^E\right| + 0.005$ cm^3·mol^{-1}), where $\left|V_{m,max}^E\right|$ stands for the maximum experimental value of V_m^E with respect to the mole fraction. The standard uncertainty of c^E is estimated to be 0.8 m·s^{-1}.

Refractive indices were measured using a refractometer model RFM970 from Bellingham+Stanley, with the temperature controlled by means of Peltier modules. The measurement technique is based on the optical detection of the critical angle at the wavelength of the sodium D line (589.6 nm). Calibration of the apparatus was undertaken using 2,2,4-trimethylpentane and toluene at (293.15-303.15) K, the working temperatures, as indicated by Marsh [30]. The temperature stability is 0.02 K, the repeatability of the n_D measurements is 0.00004 and the relative standard uncertainty is 0.0015.

3. Equations

The densimeter and sound analyzer Anton Paar DSA 5000 allows to obtain in straight form ρ, the molar volume, V_m, the coefficient of thermal expansion, $\alpha_p = -\left(1/\rho\right)\left(\partial\rho/\partial T\right)_p$ and the

Table 2. Physical properties of pure compounds at temperature T and pressure p = 0.1 MPa. [a]

Property	T/K	DMF	DPA	DBA	BA	HxA
ρ^* /g·cm^{-3}	293.15	0.948881	0.738194	0.759695	0.737048	0.764423
		0.948922[b]	0.738188[c]	0.759571[c]		
	298.15	0.944081	0.733618	0.755525	0.732231	0.760073
		0.944163[b]	0.733683[c]	0.755457[c]	0.7327[d]	0.76013[e]
	303.15	0.939361	0.729098	0.751458	0.727452	0.755848
		0.939390[b]	0.729087[c]	0.751329[c]		
c^*/m·s^{-1}	293.15	1476.8	1209.4	1261.1	1268.3	1324.0
		1477.8[b]	1209[c]	1261.2[c]		
	298.15	1457.2	1187.7	1241.5	1246.0	1303.6
		1458.5[b]	1198[f]	1248[f]	1247.8[d]	1304.7[e]
		1458.6[g]				
	303.15	1438.2	1167.2	1222.5	1224.6	1283.6
		1439[b]	1174[f]	1227[f]	1227[f]	1285[f]
		1440.3[g]				
α_p^* /10^{-3}K^{-1}	298.15	1.008	1.240	1.090	1.311	1.128
		1.010[g]	1.29[h]	1.12[h]	1.314[f]	1.13[e]
κ_S^* /TPa^{-1}	293.15	483.2	926.2	827.7	843.4	746.3
		485[b]	926.5[f]			
	298.15	498.8	966.3	858.7	879.7	774.2
		498.7[i]	947[f]	849[f]	876.6[d]	773[e]
		497.9[b]				
	303.15	514.7	1006.7	890.4	916.7	802.9
		514[b]	992[f]	883[f]	912[f]	800[f]
		512.9[g]				
κ_T^* /TPa^{-1}	298.15	659.4	1216.4	1059.4	1151.9	974.6
		650[h]	1183[f]	1039[f]	1145[f]	975[e]
		662[j]				
$C_{p\mathrm{m}}^*$ /J·mol^{-1}·K^{-1}	298.15	146.05[k]	252.84[h]	302[f]	188[l]	252[l]
n_{D}^*	293.15	1.43055	1.40432	1.41724	1.40060	
		1.43047[h]	1.4043[h]	1.4177[h]	1.40106[n]	
		1.4281[m]				
	298.15	1.42828	1.40139	1.41488	1.39786	1.41577
		1.42817[h]	1.4053[f]	1.4152[h]	1.3987[h]	1.4160[f]
		1.4280[j]				
	303.15	1.42603	1.39883	1.41253	1.39500	
		1.4267[o]	1.4022[f]	1.4143[f]	1.3978[f]	
		1.4271[j]			1.39744[n]	

[a] ρ^*, density; c^*, speed of sound; α_p^*, isobaric thermal expansion coefficient; κ_S^*, adiabatic compressibility; κ_T^*, isothermal compressibility; $C_{p\mathrm{m}}^*$, isobaric molar heat capacity; and n_{D}^*, refractive index. Standard uncertainties, u, are: $u(T) = 0.02$ K (for n_D^* values, $u(T) = 0.03$ K); $u(p) = 1$ kPa; $u(c^*) = 0.4$ m·s^{-1}. Relative standard uncertainties, u_{r}, are: $u_{\mathrm{r}}(\rho^*) = 0.0012$; $u_{\mathrm{r}}(\alpha_p^*) = 0.028$; $u_{\mathrm{r}}(\kappa_S^*) = 0.002$; $u_{\mathrm{r}}(\kappa_T^*) = 0.015$; $u_{\mathrm{r}}(n_D^*) = 0.0015$. [b]Ref. [67]; [c]Ref. [68]; [d]Ref. [69]; [e]Ref. [70]; [f]Ref. [71]; [g]Ref. [72]; [h]Ref. [73]; [i]Ref. [74]; [j]Ref. [75]; [k]Ref. [76]; [l]Ref. [77]; [m]Ref. [78]; [n]Ref. [79]; [o]Ref. [80].

isentropic compressibility, κ_S. As in other previous applications, α_p values were determined assuming that ρ changes linearly with T. In addition, κ_S can be determined from the Newton-Laplace equation assuming that the absorption of the acoustic wave is negligible:

$$\kappa_S = \frac{1}{\rho c^2} \tag{1}$$

The values F^{id} of a given thermodynamic property, F, for an ideal mixture at the same temperature and pressure as the investigated solution, are calculated by means of the well-established equations [31-33]:

$$F^{\mathrm{id}} = x_1 F_1^* + x_2 F_2^* \qquad (F = V_{\mathrm{m}}, C_{p\mathrm{m}}) \tag{2}$$

$$F^{\mathrm{id}} = \phi_1 F_1^* + \phi_2 F_2^* \qquad (F = \alpha_p, \kappa_T) \tag{3}$$

where F_i^* is the value of the property F of pure component i, and $C_{p\mathrm{m}}$ is the molar isobaric heat capacity. In equation (3), $\phi_i = x_i V_{\mathrm{m}i}^* / V_{\mathrm{m}}^{\mathrm{id}}$ represents the volume fraction of component i, where $V_{\mathrm{m}i}^*$ is the molar volume of that component. Ideal values of κ_S and c are calculated from the expressions [31]:

$$\kappa_S^{\mathrm{id}} = \kappa_T^{\mathrm{id}} - \frac{T V_{\mathrm{m}}^{\mathrm{id}} (\alpha_p^{\mathrm{id}})^2}{C_{p\mathrm{m}}^{\mathrm{id}}} \tag{4}$$

$$c^{\mathrm{id}} = \left(\frac{1}{\rho^{\mathrm{id}} \kappa_S^{\mathrm{id}}} \right)^{1/2} \tag{5}$$

being $\rho^{\mathrm{id}} = (x_1 M_1 + x_2 M_2) / V_{\mathrm{m}}^{\mathrm{id}}$ (M_i, molar mass of the i component). Finally, the ideal values of n_{D} are determined using the equation proposed by Reis *et al.* [34]:

$$n_{\mathrm{D}}^{\mathrm{id}} = \left[\phi_1 \left(n_{\mathrm{D}1}^* \right)^2 + \phi_2 \left(n_{\mathrm{D}2}^* \right)^2 \right]^{1/2} \tag{6}$$

The excess functions are then determined from the equation:

$$F^{\mathrm{E}} = F - F^{\mathrm{id}} \qquad (F = V_{\mathrm{m}}, \kappa_S, c, \alpha_p, n_{\mathrm{D}}) \tag{7}$$

4. Experimental results

Values, at the considered temperatures, of ρ and c vs. x_1, the mole fraction of DMF, are collected in Table 3, while n_{D} results are shown in Table 4. Derived properties, as excess functions, are given in the supporting information: $V_{\mathrm{m}}^{\mathrm{E}}$ (Table S1); α_p and α_p^{E} at 298.15 K (Table S2); κ_S^{E} and c^{E} at 298.15 K (Table S3) and $n_{\mathrm{D}}^{\mathrm{E}}$ (Table S4). These results are shown graphically in Figures 1-7. We have not found data available in the literature for comparison. The current data were fitted by unweighted least-squares polynomial regressions to the Redlich-Kister equation:

Table 3. Densities, ρ , and speeds of sound, c, for *N,N*-dimethylformamide (1) + amine (2) mixtures at temperature T and pressure p = 0.1 MPa. [a]

x_1	ρ /g·cm^{-3}	c /m·s^{-1}	x_1	ρ /g·cm^{-3}	c /m·s^{-1}
		DMF (1) + DPA (2) ; T/K = 293.15 K			
0.0600	0.745894	1218.2	0.4974	0.815656	1299.2
0.1071	0.752141	1225.0	0.5487	0.825989	1312.0
0.1560	0.758933	1232.9	0.6562	0.849651	1342.1
0.1975	0.764870	1239.3	0.7514	0.873097	1373.4
0.2490	0.772540	1248.1	0.8216	0.892212	1399.8
0.3099	0.782194	1259.4	0.8501	0.900523	1411.2
0.3463	0.788151	1266.2	0.9025	0.916508	1433.3
0.3985	0.797199	1276.9	0.9486	0.931283	1453.4
0.4480	0.806192	1287.6			
		DMF (1) + DPA (2) ; T/K = 298.15 K			
0.0626	0.741577	1196.9	0.5386	0.819199	1288.9
0.1083	0.747697	1204.0	0.6082	0.833997	1307.9
0.1544	0.754025	1211.2	0.6527	0.844084	1321.1
0.2541	0.768732	1228.1	0.7477	0.867448	1352.4
0.3148	0.778293	1239.3	0.8063	0.883226	1374.0
0.3609	0.786012	1248.3	0.9020	0.911457	1413.1
0.4077	0.794223	1258.2	0.9482	0.926367	1433.5
0.4966	0.810800	1278.5			
		DMF (1) + DPA (2) ; T/K = 303.15 K			
0.0453	0.734885	1174.0	0.5415	0.815193	1270.3
0.1034	0.742550	1183.0	0.6016	0.827909	1286.6
0.1963	0.755529	1198.0	0.6517	0.839209	1301.4
0.2582	0.764775	1208.8	0.7502	0.863388	1334.0
0.3559	0.780614	1227.6	0.8498	0.890941	1372.0
0.4099	0.790030	1239.0	0.9000	0.906165	1393.2
0.4565	0.798539	1249.4	0.9498	0.922203	1415.2
		DMF (1) + DBA (2) ; T/K = 298.15 K			
0.0642	0.761171	1246.4	0.5574	0.823977	1307.9
0.1134	0.765782	1250.5	0.5996	0.831688	1316.3
0.1647	0.770882	1255.0	0.6514	0.842013	1328.1
0.2121	0.775872	1259.5	0.6869	0.849571	1336.8
0.2734	0.782835	1266.1	0.7361	0.860924	1350.4
0.3213	0.788624	1271.6	0.7904	0.874714	1367.5
0.4114	0.800702	1283.5	0.8418	0.889103	1385.9
0.4526	0.806766	1289.7	0.8921	0.904666	1406.1
0.5072	0.815344	1298.6	0.9471	0.923650	1431.0

		DMF (1) + BA (2) ; T/K = 293.15 K			
0.0599	0.747390	1277.7	0.5483	0.842154	1368.9
0.1056	0.755445	1285.0	0.6569	0.866102	1393.7
0.1591	0.765035	1293.8	0.6999	0.875844	1404.0
0.2505	0.782005	1309.6	0.7537	0.888314	1416.7
0.3017	0.791811	1318.9	0.8036	0.900101	1429.0
0.3583	0.802880	1329.6	0.8579	0.913315	1442.3
0.3992	0.811114	1337.8	0.9048	0.924751	1453.7
0.5059	0.833130	1359.6	0.9546	0.937212	1465.6
		DMF (1) + BA (2) ; T/K = 298.15 K			
0.0575	0.742224	1255.4	0.4381	0.814268	1324.9
0.1092	0.751333	1263.9	0.5028	0.827736	1338.6
0.1519	0.759015	1271.1	0.6005	0.848795	1360.6
0.2043	0.768674	1280.1	0.6934	0.869781	1382.5
0.2448	0.776215	1287.4	0.7572	0.884516	1398.0
0.3090	0.788510	1299.3	0.8056	0.895958	1410.0
0.3558	0.797705	1308.4	0.9076	0.920837	1435.1
0.3986	0.806285	1317.0	0.9553	0.932723	1446.6
		DMF (1) + BA (2) ; T/K = 303.15 K			
0.0505	0.736213	1233.0	0.5281	0.828281	1324.0
0.1477	0.753539	1249.4	0.6056	0.845104	1341.6
0.2019	0.763466	1259.0	0.6960	0.865473	1363.2
0.2410	0.770708	1266.0	0.7558	0.879286	1377.7
0.3024	0.782423	1277.5	0.8006	0.889962	1389.0
0.3558	0.792882	1287.8	0.8544	0.902880	1402.3
0.4358	0.808960	1304.1	0.8998	0.914033	1413.7
0.5114	0.824673	1320.3	0.9466	0.925732	1425.2
		DMF (1) + HxA (2) ; T/K = 298.15 K			
0.0506	0.765582	1307.1	0.6022	0.846551	1368.3
0.0992	0.771096	1310.8	0.7056	0.867688	1387.1
0.1725	0.779897	1316.7	0.7996	0.889217	1406.8
0.2548	0.790546	1324.2	0.8492	0.901602	1418.4
0.3476	0.803611	1333.7	0.8982	0.914549	1430.4
0.4461	0.818861	1345.5	0.9530	0.929990	1444.7
0.5500	0.836751	1360.1			

[a] The standard uncertainties, u , are: $u(x_1) = 0.0008$; $u(p) = 1$ kPa; $u(T) = 0.02$ K. The combined expanded standard uncertainties (0.95 level of confidence) are: $U_{rc}(\rho) = 0.0024$ (relative value); $U_c(c) = 0.8\,\mathrm{m{\cdot}s^{-1}}$.

Table 4. Refractive indices, n_D, of *N,N*-dimethylformamide (1) + amine (2) mixtures at temperature T and pressure $p = 0.1$ MPa. [a]

x_1	n_D	x_1	n_D
	DMF (1) + DPA (2) ; T/K = 293.15 K		
0.0600	1.40543	0.5487	1.41645
0.1556	1.40725	0.6018	1.41789
0.2614	1.40952	0.7033	1.42079
0.3463	1.41140	0.8216	1.42444
0.3985	1.41266	0.8844	1.42653
0.4554	1.41402	0.9486	1.42882
	DMF (1) + DPA (2) ; T/K = 298.15 K		
0.0626	1.40259	0.4966	1.41247
0.1083	1.40358	0.6527	1.41673
0.1544	1.40443	0.7477	1.41960
0.2541	1.40662	0.8063	1.42147
0.3148	1.40796	0.9020	1.42478
0.3609	1.40908	0.9482	1.42645
0.4077	1.41017		
	DMF (1) + DPA (2) ; T/K = 303.15 K		
0.0453	1.39971	0.6016	1.41295
0.1034	1.40091	0.7502	1.41745
0.1963	1.40293	0.8498	1.42070
0.2582	1.40419	0.9000	1.42246
0.3559	1.40647	0.9498	1.42417
0.4099	1.40779		
	DMF (1) + DBA (2) ; T/K = 298.15 K		
0.1038	1.41553	0.7709	1.42323
0.2076	1.41628	0.8398	1.42459
0.3608	1.41761	0.8989	1.42587
0.4897	1.41900	0.9497	1.42706
0.5933	1.42034	0.9738	1.42765
0.6880	1.42178		
	DMF (1) + BA (2) ; T/K = 293.15 K		
0.0599	1.40222	0.5059	1.41521
0.1056	1.40348	0.6043	1.41829
0.1591	1.40498	0.6569	1.41992
0.2010	1.40619	0.6999	1.42126
0.2505	1.40760	0.7537	1.42292
0.3017	1.40911	0.8036	1.42448
0.3583	1.41079	0.8579	1.42618
0.3992	1.41200	0.9048	1.42763
0.4401	1.41322	0.9546	1.42915

	DMF (1) + BA (2) ; T/K = 298.15 K		
0.0575	1.39946	0.6005	1.41578
0.1092	1.40093	0.6608	1.41769
0.1519	1.40215	0.6934	1.41871
0.2043	1.40367	0.7572	1.42076
0.2448	1.40485	0.8056	1.42230
0.3090	1.40680	0.8546	1.42383
0.3558	1.40820	0.9076	1.42553
0.5028	1.41274	0.9553	1.42705
	DMF (1) + BA (2) ; T/K = 303.15 K		
0.0505	1.39644	0.5281	1.41094
0.1477	1.39927	0.6056	1.41337
0.2019	1.40087	0.6574	1.41502
0.2410	1.40209	0.6960	1.41625
0.3024	1.40392	0.7558	1.41820
0.3558	1.40552	0.8006	1.41964
0.3992	1.40686	0.8544	1.42138
0.4358	1.40802	0.8998	1.42282
0.5114	1.41041	0.9466	1.42431
	DMF (1) + HxA (2) ; T/K = 298.15 K		
0.0506	1.41613	0.5500	1.42107
0.1725	1.41707	0.6558	1.42257
0.2548	1.41779	0.7573	1.42411
0.3476	1.41870	0.8492	1.42564
0.4461	1.41980	0.9530	1.42747

[a] The standard uncertainties, u, are: $u(x_1) = 0.0008$; $u(T) = 0.03$ K; $u(p) = 1$ kPa. The relative combined expanded standard uncertainty (0.95 level of confidence), U_{rc}, is: $U_{rc}(n_D) = 0.0030$.

$$F^E = x_1(1-x_1)\sum_{i=0}^{k-1} A_i(2x_1-1)^i \tag{8}$$

where $F = V_m, \kappa_S, c, \alpha_p, n_D$. For each mixture, the number of the needed coefficients, k, in equation (8) was determined by applying an F-test of additional term [35] at the 99.5 % confidence level. Table 5 lists the parameters A_i obtained along the adjustments, and the corresponding standard deviations $\sigma(F^E)$, calculated from the expression:

$$\sigma(F^E) = \left[\frac{1}{N-k} \sum \left(F^E_{cal} - F^E_{exp} \right)^2 \right]^{1/2} \tag{9}$$

where N is the number of direct experimental values.

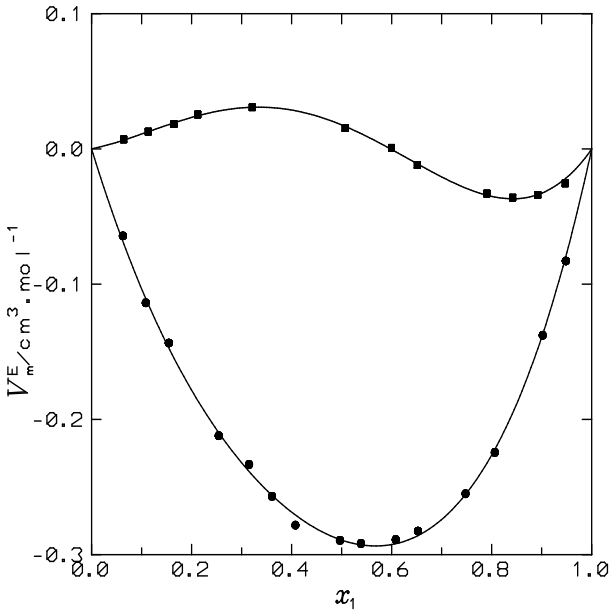

Figure 1: Excess molar volumes, V_m^E, for DMF (1) + DPA (2), or + DBA (2) systems at atmospheric pressure and 298.15 K. Full symbols, experimental values (this work): (●), DPA; (■), DBA. Solid lines, calculations with equation (8) using the coefficients from Table 5.

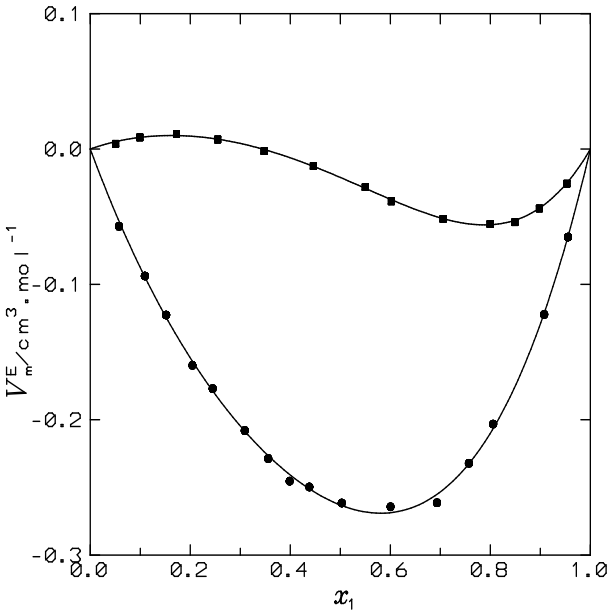

Figure 2: Excess molar volumes, V_m^E, for DMF (1) + BA (2), or + HxA (2) systems at atmospheric pressure and 298.15 K. Full symbols, experimental values (this work): (●), BA; (■), HxA. Solid lines, calculations with equation (8) using the coefficients from Table 5.

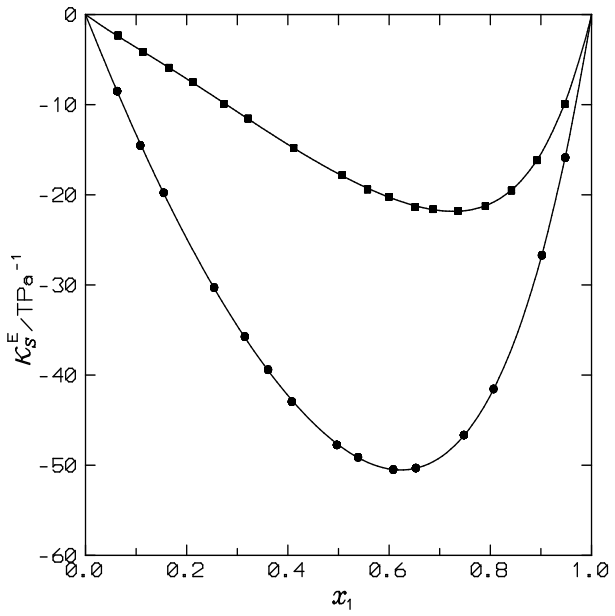

Figure 3: Excess isentropic compressibilities, κ_S^E, for DMF (1) + DPA (2), or + DBA (2) systems at atmospheric pressure and 298.15 K. Full symbols, experimental values (this work): (●), DPA; (■), DBA. Solid lines, calculations with equation (8) using the coefficients from Table 5.

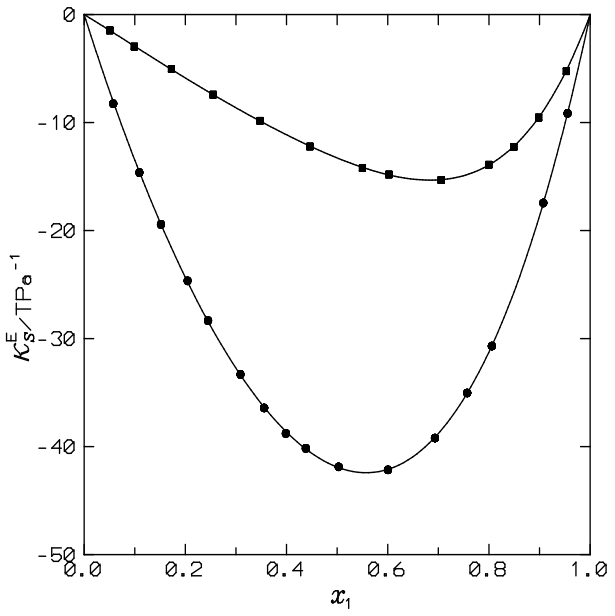

Figure 4: Excess isentropic compressibilities, κ_S^E, for DMF (1) + BA (2), or + HxA (2) systems at atmospheric pressure and 298.15 K. Full symbols, experimental values (this work): (●), BA; (■), HxA. Solid lines, calculations with equation (8) using the coefficients from Table 5.

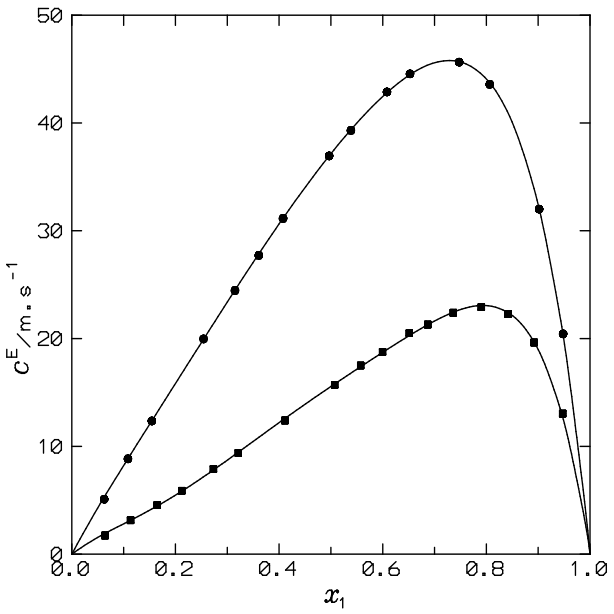

Figure 5: Excess speeds of sound, c^{E}, for DMF (1) + DPA (2), or + DBA (2) systems at atmospheric pressure and 298.15 K. Full symbols, experimental values (this work): (●), DPA; (■), DBA. Solid lines, calculations with equation (8) using the coefficients from Table 5.

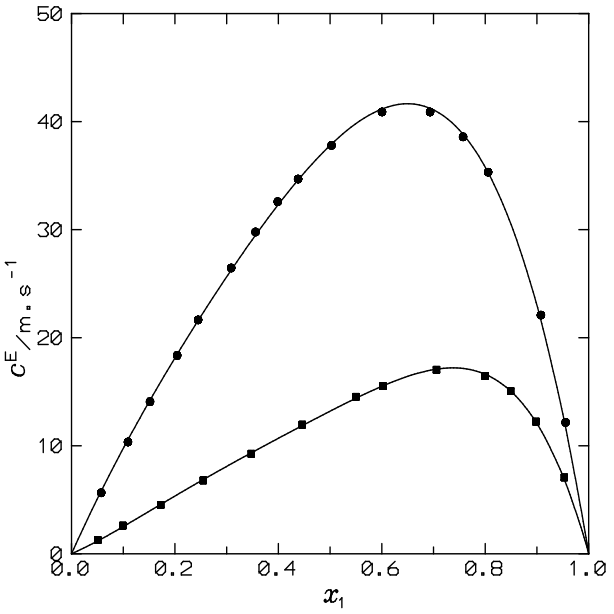

Figure 6: Excess speeds of sound, c^{E}, for DMF (1) + BA (2), or + HxA (2) systems at atmospheric pressure and 298.15 K. Full symbols, experimental values (this work): (●), BA; (■), HxA. Solid lines, calculations with equation (8) using the coefficients from Table 5.

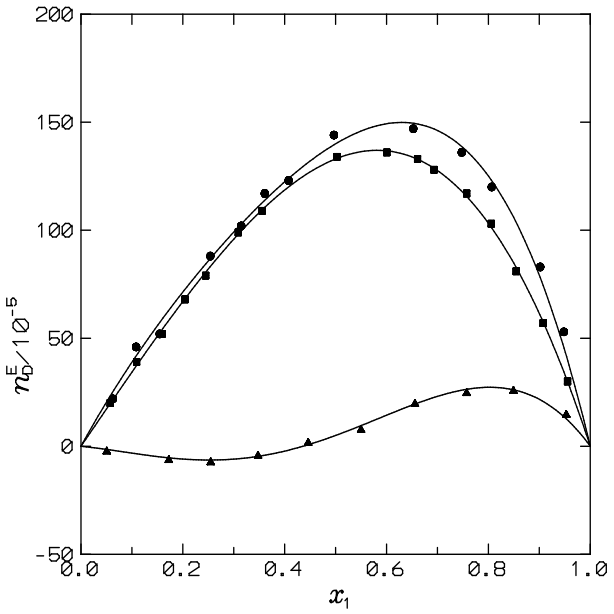

Figure 7: Excess refractive indices, $n_{\mathrm{D}}^{\mathrm{E}}$, for DMF (1) + amine (2) systems at atmospheric pressure and 298.15 K. Full symbols, experimental values (this work): (●), DPA; (■), BA; (▲), HxA. Solid lines, calculations with equation (8) using the coefficients from Table 5.

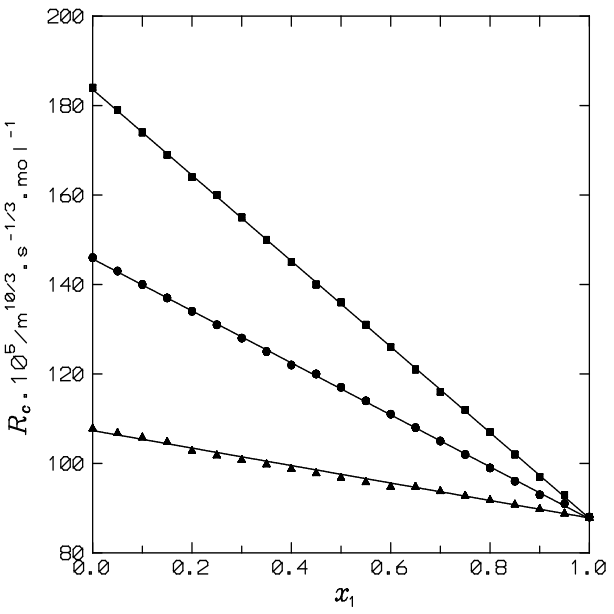

Figure 8: Rao's constant, R_c, for DMF (1) + amine (2) systems at atmospheric pressure and 298.15 K (this work): (●), DPA; (■), DBA; (▲), BA.

Table 5. Coefficients A_i and standard deviations, $\sigma\left(F^E\right)$ (equation (9)), for the representation of the F^E property at temperature T and pressure p = 0.1 MPa for *N,N*-dimethylformamide (1) + amine (2) systems by equation (8).

System	T/K	Property [a] F^E	A_0	A_1	A_2	A_3	A_4	$\sigma\left(F^E\right)$
DMF + DPA	293.15	V_m^E	–1.121	–0.23	–0.37			0.005
		n_D^E	0.00540	0.0033	0.0013			0.00004
	298.15	V_m^E	–1.157	–0.25	–0.30			0.004
		κ_S^E	–191.0	–84.2	–52.2	–18		0.11
		c^E	148.6	120.2	90	75	48	0.10
		α_p^E	–52.5					0.5
		n_D^E	0.0056	0.0028	0.0015			0.00004
	303.15	V_m^E	–1.192	–0.21	–0.37			0.005
		n_D^E	0.00583	0.0032	0.0020			0.00003
DMF + DBA	298.15	V_m^E	0.071	–0.304	–0.30			0.0015
		κ_S^E	–70.7	–59.6	–38	–35	–27	0.08
		c^E	62.2	65	53	74	61	0.15
		n_D^E	0.00020	0.00109	0.0010	0.0010	0.0008	0.000004
DMF + BA	293.15	V_m^E	–0.978	–0.29	–0.12			0.003
		n_D^E	0.00527	0.00229				0.00002
	298.15	V_m^E	–1.052	–0.29	–0.24			0.003
		κ_S^E	–167.6	–36.0	–17.0			0.09
		c^E	151.2	92	48			0.3
		α_p^E	–86	56	–195	–44		0.6
		n_D^E	0.00532	0.00189				0.00001
	303.15	V_m^E	–1.060	–0.23	–0.28			0.003
		n_D^E	0.00578	0.00197				0.00002
DMF + HxA	298.15	V_m^E	–0.084	–0.316	–0.17	–0.07		0.0010
		κ_S^E	–53.1	–38.0	–24.4	–11		0.05
		c^E	52.8	49	44	27		0.12
		n_D^E	0.00020	0.00173	0.0013			0.000014

[a] $F^E = V_m^E$, units: $cm^3 \cdot mol^{-1}$; $F^E = c^E$, units: $m \cdot s^{-1}$; $F^E = \kappa_S^E$ units: TPa^{-1}; $F^E = \alpha_p^E$, units: $10^{-6} \cdot K^{-1}$.

5. Discussion

Along this section, we are referring to values of the excess functions and of the thermophysical properties at 298.15 K and at $x_1 = 0.5$, except in specific cases duly indicated.

As we have previously mentioned, DMF is a very polar substance. As a consequence, its alkane mixtures show immiscibility regions up to rather high temperatures. For example, the upper critical solution temperatures of systems involving heptane or hexadecane are, respectively, 342.55 K [36] and 385.15 K [37].

Linear primary or secondary amines are weakly self-associated compounds with rather low dipole moments. For the amines considered, the values of this quantity are (in D): 1.3 (BA) [38], 1.3 (HxA) [1], 1.0 (DPA) [38], or 1.1 (DBA) [38]. H_m^E/J·mol^{-1} values of mixtures including a given alkane, say heptane, are: 1192 (BA) [39], 962 (HxA) [39], 424 (DPA) [40], and 317 (DBA) [40]. These positive H_m^E values can be explained in terms of the disruption of amine-amine interactions along the mixing process. We note that H_m^E decreases when the self-association of the amine becomes weaker, as the amine group is more sterically hindered in longer amines, and in secondary amines than in primary amines. On the other hand, it is well stated that positive V_m^E values are related to the breaking of interactions between like molecules, while negative values come from the creation of solute-solvent interactions and/or structural effects (geometrical factors including differences in size and shape between the mixture compounds [41-43] or interstitial accommodation [44]). The V_m^E(heptane)/cm^3·mol^{-1} values are: 0.7171 (BA) [45], 0.3450 (HxA) [45], 0.2752 (DPA) [46], and 0.0675 (DBA) [46]. Interestingly, the H_m^E and V_m^E values are positive and change in line, which reveals that the most important contribution to V_m^E comes from the disruption of amine-amine interactions upon mixing. However, structural effects may also be present. The low V_m^E value of DBA + heptane system, and the negative value of the DBA + hexane mixture (–0.185 cm^3·mol^{-1}) [47] support this statement, as positive H_m^E values and those negative of V_m^E for a given solution suggest that the most relevant contribution to the latter excess function arises from structural effects [43].

In view of the mentioned features, the negative V_m^E/cm^3·mol^{-1} values of DMF + amine mixtures for systems containing DPA (–0.289), BA (–0.263) or HxA (–0.021) and the low V_m^E positive value for the DBA solution (0.018 cm^3·mol^{-1}) can be ascribed to the existence of DMF-amine interactions as well as to structural effects. It must be noted that the increase of the amine size along a homologous series leads to increased V_m^E values. This means that the contributions that increase V_m^E (larger number of DMF-DMF interactions broken by the longer amines and the weakening of the amide-amine interactions related to the fact that the amine group is more sterically hindered in such amines) are predominant over those decreasing V_m^E (difference in size between components, lower positive contribution from the disruption of the amine-amine interactions).

The replacement of a primary linear amine (HxA) by a linear secondary amine (DPA) leads to decreased V_m^E values. It is remarkable that the same behavior is encountered for HxA or DPA + heptane mixtures (see above). Therefore, the observed variation in DMF solutions can be ascribed to a lower positive contribution to V_m^E from the breaking of the amine-amine

interactions. A similar trend is encountered in 1-alkanol + HxA, or + DPA systems [48, 49]. The more negative V_m^E value of the DMF + aniline mixture (–0.6931 $cm^3 \cdot mol^{-1}$) [20] compared to those of the systems with HxA or DPA suggests that the presence of an aromatic ring leads to stronger interactions between unlike molecules, which is in agreement with the largely negative H_m^E value of this system (see Introduction). Solutions including DPA or BA show negative values of $A_p = \left(\Delta V_m^E / \Delta T\right)_p$ and α_p^E (Table S2). Thus, the use of V_m^E ($x_1 = 0.5$) values obtained at different temperatures gives A_p /$cm^3 \cdot mol^{-1} \cdot K^{-1}$ = $-1.8 \cdot 10^{-3}$ (DPA); $-2 \cdot 10^{-4}$ (BA). This means that the structure of the mixture is more difficult to be broken than that of the pure liquids, which may be considered as an evidence of the existence of interactions between unlike molecules. In fact, values of A_p and α_p^E are positive at any composition for solutions where strong interactions between like molecules are present. This is the case, e.g, of the 2-ethoxyethanol + octane [50] or the pentan-1-ol + cyclohexane [51] systems (A_p /$cm^3 \cdot mol^{-1} \cdot K^{-1}$ = $7.6 \cdot 10^{-3}$; $2.3 \cdot 10^{-3}$, respectively). However, A_p values are also negative for solutions characterized by relevant structural effects ($-1.3 \cdot 10^{-2}$ $cm^3 \cdot mol^{-1} \cdot K^{-1}$ for the hexane + hexadecane mixture [52]). Taking into account the different molar volumes of DPA (137.93 $cm^3 \cdot mol^{-1}$) and BA (99.88 $cm^3 \cdot mol^{-1}$), the more negative A_p value of the DPA system may be related, at least partially, to structural effects. On the other hand, A_p(DMF + aniline) [20] = $-2.9 \cdot 10^{-3}$ $cm^3 \cdot mol^{-1} \cdot K^{-1}$, which is a more negative value than that of the DPA solution. This supports our previous statement, that DMF-amine interactions are stronger in the aniline system. The κ_S^E values can be also interpreted in terms of structural and interactional effects [53]. Structural effects and interactions between unlike molecules lead to negative values of this magnitude (κ_S^E /TPa^{-1}= –142 (aniline + propanone) [54]). Positive values are encountered in solutions where interactions between like molecules are predominant (κ_S^E /TPa^{-1} = 15.3 (2-ethoxyethanol + *n*-octane) [55]). For the systems under study, κ_S^E /TPa^{-1} = -47.8 (DPA); -17.7 (DBA); -41.9 (BA); -13.3 (HxA), which is consistent with the trends mentioned above. In addition, the consistency between the signs of the V_m^E, κ_S^E and c^E functions must be remarked, as V_m^E, κ_S^E are negative and c^E is positive (Tables S1 and S3; Figures 1-6). The DBA mixture slightly separates from this trend and V_m^E is small and positive. However, we underline the strong asymmetry of the κ_S^E curve, with a minimum in the region where V_m^E shows negative values (Figures 1 and 3).

We have also determined the internal pressures, P_{int} [56-59]:

$$P_{int} = \frac{\alpha_p T}{\kappa_T} - p \tag{10}$$

and the excess internal pressures, $P_{int}^E = P_{int} - P_{int}^{id}$, with $P_{int}^{id} = \alpha_p^{id} T / \kappa_T^{id} - p$ [60]. The κ_T values of the mixtures were obtained from

$$\kappa_T = \kappa_S + \frac{T V_m \alpha_p^2}{C_{p,m}} \tag{11}$$

assuming that $C_{pm}^{E} = 0$, and that $\alpha_p = \alpha_p^{id}$ (equation (3)) when experimental data are not available. For pure compounds, we have P_{int} /MPa = 455.7 (DMF); 303.9 (DPA); 306.7 (DBA); 339.2 (BA); 345 (HxA), and for the DMF mixtures, P_{int} /MPa = 353.9 (DPA); 345.9 (DBA); 389.4 (BA); 382.2 (HxA). Because the main contributions to P_{int} are related to dispersion forces and weak dipole-dipole interactions [58], these values suggest that dipolar interactions between unlike molecules are more relevant in systems including linear primary amines. On the other hand, P_{int}^{E} /MPa = 14.6 (DPA); 6.5 (DBA); 14.4 (BA); 5.9 (HxA). Large positive P_{int}^{E} values are encountered in systems characterized by strong interactions between unlike molecules. For example, P_{int}^{E} (aniline + propanone) = 61.4 MPa [54]. It is rather clear that the higher P_{int}^{E} value of the DPA system compared to that of the HxA mixture cannot be ascribed to stronger interactions between unlike molecules but to structural effects.

On the other hand, P_{int} values can be calculated using the equation [57]:

$$P_{int} = \frac{RT}{x_1 v_{f1} + x_2 v_{f2} + V_m^E} - p \tag{12}$$

In this expression, v_{fi} denotes the molar free volume of component i, obtained from $v_{fi} = RT/(p + P_{int,i})$ [57]. Results on P_{int} /MPa from equation (12) are: 380.7 (DPA), 365.7 (DBA), 389.4 (BA) and 394.1 (HxA). The differences with the experimental values (equation. (10)) are: 7.6%, 5.7%, 4.2% and 3.1%, respectively. This demonstrates that the van der Waals equation holds to a rather large extent for the investigated solutions, as equation (12) is derived from this equation of state [57].

The Rao's constant [61], R_c, (also termed molar sound velocity, $R_c = V_m c^{1/3}$) is a quantity commonly used to investigate molecular interactions in liquid mixtures from ultrasonic measurements. In fact, if there is no association, or if the degree of association does not depend on concentration, R_c changes linearly on the mole fractions of the components and one can write [62-64]: $R_c = x_1 R_{c1} + x_2 R_{c2}$ Systems where complex formation is present show deviations from this behavior [64]. For the actual mixtures under study, R_c varies linearly with x_1 (Figure 8), and this indicates that there is no complex formation [62, 63].

Finally, the n_D values can be used for the determination of the molar refraction R_m, a quantity closely related to the dispersion forces of the considered system, as n_D at optical wavelengths is related to the mean electronic polarizability [65]. R_m can be calculated using the Lorentz-Lorenz equation [65, 66]:

$$R_m = \frac{n_D^2 - 1}{n_D^2 + 2} V_m \tag{13}$$

We have R_m (DMF)/cm^3·mol^{-1} = 26.7 (DPA); 31.4 (DBA); 22.0 (BA); 26.7 (HxA). These results allow to state that: (i) as expected, dispersive interactions become more relevant when the amine size increases along a homologous series; (ii) dispersive interactions are more or less similar in DPA and HxA mixtures, which means that such solutions mainly differ in dipolar interactions.

6. Conclusions

Data on ρ, c and n_{D} for DMF + DPA, + DBA, + BA or + HxA mixtures at different temperatures have been reported, and the excess functions $V_{\mathrm{m}}^{\mathrm{E}}$, κ_S^{E}, c^{E}, α_p^{E} and $n_{\mathrm{D}}^{\mathrm{E}}$ have been calculated. The data show the existence of interactions between unlike molecules and of structural effects in the investigated systems. $V_{\mathrm{m}}^{\mathrm{E}}$ values of mixtures including linear secondary amines are lower than those of systems with linear primary amines, as for the latter solutions the contribution to $V_{\mathrm{m}}^{\mathrm{E}}$ from the breaking of amine-amine interactions is larger. Mixtures with DPA or HxA differ essentially in dipolar interactions.

Supporting information

This material contains values of $V_{\mathrm{m}}^{\mathrm{E}}$ and $n_{\mathrm{D}}^{\mathrm{E}}$ at the working temperatures and values of α_p, α_p^{E}, κ_S^{E}, c^{E} at 298.15 K.

References

[1] A.L. McClellan, *Tables of Experimental Dipole Moments.* Vols. 1,2,3, Rahara Enterprises, El Cerrito, US, 1974.

[2] P. Venkatesu, *Thermophysical contribution of N,N-dimethylformamide in the molecular interactions with other solvents.* Fluid Phase Equilib. **298** (2010) 173-191. https://doi.org/10.1016/j.fluid.2010.07.010

[3] B. Blanco, M.T. Sanz, S. Beltrán, J.L. Cabezas, J. Coca, *Vapor–liquid equilibria for the ternary system benzene+n-heptane+N,N-dimethylformamide at 101.33 kPa.* Fluid Phase Equilib. **175** (2000) 117-124. https://doi.org/10.1016/S0378-3812(00)00438-6

[4] H.J. Noh, S.J. Park, S.J. In, *Excess molar volumes and deviations of refractive indices at 298.15 K for binary and ternary mixtures with pyridine or aniline or quinoline.* J. Ind. Eng. Chem. **16** (2010) 200-206. https://doi.org/10.1016/j.jiec.2010.01.038

[5] F. Inam, H. Yan, M.J. Reece, T. Peijs, *Dimethylformamide: an effective dispersant for making ceramic–carbon nanotube composites.* Nanotech. **19** (2008) 195710. https://doi.org/10.1088/0957-4484/19/19/195710

[6] T.T. Nguyen, S.U. Nguyen, D.T. Phuong, D.C. Nguyen, A.T. Mai, *Dispersion of denatured carbon nanotubes by using a dimethylformamide solution.* Adv. Nat. Sci.: Nanosci. Nanotech. **2** (2011) 035015. https://doi.org/10.1088/2043-6262/2/3/035015

[7] Y. Chen, B. Zhang, Z. Gao, C. Chen, S. Zhao, Y. Qin, *Functionalization of multiwalled carbon nanotubes with uniform polyurea coatings by molecular layer deposition.* Carbon **82** (2015) 470-478. https://doi.org/10.1016/j.carbon.2014.10.090

[8] E.S. Eberhardt, R.T. Raines, *Amide-Amide and Amide-Water Hydrogen Bonds: Implications for Protein Folding and Stability.* J. Am. Chem. Soc. **116** (1994) 2149-2150. https://doi.org/10.1021/ja00084a067

[9] G.-Z. Jia, K.-M. Huang, L.-J. Yang, X.-Q. Yang, *Composition-Dependent Dielectric Properties of DMF-Water Mixtures by Molecular Dynamics Simulations.* Int. J. Mol. Sci. **10** (2009) 1590-1600. https://doi.org/10.3390/ijms10041590

[10] G.R. Desiraju, T. Steiner, *The Weak Hydrogen Bond in Structural Chemistry and Biology*. Oxford University Press, Oxford, UK, 1999.

[11] W.L. Jorgensen, C.J. Swenson, *Optimized intermolecular potential functions for amides and peptides. Structure and properties of liquid amides.* J. Am. Chem. Soc. **107** (1985) 569-578. https://doi.org/10.1021/ja00289a008

[12] J.A. Gonzalez, J.C. Cobos, I. García de la Fuente, *Thermodynamics of liquid mixtures containing a very strongly polar compound: Part 6. DISQUAC characterization of N,N-dialkylamides.* Fluid Phase Equilib. **224** (2004) 169-183. https://doi.org/10.1016/j.fluid.2004.02.007

[13] J.S. Rowlinson, F.L. Swinton, *Liquids and Liquid Mixtures*. 3rd Edition, Butterworths, G. B., 1982.

[14] J.A. González, I. García de la Fuente, J.C. Cobos, *Thermodynamics of mixtures with strongly negative deviations from Raoult's Law: Part 4. Application of the DISQUAC model to mixtures of 1-alkanols with primary or secondary linear amines. Comparison with Dortmund UNIFAC and ERAS results.* Fluid Phase Equilib. **168** (2000) 31-58. https://doi.org/10.1016/S0378-3812(99)00326-X

[15] U. Domańska, M. Marciniak, *Volumetric and Solid + Liquid Equilibrium Data for Linear 1-Alkanol + Decylamine Mixtures. Analysis in Terms of ERAS, DISQUAC, and Modified UNIFAC†.* Ind. Eng. Chem. Res. **43** (2004) 7647-7656. https://doi.org/10.1021/ie0401206

[16] F.F. Liew, T. Hasegawa, M. Fukuda, E. Nakata, T. Morii, *Construction of dopamine sensors by using fluorescent ribonucleopeptide complexes.* Bioorg. Med. Chem. **19** (2011) 4473-4481. https://doi.org/10.1016/j.bmc.2011.06.031

[17] J.M. Sonner, R.S. Cantor, *Molecular Mechanisms of Drug Action: An Emerging View.* Annu. Rev. Biophys. **42** (2013) 143-167. https://doi.org/10.1146/annurev-biophys-083012-130341

[18] D.L. Nelson, M.M. Cox, *Lehninger Principles of Biochemistry*. 3rd ed., Worth Publishing, New York, 2000.

[19] M. Götz, R. Reimert, S. Bajohr, H. Schnetzer, J. Wimberg, T.J.S. Schubert, *Long-term thermal stability of selected ionic liquids in nitrogen and hydrogen atmosphere.* Thermochim. Acta **600** (2015) 82-88. https://doi.org/10.1016/j.tca.2014.11.005

[20] P.S. Nikam, S.J. Kharat, *Excess Molar Volumes and Deviations in Viscosity of Binary Mixtures of N,N-Dimethylformamide with Aniline and Benzonitrile at (298.15, 303.15, 308.15, and 313.15) K.* J. Chem. Eng. Data **48** (2003) 972-976. https://doi.org/10.1021/je030101n

[21] T.E. Vittal Prasad, A. Adi Sankara Reddy, S. Kailash, D.H.L. Prasad, *Activity coefficients and excess Gibbs energy of binary mixtures of N,N-dimethyl formamide with selected compounds at 95.5 kPa.* Fluid Phase Equilib. **273** (2008) 52-58. https://doi.org/10.1016/j.fluid.2008.07.018

[22] R.S. Ramadevi, P. Venkatesu, M.V. Prabhakara Rao, M.R. Krishna, *Excess enthalpies of binary mixtures of N,N-dimethylformamide with substituted benzenes at 298.15 K.* Fluid Phase Equilib. **114** (1996) 189-197. https://doi.org/10.1016/0378-3812(95)02816-1

[23] A.B. de Haan, J. Gmehling, *Excess Enthalpies for Various Binary Mixtures with N-Methylacetamide or Acetic Anhydride.* J. Chem. Eng. Data **41** (1996) 474-478. https://doi.org/10.1021/je950294h

[24] M. Wieser, N. Holden, T.B. Coplen, J.K. Böhlke, M. Berglund, W.A. Brand, P. De Bièvre, G. M., R.D. Loss, J. Meija, T. Hirata, T. Prohaska, R. Schoenberg, G. O'Connor,

T. Walczyk, S. Yoneda, Z. X-K, *Atomic weights of the elements 2011 (IUPAC Technical Report).* Pure Appl. Chem. **85** (2013) 1047-1078. https://doi.org/10.1351/PAC-REP-13-03-02

[25] J.A. González, I. Alonso, I. Mozo, I. García de la Fuente, J.C. Cobos, *Thermodynamics of (ketone + amine) mixtures. Part VI. Volumetric and speed of sound data at (293.15, 298.15, and 303.15) K for (2-heptanone + dipropylamine, +dibutylamine, or +triethylamine) systems.* J. Chem. Thermodyn. **43** (2011) 1506-1514. https://doi.org/10.1016/j.jct.2011.05.003

[26] D. Schneditz, T. Kenner, H. Heimel, H. Stabinger, *A sound-speed sensor for the measurement of total protein concentration in disposable, blood-perfused tubes.* J. Acoust. Soc. Am. **86** (1989) 2073-2080. https://doi.org/10.1121/1.398466

[27] E. Junquera, G. Tardajos, E. Aicart, *Speeds of sound and isentropic compressibilities of (cyclohexane + benzene and (1-chlorobutane + n-hexane or n-heptane or n-octane or n-decane) at 298.15 K.* J. Chem. Thermodyn. **20** (1988) 1461-1467. https://doi.org/10.1016/0021-9614(88)90041-9

[28] K. Tamura, K. Ohomuro, S. Murakami, *Speeds of sound, isentropic and isothermal compressibilities, and isochoric heat capacities of {xc-C6H12+(1−x)C6H6}, x{CCl4+(1−x)C6H6}, and x{C7H16+(1−x)C6H6} at 298.15 K.* J. Chem. Thermodyn. **15** (1983) 859-868. https://doi.org/10.1016/0021-9614(83)90092-7

[29] K. Tamura, S. Murakami, *Speeds of sound, isentropic and isothermal compressibilities, and isochoric heat capacities of {xc-C6H12 + (1 − x)C6H6} from 293.15 to 303.15 K.* J. Chem. Thermodyn. **16** (1984) 33-38. https://doi.org/10.1016/0021-9614(84)90072-7

[30] K.N. Marsh, *Recommended reference materials for the realization of physicochemical properties.* Blackwell Scientific Publications, Oxford, UK, 1987.

[31] G.C. Benson, C.J. Halpin, A.J. Treszczanowicz, *Excess volumes and isentropic compressibilities for (2-ethoxyethanol + n-heptane) at 298.15 K.* J. Chem. Thermodyn. **13** (1981) 1175-1183. https://doi.org/10.1016/0021-9614(81)90017-3

[32] G. Douhéret, M.I. Davis, J.C.R. Reis, M.J. Blandamer, *Isentropic Compressibilities—Experimental Origin and the Quest for their Rigorous Estimation in Thermodynamically Ideal Liquid Mixtures.* ChemPhysChem **2** (2001) 148-161. https://doi.org/10.1002/1439-7641(20010316)2:3<148::AID-CPHC148>3.0.CO;2-J

[33] G. Douhéret, C. Moreau, A. Viallard, *Excess thermodynamic quantities in binary systems of non electrolytes.: Different ways of calculating excess compressibilities.* Fluid Phase Equilib. **22** (1985) 277-287. https://doi.org/10.1016/0378-3812(85)87027-8

[34] J.C.R. Reis, I.M.S. Lampreia, Â.F.S. Santos, M.L.C.J. Moita, G. Douhéret, *Refractive Index of Liquid Mixtures: Theory and Experiment.* ChemPhysChem **11** (2010) 3722-3733. https://doi.org/10.1002/cphc.201000566

[35] P.R. Bevington, *Data Reduction and Error Analysis for the Physical Sciences.* McGraw-Hill, New York, 1969.

[36] J. Lobos, I. Mozo, M. Fernández Regúlez, J.A. González, I. García de la Fuente, J.C. Cobos, *Thermodynamics of Mixtures Containing a Strongly Polar Compound. 8. Liquid−Liquid Equilibria for N,N-Dialkylamide + Selected N-Alkanes.* J. Chem. Eng. Data **51** (2006) 623-627. https://doi.org/10.1021/je050428j

[37] M. Rogalski, R. Stryjek, *Mutual solubility of binary n-hexadecane and polar compound systems.* Bull. Acad. Pol. Sci., Ser. Sci. Chim. **28** (1980) 139-147.

[38] R.C. Reid, J.M. Prausnitz, B.E. Poling, *The Properties of Gases and Liquids.* McGraw-Hill, New York, US, 1987.

[39] E. Matteoli, L. Lepori, A. Spanedda, *Thermodynamic study of heptane + amine mixtures: I. Excess and solvation enthalpies at 298.15 K.* Fluid Phase Equilib. **212** (2003) 41-52. https://doi.org/10.1016/S0378-3812(03)00260-7

[40] E. Matteoli, P. Gianni, L. Lepori, *Thermodynamic study of heptane + secondary, tertiary and cyclic amines mixtures. Part IV. Excess and solvation enthalpies at 298.15 K.* Fluid Phase Equilib. **306** (2011) 234-241. https://doi.org/10.1016/j.fluid.2011.04.013

[41] D. Patterson, *Free Volume and Polymer Solubility. A Qualitative View.* Macromolecules **2** (1969) 672-677. https://doi.org/10.1021/ma60012a021

[42] S.N. Bhattacharyya, M. Costas, D. Patterson, H.V. Tra, *Thermodynamics of mixtures containing alkanes.* Fluid Phase Equilib. **20** (1985) 27-45. https://doi.org/10.1016/0378-3812(85)90019-6

[43] L. Lepori, P. Gianni, E. Matteoli, *The Effect of the Molecular Size and Shape on the Volume Behavior of Binary Liquid Mixtures. Branched and Cyclic Alkanes in Heptane at 298.15 K.* J. Solution Chem. **42** (2013) 1263-1304. https://doi.org/10.1007/s10953-013-0023-9

[44] A.J. Treszczanowicz, G.C. Benson, *Excess volumes for n-alkanols + n-alkanes II. Binary mixtures of n-pentanol, n-hexanol, n-octanol, and n-decanol + n-heptane.* J. Chem. Thermodyn. **10** (1978) 967-974. https://doi.org/10.1016/0021-9614(78)90058-7

[45] L. Lepori, P. Gianni, A. Spanedda, E. Matteoli, *Thermodynamic study of (heptane + amine) mixtures. II. Excess and partial molar volumes at 298.15 K.* J. Chem. Thermodyn. **43** (2011) 805-813. https://doi.org/10.1016/j.jct.2010.12.025

[46] L. Lepori, P. Gianni, A. Spanedda, E. Matteoli, *Thermodynamic study of (heptane + amine) mixtures. III: Excess and partial molar volumes in mixtures with secondary, tertiary, and cyclic amines at 298.15 K.* J. Chem. Thermodyn. **43** (2011) 1453-1462. https://doi.org/10.1016/j.jct.2011.04.017

[47] T.M. Letcher, *Thermodynamics of aliphatic amine mixtures I. The excess volumes of mixing for primary, secondary, and tertiary aliphatic amines with benzene and substituted benzene compounds.* J. Chem. Thermodyn. **4** (1972) 159-173. https://doi.org/10.1016/S0021-9614(72)80021-1

[48] S. Villa, N. Riesco, I. García de la Fuente, J.A. González, J.C. Cobos, *Thermodynamics of mixtures with strongly negative deviations from Raoult's law: Part 5. Excess molar volumes at 298.15 K for 1-alkanols+dipropylamine systems: characterization in terms of the ERAS model.* Fluid Phase Equilib. **190** (2001) 113-125. https://doi.org/10.1016/S0378-3812(01)00595-7

[49] S. Villa, N. Riesco, I. García de la Fuente, J.A. González, J.C. Cobos, *Thermodynamics of mixtures with strongly negative deviations from Raoult's law. Part 8. Excess molar volumes at 298.15 K for 1-alkanol + isomeric amine (C6H15N) systems: Characterization in terms of the ERAS model.* Fluid Phase Equilib. **216** (2004) 123-133. https://doi.org/10.1016/j.fluid.2003.10.008

[50] H. Ohji, H. Ogawa, S. Murakami, K. Tamura, J.-P.E. Grolier, *Excess volumes and excess thermal expansivities for binary mixtures of 2-ethoxyethanol with non-polar solvents at temperatures between 283.15 K and 328.15 K.* Fluid Phase Equilib. **156** (1999) 101-114. https://doi.org/10.1016/S0378-3812(99)00035-7

[51] O. Hiroyuki, *Excess volumes of (1-pentanol + cyclohexane or benzene) at temperatures between 283.15 K and 328.15 K.* J. Chem. Thermodyn. **34** (2002) 849-859. https://doi.org/10.1006/jcht.2001.0940

[52] M.F. Bolotnikov, Y.A. Neruchev, Y.F. Melikhov, V.N. Verveyko, M.V. Verveyko, *Temperature Dependence of the Speed of Sound, Densities, and Isentropic Compressibilities of Hexane + Hexadecane in the Range of (293.15 to 373.15) K.* J. Chem. Eng. Data **50** (2005) 1095-1098. https://doi.org/10.1021/je050060q

[53] L. Venkatramana, R.L. Gardas, K. Sivakumar, K. Dayananda Reddy, *Thermodynamics of binary mixtures: The effect of substituents in aromatics on their excess properties with benzylalcohol.* Fluid Phase Equilib. **367** (2014) 7-21. https://doi.org/10.1016/j.fluid.2014.01.019

[54] I. Alonso, V. Alonso, I. Mozo, I. García de la Fuente, J.A. González, J.C. Cobos, *Thermodynamics of Ketone + Amine Mixtures. I. Volumetric and Speed of Sound Data at (293.15, 298.15, and 303.15) K for 2-Propanone + Aniline, + N-Methylaniline, or + Pyridine Systems.* J. Chem. Eng. Data **55** (2010) 2505-2511. https://doi.org/10.1021/je900874z

[55] K. Tamura, A. Osaki, S. Murakami, B. Laurent, J.-P.E. Grolier, *Thermodynamic properties of binary mixtures {x(2-alkoxyethanol)+(1−x)n-octane}: densities at 298.15 and 303.15 K and speeds of sound at 298.15 K.* Fluid Phase Equilib. **173** (2000) 285-296. https://doi.org/10.1016/S0378-3812(00)00434-9

[56] E.B. Bagley, T.P. Nelson, J.W. Barlow, S.A. Chen, *Internal Pressure Measurements and Liquid-State Energies.* Ind. Eng. Chem. Fundamen. **9** (1970) 93-97. https://doi.org/10.1021/i160033a015

[57] E.B. Bagley, T.P. Nelson, J.M. Scigliano, *Internal pressures of liquids and their relation to the enthalpies and entropies of mixing in nonelectrolyte solutions.* J. Phys. Chem. **77** (1973) 2794-2798. https://doi.org/10.1021/j100641a016

[58] M.R.J. Dack, *Solvent structure. The use of internal pressure and cohesive energy density to examine contributions to solvent-solvent interactions.* Aust. J. Chem. **28** (1975) 1643-1648. https://doi.org/10.1071/CH9751643

[59] E. Zorebski, *Internal pressure studies of alcohols on the basis of ultrasonic measurements.* Mol. Quantum Acoust. **26** (2005) 317–326.

[60] R. Dey, A.K. Singh, J.D. Pandey, *A new theoretical approach for estimating excess internal pressure.* J. Mol. Liq. **124** (2006) 121-123. https://doi.org/10.1016/j.molliq.2005.09.005

[61] O. Nomoto, *Molecular Sound Velocity and Molecular Compressibility of Liquid Mixtures.* J. Chem. Phys. **21** (1953) 950-951. https://doi.org/10.1063/1.1699084

[62] O. Nomoto, *Deviation from Linearity of the Concentration Dependence of the Molecular Sound Velocity in Liquid Mixtures.* J. Phys. Soc. Jpn. **13** (1958) 1524-1528. https://doi.org/10.1143/JPSJ.13.1524

[63] R. Abraham, M. Abdulkhadar, C.V. Asokan, *Ultrasonic investigation of molecular interaction in binary mixtures of nitriles with methanol/toluene.* J. Chem. Thermodyn. **32** (2000) 1-16. https://doi.org/10.1006/jcht.1999.0608

[64] S.L. Oswal, P. Oswal, J.P. Dave, *Speed of sound and isentropic compressibility of binary mixtures containing alkyl acetate or ethyl alkanoate, or ethyl bromo-alkanoate with hexane.* J. Mol. Liq. **94** (2001) 203-219. https://doi.org/10.1016/S0167-7322(01)00269-0

[65] A. Chelkowski, *Dielectric Physics*. Elsevier, Amsterdam, 1980.

[66] P. Brocos, A. Piñeiro, R. Bravo, A. Amigo, *Refractive indices, molar volumes and molar refractions of binary liquid mixtures: concepts and correlations.* Phys. Chem. Chem. Phys. **5** (2003) 550-557. https://doi.org/10.1039/B208765K

[67] D. Keshapolla, V. Singh, R.L. Gardas, *Volumetric, acoustic and transport properties of binary mixtures of benzyldimethylammonium based ionic liquids with N,N-dimethylformamide at temperature from 293.15 to 328.15 K.* J. Mol. Liq. **199** (2014) 330-338. https://doi.org/10.1016/j.molliq.2014.09.030

[68] I. Alonso, I. Mozo, I.G. de la fuente, J.A. González, J.C. Cobos, *Thermodynamics of ketone + amine mixtures Part IV. Volumetric and speed of sound data at (293.15; 298.15 and 303.15 K) for 2-butanone +dipropylamine, +dibutylamine or +triethylamine systems.* Thermochim. Acta **512** (2011) 86-92. https://doi.org/10.1016/j.tca.2010.09.004

[69] M. Domínguez, H. Artigas, P. Cea, M.C. López, J.S. Urieta, *Speed of sound and isentropic compressibility of the ternary mixture (2-Butanol + n-Hexane + 1-Butylamine) and the constituent binary mixtures at 298.15 K and 313.15 K.* J. Mol. Liq. **88** (2000) 243-258. https://doi.org/10.1016/S0167-7322(00)00143-4

[70] P. Góralski, M. Wasiak, A. Bald, *Heat Capacities, Speeds of Sound, and Isothermal Compressibilities of Some n-Amines and Tri-n-amines at 298.15 K.* J. Chem. Eng. Data **47** (2002) 83-86. https://doi.org/10.1021/je010206v

[71] S.L. Oswal, P. Oswal, R.L. Gardas, S.G. Patel, R.G. Shinde, *Acoustic, volumetric, compressibility and refractivity properties and reduction parameters for the ERAS and Flory models of some homologous series of amines from 298.15 to 328.15 K.* Fluid Phase Equilib. **216** (2004) 33-45. https://doi.org/10.1016/j.fluid.2003.09.007

[72] Neeti, S.K. Jangra, J.S. Yadav, Dimple, V.K. Sharma, *Thermodynamic investigations of ternary o-toluidine + tetrahydropyran + N,N-dimethylformamide mixture and its binaries at 298.15, 303.15 and 308.15 K.* J. Mol. Liq. **163** (2011) 36-45. https://doi.org/10.1016/j.molliq.2011.07.008

[73] J.A. Riddick, W.B. Bunger, T.K. Sakano, *Organic solvents: physical properties and methods of purification.* Wiley, New York, 1986.

[74] S. Miyanaga, K. Tamura, S. Murakami, *Excess molar volumes, isentropic and isothermal compressibilities, and isochoric heat capacities of (acetonitrile + benzene), (benzene + dimethylformamide), and (acetonitrile + dimethylformamide) at the temperature 298.15 K.* J. Chem. Thermodyn. **24** (1992) 1077-1086. https://doi.org/10.1016/S0021-9614(05)80018-7

[75] M.S. AlTuwaim, K.H.A.E. Alkhaldi, A.S. Al-Jimaz, A.A. Mohammad, *Comparative study of physico-chemical properties of binary mixtures of N,N-dimethylformamide with 1-alkanols at different temperatures.* J. Chem. Thermodyn. **48** (2012) 39-47. https://doi.org/10.1016/j.jct.2011.12.002

[76] J.P.E. Grolier, G. Roux-Desgranges, M. Berkane, E. Jiménez, E. Wilhelm, *Heat capacities and densities of mixtures of very polar substances 2. Mixtures containing N, N-dimethylformamide.* J. Chem. Thermodyn. **25** (1993) 41-50. https://doi.org/10.1006/jcht.1993.1005

[77] J. Konicek, I. Wadso, *Thermochemical Properties of Some Carboxylic Acids, Amines and N-Substituted Amides in Aqueous Solution.* Acta Chem. Scand. **25** (1971) 1541-1551. https://doi.org/10.3891/acta.chem.scand.25-1541

[78] H. Iloukhani, Z. Rostami, *Measurement of Some Thermodynamic and Acoustic Properties of Binary Solutions of N,N-Dimethylformamide with 1-Alkanols at 30°C and Comparison with Theories.* J. Solution Chem. **32** (2003) 451-462. https://doi.org/10.1023/A:1024524928767

[79] C.M. Kinart, W.J. Kinart, D. Chęcińska-Majak, *Relative Permittivity, Viscosity, and Speed of Sound for 2-Methoxyethanol + Butylamine Mixtures.* J. Chem. Eng. Data **48** (2003) 1037-1039. https://doi.org/10.1021/je030127e

[80] T.M. Aminabhavi, V.B. Patil, *Density, Viscosity, Refractive Index, and Speed of Sound in Binary Mixtures of Ethenylbenzene with N,N-Dimethylacetamide, Tetrahydrofuran, N,N-Dimethylformamide, 1,4-Dioxane, Dimethyl Sulfoxide, Chloroform, Bromoform, and 1-Chloronaphthalene in the Temperature Interval (298.15−308.15) K.* J. Chem. Eng. Data **43** (1998) 497-503. https://doi.org/10.1021/je980031y

Supporting information for:

Thermodynamics of amide + amine mixtures. 1. Volumetric, speed of sound and refractive index data for *N*,*N*-dimethylformamide + *N*-propylpropan-1-amine, + *N*-butylbutan-1-amine, + butan-1-amine, or + hexan-1-amine systems at several temperatures

Fernando Hevia, Ana Cobos, Juan Antonio González*, Isaías García de la Fuente, Luis Felipe Sanz

G.E.T.E.F., Departamento de Física Aplicada, Facultad de Ciencias, Universidad de Valladolid, Paseo de Belén, 7, 47011 Valladolid, Spain

*e-mail: jagl@termo.uva.es; Tel: +34 983 423757

Reference of the article:

F. Hevia, A. Cobos, J.A. González, I. García de la Fuente, L.F. Sanz. J. Chem. Eng. Data **61** (2016) 1468-1478. https://doi.org/10.1021/acs.jced.5b00802.

Table S1. Excess molar volumes, V_m^E, for DMF (1) + amine (2) mixtures at temperature T and pressure p = 0.1 MPa. [a]

x_1	V_m^E /cm^3·mol^{-1}	x_1	V_m^E /cm^3·mol^{-1}
	DMF (1) + DPA (2) ; T/ K = 293.15 K		
0.0600	−0.0724	0.4974	−0.2847
0.1071	−0.1116	0.5487	−0.2869
0.1560	−0.1539	0.6562	−0.2787
0.1975	−0.1765	0.7514	−0.2413
0.2490	−0.1986	0.8216	−0.2017
0.3099	−0.2341	0.8501	−0.1875
0.3463	−0.2397	0.9025	−0.1447
0.3985	−0.2621	0.9486	−0.0800
0.4480	−0.2741		
	DMF (1) + DPA (2) ; T/ K = 298.15 K		
0.0626	−0.0642	0.5386	−0.2917
0.1083	−0.1137	0.6082	−0.2889
0.1544	−0.1435	0.6527	−0.2826
0.2541	−0.2120	0.7477	−0.2549
0.3148	−0.2333	0.8063	−0.2244
0.3609	−0.2569	0.9020	−0.1378
0.4077	−0.2782	0.9482	−0.0828
0.4966	−0.2895		
	DMF (1) + DPA (2) ; T/ K = 303.15 K		
0.0453	−0.0626	0.5415	−0.3027
0.1034	−0.1218	0.6016	−0.2975
0.1963	−0.1857	0.6517	−0.2908
0.2582	−0.2163	0.7502	−0.2558
0.3559	−0.2677	0.8498	−0.1931
0.4099	−0.2877	0.9000	−0.1465
0.4565	−0.2954	0.9498	−0.0838
	DMF (1) + DBA (2) ; T/ K = 298.15 K		
0.0642	0.0070	0.5996	0.0009
0.1134	0.0128	0.6514	−0.0120
0.1647	0.0184	0.7904	−0.0330
0.2121	0.0255	0.8418	−0.0360
0.3213	0.0307	0.8921	−0.0340
0.5072	0.0153	0.9471	−0.0255
	DMF (1) + BA (2) ; T/ K = 293.15 K		
0.0599	−0.0476	0.5483	−0.2483

0.1056	−0.0798	0.6569	−0.2449
0.1591	−0.1094	0.6999	−0.2320
0.2505	−0.1610	0.7537	−0.2128
0.3017	−0.1860	0.8036	−0.1858
0.3583	−0.2066	0.8579	−0.1587
0.3992	−0.2259	0.9048	−0.1102
0.5059	−0.2465	0.9546	−0.0587
	DMF (1) + BA (2) ; T/ K = 298.15 K		
0.0575	−0.0571	0.4381	−0.2497
0.1092	−0.0938	0.5028	−0.2615
0.1519	−0.1227	0.6005	−0.2643
0.2043	−0.1598	0.6934	−0.2613
0.2448	−0.1770	0.7572	−0.2322
0.3090	−0.2080	0.8056	−0.2033
0.3558	−0.2287	0.9076	−0.1223
0.3986	−0.2454	0.9553	−0.0651
	DMF (1) + BA (2) ; T/ K = 303.15 K		
0.0505	−0.0522	0.5281	−0.2698
0.1477	−0.1338	0.6056	−0.2704
0.2019	−0.1675	0.6960	−0.2574
0.2410	−0.1816	0.7558	−0.2289
0.3024	−0.2108	0.8006	−0.2107
0.3558	−0.2335	0.8544	−0.1664
0.4358	−0.2533	0.8998	−0.1251
0.5114	−0.2621	0.9466	−0.0748
	DMF (1) + HxA (2) ; T/ K = 298.15 K		
0.0506	0.0039	0.6022	−0.0387
0.0992	0.0086	0.7056	−0.0516
0.1725	0.0112	0.7996	−0.0554
0.2548	0.0070	0.8492	−0.0541
0.3476	−0.0015	0.8982	−0.0439
0.4461	−0.0126	0.9530	−0.0256
0.5500	−0.0281		

[a] The standard uncertainties are: $u(x_1) = 0.0008$; $u(p) = 1$ kPa; $u(T) = 0.02$ K. The relative combined expanded standard uncertainty (0.95 level of confidence) is: $U_{rc}(V_m^E) = 0.025$.

Table S2. Isobaric thermal expansion coefficient, α_p, and the corresponding excess function, α_p^{E}, at temperature $T = 298.15$ K and pressure $p = 0.1$ MPa, of DMF (1) + amine (2) mixtures. [a]

x_1	ϕ_1	α_p [b] /10^{-3}K^{-1}	$\left(\frac{\partial\rho}{\partial T}\right)_p$ /kg m^{-3} K^{-1}	r[c]	α_p^{E} /10^{-6}K^{-1}
			DMF (1) + DPA(2)		
0.0626	0.0361	1.228	− 0.910953	0.999977	− 4
0.1083	0.0638	1.220	− 0.912081	0.999966	− 5
0.1544	0.0930	1.211	− 0.913352	0.999961	− 7
0.2541	0.1605	1.192	− 0.916600	0.999965	− 11
0.3148	0.2050	1.181	− 0.918932	0.999973	− 11
0.3609	0.2407	1.172	− 0.920886	0.999980	− 12
0.4077	0.2787	1.162	− 0.923030	0.999986	− 13
0.4966	0.3564	1.144	− 0.927515	0.999993	− 13
0.5386	0.3959	1.135	− 0.929800	0.999994	− 13
0.6082	0.4656	1.120	− 0.933767	0.999995	− 12
0.6527	0.5134	1.109	− 0.936379	0.999994	− 12
0.7477	0.6245	1.086	− 0.941942	0.999989	− 9
0.8063	0.7003	1.070	− 0.945181	0.999983	− 8
0.9020	0.8378	1.042	− 0.949609	0.999975	− 4
0.9482	0.9113	1.027	− 0.951097	0.999978	− 2
			DMF (1) + BA(2)		
0.0575	0.0452	1.283	− 0.952253	1.000000	− 14
0.1092	0.0868	1.262	− 0.948543	0.999999	− 23
0.1519	0.1219	1.248	− 0.947139	0.999998	− 26
0.2043	0.1660	1.232	− 0.947004	0.999995	− 29
0.2448	0.2008	1.221	− 0.947790	0.999993	− 29
0.3090	0.2574	1.205	− 0.950026	0.999988	− 28
0.3558	0.2998	1.193	− 0.952015	0.999983	− 27
0.3986	0.3394	1.183	− 0.953824	0.999978	− 25
0.4381	0.3767	1.173	− 0.955318	0.999972	− 24
0.5028	0.4394	1.156	− 0.957074	0.999959	− 22
0.6005	0.5382	1.128	− 0.957395	0.999931	− 20
0.6934	0.6368	1.098	− 0.954824	0.999901	− 20
0.7572	0.7074	1.076	− 0.951809	0.999886	− 21
0.8056	0.7626	1.059	− 0.949272	0.999885	− 21
0.9076	0.8839	1.027	− 0.945455	0.999929	− 16
0.9553	0.9431	1.014	− 0.945764	0.999968	− 11

[a] The standard uncertainties are: $u(x_1) = 0.0008$; $u(p) = 1$ kPa; $u(T) = 0.02$ K. The relative combined expanded standard uncertainty (0.95 level of confidence) is $U_{\mathrm{rc}}(\alpha_p^{\mathrm{E}}) = 0.05$. [b] Density values at 293.15 and 303.15 K at the mole fractions reported at 298.15 K were obtained from the corresponding Redlich-Kister adjustments for $V_{\mathrm{m}}^{\mathrm{E}}$. [c] Regression coefficients (absolute values) obtained when fitting densities against temperature, assuming a linear dependence between the two quantities.

Table S3. Excess functions, at temperature T = 298.15 K and pressure p = 0.1 MPa, for κ_S, adiabatic compressibility, and c, speed of sound, of DMF (1) + amine (2) mixtures. [a]

x_1	κ_S^E /TPa^{-1}	c^E /m·s^{-1}	x_1	κ_S^E /TPa^{-1}	c^E /m·s^{-1}
		DMF (1) + DPA (2)			
0.0626	− 8.5	5.1	0.5386	− 49.1	39.3
0.1083	− 14.5	8.8	0.6082	− 50.5	42.9
0.1544	− 19.8	12.4	0.6527	− 50.3	44.6
0.2541	− 30.3	19.9	0.7477	− 46.7	45.6
0.3148	− 35.7	24.5	0.8063	− 41.5	43.6
0.3609	− 39.4	27.7	0.9020	− 26.7	32.0
0.4077	− 42.9	31.1	0.9482	− 15.9	20.4
0.4966	− 47.7	36.9			
		DMF (1) + DBA (2)			
0.0642	− 2.3	1.7	0.5574	− 19.4	17.5
0.1134	− 4.1	3.1	0.5996	− 20.2	18.8
0.1647	− 5.9	4.5	0.6514	− 21.4	20.5
0.2121	− 7.5	5.9	0.6869	− 21.6	21.3
0.2734	− 9.9	7.9	0.7361	− 21.8	22.4
0.3213	− 11.5	9.4	0.7904	− 21.2	22.9
0.4114	− 14.8	12.4	0.8418	− 19.5	22.3
0.4526	− 16.2	13.9	0.8921	− 16.2	19.6
0.5072	− 17.8	15.7	0.9471	− 9.9	13.0
		DMF (1) + BA (2)			
0.0575	− 8.2	5.6	0.4381	− 40.2	34.7
0.1092	− 14.6	10.3	0.5028	− 41.9	37.8
0.1519	− 19.4	14.1	0.6005	− 42.1	40.9
0.2043	− 24.6	18.4	0.6934	− 39.2	40.9
0.2448	− 28.3	21.6	0.7572	− 35.0	38.6
0.3090	− 33.3	26.5	0.8056	− 30.7	35.3
0.3558	− 36.4	29.8	0.9076	− 17.4	22.1
0.3986	− 38.8	32.6	0.9553	− 9.1	12.2
		DMF (1) + HxA (2)			
0.0506	− 1.5	1.3	0.6022	− 14.8	15.5
0.0992	− 2.9	2.6	0.7056	− 15.3	17.0
0.1725	− 5.0	4.5	0.7996	− 13.9	16.5
0.2548	− 7.4	6.8	0.8492	− 12.2	15.1
0.3476	− 9.8	9.3	0.8982	− 9.5	12.2
0.4461	− 12.2	11.9	0.9530	− 5.2	7.1
0.5500	− 14.2	14.5			

[a] The standard uncertainties, u, are: $u(x_1) = 0.0008$; $u(p) = 1$ kPa; $u(T) = 0.02$ K. The combined expanded standard uncertainties (0.95 level of confidence) are: $U_{rc}(c^E) = 0.0015$; $U_{rc}(\kappa_S^E) = 0.05$.

Table S4. Excess refractive indices, $n_{\mathrm{D}}^{\mathrm{E}}$, of DMF (1) + amine (2) mixtures at temperature T and pressure $p = 0.1$ MPa. [a]

x_1	$n_{\mathrm{D}}^{\mathrm{E}}$	x_1	$n_{\mathrm{D}}^{\mathrm{E}}$
	DMF (1) + DPA (2) ; T/ K = 293.15 K		
0.0600	0.00019	0.5487	0.00142
0.1556	0.00045	0.6018	0.00146
0.2614	0.00081	0.7033	0.00143
0.3463	0.00102	0.8216	0.00115
0.3985	0.00118	0.8844	0.00089
0.4554	0.00126	0.9486	0.00056
	DMF (1) + DPA (2) ; T/ K = 298.15 K		
0.0626	0.00022	0.4966	0.00144
0.1083	0.00046	0.6527	0.00147
0.1544	0.00052	0.7477	0.00136
0.2541	0.00088	0.8063	0.00120
0.3148	0.00102	0.9020	0.00083
0.3609	0.00117	0.9482	0.00053
0.4077	0.00123		
	DMF (1) + DPA (2) ; T/ K = 303.15 K		
0.0453	0.00017	0.6016	0.00158
0.1034	0.00041	0.7502	0.00149
0.1963	0.00080	0.8498	0.00114
0.2582	0.00088	0.9000	0.00089
0.3559	0.00116	0.9498	0.00046
0.4099	0.00128		
	DMF (1) + DBA (2) ; T/ K = 298.15 K		
0.1038	−0.00002	0.7709	0.00023
0.2076	−0.00003	0.8398	0.00026
0.3608	−0.00001	0.8989	0.00023
0.4897	0.00004	0.9497	0.00016
0.5933	0.00011	0.9738	0.00010
0.6880	0.00018		
	DMF (1) + BA (2) ; T/ K = 293.15 K		
0.0599	0.00019	0.5059	0.00128
0.1056	0.00034	0.6043	0.00137
0.1591	0.00051	0.6569	0.00135
0.2010	0.00066	0.6999	0.00131
0.2505	0.00078	0.7537	0.00119
0.3017	0.00093	0.8036	0.00106

0.3583	0.00107	0.8579	0.00087
0.3992	0.00114	0.9048	0.00064
0.4401	0.00120	0.9546	0.00033
	DMF (1) + BA (2) ; T/ K = 298.15 K		
0.0575	0.00020	0.6005	0.00136
0.1092	0.00039	0.6608	0.00133
0.1519	0.00052	0.6934	0.00128
0.2043	0.00068	0.7572	0.00117
0.2448	0.00079	0.8056	0.00103
0.3090	0.00099	0.8546	0.00081
0.3558	0.00109	0.9076	0.00057
0.5028	0.00134	0.9553	0.00030
	DMF (1) + BA (2) ; T/ K = 303.15 K		
0.0505	0.00020	0.5281	0.00147
0.1477	0.00057	0.6056	0.00146
0.2019	0.00075	0.6574	0.00142
0.2410	0.00092	0.6960	0.00136
0.3024	0.00107	0.7558	0.00127
0.3558	0.00117	0.8006	0.00113
0.3992	0.00126	0.8544	0.00093
0.4358	0.00134	0.8998	0.00069
0.5114	0.00146	0.9466	0.00040
	DMF (1) + HxA (2) ; T/ K = 298.15 K		
0.0506	−0.00002	0.5500	0.00008
0.1725	−0.00006	0.6558	0.00020
0.2548	−0.00007	0.7573	0.00025
0.3476	−0.00004	0.8492	0.00026
0.4461	0.00002	0.9530	0.00015

[a] The standard uncertainties, u, are: $u(x_1) = 0.0008$; $u(T) = 0.03$ K; $u(p) = 1$ kPa. The relative combined expanded standard uncertainty (0.95 level of confidence), U_{rc}, is: $U_{rc}(n_D^E) = 0.04$.

Thermodynamics of amide + amine mixtures. 2. Volumetric, speed of sound and refractive index data for *N,N*-dimethylacetamide + *N*-propylpropan-1-amine, + *N*-butylbutan-1-amine, + butan-1-amine, or + hexan-1-amine systems at several temperatures

Fernando Hevia, Ana Cobos, Juan Antonio González*, Isaías García de la Fuente, Víctor Alonso

G.E.T.E.F., Departamento de Física Aplicada, Facultad de Ciencias, Universidad de Valladolid, Paseo de Belén, 7, 47011 Valladolid, Spain

*e-mail: jagl@termo.uva.es; Tel: +34 983 423757

Abstract

Data on density, ρ, speed of sound, c, and refractive index, n_D, of binary systems containing *N,N*-dimethylacetamide (DMA) + *N*-propylpropan-1-amine (DPA) or + butan-1-amine (BA) at 293.15 K, 298.15 K and 303.15 K, and + *N*-butylbutan-1-amine (DBA) or + hexan-1-amine (HxA) at 298.15 K are reported. A densimeter and sound analyzer Anton Paar DSA 5000 has been used for the measurement of ρ and c, whereas n_D values have been obtained by means of a refractometer RFM970 from Bellingham+Stanley. Also, values of excess molar volumes, V_m^E, excess isentropic compressibilities, κ_S^E, excess speeds of sound, c^E, excess isobaric thermal expansion coefficients, α_p^E, and of excess refractive indices, n_D^E, have been determined from these data. The investigated systems are characterized by amide-amine interactions and structural effects, as it is shown by their negative or low positive V_m^E values and by the results from the application of the Prigogine-Flory-Patterson (PFP) model. The breaking of amine-amine interactions is more relevant in systems containing linear primary amines than in those with linear secondary amines, and the V_m^E values are lower for the latter systems. Molar refraction has been used to evaluate the dispersive interactions in the mixtures under study, yielding the result that DPA and HxA systems present similar dispersive interactions and mainly differ in their dipolar character. Steric hindrance of the amide group in DMA leads to weaker amide-amine interactions than in the corresponding *N,N*-dimethylformamide (DMF) + amine systems.

Adapted by permission from Springer Nature: Springer, Journal of Solution Chemistry. F. Hevia, A. Cobos, J.A. González, I. García de la Fuente, V. Alonso, *Thermodynamics of amide + amine mixtures. 2. Volumetric, speed of sound and refractive index data for N,N-dimethylacetamide + N-propylpropan-1-amine, + N-butylbutan-1-amine, + butan-1-amine, or + hexan-1-amine systems at several temperatures*, J. Solution Chem. **46** (2017) 150-174. https://doi.org/10.1007/s10953-016-0560-0.

1. Introduction

N,N-dimethylformamide (DMF) and *N,N*-dimethylacetamide (DMA) are very polar compounds (their dipole moment is 3.7 D [1, 2]) widely used in the industry, since they are aprotic protophilic substances with excellent donor-acceptor properties and solubility. In addition, they are employed for the separation of aromatic compounds and petroleum hydrocarbons. Amides are very common in nature and are found in proteins, RNA, DNA, amino acids, hormones and vitamins. The knowledge of liquid mixtures containing the amide functional group is necessary for a deeper understanding of more complex molecules, as those of biological interest [3]. Moreover, amides deserve to be investigated, as in pure state they show a significant local order [4]. In the case of *N,N*-dialkylamides, due to the absence of hydrogen bonds, this has been attributed to the existence of strong dipolar interactions [5].

Linear primary and secondary amines can form hydrogen bonds, appearing self-associated complexes and even heterocomplexes in mixtures with other associated compounds [6-8]. The amine group is also present in compounds of great biological significance. The proteins usually bound to DNA polymers contain various amine groups [9]. Histamine and dopamine are amines with the role of neurotransmitters [8, 10], and the breaking of amino acids releases amines. On the other hand, the ions of many ionic liquids used in technical applications are related to amines [11].

In earlier works, we have studied the thermodynamic properties of mixtures containing ketones and amines [12-19]. It is interesting to examine the effect of replacing a ketone, a moderately polar compound, by a more polar one, such as an amide. In our previous study [20], we have reported data on density, ρ, speed of sound, c, and refractive index, n_{D} of the binary systems DMF + *N*-propylpropan-1-amine (DPA) or + butan-1-amine (BA) at (293.15-303.15) K, and + *N*-butylbutan-1-amine (DBA) or + hexan-1-amine (HxA) at 298.15 K. Now, we continue this series of works by replacing DMF by DMA, and treating these systems by means of the Prigogine-Flory-Patterson (PFP) model [21]. A survey of literature data shows that there are no experimental data on the considered mixtures. Nevertheless, DMF, or DMA + aniline or pyridine mixtures have been investigated rather extensively, reporting calorimetric, volumetric, vapor-liquid equilibria, c, or n_{D} data [22-27]. Interestingly, at equimolar composition and 298.15 K, the excess molar enthalpies ($H_{\mathrm{m}}^{\mathrm{E}}$) of the DMF or DMA + aniline systems are, respectively, –2946 J·mol^{-1} [25] and –352 J·mol^{-1} [27], which underlines the importance of interactions between unlike molecules in such systems.

2. Experimental

2.1. Materials

Table 1 contains information about the source and the purity of the compounds, which have been used without further purification. Table 2 lists experimental values of ρ, c, n_{D}, thermal expansion coefficient, α_p, isentropic compressibility, κ_S, and isothermal compressibility, κ_T, for the pure compounds. Our values are in good agreement with the literature data.

2.2. Apparatus and procedure

Binary mixtures have been prepared by mass in small vessels of about 10 cm^3, using an analytical balance HR-202 (weighing accuracy 0.01 mg), with all weighings corrected for buoyancy effects. The standard uncertainty in the final mole fraction is estimated to be 0.0001. Molar quantities were calculated using the relative atomic mass Table of 2015 issued by the Commission on Isotopic Abundances and Atomic Weights (IUPAC) [28].

Temperatures were measured using Pt-100 resistances, calibrated according to the ITS-90 scale of temperature, against the triple point of water and the melting point of Ga. The standard uncertainty of the equilibrium temperature measurements is 0.01 K and 0.02 K for ρ and n_D measurements, respectively.

Densities and speeds of sound have been measured using a vibrating-tube densimeter and sound analyzer DSA 5000 from Anton Paar, which is automatically thermostated within 0.01 K. The calibration of the device has been described in a previous work [14]. The repeatability of the ρ measurements is 0.005 $kg{\cdot}m^{-3}$, whereas their overall standard uncertainty is $1 \cdot 10^{-2}$ $kg \cdot m^{-3}$. The determination of the speed of sound is based on the measurement of the time of propagation of short acoustic pulses, whose central frequency is 3 MHz [29], and which are transmitted repeatedly through the sample. The repeatability of these c measurements is 0.1 $m{\cdot}s^{-1}$ and their standard uncertainty is 0.2 $m{\cdot}s^{-1}$. The excess volume, V_m^E, and the excess speed of sound, c^E, of the system cyclohexane + benzene have been measured at (293.15-303.15) K to check the experimental technique. The experimental results and published values [30-32] are in good agreement. The standard uncertainty of V_m^E is $(0.010\left|V_{m,max}^E\right| + 0.005\ cm^3{\cdot}mol^{-1})$, where $\left|V_{m,max}^E\right|$ stands for the maximum absolute experimental value of V_m^E respect to the composition. The standard uncertainty of c^E is estimated to be 0.4 $m{\cdot}s^{-1}$.

A refractometer RFM970 from Bellingham+Stanley has been used for the n_D measurements. The technique is based on the optical detection of the critical angle at the wavelength of the sodium D line (589.3 nm). The temperature is controlled by means of Peltier modules and its stability is 0.02 K. The refractometer has been calibrated using 2,2,4-trimethylpentane and toluene at the working temperatures (293.15-303.15) K, as recommended by Marsh [33]. The repeatability of the measurements is 0.00004, and the standard uncertainty is 0.00008.

Table 1. Sample description.

Chemical	CAS number	Source	Purification method	Purity	Analysis method
N,N-dimethyacetamide (DMA)	127-19-5	Sigma-Aldrich	none	≥ 0.995	GC[a]
N-propylpropan-1-amine (DPA)	142-84-7	Aldrich	none	≥ 0.99	GC[a]
N-butylbutan-1-amine (DBA)	111-92-2	Aldrich	none	≥ 0.995	GC[a]
butan-1-amine (BA)	109-73-9	Sigma--Aldrich	none	≥ 0.995	GC[a]
hexan-1-amine (HxA)	111-26-2	Aldrich	none	≥ 0.995	GC[a]

[a] In mole fraction. [b] Gas Chromatography

Table 2. Physical properties of pure compounds at temperature T and pressure p = 0.1 MPa. [a]

Property	T/K	DMF	DPA	DBA	BA	HxA
ρ^* /g·cm^{-3}	293.15	0.94087	0.73778	0.75970	0.73705	0.76439
		0.940846 [63]	0.7375 [1]	0.759571 [17]	0.73712 [64]	0.7651 [65]
	298.15	0.93630	0.73322	0.75553	0.73233	0.76019
		0.936233 [63]]	0.73321 [66]	0.755457 [17]	0.73233 [64]	0.76013 [67]
	303.15	0.93169	0.72870	0.75146	0.72750	0.75589
		0.931618 [63]	0.729087 [17]	0.751329 [17]	0.72751 [64]	0.7562 [65]
c^*/m·s^{-1}	293.15	1475.1	1208.7	1261.1	1268.1	1323.9
			1209 [17]	1261.2 [17]		
	298.15	1455.7	1187.3	1241.5	1246.1	1303.8
		1455.37 [68]	1198 [70]	1248 [70]	1247.8 [71]	1304.7 [67]
		1458 [69]				
	303.15	1435.7	1166.7	1222.5	1224.5	1283.5
		1441 [72]	1174 [70]	1227 [70]	1227 [70]	1285 [70]
α_p^* /10^{-3}K^{-1}	298.15	0.980	1.239	1.090	1.304	1.119
		0.960 [73]	1.29 [1]	1.12 [1]	1.314 [70]	1.13 [67]
κ_S^* /TPa^{-1}	293.15	488.5	927.8	827.7	843.7	746.4
			926.5 [70]			
	298.15	504.0	967.5	858.7	879.4	773.9
		504.29 [68]	947 [70]	849 [70]	876.6 [71]	773 [67]
	303.15	520.7	1008.2	890.4	916.7	803.1
		516 [72]	992 [70]	883 [70]	912 [70]	800 [70]
κ_T^* /TPa^{-1}	298.15	653.5	1217.3	1059.4	1148.7	971.1
		671 [74]	1183 [70]	1039 [70]	1145 [70]	975 [67]
C_{pm}^* /J·mol^{-1}·K^{-1}	298.15	178.2 [75]	252.84 [1]	302 [70]	188 [76]	252 [76]
n_{D}^*	293.15	1.43814	1.40398		1.40059	
		1.4384 [1]	1.4043 [1]			
	298.15	1.43595	1.40135	1.41488	1.39789	1.41571
		1.4363 [69]	1.40132 [77]	1.4152 [1]	1.3987 [1]	1.4160 [70]
	303.15	1.43382	1.39871		1.39507	
		1.4342 [69]	1.4022 [70]		1.3978 [70]	

[a] ρ^*, density; c^*, speed of sound; α_p^*, isobaric thermal expansion coefficient; κ_S^*, adiabatic compressibility; κ_T^*, isothermal compressibility; C_{pm}^*, isobaric molar heat capacity; and n_{D}^*, refractive index. The standard uncertainties are: $u(T) = 0.01$ K (for n_D^* values, $u(T) = 0.02$ K); $u(p) = 1$ kPa; $u(c^*) = 0.2$ m·s^{-1}; $u(\rho^*) = 0.00005$ g·cm^{-3}; $u(n_D^*) = 0.00008$ and (relative values) $u_{\mathrm{r}}(\alpha_p^*) = 0.015$; $u_{\mathrm{r}}(\kappa_S^*) = 0.002$; $u_{\mathrm{r}}(\kappa_T^*) = 0.012$.

3. Equations

The experimental values of ρ, molar volume, V_{m}, α_p, and κ_S, can be obtained by means of a densimeter and sound analyzer rather directly. The values of $\alpha_p = -(1/\rho)(\partial\rho/\partial T)_p$ have been calculated under the assumption that ρ depends linearly on T in the range of temperatures

considered. Moreover, as long as it is possible to neglect the dispersion and absorption of the acoustic wave, κ_S can be determined using ρ and c values through the Newton-Laplace equation:

$$\kappa_S = \frac{1}{\rho c^2} \tag{1}$$

The values F^{id} of a quantity, F, for an ideal mixture at the same temperature and pressure as the investigated solution are calculated from the relations:

$$F^{\mathrm{id}} = x_1 F_1^* + x_2 F_2^* \qquad (F = V_{\mathrm{m}}, C_{p\mathrm{m}}) \tag{2}$$

$$F^{\mathrm{id}} = \phi_1 F_1^* + \phi_2 F_2^* \qquad (F = \alpha_p, \kappa_T) \tag{3}$$

where F_i^* denotes the property for the pure component i, $C_{p\mathrm{m}}$ is the molar heat capacity at constant pressure, κ_T is the isothermal compressibility and $\phi_i = x_i V_{\mathrm{m}i}^* / V_{\mathrm{m}}^{\mathrm{id}}$ represents the ideal volume fraction. In the case of κ_S and c, the following expressions are used:

$$\kappa_S^{\mathrm{id}} = \kappa_T^{\mathrm{id}} - \frac{T V_{\mathrm{m}}^{\mathrm{id}} (\alpha_p^{\mathrm{id}})^2}{C_{p\mathrm{m}}^{\mathrm{id}}} \tag{4}$$

$$c^{\mathrm{id}} = \left(\frac{1}{\rho^{\mathrm{id}} \kappa_S^{\mathrm{id}}} \right)^{1/2} \tag{5}$$

being $\rho^{\mathrm{id}} = (x_1 M_1 + x_2 M_2) / V_{\mathrm{m}}^{\mathrm{id}}$ the ideal density, and M_i the molar mass of the pure component i. For the refractive index, n_{D}, the ideal values are obtained from the equation [34]:

$$n_{\mathrm{D}}^{\mathrm{id}} = \left[\phi_1 \left(n_{\mathrm{D}1}^* \right)^2 + \phi_2 \left(n_{\mathrm{D}2}^* \right)^2 \right]^{1/2} \tag{6}$$

The excess properties, F^{E}, are then obtained from the relation:

$$F^{\mathrm{E}} = F - F^{\mathrm{id}} \qquad (F = V_{\mathrm{m}}, \kappa_S, c, \alpha_p, n_{\mathrm{D}}) \tag{7}$$

4. Results

Values of ρ, c, and $V_{\mathrm{m}}^{\mathrm{E}}$ as functions of x_1, the mole fraction of DMA, and at the considered temperatures are included in Table 3. For DBA or HxA mixtures, the measurements were made at 298.15 K only, due to: (i) their low $|V_{\mathrm{m}}^{\mathrm{E}}|$ values; (ii) the weak temperature dependence of $V_{\mathrm{m}}^{\mathrm{E}}$ encountered for the systems with BA or DPA. The corresponding results of κ_S^{E}, c^{E}, and α_p^{E} at 298.15 K are given in Table 4. The n_{D} values and their corresponding excess functions, $n_{\mathrm{D}}^{\mathrm{E}}$, are collected in Table 5. Our experimental method is not accurate enough to determine $n_{\mathrm{D}}^{\mathrm{E}}$ values for the systems containing DBA or HxA. Some of these results are represented in Figures 1-7. We have not found literature data for comparison.

The data have been fitted by an unweighted linear least-squares regression to a Redlich-Kister equation [35]:

Table 3. Densities, ρ, excess molar volumes, V_m^E, and speeds of sound, c, for *N,N*-dimethylacetamide (1) + amine (2) mixtures at temperature T and pressure p = 0.1 MPa. [a]

x_1	ρ /g·cm^{-3}	V_m^E /cm^3·mol^{-1}	c /m·s^{-1}	x_1	ρ /g·cm^{-3}	V_m^E /cm^3·mol^{-1}	c /m·s^{-1}
DMA (1) + DPA (2); T/K= 293.15							
0.0000	0.73778		1208.7	0.4914	0.81947	–0.2137	1304.1
0.0621	0.74684	–0.0656	1218.8	0.5582	0.83282	–0.2096	1321.1
0.1201	0.75556	–0.1122	1228.6	0.6520	0.85273	–0.1936	1347.3
0.1432	0.75911	–0.1272	1232.6	0.7141	0.86668	–0.1719	1366.3
0.2142	0.77035	–0.1659	1245.4	0.7604	0.87751	–0.1495	1381.5
0.2434	0.77511	–0.1780	1250.8	0.8012	0.88743	–0.1312	1395.5
0.3154	0.78722	–0.1971	1264.9	0.8494	0.89962	–0.1098	1413.2
0.3398	0.79148	–0.2052	1269.9	0.9017	0.91334	–0.0754	1433.4
0.4140	0.80484	–0.2178	1286.0	0.9457	0.92538	–0.0441	1451.5
0.4668	0.81475	–0.2175	1298.2	1.0000	0.94087		1475.1
DMA (1) + DPA (2); T/K= 298.15							
0.0000	0.73322		1187.3	0.5678	0.83024	–0.2214	1303.8
0.0668	0.74299	–0.0767	1198.4	0.5999	0.83691	–0.2120	1312.5
0.1010	0.74814	–0.1103	1204.2	0.6543	0.84864	–0.1998	1328.2
0.1466	0.75510	–0.1400	1212.2	0.7153	0.86240	–0.1823	1347.1
0.2032	0.76403	–0.1719	1222.5	0.7605	0.87301	–0.1619	1362.0
0.2606	0.77342	–0.1967	1233.5	0.8006	0.88277	–0.1440	1375.9
0.3112	0.78198	–0.2125	1243.6	0.8576	0.89720	–0.1137	1396.8
0.3584	0.79022	–0.2214	1253.4	0.8960	0.90729	–0.0875	1411.8
0.3933	0.79648	–0.2258	1261.1	0.9495	0.92191	–0.0469	1433.8
0.4622	0.80932	–0.2314	1277.0	1.0000	0.93630		1455.7
0.5019	0.81700	–0.2303	1286.7				
DMA (1) + DPA (2); T/K= 303.15							
0.0000	0.72870		1166.7	0.5632	0.82479	–0.2412	1282.9
0.0609	0.73755	–0.0658	1176.8	0.5926	0.83089	–0.2360	1290.9
0.1008	0.74351	–0.1011	1183.7	0.6511	0.84343	–0.2204	1307.7
0.1975	0.75853	–0.1674	1201.1	0.7089	0.85641	–0.2019	1325.4
0.2416	0.76569	–0.1905	1209.6	0.7618	0.86882	–0.1802	1342.8
0.2915	0.77407	–0.2173	1219.5	0.7881	0.87517	–0.1655	1351.9
0.3409	0.78258	–0.2288	1229.8	0.8571	0.89250	–0.1226	1376.9
0.3957	0.79240	–0.2427	1241.8	0.9026	0.90448	–0.0903	1394.6
0.4536	0.80316	–0.2476	1255.2	0.9464	0.91644	–0.0520	1412.6
0.4910	0.81033	–0.2451	1264.2	1.0000	0.93169		1435.7
DMA (1) + DBA (2); T/K= 298.15							
0.0000	0.75553		1241.5	0.5040	0.81954	0.0540	1304.4
0.0556	0.76111	0.0057	1246.5	0.6059	0.83747	0.0568	1324.5
0.1101	0.76685	0.0150	1251.6	0.6466	0.84529	0.0572	1333.6
0.1416	0.77031	0.0202	1254.8	0.6971	0.85562	0.0542	1346.1
0.2017	0.77724	0.0263	1261.3	0.7538	0.86809	0.0502	1361.6
0.2645	0.78493	0.0327	1268.7	0.7900	0.87660	0.0437	1372.5

0.3006	0.78956	0.0411	1273.2	0.8612	0.89469	0.0332	1396.6
0.3448	0.79551	0.0436	1279.2	0.8925	0.90328	0.0271	1408.3
0.3993	0.80324	0.0513	1287.1	0.9566	0.92228	0.0106	1435.3
0.4461	0.81028	0.0526	1294.4	1.0000	0.93629		1455.7
			DMA (1) + BA (2); T/K= 293.15				
0.0000	0.73705		1268.1	0.5968	0.85698	–0.1771	1383.5
0.0490	0.74668	–0.0355	1276.6	0.6577	0.86951	–0.1624	1396.8
0.1067	0.75803	–0.0680	1286.8	0.7542	0.88954	–0.1354	1418.5
0.1477	0.76612	–0.0867	1294.1	0.8499	0.90960	–0.1022	1440.4
0.2508	0.78662	–0.1253	1313.2	0.9063	0.92143	–0.0716	1453.5
0.3494	0.80649	–0.1611	1332.2	0.9420	0.92898	–0.0526	1461.8
0.4513	0.82709	–0.1687	1352.7	1.0000	0.94108		1475.2
0.5505	0.84739	–0.1736	1373.5				
			DMA (1) + BA (2); T/K= 298.15				
0.0000	0.73233		1246.1	0.5646	0.84566	–0.1948	1356.4
0.0536	0.74283	–0.0378	1255.7	0.6946	0.87259	–0.1823	1385.3
0.1214	0.75625	–0.0862	1268.1	0.7540	0.88492	–0.1607	1398.7
0.1929	0.77041	–0.1198	1281.2	0.8534	0.90573	–0.1210	1421.8
0.2540	0.78258	–0.1418	1292.8	0.9055	0.91672	–0.0960	1434.2
0.3630	0.80457	–0.1808	1314.3	0.9446	0.92485	–0.0606	1443.0
0.4684	0.82594	–0.1925	1335.9	1.0000	0.93633		1455.6
0.5051	0.83343	–0.1938	1343.6				
			DMA (1) + BA (2); T/K= 303.15				
0.0000	0.72750		1224.5	0.4971	0.82713	–0.2009	1321.7
0.0517	0.73770	–0.0456	1233.9	0.6574	0.86025	–0.1930	1356.9
0.1082	0.74889	–0.0875	1244.3	0.7957	0.88919	–0.1582	1388.8
0.1535	0.75783	–0.1083	1252.8	0.8498	0.90040	–0.1161	1401.1
0.2556	0.77826	–0.1617	1272.3	0.9090	0.91297	–0.0918	1415.1
0.2921	0.78562	–0.1783	1279.6	0.9404	0.91948	–0.0590	1422.3
0.3582	0.79885	–0.1832	1292.6	1.0000	0.93195		1436.1
0.4583	0.81922	–0.2014	1313.3				
			DMA (1) + HxA (2); T/K= 298.15				
0.0000	0.76019		1303.8	0.6130	0.85274	0.0027	1374.5
0.0575	0.76737	0.0052	1308.5	0.6994	0.86931	–0.0020	1389.5
0.1197	0.77545	0.0052	1314.0	0.7620	0.88202	–0.0064	1401.2
0.1582	0.78060	0.0084	1317.5	0.8060	0.89133	–0.0094	1410.3
0.2079	0.78743	0.0114	1322.4	0.8544	0.90192	–0.0086	1420.5
0.2450	0.79271	0.0087	1326.1	0.8959	0.91134	–0.0090	1430.2
0.3068	0.80176	0.0082	1333.0	0.9467	0.92330	–0.0066	1442.2
0.4037	0.81674	0.0063	1344.4	1.0000	0.93637		1455.8
0.5122	0.83471	0.0068	1359.1				

[a] The standard uncertainties are: $u(x_1) = 0.0001$; $u(p) = 1$ kPa; $u(T) = 0.01$ K. The standard uncertainties are: $u(\rho) = 0.00005$ g·cm^{-3}; $u\left(V_m^E\right) = (0.010\left|V_{m,max}^E\right| + 0.005$ cm^3·mol^{-1}); $u(c) = 0.2$ m·s^{-1}.

Table 4. Excess functions, at temperature T = 298.15 K and pressure p = 0.1 MPa, for κ_S, adiabatic compressibility, c, speed of sound, and α_p, isobaric thermal expansion coefficient, of *N,N*-dimethylacetamide (1) + amine (2) mixtures. [a]

x_1	κ_S^E /TPa^{-1}	c^E /m·s^{-1}	α_p^E /10^{-6}·K^{-1} [b]	x_1	κ_S^E /TPa^{-1}	c^E /m·s^{-1}	α_p^E /10^{-6}·K^{-1} [b]
			DMA (1) + DPA (2)				
0.0668	–9.7	5.8	–1	0.5678	–45.0	38.3	–26
0.1010	–14.1	8.6	–2	0.5999	–44.6	39.1	–26
0.1466	–19.5	12.3	–4	0.6543	–43.4	39.9	–26
0.2032	–25.6	16.7	–7	0.7153	–40.5	39.7	–26
0.2606	–31.1	21.0	–10	0.7605	–37.3	38.3	–24
0.3112	–35.1	24.5	–14	0.8006	–33.6	36.1	–22
0.3584	–38.2	27.6	–16	0.8576	–26.7	30.7	–18
0.3933	–40.3	29.8	–19	0.8960	–20.9	25.4	–14
0.4622	–43.2	33.7	–22	0.9495	–11.2	14.7	–7
0.5019	–44.3	35.7	–24				
			DMA (1) + DBA (2)				
0.0556	–2.3	1.7		0.5040	–16.7	15.2	
0.1101	–4.3	3.3		0.6059	–18.1	17.5	
0.1416	–5.5	4.3		0.6466	–18.2	18.1	
0.2017	–7.8	6.2		0.6971	–18.1	18.8	
0.2645	–10.1	8.1		0.7538	–17.2	18.7	
0.3006	–11.2	9.2		0.7900	–16.2	18.3	
0.3448	–12.7	10.6		0.8612	–13.1	15.9	
0.3993	–14.3	12.3		0.8925	–11.0	13.9	
0.4461	–15.4	13.6		0.9566	–5.4	7.4	
			DMA (1) + BA (2)				
0.0536	–7.7	5.4	–11	0.5646	–35.9	35.0	–31
0.1214	–16.2	11.7	–20	0.6946	–31.3	33.6	–31
0.1929	–23.1	17.5	–25	0.7540	–27.4	30.8	–31
0.2540	–27.9	22.0	–27	0.8534	–18.8	22.9	–26
0.3630	–33.9	28.7	–29	0.9055	–13.2	16.8	–22
0.4684	–36.4	33.1	–30	0.9446	–8.1	10.6	–16
0.5051	–36.5	34.1	–30				
			DMA (1) + HxA (2)				
0.0575	–1.8	1.6		0.6130	–12.2	13.3	
0.1197	–3.8	3.4		0.6994	–11.7	13.5	
0.1582	–4.9	4.3		0.7620	–10.6	12.6	
0.2079	–6.3	5.7		0.8060	–9.7	11.9	
0.2450	–7.1	6.6		0.8544	–7.9	10.0	
0.3068	–8.8	8.3		0.8959	–6.4	8.3	
0.4037	–10.5	10.3		0.9467	–3.5	4.8	
0.5122	–11.9	12.3					

[a] The standard uncertainties are: $u(x_1) = 0.0001$; $u(p) = 1$ kPa; $u(T) = 0.01$ K. The standard uncertainties are: $u(c^E) = 0.4$; and (relative values) $u_r(\kappa_S^E) = 0.015$; $u_r(\alpha_p^E) = 0.025$. [b] Density values at 293.15 K and 303.15 K at the mole fractions reported at 298.15 K were obtained from the corresponding Redlich-Kister adjustments for V_m^E.

Table 5. Refractive indices, n_D, and the corresponding excess values, n_D^E, of *N,N*-dimethylacetamide (1) + amine (2) mixtures at temperature T and pressure $p = 0.1$ MPa. [a]

x_1	n_D	$n_D^E/10^{-5}$	x_1	n_D	$n_D^E/10^{-5}$
		DMA (1) + DPA (2); T/K = 293.15			
0.0000	1.40398		0.5582	1.42085	104
0.0621	1.40569	23	0.6520	1.42418	102
0.1201	1.40731	42	0.7141	1.42649	97
0.1432	1.40797	49	0.7604	1.42826	90
0.2142	1.41003	69	0.8012	1.42986	82
0.3154	1.41303	87	0.8494	1.43179	69
0.3398	1.41376	89	0.9017	1.43396	52
0.4140	1.41609	99	0.9457	1.43581	32
0.4668	1.41780	103	1.0000	1.43814	
0.4914	1.41860	104			
		DMA (1) + DPA (2); T/K = 298.15			
0.0000	1.40135		0.4622	1.41524	110
0.0668	1.40324	28	0.5678	1.41882	111
0.1010	1.40422	41	0.6543	1.42192	107
0.1466	1.40554	56	0.7153	1.42421	101
0.2032	1.40720	72	0.7605	1.42597	94
0.2606	1.40892	86	0.8006	1.42755	85
0.3112	1.41045	95	0.8576	1.42988	70
0.3584	1.41191	101	0.9495	1.43376	31
0.3933	1.41302	106	1.0000	1.43595	
		DMA (1) + DPA (2); T/K = 303.15			
0.0000	1.39871		0.5632	1.41619	105
0.0609	1.40041	21	0.5926	1.41723	104
0.1008	1.40155	35	0.6511	1.41934	97
0.1975	1.40440	65	0.7089	1.42153	91
0.2416	1.40577	79	0.7881	1.42468	79
0.2915	1.40727	87	0.8571	1.42755	63
0.3409	1.40885	99	0.9026	1.42948	46
0.3957	1.41059	104	0.9464	1.43142	29
0.4536	1.41246	106	1.0000	1.43382	
0.4910	1.41370	106			
		DMA (1) + DBA (2); T/K = 298.15			
0.0000	1.41495		0.5543	1.42341	
0.0554	1.41559		0.6061	1.42456	
0.1101	1.41627		0.6466	1.42545	
0.1413	1.41667		0.6971	1.42667	
0.2106	1.41761		0.7538	1.42813	
0.2645	1.41838		0.7900	1.42907	
0.3006	1.41893		0.8613	1.43120	
0.3448	1.41961		0.8925	1.43216	
0.3993	1.42053		0.9566	1.43436	
0.4461	1.42137		1.0000	1.43592	
0.5040	1.42243				

		DMA (1) + BA (2); T/K = 293.15			
0.0000	1.40059		0.5505	1.42171	98
0.0490	1.40249	16	0.5968	1.42344	96
0.1067	1.40474	34	0.6577	1.42571	91
0.1477	1.40633	46	0.6982	1.42722	87
0.1916	1.40804	58	0.7542	1.42931	80
0.2508	1.41031	70	0.8499	1.43280	58
0.2962	1.41207	79	0.9063	1.43483	40
0.3494	1.41411	88	0.9420	1.43611	28
0.4513	1.41796	95	1.0000	1.43813	
0.5007	1.41983	97			
		DMA (1) + BA (2); T/K = 298.15			
0.0000	1.39789		0.5979	1.42105	93
0.0536	1.39999	17	0.6554	1.42323	89
0.1214	1.40265	37	0.6946	1.42471	85
0.1929	1.40547	57	0.7540	1.42698	80
0.2540	1.40786	71	0.7912	1.42837	73
0.2974	1.40955	79	0.8534	1.43067	58
0.4027	1.41359	90	0.9055	1.43259	43
0.4684	1.41610	93	0.9446	1.43399	27
0.5051	1.41751	94	1.0000	1.43595	
0.5646	1.41978	94			
		DMA (1) + BA (2); T/K = 303.15			
0.0000	1.39507		0.5583	1.41717	107
0.0517	1.39714	18	0.5962	1.41864	106
0.1082	1.39943	39	0.6574	1.42099	101
0.1535	1.40125	53	0.6970	1.42250	96
0.1894	1.40271	66	0.7537	1.42467	88
0.2556	1.40535	82	0.7957	1.42629	82
0.2921	1.40678	88	0.8498	1.42834	70
0.3582	1.40941	100	0.9090	1.43054	50
0.4583	1.41329	106	0.9404	1.43168	37
0.4971	1.41479	106	1.0000	1.43375	
		DMA (1) + HxA (2); T/K = 298.15			
0.0000	1.41571		0.6130	1.42641	
0.0575	1.41652		0.6994	1.42832	
0.1197	1.41744		0.7620	1.42978	
0.1582	1.41804		0.8060	1.43085	
0.2079	1.41882		0.8544	1.43205	
0.2450	1.41942		0.8959	1.43310	
0.3068	1.42049		0.9467	1.43445	
0.4037	1.42224		1.0000	1.43590	
0.5122	1.42433				

[a] The standard uncertainties are: $u(x_1) = 0.0001$; $u(T) = 0.02$ K; $u(p) = 1$ kPa. ; $u(n_D) = 0.00008$; $u(n_D^E) = 0.0002$.

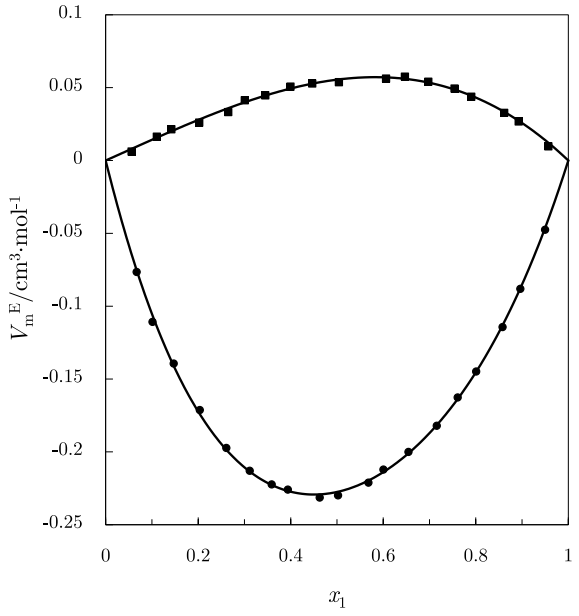

Figure 1: Excess molar volumes, V_m^E, for DMA (1) + DPA (2), or + DBA (2) systems at 0.1 MPa and 298.15 K. Full symbols, experimental values (this work): (●), DPA; (■), DBA. Solid lines, calculations with equation (8) using the coefficients from Table 6.

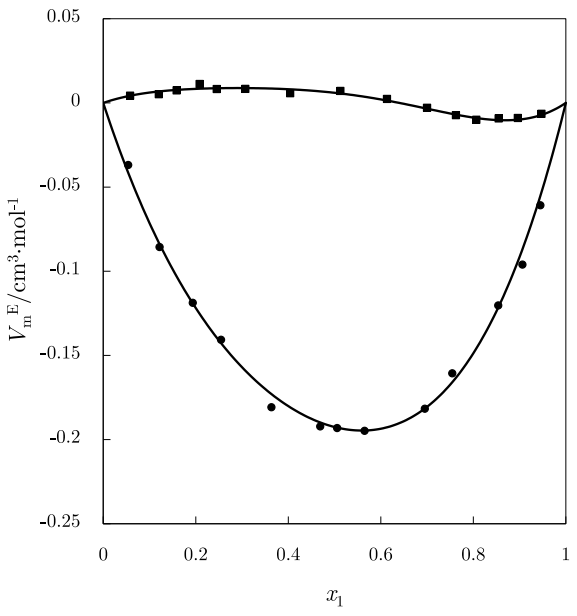

Figure 2: Excess molar volumes, V_m^E, for DMA (1) + BA (2), or + HxA (2) systems at 0.1 MPa and 298.15 K. Full symbols, experimental values (this work): (●), BA; (■), HxA. Solid lines, calculations with equation (8) using the coefficients from Table 6.

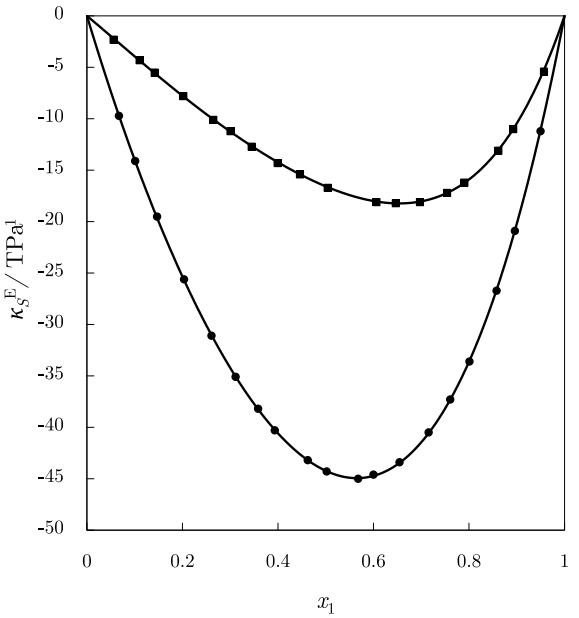

Figure 3: Excess isentropic compressibilities, κ_S^E, for DMA (1) + DPA (2), or + DBA (2) systems at 0.1 MPa and 298.15 K. Full symbols, experimental values (this work): (●), DPA; (■), DBA. Solid lines, calculations with equation (8) using the coefficients from Table 6.

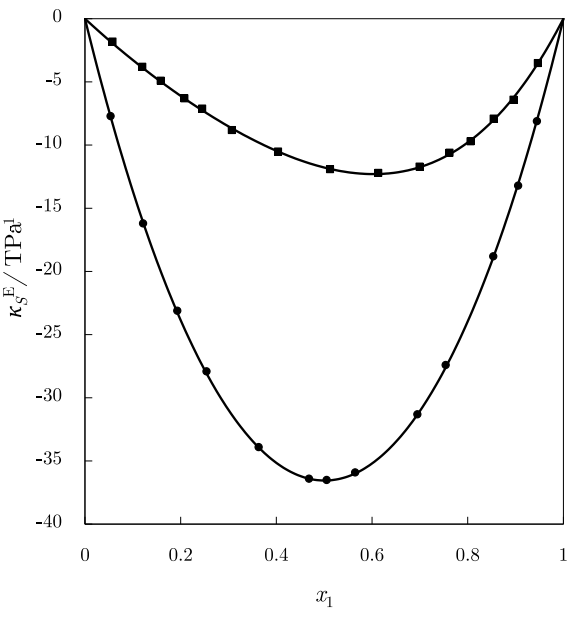

Figure 4: Excess isentropic compressibilities, κ_S^E, for DMA (1) + BA (2), or + HxA (2) systems at 0.1 MPa and 298.15 K. Full symbols, experimental values (this work): (●), BA; (■), HxA. Solid lines, calculations with equation (8) using the coefficients from Table 6.

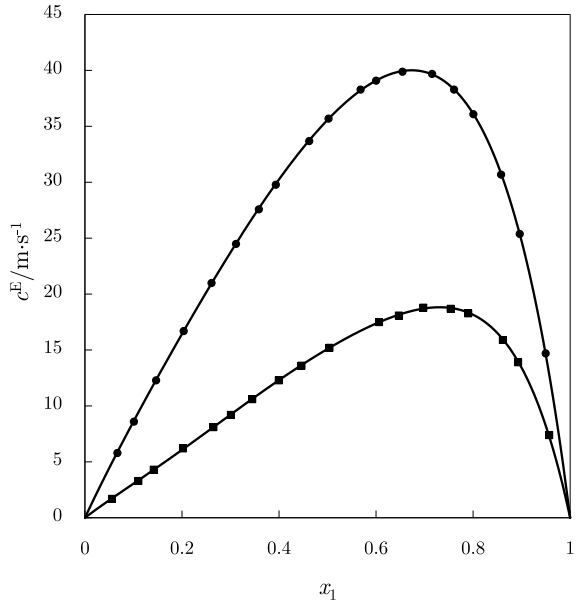

Figure 5: Excess speeds of sound, c^E, for DMA (1) + DPA (2), or + DBA (2) systems at 0.1 MPa and 298.15 K. Full symbols, experimental values (this work): (●), DPA; (■), DBA. Solid lines, calculations with equation (8) using the coefficients from Table 6.

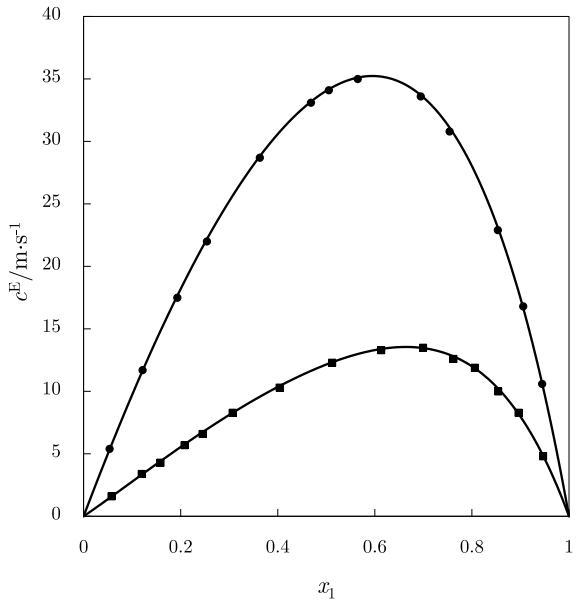

Figure 6: Excess speeds of sound, c^E, for DMA (1) + BA (2), or + HxA (2) systems at 0.1 MPa and 298.15 K. Full symbols, experimental values (this work): (●), BA; (■), HxA. Solid lines, calculations with equation (8) using the coefficients from Table 6.

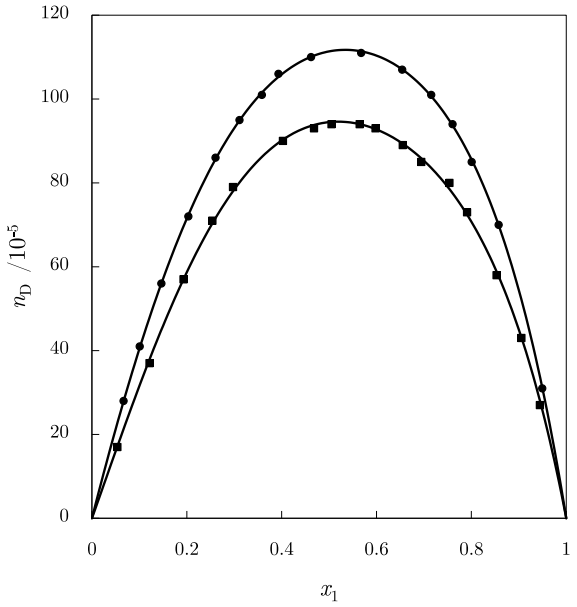

Figure 7: Excess refractive indices, n_D^E, for DMA (1) + amine (2) systems at 0.1 MPa and 298.15 K. Full symbols, experimental values (this work): (●), DPA; (■), BA. Solid lines, calculations with equation (8) using the coefficients from Table 6.

Table 6. Coefficients A_i and standard deviations, $\sigma\left(F^{\mathrm{E}}\right)$ (equation (9)), for the representation of the F^{E} property at temperature T and pressure $p = 0.1$ MPa for *N,N*-dimethylacetamide (1) + amine (2) systems by equation (8).

System	T/K	Property [a] F^{E}	A_0	A_1	A_2	A_3	A_4	$\sigma\left(F^{\mathrm{E}}\right)$
DMA + DPA	293.15	$V_{\mathrm{m}}^{\mathrm{E}}$	–0.861	0.132	–0.15			0.002
		$n_{\mathrm{D}}^{\mathrm{E}} / 10^{-5}$	416	69	118	69		0.7
	298.15	$V_{\mathrm{m}}^{\mathrm{E}}$	–0.910	0.140	–0.23			0.0018
		κ_S^{E}	–176.9	–43.1	–20.5			0.07
		c^{E}	142.3	90.7	54	33	20	0.06
		$\alpha_p^{\mathrm{E}} / 10^{-6}$	–94.8	–79	14			0.4
		$n_{\mathrm{D}}^{\mathrm{E}} / 10^{-5}$	445.5	43	127	85		0.4
	303.15	$V_{\mathrm{m}}^{\mathrm{E}}$	–0.983	0.063	–0.12			0.0017
		$n_{\mathrm{D}}^{\mathrm{E}} / 10^{-5}$	428	–17	50	176		1.1
DMA + DBA	298.15	$V_{\mathrm{m}}^{\mathrm{E}}$	0.222	0.08				0.0015
		κ_S^{E}	–66.4	–38.7	–21.1	–11		0.06
		c^{E}	60.4	51.4	35	32	21	0.06
DMA + BA	293.15	$V_{\mathrm{m}}^{\mathrm{E}}$	–0.696	–0.07	–0.11			0.004
		$n_{\mathrm{D}}^{\mathrm{E}} / 10^{-5}$	390	32	44	67		0.7
	298.15	$V_{\mathrm{m}}^{\mathrm{E}}$	–0.77	–0.14	–0.21			0.005
		κ_S^{E}	–145.9	–0.6	–9.0			0.12
		c^{E}	135.7	48	23	9		0.13
		$\alpha_p^{\mathrm{E}} / 10^{-6}$	–119	–25	–156			1
		$n_{\mathrm{D}}^{\mathrm{E}} / 10^{-5}$	378	23	74	110		0.8
	303.15	$V_{\mathrm{m}}^{\mathrm{E}}$	–0.81	–0.07	–0.24			0.005
		$n_{\mathrm{D}}^{\mathrm{E}} / 10^{-5}$	429	3	105	189		1
DMA + HxA	298.15	$V_{\mathrm{m}}^{\mathrm{E}}$	0.024	–0.06	–0.07	–0.08		0.0014
		κ_S^{E}	–47.0	–19.3	–6.7			0.1
		c^{E}	48.3	30.7	17.3	8		0.1

[a] $F^{\mathrm{E}} = V_{\mathrm{m}}^{\mathrm{E}}$, units: $\mathrm{cm^3 \cdot mol^{-1}}$; $F^{\mathrm{E}} = c^{\mathrm{E}}$, units: $\mathrm{m \cdot s^{-1}}$; $F^{\mathrm{E}} = \kappa_S^{\mathrm{E}}$ units: $\mathrm{TPa^{-1}}$; $F^{\mathrm{E}} = \alpha_p^{\mathrm{E}} / 10^{-6}$, units: $\mathrm{K^{-1}}$.

$$F^{\mathrm{E}} = x_1(1-x_1)\sum_{i=0}^{k-1} A_i(2x_1-1)^i \qquad \left(F = V_{\mathrm{m}}, \kappa_S, c, \alpha_p, n_{\mathrm{D}}\right) \tag{8}$$

For each system and property, the number, k, of necessary coefficients for this regression has been determined by applying an F-test of additional term [36] at 99.5% confidence level. Table 6 includes the parameters A_i obtained, and the standard deviations $\sigma\left(F^{\mathrm{E}}\right)$, defined by:

$$\sigma\left(F^{\mathrm{E}}\right)=\left[\frac{1}{N-k}\sum_{j=1}^{N}\left(F_{\mathrm{cal},j}^{\mathrm{E}}-F_{\mathrm{exp},j}^{\mathrm{E}}\right)^{2}\right]^{1/2} \tag{9}$$

where the index j takes one value for each of the N experimental data $F_{\mathrm{exp},j}^{\mathrm{E}}$, and $F_{\mathrm{cal},j}^{\mathrm{E}}$ is the corresponding value of the excess property F^{E} calculated from equation (8).

5. Prigogine-Flory-Patterson model

In this version of the Flory theory, the excess volumes can be expressed as the sum of three terms [21]: an interactional contribution, proportional to χ_{12} (the interactional Flory parameter); a free volume contribution (the so-called curvature term), related to the difference in the degree of thermal expansion between the two components, and a p^* contribution which arises from the differences in the internal pressures of the components. The mentioned terms are given, respectively, by:

$$\frac{V_{\mathrm{m,interac}}^{\mathrm{E}}}{x_1V_{\mathrm{m},1}^{*}+x_2V_{\mathrm{m},2}^{*}}=\frac{(\tilde{V}^{1/3}-1)\tilde{V}^{2/3}\Psi_1\theta_2(\chi_{12}/p_1^{*})}{\frac{4}{3}\tilde{V}^{-1/3}-1} \tag{10}$$

$$\frac{V_{\mathrm{m,curvature}}^{\mathrm{E}}}{x_1V_{\mathrm{m},1}^{*}+x_2V_{\mathrm{m},2}^{*}}=-\frac{(\tilde{V}_1-\tilde{V}_2)^2\left(\frac{14}{9}\tilde{V}^{-1/3}-1\right)\Psi_1\Psi_2}{\left(\frac{4}{3}\tilde{V}^{-1/3}-1\right)\tilde{V}} \tag{11}$$

$$\frac{V_{\mathrm{m},p^*\mathrm{effect}}^{\mathrm{E}}}{x_1V_{\mathrm{m},1}^{*}+x_2V_{\mathrm{m},2}^{*}}=\frac{(\tilde{V}_1-\tilde{V}_2)(p_1^{*}-p_2^{*})\Psi_1\Psi_2}{p_2^{*}\Psi_1+p_1^{*}\Psi_2} \tag{12}$$

In these equations the contact energy fraction Ψ_i is defined by:

$$\Psi_i=\frac{\varphi_i p_i^{*}}{\varphi_1 p_1^{*}+\varphi_2 p_2^{*}} \tag{13}$$

The remaining symbols have their usual meaning [37-39]. $\tilde{V}=V_{\mathrm{m}}/V_{\mathrm{m}}^{*}$ and $\tilde{V}_i=V_{\mathrm{m},i}/V_{\mathrm{m},i}^{*}$ are the reduced volume of the mixture and of component i, respectively; $V_{\mathrm{m},i}^{*}$, p_i^{*} and T_i^{*} are the characteristic parameters (reduction parameters) of the pure liquids which are obtained from experimental data, such as $\alpha_{p,i}$ and $\kappa_{T,i}$. For mixtures, the corresponding parameters are calculated as follows [38, 39]:

$$V_{\mathrm{m}}^{*}=x_1V_{\mathrm{m},1}^{*}+x_2V_{\mathrm{m},2}^{*} \tag{14}$$

$$T^{*}=\frac{\varphi_1 p_1^{*}+\varphi_2 p_2^{*}-\varphi_1\theta_2\chi_{12}}{\frac{\varphi_1 p_1}{T_1^{*}}+\frac{\varphi_2 p_2}{T_2^{*}}} \tag{15}$$

$$p^{*}=\varphi_1 p_1^{*}+\varphi_2 p_2^{*}-\varphi_1\theta_2\chi_{12} \tag{16}$$

Finally, $\varphi_i = x_i V^*_{m,i} / \sum x_j V^*_{m,j}$ is the segment fraction and θ_2 is site fraction ($= \varphi_2 / (\varphi_2 + S_{12}\varphi_1)$). S_{12} is the so-called geometrical parameter of the mixture, which, assuming that the molecules are spherical, is calculated as $S_{12} = \left(V^*_{m,1} / V^*_{m,2}\right)^{-1/3}$.

Table 7. Values of molar volume, $V_{m,i}$, and Flory reduction parameters for volume, $V^*_{m,i}$, and pressure, P^*_i, at 298.15 K of pure compounds.

Compound	$V_{m,i}$ /cm^3·mol^{-1}	$V^*_{m,i}$ / cm^3· mol^{-1}	p^*_i /J·cm^{-3}
DMF[b]	77.42	61.97	711.4
DMA	93.05	74.82	691.4
DPA	138.00	106.59	508.8
DBA	171.13	135.82	491.7
BA	99.87	76.42	578.0
HxA	133.11	104.68	555.6

[a] Values determined using densities, thermal expansion coefficients and isothermal compressibilities given in Table 2 and in reference [20]. [b] *N,N*-dimethylformamide.

Table 8. Values of the contributions to V^E_m, at 298.15 K and equimolar composition, for DMF or DMA + amine systems calculated according to the PFP model (equations (10)-(12)) using the interaction parameters, χ_{12}, also listed.

System[a]	χ^b_{12} /J·cm^{-3}	V^E_m contributions / cm^3·mol^{-1}		
		Interactional term	Curvature term	p^* effect term
DMF + BA	2.5	0.0284	–0.085	–0.206
DMF + HxA	8.4	0.1001	–0.015	–0.110
DMF + DPA	6.2	0.0837	–0.064	–0.308
DMF + DBA	8.15	0.1110	–0.004	–0.089
DMA + BA	9.3	0.1180	–0.111	–0.214
DMA + HxA	12.42	0.1680	–0.026	–0.135
DMA + DPA	13.45	0.2035	–0.088	–0.351
DMA + DBA	13.45	0.2069	–0.010	–0.140

[a] DMF, *N,N*-dimethylformamide. [b] Determined from V^E_m data at equimolar composition [20], this work.

5.1. Theoretical results

Table 7 lists the values of $V^*_{m,i}$ and p^*_i used in this work. χ_{12} values determined from V^E_m at 298.15 K and equimolar composition are given in Table 8, which also contains the different contributions to V^E_m calculated according to equations (10)-(12). A comparison between experimental and theoretical results is shown, for some selected mixtures, in Figures 8 and 9.

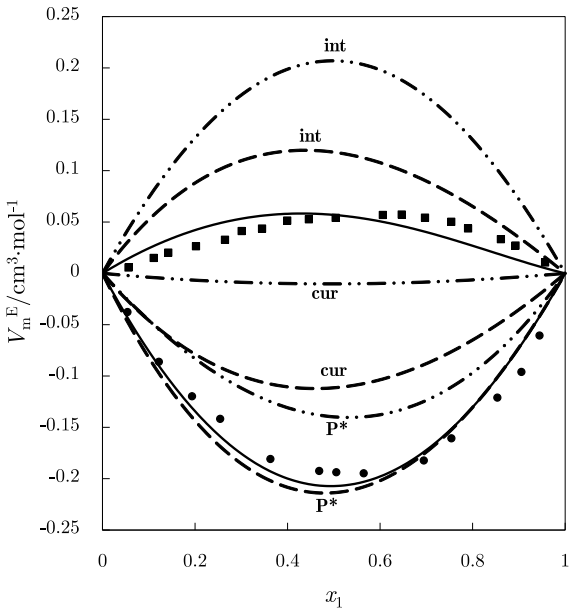

Figure 8: Excess molar volumes, V^E_m, for DMA (1) + amine (2) systems at 0.1 MPa and 298.15 K. Full symbols, experimental values (this work): (●), BA; (■), DBA. Solid lines, Flory results. Dashed lines, contributions to V^E_m according to the Prigogine-Flory-Patterson model ("int", interactional; "cur", curvature; "*P**", p^* effect): (– – –), BA; (– · · –), DBA.

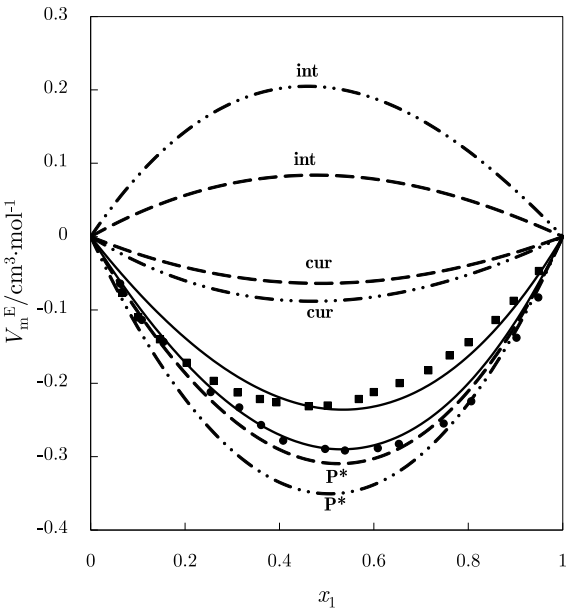

Figure 9: Excess molar volumes, V^E_m, for amide (1) + DPA (2) systems at 0.1 MPa and 298.15 K. Full symbols, experimental values: (●), DMF [20]; (■), DMA (this work). Solid lines, Flory results. Dashed lines, contributions to V^E_m according to the Prigogine-Flory-Patterson model ("int", interactional; "cur", curvature; "*P**", p^* effect): (– – –), DMF; (– · · –), DMA.

6. Discussion

In the present section, the values of the thermophysical properties and the excess functions are referred to $T = 298.15$ K and $x_1 = 0.5$.

DMA is a strongly polar compound (dipole moment μ / D = 3.7 [1]). This is reflected in the fact that DMA + alkane mixtures present miscibility gaps up to quite high temperatures. For instance, the upper critical solution temperature of the heptane system is 309.8 K [40].

The amines considered in this work are linear, either primary or secondary. They are weakly self-associated and their dipole moments μ / D are low: 1.3 (BA) [41], 1.3 (HxA) [2], 1.0 (DPA)

[41], and 1.1 (DBA) [41]. The values of the excess molar enthalpy, H_m^E / J·mol^{-1}, for the heptane mixtures are: 1192 (BA) [42], 962 (HxA) [42], 424 (DPA) [43], and 317 (DBA) [43]. These values can be explained in terms of the breaking of amine-amine interactions upon mixing. We note that H_m^E values are lower for systems with secondary amines, as the amine group is more sterically hindered and self-association is lower in such amines. The corresponding values of V_m^E(heptane) / cm^3·mol^{-1} are: 0.7171 (BA) [44], 0.3450 (HxA) [44], 0.2752 (DPA) [45], and 0.0675 (DBA) [45]. It is well stated that positive V_m^E values arise from the disruption of interactions between like molecules, whereas negative ones appear when interactions between unlike molecules are created and/or when structural effects (differences in size and shape [46-48] or interstitial accommodation [49]) exist. The parallel change of H_m^E and V_m^E indicates that the disruption of amine-amine interactions upon mixing is the main contribution to V_m^E. Nevertheless, the low value of V_m^E in the DBA + heptane system and the negative one of the DBA + hexane system, –0.1854 cm^3·mol^{-1} [50], allow to state that structural effects are present, since this is suggested to be the most relevant contribution when a positive H_m^E value is together with a negative V_m^E value [48].

For the DMA + amine mixtures, we have obtained here either negative or small and positive V_m^E / cm^3·mol^{-1} values (Figures 1, 2): –0.1940 (BA); –0.2275 (DPA), 0.0063 (HxA); 0.0553 (DBA), which point to the existence of interactions between unlike molecules and structural effects. On the other hand, along a given homologous series, V_m^E increases with the amine size (Figures 1, 2). This means that, other than the phenomena which decrease V_m^E (differences in size between components and lower positive contributions because of the disruption of amine-amine interactions), the predominant effects are: i) the higher number of broken interactions between DMA molecules by longer amines; and ii) the lower number and weaker DMA-amine interactions created in systems involving larger amines, as then the amine group is more sterically hindered. The replacement of HxA by DPA leads to a lower V_m^E value, as in the case of the HxA or DPA + heptane mixtures (see above). Therefore, this trend can be explained by the decrease of the positive contribution to V_m^E related to the breaking of interactions between like molecules when a secondary amine is involved. Interestingly, the same behavior is encountered in 1-alkanol + HxA or + DPA systems [51, 52]. The small positive V_m^E values of the DBA solution over the whole concentration range underline the importance of the positive contribution to V_m^E from the breaking of DMA-DMA interactions by the large aliphatic surface of DBA. In fact, the corresponding V_m^E curve, skewed to higher x_1 values (Figure 1), reveals that DBA is a good breaker of the interactions between DMA molecules. The mentioned surface is smaller for HxA and then very small positive V_m^E values are encountered at lower DMA concentrations (Figure 2). Negative V_m^E values at the other side of the concentration range (Figure 2) suggest that interactions between unlike molecules are more favorable. This is consistent with the observed V_m^E minimum of the BA mixture at $x_1 \approx 0.56$ (Figure 2). Interestingly, the symmetry of the V_m^E curve of the DPA system is opposite to that of the BA solution (Figure 1). This feature together with V_m^E(DMA + DPA) < V_m^E(DMA + BA) (Table 3) suggest that structural effects become relevant in the system with DPA. Calculations using the PFP model are in agreement with this statement (see below).

The values of the derived properties κ_S^E, α_p^E are negative, while those of c^E are positive (Figures 3-6, Table 6). In any case, all of them are rather small in absolute value, indicating that the studied systems show a nearly ideal behavior with respect to these properties. Nevertheless, it should be mentioned that negative values of κ_S^E, α_p^E and $A_p = \left(\Delta V_m^E / \Delta T\right)_p$ (–$3{\cdot}10^{-3}$ $cm^3{\cdot}mol^{-1}{\cdot}K^{-1}$ (DPA); –$2.8{\cdot}10^{-3}$ $cm^3{\cdot}mol^{-1}{\cdot}K^{-1}$ (BA)) are characteristic of systems where relevant interactions between unlike molecules and/or structural effects exist [19, 53]. On the other hand, the quantities V_m^E and κ_S^E change in line along a homologous series, while c^E shows an opposite variation. The same behavior is observed when replacing HxA by DPA.

6.1. Internal pressures

The internal pressure [54-57], P_{int}, is an adequate quantity to examine the intermolecular forces in liquids and liquid mixtures:

$$P_{int} = T\frac{\alpha_p}{\kappa_T} - p \tag{17}$$

Here, the κ_T values of the mixtures have been obtained from

$$\kappa_T = \kappa_S + \frac{TV_m(\alpha_p)^2}{C_{pm}} \tag{18}$$

assuming $C_{pm}^E = 0$ [58], and $\alpha_p^E = 0$ when experimental data are not available. For the pure compounds studied, P_{int}^* / MPa = 447.0 (DMA), 338.3 (BA), 343.5 (HxA), 303.4 (DPA), and 306.7 (DBA), whereas for the DMA mixtures P_{int} / MPa = 386.8 (BA), 381.9 (HxA), 353.2 (DPA), and 348.2 (DBA). The most important contributions to P_{int} arise from dispersion forces and weak dipole-dipole interactions [56], and therefore these results suggest that dipolar interactions are stronger in the systems with linear primary amines.

We have also determined the excess internal pressures, $P_{int}^E = P_{int} - P_{int}^{id}$, ($P_{int}^{id} = T\alpha_p^{id} / \kappa_T^{id} - p$ [59]). Thus, $P_{int}^E(\text{DMA}) / \text{MPa} = 10.8$ (BA), 5.3 (HxA), 11.7 (DPA), and 6.3 (DBA). Systems with strong interactions between unlike molecules show large P_{int}^E values. For example, P_{int}^E = 61.4 MPa for the aniline + 2-propanone system [19]. This is seen to be verified by the above results, although the fact that the value for the HxA mixture is lower than for the DPA system may be due, at least partially, to structural effects, as they are similar to the hexane + hexadecane mixture (6.5 MPa [1, 60]). This is also consistent with the observed trend for their V_m^E values [12-15, 17, 19].

The Van der Waals model allows to obtain the internal pressure from [55]:

$$P_{int}^{VDW} = \frac{RT}{x_1V_{fm,1}^* + x_2V_{fm,2}^* + V_m^E} - p \tag{19}$$

where $V_{fm,i}^* = RT / \left(p + P_{int,i}^*\right)$ is the free molar volume of the pure component i. The relative deviations of the results obtained from equation (19) and the experimental ones,

$\left(P_{\text{int}}^{\text{VDW}} - P_{\text{int}}\right) / P_{\text{int}}$, for the DMA mixtures are 2.7% (BA), 1.6% (HxA), 5.8% (DPA), and 3.6% (DBA). One can conclude that the Van der Waals equation is useful for the P_{int} calculation of the studied solutions.

6.2. Molar refractions

The refractive index at optical wavelengths is closely related to dispersion forces, since the molar refraction (or molar refractivity), R_{m}, defined by the Lorentz-Lorenz equation [61, 62]:

$$R_{\text{m}} = \frac{n_{\text{D}}^2 - 1}{n_{\text{D}}^2 + 2} V_{\text{m}} = \frac{N_A \alpha_e}{3\varepsilon_0} \tag{20}$$

(where N_A and ε_0 stand for Avogadro's constant and the vacuum permittivity, respectively) is proportional to the mean electronic contribution, α_e, to the polarizability, [61]. The values of $R_{\text{m}} / \text{cm}^3 \cdot \text{mol}^{-1}$ for the investigated systems are 24.7 (BA), 28.2 (HxA), 29.0 (DPA), and 33.6 (DBA). Clearly, dispersive interactions are more important for larger amines in a homologous series. Moreover, it can be stated that these forces are quite similar for the HxA and DPA systems, and therefore the corresponding difference in their P_{int} values is principally due to dipolar interactions.

6.3. Comparison with other systems

For the considered amines, and also for aniline, mixtures with DMF are characterized by lower $V_{\text{m}}^{\text{E}} / \text{cm}^3 \cdot \text{mol}^{-1}$ values: –0.2630 (BA), –0.0210 (HxA), –0.2893 (DPA), and 0.0178 (DBA) [20]; –0.6615 (aniline) [22], and –0.6092 $\text{cm}^3 \cdot \text{mol}^{-1}$ at 303.15 K for DMA + aniline [26]. This allows to conclude that amide-amine interactions are stronger in mixtures with DMF. Interestingly, deviations between experimental P_{int} values and results from equation (12) are slightly larger for DMF systems: 7.6% (BA), 5.7% (HxA), 4.2% (DPA) and 3.1% (DBA) [20], which suggests that dipolar interactions are more relevant in such solutions. Finally, it is noteworthy that V_{m}^{E} values are much lower for the mixture including aniline; this reveals that interactions between unlike molecules are strengthened when aniline is involved. The same trend is encountered for 2-alkanone + DPA or + aniline systems [12-19].

It is here pertinent to examine the effect of replacing a *N,N*-dialkylamide (DMF or DMA) by a 2-alkanone of similar size (2-propanone or 2-butanone). V_{m}^{E} values of 2-propanone or 2-butanone + DPA, or + DBA mixtures are higher than those of the corresponding systems with DMF or DMA. For example, $V_{\text{m}}^{\text{E}}(\text{DPA}) / \text{cm}^3 \cdot \text{mol}^{-1} =$ 0.243 (2-propanone) [12], 0.144 (2-butanone) [17] and $V_{\text{m}}^{\text{E}}(\text{DBA}) / \text{cm}^3 \cdot \text{mol}^{-1} =$ 0.417 (2-propanone) [12]; 0.265 (2-butanone) [17]. In addition, the H_{m}^{E} values of these 2-alkanone mixtures are positive [16]. All this suggests that amide-amine interactions are stronger than alkanone-amine interactions in mixtures containing a linear secondary amine. Interestingly, aniline mixtures show a rather different behavior. For the 2-alkanone + aniline mixtures, we have $H_{\text{m}}^{\text{E}} / \text{J} \cdot \text{mol}^{-1} =$ –1236 (2-propanone); –1165 (2-butanone) [18] and $V_{\text{m}}^{\text{E}} / \text{cm}^3 \cdot \text{mol}^{-1} =$ –1.183 (2-propanone) [19]; –1.246 (2-butanone) [13]. The lower V_{m}^{E} and the higher H_{m}^{E} values of the 2-propanone mixture compared to those of the DMF

system indicate that interactions between unlike molecules are stronger in the latter solution and that structural effects are more relevant in the 2-propanone system. Surprisingly, DMA-aniline interactions seem to be weaker than (2-butanone)-aniline interactions (see the corresponding $H_{\mathrm{m}}^{\mathrm{E}}$ values of these systems). This matter deserves a careful investigation, currently undertaken.

6.4. Prigogine-Flory-Patterson theory

In the framework of this theory, calculations show that χ_{12} increases when replacing DMF by DMA in systems with a given amine (component 2) (Table 8). In the original Flory model [37], χ_{12} is proportional to $\Delta\eta / v_s^*$, being v_s^* the reduction volume of a segment and $\Delta\eta = \eta_{11} + \eta_{22} - 2\eta_{12}$. The positive η_{ij} magnitudes characterize the energy of interaction for a pair of neighboring sites. As η_{22} remains constant, the χ_{12} value increase may be due to the predominance of the η_{12} decrease over that of η_{11}. The latter is linked to a weakening of the amide-amide interactions; the former merely reflects a weakening of the interactions between unlike molecules. Similar trends are also valid when BA is replaced by HxA in DMF solutions. Interestingly, the DMA + DPA or + DBA systems are characterized by the same χ_{12} value (Table 8), which suggests that such mixtures essentially differ in size effects. Finally, an inspection of the different contributions to $V_{\mathrm{m}}^{\mathrm{E}}$ listed in Table 8 shows that $(V_{\mathrm{m,curvature}}^{\mathrm{E}} + V_{\mathrm{m},p^*\mathrm{effect}}^{\mathrm{E}}) / V_{\mathrm{m}}^{\mathrm{E}}$ is much higher (in absolute value) for systems with DPA. This indicates that structural effects are more important for such a type of solution.

Regarding the composition dependence of $V_{\mathrm{m}}^{\mathrm{E}}$, the model describes fairly well this excess function for the systems DMF or DMA + BA, or + DPA (Figures 8,9) . Results for the mixtures with DBA or HxA are somewhat poorer as the representation of low $V_{\mathrm{m}}^{\mathrm{E}}$ values is a very difficult task for any theoretical model.

7. Conclusions

Binary systems of DMA + BA, + HxA, + DPA or + DBA have been studied at different temperatures, reporting values of ρ, c, n_{D} and of the excess functions ($V_{\mathrm{m}}^{\mathrm{E}}$, κ_S^{E}, c^{E}, α_p^{E} and $n_{\mathrm{D}}^{\mathrm{E}}$) determined from these ones. Negative and low positive $V_{\mathrm{m}}^{\mathrm{E}}$ values for the investigated mixtures point out to the existence of interactions between unlike molecules, as well as of structural effects. This is also supported by results from the PFP model. $V_{\mathrm{m}}^{\mathrm{E}}$ values are higher in the case of systems with linear primary amines, as the breaking of amine-amine interactions is more relevant than when linear secondary amines are involved. Steric hindrance of the amide group appears to be relevant, since comparisons with results of systems including amines and DMF or DMA show that interactions between unlike molecules are stronger in the former systems. The main differences between mixtures containing DPA and HxA come essentially from dipolar interactions. Dispersive interactions increase with the amine size in systems with a given amide.

Acknowledgements

F. Hevia gratefully acknowledges the grant received from the program 'Ayudas para la Formación de Profesorado Universitario (convocatoria 2014), de los subprogramas de Formación y de Movilidad incluidos en el Programa Estatal de Promoción del Talento y su Empleabilidad, en el marco del Plan Estatal de Investigación Científica y Técnica y de Innovación 2013-2016, de la Secretaría de Estado de Educación, Formación Profesional y Universidades, Ministerio de Educación, Cultura y Deporte, Gobierno de España'.

References

[1] J.A. Riddick, W.B. Bunger, T.K. Sakano, *Organic solvents: physical properties and methods of purification*. Wiley, New York, 1986.

[2] A.L. McClellan, *Tables of Experimental Dipole Moments*. Vols. 1,2,3, Rahara Enterprises, El Cerrito, US, 1974.

[3] E.S. Eberhardt, R.T. Raines, *Amide-Amide and Amide-Water Hydrogen Bonds: Implications for Protein Folding and Stability*. J. Am. Chem. Soc. **116** (1994) 2149-2150. https://doi.org/10.1021/ja00084a067

[4] W.L. Jorgensen, C.J. Swenson, *Optimized intermolecular potential functions for amides and peptides. Structure and properties of liquid amides*. J. Am. Chem. Soc. **107** (1985) 569-578. https://doi.org/10.1021/ja00289a008

[5] J.A. Gonzalez, J.C. Cobos, I. García de la Fuente, *Thermodynamics of liquid mixtures containing a very strongly polar compound: Part 6. DISQUAC characterization of N,N-dialkylamides*. Fluid Phase Equilib. **224** (2004) 169-183. https://doi.org/10.1016/j.fluid.2004.02.007

[6] J.A. González, I. García de la Fuente, J.C. Cobos, *Thermodynamics of mixtures with strongly negative deviations from Raoult's Law: Part 4. Application of the DISQUAC model to mixtures of 1-alkanols with primary or secondary linear amines. Comparison with Dortmund UNIFAC and ERAS results*. Fluid Phase Equilib. **168** (2000) 31-58. https://doi.org/10.1016/S0378-3812(99)00326-X

[7] U. Domańska, M. Marciniak, *Volumetric and Solid + Liquid Equilibrium Data for Linear 1-Alkanol + Decylamine Mixtures. Analysis in Terms of ERAS, DISQUAC, and Modified UNIFAC†*. Ind. Eng. Chem. Res. **43** (2004) 7647-7656. https://doi.org/10.1021/ie0401206

[8] F.F. Liew, T. Hasegawa, M. Fukuda, E. Nakata, T. Morii, *Construction of dopamine sensors by using fluorescent ribonucleopeptide complexes*. Bioorg. Med. Chem. **19** (2011) 4473-4481. https://doi.org/10.1016/j.bmc.2011.06.031

[9] D.L. Nelson, M.M. Cox, *Lehninger Principles of Biochemistry*. 3rd ed., Worth Publishing, New York, 2000.

[10] J.M. Sonner, R.S. Cantor, *Molecular Mechanisms of Drug Action: An Emerging View*. Annu. Rev. Biophys. **42** (2013) 143-167. https://doi.org/10.1146/annurev-biophys-083012-130341

[11] M. Götz, R. Reimert, S. Bajohr, H. Schnetzer, J. Wimberg, T.J.S. Schubert, *Long-term thermal stability of selected ionic liquids in nitrogen and hydrogen atmosphere*. Thermochim. Acta **600** (2015) 82-88. https://doi.org/10.1016/j.tca.2014.11.005

[12] I. Alonso, V. Alonso, I. Mozo, I. García de la Fuente, J.A. González, J.C. Cobos, *Thermodynamics of ketone + amine mixtures: Part II. Volumetric and speed of sound*

data at (293.15, 298.15 and 303.15) K for 2-propanone + dipropylamine, + dibutylamine or + triethylamine systems. J. Mol. Liq. **155** (2010) 109-114. https://doi.org/10.1016/j.molliq.2010.05.022

[13] I. Alonso, I. Mozo, I.G. de la Fuente, J.A. González, J.C. Cobos, *Thermodynamics of Ketone + Amine Mixtures. Part III. Volumetric and Speed of Sound Data at (293.15, 298.15, and 303.15) K for 2-Butanone + Aniline, + N-Methylaniline, or + Pyridine Systems.* J. Chem. Eng. Data **55** (2010) 5400-5405. https://doi.org/10.1021/je100472t

[14] J.A. González, I. Alonso, I. Mozo, I. García de la Fuente, J.C. Cobos, *Thermodynamics of (ketone + amine) mixtures. Part VI. Volumetric and speed of sound data at (293.15, 298.15, and 303.15) K for (2-heptanone + dipropylamine, +dibutylamine, or +triethylamine) systems.* J. Chem. Thermodyn. **43** (2011) 1506-1514. https://doi.org/10.1016/j.jct.2011.05.003

[15] I. Alonso, I. Mozo, I.G. De La Fuente, J.A. González, J.C. Cobos, *Thermodynamics of ketone + amine mixtures 7. Volumetric and speed of sound data at (293.15, 298.15 and 303.15) K for 2-pentanone + aniline, + N-methylaniline, or + pyridine systems.* J. Mol. Liq. **160** (2011) 180-186. https://doi.org/10.1016/j.molliq.2011.03.015

[16] J.A. González, I. Alonso, I. García De La Fuente, J.C. Cobos, *Thermodynamics of ketone + amine mixtures. Part IX. Excess molar enthalpies at 298.15 K for dipropylamine, or dibutylamine + 2-alkanone systems and modeling of linear or aromatic amine + 2-alkanone mixtures in terms of DISQUAC and ERAS.* Fluid Phase Equilib. **343** (2013) 1-12. https://doi.org/10.1016/j.fluid.2013.01.011

[17] I. Alonso, I. Mozo, I.G. de la fuente, J.A. González, J.C. Cobos, *Thermodynamics of ketone + amine mixtures Part IV. Volumetric and speed of sound data at (293.15; 298.15 and 303.15 K) for 2-butanone +dipropylamine, +dibutylamine or +triethylamine systems.* Thermochim. Acta **512** (2011) 86-92. https://doi.org/10.1016/j.tca.2010.09.004

[18] I. Alonso, I. Mozo, I. García de la Fuente, J.A. González, J.C. Cobos, *Thermodynamics of Ketone + Amine Mixtures. Part VIII. Molar Excess Enthalpies at 298.15 K for n-Alkanone + Aniline or + N-Methylaniline Systems.* J. Chem. Eng. Data **56** (2011) 3236-3241. https://doi.org/10.1021/je200333p

[19] I. Alonso, V. Alonso, I. Mozo, I. García de la Fuente, J.A. González, J.C. Cobos, *Thermodynamics of Ketone + Amine Mixtures. I. Volumetric and Speed of Sound Data at (293.15, 298.15, and 303.15) K for 2-Propanone + Aniline, + N-Methylaniline, or + Pyridine Systems.* J. Chem. Eng. Data **55** (2010) 2505-2511. https://doi.org/10.1021/je900874z

[20] F. Hevia, A. Cobos, J.A. González, I. García de la Fuente, L.F. Sanz, *Thermodynamics of Amide + Amine Mixtures. 1. Volumetric, Speed of Sound, and Refractive Index Data for N,N-Dimethylformamide + N-Propylpropan-1-amine, + N-Butylbutan-1-amine, + Butan-1-amine, or + Hexan-1-amine Systems at Several Temperatures.* J. Chem. Eng. Data **61** (2016) 1468-1478. https://doi.org/10.1021/acs.jced.5b00802

[21] H. Van Tra, D. Patterson, *Volumes of mixing and the P * effect: Part I. Hexane isomers with normal and branched hexadecane.* J. Solution Chem. **11** (1982) 793-805. https://doi.org/10.1007/BF00650519

[22] H.J. Noh, S.J. Park, S.J. In, *Excess molar volumes and deviations of refractive indices at 298.15 K for binary and ternary mixtures with pyridine or aniline or quinoline.* J. Ind. Eng. Chem. **16** (2010) 200-206. https://doi.org/10.1016/j.jiec.2010.01.038

[23] P.S. Nikam, S.J. Kharat, *Excess Molar Volumes and Deviations in Viscosity of Binary Mixtures of N,N-Dimethylformamide with Aniline and Benzonitrile at (298.15, 303.15,*

308.15, and 313.15) K. J. Chem. Eng. Data **48** (2003) 972-976. https://doi.org/10.1021/je030101n

[24] T.E. Vittal Prasad, A. Adi Sankara Reddy, S. Kailash, D.H.L. Prasad, *Activity coefficients and excess Gibbs energy of binary mixtures of N,N-dimethyl formamide with selected compounds at 95.5 kPa.* Fluid Phase Equilib. **273** (2008) 52-58. https://doi.org/10.1016/j.fluid.2008.07.018

[25] R.S. Ramadevi, P. Venkatesu, M.V. Prabhakara Rao, M.R. Krishna, *Excess enthalpies of binary mixtures of N,N-dimethylformamide with substituted benzenes at 298.15 K.* Fluid Phase Equilib. **114** (1996) 189-197. https://doi.org/10.1016/0378-3812(95)02816-1

[26] G. Chandrasekhar, P. Venkatesu, M.V. Prabhakara Rao, *Excess Volumes and Ultrasonic Studies of n,n-Dimethyl Acetamide with Substituted Benzenes at 303.15 k.* Phys. Chem. Liq. **40** (2002) 181-189. https://doi.org/10.1080/00319100208086661

[27] G. Chandra Sekhar, M.V. Prabhakara Rao, D.H.L. Prasad, Y.V.L. Ravi Kumar, *Excess molar enthalpies of N,N-dimethylacetamide with substituted benzenes at 298.15 K.* Thermochim. Acta **402** (2003) 99-103. https://doi.org/10.1016/S0040-6031(02)00542-7

[28] CIAAW, *Atomic weights of the elements 2015.* ciaaw.org/atomic-weights.htm (accessed 2015)

[29] D. Schneditz, T. Kenner, H. Heimel, H. Stabinger, *A sound-speed sensor for the measurement of total protein concentration in disposable, blood-perfused tubes.* J. Acoust. Soc. Am. **86** (1989) 2073-2080. https://doi.org/10.1121/1.398466

[30] E. Junquera, G. Tardajos, E. Aicart, *Speeds of sound and isentropic compressibilities of (cyclohexane + benzene and (1-chlorobutane + n-hexane or n-heptane or n-octane or n-decane) at 298.15 K.* J. Chem. Thermodyn. **20** (1988) 1461-1467. https://doi.org/10.1016/0021-9614(88)90041-9

[31] K. Tamura, K. Ohomuro, S. Murakami, *Speeds of sound, isentropic and isothermal compressibilities, and isochoric heat capacities of {xc-C6H12+(1−x)C6H6}, x{CCl4+(1−x)C6H6}, and x{C7H16+(1−x)C6H6} at 298.15 K.* J. Chem. Thermodyn. **15** (1983) 859-868. https://doi.org/10.1016/0021-9614(83)90092-7

[32] K. Tamura, S. Murakami, *Speeds of sound, isentropic and isothermal compressibilities, and isochoric heat capacities of {xc-C6H12 + (1 − x)C6H6} from 293.15 to 303.15 K.* J. Chem. Thermodyn. **16** (1984) 33-38. https://doi.org/10.1016/0021-9614(84)90072-7

[33] K.N. Marsh, *Recommended reference materials for the realization of physicochemical properties.* Blackwell Scientific Publications, Oxford, UK, 1987.

[34] J.C.R. Reis, I.M.S. Lampreia, Â.F.S. Santos, M.L.C.J. Moita, G. Douhéret, *Refractive Index of Liquid Mixtures: Theory and Experiment.* ChemPhysChem **11** (2010) 3722-3733. https://doi.org/10.1002/cphc.201000566

[35] O. Redlich, A.T. Kister, *Algebraic Representation of Thermodynamic Properties and the Classification of Solutions.* Ind. & Eng. Chem. **40** (1948) 345-348. https://doi.org/10.1021/ie50458a036

[36] P.R. Bevington, D.K. Robinson, *Data Reduction and Error Analysis for the Physical Sciences.* McGraw-Hill, New York, 2000.

[37] P.J. Flory, *Statistical Thermodynamics of Liquid Mixtures.* J. Am. Chem. Soc. **87** (1965) 1833-1838. https://doi.org/10.1021/ja01087a002

[38] R. Bravo, M. Pintos, A. Amigo, *Dependence upon temperature of the excess molar volumes of tetrahydropyran + n-alkane mixtures.* Can. J. Chem. **73** (1995) 375-379. https://doi.org/10.1139/v95-049

[39] J.A. González, N. Riesco, I. Mozo, I. García De La Fuente, J.C. Cobos, *Thermodynamics of Mixtures Containing Alkoxyethanols. XXI. Application of the Flory Theory to the Study of Orientational Effects in Systems with Dibutyl Ether or 1-Butanol.* Ind. Eng. Chem. Res. **46** (2007) 1350-1359. https://doi.org/10.1021/ie0609012

[40] X. An, H. Zhao, F. Jiang, W. Shen, *The (liquid + liquid) critical phenomena of (a polar liquid + an n-alkane) V. Coexistence curves of (N,N-dimethylacetamide + heptane).* J. Chem. Thermodyn. **28** (1996) 1221-1232. https://doi.org/10.1006/jcht.1996.0109

[41] R.C. Reid, J.M. Prausnitz, B.E. Poling, *The Properties of Gases and Liquids.* McGraw-Hill, New York, US, 1987.

[42] E. Matteoli, L. Lepori, A. Spanedda, *Thermodynamic study of heptane + amine mixtures: I. Excess and solvation enthalpies at 298.15 K.* Fluid Phase Equilib. **212** (2003) 41-52. https://doi.org/10.1016/S0378-3812(03)00260-7

[43] E. Matteoli, P. Gianni, L. Lepori, *Thermodynamic study of heptane + secondary, tertiary and cyclic amines mixtures. Part IV. Excess and solvation enthalpies at 298.15 K.* Fluid Phase Equilib. **306** (2011) 234-241. https://doi.org/10.1016/j.fluid.2011.04.013

[44] L. Lepori, P. Gianni, A. Spanedda, E. Matteoli, *Thermodynamic study of (heptane + amine) mixtures. II. Excess and partial molar volumes at 298.15 K.* J. Chem. Thermodyn. **43** (2011) 805-813. https://doi.org/10.1016/j.jct.2010.12.025

[45] L. Lepori, P. Gianni, A. Spanedda, E. Matteoli, *Thermodynamic study of (heptane + amine) mixtures. III: Excess and partial molar volumes in mixtures with secondary, tertiary, and cyclic amines at 298.15 K.* J. Chem. Thermodyn. **43** (2011) 1453-1462. https://doi.org/10.1016/j.jct.2011.04.017

[46] D. Patterson, *Free Volume and Polymer Solubility. A Qualitative View.* Macromolecules **2** (1969) 672-677. https://doi.org/10.1021/ma60012a021

[47] S.N. Bhattacharyya, M. Costas, D. Patterson, H.V. Tra, *Thermodynamics of mixtures containing alkanes.* Fluid Phase Equilib. **20** (1985) 27-45. https://doi.org/10.1016/0378-3812(85)90019-6

[48] L. Lepori, P. Gianni, E. Matteoli, *The Effect of the Molecular Size and Shape on the Volume Behavior of Binary Liquid Mixtures. Branched and Cyclic Alkanes in Heptane at 298.15 K.* J. Solution Chem. **42** (2013) 1263-1304. https://doi.org/10.1007/s10953-013-0023-9

[49] A.J. Treszczanowicz, G.C. Benson, *Excess volumes for n-alkanols + n-alkanes II. Binary mixtures of n-pentanol, n-hexanol, n-octanol, and n-decanol + n-heptane.* J. Chem. Thermodyn. **10** (1978) 967-974. https://doi.org/10.1016/0021-9614(78)90058-7

[50] T.M. Letcher, *Thermodynamics of aliphatic amine mixtures I. The excess volumes of mixing for primary, secondary, and tertiary aliphatic amines with benzene and substituted benzene compounds.* J. Chem. Thermodyn. **4** (1972) 159-173. https://doi.org/10.1016/S0021-9614(72)80021-1

[51] S. Villa, N. Riesco, I. García de la Fuente, J.A. González, J.C. Cobos, *Thermodynamics of mixtures with strongly negative deviations from Raoult's law: Part 5. Excess molar volumes at 298.15 K for 1-alkanols+dipropylamine systems: characterization in terms of the ERAS model.* Fluid Phase Equilib. **190** (2001) 113-125. https://doi.org/10.1016/S0378-3812(01)00595-7

[52] S. Villa, N. Riesco, I. García de la Fuente, J.A. González, J.C. Cobos, *Thermodynamics of mixtures with strongly negative deviations from Raoult's law. Part 8. Excess molar volumes at 298.15 K for 1-alkanol + isomeric amine (C6H15N) systems:*

Characterization in terms of the ERAS model. Fluid Phase Equilib. **216** (2004) 123-133. https://doi.org/10.1016/j.fluid.2003.10.008

[53] L. Venkatramana, R.L. Gardas, K. Sivakumar, K. Dayananda Reddy, *Thermodynamics of binary mixtures: The effect of substituents in aromatics on their excess properties with benzylalcohol.* Fluid Phase Equilib. **367** (2014) 7-21. https://doi.org/10.1016/j.fluid.2014.01.019

[54] E.B. Bagley, T.P. Nelson, J.W. Barlow, S.A. Chen, *Internal Pressure Measurements and Liquid-State Energies.* Ind. Eng. Chem. Fundamen. **9** (1970) 93-97. https://doi.org/10.1021/i160033a015

[55] E.B. Bagley, T.P. Nelson, J.M. Scigliano, *Internal pressures of liquids and their relation to the enthalpies and entropies of mixing in nonelectrolyte solutions.* J. Phys. Chem. **77** (1973) 2794-2798. https://doi.org/10.1021/j100641a016

[56] M.R.J. Dack, *Solvent structure. The use of internal pressure and cohesive energy density to examine contributions to solvent-solvent interactions.* Aust. J. Chem. **28** (1975) 1643-1648. https://doi.org/10.1071/CH9751643

[57] E. Zorebski, *Internal pressure studies of alcohols on the basis of ultrasonic measurements.* Mol. Quantum Acoust. **26** (2005) 317–326.

[58] W. Marczak, K. Kielek, *Internal Pressure in Binary Mixtures of Methylpyridine Isomers with H2O and D2O.* Int. J. Thermophys. **31** (2009) 85-96. https://doi.org/10.1007/s10765-009-0615-1

[59] R. Dey, A.K. Singh, J.D. Pandey, *A new theoretical approach for estimating excess internal pressure.* J. Mol. Liq. **124** (2006) 121-123. https://doi.org/10.1016/j.molliq.2005.09.005

[60] M.F. Bolotnikov, Y.A. Neruchev, Y.F. Melikhov, V.N. Verveyko, M.V. Verveyko, *Temperature Dependence of the Speed of Sound, Densities, and Isentropic Compressibilities of Hexane + Hexadecane in the Range of (293.15 to 373.15) K.* J. Chem. Eng. Data **50** (2005) 1095-1098. https://doi.org/10.1021/je050060q

[61] A. Chelkowski, *Dielectric Physics.* Elsevier, Amsterdam, 1980.

[62] P. Brocos, A. Piñeiro, R. Bravo, A. Amigo, *Refractive indices, molar volumes and molar refractions of binary liquid mixtures: concepts and correlations.* Phys. Chem. Chem. Phys. **5** (2003) 550-557. https://doi.org/10.1039/B208765K

[63] J. Krakowiak, H. Koziel, W. Grzybkowski, *Apparent molar volumes of divalent transition metal perchlorates and chlorides in N,N-dimethylacetamide.* J. Mol. Liq. **118** (2005) 57-65. https://doi.org/10.1016/j.molliq.2004.07.013

[64] S.S. Bittencourt, R.B. Torres, *Volumetric properties of binary mixtures of (acetonitrile + amines) at several temperatures with application of the ERAS model.* J. Chem. Thermodyn. **93** (2016) 222-241. https://doi.org/10.1016/j.jct.2015.09.002

[65] Y. Miyake, A. Baylaucq, F. Plantier, D. Bessières, H. Ushiki, C. Boned, *High-pressure (up to 140 MPa) density and derivative properties of some (pentyl-, hexyl-, and heptyl-) amines between (293.15 and 353.15) K.* J. Chem. Thermodyn. **40** (2008) 836-845. https://doi.org/10.1016/j.jct.2008.01.006

[66] F. Sarmiento, M.I. Paz Andrade, J. Fernandez, R. Bravo, M. Pintos, *Excess enthalpies of 1-heptanol + n-alkane and di-n-propylamine + normal alcohol mixtures at 298.15 K.* J. Chem. Eng. Data **30** (1985) 321-323. https://doi.org/10.1021/je00041a025

[67] P. Góralski, M. Wasiak, A. Bald, *Heat Capacities, Speeds of Sound, and Isothermal Compressibilities of Some n-Amines and Tri-n-amines at 298.15 K.* J. Chem. Eng. Data **47** (2002) 83-86. https://doi.org/10.1021/je010206v

[68] D. Warmińska, A. Płaczek, H. Koziel, W. Grzybkowski, *Adiabatic Compressibilities of Divalent Transition-Metal Perchlorates and Chlorides in N,N-Dimethylacetamide and Dimethylsulfoxide.* J. Chem. Eng. Data **54** (2009) 745-751. https://doi.org/10.1021/je8004134

[69] J.G. Baragi, M.I. Aralaguppi, T.M. Aminabhavi, M.Y. Kariduraganavar, S.S. Kulkarni, *Density, Viscosity, Refractive Index, and Speed of Sound for Binary Mixtures of 1,4-Dioxane with Different Organic Liquids at (298.15, 303.15, and 308.15) K.* J. Chem. Eng. Data **50** (2005) 917-923. https://doi.org/10.1021/je049609w

[70] S.L. Oswal, P. Oswal, R.L. Gardas, S.G. Patel, R.G. Shinde, *Acoustic, volumetric, compressibility and refractivity properties and reduction parameters for the ERAS and Flory models of some homologous series of amines from 298.15 to 328.15 K.* Fluid Phase Equilib. **216** (2004) 33-45. https://doi.org/10.1016/j.fluid.2003.09.007

[71] M. Domínguez, H. Artigas, P. Cea, M.C. López, J.S. Urieta, *Speed of sound and isentropic compressibility of the ternary mixture (2-Butanol + n-Hexane + 1-Butylamine) and the constituent binary mixtures at 298.15 K and 313.15 K.* J. Mol. Liq. **88** (2000) 243-258. https://doi.org/10.1016/S0167-7322(00)00143-4

[72] S.L. Oswal, N.B. Patel, *Speeds of Sound, Isentropic Compressibilities, and Excess Volumes of Binary Mixtures of Acrylonitrile with Organic Solvents.* J. Chem. Eng. Data **45** (2000) 225-230. https://doi.org/10.1021/je980305h

[73] P. Scharlin, K. Steinby, *Excess thermodynamic properties of binary mixtures of N,N-dimethylacetamide with water or water-d2 at temperatures from 277.13 K to 318.15 K.* J. Chem. Thermodyn. **35** (2003) 279-300. https://doi.org/10.1016/S0021-9614(02)00359-2

[74] P. García-Giménez, J.F. Martínez-López, S.T. Blanco, I. Velasco, S. Otín, *Densities and Isothermal Compressibilities at Pressures up to 20 MPa of the Systems N,N-Dimethylformamide or N,N-Dimethylacetamide + a,ω-Dichloroalkane.* J. Chem. Eng. Data **52** (2007) 2368-2374. https://doi.org/10.1021/je700339f

[75] J.P.E. Grolier, G. Roux-Desgranges, M. Berkane, E. Jiménez, E. Wilhelm, *Heat capacities and densities of mixtures of very polar substances 2. Mixtures containing N, N-dimethylformamide.* J. Chem. Thermodyn. **25** (1993) 41-50. https://doi.org/10.1006/jcht.1993.1005

[76] J. Konicek, I. Wadso, *Thermochemical Properties of Some Carboxylic Acids, Amines and N-Substituted Amides in Aqueous Solution.* Acta Chem. Scand. **25** (1971) 1541-1551. https://doi.org/10.3891/acta.chem.scand.25-1541

[77] J.M. Resa, C. González, S. Ortiz de Landaluce, J. Lanz, *Vapor−Liquid Equilibrium of Binary Mixtures Containing Diethylamine + Diisopropylamine, Diethylamine + Dipropylamine, and Chloroform + Diisopropylamine at 101.3 kPa, and Vapor Pressures of Dipropylamine.* J. Chem. Eng. Data **45** (2000) 867-871. https://doi.org/10.1021/je000020g

Journal of Molecular Liquids 238 (2017) 440–446

Contents lists available at ScienceDirect

Journal of Molecular Liquids

journal homepage: www.elsevier.com/locate/molliq

Thermodynamics of amide + amine mixtures. 3. Relative permittivities of *N*,*N*-dimethylformamide + *N*-propylpropan-1-amine, + *N*-butylbutan-1-amine, + butan-1-amine, or + hexan-1-amine systems at several temperatures

Fernando Hevia, Juan Antonio González *, Isaías García de la Fuente, Luis Felipe Sanz, José Carlos Cobos

G.E.T.E.F., Departamento de Física Aplicada, Facultad de Ciencias, Universidad de Valladolid, Paseo de Belén, 7, 47011 Valladolid, Spain

ARTICLE INFO

Article history:
Received 1 December 2016
Received in revised form 13 April 2017
Accepted 6 May 2017
Available online 7 May 2017

Keywords:
DMF
Amine
Permittivity
Orientational polarizability
Kirkwood correlation factor

ABSTRACT

Relative permittivities at 1 MHz, ε_r, and at (293.15–303.15) K, are reported for the binary systems *N*,*N*-dimethylformamide (DMF) + *N*-propylpropan-1-amine (DPA), + *N*-butylbutan-1-amine (DBA), + butan-1-amine (BA) or + hexan-1-amine (HxA). The values of the excess relative permittivities, ε_r^E, have also been determined for these solutions. The measurements were realized by means of a precision impedance analyser 4294A, to which a 16452A cell connected using a 16048G test lead, all of them from Agilent. The ε_r^E values are large and negative, and diminish when the size of the amine increases along a homologous series, which has been ascribed mainly to the rupture of interactions between like molecules along mixing. Calculations on excess molar orientational polarizabilities support this conclusion, indicating a dominant contribution to ε_r^E from the orientational polarizability of the molecules in the mixture. The analysis of excess relative Kirkwood correlation factors shows that the correlation between dipoles is effectively decreased along the mixing process.

1. Introduction

N,*N*-dimethylformamide (DMF) is a very polar compound (3.7 D [1]) able to dissolve many organic substances, as it is an aprotic protophilic substance with excellent donor-acceptor properties. Consequently, DMF has many applications: in the industry [2–4], Nanotechnology [5,6], or in electrochemical investigation [7,8], where it is a valuable solvent due to its non-ionic character and high dielectric constant (37.398 at 298.15 K, this work). The knowledge of liquid mixtures containing the amide functional group is also necessary for a deeper understanding of more complex molecules, as those of biological interest [9]. For example, as the chemical environment of proteins is very complex, it is reasonable to pay attention to small molecules similar to the functional groups that constitute the biomolecule. This approach is useful to evaluate interactions in condensed phase environments from thermodynamic, transport, or dielectric properties that are readily available for many organic compounds. On the other hand, it is well known that peptide bond plays a crucial role in the stabilization of secondary structural elements of proteins. The study of the peptide bond is linked to that on the ability of amides to form hydrogen bonds. In fact, amides, in pure state, show a significant local order [10], which, in the case of *N*,*N*-dialkylamides, has been attributed to the existence of strong dipolar interactions [11], as such compounds are not self-associated.

In contrast, linear primary and secondary amines can form hydrogen bonds, appearing self-associated complexes and even heterocomplexes in mixtures with other associated compounds [12–14]. The amine group is also present in substances of great biological significance. The proteins usually bound to DNA polymers contain various amine groups [15]. Histamine and dopamine are amines with the role of neurotransmitters [14,16], and the breaking of amino acids releases amines. In addition, the ions of many ionic liquids used in technical applications are related to amines [17].

In a previous study [18], we have reported data of density, ρ, speed of sound, c, and refractive index, n_D, for the binary systems DMF + *N*-propylpropan-1-amine (DPA) or + butan-1-amine (BA) at (293.15–303.15) K, and + *N*-butylbutan-1-amine (DBA) or + hexan-1-amine at 298.15 K. Now, we continue the characterization of these systems providing low-frequency relative permittivities at (293.15–303.15) K. A literature survey shows that ε_r measurements for DMF + linear primary or secondary amine mixtures are not available. In fact, the ε_r database for DMF solutions is rather limited. Nevertheless, experimental ε_r values have been reported for this type of systems including solvents such as: alkanols [19–22], dimethylsulfoxide [23,24] 1,4-dioxane [23] or propylene glycol [25]. The present ε_r data, together with our previous ρ and n_D measurements [18] for DMF + amine solutions are used here to determine the corresponding orientational and induced polarizabilities

* Corresponding author.
E-mail address: jagl@termo.uva.es (J.A. González).

http://dx.doi.org/10.1016/j.molliq.2017.05.025
0167-7322/

according to the Kirkwood-Fröhlich model [26–28] and the Balankina relative excess Kirkwood correlation factors [29], quantities which are useful to gain insight into the dipole correlations present in the mixtures under consideration.

2. Experimental

2.1. Materials

All the compounds were used without further purification. Information regarding their source and purity is collected in Table 1. Their ε_r values at 1 MHz and 0.1 MPa are listed in Table 2; they are in good agreement with the literature data.

2.2. Apparatus and procedure

Binary mixtures have been prepared by mass in small vessels of about 10 cm^3, using an analytical balance HR-202 (weighing accuracy 0.01 mg), with all weighings corrected for buoyancy effects. The standard uncertainty in the final mole fraction is estimated to be 0.0001. For the calculation of molar quantities, the relative atomic mass table of 2015 issued by the Commission on Isotopic Abundances and Atomic Weights (IUPAC) [30] was used.

Temperatures were measured using Pt-100 resistances, calibrated according to the ITS-90 scale of temperature, against the triple point of the water and the fusion point of Ga. The repeatability of the equilibrium temperature measurements is 0.01 K, and the corresponding standard uncertainty is 0.02 K.

The ε_r measurements were realized using a 16452A cell (parallel-plate capacitor) connected, by means of a 16048G test lead, to a precision impedance analyser 4294A; the three of them are from Agilent. The 16452A cell is made of Nickel-plated cobalt (54% Fe, 17% Co, 29% Ni) with a ceramic insulator (alumina, Al_2O_3). The volume of the sample filling the cell is ≈4.8 cm^3. The temperature was controlled by a thermostatic bath LAUDA RE304, with a temperature stability of 0.02 K. Details about the device configuration and calibration are given elsewhere [31]. The relative standard uncertainty of the ε_r measurements is 0.0001. The relative total uncertainty was estimated to be 0.003 from the differences between our data and values available in the literature for the following pure liquids in the temperature range (288.15–333.15) K: water, benzene, cyclohexane, hexane, nonane, decane, dimethyl carbonate, diethyl carbonate, methanol, 1-propanol, 1-pentanol, 1-hexanol, 1-heptanol, 1-octanol, 1-nonanol and 1-decanol.

3. Results

The relative permittivity of an ideal mixture at the same temperature and pressure as the solution under study, ε_r^{id}, is calculated from the expression [32]:

$$\varepsilon_r^{id} = \phi_1 \varepsilon_{r1}^* + \phi_2 \varepsilon_{r2}^* \quad (1)$$

where the volume fraction of component i is defined as $\phi_i = x_i V_{mi}^* / V_m^{id}$. Here, x_i represents the mole fraction of component i, V_{mi}^* and ε_{ri}^* stand for the molar volume and relative permittivity of pure component i respectively, and $V_m^{id} = x_1 V_{m1}^* + x_2 V_{m2}^*$ is the ideal molar volume of the mixture at the same temperature and pressure. The excess relative permittivity, ε_r^E, is obtained as

$$\varepsilon_r^E = \varepsilon_r - \varepsilon_r^{id} \quad (2)$$

where ε_r is the permittivity of the mixture. The necessary volumetric properties were obtained in an earlier work [18].

Volume fractions of DMF (ϕ_1), ε_r, and ε_r^E values are listed in Table 3 for DMF (1) + amine (2) systems as functions of the mole fraction of DMF, x_1, in the temperature range (293.15–303.15) K.

The ε_r^E data have been fitted by an unweighted linear least-squares regression to a Redlich-Kister equation [33]:

$$\varepsilon_r^E = x_1(1-x_1)\sum_{i=0}^{k-1} A_i (2x_1 - 1)^i \quad (3)$$

For each system and temperature, the number, k, of necessary coefficients for this regression has been determined by applying an F-test of additional term [34] at 99.5% confidence level. Table 4 includes the parameters A_i obtained, and the standard deviations $\sigma(\varepsilon_r^E)$, defined by:

$$\sigma(\varepsilon_r^E) = \left[\frac{1}{N-k}\sum_{j=1}^{N}\left(\varepsilon_{r,cal,j}^E - \varepsilon_{r,\,exp,j}^E\right)^2\right]^{1/2} \quad (4)$$

where the index j takes one value for each of the N experimental data $\varepsilon_{r,exp,j}^E$, and $\varepsilon_{r,cal,j}^E$ is the corresponding value of the excess property ε_r^E calculated from Eq. (3).

Table 2
Relative permittivity, ε_r^*, of pure compounds at temperature T, pressure $p = 0.1$ MPa and frequency $\nu = 1$ MHz.[a]

Compound	T/K	ε_r^* Exp.	Lit.
DMF	293.15	38.268	38.30 [22]
	298.15	37.398	37.65 [42]
	303.15	36.521	36.55 [43]
DPA	293.15	3.160	3.31 [44]
			3.068 [45]
	298.15	3.106	3.24 [44]
	303.15	3.053	3.18 [44]
DBA	293.15	2.943	2.978 [45]
			2.765 [46]
	298.15	2.903	
	303.15	2.863	2.697 [46]
BA	293.15	4.733	4.71 [47]
			4.88 [45]
			4.91 [48]
	298.15	4.639	4.62 [48]
	303.15	4.546	4.57 [47]
			4.48 [48]
HxA	293.15	3.966	3.94 [49]
	298.15	3.904	
	303.15	3.841	3.83 [49]

[a] The standard uncertainties are: $u(T) = 0.02$ K; $u(p) = 1$ kPa; $u(\nu) = 20$ Hz. The relative standard uncertainty is: $u_r(\varepsilon_r^*) = 0.0001$. The ε_r^* relative total uncertainty is 0.003.

Table 1
Sample description.

Chemical name	CAS number	Source	Purification method	Purity[a]	Analysis method
N,*N*-dimethylformamide (DMF)	68-12-2	Sigma-Aldrich	none	≥0.999	GC[b]
N-propylpropan-1-amine (DPA)	142-84-7	Fluka	none	≥0.99	GC[b]
N-butylbutan-1-amine (DBA)	111-92-2	Aldrich	none	≥0.995	GC[b]
Butan-1-amine (BA)	109-73-9	Sigma-Aldrich	none	≥0.995	GC[b]
Hexan-1-amine (HxA)	111-26-2	Aldrich	none	≥0.995	GC[b]

[a] In mole fraction.
[b] Gas chromatography.

Table 3
Volume fractions of DMF, ϕ_1, relative permittivities, ε_r, and excess relative permittivities, ε_r^E, of DMF (1) + amine (2) mixtures as functions of the mole fraction of DMF, x_1, at temperature T, pressure $p = 0.1$ MPa and frequency $\nu = 1$ MHz.[a]

x_1	ϕ_1	ε_r	ε_r^E	x_1	ϕ_1	ε_r	ε_r^E
DMF (1) + DPA (2); T/K = 293.15							
0.0000	0.0000	3.160		0.5443	0.4016	15.752	−1.507
0.0604	0.0349	4.144	−0.241	0.6001	0.4575	17.766	−1.456
0.1068	0.0630	4.914	−0.458	0.6582	0.5197	20.054	−1.352
0.1538	0.0927	5.754	−0.661	0.6963	0.5630	21.699	−1.227
0.1874	0.1147	6.390	−0.797	0.7563	0.6356	24.447	−1.028
0.2539	0.1605	7.773	−1.022	0.8105	0.7062	27.175	−0.778
0.3117	0.2029	9.056	−1.227	0.8534	0.7659	29.466	−0.583
0.3921	0.2660	11.092	−1.407	0.8993	0.8338	32.048	−0.385
0.4580	0.3220	12.962	−1.503	0.9520	0.9177	35.221	−0.158
0.5045	0.3639	14.398	−1.538	1.0000	1.0000	38.268	
DMF (1) + DPA (2); T/K = 298.15							
0.0000	0.0000	3.106		0.5443	0.4014	15.380	−1.491
0.0604	0.0348	4.061	−0.238	0.6001	0.4572	17.344	−1.440
0.1068	0.0629	4.811	−0.452	0.6582	0.5194	19.579	−1.338
0.1538	0.0926	5.633	−0.648	0.6963	0.5627	21.181	−1.221
0.1874	0.1146	6.253	−0.783	0.7563	0.6353	23.849	−1.043
0.2539	0.1604	7.601	−1.005	0.8105	0.7059	26.516	−0.797
0.3117	0.2027	8.851	−1.206	0.8534	0.7657	28.762	−0.601
0.3921	0.2658	10.836	−1.385	0.8993	0.8337	31.286	−0.409
0.4580	0.3217	12.651	−1.487	0.9520	0.9176	34.389	−0.183
0.5045	0.3637	14.069	−1.509	1.0000	1.0000	37.398	
DMF (1) + DPA (2); T/K = 303.15							
0.0000	0.0000	3.053		0.5443	0.4011	15.004	−1.473
0.0604	0.0348	3.974	−0.244	0.6001	0.4569	16.914	−1.431
0.1068	0.0628	4.709	−0.446	0.6582	0.5191	19.090	−1.336
0.1538	0.0925	5.510	−0.639	0.6963	0.5624	20.660	−1.215
0.1874	0.1145	6.112	−0.773	0.7563	0.6350	23.252	−1.053
0.2539	0.1602	7.422	−0.993	0.8105	0.7057	25.872	−0.799
0.3117	0.2025	8.650	−1.180	0.8534	0.7655	28.051	−0.622
0.3921	0.2656	10.585	−1.357	0.8993	0.8335	30.513	−0.436
0.4580	0.3215	12.362	−1.451	0.9520	0.9175	33.552	−0.208
0.5045	0.3634	13.730	−1.485	1.0000	1.0000	36.521	
DMF (1) + DBA (2); T/K = 293.15							
0.0000	0.0000	2.943		0.5495	0.3558	13.618	−1.909
0.0622	0.0292	3.733	−0.243	0.5944	0.3989	15.155	−1.896
0.1117	0.0539	4.394	−0.455	0.6458	0.4522	17.062	−1.874
0.1954	0.0991	5.628	−0.820	0.7069	0.5220	19.694	−1.711
0.2481	0.1300	6.494	−1.047	0.7550	0.5825	21.998	−1.547
0.3044	0.1654	7.531	−1.262	0.8058	0.6526	24.672	−1.352
0.3621	0.2045	8.691	−1.485	0.8446	0.7111	26.989	−1.104
0.3984	0.2307	9.507	−1.595	0.8946	0.7935	30.244	−0.764
0.4462	0.2673	10.675	−1.722	0.9517	0.8992	34.374	−0.372
0.5136	0.3235	12.533	−1.852	1.0000	1.0000	38.311	
DMF (1) + DBA (2); T/K = 298.15							
0.0000	0.0000	2.903		0.5495	0.3557	13.331	−1.850
0.0622	0.0291	3.672	−0.236	0.5944	0.3988	14.817	−1.852
0.1117	0.0538	4.314	−0.446	0.6458	0.4521	16.687	−1.822
0.1954	0.0990	5.521	−0.799	0.7069	0.5219	19.252	−1.666
0.2481	0.1299	6.366	−1.021	0.7550	0.5824	21.481	−1.526
0.3044	0.1653	7.378	−1.231	0.8058	0.6525	24.118	−1.309
0.3621	0.2044	8.521	−1.438	0.8446	0.7110	26.355	−1.091
0.3984	0.2306	9.310	−1.553	0.8946	0.7935	29.534	−0.760
0.4462	0.2672	10.445	−1.681	0.9517	0.8992	33.603	−0.339
0.5136	0.3234	12.260	−1.806	1.0000	1.0000	37.422	
DMF (1) + DBA (2); T/K = 303.15							
0.0000	0.0000	2.863		0.5495	0.3556	13.031	−1.803
0.0622	0.0291	3.610	−0.233	0.5944	0.3987	14.481	−1.804
0.1117	0.0538	4.237	−0.437	0.6458	0.4520	16.306	−1.774
0.1954	0.0990	5.412	−0.784	0.7069	0.5218	18.800	−1.629
0.2481	0.1299	6.236	−1.000	0.7550	0.5823	20.971	−1.495
0.3044	0.1653	7.225	−1.203	0.8058	0.6524	23.534	−1.292
0.3621	0.2043	8.338	−1.403	0.8446	0.7109	25.713	−1.082
0.3984	0.2305	9.112	−1.511	0.8946	0.7934	28.815	−0.758
0.4462	0.2671	10.218	−1.637	0.9517	0.8991	32.785	−0.346
0.5136	0.3233	11.986	−1.761	1.0000	1.0000	36.528	
DMF (1) + BA (2); T/K = 293.15							
0.0000	0.0000	4.733		0.4992	0.4362	18.425	−0.926
0.0467	0.0366	5.756	−0.204	0.5956	0.5334	21.782	−0.827
0.1016	0.0807	6.990	−0.447	0.6458	0.5860	23.618	−0.754
0.1505	0.1209	8.192	−0.593	0.6990	0.6432	25.663	−0.626
0.2030	0.1651	9.522	−0.744	0.7895	0.7443	29.231	−0.446
0.2442	0.2005	10.603	−0.849	0.8476	0.8119	31.649	−0.293
0.3014	0.2509	12.198	−0.943	0.8959	0.8698	33.690	−0.193
0.3552	0.2995	13.811	−0.959	0.9490	0.9353	36.001	−0.077
0.4466	0.3852	16.683	−0.959	1.0000	1.0000	38.246	
DMF (1) + BA (2); T/K = 298.15							
0.0000	0.0000	4.639		0.4992	0.4359	17.983	−0.926
0.0467	0.0366	5.632	−0.205	0.5956	0.5331	21.269	−0.822
0.1016	0.0806	6.840	−0.438	0.6458	0.5856	23.068	−0.741
0.1505	0.1207	8.004	−0.586	0.6990	0.6429	25.059	−0.626
0.2030	0.1649	9.305	−0.732	0.7895	0.7441	28.564	−0.434
0.2442	0.2003	10.363	−0.833	0.8476	0.8117	30.905	−0.306
0.3014	0.2506	11.917	−0.926	0.8959	0.8696	32.912	−0.194
0.3552	0.2992	13.487	−0.947	0.9490	0.9352	35.165	−0.089
0.4466	0.3848	16.277	−0.959	1.0000	1.0000	37.375	
DMF (1) + BA (2); T/K = 303.15							
0.0000	0.0000	4.546		0.4992	0.4355	17.533	−0.916
0.0467	0.0365	5.504	−0.207	0.5956	0.5327	20.735	−0.817
0.1016	0.0805	6.687	−0.429	0.6458	0.5853	22.487	−0.744
0.1505	0.1206	7.807	−0.589	0.6990	0.6425	24.428	−0.629
0.2030	0.1647	9.076	−0.728	0.7895	0.7438	27.855	−0.436
0.2442	0.2000	10.120	−0.811	0.8476	0.8115	30.162	−0.290
0.3014	0.2503	11.632	−0.905	0.8959	0.8695	32.127	−0.177
0.3552	0.2989	13.152	−0.936	0.9490	0.9351	34.330	−0.068
0.4466	0.3845	15.865	−0.956	1.0000	1.0000	36.470	
DMF (1) + HxA (2); T/K = 293.15							
0.0000	0.0000	3.966		0.5571	0.4226	17.096	−1.369
0.0559	0.0333	4.841	−0.267	0.6043	0.4705	18.792	−1.316
0.1089	0.0664	5.734	−0.510	0.6439	0.5127	20.311	−1.245
0.1672	0.1046	6.807	−0.748	0.7060	0.5829	22.872	−1.093
0.2106	0.1344	7.678	−0.899	0.7438	0.6282	24.506	−1.013
0.2553	0.1663	8.627	−1.045	0.7954	0.6935	26.946	−0.813
0.3031	0.2020	9.710	−1.186	0.8467	0.7627	29.497	−0.636
0.3520	0.2402	10.936	−1.271	0.8948	0.8319	32.073	−0.435
0.4062	0.2847	12.386	−1.348	0.9508	0.9183	35.291	−0.181
0.4504	0.3229	13.644	−1.400	1.0000	1.0000	38.275	
0.5074	0.3748	15.427	−1.398				
DMF (1) + HxA (2); T/K = 298.15							
0.0000	0.0000	3.904		0.5571	0.4225	16.715	−1.351
0.0559	0.0333	4.759	−0.261	0.6043	0.4704	18.362	−1.309
0.1089	0.0664	5.629	−0.501	0.6439	0.5126	19.846	−1.240
0.1672	0.1046	6.681	−0.729	0.7060	0.5828	22.334	−1.105
0.2106	0.1343	7.523	−0.883	0.7438	0.6281	23.949	−1.008
0.2553	0.1662	8.455	−1.020	0.7954	0.6934	26.304	−0.842
0.3031	0.2019	9.518	−1.153	0.8467	0.7626	28.833	−0.633
0.3520	0.2401	10.701	−1.251	0.8948	0.8319	31.328	−0.460
0.4062	0.2846	12.113	−1.331	0.9508	0.9183	34.469	−0.215
0.4504	0.3228	13.350	−1.374	1.0000	1.0000	37.423	
0.5074	0.3747	15.080	−1.384				
DMF (1) + HxA (2); T/K = 303.15							
0.0000	0.0000	3.841		0.5571	0.4223	16.326	−1.317
0.0559	0.0333	4.675	−0.254	0.6043	0.4702	17.927	−1.281
0.1089	0.0663	5.526	−0.482	0.6439	0.5124	19.376	−1.211
0.1672	0.1045	6.549	−0.707	0.7060	0.5826	21.803	−1.079
0.2106	0.1343	7.371	−0.859	0.7438	0.6279	23.372	−0.990
0.2553	0.1662	8.278	−0.995	0.7954	0.6932	25.663	−0.833
0.3031	0.2018	9.315	−1.121	0.8467	0.7625	28.132	−0.629
0.3520	0.2400	10.470	−1.215	0.8948	0.8318	30.585	−0.441
0.4062	0.2845	11.844	−1.295	0.9508	0.9183	33.628	−0.225
0.4504	0.3227	13.047	−1.340	1.0000	1.0000	36.523	
0.5074	0.3745	14.739	−1.341				

[a] The standard uncertainties are: $u(T) = 0.02$ K; $u(p) = 1$ kPa; $u(\nu) = 20$ Hz; $u(x_1) = 0.0001$; $u(\phi_1) = 0.0002$. The relative standard uncertainty is $u_r(\varepsilon_r) = 0.0001$. The relative combined standard uncertainty is $U_{rc}(\varepsilon_r^E) = 0.03$.

4. Discussion

Along the present section, the values of the thermophysical properties and the excess functions are referred to $T = 298.15$ K and $\phi_1 = 0.5$.

Table 4
Coefficients A_i and standard deviations, $\sigma(\varepsilon_r^E)$ (Eq. (4)), for the representation of ε_r^E at temperature T and pressure $p = 0.1$ MPa for DMF (1) + amine (2) systems by Eq. (3).

System	T/K	A_0	A_1	A_2	A_3	$\sigma(\varepsilon_r^E)$
DMF + DPA	293.15	−6.12	−0.40	2.54	1.2	0.011
	298.15	−6.03	−0.45	2.25	0.9	0.010
	303.15	−5.92	−0.57	1.93	0.8	0.012
DMF + DBA	293.15	−7.36	−3.16	1.5	1.3	0.013
	298.15	−7.17	−3.12	1.37	1.3	0.011
	303.15	−6.97	−3.01	1.14	1.1	0.011
DMF + BA	293.15	−3.76	1.72	0.5		0.014
	298.15	−3.73	1.66	0.48		0.008
	303.15	−3.71	1.64	0.60		0.010
DMF + HxA	293.15	−5.61	0.32	1.09		0.011
	298.15	−5.53	0.15	0.90		0.006
	303.15	−5.39	0.09	0.82		0.007

The value of ε_r is determined by a number of factors, such as the permanent dipole moment of the molecules, their polarizability or the nature of the liquid structure and collective dynamics. In addition to the fact that DMF has a high molecular dipole moment (3.7 D [1]), its marked polar character is well demonstrated by the relatively high upper critical solution temperatures of DMF + heptane (342.55 K) [35] and DMF + hexadecane (385.15 K) [36] systems. The orientational contribution to ε_r of strongly polar substances tends to be high and predominant; accordingly, the ε_r value encountered for DMF is rather large (37.398).

Linear primary and secondary amines are weakly self-associated, which is reflected in the positive $H_m^E(x_1 = 0.5)/\mathrm{J\cdot mol^{-1}}$ values of heptane mixtures: 424 (DPA) [37], 317 (DBA) [37], 1192 (BA) [38], and 962 (HxA) [38]. These values can be ascribed to the disruption of amine-amine interactions along mixing. However, their polarity is rather weak, as shown by their relative permittivities: 3.106 (DPA), 2.903 (DBA), 4.639 (BA), and 3.904 (HxA). It is seen that ε_r is lower when the amine group is more sterically hindered, i.e., when dipolar interactions are weaker, which suggests that the differences between the permittivity of these amines are mainly of the orientational type (see also the discussion below about molar polarizability).

It is known that the disruption of interactions between like molecules, here the breaking of DMF-DMF and amine-amine interactions, contributes negatively to ε_r^E. The relative ε_r values of amines show that such contribution decreases when replacing BA by HxA, DPA by DBA, or HxA by DPA. In addition, it is expected that interactions between DMF molecules be more easily broken by those amines with larger aliphatic surfaces. In contrast, the creation of interactions between unlike molecules might have either a positive or a negative contribution to ε_r^E. A positive contribution is encountered when interactions between unlike molecules lead to an increased number of effective dipole moments in the system. Negative contributions arise when interactions between unlike molecules lead to a loss of structure of the liquid with a decrease of the number of effective dipole moments. The mixtures under study are characterized by negative ε_r^E values (Figs. 1 and 2): −1.372 (DPA), −1.733 (DBA), −0.864 (BA), and −1.262 (HxA). Therefore, the dominant contributions arise from the breaking of interactions between like molecules. Interestingly, the ε_r^E value of the DMF + heptane mixture at $\phi_1 = 0.0171$ and 293.15 K is slightly lower (−0.24, calculated from data of the literature [39]) than the values of the corresponding systems with amines at the same conditions: −0.129 (DPA), −0.146 (DBA), −0.104 (BA), and −0.137 (HxA). This reveals that the formation of DMF-amine interactions contributes positively to ε_r^E. On the basis of these considerations, the fact that ε_r^E (DPA) < ε_r^E (HxA) can be explained as follows. Firstly, it is possible to assume that the negative contribution to ε_r^E from the disruption of DMF-DMF interactions is similar in both systems as HxA and DPA have similar aliphatic surfaces. If one takes into account that the negative contribution to ε_r^E (in absolute value) is larger in the case of HxA, this means that the positive contribution to ε_r^E due to the creation of interactions between unlike molecules is higher in the case of the HxA mixture. The observed ε_r^E decrease when replacing BA by HxA, or DPA by DBA, can be explained in similar terms.

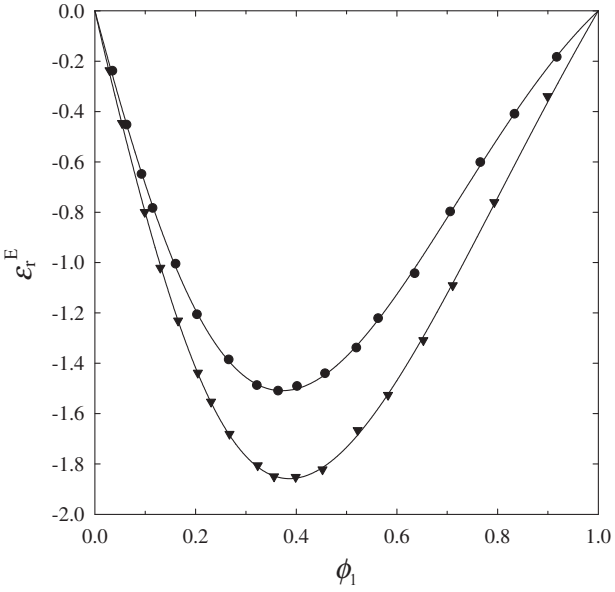

Fig. 1. Excess relative permittivities, ε_r^E, for DMF (1) + DPA (2), or + DBA (2) systems at 0.1 MPa, 298.15 K and 1 MHz. Full symbols, experimental values (this work): (●), DPA; (▼), DBA. Solid lines, calculations with Eq. (3) using the coefficients from Table 4.

In a previous article [18], we reported ultrasonic, volumetric and refractive index (at the wavelength of the sodium D line), n_D, data for the mixtures under study. We also evaluated the molar refractivities, which are related to the mean electronic polarizability and dispersive interactions [28,40]. Using values reported there and ε_r data determined in this work, the molar orientational polarizabilities (also termed molar orientational polarizations or molar polarizability volumes), Π_m^{or}, can be calculated. According to the Kirkwood-Fröhlich equation, this quantity can be written as [26–28]

$$\Pi_m^{or} = \frac{N_A \alpha_{or}}{3\varepsilon_0} = \frac{(\varepsilon_r - \varepsilon_{r\infty})(2\varepsilon_r + \varepsilon_{r\infty})}{9\varepsilon_r} V_m \quad (5)$$

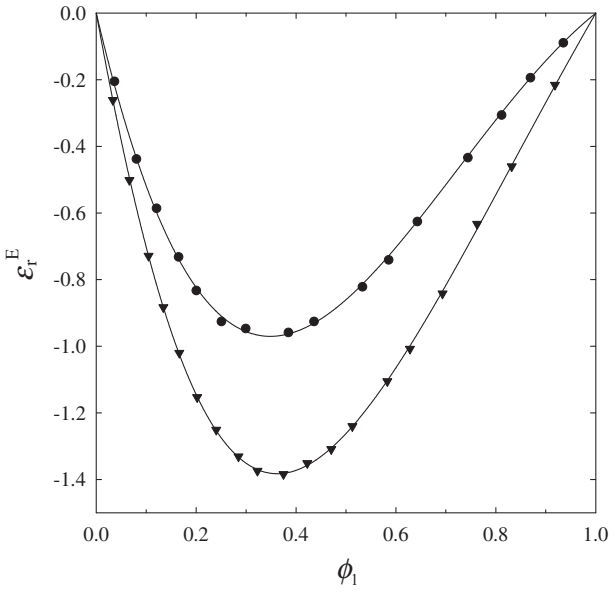

Fig. 2. Excess relative permittivities, ε_r^E, for DMF (1) + BA (2), or + HxA (2) systems at 0.1 MPa, 298.15 K and 1 MHz. Full symbols, experimental values (this work): (●), BA; (▼), HxA. Solid lines, calculations with Eq. (3) using the coefficients from Table 4.

where α_{or} stands for the orientational polarizability (in the case of mixtures, a one-fluid approach is implicit [29]), ε_0 represents the vacuum permittivity, N_A is Avogadro's constant, and $\varepsilon_{r\infty}$ symbolizes the relative permittivity at a frequency at which only the induced (atomic and electronic) polarizability contributes. It has been estimated from the relation [41] $\varepsilon_{r\infty} = 1.1 n_D^2$. Also, the Kirkwood-Fröhlich model provides for the molar induced polarizabilities, Π_m^{ind}, the following expression:

$$\Pi_m^{ind} = \frac{N_A \alpha_{ind}}{3\varepsilon_0} = \frac{(\varepsilon_{r\infty} - 1)(2\varepsilon_r + \varepsilon_{r\infty})}{9\varepsilon_r} V_m \tag{6}$$

with α_{ind} meaning the induced polarizability. For the pure compounds, $(\Pi_m^{or})^*/cm^3 \cdot mol^{-1} = 623.0$ (DMF), 39.1 (DPA), 36.8 (DBA), 68.1 (BA), and 64.5 (HxA). On the other hand, $(\Pi_m^{ind})^*/cm^3 \cdot mol^{-1} = 22.0$ (DMF), 47.9 (DPA), 63.0 (DBA), 31.4 (BA), and 45.7 (HxA). The Kirkwood-Fröhlich model then supports our previous statements about the permittivity of the pure compounds, namely: i) ε_r of DMF arises predominantly from the orientational contribution; and ii) the differences between ε_r of the pure amines are primarily due to orientational effects, as $(\Pi_m^{or})^*$ and ε_r vary in the same sense and $(\Pi_m^{ind})^*$ in the opposite.

Using smoothed values for V_m^E, n_D^E and ε_r^E at $\Delta x_1 = 0.01$, we have also determined the excess molar orientational polarizabilities of the mixtures, $(\Pi_m^{or})^E = \Pi_m^{or} - (\Pi_m^{or})^{id}$, as functions of composition, where $(\Pi_m^{or})^{id}$ is calculated substituting the ideal values in Eq. (5). The results are shown graphically in Fig. 3. The values of $(\Pi_m^{or})^E/cm^3 \cdot mol^{-1}$ are: −31.6 (DPA), −41.4 (DBA), −18.0 (BA) and −27.8 (HxA). These values change in line with those of ε_r^E, pointing out that the main contribution to ε_r^E arises from effects on the orientational polarizability of the molecules. Note the similar shape of the ε_r^E and $(\Pi_m^{or})^E$ curves (Figs. 1–3). The variation of Π_m^{or} contrasts with that of the corresponding molar refractivities, whose values increase with the size of the amine [18], indicating that dispersive interactions become more relevant in the same order.

The Balankina relative excess Kirkwood correlation factors [29], $g_{k,rel}^E = (g_k - g_k^{id})/g_k^{id}$, where g_k and g_k^{id} account respectively for the real and ideal Kirkwood correlation factors, are a useful tool to probe into the structure of the mixtures:

$$g_{k,rel}^E = \frac{V_m(\varepsilon_r - \varepsilon_{r\infty})(2\varepsilon_r + \varepsilon_{r\infty})\varepsilon_r^{id}(\varepsilon_{r\infty}^{id} + 2)^2}{V_m^{id}(\varepsilon_r^{id} - \varepsilon_{r\infty}^{id})(2\varepsilon_r^{id} + \varepsilon_{r\infty}^{id})\varepsilon_r(\varepsilon_{r\infty} + 2)^2} - 1 \tag{7}$$

In the ideal mixture, neither correlations between like dipoles are destroyed nor are new correlations between unlike dipoles created. Therefore, the negative $g_{k,rel}^E$ curves (Fig. 4) for DMF + amine systems indicate that the mean correlation between dipoles is destroyed upon mixing. The $g_{k,rel}^E$ values vary in the same order as the ε_r^E and $(\Pi_m^{or})^E$ magnitudes: − 0.08 (DPA), − 0.09 (DBA), −0.05 (BA), and − 0.07 (HxA), which can be interpreted in similar terms. The minima of the $g_{k,rel}^E$ curves is reached at lower volume fractions of DMF than in the ε_r^E and $(\Pi_m^{or})^E$ curves (Table 5). Thus, according to the Kirkwood-Fröhlich model, the destruction of dipole correlations is not the only responsible for the ε_r^E minima, suggesting the importance of other related effects, such as the number and intensity of interactions created and disrupted upon mixing.

The structure induced in the liquid by the electric field is gradually destroyed as thermal agitation increases. Accordingly, the polarization diminishes with increasing T and the observed values of $(\partial\varepsilon_r^*/\partial T)_p$ are negative. For the pure compounds, $(\partial\varepsilon_r^*/\partial T)_p/K^{-1} = -0.175$ (DMF), −0.011 (DPA), −0.008 (DBA), −0.019 (BA) and −0.013 (HxA). These results point out that the loss of structure is higher when the polar character of the liquid becomes stronger. Similarly, for the DMF mixtures, $(\partial\varepsilon_r/\partial T)_p/K^{-1} = -0.090$ (DPA), −0.085 (DBA), −0.097 (BA) and −0.091 (HxA). The values of $(\partial\varepsilon_r^E/\partial T)_p$ are slightly positive. The largest value is encountered for the DBA system ($\approx 0.01\ K^{-1}$). As the DBA is the pure compound which shows the weakest temperature dependence of ε_r, this result suggests that, in the DMF + DBA system, the contribution to ε_r from the amide-amine interactions with respect to those from the breaking of interactions between like molecules has a more relevant weight when T increases.

5. Conclusions

Values of ε_r and ε_r^E over the temperature range (293.15–303.15) K have been reported for the systems DMF + DPA, + DBA, + BA or + HxA. The ε_r^E values are rather large and negative, and decrease when the size of the amine increases along a homologous series. This behaviour has been attributed to a dominant contribution related to the rupture of interactions between like molecules. The mixtures have also been investigated in terms of the excess molar orientational polarizabilities and excess relative Kirkwood correlation factors. This study supports the previous conclusion, pointing out to a dominant

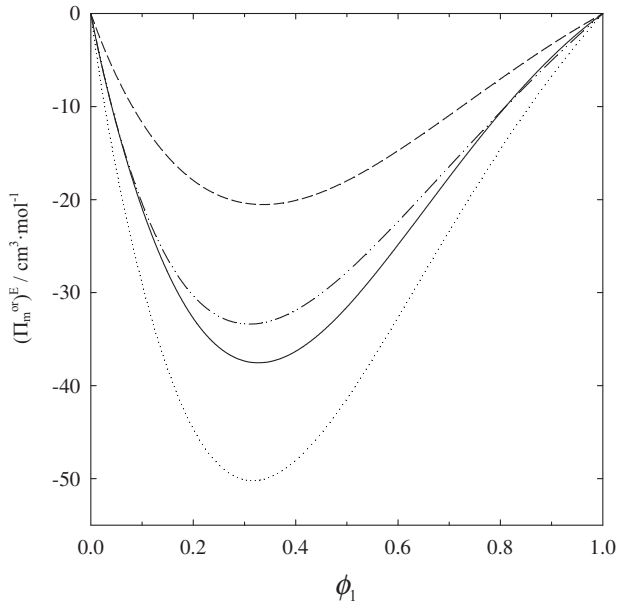

Fig. 3. Excess molar orientational polarizability, $(\Pi_m^{or})^E$, for DMF (1) + amine (2) systems at 0.1 MPa and 298.15 K: DPA (—); DBA (·····); BA (– – – –); HxA (–·–·–·–).

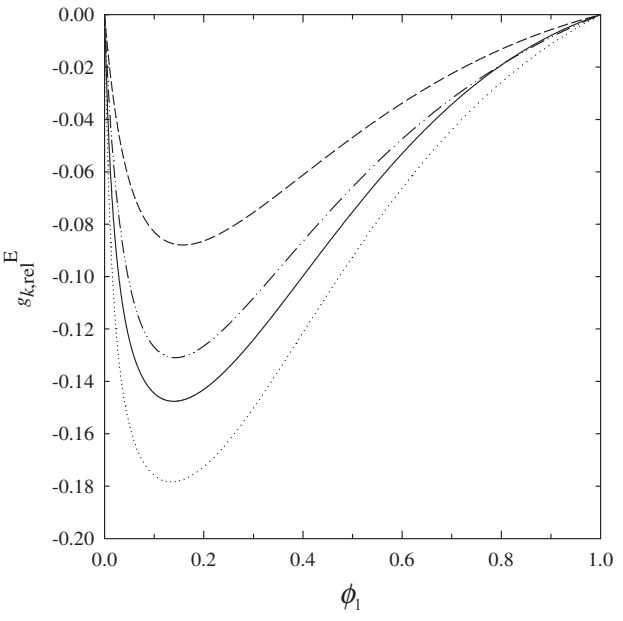

Fig. 4. Relative excess Kirkwood correlation factors, $g_{k,rel}^E$, for DMF (1) + amine (2) systems at 0.1 MPa and 298.15 K: DPA (—); DBA (·····); BA (– – – –); HxA (–·–·–·–).

Table 5
Compositions of DMF (x_1, mole fraction; ϕ_1, volume fraction) and values of the minima of the excess relative permittivity, ε_r^E, excess molar orientational polarizability, $(\Pi_m^{or})^E$, and relative excess Kirkwood correlation factors, $g_{k,rel}^E$ (Eq. (7)), curves at temperature $T = 298.15$ K and pressure $p = 0.1$ MPa for DMF (1) + amine (2) systems.

System	ε_r^E minimum			$(\Pi_m^{or})^E$ minimum			$g_{k,rel}^E$ minimum		
	x_1	ϕ_1	ε_r^E	x_1	ϕ_1	$(\Pi_m^{or})^E/cm^3 \cdot mol^{-1}$	x_1	ϕ_1	$g_{k,rel}^E$
DMF + DPA	0.51	0.37	−1.509	0.46	0.32	−37.5	0.22	0.14	−0.15
DMF + DBA	0.58	0.38	−1.858	0.51	0.32	−50.2	0.26	0.14	−0.18
DMF + BA	0.41	0.35	−0.972	0.40	0.34	−20.5	0.20	0.16	−0.09
DMF + HxA	0.49	0.36	−1.383	0.44	0.31	−33.4	0.22	0.14	−0.13

contribution to ε_r^E from the effects on the orientational polarizability of the molecules and an effective loss of correlation between dipoles along mixing.

Funding

F. Hevia gratefully acknowledges the grant FPU14/04104 received from the program 'Ayudas para la Formación de Profesorado Universitario (convocatoria 2014), Ministerio de Educación, Cultura y Deporte, Gobierno de España'.

References

[1] A.L. McClellan, Tables of Experimental Dipole Moments, vols. 1, 2, 3, Rahara Enterprises, El Cerrito, US, 1974.
[2] P. Venkatesu, Thermophysical contribution of *N*,*N*-dimethylformamide in the molecular interactions with other solvents, Fluid Phase Equilib. 298 (2010) 173–191.
[3] B. Blanco, M.T. Sanz, S. Beltrán, J.L. Cabezas, J. Coca, Vapor–liquid equilibria for the ternary system benzene + *n*-heptane + *N*,*N*-dimethylformamide at 101.33 kPa, Fluid Phase Equilib. 175 (2000) 117–124.
[4] H.J. Noh, S.J. Park, S.J. In, Excess molar volumes and deviations of refractive indices at 298.15 K for binary and ternary mixtures with pyridine or aniline or quinoline, J. Ind. Eng. Chem. 16 (2010) 200–206.
[5] F. Inam, H. Yan, M.J. Reece, T. Peijs, Dimethylformamide: an effective dispersant for making ceramic–carbon nanotube composites, Nanotechnology 19 (2008) 195710.
[6] T.T. Nguyen, S.U. Nguyen, D.T. Phuong, D.C. Nguyen, A.T. Mai, Dispersion of denatured carbon nanotubes by using a dimethylformamide solution, Adv. Nat. Sci. Nanosci. Nanotechnol. 2 (2011), 035015.
[7] K. Fujii, H. Wakamatsu, Y. Todorov, N. Yoshimoto, M. Morita, Structural and electrochemical properties of Li ion solvation complexes in the salt-concentrated electrolytes using an aprotic donor solvent, *N*,*N*-dimethylformamide, J. Phys. Chem. C 120 (2016) 17196–17204.
[8] S. Mu, The electrochemical synthesis and properties of poly(aniline-*co*-diphenylamine and 5-aminosalicylic acid) with p-type doping and n-type doping, Electrochim. Acta 144 (2014) 243–253.
[9] E.S. Eberhardt, R.T. Raines, Amide-amide and amide-water hydrogen bonds: implications for protein folding and stability, J. Am. Chem. Soc. 116 (1994) 2149–2150.
[10] W.L. Jorgensen, C.J. Swenson, Optimized intermolecular potential functions for amides and peptides. Structure and properties of liquid amides, J. Am. Chem. Soc. 107 (1985) 569–578.
[11] J.A. Gonzalez, J.C. Cobos, I. García de la Fuente, Thermodynamics of liquid mixtures containing a very strongly polar compound: part 6. DISQUAC characterization of *N*,*N*-dialkylamides, Fluid Phase Equilib. 224 (2004) 169–183.
[12] J.A. González, I. García de la Fuente, J.C. Cobos, Thermodynamics of mixtures with strongly negative deviations from Raoult's Law: part 4. Application of the DISQUAC model to mixtures of 1-alkanols with primary or secondary linear amines. Comparison with Dortmund UNIFAC and ERAS results, Fluid Phase Equilib. 168 (2000) 31–58.
[13] U. Domańska, M. Marciniak, Volumetric and solid + liquid equilibrium data for linear 1-alkanol + decylamine mixtures. Analysis in terms of ERAS, DISQUAC, and modified UNIFAC, Ind. Eng. Chem. Res. 43 (2004) 7647–7656.
[14] F.F. Liew, T. Hasegawa, M. Fukuda, E. Nakata, T. Morii, Construction of dopamine sensors by using fluorescent ribonucleopeptide complexes, Bioorg. Med. Chem. 19 (2011) 4473–4481.
[15] D.L. Nelson, M.M. Cox, Lehninger Principles of Biochemistry, third ed. Worth Publishing, New York, 2000.
[16] J.M. Sonner, R.S. Cantor, Molecular mechanisms of drug action: an emerging view, Annu. Rev. Biophys. 42 (2013) 143–167.
[17] M. Götz, R. Reimert, S. Bajohr, H. Schnetzer, J. Wimberg, T.J.S. Schubert, Long-term thermal stability of selected ionic liquids in nitrogen and hydrogen atmosphere, Thermochim. Acta 600 (2015) 82–88.
[18] F. Hevia, A. Cobos, J.A. González, I. García de la Fuente, L.F. Sanz, Thermodynamics of amide + amine mixtures. 1. Volumetric, speed of sound, and refractive index data for *N*,*N*-dimethylformamide + *N*-propylpropan-1-amine, + *N*-butylbutan-1-amine, + butan-1-amine, or + hexan-1-amine systems at several temperatures, J. Chem. Eng. Data 61 (2016) 1468–1478.
[19] R.J. Sengwa, V. Khatri, Study of static permittivity and hydrogen bonded structures in amide–alcohol mixed solvents, Thermochim. Acta 506 (2010) 47–51.
[20] M.S. Bakshi, G. Kaur, Thermodynamic behavior of mixtures. 4. Mixtures of methanol with pyridine and *N*,*N*-dimethylformamide at 25 °C, J. Chem. Eng. Data 42 (1997) 298–300.
[21] C.M. Kinart, *N*,*N*-dimethylformamide-methanol binary mixtures and their assumed internal structures, Phys. Chem. Liq. 27 (1994) 115–121.
[22] C.M. Kinart, W.J. Kinart, Study on the internal structures of liquid *N*,*N*-dimethylformamide-benzyl alcohol mixtures, Phys. Chem. Liq. 31 (1996) 1–8.
[23] R.J. Sengwa, S. Sankhla, V. Khatri, Dielectric characterization and molecular interaction behaviour in binary mixtures of amides with dimethylsulphoxide and 1,4-dioxane, J. Mol. Liq. 151 (2010) 17–22.
[24] C.M. Kinart, A. Bald, W.J. Kinart, A. Kolasinski, Dimethylsulfoxide - *N*,*N*-dimethylformamide binary mixtures and their physicochemical properties, Phys. Chem. Liq. 36 (1998) 245–256.
[25] V.V. Navarkhele, M.K. Bhanarkar, Microwave dielectric response of binary mixture of *N*,*N*-dimethylformamide with propylene glycol using TDR method, Mol. Phys. 107 (2009) 1823–1830.
[26] C. Moreau, G. Douhéret, Thermodynamic and physical behaviour of water + acetonitrile mixtures. Dielectric properties, J. Chem. Thermodyn. 8 (1976) 403–410.
[27] P. Bordewijk, On the derivation of the Kirkwood-Fröhlich equation, Physica 69 (1973) 422–432.
[28] A. Chelkowski, Dielectric Physics, Elsevier, Amsterdam, 1980.
[29] J.C.R. Reis, T.P. Iglesias, Kirkwood correlation factors in liquid mixtures from an extended Onsager-Kirkwood-Fröhlich equation, Phys. Chem. Chem. Phys. 13 (2011) 10670–10680.
[30] CIAAW, Atomic Weights of the Elements, 2015 ciaaw.org/atomic-weights.htm (accessed 2015).
[31] V. Alonso, J.A. González, I. García de la Fuente, J.C. Cobos, Dielectric and refractive index measurements for the systems 1-pentanol + octane, or + dibutyl ether or for dibutyl ether + octane at different temperatures, Thermochim. Acta 543 (2012) 246–253.
[32] J.C.R. Reis, T.P. Iglesias, G. Douhéret, M.I. Davis, The permittivity of thermodynamically ideal liquid mixtures and the excess relative permittivity of binary dielectrics, Phys. Chem. Chem. Phys. 11 (2009) 3977–3986.
[33] O. Redlich, A.T. Kister, Algebraic representation of thermodynamic properties and the classification of solutions, Ind. Eng. Chem. 40 (1948) 345–348.
[34] P.R. Bevington, D.K. Robinson, Data Reduction and Error Analysis for the Physical Sciences, McGraw-Hill, New York, 2000.
[35] J. Lobos, I. Mozo, M. Fernández Regúlez, J.A. González, I. García de la Fuente, J.C. Cobos, Thermodynamics of mixtures containing a strongly polar compound. 8. Liquid−liquid equilibria for *N*,*N*-dialkylamide + selected *n*-alkanes, J. Chem. Eng. Data 51 (2006) 623–627.
[36] M. Rogalski, R. Stryjek, Mutual solubility of binary *n*-hexadecane and polar compound systems, Bull. Acad. Pol. Sci., Ser. Sci. Chim. 28 (1980) 139–147.
[37] E. Matteoli, P. Gianni, L. Lepori, Thermodynamic study of heptane + secondary, tertiary and cyclic amines mixtures. Part IV. Excess and solvation enthalpies at 298.15 K, Fluid Phase Equilib. 306 (2011) 234–241.
[38] E. Matteoli, L. Lepori, A. Spanedda, Thermodynamic study of heptane + amine mixtures: I. Excess and solvation enthalpies at 298.15 K, Fluid Phase Equilib. 212 (2003) 41–52.
[39] C. Wohlfahrt, Static Dielectric Constants of Pure Liquids and Binary Liquid Mixtures. Landolt-Börnstein - Group IV Physical Chemistry, vol. 6, Springer Berlin, Heidelberg, Berlin, 1991.
[40] P. Brocos, A. Piñeiro, R. Bravo, A. Amigo, Refractive indices, molar volumes and molar refractions of binary liquid mixtures: concepts and correlations, Phys. Chem. Chem. Phys. 5 (2003) 550–557.
[41] Y. Marcus, The structuredness of solvents, J. Solut. Chem. 21 (1992) 1217–1230.
[42] R.J. Sengwa, Madhvi, S. Sankhla, H-bonded molecular interaction study on binary mixtures of mono alkyl ethers of ethylene glycol with different polar solvents by concentration dependent dielectric analysis, Phys. Chem. Liq. 44 (2006) 637–653.
[43] R.J. Sengwa, S. Sankhla, V. Khatri, Dielectric constant and molecular association in binary mixtures of *N*,*N*-dimethylethanolamine with alcohols and amides, Fluid Phase Equilib. 285 (2009) 50–53.
[44] C.M. Kinart, A. Ćwiklińska, W.J. Kinart, A. Bald, Density and relative permittivity of 2-methoxyethanol + dipropylamine mixtures at various temperatures, J. Chem. Eng. Data 49 (2004) 1425–1428.
[45] J.A. Riddick, W.B. Bunger, T.K. Sakano, Organic Solvents: Physical Properties and Methods of Purification, Wiley, New York, 1986.

[46] F. Ratkovics, L. Domonkos, Properties of alcohol-amine mixtures. 9, Acta Chim. Acad. Sci. Hung. 89 (1976) 325–330.
[47] F.J. Arcega Solsona, J.M. Fornies-Marquina, Dielectric properties of ten primary amines at microwave frequencies as a function of temperature, J. Phys. D. Appl. Phys. 15 (1982) 1783–1793 (cf. [39]).
[48] C.M. Kinart, W.J. Kinart, D. Chęcińska-Majak, Relative permittivity, viscosity, and speed of sound for 2-methoxyethanol + butylamine mixtures, J. Chem. Eng. Data 48 (2003) 1037–1039.
[49] S. Otín, J. Fernández, J.M. Embid, I. Velasco, C.G. Losa, Thermodynamic and dielectric properties of binary polar + non-polar mixtures I. Static dielectric constants and excess molar enthalpies of *n*-alkylamine + *n*-dodecane systems, Ber. Bunsenges. Phys. Chem. 90 (1986) 1179–1183.

J. Chem. Thermodynamics 118 (2018) 175–187

Contents lists available at ScienceDirect

J. Chem. Thermodynamics

journal homepage: www.elsevier.com/locate/jct

Thermodynamics of amide + amine mixtures. 4. Relative permittivities of *N*,*N*-dimethylacetamide + *N*-propylpropan-1-amine, + *N*-butylbutan-1-amine, + butan-1-amine, or + hexan-1-amine systems and of *N*,*N*-dimethylformamide + aniline mixture at several temperatures. Characterization of amine + amide systems using ERAS

Fernando Hevia, Juan Antonio González *, Ana Cobos, Isaías García de la Fuente, Luis Felipe Sanz

G.E.T.E.F., Departamento de Física Aplicada, Facultad de Ciencias, Universidad de Valladolid, Paseo de Belén, 7, 47011 Valladolid, Spain

ARTICLE INFO

Article history:
Received 2 June 2017
Received in revised form 6 November 2017
Accepted 20 November 2017
Available online 22 November 2017

Keywords:
Amides
Amines
Permittivity, Kirkwood correlation factor
Excess functions
ERAS

ABSTRACT

Relative permittivities at 1 MHz, ε_r, and at (293.15–303.15) K are reported for the binary systems *N*,*N*-dimethylacetamide (DMA) + *N*-propylpropan-1-amine (DPA), + *N*-butylbutan-1-amine (DBA), + butan-1-amine (BA) or + hexan-1-amine (HxA) and for *N*,*N*-dimethylformamide (DMF) + aniline. The excess permittivities, ε_r^E, are large and negative for systems with DMA, whereas they are large and positive for the aniline mixture. From the analysis of these ε_r^E data and of measurements previously reported, it is concluded: (i) the main contribution to ε_r^E in systems with linear amines arises from the breaking of interactions between like molecules; (ii) in the DMF + aniline mixture, interactions between unlike molecules contribute positively to ε_r^E, and such a contribution is dominant; (iii) longer linear amines are better breakers of the amide-amide interactions; (iv) interactions between unlike molecules are more easily formed when shorter linear amines, or DMF, participate. These findings are confirmed by a general study conducted in terms of excess values of molar orientational and induced polarizabilities and of the relative Kirkwood correlation factors for systems and components. The ERAS model is also applied to amide + amine mixtures. ERAS represents rather accurately the excess enthalpies and volumes of the mentioned systems. The variation of the cross-association equilibrium constants, determined using ERAS, with the molecular structure is in agreement with that observed for ε_r^E.

1. Introduction

The chemical environment of proteins is highly complex. A suitable approach for its investigation is to focus on small organic molecules which are more or less similar to the functional groups which constitute the biomolecule [1]. In this framework, the determination of thermodynamic, transport and dielectric properties for the mentioned molecules and for their mixtures is necessary, as information on interactions in condensed phase environments can be inferred from these properties.

Amides are a very important class of organic solvents due to their high polarity (the dipole moment of *N*,*N*-dimethylformamide (DMF) and *N*,*N*-dimethylacetamide (DMA) is 3.7 D [2,3]), strong solvating power and liquid state range [4]. The latter is strongly linked to the ability of amides to form hydrogen bonds. It is well known that primary and secondary amides are self-associated species, while tertiary amides show a relevant local order due to the existence of strong dipolar interactions between their molecules [5,6]. This makes amides useful as model systems for peptides [6].

The amine group is also encountered in substances of great biological interest. For example, histamine and dopamine act as neurotransmitters [7,8], and the breaking of amino acids releases amines. On the other hand the proteins usually bound to DNA polymers contain various amine groups [9]. Interestingly, primary and secondary amines are self-associated compounds [10–14] with low dipole moments in the case of linear amines (1.3 D for BA and 1.0 D for DPA [15]). The dipole moment of aniline (1.51 D [3]) is higher and proximity effects between the phenyl ring and the amine group lead to strong dipolar interactions between aniline molecules. As a consequence, aniline + *n*-alkane mixtures are characterized by relatively high upper critical solution temperatures (343.1 K for the heptane solution [16]).

* Corresponding author.
E-mail address: jagl@termo.uva.es (J.A. González).

https://doi.org/10.1016/j.jct.2017.11.011
0021-9614/

The study of amine + amide systems is then relevant as it allows to gain insight into the amide group behaviour when it is surrounded by different environments. In fact, the hydrogen-bonded structures where the amide group is involved can show very different biological activities depending on the mentioned environments [17].

The few data available in the literature on excess molar enthalpies, H^E_m, for amine + amide mixtures underline the importance of interactions between unlike molecules in such systems. For example, at equimolar composition, we have $H^E_m/J \cdot mol^{-1} = -2946$ (aniline + DMF, T = 298.15 K) [18]; −352 (aniline + DMA, T = 298.15 K) [19], −1000 (HxA + *N*-methylacetamide (NMA), T = 363.15 K) [20]. Interestingly, H^E_m /J·mol^{-1} values of methanol + NMA (−76, T = 313.15 K) [21], or + DMA (−737; T = 298.15 K) [22] are very different.

In previous studies, we have reported data on density, ρ, speed of sound, c, and refractive index, n_D, for the binary systems DMF [23], or DMA [24] + *N*-propylpropan-1-amine (DPA) or + butan-1-amine (BA) at (293.15–303.15) K, and + *N*-butylbutan-1-amine (DBA) or + hexan-1-amine (HxA) at 298.15 K. These data have been interpreted in terms of solute-solvent interactions and structural effects [23,24]. On the other hand, we have also reported permittivity measurements for the DMF + BA, + HxA, + DPA, + DBA systems at (293.15–303.15) K [25]. As a continuation of these works, we provide now low-frequency relative permittivities, ε_r, for the DMA + BA, + HxA, + DPA, + DBA mixtures, and for the DMF + aniline system at the same temperature range. The replacement of DMF by DMA in the mentioned systems including linear amines may be useful to investigate steric/size effects on the excess ε_r values. The aniline + DMF system has been selected on the basis of its very large and negative H^E_m value. The present study is completed by the application of different theories. Firstly, amine + amide mixtures are studied using the ERAS model [26]. Secondly, the ε_r data reported here are used together with the corresponding ρ and n_D values available in the literature [23,24,27] to determine orientational and induced polarizabilities according to the Kirkwood-Fröhlich model [28–31] and the Balankina relative excess Kirkwood correlation factors [32], very useful quantities to gain insight into the dipole correlations present in the mixtures under consideration.

2. Experimental

2.1. Materials

Table 1 collects information regarding the source and purity of the pure compounds, which have been used with no further purification.

2.2. Apparatus and procedure

Binary mixtures were prepared by mass in small vessels of about 10 cm^3, using an analytical balance Sartorius MSU125p (weighing accuracy 0.01 mg), with all weighings corrected for buoyancy effects. The standard uncertainty in the final mole fraction is estimated to be 0.0010. Molar quantities were calculated using the relative atomic mass Table of 2015 issued by the Commission on Isotopic Abundances and Atomic Weights (IUPAC) [33]. In order to minimize the effects of the interaction of amines with air components, they were stored with 4 Å molecular sieves; also, the measurement cell (see below) was completely filled with the samples and appropriately closed. Different density measurements of pure compounds, conducted along experiments, showed that this quantity remained unchanged within the experimental uncertainty.

Temperatures were measured by means of Pt-100 resistances, calibrated according to the ITS-90 scale of temperature, against two fixed points: the triple point of water and the fusion point of Ga. The standard uncertainty of the equilibrium temperature measurements is 0.01 K and the corresponding accuracy is 0.02 K.

Permittivity measurements were conducted using a 16452A cell (parallel-plate capacitor) connected, by means of a 16048G test lead, to a precision impedance analyser 4294A; all of them are from Agilent. The 16452A cell is made of Nickel-plated cobalt (54% Fe, 17% Co, 29% Ni) with a ceramic insulator (alumina, Al_2O_3). The volume of the sample filling the cell is ≈ 4.8 cm^3. The temperature was controlled by a thermostatic bath LAUDA RE304, (temperature stability: 0.02 K). Details about the device configuration and calibration can be found elsewhere [34]. The relative standard uncertainty of the ε_r measurements (i.e. the repeatability) is 0.0001. The total relative standard uncertainty of ε_r was estimated to be 0.003 from the differences between our data and values available in the literature for the following pure liquids in the temperature range (288.15–333.15) K: water, benzene, cyclohexane, hexane, nonane, decane, dimethyl carbonate, diethyl carbonate, methanol, 1-propanol, 1-pentanol, 1-hexanol, 1-heptanol, 1-octanol, 1-nonanol and 1-decanol.

Our experimental ε_r values, at 1 MHz and 0.1 MPa, of pure compounds, together with literature data, are shown in Table 2. We note the excellent agreement encountered between them for DMF and DMA. Larger discrepancies between such data are observed for amines, which may be ascribed to the different source and purity of the amines used in the literature. In fact, inspection of Table 2 shows that, for example, some ε_r values of aniline taken from the literature are not sure as they do not change consistently with temperature. In contrast, our ε_r values correctly decrease with the increasing of temperature, and the density measurements are in good agreement with literature data (Table S1, supplementary material; see also [23,24] for the remaining amines).

3. Experimental results

The relative permittivity of an ideal mixture at the same temperature and pressure as the solution under study, ε_r^{id}, is calculated from the expression [35]:

$$\varepsilon_r^{id} = \phi_1 \varepsilon_{r1}^* + \phi_2 \varepsilon_{r2}^* \quad (1)$$

Table 1
Sample description.

Chemical name	CAS Number	Source	Purification method	Purity[a]
N,*N*-dimethylacetamide (DMA)	127-19-5	Sigma-Aldrich	None	0.9998
N,*N*-dimethylformamide (DMF)	68-12-2	Sigma-Aldrich	None	0.9995
N-propylpropan-1-amine (DPA)	142-84-7	Aldrich	None	0.996
N-butylbutan-1-amine (DBA)	111-92-2	Aldrich	None	0.9974
butan-1-amine (BA)	109-73-9	Sigma-Aldrich	None	0.9996
Hexan-1-amine (HxA)	111-26-2	Aldrich	None	0.999
Aniline	62-53-3	Sigma-Aldrich	None	0.999

[a] In mole fraction. Provided by the supplier by gas chromatography.

Table 2
Relative permittivity, ε_r^*, of pure compounds at temperature T, pressure $p = 0.1$ MPa and frequency $\nu = 1$ MHz.[a]

Compound[b]	T/K	ε_r^*		$V_m \frac{\partial \varepsilon_r^*}{\partial T}$/cm$^3 \cdot$ mol$^{-1} \cdot$ K^{-1}	μ/D
		Exp.	Lit.		
DMA	293.15	39.695			
	298.15	38.586	38.60 [59]; 43.00 [60], 37.78 [61]	−20.47[c]	3.7 [2]
	303.15	37.499	37.72 [62]; 38.67 [63]		
DMF	293.15	38.334	38.30 [64]		
	298.15	37.440	37.65 [65], 37.6 [50]	−13.55[d]	3.7 [3]
	303.15	36.580	36.55 [66]		
DPA	293.15	3.148	3.31 [67]; 3.068 [3]		
	298.15	3.093	3.24 [67]	−1.52[c]	1.0 [15]
	303.15	3.037	3.18 [3]		
DBA	293.15	2.938	2.978 [3]; 2.765 [68]		
	298.15	2.896		−1.37[c]	1.1 [15]
	303.15	2.858	2.697 [68]		
BA	293.15	4.729	4.71 [69]; 4.88 [3]; 4.91 [70]; 5.34 [71]; 4.70 [47]		
	298.15	4.636	4.62 [70]; 5.16 [71]	−1.90[c]	1.3 [15]
	303.15	4.547	4.57 [70]; 4.48 [71]		
HxA	293.15	3.955	3.94 [47]		
	298.15	3.893		−1.73[c]	1.3 [2]
	303.15	3.835	3.83 [47]		
Aniline[e]	293.15	7.117	6.48 [72]; 6.55 [73]		
	298.15	6.984	6.774 [74], 6.59 [75]	−2.39[e]	1.51 [3]
	303.15	6.856	6.09 [72]; 6.0 [73]; 6.71 [3]; 6.88 [76]; 6.857 [77]; 6.055 [78]		

[a] The standard uncertainties are: $u(T) = 0.02$ K; $u(p) = 1$ kPa; $u(\nu) = 20$ Hz. The total relative standard uncertainty is: $u_r(\varepsilon_r^*) = 0.003$.
[b] For symbols, see Table 1.
[c] Molar volume, V_m, taken from Ref. [24].
[d] V_m taken from Ref. [23].
[e] V_m taken from Table S1.

where the volume fraction of component i is defined as $\phi_i = x_i V_{mi}^* / V_m^{id}$; x_i represents the mole fraction of component i, V_{mi}^* and ε_{ri}^* stand for the molar volume and relative permittivity of pure component i respectively, and $V_m^{id} = x_1 V_{m1}^* + x_2 V_{m2}^*$ is the ideal molar volume of the mixture at the same temperature and pressure. The excess relative permittivity, ε_r^E, is obtained as

$$\varepsilon_r^E = \varepsilon_r - \varepsilon_r^{id} \quad (2)$$

where ε_r is the permittivity of the mixture. The necessary volumetric properties were obtained from the literature [23,24,27] (see also footnote of Table 2). Table 3 lists ϕ_1, ε_r and ε_r^E values for DMA (1) + amine (2), or DMF (1) + aniline (2) systems as functions of the mole fraction of the amide, x_1, in the temperature range (293.15–303.15) K. Results are shown graphically in Figs. 1–3 (see also Fig. S1, supplementary material). The only data available in the literature [36] for comparison are those for the DMF + aniline system at 303.15 K. They largely differ from our measurements (Fig. S2, supplementary material).

The ε_r^E data have been fitted by an unweighted linear least-squares regression to a Redlich-Kister equation:

$$\varepsilon_r^E = x_1(1 - x_1)\sum_{i=0}^{k-1} A_i (2x_1 - 1)^i \quad (3)$$

For each system, the number, k, of necessary coefficients for this regression has been determined by applying an F-test of additional term [37] at 99.5% confidence level. Table 4 includes the parameters A_i obtained, and the standard deviations $\sigma(\varepsilon_r^E)$, defined by:

$$\sigma(\varepsilon_r^E) = \left[\frac{1}{N-k}\sum_{j=1}^{N}(\varepsilon_{r,cal,j}^E - \varepsilon_{r,exp,j}^E)^2\right]^{1/2} \quad (4)$$

where N is the number of $\varepsilon_{r,exp,j}^E$ experimental data, and $\varepsilon_{r,cal,j}^E$ is the corresponding value of the excess property ε_r^E calculated from Eq. (3).

4. ERAS model

Some important features of this model are now given. (i) The excess functions are calculated as the sum of two contributions. The chemical contribution, $F_{m,chem}^E$, arises from hydrogen-bonding; the physical contribution, $F_{m,phys}^E$, is related to non-polar Van der Waals' interactions including free volume effects. Expressions for the molar excess functions $F_m^E = H_m^E$ (enthalpy); V_m^E (volume) can be found elsewhere [38,39]. (ii) It is assumed that only consecutive linear association occurs. Such an association is described by a chemical equilibrium constant (K_A) independent of the chain length of the associated species (amines), according to the equation:

$$A_m + A \leftrightarrow A_{m+1} \quad (5)$$

with m ranging from 1 to ∞. The cross-association between a self-associated species A_m and a non self-associated compound B (in this study, tertiary amides) is represented by

$$A_m + B \overset{K_{AB}}{\leftrightarrow} A_m B \quad (6)$$

Linear secondary amides (N-methylacetamide is also considered in this work) are also self-associated and their association is described by an equation similar to Eq. (5):

$$B_n + B \leftrightarrow B_{n+1} \quad (7)$$

with n ranging from 1 to ∞. The cross-association is then represented by:

Table 3
Volume fractions of amide, ϕ_1, relative permittivities, ε_r, and excess relative permittivities, ε_r^E, of DMA (1) + amine (2) and DMF (1) + aniline (2)[a] mixtures as functions of the mole fraction of amide, x_1, at temperature T, pressure p = 0.1 MPa and frequency $\nu = 1$ MHz.[b]

x_1	ϕ_1	ε_r	ε_r^E	x_1	ϕ_1	ε_r	ε_r^E
DMA (1) + DPA (2); T/K = 293.15							
0.0000	0.0000	3.148		0.6398	0.5453	20.725	−2.352
0.0600	0.0413	4.165	−0.492	0.6985	0.6100	23.242	−2.200
0.1099	0.0769	5.107	−0.851	0.7479	0.6670	25.568	−1.957
0.1494	0.1060	5.897	−1.125	0.7948	0.7234	27.856	−1.730
0.2122	0.1539	7.264	−1.509	0.8464	0.7881	30.535	−1.416
0.3021	0.2261	9.460	−1.951	0.8928	0.8490	33.134	−1.042
0.4041	0.3140	12.353	−2.271	0.9494	0.9268	36.494	−0.526
0.4917	0.3951	15.141	−2.447	1.0000	1.0000	39.695	
0.5905	0.4933	18.754	−2.423				
DMA (1) + DPA (2); T/K = 298.15							
0.0000	0.0000	3.093		0.6398	0.5450	20.156	−2.281
0.0600	0.0413	4.083	−0.476	0.6985	0.6097	22.613	−2.120
0.1099	0.0768	4.990	−0.829	0.7479	0.6667	24.852	−1.904
0.1494	0.1059	5.757	−1.095	0.7948	0.7231	27.082	−1.676
0.2122	0.1537	7.088	−1.460	0.8464	0.7879	29.694	−1.364
0.3021	0.2259	9.217	−1.894	0.8928	0.8488	32.205	−1.014
0.4041	0.3138	12.018	−2.213	0.9494	0.9267	35.464	−0.520
0.4917	0.3947	14.741	−2.361	1.0000	1.0000	38.586	
0.5905	0.4930	18.239	−2.352				
DMA (1) + DPA (2); T/K = 303.15							
0.0000	0.0000	3.037		0.6398	0.5446	19.598	−2.207
0.0600	0.0412	3.999	−0.458	0.6985	0.6094	21.993	−2.045
0.1099	0.0768	4.873	−0.811	0.7479	0.6664	24.135	−1.867
0.1494	0.1058	5.619	−1.064	0.7948	0.7229	26.324	−1.626
0.2122	0.1535	6.912	−1.415	0.8464	0.7877	28.874	−1.309
0.3021	0.2257	8.980	−1.835	0.8928	0.8487	31.293	−0.992
0.4041	0.3135	11.690	−2.151	0.9494	0.9267	34.462	−0.511
0.4917	0.3944	14.338	−2.291	1.0000	1.0000	37.499	
0.5905	0.4926	17.732	−2.281				
DMA (1) + DBA (2); T/K = 293.15							
0.0000	0.0000	2.938		0.6015	0.4510	16.820	−2.695
0.0896	0.0508	4.186	−0.619	0.6429	0.4949	18.472	−2.657
0.1507	0.0881	5.155	−1.021	0.7094	0.5706	21.390	−2.522
0.2190	0.1324	6.372	−1.433	0.7469	0.6163	23.221	−2.370
0.3109	0.1971	8.266	−1.917	0.7992	0.6842	25.981	−2.106
0.3974	0.2641	10.350	−2.296	0.8428	0.7448	28.506	−1.809
0.4353	0.2956	11.384	−2.419	0.8963	0.8247	31.920	−1.331
0.4940	0.3470	13.117	−2.576	0.9456	0.9044	35.389	−0.792
0.5505	0.4000	14.971	−2.670	1.0000	1.0000	39.695	
DMA (1) + DBA (2); T/K = 298.15							
0.0000	0.0000	2.896		0.6015	0.4509	16.376	−2.613
0.0896	0.0508	4.106	−0.603	0.6429	0.4948	17.967	−2.588
0.1507	0.0880	5.045	−0.992	0.7094	0.5704	20.804	−2.450
0.2190	0.1323	6.224	−1.394	0.7469	0.6161	22.565	−2.320
0.3109	0.1970	8.063	−1.864	0.7992	0.6840	25.246	−2.062
0.3974	0.2640	10.085	−2.233	0.8428	0.7446	27.715	−1.756
0.4353	0.2954	11.084	−2.355	0.8963	0.8246	31.031	−1.295
0.4940	0.3468	12.766	−2.507	0.9456	0.9043	34.398	−0.772
0.5505	0.3998	14.575	−2.590	1.0000	1.0000	38.586	
DMA (1) + DBA (2); T/K = 303.15							
0.0000	0.0000	2.858		0.6015	0.4507	15.942	−2.529
0.0896	0.0508	4.033	−0.585	0.6429	0.4946	17.504	−2.487
0.1507	0.0880	4.942	−0.964	0.7094	0.5703	20.253	−2.361
0.2190	0.1323	6.086	−1.355	0.7469	0.6160	21.966	−2.231
0.3109	0.1970	7.871	−1.811	0.7992	0.6839	24.579	−1.970
0.3974	0.2639	9.833	−2.167	0.8428	0.7446	26.984	−1.668
0.4353	0.2953	10.809	−2.278	0.8963	0.8245	30.209	−1.211
0.4940	0.3467	12.440	−2.428	0.9456	0.9043	33.491	−0.693
0.5505	0.3997	14.195	−2.509	1.0000	1.0000	37.499	
DMA (1) + BA (2); T/K = 293.15							
0.0000	0.0000	4.729		0.5989	0.5822	23.127	−1.935
0.0584	0.0547	6.126	−0.513	0.6947	0.6798	26.781	−1.689
0.1069	0.1005	7.365	−0.874	0.7906	0.7789	30.606	−1.325
0.1973	0.1866	9.841	−1.405	0.8404	0.8309	32.664	−1.083
0.3034	0.2890	13.000	−1.822	0.8970	0.8904	35.070	−0.755
0.4037	0.3872	16.238	−2.014	0.9491	0.9457	37.354	−0.403
0.4978	0.4805	19.477	−2.033	1.0000	1.0000	39.653	

Table 3 (*continued*)

x_1	ϕ_1	ε_r	ε_r^E	x_1	ϕ_1	ε_r	ε_r^E
DMA (1) + BA (2); T/K = 298.15							
0.0000	0.0000	4.636		0.5989	0.5818	22.511	−1.842
0.0584	0.0546	5.989	−0.497	0.6947	0.6795	26.066	−1.598
0.1069	0.1003	7.194	−0.841	0.7906	0.7786	29.779	−1.244
0.1973	0.1863	9.596	−1.354	0.8404	0.8307	31.779	−1.009
0.3034	0.2887	12.665	−1.755	0.8970	0.8903	34.105	−0.703
0.4037	0.3868	15.823	−1.922	0.9491	0.9456	36.315	−0.367
0.4978	0.4801	18.954	−1.953	1.0000	1.0000	38.526	
DMA (1) + BA (2); T/K = 303.15							
0.0000	0.0000	4.547		0.5989	0.5814	21.946	−1.769
0.0584	0.0545	5.863	−0.481	0.6947	0.6791	25.392	−1.544
0.1069	0.1002	7.034	−0.816	0.7906	0.7784	28.998	−1.211
0.1973	0.1861	9.380	−1.302	0.8404	0.8304	30.943	−0.981
0.3034	0.2883	12.352	−1.700	0.8970	0.8901	33.220	−0.672
0.4037	0.3864	15.431	−1.855	0.9491	0.9455	35.362	−0.356
0.4978	0.4797	18.478	−1.884	1.0000	1.0000	37.515	
DMA (1) + HxA (2); T/K = 293.15							
0.0000	0.0000	3.955		0.6944	0.6138	23.705	−2.183
0−.1027	0.0741	5.810	−0.793	0.7581	0.6867	26.548	−1.945
0.1921	0.1426	7.690	−1.361	0.8028	0.7401	28.677	−1.724
0.3016	0.2320	10.349	−1.896	0.8528	0.8021	31.226	−1.390
0.3994	0.3175	13.099	−2.201	0.8986	0.8611	33.671	−1.054
0.5066	0.4180	16.508	−2.383	0.9529	0.9340	36.812	−0.518
0.6030	0.5151	20.011	−2.350	1.0000	1.0000	39.688	
DMA (1) + HxA (2); T/K = 298.15							
0.0000	0.0000	3.893		0.6944	0.6137	23.075	−2.118
0.1027	0.0741	5.694	−0.771	0.7581	0.6866	25.835	−1.888
0−.1921	0.1425	7.522	−1.317	0.8028	0.7400	27.897	−1.679
0.3016	0.2319	10.096	−1.846	0.8528	0.8020	30.358	−1.370
0.3994	0.3173	12.772	−2.134	0.8986	0.8610	32.742	−1.034
0.5066	0.4178	16.083	−2.311	0.9529	0.9340	35.798	−0.511
0.6030	0.5150	19.493	−2.274	1.0000	1.0000	38.600	
DMA (1) + HxA (2); T/K = 303.15							
0.0000	0.0000	3.835		0.6944	0.6135	22.498	−2.022
0.1027	0.0740	5.588	−0.742	0.7581	0.6864	25.163	−1.815
0−.1921	0.1424	7.362	−1.274	0.8028	0.7398	27.182	−1.597
0.3016	0.2317	9.866	−1.781	0.8528	0.8019	29.567	−1.306
0.3994	0.3172	12.465	−2.065	0.8986	0.8609	31.893	−0.969
0.5066	0.4177	15.690	−2.229	0.9529	0.9339	34.820	−0.503
0.6030	0.5148	19.005	−2.188	1.0000	1.0000	37.552	
DMF (1) + aniline (2); T/K = 293.15							
0.0000	0.0000	7.117		0.5999	0.5589	26.184	1.620
0.0533	0.0454	8.910	0.376	0.6989	0.6624	28.955	1.160
0.1046	0.0899	10.653	0.730	0.7931	0.7641	31.604	0.634
0.1562	0.1353	12.414	1.073	0.8431	0.8195	33.120	0.421
0.2033	0.1774	14.004	1.349	0.8982	0.8818	34.833	0.189
0.3015	0.2673	17.269	1.808	0.9459	0.9366	36.439	0.084
0.4071	0.3672	20.625	2.045	1.0000	1.0000	38.334	
0.5013	0.4593	23.428	1.973				
DMF (1) + aniline (2); T/K = 298.15							
0.0000	0.0000	6.984		0.5999	0.5592	25.601	1.586
0.0533	0.0455	8.729	0.359	0.6989	0.6626	28.310	1.146
0.1046	0.0899	10.426	0.704	0.7931	0.7643	30.920	0.658
0.1562	0.1354	12.144	1.036	0.8431	0.8197	32.402	0.453
0.2033	0.1775	13.689	1.299	0.8982	0.8819	34.071	0.228
0.3015	0.2675	16.874	1.743	0.9459	0.9367	35.620	0.108
0.4071	0.3674	20.146	1.972	1.0000	1.0000	37.440	
0.5013	0.4596	22.895	1.913				
DMF (1) + aniline (2); T/K = 303.15							
0.0000	0.0000	6.856		0.5999	0.5593	25.026	1.545
0.0533	0.0455	8.557	0.349	0.6989	0.6627	27.687	1.133
0.1046	0.0900	10.200	0.669	0.7931	0.7644	30.246	0.669
0.1562	0.1355	11.876	0.992	0.8431	0.8198	31.690	0.466
0.2033	0.1777	13.383	1.245	0.8982	0.8819	33.315	0.245
0.3015	0.2676	16.485	1.675	0.9459	0.9367	34.821	0.123
0.4071	0.3676	19.678	1.895	1.0000	1.0000	36.580	
0.5013	0.4597	22.371	1.851				

[a] For symbols, see Table 1.

[b] The standard uncertainties are: $u(T) = 0.02$ K; $u(p) = 1$ kPa; $u(v) = 20$ Hz; $u(x_1) = 0.0010$; $u(\phi_1) = 0.0040$. The relative standard uncertainty is: $u_r(\varepsilon_r) = 0.003$; and the relative combined expanded uncertainty (0.95 level of confidence) is $U_{rc}(\varepsilon_r^E) = 0.03$.

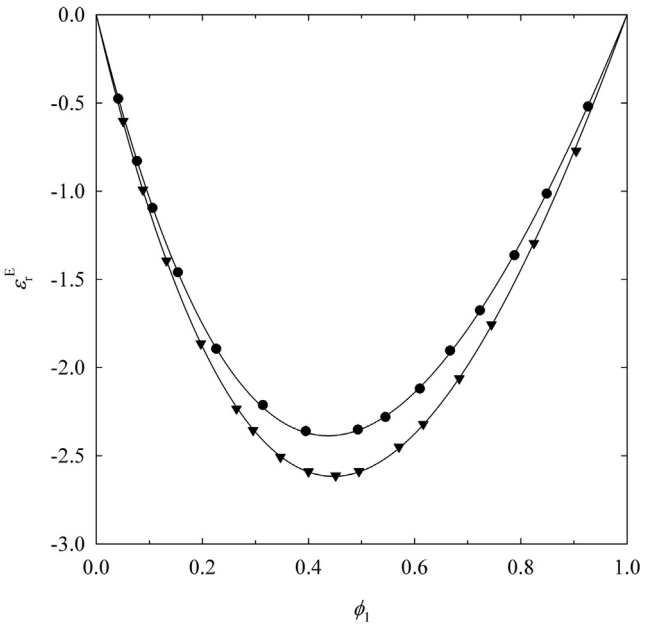

Fig. 1. Excess relative permittivities, ε_r^E, for DMA (1) + DPA (2), or + DBA (2) systems at 0.1 MPa, 298.15 K and 1 MHz. Full symbols, experimental values (this work): (●), DPA; (▼), DBA. Solid lines, calculations with Eq. (3) using the coefficients from Table 4.

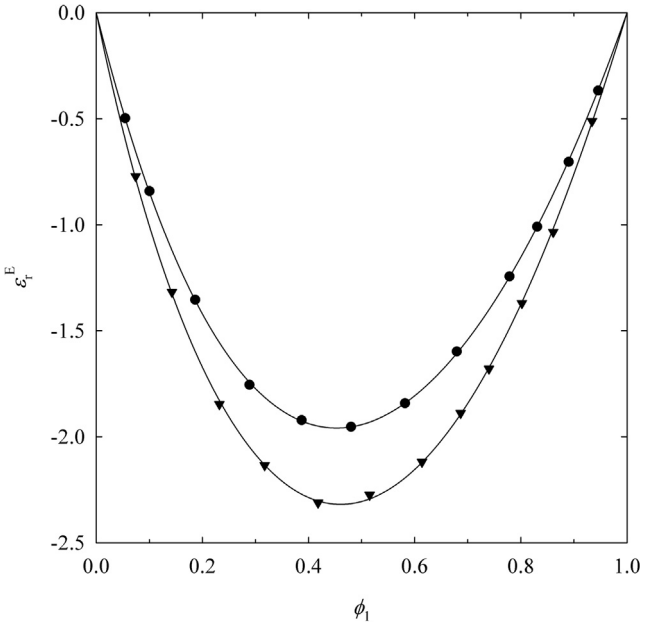

Fig. 2. Excess relative permittivities, ε_r^E, for DMA (1) + BA (2), or + HxA (2) systems at 0.1 MPa, 298.15 K and 1 MHz. Full symbols, experimental values (this work): (●), BA; (▼), HxA. Solid lines, calculations with Eq. (3) using the coefficients from Table 4.

$$A_m + B_n \overset{K_{AB}}{\leftrightarrow} A_m B_n \tag{8}$$

The cross-association constants (K_{AB}) of Eqs. (6) and (8) are also considered to be independent of the chain length. Eqs. (5)–(8) are characterized by Δh_i^*, the enthalpy of the reaction that corresponds to the hydrogen-bonding energy, and by the volume change (Δv_i^*) related to the formation of the linear chains. (iii) The $F_{m,phys}^E$ term is derived from the Flory's equation of state [40], which is assumed to be valid not only for pure compounds but also for the mixture [41,42]:

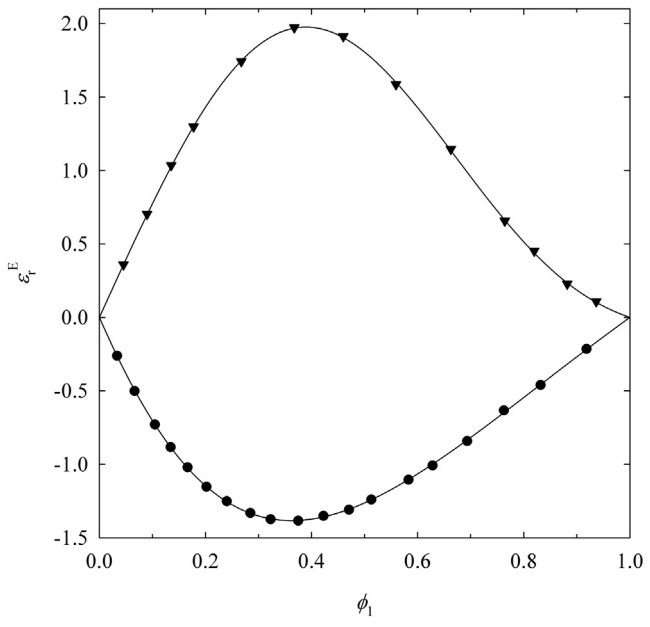

Fig. 3. Excess relative permittivities, ε_r^E, for DMF (1) + amine (2) systems at 0.1 MPa, 298.15 K and 1 MHz. Full symbols, experimental values: (▼), aniline (this work); (●), HxA [25]. Solid lines, calculations with Eq. (3) using the coefficients from Table 4 or from the literature [25].

$$\frac{\bar{P}_i \bar{V}_i}{\bar{T}_i} = \frac{\bar{V}_i^{1/3}}{\bar{V}_i^{1/3} - 1} - \frac{1}{\bar{V}_i \bar{T}_i} \tag{9}$$

where i = A,B or M (mixture). In Eq. (9), $\bar{V}_i = V_{mi}/V_i^*$; $\bar{P}_i = P/P_i^*$; $\bar{T}_i = T/T_i^*$ are the reduced properties for volume, pressure and temperature, respectively. The pure component reduction parameters V_i^*, P_i^*, T_i^* are obtained from *P-V-T* data (density, α_p, isobaric thermal expansion coefficient, and isothermal compressibility, κ_T), and association parameters [41,42]. The reduction parameters for the mixture P_M^* and T_M^* are calculated from mixing rules [41,42]. The total relative molecular volumes and surfaces of the compounds were calculated additively on the basis of the group volumes and surfaces recommended by Bondi [43].

4.1. Adjustment of ERAS parameters

Values of V_{mi}, V_i^* and P_i^* of pure compounds at T = 298.15 K, needed for calculations, are listed in Table S2 of supplementary material. K_A, Δh_A^*, and Δv_A^* of the self-associated amines and of *N*-methylacetamide are known from H_m^E and V_m^E data for the corresponding mixtures with alkanes [11–13,44]. The binary parameters to be fitted against H_m^E [18–20] and V_m^E [23,24,27,45] data available in the literature for amine + amide systems are then K_{AB}, Δh_{AB}^*, Δv_{AB}^* and X_{AB}. They are collected in Table 5.

4.2. Results

ERAS results are shown in Table 6 and Figs. 4 and 5 (see also Figs. S3 and S4 of supplementary material). We must underline that the model describes, rather correctly, the H_m^E and V_m^E functions of the amine + amide systems under study using parameters which smoothly change with the molecular structure (Table 5).

Table 4
Coefficients A_i and standard deviations, $\sigma(\varepsilon_r^E)$ (Eq. (4)), for the representation of ε_r^E at temperature T and pressure p = 0.1 MPa for DMA (1) + amine (2) and DMF (1) + aniline (2) systems by Eq. (3).

System[a]	T/K	A_0	A_1	A_2	A_3	A_4	$\sigma(\varepsilon_r^E)$
DMA + DPA	293.15	−9.79	−1.40				0.012
	298.15	−9.50	−1.34				0.007
	303.15	−9.21	−1.30				0.007
DMA + DBA	293.15	−10.35	−4.09	−1.03			0.011
	298.15	−10.06	−4.00	−1.06			0.009
	303.15	−9.76	−3.70	−0.69			0.006
DMA + BA	293.15	−8.16	0.72	−0.81			0.008
	298.15	−7.81	0.86	−0.64			0.006
	303.15	−7.53	0.83	−0.67			0.008
DMA + HxA	293.15	−9.49	−1.70	−0.9			0.010
	298.15	−9.19	−1.68	−1.0			0.012
	303.15	−8.86	−1.52	−0.9			0.011
DMF + aniline	293.15	7.87	−4.1	−5.6	1.0	1.7	0.012
	298.15	7.63	−3.83	−5.2	1.2	1.7	0.010
	303.15	7.38	−3.48	−4.8	1.2	1.7	0.009

[a] For symbols, see Table 1.

Table 5
ERAS parameters[a] for amine (1) + amide (2) mixtures at 298.15 K.

System[b]	K_{AB}	Δh^*_{AB}/kJ·mol^{-1}	Δv^*_{AB}/cm^3·mol^{-1}	X_{AB}/J·cm^{-3}
BA + DMF	1.2	−22	−2.5	10
HxA + DMF	0.65	−22	−2.5	10
DPA + DMF	0.6	−22	−3.1	10
DBA + DMF	0.20	−22	−3.1	17.45
BA + DMA	0.75	−22	−2.5	10
HxA + DMA	0.50	−22	−2.5	10
DPA + DMA	0.25	−22	−3.9	10
DBA + DMA	0.12	−22	−3.9	17.45
Aniline + DMF	70	−22	−11.1	4
Aniline + DMA	2.20	−22	−20	3.2
HxA + NMA[c]	20	−25.	−3.2	5

[a] K_{AB}, association constant of component A with component B; Δh^*_{AB}, association enthalpy of component A with component B; Δv^*_{AB}, association volume of component A with component B; X_{AB}, physical parameter.
[b] For symbols, see Table 1.
[c] T = 363.15 K.

Table 6
Excess molar volumes, V^E_m, at 298.15, equimolar composition and 0.1 MPa for amine (1) + *N*,*N*-dialkylamide (2) mixtures. Comparison of experimental results (exp) with ERAS calculations; the physical ($V^E_{m,phys}$) and chemical ($V^E_{m,chem}$) contributions are also listed.

System[a]	V^E_m				Ref.
	Exp.	ERAS[b]	$V^E_{m,phys}$	$V^E_{m,chem}$	
BA + DMA	−0.192	−0.208	−0.177	−0.031	[24]
HxA + DMA	0.006	0.006	0.043	−0.036	[24]
DPA + DMA	−0.227	−0.232	−0.242	0.01	[24]
DBA + DMA	0.056	0.051	0.116	−0.065	[24]
BA + DMF	−0.263	−0.270	−0.132	−0.139	[23]
HxA + DMA	−0.021	−0.024	0.075	−0.099	[23]
DPA + DMF	−0.289	−0.291	−0.181	−0.110	[23]
DBA + DMF	0.018	0.015	0.126	−0.111	[23]
Aniline + DMA	−0.609[c]	−0.634	0.264	−0.898	[45]
Aniline + DMF	−0.662	−0.662	0.241	−0.903	[27]
	−0.693				[79]

[a] For symbols, see Table 1.
[b] Results using ERAS parameters from Table 5.
[c] T = 303.15 K; X_{AB} = 5 J·cm^{-3}.

5. Kirkwood-Fröhlich model

Some relevant hypotheses of the model are: (i) molecules of a given polar compound are assumed to be spherical (i.e., an intrinsic dipole moment inside a spherical cavity), (ii) the effect of the induced polarization of the molecules is treated in macroscopic way, assuming that the cavity is filled by a continuous medium of relative permittivity ε_r^∞ (the value of the permittivity at a high frequency at which only the induced polarizability contributes); (iii) long-range interactions are taken into account macroscopically by considering the outside of the cavity as a continuous dielectric of permittivity ε_r, leading to the Onsager local field; (iv) short-

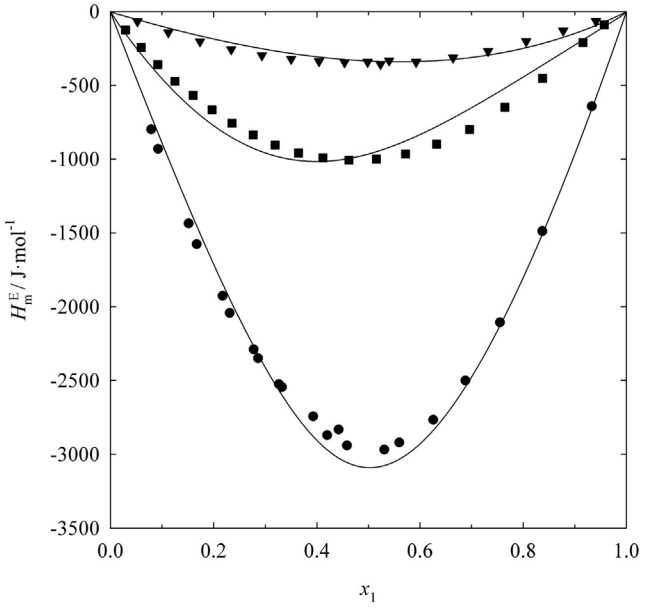

Fig. 4. Excess molar enthalpies, H_m^E for amine (1) + amide (2) mixtures at 0.1 MPa. Points experimental results: (●), aniline (1) + DMF (2) (T = 298.15 K) [18]; (■), HxA (1) + NMA (2) (T = 363.15 K) [20]; (▲), aniline (1) + DMA (2) (T = 298.15 K) [19]. Solid lines, ERAS calculations with parameters from Table 5.

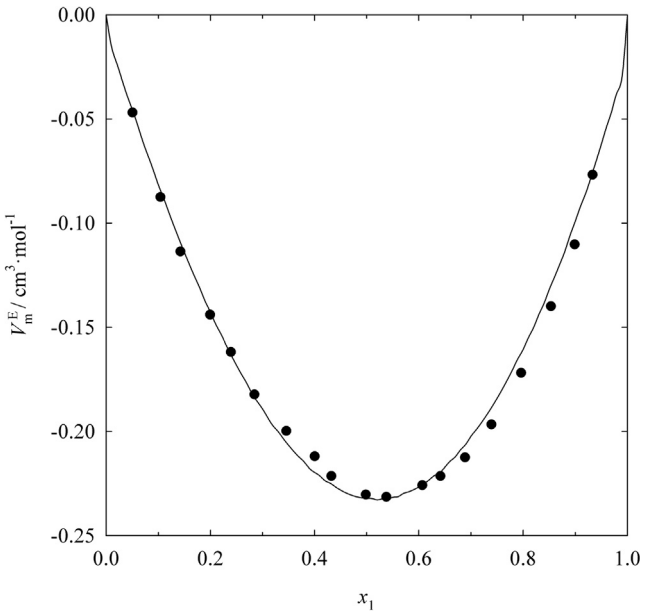

Fig. 5. Excess molar volume, V_m^E for DPA (1) + DMA (2) mixture at 298.15 K and 0.1 MPa. Points experimental results [24]. Solid line, ERAS calculations with parameters from Table 5.

range interactions are not neglected. A central magnitude of the theory is the so-called Kirkwood correlation factor, g_K, which provides information of the deviations from randomness of the orientation of a dipole with respect to its neighbours. This is an important parameter, as it provides information on specific interactions in the liquid state. For a mixture, g_K can be determined, in the context of a one-fluid model [32], from macroscopic physical properties according to the expression [28,29,31,32]:

$$g_K = \frac{9k_B T V_m \varepsilon_0 (\varepsilon_r - \varepsilon_r^\infty)(2\varepsilon_r + \varepsilon_r^\infty)}{N_A \mu^2 \varepsilon_r (\varepsilon_r^\infty + 2)^2} \quad (10)$$

Here, k_B is Boltzmann's constant; N_A, Avogadro's constant; ε_0, the vacuum permittivity; and V_m, the molar volume of the liquid at the working temperature, T. For polar compounds, ε_r^∞ is estimated from the relation $\varepsilon_r^\infty = 1.1 n_D^2$ [46]. μ represents the gas phase dipole moment of the solution, estimated from the equation [32]:

$$\mu^2 = x_1 \mu_1^2 + x_2 \mu_2^2 \quad (11)$$

where μ_i stands for the dipole moment of component i (=1,2) (Table 2).

The molar orientational polarizabilities (molar orientational polarizations or molar polarizability volumes), Π_m^{or}, are determined from [29–31]:

$$\Pi_m^{or} = \frac{N_A \alpha_{or}}{3\varepsilon_0} = \frac{(\varepsilon_r - \varepsilon_r^\infty)(2\varepsilon_r + \varepsilon_r^\infty)}{9\varepsilon_r} V_m \quad (12)$$

where α_{or} stands for the orientational polarizability (in the case of mixtures, a one-fluid approach is implicit).

Molar induced polarizabilities, Π_m^{ind}, can be calculated in the framework of the Kirkwood-Fröhlich model by means of the expression:

$$\Pi_m^{ind} = \frac{N_A \alpha_{ind}}{3\varepsilon_0} = \frac{(\varepsilon_r^\infty - 1)(2\varepsilon_r + \varepsilon_r^\infty)}{9\varepsilon_r} V_m \quad (13)$$

with α_{ind} meaning the induced polarizability. Excess values of Π_m^{or} and Π_m^{ind} (Table 7, Figs. 6 and S5, and S6 of supplementary material) have been obtained from the equation:

$$F^E = F - F^{id} \qquad (F = \Pi_m^{or} \text{ or } \Pi_m^{ind}) \quad (14)$$

with F^{id} values determined from Eqs. (12) or (13) using ideal values for the involved quantities in the mentioned equations. Particularly, calculations have been conducted using smoothed values of V_m^E [23,24,27,45], n_D^E [23,24,27] and ε_r^E (this work) at $\Delta x_1 = 0.01$.

6. Discussion

Along the present section, the values of the physical properties which involve some permittivity measurements and of their excess functions are referred to 298.15 K and $\phi_1 = 0.5$. Values of H_m^E and V_m^E are referred to 298.15 K and equimolar composition.

It is known that the disruption of interactions between like molecules, in the present case amide-amide and amine-amine interactions, contributes negatively to ε_r^E. For instance, the ε_r^E values of n-alkylamine + n-C_{12} systems at 293.15 K are: −0.314 (propylamine) < −0.243 (BA) < −0.133 (HxA) [47]. This negative contribution diminishes when increasing the chain length of the amine, as the amine group is then more sterically hindered, in such a way that the effective polarity of longer amines becomes weaker. The creation of interactions between unlike molecules along the mixing process may lead either to a positive or to a negative contribution to ε_r^E [48]. A positive contribution is encountered when interactions between unlike molecules lead to an increased number of effective dipole moments in the system. Negative contributions arise when interactions between unlike molecules lead to a loss of the polar structure of the liquid, and therefore to a decreased number of effective dipole moments.

The large and negative ε_r^E values of DMA + linear amine mixtures reveal that the negative contributions from the breaking of interactions between like molecules are dominant. It is noteworthy that the ε_r^E values of n-alkylamine + n-C_{12} systems at 293.15 K are much less negative than those of DMA + n-alkylamine, e.g., −2.447 for the DPA system (see above). This suggests that ε_r^E of DMA solutions is determined, to a large extent, by the breaking of the dipolar interactions between DMA molecules. On the other

Table 7
Excess functions, permittivity, ε_r^E, orientational polarizability, $(\Pi_m^{or})^E$, and relative Kirkwood's correlation factors ($g_{K,rel}^E$, $g_{K,rel,i}^E$, i = 1,2) for *N*,*N*-dialkylamide (1) + amine (2) mixtures at $\phi_1 = 0.5$ and 298.15 K. The minimum and maximum values of ε_r^E, $g_{K,rel}^E$, $g_{K,rel,i}^E$ (i = 1,2) and the corresponding compositions are also listed.

System[a]	ε_r^E	$(\Pi_m^{or})^E$/cm^3·mol^{-1}	$g_{K,rel}^E$	$g_{K,rel,1}^E$	$g_{K,rel,2}^E$
$\phi_1 = 0.5$					
DMA + BA	−1.943	−42.6	−0.10	−0.10	−0.10
DMA + HxA	−2.305	−56.4	−0.12	−0.12	−0.12
DMA + DPA	−2.348	−59.2	−0.12	−0.12	−0.12
DMA + DBA	−2.586	−69.5	−0.13	−0.13	−0.13
DMF + BA	−0.864	−18.0	−0.05	−0.05	−0.05
DMF + HxA	−1.262	−27.8	−0.07	−0.07	−0.06
DMF + DPA	−1.372	−31.6	−0.08	−0.08	−0.08
DMF + DBA	−1.733	−41.4	−0.09	−0.09	−0.09
DMF + aniline	1.806	30.5	0.10	0.08	0.08

Minimum or maximum values

	ϕ_1	ε_r^E	ϕ_1	$g_{K,rel}^E$	ϕ_1	$g_{K,rel1}^E$	ϕ_1	$g_{K,rel2}^E$
DMA + BA	0.45	−1.98	0.19	−0.14	0.17	−0.15	0.18	−0.14
DMA + HxA	0.46	−2.32	0.20	−0.18	0.15	−0.19	0.15	−0.18
DMA + DPA	0.43	−2.39	0.17	−0.21	0.11	−0.22	0.12	−0.21
DMA + DBA	0.45	−2.62	0.18	−0.24	0.10	−0.24	0.11	−0.24
DMF + BA	0.35	−0.97	0.20	−0.09	0.15	−0.09	0.15	−0.09
DMF + HxA	0.36	−1.38	0.22	−0.13	0.14	−0.13	0.14	−0.13
DMF + DPA	0.37	−1.51	0.22	−0.15	0.12	−0.16	0.14	−0.15
DMF + DBA	0.38	−1.86	0.26	−0.18	0.14	−0.18	0.14	−0.18
DMF + aniline	0.39	1.976	0.25	0.12	0.28	0.11	0.25	0.13

[a] For symbols, see Table 1.

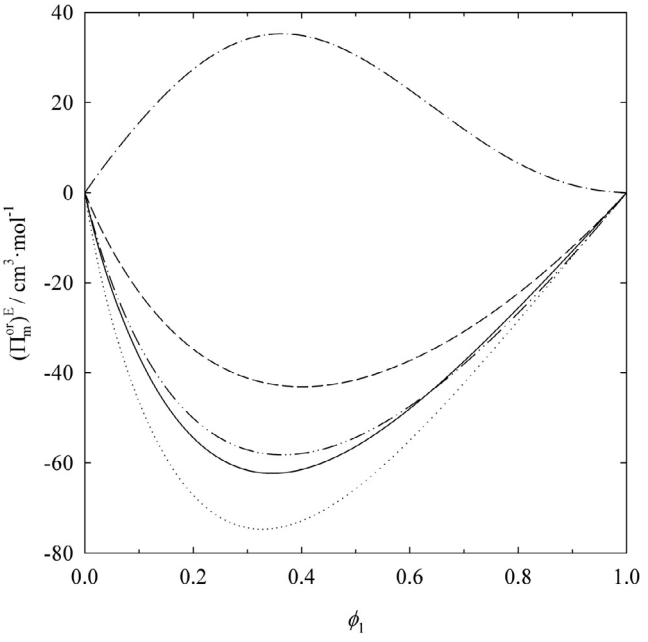

Fig. 6. Excess molar orientational polarizability, $(\Pi_m^{or})^E$, for DMA (1) + linear amine (2), or DMF (1) + aniline (2) systems at 0.1 MPa and 298.15 K. (− − −), DMA + DPA; (···), DMA + DBA; (− − −), DMA + BA; (···−···), DMA + HxA; (·−·), DMF + aniline.

hand, one can expect that interactions between unlike molecules contribute positively to ε_r^E. In fact, the ε_r^E value of the DMF + heptane mixture at $\phi_1 = 0.0171$ and 293.15 K is lower (−0.24, calculated from data of the literature [49]) than the values of the corresponding systems with amines at the same conditions: −0.129 (DPA), −0.146 (DBA), −0.104 (BA), and −0.137 (HxA) [47]. Interestingly, ε_r^E is positive for the DMF + aniline mixture. This clearly indicates that ε_r^E is now mainly determined by the positive contribution related to the aniline-DMF interactions created upon mixing. Other systems as methanol + DMF (2.57 [50]); + DMA (0.52 [51]); + pyridine (2.85 [50]), or + cyclohexylamine (1.13 [52]) also show positive ε_r^E values.

We note that, in DMA solutions, ε_r^E (DBA) < ε_r^E (DPA) and ε_r^E (HxA) < ε_r^E (BA) (Table 7, Figs. 1, 2). This can be explained as follows: (i) longer amines are better breakers of the DMA-DMA interactions due to their large aliphatic surface; (ii) the formation of interactions between unlike molecules becomes easier when shorter amines are involved, as the amine group is then less sterically hindered. It is remarkable that ε_r^E (HxA) ≈ ε_r^E (DPA), which suggests that the ε_r decrease when HxA is replaced by DPA (note that ε_r^* (HxA) = 3.893 > ε_r^* (DPA) = 3.093, Table 2) is compensated by the creation of a larger number of interactions between unlike molecules in the case of the HxA mixture. Similar trends are observed for the corresponding systems with DMF, but an interesting difference is that ε_r^E (HxA) = −1.383 > ε_r^E (DPA) = −1.509 [25]. It seems that interactions between unlike molecules could be now even more important, as the amide group is less sterically hindered in DMF. Comparison between ε_r^E values of mixtures with a given linear amine shows that ε_r^E (DMF) > ε_r^E (DMA). In addition, ε_r^E curves of the DMA systems are more skewed towards larger ϕ_1 values (Table 7). This suggests that linear amines can disrupt more easily DMA-DMA interactions and that the creation of amide-amine interactions is favoured when DMF molecules participate.

Finally, we must remark that the replacement of HxA ($\varepsilon_r^E = -1.383$) by aniline ($\varepsilon_r^E = 1.806$) in DMF solutions has a large impact on the ε_r^E values of these mixtures, which show opposite signs. Therefore, the aromaticity effect leads here to an increase of the number of effective dipole moments in the aniline system.

6.1. Temperature dependence of ε_r

Some important information on interactions and structure of a liquid can be inferred from the temperature dependence of ε_r. Of particular interest is the investigation of entropic effects induced in the liquid by the external electric field applied, $\vec{E}$. The relationship between $(\partial\varepsilon_r/\partial T)$ and the entropy increment per volume unit is given by [28,53–55]:

$$\frac{\Delta S}{\vec{E}^2} = \frac{S(T,\vec{E}) - S_0(T)}{\vec{E}^2} = \frac{\varepsilon_0}{2}\left(\frac{\partial \varepsilon_r}{\partial T}\right) \quad (15)$$

In this expression, $S(T,\vec{E})$ is the entropy per volume unit of the system at temperature T under the application of $\vec{E}$, and $S_0(T)$ is the entropy per volume unit of the solution in absence of $\vec{E}$. The data analysis is more properly conducted on the basis of the $\frac{\Delta S}{\vec{E}^2}V_m$ magnitude as then one is considering along the discussion a number of molecules equal to N_A [54,55]. Within this treatment, volume variations with T have been neglected. We must note that $\Delta S < 0$ corresponds to the dipolar ordering action of $\vec{E}$, which is the normal behaviour of common liquids. All the pure compounds and systems along the present work follow this trend (Tables 2 and 8). From our results, some conclusions can be stated. (i) The molar entropy increments induced in amides are much more negative than those induced in amines (Table 2). This remarks the existence of strong dipolar interactions between amide molecules, which lead to the formation of entities of high polarity. Such entities are better oriented by the application of $\vec{E}$. (ii) For linear amines, the molar entropy increments become less negative in the sequence: BA > HxA > DPA > DBA (Table 2). Clearly, it can be ascribed to a meaningful decrease of the orientational polarizability of the amines in the same order (see below). Aniline shows the largest $\left|\frac{\Delta S}{\vec{E}^2}V_m\right|$ value, as a consequence of its stronger polar character. (iii) Interestingly, $\frac{\Delta S}{\vec{E}^2}V_m$ is more negative for DMA than for DMF (Table 2). This suggests that the ability of the DMA entities to respond to the ordering action of $\vec{E}$ is higher, a behaviour that can be attributed to weaker dipolar interactions between DMA molecules. This is supported experimentally by liquid-liquid equilibrium measurements, as the upper critical solution temperatures of heptane systems are 342.55 K (DMF) [56] >309.8 K (DMA) [57] (see also the results from the Kirkwood-Fröhlich model below). (iv) A similar analysis is still valid for the considered mixtures (Table 8). For example, $\frac{\Delta S}{\vec{E}^2}V_m$ values of DMA solutions decrease in the sequence BA > DBA. This can be explained assuming, as previously, that DBA is a better breaker of interactions between amide molecules leading to a higher loss of the polar structure of DMA. This makes that the remaining DMA entities, of smaller size than those in pure amide, can be more easily oriented by the action of $\vec{E}$. It must be also remarked that the higher polar structure of the DMF + aniline system compared to that of the HxA system leads to a lower $\frac{\Delta S}{\vec{E}^2}V_m$ value for the former solution.

6.2. Results from ERAS model

The application of the ERAS model is useful to complete the description given above. Some important features are now given. (i) Amine-amide interactions are rather strong, as $\Delta h^*_{AB} = -22$ kJ mol^{-1}, is a value not far from that used for 1-alkanol self-association (-25.1 kJ·mol^{-1}) in applications of the ERAS model [10,26,39,58]. It must be remarked that the same Δh^*_{AB} parameter is valid for all the tertiary amide + amine mixtures under consideration. (ii) Negative V^E_m values of BA, or DPA + DMA system arise from structural effects, as it is suggested by $V^E_{m,phys} < 0$ (Table 6) and positive X_{AB} values (Table 5). The $V^E_{m,chem}$ term (i.e., interactions between unlike molecules) is also relevant for the BA or DPA + DMF mixtures. Structural effects contribute more largely to V^E_m in DPA systems. (iii) The large $|V^E_{m,chem}|$ values of aniline mixtures may be indicative that the model overestimates this contribution. In fact, the V^E_m values of such systems are rather similar (V^E_m/cm^3·mol^{-1} = −0.662 (DMF) [27]; −0.636 (DMA) [45], T = 303.15 K), while the corresponding H^E_m values are very different (see above); (iv) The equilibrium constant K_{AB} decreases in the sequences: BA > HxA and DPA > DBA. In addition, for mixtures with a given amine, K_{AB} (DMF) > K_{AB} (DMA). If one takes into account that, in the ERAS model, self-association or solvation effects are described by means of linear chains formed by the system components, the relative variation of K_{AB} agrees with that encountered for ε^E_r.On the other hand, the large K_{AB} value for the DMF + aniline mixture is to be noted, as it remarks that interactions between unlike molecules become here rather important.

Table 8
Values of $V_m\frac{\partial \varepsilon^*_r}{\partial T}$/cm^3 · mol^{-1} · K^{-1} at 298.15 K for *N*,*N*-dialkylamide (1) + amine (2) mixtures at 298.15 K and $\phi_1 = 0.5$.

Amide	BA	HxA	DPA	DBA	Aniline
DMA	−9.86	−10.9	−11.1	−11.6	
DMF	−8.27	−8.80	−8.90	−8.81	−9.31

6.3. Results from Kirkwood-Fröhlich's theory

Firstly, we give values of $(\Pi^{or}_m)^*$ and of $(\Pi^{ind}_m)^*$ for pure compounds: $(\Pi^{or}_m)^*$/cm^3·mol^{-1} = 623.0 (DMF); 773.0 (DMA); 68.0 (BA); 64.1 (HxA); 38.6 (DPA); 36.3 (DBA), 103.0 (aniline) and $(\Pi^{ind}_m)^*$/cm^3·mol^{-1} = 22.0 (DMF); 27.0 (DMA); 31.4 (BA); 45.7 (HXA); 47.9 (DPA); 63.0 (DBA), 42,7 (aniline). It is remarkable that $(\Pi^{or}_m)^*$ of DMA is much larger than $(\Pi^{ind}_m)^*$. It is also important to consider the sum of these two quantities (i.e. the total molar polarizability); in the same units: 645.0 (DMF); 800.0 (DMA); 99.4 (BA); 109.8 (HxA); 86.5 (DPA); 99.3 (DBA). These results indicate that DMA molecules are more easily oriented by the application of an electric field than DMF molecules, and underline that dipolar interactions between DMA molecules are weaker than in DMF. This was suggested by their $\frac{\Delta S}{\vec{E}^2}V_m$ values (see above). Interestingly, the total molar polarizability of the compounds does not vary in the same sense as ε^*_r. Nevertheless, it must be taken into account that, when applying a certain electric field, $(\varepsilon^*_r - 1)$ is proportional to the macroscopic dipole moment per unit volume, and therefore the trend of ε^*_r can be explained as arising from volume effects. In fact, the total molar polarizability per unit volume does vary accordingly to ε^*_r: 8.331 (DMF); 8.600 (DMA); 0.995 (BA); 0.825 (HxA); 0.627 (DPA); 0.580 (DBA); 1.54 (aniline).

Results for $(\Pi^{or}_m)^E$/(in cm^3·mol^{-1}) of DMA systems are: −42.6 (BA) > −56.4 (HxA) > −59.2 (DPA) > −69.5 (DBA). These $(\Pi^{or}_m)^E$ values change in line with those of ε^E_r (Table 7), pointing out to a main contribution to ε^E_r arising from effects related to the orientational polarizability of the molecules. The same trend is observed for $(\Pi^{or}_m)^E$/cm^3·mol^{-1} of DMF mixtures: 30.5 (aniline) > −18.0 (BA) > −27.8 (HxA) > −31.6 (DPA) > −41.4 (DBA). It seems to be clear that there is a loss of effective dipole moments in DMA + linear amines mixtures with regards to those involving DMF. In contrast, there is a meaningful increment of the effective dipole moments when HxA is replaced by aniline in DMF solutions. Interestingly, the $(\Pi^{ind}_m)^E$ curves (Figs. S5 and S6 of supplementary material) of *n*-alkylamine systems show a maximum at the concentrations where a minimum exists for the $(\Pi^{or}_m)^E$ curves (Fig. 6). This is a consistent result, as it indicates that the decrease of orientational polarization effects is linked to an increase of Π^{ind}_m, that is, roughly speaking, to an increase of dispersive interactions. For a given linear amine, the $(\Pi^{ind}_m)^E$ maximum changes in the order: DMF < DMA, which also supports the more polar character of DMF solutions (Figures S5 and S6). In systems with a fixed amide, the mentioned maximum

changes in the sequence: DBA > DPA > HxA > BA. That is, it decreases when the polarity of the mixture increases. It is to be noted that the increase of polarity in the DMF + aniline system is accompanied by a decrease in the dispersive interactions (Figs. 6 and S6, supplementary material).

The Balankina relative excess Kirkwood correlation factors [32], $g^{E}_{K,rel} = (g_K - g^{id}_K)/g^{id}_K$, where g_K and g^{id}_K account respectively for the real and ideal Kirkwood correlation factors, are a useful tool to probe into the structure of the mixtures:

$$g^{E}_{K,rel} = \frac{V_m(\varepsilon_r - \varepsilon_r^{\infty})(2\varepsilon_r + \varepsilon_r^{\infty})\varepsilon_r^{id}(\varepsilon_r^{id,\infty} + 2)^2}{V_m^{id}(\varepsilon_r^{id} - \varepsilon_r^{id,\infty})(2\varepsilon_r^{id} + \varepsilon_r^{id,\infty})\varepsilon_r(\varepsilon_r^{\infty} + 2)^2} - 1 \quad (16)$$

It is also possible to develop a two-liquid model [32], in which liquid i (i = 1,2) is defined by molecules of pure substance i located in spherical cavities of volume $\bar{V}_{mi}/N_A$ (where $\bar{V}_{mi}$ stands for the partial molar volume of component i) and embedded in a dielectric continuum formed by the real mixture at the same composition. This approach leads to the definition of the relative excess Kirkwood correlation factor of liquid i, which is given by:

$$g^{E}_{K,rel,i} = \frac{\bar{V}_{mi}(\varepsilon_r - \varepsilon_{ri}^{\infty})(2\varepsilon_r + \varepsilon_{ri}^{\infty})\varepsilon_r^{id}}{V_{mi}(\varepsilon_r^{id} - \varepsilon_r^{\infty})(2\varepsilon_r^{id} + \varepsilon_{ri}^{\infty})\varepsilon_r} - 1 \quad (17)$$

Values of $g^{E}_{K,rel}$ and $g^{E}_{K,rel,i}$ are collected in Table 7 (Figs. 7–10). From inspection of the results obtained some conclusions regarding systems with linear amines can be stated. (i) The $g^{E}_{K,rel}$ values are negative over the whole composition range. As in the ideal mixture neither correlations between like dipoles are destroyed nor are new correlations between unlike dipoles created, these results show that there is a destruction of the structure in the solution with regards to that of the ideal mixture. (ii) Interestingly, the $g^{E}_{K,rel}$ curves are skewed towards low ϕ_1 values (Figs. 7 and 8). This suggests that the amide structure is better destroyed at such concentrations. (iii) An interesting result is that the minima of the $g^{E}_{K,rel}$ curves is reached at lower volume fractions of the amide than in the ε^{E}_r and $(\Pi^{or}_m)^E$ curves (Table 7). Thus, according to the Kirkwood-Fröhlich model, the destruction of dipole correlations is not the only responsible for the ε^{E}_r minima, but other related effects, such as the number and strength of interactions created and disrupted upon mixing, are also important. (iv) The minimum values change in similar order to that encountered for ε^{E}_r. For example, $g^{E}_{K,rel}$ (DMA) = −0.14 (BA) > −0.18 (HxA) > −0.21 (DPA) > −0.24 (DBA). The BA mixture is the most structured, which can be ascribed to a higher relevance of the creation of interactions between unlike molecules. (v) Similarly, systems with DMF are also more structured than those with DMA. (vi) For a given mix-

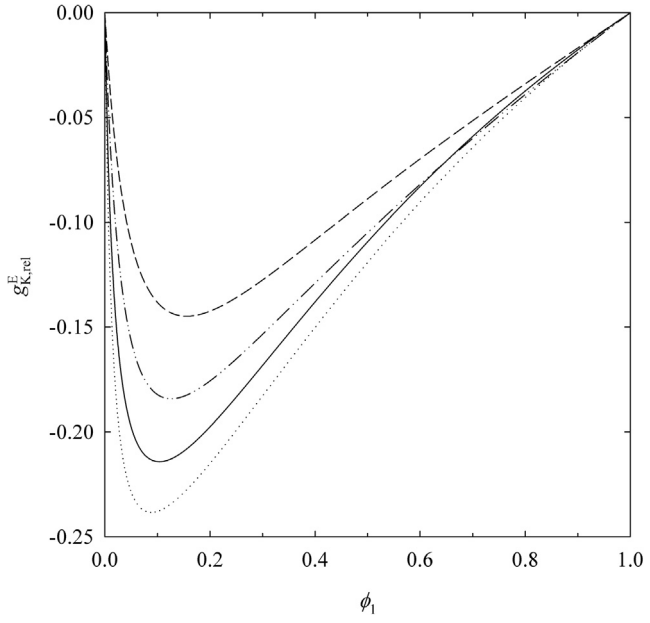

Fig. 7. Excess relative Kirkwood correlation factors, $g^{E}_{K,rel}$, of DMA (1) + amine (2) systems at 0.1 MPa and 298.15 K. (– – –), DMA + DPA; (···), DMA + DBA; (– – –), DMA + BA; (·–·–·), DMA + HxA.

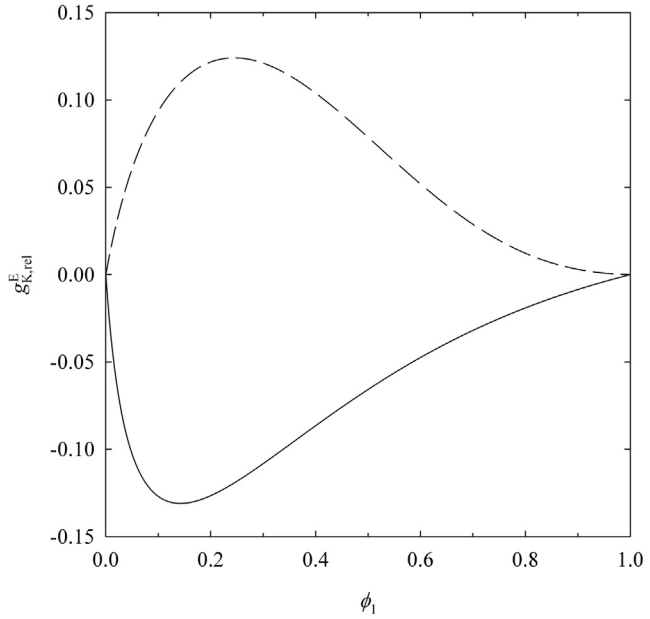

Fig. 8. Excess relative Kirkwood correlation factors, $g^{E}_{K,rel}$, of DMF (1) + amine (2) systems at 0.1 MPa and 298.15 K. (– – –), HxA [25]; (– – –), aniline (this work).

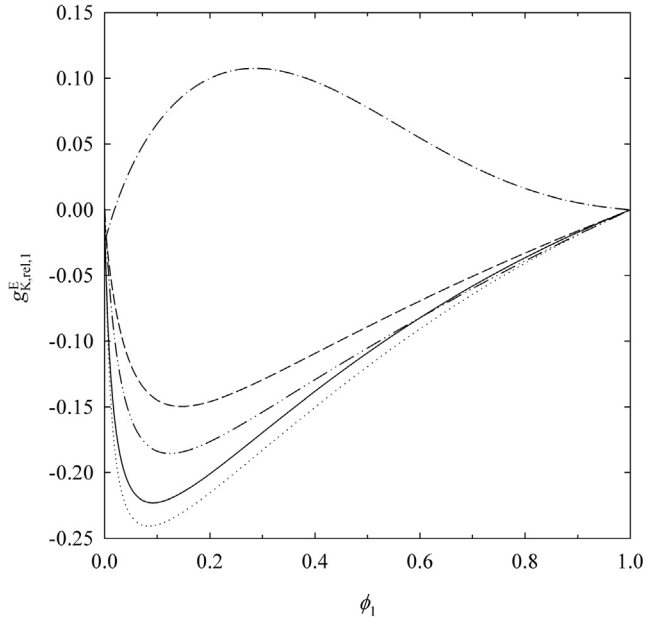

Fig. 9. Excess relative Kirkwood correlation factors of liquid 1, $g^{E}_{K,rel,1}$, for DMA (1) + linear amine (2), or DMF (1) + aniline (2) systems at 0.1 MPa and 298.15 K. (– – –), DMA + DPA; (···), DMA + DBA; (– – –), DMA + BA; (·–·–·), DMA + HxA; (·–·), DMF + aniline.

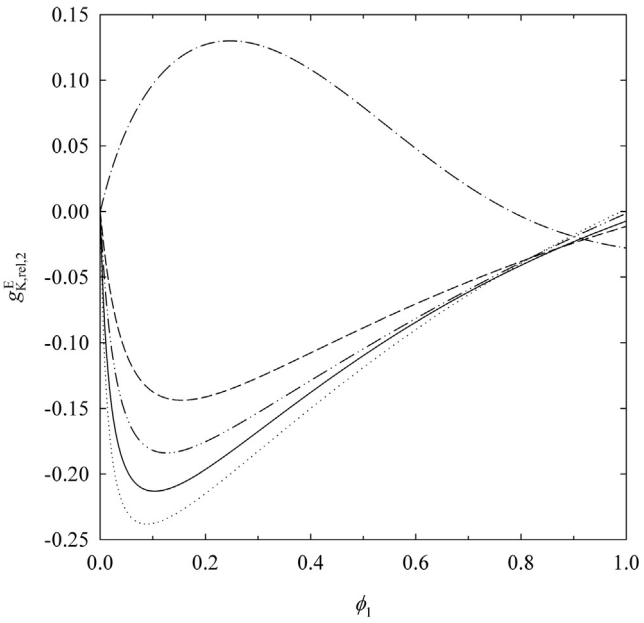

Fig. 10. Excess relative Kirkwood correlation factors of liquid 2, $g^E_{K,rel,2}$, for DMA (1) + linear amine (2), or DMF (1) + aniline (2) systems at 0.1 MPa and 298.15 K. (– – –), DMA + DPA; (···), DMA + DBA; (– – –), DMA + BA; (·–·–·), DMA + HxA; (·–·), DMF + aniline.

ture, the $g^E_{K,rel,i}$ values are practically independent of the component considered and are similar to $g^E_{K,rel}$ values (Table 7). This may mean than interaction between unlike molecules partially compensate the loss of structure of the components. (vi) The $|g^E_{K,rel,1}|$ values are larger for DMA than for DMF in systems with a given linear amine. That is, the loss of order in the liquid state is higher in the vicinity of a DMA molecule than around a DMF molecule.

Finally, we must remark the positive values of $g^E_{K,rel}$ and $g^E_{K,rel,i}$ for the DMF + aniline mixture. They show that the passage from an ideal to a real mixture leads here to an increment of the order in the liquid state, which, in addition, is higher in the neighbourhood of the aniline molecules. The DMF + HxA system behaves in the opposite way and there is a loss of order in the liquid state when passing from an ideal to a real mixture.

7. Conclusions

Measurements on ε_r have been reported for the systems: DMA + BA, + HxA, + DPA, or + DBA and for DMF + aniline at (293.15–303.15) K. The corresponding ε^E_r values are large and negative for mixtures with linear amines and positive for the aniline solution. In the former case, this means that the main contributions to ε^E_r come from the disruption of interactions between like molecules. In the latter case, the ε^E_r sign is determined by the positive contribution from the DMF-aniline interactions. Inspection of ε^E_r data shows that: (i) longer linear amines are better breakers of the amide-amide interactions; (ii) interactions between unlike molecules are more easily formed when shorter linear amines, or DMF, participate. Calculations on $(\Pi^{or}_m)^E$, $(\Pi^{ind}_m)^E$, $g^E_{K,rel}$ and $g^E_{K,rel,i}$, and the dependence of K_{AB} with the molecular structure are consistent with these findings.

Acknowledgements

The authors gratefully acknowledge the financial support received from the Consejería de Educación y Cultura of Junta de Castilla y León, under Project BU034U16. F. Hevia and A. Cobos are grateful to Ministerio de Educación, Cultura y Deporte for the grants FPU14/04104 and FPU15/05456 respectively.

Appendix A. Supplementary data

Supplementary data associated with this article can be found, in the online version, at https://doi.org/10.1016/j.jct.2017.11.011.

References

[1] E.S. Eberhardt, R.T. Raines, J. Am. Chem. Soc. 116 (1994) 2149–2150.
[2] A.L. McClellan, Tables of Experimental Dipole Moments, Vols. 1,2,3, Rahara Enterprises, El Cerrito, US, 1974.
[3] J.A. Riddick, W.B. Bunger, T.K. Sakano, Organic Solvents: Physical Properties and Methods of Purification, Wiley, New York, 1986.
[4] W.L. Jorgensen, C.J. Swenson, J. Am. Chem. Soc. 107 (1985) 569–578.
[5] J.A. Gonzalez, J.C. Cobos, I. García de la Fuente, Fluid Phase Equilib. 224 (2004) 169–183.
[6] J. Barthel, R. Buchner, B. Wurm, J. Mol. Liq. 98 (2002) 51–69.
[7] F.F. Liew, T. Hasegawa, M. Fukuda, E. Nakata, T. Morii, Bioorg. Med. Chem. 19 (2011) 4473–4481.
[8] J.M. Sonner, R.S. Cantor, Annu. Rev. Biophys. 42 (2013) 143–167.
[9] D.L. Nelson, M.M. Cox, Lehninger Principles of Biochemistry, third ed., Worth Publishing, New York, 2000.
[10] H. Funke, M. Wetzel, A. Heintz, Pure Appl. Chem. 61 (1989) 1429–1439.
[11] S. Villa, J.A. González, I.G. De La Fuente, N. Riesco, J.C. Cobos, J. Solution Chem. 31 (2002) 1019–1038.
[12] J.A. González, I. Mozo, I. García de la Fuente, J.C. Cobos, Can. J. Chem. 83 (2005) 1812–1825.
[13] S. Villa, N. Riesco, I. García de la Fuente, J.A. González, J.C. Cobos, Fluid Phase Equilib. 216 (2004) 123–133.
[14] J.A. González, L.F. Sanz, I. García De La Fuente, J.C. Cobos, Thermochim. Acta 573 (2013) 229–236.
[15] R.C. Reid, J.M. Prausnitz, B.E. Poling, The Properties of Gases and Liquids, McGraw-Hill, New York, US, 1987.
[16] H. Matsuda, K. Ochi, K. Kojima, J. Chem. Eng. Data 48 (2003) 184–189.
[17] T.W. Whitfield, G.J. Martyna, S. Allison, S.P. Bates, H. Vass, J. Crain, J. Phys. Chem. B 110 (2006) 3624–3637.
[18] R.S. Ramadevi, P. Venkatesu, M.V. Prabhakara Rao, M.R. Krishna, Fluid Phase Equilib. 114 (1996) 189–197.
[19] G. Chandra Sekhar, M.V. Prabhakara Rao, D.H.L. Prasad, Y.V.L. Ravi Kumar, Thermochim. Acta 402 (2003) 99–103.
[20] A.B. de Haan, J. Gmehling, J. Chem. Eng. Data 41 (1996) 474–478.
[21] L. Pikkarainen, J. Solution Chem. 16 (1987) 125–132.
[22] M. Oba, S. Murakami, R. Fujishiro, J. Chem. Thermodyn. 9 (1977) 407–414.
[23] F. Hevia, A. Cobos, J.A. González, I. García de la Fuente, L.F. Sanz, J. Chem. Eng. Data 61 (2016) 1468–1478.
[24] F. Hevia, A. Cobos, J.A. González, I.G. de la Fuente, V. Alonso, J. Solution Chem. 46 (2017) 150–174.
[25] F. Hevia, J.A. González, I. García de la Fuente, L.F. Sanz, J.C. Cobos, J. Mol. Liq. 238 (2017) 440–446.
[26] A. Heintz, Ber. Bunsenges. Phys. Chem. 89 (1985) 172–181.
[27] H.J. Noh, S.J. Park, S.J. In, J. Ind. Eng. Chem. 16 (2010) 200–206.
[28] H. Fröhlich, Theory of Dielectrics, Clarendon Press, Oxford, 1958.
[29] C. Moreau, G. Douhéret, J. Chem. Thermodyn. 8 (1976) 403–410.
[30] P. Bordewijk, Physica 69 (1973) 422–432.
[31] A. Chelkowski, Dielectric Physics, Elsevier, Amsterdam, 1980.
[32] J.C.R. Reis, T.P. Iglesias, Phys. Chem. Chem. Phys. 13 (2011) 10670–10680.
[33] CIAAW, ciaaw.org/atomic-weights.htm (accessed 2015).
[34] V. Alonso, J.A. González, I. García de la Fuente, J.C. Cobos, Thermochim. Acta 543 (2012) 246–253.
[35] J.C.R. Reis, T.P. Iglesias, G. Douhéret, M.I. Davis, Phys. Chem. Chem. Phys. 11 (2009) 3977–3986.
[36] A. Chaudhari, C.S. Patil, A.G. Shankarwar, B.R. Arbad, S.C. Mehrotra, J. Korean Chem. Soc. 45 (2001) 201–206.
[37] P.R. Bevington, D.K. Robinson, Data Reduction and Error Analysis for the Physical Sciences, McGraw-Hill, New York, 2000.
[38] J.A. González, S. Villa, N. Riesco, I. García de la Fuente, J.C. Cobos, Can. J. Chem. 81 (2003) 319–329.
[39] J.A. González, I. García de la Fuente, J.C. Cobos, Fluid Phase Equilib. 168 (2000) 31–58.
[40] P.J. Flory, J. Am. Chem. Soc. 87 (1965) 1833–1838.
[41] A. Heintz, P.K. Naicker, S.P. Verevkin, R. Pfestorf, Ber. Bunsenges. Phys. Chem. 102 (1998) 953–959.
[42] A. Heintz, D. Papaioannou, Thermochim. Acta 310 (1998) 69–76.
[43] A. Bondi, Physical Properties of Molecular Crystals, Liquids and Glasses, Wiley, New York, 1968.
[44] J.A. González, Phys. Chem. Liq. 42 (2004) 159–172.
[45] G. Chandrasekhar, P. Venkatesu, M.V. Prabhakara Rao, Phys. Chem. Liq. 40 (2002) 181–189.
[46] Y. Marcus, J. Solution Chem. 21 (1992) 1217–1230.

[47] S. Otín, J. Fernández, J.M. Embid, I. Velasco, C.G. Losa, Ber. Bunsenges. Phys. Chem. 90 (1986) 1179–1183.
[48] J.A. González, L.F. Sanz, I. García de la Fuente, J.C. Cobos, J. Chem. Thermodyn. 91 (2015) 267–278.
[49] C. Wohlfahrt, Static Dielectric Constants of Pure Liquids and Binary Liquid Mixtures. Landolt-Börnstein - Group IV Physical Chemistry Vol. 6, Springer Berlin Heidelberg, Berlin, 1991.
[50] M.S. Bakshi, G. Kaur, J. Chem. Eng. Data 42 (1997) 298–300.
[51] G. Ritzoulis, A. Fidantsi, J. Chem. Eng. Data 45 (2000) 207–209.
[52] L.F. Sanz, J.A. González, I.G. De La Fuente, J.C. Cobos, Thermochim. Acta 631 (2016) 18–27.
[53] J. Jadżyn, G. Czechowski, J.-L. Déjardin, M. Ginovska, J. Phys. Chem. A 111 (2007) 8325–8329.
[54] J. Świergiel, I. Płowaś, J. Jadżyn, J. Mol. Liq. 220 (2016) 879–882.
[55] J. Świergiel, I. Płowaś, J. Jadżyn, J. Mol. Liq. 223 (2016) 628–634.
[56] J. Lobos, I. Mozo, M. Fernández Regúlez, J.A. González, I. García de la Fuente, J.C. Cobos, J. Chem. Eng. Data 51 (2006) 623–627.
[57] X. An, H. Zhao, F. Jiang, W. Shen, J. Chem. Thermodyn. 28 (1996) 1221–1232.
[58] J.A. González, I. Alonso, C. Alonso-Tristán, I.G.D.L. Fuente, J.C. Cobos, J. Chem. Thermodyn. 56 (2013) 89–98.
[59] J. Barthel, K. Bachhuber, R. Buchner, J.B. Gill, M. Kleebauer, Chem. Phys. Lett. 167 (1990) 62–66.
[60] P. Undre, S.N. Helambe, S.B. Jagdale, P.W. Khirade, S.C. Mehrotra, J. Mol. Liq. 137 (2008) 147–151.
[61] T. Yokoyama, E. Iwamoto, T. Kumamaru, Bull. Chem. Soc. Jpn. 64 (1991) 1198–1204.
[62] R.J. Sengwa, V. Khatri, Thermochim. Acta 506 (2010) 47–51.
[63] J. Świergiel, J. Jadżyn, J. Chem. Eng. Data 54 (2009) 2296–2300.
[64] C.M. Kinart, W.J. Kinart, Phys. Chem. Liq. 31 (1996) 1–8.
[65] R.J. Sengwa, Madhvi, S. Sankhla, Phys. Chem. Liq. 44 (2006) 637–653.
[66] R.J. Sengwa, S. Sankhla, V. Khatri, Fluid Phase Equilib. 285 (2009) 50–53.
[67] C.M. Kinart, A. Ćwiklińska, W.J. Kinart, A. Bald, J. Chem. Eng. Data 49 (2004) 1425–1428.
[68] F. Ratkovics, L. Domonkos, Acta Chim. Acad. Sci. Hung. 89 (1976) 325.
[69] F.J. Arcega Solsona, J.M. Fornies-Marquina, J. Phys. D: Appl. Phys. 15 (1982) 1783–1793.
[70] C.M. Kinart, W.J. Kinart, D. Chęcińska-Majak, J. Chem. Eng. Data 48 (2003) 1037–1039.
[71] S. Murakami, R. Fujishiro, Bull. Chem. Soc. Jpn. 39 (1966) 720–725.
[72] V.A. Rana, A.D. Vyas, S.C. Mehrotra, J. Mol. Liq. 102 (2003) 379–391.
[73] S.P. Patil, A.S. Chaudhari, M.P. Lokhande, M.K. Lande, A.G. Shankarwar, S.N. Helambe, B.R. Arbad, S.C. Mehrotra, J. Chem. Eng. Data 44 (1999) 875–878.
[74] S. Lata, K.C. Singh, A. Suman, J. Mol. Liq. 147 (2009) 191–197.
[75] B.D. Watode, P.G. Hudge, M.N. Shinde, R.B. Talware, A.C. Kumbharkhane, Phys. Chem. Liq. 53 (2015) 252–263.
[76] A.N. Prajapati, V.A. Rana, A.D. Vyas, Ind. J. Pure Appl. Phys. 51 (2013) 104–111.
[77] G. Parthipan, T. Thenappan, J. Mol. Liq. 138 (2008) 20–25.
[78] T.V. Krishna, S.S. Sastry, J. Solution Chem. 39 (2010) 1377–1393.
[79] P.S. Nikam, S.J. Kharat, J. Chem. Eng. Data 48 (2003) 972–976.

JCT 17-479

Supplementary material for:

Thermodynamics of amide + amine mixtures. 4. Relative permittivities of *N,N*-dimethylacetamide + *N*-propylpropan-1-amine, + *N*-butylbutan-1-amine, + butan-1-amine, or + hexan-1-amine systems and of *N,N*-dimethylformamide + aniline mixture at several temperatures. Characterization of amine + amide systems using ERAS

Fernando Hevia, Juan Antonio González*, Ana Cobos, Isaías García de la Fuente, Luis Felipe Sanz

G.E.T.E.F., Departamento de Física Aplicada, Facultad de Ciencias, Universidad de Valladolid, Paseo de Belén, 7, 47011 Valladolid, Spain

*e-mail: jagl@termo.uva.es; Tel: +34 983 423757

Reference of the article:

F. Hevia, J.A. González, A. Cobos, I. García de la Fuente, L.F. Sanz. J. Chem. Thermodyn. **118** (2018) 175-187. https://doi.org/10.1016/j.jct.2017.11.011

Table S1. Density, ρ, of aniline at temperature T and 0.1 MPa [a]

T/K	ρ /g·cm^{-3}	
	Experimental	Literature
293.15	1.02179	1.0217 [s1]
		1.0173 [s2]
		1.02104 [s3]
298.15	1.01752	1.0174 [s1]
		1.01744 [s4]
		1.0175 [s5]
		1.0176 [s6]
303.15	1.01319	1.0130 [s1]
		1.01309 [s2]
		1.01318 [s7]

[a] Density values measured by means of a vibrating-tube densimeter and sound analyzer Anton Paar model DSA-5000. For details regarding the experimental method, see [s8,s9]. Standard uncertainties, u, are: $u(\rho) = 0.0012\rho$; $u(T) = 0.01$ K, and for pressure $u(p) = 1$ kPa..

Table S2. ERAS parameters[a] for pure compounds at 298.15 K.

Compound	V_{mi} / cm^3·mol^{-1}	α_{Pi} / 10^3·K^{-1}	κ_{Ti} / TPa^{-1}	K_i	Δh_i^* / kJ·mol^{-1}	Δv_i^* / cm^3·mol^{-1}	V_i^* / cm^3 ·mol^{-1}	P_i^* / J·cm^{-3}
DPA	138.00[b]	1.24[b]	1217[b]	0.55[c]	−7.5[c]	−2.8[c]	107.58	470.5
DBA	171.06[b]	1.09[b]	1059[b]	0.16[c]	−6.5[c]	−3.4[c]	135.59	481.0
BA	99.87[b]	1.30[b]	1149[b]	0.96[d]	−13.2[d]	−2.8[d]	77.65	515.8
HxA	133.11[b]	1.12[b]	971[b]	0.78[e]	−13.2[e]	−2.8[e]	105.99	506.2
Aniline	91.53[f]	0.85[f]	468[f]	14.8[f]	−15[f]	−12[f]	79.82	541.6
DMF	77.42[g]	1.01[g]	659.4[g]				61.97	711.4
DMA	93.05[b]	0.98[b]	653.5[b]				74.82	691.4
NMA	76.94[h]	0.869[h]	612[h]	72.5[h]	−25[h]	−3.6[h]	63.95	561.6

[a] V_{mi}, molar volume; α_{Pi}, isobaric thermal expansion coefficient; κ_{Ti}, isothermal compressibility; K_i, equilibrium constant; V_i^* and P_i^*, reduction parameters for volume and pressure, respectively; Δh_i^*, hydrogen bonding enthalpy; Δv_i^*, self-association volume; [b][s9]; [c] [s10]; [d] [s11]; [e][s12]; [f] [s13]; [g][s8]; [h][s14] (T = 303.15 K).

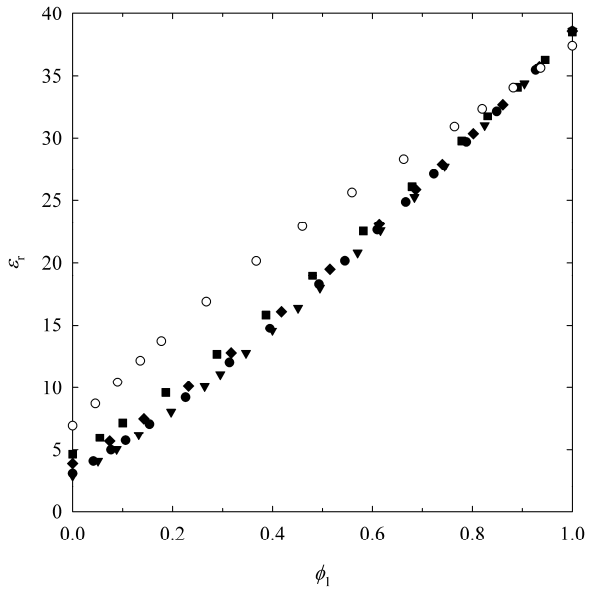

Figure S1: Relative permittivities, ε_r , of amide (1) + amine (2) systems at 0.1 MPa; 298.15 K and 1 MHz. (●), DMA + DPA; (▼), DMA + DBA; (■), DMA + BA; (◆), DMA + HxA; (○), DMF + aniline.

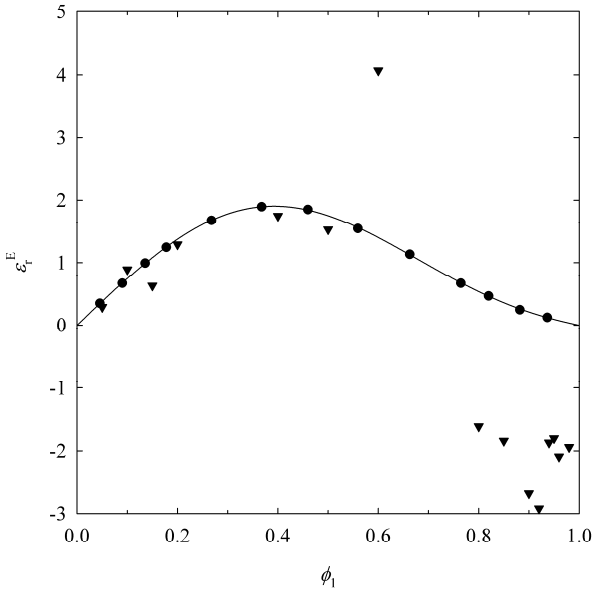

Figure S2: Excess relative permittivities, ε_r^E , for the DMF (1) + aniline (2) system at 0.1 MPa and 303.15 K. (●), this work; (▼), [s15]. Solid line, calculations with equation (3) using the coefficients from Table 4.

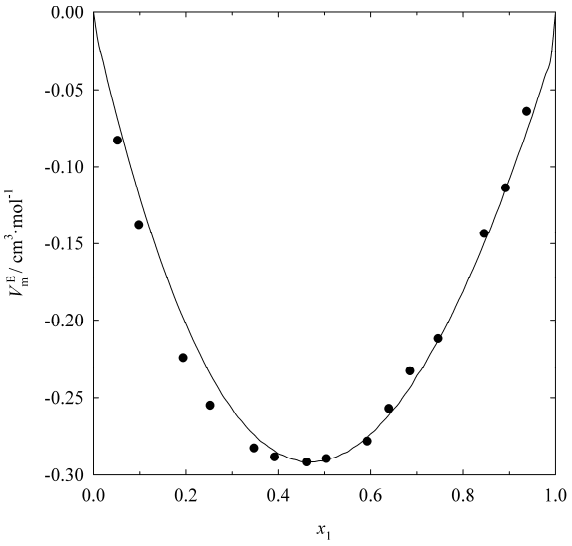

Figure S3: Excess molar volume, V_m^E for the DPA (1) + DMF (2) mixture at 298.15 K and 0.1 MPa. Points experimental results [s8]. Solid line, ERAS calculations with parameters from Table 5.

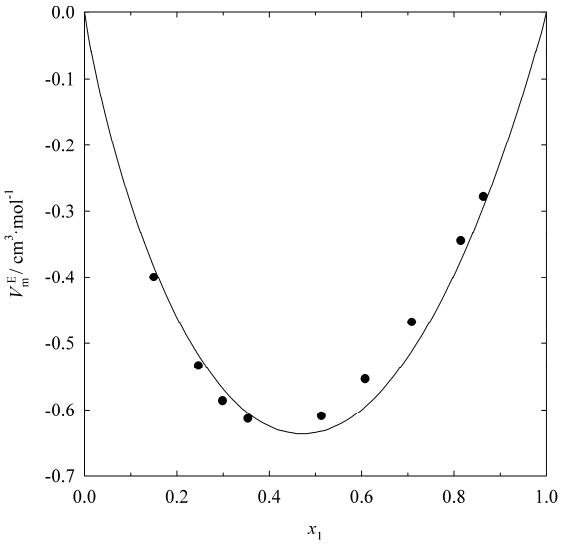

Figure S4: Excess molar volume, V_m^E for the aniline (1) + DMA (2) mixture at 303.15 K and 0.1 MPa. Points experimental results [s16]. Solid line, ERAS calculations with parameters from Table 5.

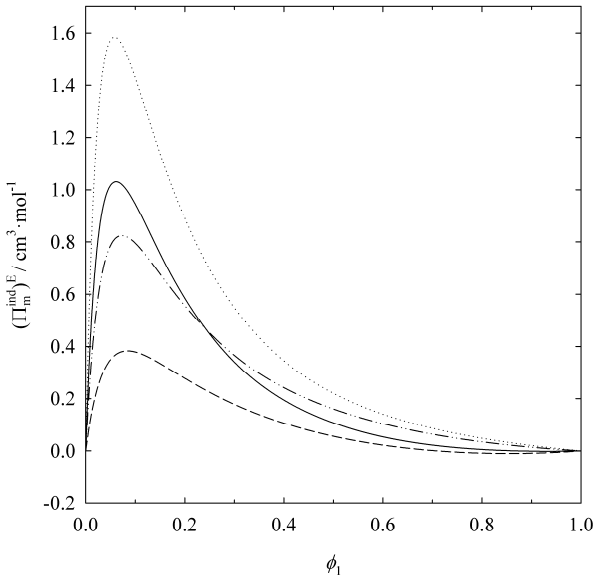

Figure S5: Excess molar induced polarizability, $(\Pi_m^{ind})^E$, for DMA (1) + linear amine (2) systems at 0.1 MPa and 298.15 K. (——), DPA; (···), DBA; (– – –), BA; (···—··), HxA.

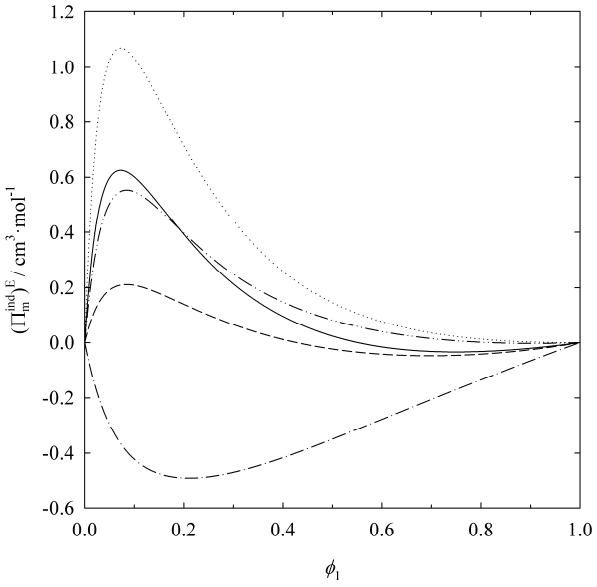

Figure S6: Excess molar induced polarizability, $(\Pi_m^{ind})^E$, for DMF (1) + linear amine (2) [s17], or + aniline (this work) systems at 0.1 MPa and 298.15 K. (——), DPA; (···), DBA; (– – –), BA; (·· –··), HxA; (·—·), aniline.

References

[s1] D. Soldatovic, J. Vukasanovic, I. Radovic, Z. Visak, M. Kijevcanin, J. Chem. Thermodyn. **109** (2017) 137-154

[s2] V.K. Sharma, S. Solanki, J. Mol. Liq. **177** (2013) 133-144.

[s3] L. Su, H. Wang, J. Chem. Thermodyn. **41** (2009) 315-322.

[s4] A.K. Naim, Int. J. Thermophys. **28** (2007) 1228-1244.

[s5] J.A. Riddick, W.B. Bunger, T.K. Sakano, Organic solvents: physical properties and methods of purification, Wiley, New York, 1986.

[s6] S.K. Jangra, J.S. Yadav, N. Saini, D. Sharma, V.K. Sharma, J. Mol. Liq. **162** (2011) 122-128.

[s7] P. Vasundhara, C. Narasimha Rao, L. Venkatramana, K. Sivakumar, P. Venkateswarlu, R.L. Gardas, J. Mol. Liq. **202** (2015) 158-164

[s8] F. Hevia, A. Cobos, J.A. González, I. García de la Fuente, L.F. Sanz, J. Chem. Eng. Data **61** (2016) 1468-1478.

[s9] F. Hevia, A. Cobos, J.A. González, I.G. de la Fuente, V. Alonso, J. Solution Chem. **46** (2017) 150-174.

[s10] S. Villa, N. Riesco, I. García de la Fuente, J.A. González, J.C. Cobos, J. Solution Chem. **32** (2003) 179-194.

[s11] J.A. González, I. García de la Fuente, J.C. Cobos, Fluid Phase Equilib. **168** (2000) 31-58.

[s12] S. Villa, N. Riesco, I. García de la Fuente, J.A. González, J.C. Cobos, Fluid Phase Equilib. **216** (2004) 123-133.

[s13] J.A. González, I. Mozo, I. García de la Fuente, J.C. Cobos, Can. J. Chem. **83** (2005) 1812-1825.

[s14] J.A. González, Phys. Chem. Liq., **42** (2004) 159-172.

[s15] A. Chaudhari, C.S. Patil, A.G. Shankarwar, B.R. Arwad, S.C. Mehrotra, J. Korean Chem. Soc. **45** (2001) 201-206.

[s16] G. Chandrasekhar, P. Venkatesu, M.V. Prabhakara Rao, Phys. Chem. Liq., **40** (2002) 181-189.

[s17] F. Hevia, J.A. González, I. García de la Fuente, L.F. Sanz, J.C. Cobos, J. Mol. Liq. **238** (2017) 440-446.

Fluid Phase Equilibria 468 (2018) 18–28

Contents lists available at ScienceDirect

Fluid Phase Equilibria

journal homepage: www.elsevier.com/locate/fluid

Thermodynamics of mixtures with strongly negative deviations from Raoult's law. XV. Permittivities and refractive indices for 1-alkanol + *n*-hexylamine systems at (293.15–303.15) K. Application of the Kirkwood-Fröhlich model

Fernando Hevia [a], Juan Antonio González [a, *], Ana Cobos [a], Isaías García de la Fuente [a], Cristina Alonso-Tristán [b]

[a] G.E.T.E.F., Departamento de Física Aplicada, Facultad de Ciencias, Universidad de Valladolid, Paseo de Belén, 7, 47011 Valladolid, Spain
[b] Unidad de Investigación Consolidada UIC-011, JCyL, Departamento de Ingeniería Electromecánica, Escuela Politécnica Superior, Universidad de Burgos, Avda. Cantabria s/n, 09006, Burgos, Spain

ARTICLE INFO

Article history:
Received 8 March 2018
Accepted 7 April 2018
Available online 10 April 2018

Keywords:
1-alkanol
n-hexylamine
Permittivity
Refractive index
Kirkwood correlation factor

ABSTRACT

Relative permittivities at 1 MHz, ε_r, and refractive indices at the sodium D-line, n_D, are reported at 0.1 MPa and at (293.15–303.15) K for the binary systems 1-alkanol + *n*-hexylamine (HxA). Also, their corresponding excess functions are calculated and correlated. Positive values of the excess permittivities, ε_r^E, are encountered for the methanol system, whereas the remaining mixtures show negative values. This reveals that interactions between unlike molecules contribute positively to ε_r^E. This contribution is dominant for the methanol mixture, while those arising from the breaking of interactions between like molecules are prevalent for the remaining mixtures. At φ_1 (volume fraction) = 0.5, ε_r^E changes in the order: methanol > 1-propanol > 1-butanol > 1-pentanol < 1-heptanol. Similar variation with the chain length of the 1-alkanol is observed for mixtures such as 1-alkanol + heptane, or + cyclohexylamine, and can be explained in terms of the lower and weaker self-association of longer 1-alkanols. The effect of the replacement of HxA by cyclohexylamine, or by aniline, is also shown. Calculations on molar refractions indicate that dispersive interactions in the systems under study increase with the length of the 1-alkanol. The mixtures are studied by means of the application of the Kirkwood-Fröhlich model, and the Kirkwood correlation factors, including the corresponding excess values, are reported.

1. Introduction

Mixtures formed by 1-alkanol and amine are a very interesting class of systems, as they show a variety of different behaviours. For example, 1-alkanol + linear primary or secondary amine systems are characterized by strongly negative excess molar enthalpies (H_m^E). Thus, at 298.15 K and equimolar composition, H_m^E/J·mol^{-1} = −3200 (methanol + *n*-hexylamine (HxA)) [1]; −4581 (methanol + diethylamine) [2]. This has been interpreted as the result of two different opposing effects. In the pure liquid state, both 1-alkanols and amines are self-associated by means of O-H—O and N-H—N bonds, respectively. When the mixing process takes place, such bonds are broken, and this process leads to a positive contribution to H_m^E. However, new interactions between unlike molecules are simultaneously created, which contributes negatively to H_m^E. Therefore, the large and negative H_m^E values reveal that the new O-H—N bonds created are stronger than the O-H—O and N-H—N bonds. Thus, the values of the enthalpy of the hydrogen bonds between methanol and amine estimated from the application of the ERAS model [3] are: −42.4 kJ·mol^{-1} (*n*-hexylamine) [4]; −45.4 kJ·mol^{-1} (diethylamine) [5]. The value used, within this model, for the enthalpy of the H bonds between alkanol molecules is higher: −25.1 kJ·mol^{-1} [3–5]. As a consequence of the strong interactions between unlike molecules, the systems are highly structured. For example, at 298.15 K and x_1 = 0.5, TS_m^E (=$H_m^E - G_m^E$; G_m^E molar excess Gibbs energy) is −3758 J·mol^{-1} for the methanol + diethylamine mixture (value determined using G_m^E = −823 J·mol^{-1} [6]). For comparison, we provide similar results for

* Corresponding author.
E-mail address: jagl@termo.uva.es (J.A. González).

https://doi.org/10.1016/j.fluid.2018.04.007
0378-3812/

Table 1
Sample description.

Chemical name	CAS Number	Source	Purification method	Purity[a]
methanol	67-56-1	Sigma-Aldrich	none	99.99%
1-propanol	71-23-8	Sigma-Aldrich	none	99.84%
1-butanol	71-36-3	Sigma-Aldrich	none	99.86%
1-pentanol	71-41-0	Sigma-Aldrich	none	99.9%
1-heptanol	111-70-6	Sigma-Aldrich	none	99.8%
n-hexylamine (HxA)	111-26-2	Aldrich	none	99.9%

[a] In mole fraction. Provided by the supplier by gas chromatography.

the 1-propanol + hexane system, TS^{E}_{m}= (533 (=H^{E}_{m}) − 1295 (=G^{E}_{m})) = −762 J·mol^{-1} [7,8]. The existence of strong interactions between unlike molecules in this type of solutions is also supported by large and negative excess molar volumes [4,9–13] and by solid-liquid equilibria measurements, as the corresponding phase diagrams show that complex formation is an important feature of systems [14]. Interestingly, the replacement of a linear primary amine by aniline leads to very different H^{E}_{m}/J·mol^{-1} values: −170 (methanol) [15]; 1020 (1-butanol) [16]. This can be explained in terms of a large contribution to H^{E}_{m} from the breaking of the strong dipolar interactions between aniline molecules upon mixing. Note that the upper critical solution temperature of the aniline + heptane system is 343.1 K [17].

We have extended the database of 1-alkanol + amine mixtures reporting excess molar volumes [4,9–13]; dynamic viscosities [11–13]; vapour-liquid equilibria [18]; permittivities (ε_r) and refractive indices (n_D) [11–13,19]. In addition, these systems have been studied by using different models as DISQUAC or ERAS [4,5,9,10,12,20–23]; the formalism of the Kirkwood-Buff integrals [24], or the concentration-concentration structure factor ($S_{CC}(0)$) formalism [25]. As a continuation, we provide now ε_r and n_D measurements over the temperature range (293.15–303.15) K for the systems 1-alkanol + HxA. In addition, the data are analyzed in terms of the Kirkwood-Fröhlich model [26–29], which is a useful approach to gain insight into the mixture structure and interactions.

2. Experimental

2.1. Materials

Information about the purity and source of the pure compounds used along the experiments is collected in Table 1. They were used without further purification. Table 2 contains their ε_r values at 1 MHz, densities (ρ) and n_D values at 0.1 MPa and at the working temperatures. These results agree well with literature data.

2.2. Apparatus and procedure

Binary mixtures were prepared by mass in small vessels of about 10 cm^3 with the aid of an analytical balance Sartorius MSU125p (weighing accuracy 0.01 mg), taking into account the corresponding corrections on buoyancy effects. The standard uncertainty in the final mole fraction is 0.0010. Molar quantities were calculated using the relative atomic mass Table of 2015 issued by the Commission on Isotopic Abundances and Atomic Weights (IUPAC) [30]. In order to minimize the effects of the interaction of the compounds with air components, they were stored with 4 Å molecular sieves (except methanol, because measurements were affected). In addition, the measurement cell (see below) was completely filled with the samples and appropriately closed. Different density measurements of pure compounds, conducted along experiments, showed that this quantity remained unchanged within the experimental uncertainty.

Temperatures were measured with Pt-100 resistances, calibrated according to the ITS-90 scale of temperature, against the triple point of the water and the fusion point of Ga. The standard uncertainty of this quantity is 0.01 K for ρ determinations, and 0.02 K for ε_r and n_D measurements.

Densities were obtained using a vibrating-tube densimeter and sound analyser Anton Paar DSA 5000, which is automatically thermostated within 0.01K. The calibration procedure has been described elsewhere [31]. The relative standard uncertainty of the ρ measurements is 0.0012.

A Bellingham + Stanley RFM970 refractometer was used for the n_D measurements. The technique is based on the optical detection of the critical angle at the wavelength of the sodium D line (589.3 nm). The temperature is controlled by Peltier modules and its stability is 0.02K. The refractometer has been calibrated using 2,2,4-trimethylpentane and toluene at (293.15–303.15) K, following the recommendations by Marsh [32]. The standard uncertainty of n_D is 0.00008.

The ε_r measurements were performed with the aid of an equipment from Agilent. A 16452A cell, which is a parallel-plate capacitor made of Nickel-plated cobalt (54% Fe, 17% Co, 29% Ni) with a ceramic insulator (alumina, Al_2O_3), is filled with a sample volume of ≈4.8 cm^3. The cell is connected by a 16048G test lead to a precision impedance analyser 4294A, and immersed in a thermostatic bath LAUDA RE304, with a temperature stability of 0.02 K. Details about the device configuration and calibration are given elsewhere [33]. The relative standard uncertainty of the ε_r measurements (i.e. the repeatability) is 0.0001. The total relative standard uncertainty of ε_r was estimated to be 0.003 from the differences between our data and values available in the literature, in the range of temperature (288.15–333.15) K, for the following pure liquids: water, benzene, cyclohexane, hexane, nonane, decane, dimethyl carbonate, diethyl carbonate, methanol, 1-propanol, 1-pentanol, 1-hexanol, 1-heptanol, 1-octanol, 1-nonanol and 1-decanol.

3. Results

From the experimental ε_r values at different temperatures, we can also determine the derivative $(\partial\varepsilon_r/\partial T)_p$ at 298.15 K as the slope of a linear regression of experimental ε_r values in the range (293.15–303.15) K.

Let us denote by x_i the mole fraction of component *i*. The corresponding volume fraction, φ_i, is given by $\varphi_i = x_i V^*_{mi}/(x_1 V^*_{m1} + x_2 V^*_{m2})$, where V^*_{mi} stands for the molar volume of component *i*. For an ideal mixture at the same temperature and pressure as the mixture under study, the relative permittivity, ε^{id}_r, the derivative $[(\partial\varepsilon_r/\partial T)_p]^{id}$, and the refractive index, n^{id}_D, are given by [34,35]:

$$\varepsilon^{id}_r = \varphi_1 \varepsilon^*_{r1} + \varphi_2 \varepsilon^*_{r2} \quad (1)$$

Table 2
Relative permittivity at frequency $\nu = 1$ MHz, ε_r^*, refractive index, n_D^*, and density, ρ^*, of pure compounds at temperature T and pressure $p = 0.1$ MPa.[a]

Compound	T/K	ε_r^*		n_D^*		$\rho^*/g\cdot cm^{-3}$	
		Exp.	Lit.	Exp.	Lit.	Exp.	Lit.
methanol	293.15	33.569	33.61 [46]	1.32862	1.32859 [47]	0.79163	0.7916 [48] 791400 [49]
	298.15	32.619	32.62 [46]	1.32654	1.32652 [50]	0.78695	0.7869 [51] 786884 [52]
	303.15	31.652	31.66 [46]	1.32439	1.32457 [53] 32410 [54]	0.78222	0.782158 [52]
1-propanol	293.15	21.150	21.15 [55]	1.38514	1.38512 [56]	0.80366	0.80361 [57]
	298.15	20.449	20.42 [55]	1.38306	1.38307 [54]	0.79968	0.79960 [57]
	303.15	19.784	19.75 [55]	1.38102	1.38104 [54]	0.79566	0.79561 [57]
1-butanol	293.15	18.192	18.19 [55]	1.39931	1.3993 [58]	0.80985	0.80982 [59] 0.8098 [60]
	298.15	17.545	17.53 [55]	1.39733	1.397336 [61]	0.80606	0.80606 [59]
	303.15	16.933	16.89 [55]	1.39529	1.3953 [62]	0.80222	0.8022 [60]
1-pentanol	293.15	15.701	15.63 [46]	1.40985	1.40986 [54]	0.81466	0.81468 [63]
	298.15	15.102	15.08 [64]	1.40793	1.40789 [54]	0.81103	0.81103 [63]
	303.15	14.536	14.44 [46]	1.40590	1.40592 [65]	0.80735	0.81737 [63]
1-heptanol	293.15	12.019	11.54 [66]	1.42425	1.42433 [67]	0.82237	0.8223 [68]
	298.15	11.504	11.45 [64]	1.42235	1.42240 [67]	0.81890	0.81881 [69]
	303.15	11.014	11.07 [70]	1.42047	1.42047 [65] 42048 [67]	0.81537	0.8153 [68]
HxA	293.15	3.964	3.94 [71]	1.41808	1.4180 [72]	0.76443	0.7651 [73]
	298.15	3.904		1.41563	1.41550 [72]	0.76019	0.76013 [74]
	303.15	3.846	3.83 [71]	1.41321	1.4131 [72]	0.75590	0.7562 [73]

[a] The standard uncertainties are: $u(T) = 0.02$K (for ρ^* measurements, $u(T) = 0.01$K); $u(p) = 1$kPa; $u(\nu) = 20$ Hz; $u(n_D^*) = 0.00008$. The relative standard uncertainties are: $u_r(\rho^*) = 0.0012$, $u_r(\varepsilon_r^*) = 0.003$.

$$n_D^{id} = \left[\varphi_1 (n_{D1}^*)^2 + \varphi_2 (n_{D2}^*)^2\right]^{1/2} \quad (2)$$

$$\left[\left(\frac{\partial \varepsilon_r}{\partial T}\right)_p\right]^{id} = \left(\frac{\partial \varepsilon_r^{id}}{\partial T}\right)_p \quad (3)$$

where ε_{ri}^* and n_{Di}^* denote the relative permittivity and the refractive index of pure species i, and $(\partial \varepsilon_r^{id}/\partial T)_p$ is calculated from linear regressions as indicated above. The corresponding excess functions, F^E, are obtained as

$$F^E = F - F^{id} \quad , \quad F = \varepsilon_r,\ n_D,\ \left(\frac{\partial \varepsilon_r}{\partial T}\right)_p \quad (4)$$

Table 3 lists φ_1, ε_r and ε_r^E values of 1-alkanol (1) + HxA (2) systems as functions of x_1, in the temperature range (293.15–303.15) K. Table 4 contains the corresponding experimental x_1, φ_1, n_D and n_D^E values. The data of $[(\partial \varepsilon_r/\partial T)_p]^E = (\partial \varepsilon_r^E/\partial T)_p$ are collected in Table S1 (supplementary material).

The F^E data were fitted to a Redlich-Kister equation [36] by an unweighted linear least-squares regression:

$$F^E = x_1(1 - x_1)\sum_{i=0}^{k-1} A_i (2x_1 - 1)^i \quad (5)$$

The number, k, of necessary coefficients for this regression has been determined, for each system and temperature, by applying an F-test of additional term [37] at 99.5% confidence level. Table 5 includes the parameters A_i obtained, and the standard deviations $\sigma(F^E)$, defined by:

$$\sigma\left(F^E\right) = \left[\frac{1}{N-k}\sum_{j=1}^{N}\left(F_{cal,j}^E - F_{exp,j}^E\right)^2\right]^{1/2} \quad (6)$$

where the index j takes one value for each of the N experimental data $F_{exp,j}^E$, and $F_{cal,j}^E$ is the corresponding value of the excess property F^E calculated from equation (5).

Values of ε_r^E, n_D^E and $(\partial \varepsilon_r^E/\partial T)_p$ versus φ_1 of 1-alkanol + amine systems at 298.15 K are plotted in Figs. 1, 2 and 3 respectively with their corresponding Redlich-Kister regressions. Data on $n_D$are plotted in Fig. S1.

4. Discussion

Unless stated otherwise, the below values of the thermophysical properties and their corresponding excess functions are referred to $T = 298.15$ K and $\varphi_1 = 0.5$. On the other hand, n stands for the number of C atoms of the 1-alkanol.

4.1. Excess relative permittivities

The rupture of interactions between molecules of the same species along mixing is associated to a negative contribution to ε_r^E. The creation of new interactions in the mixture forms multimers, whose total dipole moment can be more or less effective —in its impact on the macroscopic dipole moment under the action of an electric field— than in the ideal mixture. In the first case, the contribution to ε_r^E is positive, whereas in the second case it is negative. 1-Alkanol + heptane mixtures show rather large negative values of this quantity (Fig. 4): $\varepsilon_r^E = -1.075$ ($n = 3$), -2.225 ($n = 4$), -2.525 ($n = 5$), -2.875 ($n = 7$), -1.775 ($n = 10$) [12,38–40]. These negative values can be attributed to the breaking of 1-alkanol self-association. For methanol, there exists a partial immiscibility region [41]. The $\varepsilon_r(n)$ variation follows the sequence: 1-propanol > 1-butanol > 1-pentanol > 1-heptanol < 1-decanol. It can be explained in terms of the lower and weaker self-association of longer 1-alkanols [19]. This statement also applies for the relative variation of ε_r^E in the mixtures under study (Figs. 1 and 4): 1.480 ($n = 1$), -0.960 ($n = 3$), -1.424 ($n = 4$), -1.530 ($n = 5$), -1.295 ($n = 7$). These results are higher than those of heptane mixtures. This suggests that the formation of (1-alkanol)-HxA interactions yields a positive contribution to ε_r^E.

Table 3
Volume fractions of 1-alkanol, φ_1, relative permittivities, ε_r, and excess relative permittivities, ε_r^E, of 1-alkanol (1) + HxA (2) mixtures as functions of the mole fraction of the 1-alkanol, x_1, at temperature T, pressure $p = 0.1$ MPa and frequency $\nu = 1$ MHz.[a]

x_1	φ_1	ε_r	ε_r^E	x_1	φ_1	ε_r	ε_r^E
methanol (1) + HxA (2); T/K = 293.15							
0.0000	0.0000	3.964		0.7016	0.4182	17.646	1.301
0.0534	0.0170	4.367	− 0.100	0.8002	0.5505	21.864	1.602
0.1220	0.0408	4.964	− 0.208	0.8485	0.6313	24.251	1.597
0.1906	0.0672	5.681	− 0.272	0.8984	0.7300	26.928	1.352
0.3081	0.1198	7.244	− 0.267	0.9496	0.8521	30.037	0.847
0.3950	0.1664	8.783	− 0.107	0.9834	0.9477	32.343	0.322
0.4982	0.2329	11.109	0.250	1.0000	1.0000	33.569	
0.6035	0.3176	14.210	0.843				
methanol (1) + HxA (2); T/K = 298.15							
0.0000	0.0000	3.904		0.7016	0.4183	17.127	1.212
0.0534	0.0170	4.293	− 0.099	0.8002	0.5506	21.254	1.540
0.1220	0.0408	4.870	− 0.206	0.8485	0.6314	23.597	1.562
0.1906	0.0672	5.564	− 0.270	0.8984	0.7301	26.203	1.334
0.3081	0.1199	7.085	− 0.262	0.9496	0.8521	29.216	0.844
0.3950	0.1665	8.557	− 0.128	0.9834	0.9477	31.440	0.323
0.4982	0.2329	10.806	0.214	1.0000	1.0000	32.619	
0.6035	0.3177	13.794	0.767				
methanol (1) + HxA (2); T/K = 303.15							
0.0000	0.0000	3.964		0.7016	0.4182	17.646	1.301
0.0534	0.0170	4.367	− 0.100	0.8002	0.5505	21.864	1.602
0.1220	0.0408	4.964	− 0.208	0.8485	0.6313	24.251	1.597
0.1906	0.0672	5.681	− 0.272	0.8984	0.7300	26.928	1.352
0.3081	0.1198	7.244	− 0.267	0.9496	0.8521	30.037	0.847
0.3950	0.1664	8.783	− 0.107	0.9834	0.9477	32.343	0.322
0.4982	0.2329	11.109	0.250	1.0000	1.0000	33.569	
0.6035	0.3176	14.210	0.843				
1-propanol (1) + HxA (2); T/K = 293.15							
0.0000	0.0000	3.964		0.6097	0.4688	10.990	− 1.031
0.0708	0.0413	4.411	− 0.263	0.6977	0.5659	12.847	− 0.843
0.1073	0.0636	4.663	− 0.394	0.8044	0.6991	15.469	− 0.510
0.1470	0.0887	4.953	− 0.535	0.8406	0.7487	16.431	− 0.400
0.1935	0.1194	5.330	− 0.686	0.8989	0.8340	18.080	− 0.217
0.3070	0.2002	6.436	− 0.969	0.9504	0.9154	19.605	− 0.091
0.3941	0.2687	7.471	− 1.111	1.0000	1.0000	21.150	
0.5056	0.3662	9.113	− 1.145				
1-propanol (1) + HxA (2); T/K = 298.15							
0.0000	0.0000	3.904		0.6097	0.4686	10.649	− 1.008
0.0708	0.0412	4.336	− 0.250	0.6977	0.5658	12.426	− 0.839
0.1073	0.0635	4.578	− 0.377	0.8044	0.6989	14.948	− 0.519
0.1470	0.0887	4.857	− 0.515	0.8406	0.7486	15.885	− 0.405
0.1935	0.1193	5.222	− 0.656	0.8989	0.8339	17.478	− 0.223
0.3070	0.2001	6.286	− 0.929	0.9504	0.9154	18.955	− 0.094
0.3941	0.2686	7.279	− 1.069	1.0000	1.0000	20.449	
0.5056	0.3660	8.850	− 1.109				
1-propanol (1) + HxA (2); T/K = 303.15							
0.0000	0.0000	3.846		0.6097	0.4685	10.324	− 0.989
0.0708	0.0412	4.263	− 0.240	0.6977	0.5656	12.034	− 0.827
0.1073	0.0635	4.499	− 0.359	0.8044	0.6988	14.463	− 0.520
0.1470	0.0886	4.770	− 0.488	0.8406	0.7484	15.354	− 0.420
0.1935	0.1192	5.123	− 0.623	0.8989	0.8338	16.902	− 0.233
0.3070	0.2000	6.148	− 0.886	0.9504	0.9153	18.330	− 0.104
0.3941	0.2685	7.102	− 1.023	1.0000	1.0000	19.784	
0.5056	0.3659	8.605	− 1.073				
1-butanol (1) + HxA (2); T/K = 293.15							
0.0000	0.0000	3.965		0.5930	0.5018	9.623	− 1.481
0.0510	0.0358	4.258	− 0.216	0.6983	0.6154	11.376	− 1.344
0.0969	0.0691	4.538	− 0.410	0.8047	0.7402	13.472	− 1.024
0.1402	0.1013	4.828	− 0.578	0.8525	0.7998	14.558	− 0.786
0.2052	0.1515	5.294	− 0.826	0.9035	0.8662	15.741	− 0.547
0.3095	0.2366	6.164	− 1.167	0.9460	0.9237	16.795	− 0.311
0.4059	0.3208	7.139	− 1.390	1.0000	1.0000	18.192	
0.5054	0.4140	8.352	− 1.503				
1-butanol (1) + HxA (2); T/K = 298.15							
0.0000	0.0000	3.904		0.5930	0.5016	9.333	− 1.413
0.0510	0.0358	4.186	− 0.206	0.6983	0.6152	11.005	− 1.291
0.0969	0.0690	4.460	− 0.385	0.8047	0.7400	13.003	− 0.995
0.1402	0.1012	4.739	− 0.545	0.8525	0.7997	14.054	− 0.759
0.2052	0.1514	5.190	− 0.779	0.9035	0.8661	15.182	− 0.536
0.3095	0.2364	6.028	− 1.101	0.9460	0.9237	16.197	− 0.307
0.4059	0.3206	6.965	− 1.312	1.0000	1.0000	17.545	
0.5054	0.4138	8.121	− 1.428				
1-butanol (1) + HxA (2); T/K = 303.15							
0.0000	0.0000	3.845		0.5930	0.5014	9.058	− 1.349
0.0510	0.0358	4.120	− 0.194	0.6983	0.6150	10.656	− 1.238
0.0969	0.0689	4.385	− 0.362	0.8047	0.7398	12.566	− 0.962
0.1402	0.1012	4.656	− 0.514	0.8525	0.7996	13.565	− 0.745
0.2052	0.1512	5.094	− 0.730	0.9035	0.8660	14.656	− 0.523
0.3095	0.2363	5.898	− 1.040	0.9460	0.9236	15.632	− 0.301
0.4059	0.3204	6.797	− 1.241	1.0000	1.0000	16.933	
0.5054	0.4136	7.905	− 1.353				
1-pentanol (1) + HxA (2); T/K = 293.15							
0.0000	0.0000	3.967		0.6013	0.5521	8.827	− 1.618
0.0520	0.0429	4.248	− 0.222	0.6916	0.6470	10.025	− 1.534
0.1079	0.0900	4.563	− 0.460	0.7952	0.7604	11.649	− 1.241
0.1601	0.1348	4.876	− 0.673	0.8396	0.8106	12.419	− 1.060
0.2014	0.1709	5.146	− 0.826	0.9006	0.8810	13.582	− 0.723
0.3100	0.2686	5.924	− 1.195	0.9431	0.9313	14.457	− 0.438
0.3982	0.3510	6.653	− 1.433	1.0000	1.0000	15.701	
0.5031	0.4528	7.689	− 1.591				
1-pentanol (1) + HxA (2); T/K = 298.15							
0.0000	0.0000	3.905		0.6013	0.5519	8.567	− 1.518
0.0520	0.0429	4.176	− 0.209	0.6916	0.6468	9.702	− 1.445
0.1079	0.0899	4.485	− 0.427	0.7952	0.7602	11.246	− 1.171
0.1601	0.1347	4.785	− 0.628	0.8396	0.8104	11.973	− 1.006
0.2014	0.1708	5.047	− 0.770	0.9006	0.8809	13.084	− 0.684
0.3100	0.2684	5.796	− 1.114	0.9431	0.9312	13.913	− 0.419
0.3982	0.3508	6.494	− 1.339	1.0000	1.0000	15.102	
0.5031	0.4526	7.486	− 1.487				
1-pentanol (1) + HxA (2); T/K = 303.15							
0.0000	0.0000	3.846		0.6013	0.5516	8.319	− 1.424
0.0520	0.0428	4.110	− 0.194	0.6916	0.6465	9.397	− 1.360
0.1079	0.0898	4.408	− 0.398	0.7952	0.7600	10.864	− 1.106
0.1601	0.1345	4.701	− 0.583	0.8396	0.8102	11.555	− 0.952
0.2014	0.1706	4.957	− 0.713	0.9006	0.8808	12.610	− 0.652
0.3100	0.2682	5.675	− 1.038	0.9431	0.9311	13.397	− 0.402
0.3982	0.3505	6.348	− 1.245	1.0000	1.0000	14.536	
0.5031	0.4523	7.298	− 1.383				
1-heptanol (1) + HxA (2); T/K = 293.15							
0.0000	0.0000	3.963		0.6036	0.6191	7.425	− 1.525
0.0503	0.0535	4.202	− 0.192	0.7001	0.7136	8.239	− 1.473
0.0950	0.1008	4.414	− 0.361	0.8007	0.8109	9.272	− 1.224
0.1606	0.1696	4.731	− 0.598	0.8524	0.8604	9.877	− 1.017
0.2073	0.2182	4.970	− 0.751	0.8904	0.8966	10.381	− 0.805
0.3067	0.3207	5.497	− 1.050	0.9402	0.9438	11.091	− 0.475
0.4038	0.4196	6.064	− 1.279	1.0000	1.0000	12.019	
0.4991	0.5154	6.671	− 1.444				
1-heptanol (1) + HxA (2); T/K = 298.15							
0.0000	0.0000	3.903		0.6036	0.6188	7.224	− 1.382
0.0503	0.0534	4.133	− 0.176	0.7001	0.7133	7.981	− 1.344
0.0950	0.1006	4.339	− 0.329	0.8007	0.8107	8.951	− 1.114
0.1606	0.1694	4.644	− 0.547	0.8524	0.8603	9.521	− 0.921
0.2073	0.2180	4.882	− 0.678	0.8904	0.8965	9.983	− 0.734
0.3067	0.3205	5.392	− 0.947	0.9402	0.9437	10.642	− 0.434
0.4038	0.4193	5.934	− 1.156	1.0000	1.0000	11.504	
0.4991	0.5151	6.508	− 1.310				
1-heptanol (1) + HxA (2); T/K = 303.15							
0.0000	0.0000	3.848		0.6036	0.6185	7.035	− 1.245
0.0503	0.0534	4.070	− 0.161	0.7001	0.7131	7.746	− 1.212
0.0950	0.1005	4.271	− 0.297	0.8007	0.8105	8.651	− 1.005
0.1606	0.1692	4.567	− 0.493	0.8524	0.8601	9.177	− 0.834
0.2073	0.2178	4.796	− 0.613	0.8904	0.8964	9.607	− 0.665
0.3067	0.3202	5.291	− 0.852	0.9402	0.9436	10.222	− 0.388
0.4038	0.4190	5.811	− 1.040	1.0000	1.0000	11.014	
0.4991	0.5147	6.358	− 1.178				

[a] The standard uncertainties are: $u(T) = 0.02$K; $u(p) = 1$kPa; $u(\nu) = 20$ Hz; $u(x_1) = 0.0010$; $u(\varphi_1) = 0.004$. The relative standard uncertainty is: $u_r(\varepsilon_r) = 0.003$; and the relative combined expanded uncertainty (0.95 level of confidence) is $U_{rc}(\varepsilon_r^E) = 0.03$.

4.1.1. Effect of cyclization

Cyclohexylamine (c-HxA) is a cyclic primary amine with a slightly higher permittivity than HxA ($\varepsilon_r^* = 4.53$ [19]). The trend observed in the two series of systems 1-alkanol + heptane and + HxA is the same as for 1-alkanol + c-HxA mixtures (Fig. 4), for the

Table 4
Volume fractions of 1-alkanol, φ_1, refractive indices, n_D, and excess refractive indices, n_D^E, of 1-alkanol (1) + HxA (2) mixtures as functions of the mole fraction of the 1-alkanol, x_1, at temperature T and pressure $p = 0.1$ MPa.[a]

x_1	φ_1	n_D	$10^5 n_D^E$	x_1	φ_1	n_D	$10^5 n_D^E$
methanol (1) + HxA (2); T/K = 293.15							
0.0000	0.0000	1.41808		0.6997	0.4160	1.38836	679
0.0534	0.0170	1.41741	80	0.7995	0.5494	1.37505	540
0.0942	0.0308	1.41681	140	0.8475	0.6295	1.36685	440
0.1871	0.0657	1.41513	275	0.8978	0.7287	1.35657	309
0.2977	0.1147	1.41250	439	0.9496	0.8521	1.34385	162
0.4039	0.1716	1.40889	576	0.9834	0.9477	1.33399	54
0.4917	0.2283	1.40480	664	1.0000	1.0000	1.32862	
0.5977	0.3124	1.39790	715				
methanol (1) + HxA (2); T/K = 298.15							
0.0000	0.0000	1.41563		0.6997	0.4161	1.38615	689
0.0534	0.0170	1.41499	83	0.7995	0.5495	1.37296	557
0.0942	0.0308	1.41442	145	0.8475	0.6296	1.36479	457
0.1871	0.0658	1.41282	288	0.8978	0.7288	1.35460	332
0.2977	0.1148	1.41017	448	0.9496	0.8521	1.34182	173
0.4039	0.1717	1.40657	583	0.9834	0.9477	1.33194	59
0.4917	0.2283	1.40243	664	1.0000	1.0000	1.32654	
0.5977	0.3125	1.39550	710				
methanol (1) + HxA (2); T/K = 303.15							
0.0000	0.0000	1.41321		0.6997	0.4162	1.38372	678
0.0534	0.0170	1.41261	86	0.7995	0.5496	1.37067	556
0.0942	0.0308	1.41204	148	0.8475	0.6297	1.36257	461
0.1871	0.0658	1.41040	286	0.8978	0.7289	1.35240	335
0.2977	0.1148	1.40773	443	0.9496	0.8522	1.33968	179
0.4039	0.1717	1.40412	576	0.9834	0.9477	1.32980	62
0.4917	0.2284	1.40000	658	1.0000	1.0000	1.32439	
0.5977	0.3125	1.39316	709				
1-propanol (1) + HxA (2); T/K = 293.15							
0.0000	0.0000	1.41808		0.6040	0.4628	1.40784	491
0.0520	0.0301	1.41775	65	0.6965	0.5645	1.40408	450
0.1015	0.0600	1.41735	122	0.8013	0.6949	1.39877	350
0.1475	0.0890	1.41693	175	0.8505	0.7627	1.39588	285
0.2108	0.1311	1.41627	246	0.8953	0.8285	1.39295	211
0.2983	0.1936	1.41509	333	0.9486	0.9125	1.38914	109
0.3967	0.2708	1.41351	427	1.0000	1.0000	1.38514	
0.4998	0.3608	1.41113	485				
1-propanol (1) + HxA (2); T/K = 298.15							
0.0000	0.0000	1.41563		0.6040	0.4627	1.40551	487
0.0520	0.0300	1.41529	63	0.6965	0.5644	1.40199	466
0.1015	0.0600	1.41492	122	0.8013	0.6948	1.39675	368
0.1475	0.0890	1.41452	176	0.8505	0.7626	1.39373	288
0.2108	0.1310	1.41393	253	0.8953	0.8284	1.39085	216
0.2983	0.1935	1.41276	338	0.9486	0.9124	1.38704	111
0.3967	0.2707	1.41120	432	1.0000	1.0000	1.38306	
0.4998	0.3607	1.40876	480				
1-propanol (1) + HxA (2); T/K = 303.15							
0.0000	0.0000	1.41321		0.6040	0.4625	1.40323	482
0.0520	0.0300	1.41292	67	0.6965	0.5642	1.39964	450
0.1015	0.0599	1.41258	128	0.8013	0.6947	1.39454	361
0.1475	0.0889	1.41223	185	0.8505	0.7625	1.39168	295
0.2108	0.1310	1.41160	257	0.8953	0.8283	1.38884	224
0.2983	0.1934	1.41049	345	0.9486	0.9124	1.38505	118
0.3967	0.2706	1.40878	421	1.0000	1.0000	1.38102	
0.4998	0.3605	1.40642	473				
1-butanol (1) + HxA (2); T/K = 293.15							
0.0000	0.0000	1.41810		0.6004	0.5095	1.41298	442
0.0552	0.0388	1.41812	74	0.6977	0.6148	1.41065	407
0.0896	0.0637	1.41800	109	0.7982	0.7322	1.40746	309
0.1588	0.1155	1.41781	187	0.8451	0.7905	1.40577	250
0.1967	0.1448	1.41768	229	0.8996	0.8610	1.40359	165
0.3035	0.2315	1.41702	325	0.9461	0.9239	1.40166	91
0.4077	0.3225	1.41603	396	1.0000	1.0000	1.39931	
0.4984	0.4072	1.41487	439				
1-butanol (1) + HxA (2); T/K = 298.15							
0.0000	0.0000	1.41565		0.6004	0.5093	1.41079	444
0.0552	0.0388	1.41564	70	0.6977	0.6146	1.40845	403
0.0896	0.0637	1.41556	107	0.7982	0.7321	1.40534	308
0.1588	0.1154	1.41542	187	0.8451	0.7903	1.40368	249
0.1967	0.1447	1.41529	228	0.8996	0.8609	1.40158	169
0.3035	0.2314	1.41470	327	0.9461	0.9238	1.39965	92
0.4077	0.3223	1.41381	404	1.0000	1.0000	1.39733	
0.4984	0.4070	1.41267	445				

Table 4 (*continued*)

x_1	φ_1	n_D	$10^5 n_D^E$	x_1	φ_1	n_D	$10^5 n_D^E$
1-butanol (1) + HxA (2); T/K = 303.15							
0.0000	0.0000	1.41322		0.6004	0.5091	1.40852	440
0.0552	0.0388	1.41324	71	0.6977	0.6143	1.40621	398
0.0896	0.0636	1.41319	110	0.7982	0.7319	1.40316	304
0.1588	0.1153	1.41306	190	0.8451	0.7902	1.40155	248
0.1967	0.1446	1.41294	230	0.8996	0.8608	1.39949	169
0.3035	0.2312	1.41240	331	0.9461	0.9238	1.39765	99
0.4077	0.3221	1.41148	401	1.0000	1.0000	1.39529	
0.4984	0.4068	1.41040	445				
1-pentanol (1) + HxA (2); T/K = 293.15							
0.0000	0.0000	1.41813		0.6005	0.5513	1.41756	399
0.0472	0.0389	1.41838	57	0.7122	0.6692	1.41609	350
0.1005	0.0837	1.41862	118	0.7963	0.7616	1.41463	280
0.1648	0.1389	1.41884	186	0.8457	0.8175	1.41364	228
0.2022	0.1716	1.41896	225	0.8982	0.8782	1.41246	160
0.3102	0.2688	1.41908	317	0.9362	0.9230	1.41153	104
0.3982	0.3510	1.41895	372	1.0000	1.0000	1.40985	
0.5002	0.4500	1.41846	405				
1-pentanol (1) + HxA (2); T/K = 298.15							
0.0000	0.0000	1.41563		0.6005	0.5510	1.41543	404
0.0472	0.0389	1.41592	59	0.7122	0.6689	1.41403	355
0.1005	0.0836	1.41622	123	0.7963	0.7614	1.41259	282
0.1648	0.1388	1.41649	193	0.8457	0.8174	1.41164	230
0.2022	0.1715	1.41660	229	0.8982	0.8781	1.41048	161
0.3102	0.2686	1.41679	322	0.9362	0.9230	1.40957	105
0.3982	0.3508	1.41671	378	1.0000	1.0000	1.40793	
0.5002	0.4497	1.41623	406				
1-pentanol (1) + HxA (2); T/K = 303.15							
0.0000	0.0000	1.41324		0.6005	0.5508	1.41329	409
0.0472	0.0388	1.41360	64	0.7122	0.6687	1.41193	359
0.1005	0.0835	1.41392	129	0.7963	0.7612	1.41054	288
0.1648	0.1386	1.41424	202	0.8457	0.8172	1.40958	234
0.2022	0.1713	1.41438	239	0.8982	0.8780	1.40844	164
0.3102	0.2683	1.41458	331	0.9362	0.9229	1.40754	107
0.3982	0.3505	1.41451	384	1.0000	1.0000	1.40590	
0.5002	0.4494	1.41407	412				
1-heptanol (1) + HxA (2); T/K = 293.15							
0.0000	0.0000	1.41807		0.6020	0.6175	1.42550	361
0.0560	0.0596	1.41916	72	0.7029	0.7163	1.42563	313
0.1018	0.1079	1.41999	125	0.7979	0.8082	1.42545	238
0.1463	0.1546	1.42077	174	0.8534	0.8614	1.42521	181
0.2047	0.2155	1.42171	231	0.8986	0.9044	1.42496	130
0.3044	0.3184	1.42310	306	0.9472	0.9504	1.42464	70
0.4059	0.4217	1.42423	355	1.0000	1.0000	1.42425	
0.5044	0.5207	1.42503	374				
1-heptanol (1) + HxA (2); T/K = 298.15							
0.0000	0.0000	1.41563		0.6020	0.6172	1.42331	353
0.0560	0.0595	1.41674	71	0.7029	0.7161	1.42351	306
0.1018	0.1078	1.41761	125	0.7979	0.8080	1.42339	233
0.1463	0.1545	1.41840	173	0.8534	0.8612	1.42320	178
0.2047	0.2153	1.41937	229	0.8986	0.9043	1.42299	128
0.3044	0.3181	1.42080	303	0.9472	0.9503	1.42271	69
0.4059	0.4214	1.42197	350	1.0000	1.0000	1.42235	
0.5044	0.5204	1.42280	367				
1-heptanol (1) + HxA (2); T/K = 303.15							
0.0000	0.0000	1.41321		0.6020	0.6169	1.42116	347
0.0560	0.0594	1.41434	70	0.7029	0.7158	1.42142	301
0.1018	0.1077	1.41523	124	0.7979	0.8078	1.42136	228
0.1463	0.1543	1.41604	171	0.8534	0.8611	1.42120	174
0.2047	0.2151	1.41703	226	0.8986	0.9042	1.42103	125
0.3044	0.3178	1.41853	301	0.9472	0.9502	1.42079	68
0.4059	0.4211	1.41974	347	1.0000	1.0000	1.42047	
0.5044	0.5200	1.42062	363				

[a] The standard uncertainties are: $u(T) = 0.02$K; $u(p) = 1$kPa; $u(x_1) = 0.0008$; $u(\varphi_1) = 0.004$, $u(n_D) = 0.00008$. The combined expanded uncertainty (0.95 level of confidence) is $U_{rc}(n_D^E) = 0.0002$.

same reasons: $\varepsilon_r^E = 2.218$ ($n = 1$ [13]), −0.269 ($n = 3$ [19]), −0.848 ($n = 4$ [19]), −0.915 ($n = 7$ [19]) −0.411 ($n = 10$ [19]). Therefore, cyclization of the amine leads to increased ε_r^E values compared to those of systems with HxA; i.e., multimers formed by unlike molecules contribute more positively to ε_r^E in cyclohexylamine solutions.

Table 5
Coefficients A_i and standard deviations, $\sigma(F^E)$ (equation (6)), for the representation of F^E at temperature T and pressure $p = 0.1$ MPa for 1-alkanol (1) + HxA (2) systems by equation (5).

Property F^E	System	T/K	A_0	A_1	A_2	A_3	A_3	$\sigma(F^E)$
ε_r^E	methanol + HxA	293.15	1.12	9.1	8.4	2.2		0.016
		298.15	0.92	8.4	8.5	3.1		0.017
		303.15	0.82	8.0	8.6	3.4		0.013
	1-propanol + HxA	293.15	− 4.59	0.66	2.08	0.65		0.004
		298.15	− 4.45	0.44	1.92	0.8		0.005
		303.15	− 4.30	0.23	1.74	0.8		0.005
	1-butanol + HxA	293.15	− 6.00	− 1.1	0.8			0.012
		298.15	− 5.70	− 1.17	0.6			0.013
		303.15	− 5.41	− 1.25	0.49			0.011
	1-pentanol + HxA	293.15	− 6.38	− 2.08				0.006
		298.15	− 5.98	− 2.02				0.008
		303.15	− 5.55	− 1.98	− 0.24			0.006
	1-heptanol + HxA	293.15	− 5.81	− 2.6	− 0.79			0.007
		298.15	− 5.26	− 2.38	− 0.77			0.007
		303.15	− 4.73	− 2.15	− 0.73			0.008
$10^5 n_D^E$	methanol + HxA	293.15	2694	1518	− 255	− 670		2
		298.15	2694	1454	− 22	− 427		4
		303.15	2663	1443	64	− 385		0.8
	1-propanol + HxA	293.15	1922	614	− 230			5
		298.15	1898	644				8
		303.15	1892	609				1
	1-butanol + HxA	293.15	1755	551	− 215	− 406		3
		298.15	1772	491	− 264	− 260		1.5
		303.15	1761	363	− 218			4
	1-pentanol + HxA	293.15	1615	283	− 146			0.9
		298.15	1631	268	− 119			1.5
		303.15	1653	243	− 62			1.2
	1-heptanol + HxA	293.15	1495	50	− 147			1.5
		298.15	1468	33	− 126			0.9
		303.15	1451	20	− 138			0.6
$\left(\frac{\partial \varepsilon_r^E}{\partial T}\right)_p$ /K^{-1}	methanol + HxA	298.15	− 0.028	− 0.105	− 0.01	0.11	0.05	0.0007
	1-propanol + HxA	298.15	0.0284	− 0.038	− 0.032			0.0003
	1-butanol + HxA	298.15	0.060	− 0.015	− 0.034			0.0005
	1-pentanol + HxA	298.15	0.082	0.010	− 0.017			0.0005
	1-heptanol + HxA	298.15	0.109	0.045				0.0007

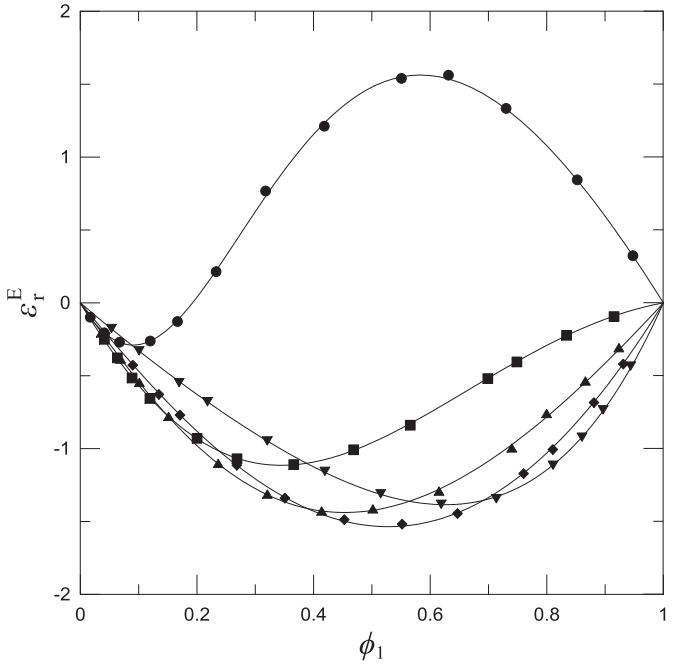

Fig. 1. Excess relative permittivities, ε_r^E, of 1-alkanol (1) + HxA (2) systems at 0.1 MPa, 298.15 K and 1 MHz. Full symbols, experimental values (this work): (●), methanol; (■), 1-propanol; (▲), 1-butanol; (◆), 1-pentanol; (▼), 1-heptanol. Solid lines, calculations with equation (5) using the coefficients from Table 5.

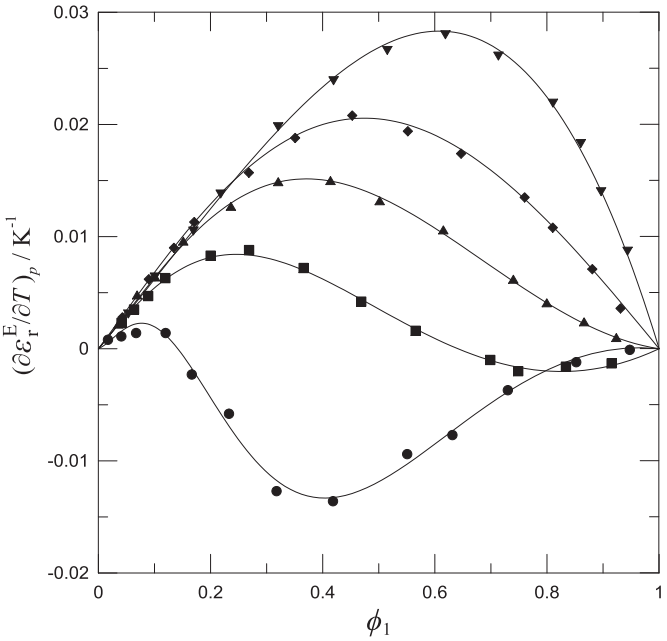

Fig. 2. Derivative of the excess relative permittivity of 1-alkanol (1) + HxA (2) systems at 0.1 MPa, 298.15 K and 1 MHz. Full symbols, experimental values (this work): (●), methanol; (■), 1-propanol; (▲), 1-butanol; (◆), 1-pentanol; (▼), 1-heptanol. Solid lines, calculations with equation (5) using the coefficients from Table 5.

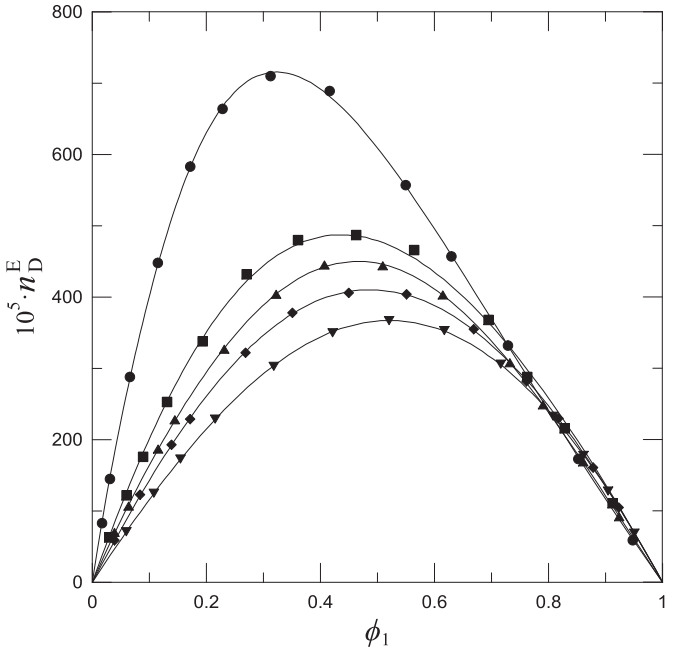

Fig. 3. Excess refractive index, n_D^E, of 1-alkanol (1) + HxA (2) systems at 0.1 MPa, 298.15 K and 1 MHz. Full symbols, experimental values (this work): (●), methanol; (■), 1-propanol; (▲), 1-butanol; (◆), 1-pentanol; (▼), 1-heptanol. Solid lines, calculations with equation (5) using the coefficients from Table 5.

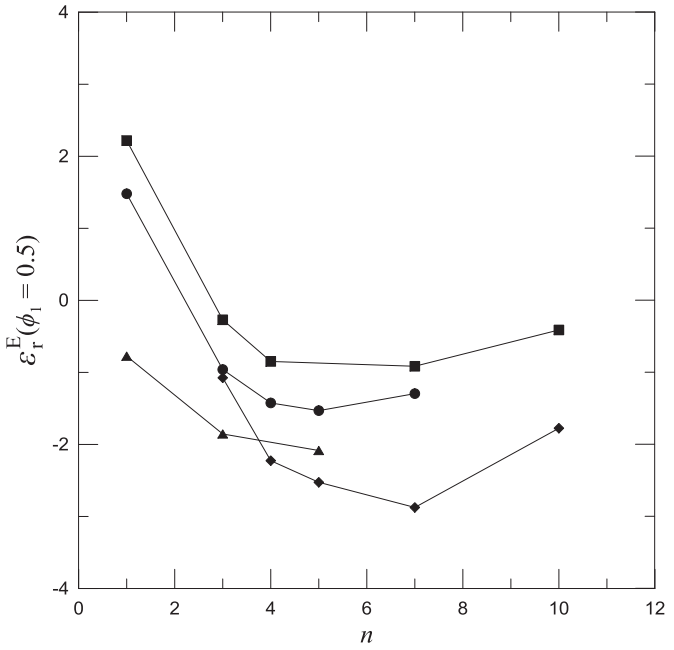

Fig. 4. Excess relative permittivities at φ_1 = 0.5of 1-alkanol (1) + amine (2) or + heptane (2) systems as functions of the number of carbon atoms of the 1-alkanol, at 0.1 MPa, 298.15 K and 1 MHz: (●), HxA (this work); (■), c-HxA [13, 19]; (▲), aniline [42]; (◆), heptane [12, 38–40].

4.1.2. Effect of aromaticity

The effect of aromaticity is more dramatic than that of cyclization. In fact, aniline ($\varepsilon_r^* = 7.004$ [42]) shows a greater value of the relative permittivity, underlining the importance of aniline-aniline interactions and the polarizability of the aromatic ring. The values of the corresponding excess property are of course negative [42] (Fig. 4): −0.775 ($n = 1$), −1.854 ($n = 3$), −2.084 ($n = 5$). In addition, they are lower than those of the mixtures with HxA or c-HxA. This may be explained taking into account that the breaking of the dipolar interactions between aniline molecules contributes more negatively to ε_r^E.

4.2. Entropy change with the electric field

ε_r is a collective property and its magnitude in a liquid depends on its structure, the permanent dipole moment of its molecules and their polarizability. It must be highlighted that it is also affected by volume effects. In fact, let $\vec{B}$ denote the macroscopic dipole moment and V the volume. The polarization (macroscopic dipole moment per unit volume) of the liquid, $\vec{B}/V$, is related to the intensity of the electric field, $\vec{E}$, through the equation $\vec{B}/V = (\varepsilon_r - 1)\varepsilon_0 \vec{E}$ (ε_0 = vacuum permittivity). In order to compare the response of different liquids to an electric field, it is desirable to work with the molar susceptibility, $\chi_m = (\varepsilon_r - 1)V_m$. This quantity, for a given electric field, is proportional to the macroscopic dipole moment resulting from a fixed amount (1 mol) of molecules. For a linear, isotropic and homogeneous dielectric at constant composition, the molar macroscopic dipole moment B_m is related to χ_m and E by:

$$\frac{1}{\varepsilon_0 E} B_m = \chi_m \tag{7}$$

The T-dependence of χ_m is linked to the change of the molar entropy, S_m, with a variation of E through the Schwarz relation (p = pressure):

$$\frac{1}{\varepsilon_0 E}\left(\frac{\partial S_m}{\partial E}\right)_{T,p} = \left(\frac{\partial S_m}{\partial(\varepsilon_0 E^2/2)}\right)_{T,p} = \left(\frac{\partial \chi_m}{\partial T}\right)_p \tag{8}$$

This variation is usually negative in common liquids like the ones considered in this work (Table 6), as it is associated with structure creation (dipolar ordering) by an increase of the electric field and a consequent negative variation of the entropy. It can be calculated from linear regressions of χ_m values in the temperature range (293.15–303.15) K. In the following discussion, we will use the notation $\eta_{m,p} = -\left(\frac{\partial \chi_m}{\partial T}\right)_p$.

The values of $\eta^*_{m,p}$ for the pure 1-alkanols increase with n (Table 6). It indicates that a high self-association (in the absence of an electric field) decreases the ability of the electric field to create structure by orientating the dipoles of individual molecules, as the multimers present in the liquid are more stable and the rotational degrees of freedom are more constricted. The lower $\eta^*_{m,p}$ values of the amines seem to be due to their lower μ. As HxA and c-HxA have similar dipole moments (Table 6), the fact that $\eta^*_{m,p}$(HxA) < $\eta^*_{m,p}$(c-HxA) indicates more freedom of rotation of the c-HxA molecules. Also, $\eta^*_{m,p}$(c-HxA) < $\eta^*_{m,p}$(aniline), which can be ascribed to an extra contribution to the polarizability of the molecules of aniline due to the presence of the aromatic ring.

It is interesting to analyse the $\eta_{m,p}(\varphi_1)$ curves for 1-alkanol + HxA systems (Fig. 5). The necessary volumetric properties to compute them have been taken from a previous work [4]. Due to the absence of experimental volumetric data in the whole range of temperature necessary for the complete set of studied systems, we have neglected the contribution from the temperature dependence of the excess molar volume; this approximation does not appreciably affect the $\eta_{m,p}$ results, as can be seen by performing the exact calculation for the system 1-butanol + HxA [43]. At low HxA concentrations, $\eta_{m,p}$ varies more rapidly when the 1-alkanol is longer. This shows that, in this region, the difficulty for the electric field to rotate the dipoles decreases more rapidly with

Table 6
Intrinsic dipole moment, μ, and molar dielectric properties of pure liquids at $p = 0.1$ MPa: χ^*_m, molar dielectric susceptibility; $\eta^*_{m,p} = -(\partial\chi^*_m/\partial T)_p$.

Compound	μ/D	χ^*_m/cm$^3\cdot$mol^{-1}			$\eta^*_{m,p}$/cm$^3\cdot$mol$^{-1}\cdot$K^{-1}
		$T = 293.15$ K	$T = 298.15$ K	$T = 303.15$ K	$T = 298.15$ K
methanol	1.664 [75]	1318	1287	1256	6.2
1-propanol	1.629 [75]	1507	1462	1419	8.8
1-butanol	1.614 [75]	1574	1521	1472	10.2
1-pentanol	1.598 [75]	1591	1533	1478	11.3
1-heptanol	1.583 [75]	1557	1491	1427	13.0
1-decanol	1.566 [75]	1413[a]	1342[a]	1277[a]	13.6[a]
HxA	1.3 [76]	392	387	381	1.1
c-HxA	1.26 [77]	418[a]	409[a]	401[a]	1.7[a]
aniline	1.51 [40]	558[b]	548[b]	538[b]	2.0[b]

[a] Calculated from data of ref. [19].
[b] Calculated from data of ref. [78].

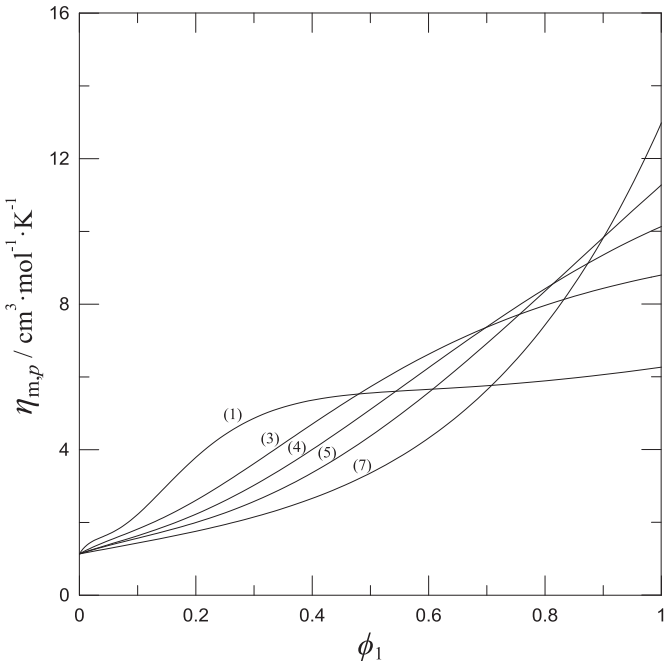

Fig. 5. $\eta_{m,p} = -\left(\frac{\partial\chi_m}{\partial T}\right)_p$ of 1-alkanol (1) + HxA (2) systems at 0.1 MPa, 298.15 K and 1 MHz. Numbers in parentheses indicate the number of atoms of the 1-alkanol.

concentration when the 1-alkanol self-association is lower and weaker.

4.3. Molar refraction

The refractive index at optical wavelengths is closely related to dispersion forces, since the molar refraction (or molar refractivity), R_m, defined by the Lorentz-Lorenz equation [29,44]:

$$R_m = \frac{n_D^2 - 1}{n_D^2 + 2} V_m = \frac{N_A \alpha_e}{3\varepsilon_0} \tag{9}$$

(where N_A and ε_0 stand for Avogadro's constant and the vacuum permittivity, respectively) is proportional to the mean electronic contribution, α_e, to the polarizability, [29]. For the investigated systems, the values of R_m/cm$^3\cdot$mol^{-1} at $x_1 = 0.5$ are (Fig. S2): 20.5 ($n = 1$), 25.2 ($n = 3$), 27.5 ($n = 4$), 29.8 ($n = 5$), 34.5 ($n = 7$). It is clear that dispersive interactions are more important in longer 1-alkanols. We have calculated the corresponding excess values, $R_m^E = R_m - R_m^{id}$, with R_m^{id} evaluated substituting ideal values in equation (9). The curves are negative, which means a loss in dispersive interactions along mixing with respect to the ideal state, in which dipoles of different components do not interact. The minimum values occur at $x_1 \approx 0.5$; in the same units: −0.37 ($n = 1$), −0.28 ($n = 3,4,5,7$). The lower value of the methanol system can be ascribed to a larger number of hydrogen bonds formed by the two species along the mixing process.

4.4. Kirkwood-Fröhlich model

Some relevant hypotheses of the model are: (i) a molecule of a given polar compound is modelled as a dipole moment inside a spherical cavity; (ii) the effect of the induced polarization of the molecules is treated in macroscopic way, assuming that the dipole is rigid (it only rotates) and the cavity is filled by a continuous medium of relative permittivity ε_r^∞ (the value of the permittivity at a high frequency at which only the induced polarizability contributes); (iii) long-range interactions are considered macroscopically by assuming that the outside of the cavity is a continuous dielectric of permittivity ε_r; (iv) short-range interactions are not neglected, and they are brought on stage by means of the so-called Kirkwood correlation factor, g_K, which provides information of the deviations from randomness of the orientation of a dipole with respect to its neighbours. This is an important parameter, as it provides information about specific interactions in the liquid state. For a mixture, g_K can be determined, in the context of a one-fluid model [26], from macroscopic physical properties according to the expression [26–29]:

$$g_K = \frac{9k_B T V_m \varepsilon_0 (\varepsilon_r - \varepsilon_r^\infty)(2\varepsilon_r + \varepsilon_r^\infty)}{N_A \mu^2 \varepsilon_r (\varepsilon_r^\infty + 2)^2} \tag{10}$$

Here, k_B is Boltzmann's constant; N_A, Avogadro's constant; ε_0, the vacuum permittivity; and V_m, the molar volume of the liquid at the working temperature, T. For polar compounds, ε_r^∞ is estimated from the relation $\varepsilon_r^\infty = 1.1 n_D^2$ [45]. μ represents the dipole moment of the solution, estimated from the equation [26]:

$$\mu^2 = x_1 \mu_1^2 + x_2 \mu_2^2 \tag{11}$$

where μ_i stands for the dipole moment of component i (=1,2). Calculations have been conducted using smoothed values of V_m^E [4], n_D^E(this work) and ε_r^E (this work) at $\Delta x_1 = 0.01$. The source and values of μ_i are collected in Table 6.

Our calculations on g_K curves for 1-alkanol + HxA systems can be seen in Fig. 6. They support the conclusions extracted from the analysis of $\eta_{m,p}$, indicating that the mixture structure varies very rapidly with the HxA concentration for $n = 3$, 4, 5, 7. In contrast, for the methanol system g_K changes slowly from $\varphi_1 > 0.6$ approximately, and this indicates that HxA is not able to break effectively

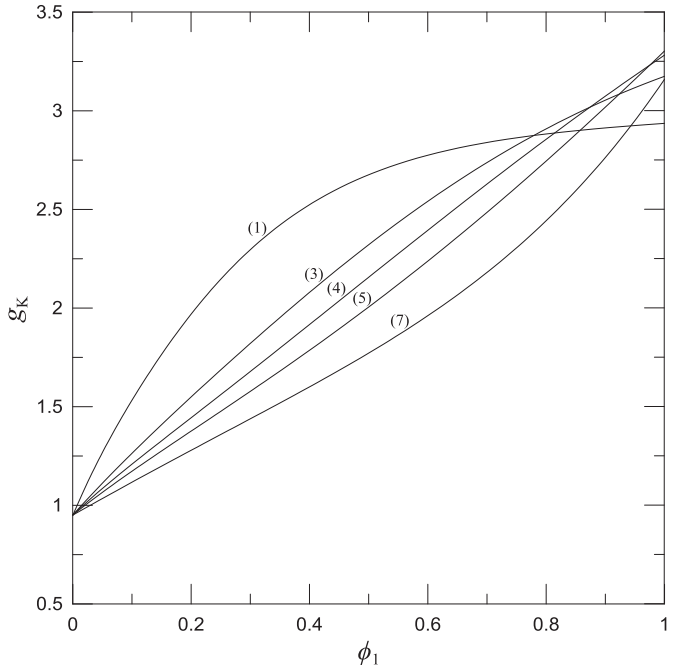

Fig. 6. Kirkwood correlation factor, g_K, of 1-alkanol (1) + HxA (2) systems at 0.1 MPa, 298.15 K and 1 MHz. Numbers in parentheses indicate the number of atoms of the 1-alkanol.

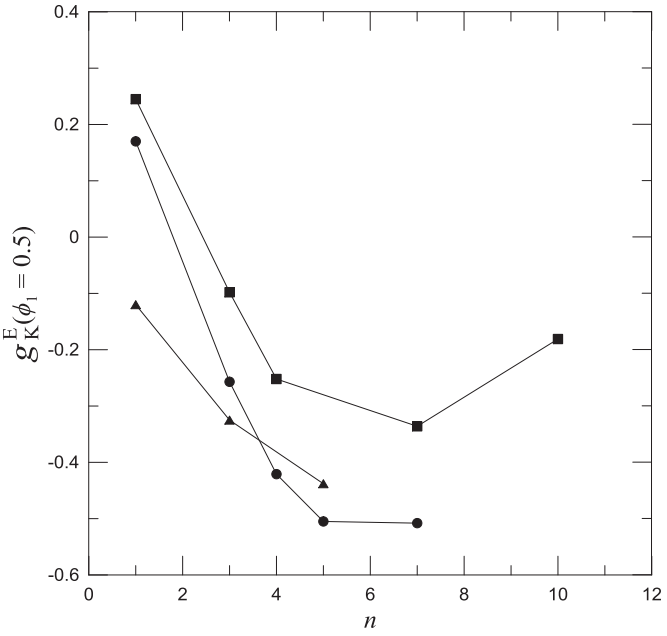

Fig. 8. Excess Kirkwood correlation factors at $\varphi_1 = 0.5$ of 1-alkanol (1) + amine (2) systems as functions of the number of carbon atoms of the 1-alkanol, at 0.1 MPa, 298.15 K and 1 MHz: (●), HxA (this work); (■), c-HxA [13,19]; (▲), aniline [42].

the methanol self-association at such concentrations. This phenomenon remarks the strong relationship between the magnitude of the rupture of the 1-alkanol self-association by the amine and the dielectric behaviour of the mixtures.

We have also evaluated the excess Kirkwood correlation factors, $g_K^E = g_K - g_K^{id}$, where g_K^{id} is calculated substituting the real quantities by ideal ones in equation (10). The values for 1-alkanol + HxA systems are (Fig. 7 and 8): 0.170 ($n = 1$), −0.257 ($n = 3$), −0.421 ($n = 4$), −0.505 ($n = 5$), −0.508 ($n = 7$). The positive value for the methanol mixture can be justified by the formation of strong methanol-HxA interactions, which is consistent with the above analyses. The minima of the g_K^E curves occurs at lower φ_1 than in the ε_r^E curves. For the minimum of the curves, g_K^E(1-pentanol) > g_K^E(1-heptanol), while the opposite behaviour is encountered for ε_r^E. Thus, according to the Kirkwood-Fröhlich model, the destruction of the correlations of the dipoles is not the only responsible for the ε_r^E minima, but there are other effects involved. For c-HxA systems, g_K^E values are higher (Fig. 8), indicating that in these mixtures the balance of destruction and creation of correlations is more inclined to the latter than in the case 1-alkanol + HxA. Aniline systems are quite interesting, as g_K^E(HxA) < g_K^E(aniline) for the 1-pentanol mixtures (Fig. 8). This phenomenon may be related to the higher importance of the rupture of interactions between like molecules in 1-alkanol + aniline solutions, as showed by ε_r^E values and also H_m^E (see introduction).

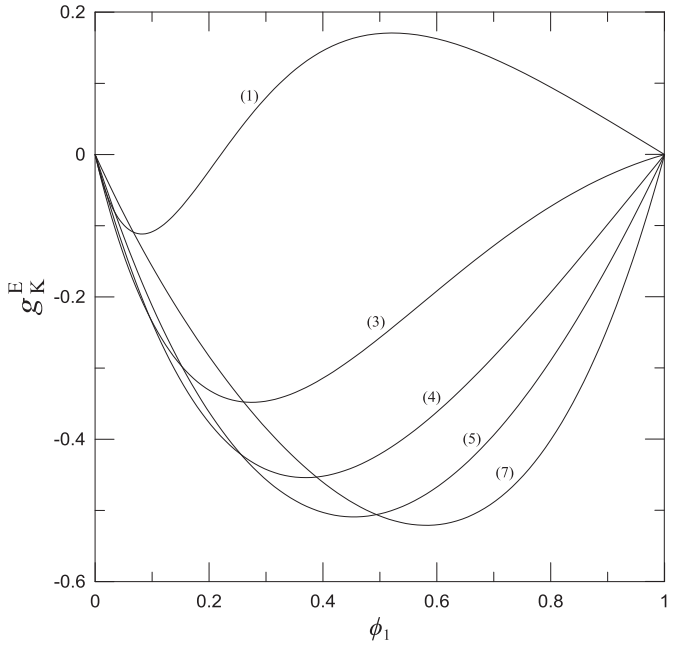

Fig. 7. Excess Kirkwood correlation factor, g_K^E, of 1-alkanol (1) + HxA (2) systems at 0.1 MPa, 298.15 K and 1 MHz. Numbers in parentheses indicate the number of atoms of the 1-alkanol.

5. Conclusions

ε_r and n_D measurements have been reported for the 1-alkanol + *n*-hexylamine systems at (293.15–303.15) K. The formation of multimers built by unlike molecules contributes positively to ε_r^E. Such contribution is dominant for the methanol mixture and ε_r^E is positive. For the remaining systems, the dominant contributions arise from the breaking of interactions between like molecules, and ε_r^E values are negative. For a given 1-alkanol, ε_r^E changes in the sequence: cyclohexylamine > *n*-hexylamine > aniline. The application of the Kirkwood-Fröhlich model confirms these findings. Calculations on R_m show that dispersive interactions in the studied mixtures increase with the length of the 1-alkanol.

Acknowledgements

F. Hevia and A. Cobos are grateful to Ministerio de Educación, Cultura y Deporte for the grants FPU14/04104 and FPU15/05456 respectively. The authors gratefully acknowledge the financial

support received from the Consejería de Educación y Cultura of Junta de Castilla y León, under Project BU034U16.

Appendix A. Supplementary data

Supplementary data related to this article can be found at https://doi.org/10.1016/j.fluid.2018.04.007.

References

[1] A. Heintz, P.K. Naicker, S.P. Verevkin, R. Pfestorf, Thermodynamics of alkanol + amine mixtures. Experimental results and ERAS model calculations of the heat of mixing, Ber. Bunsenges. Phys. Chem. 102 (1998) 953–959, https://doi.org/10.1002/bbpc.19981020707.

[2] K. Nakanishi, H. Touhara, N. Watanabe, Studies on associated solutions. II. Heat of mixing of methanol with aliphatic amines, Bull. Chem. Soc. Jpn. 43 (1970) 2671–2676, https://doi.org/10.1246/bcsj.43.2671.

[3] A. Heintz, A new theoretical approach for predicting excess properties of alkanol/alkane mixtures, Ber. Bunsenges. Phys. Chem. 89 (1985) 172–181, https://doi.org/10.1002/bbpc.19850890217.

[4] S. Villa, N. Riesco, I. Garcıa de la Fuente, J.A. González, J.C. Cobos, Thermodynamics of mixtures with strongly negative deviations from Raoult's law. Part 8. Excess molar volumes at 298.15 K for 1-alkanol + isomeric amine (C6H15N) systems: characterization in terms of the ERAS model, Fluid Phase Equil. 216 (2004) 123–133, https://doi.org/10.1016/j.fluid.2003.10.008.

[5] J.A. González, I. García de la Fuente, J.C. Cobos, Thermodynamics of mixtures with strongly negative deviations from Raoult's Law: Part 4. Application of the DISQUAC model to mixtures of 1-alkanols with primary or secondary linear amines. Comparison with Dortmund UNIFAC and ERAS results, Fluid Phase Equil. 168 (2000) 31–58, https://doi.org/10.1016/S0378-3812(99)00326-X.

[6] R. Srivastava, B.D. Smith, Total-pressure vapor-liquid equilibrium data for binary systems of diethylamine with acetone, acetonitrile, and methanol, J. Chem. Eng. Data 30 (1985) 308–313, https://doi.org/10.1021/je00041a022.

[7] L. Wang, G.C. Benson, B.C.Y. Lu, Excess enthalpies of 1-propanol + n-hexane + n-decane or n-dodecane at 298.15 K, J. Chem. Eng. Data 37 (1992) 403–406, https://doi.org/10.1021/je00008a007.

[8] S.-c. Hwang, R.L. Robinson, Vapor-liquid equilibria at 25 °C for nine alcohol-hydrocarbon binary systems, J. Chem. Eng. Data 22 (1977) 319–325, https://doi.org/10.1021/je60074a025.

[9] S. Villa, N. Riesco, I. Garcıa de la Fuente, J.A. González, J.C. Cobos, Thermodynamics of mixtures with strongly negative deviations from Raoult's law: Part 5. Excess molar volumes at 298.15 K for 1-alkanols+dipropylamine systems: characterization in terms of the ERAS model, Fluid Phase Equil. 190 (2001) 113–125, https://doi.org/10.1016/S0378-3812(01)00595-7.

[10] S. Villa, N. Riesco, I. Garcıa de la fuente, J.A. González, J.C. Cobos, Thermodynamics of mixtures with strongly negative deviations from Raoult's law: Part 6. Excess molar volumes at 298.15 K for 1-alkanols + dibutylamine systems. Characterization in terms of the ERAS model, Fluid Phase Equil. 198 (2002) 313–329, https://doi.org/10.1016/S0378-3812(01)00808-1.

[11] L.F. Sanz, J.A. González, I. García De La Fuente, J.C. Cobos, Thermodynamics of mixtures with strongly negative deviations from Raoult's law. XI. Densities, viscosities and refractives indices at (293.15–303.15) K for cyclohexylamine + 1-propanol, or +1-butanol systems, J. Mol. Liq. 172 (2012) 26–33, https://doi.org/10.1016/j.molliq.2012.05.003.

[12] L.F. Sanz, J.A. González, I. García de la Fuente, J.C. Cobos, Thermodynamics of mixtures with strongly negative deviations from Raoult's law. XII. Densities, viscosities and refractive indices at T = (293.15 to 303.15) K for (1-heptanol, or 1-decanol + cyclohexylamine) systems. Application of the ERAS model to (1-alkanol + cyclohexylamine) mixtures, J. Chem. Thermodyn. 80 (2015) 161–171, https://doi.org/10.1016/j.jct.2014.09.005.

[13] L.F. Sanz, J.A. González, I.G. De La Fuente, J.C. Cobos, Thermodynamics of mixtures with strong negative deviations from raoult's law. XIV. density, permittivity, refractive index and viscosity data for the methanol + cyclohexylamine mixture at (293.15–303.15) K, Thermochim. Acta 631 (2016) 18–27, https://doi.org/10.1016/j.tca.2016.03.002.

[14] U. Domańska, M. Głoskowska, Experimental solid + liquid equilibria and excess molar volume of alkanol + octylamine mixtures. Analysis in terms of ERAS, DISQUAC, and modified UNIFAC, J. Chem. Eng. Data 49 (2004) 101–108, https://doi.org/10.1021/je0301895.

[15] K. Nakanishi, H. Touhara, Excess molar enthalpies of (methanol + aniline), (methanol + N-methylaniline), and (methanol + N,N-dimethylaniline), J. Chem. Thermodyn. 18 (1986) 657–660, https://doi.org/10.1016/0021-9614(86)90067-4.

[16] I. Nagata, Excess enthalpies of (aniline + butan-1-ol) and of (aniline + butan-1-ol + benzene) at the temperature 298.15 K, J. Chem. Thermodyn. 25 (1993) 1281–1285, https://doi.org/10.1006/jcht.1993.1127.

[17] H. Matsuda, K. Ochi, K. Kojima, Determination and correlation of LLE and SLE data for the methanol + cyclohexane, aniline + heptane, and phenol + hexane system, J. Chem. Eng. Data 48 (2003) 184–189, https://doi.org/10.1021/je020156+.

[18] S. Villa, R. Garriga, P. Pérez, M. Gracia, J.A. González, I.G. de la Fuente, J.C. Cobos, Thermodynamics of mixtures with strongly negative deviations from Raoult's law: Part 9. Vapor–liquid equilibria for the system 1-propanol + di-n-propylamine at six temperatures between 293.15 and 318.15 K, Fluid Phase Equil. 231 (2005) 211–220, https://doi.org/10.1016/j.fluid.2005.01.013.

[19] J.A. González, L.F. Sanz, I. García de la Fuente, J.C. Cobos, Thermodynamics of mixtures with strong negative deviations from Raoult's law. XIII. Relative permittivities for (1-alkanol + cyclohexylamine) systems, and dielectric study of (1-alkanol + polar) compound (amine, amide or ether) mixtures, J. Chem. Thermodyn. 91 (2015) 267–278, https://doi.org/10.1016/j.jct.2015.07.032.

[20] J.A. González, I.G. de la Fuente, J.C. Cobos, Thermodynamics of mixtures with strongly negative deviations from Raoult's law. Part 3. Application of the DISQUAC model to mixtures of triethylamine with alkanols. Comparison with Dortmund UNIFAC and ERAS results, Can. J. Chem. 78 (2000) 1272–1284, https://doi.org/10.1139/v00-114.

[21] J.A. González, I. Mozo, I. García de la Fuente, J.C. Cobos, Thermodynamics of organic mixtures containing amines. IV. Systems with aniline, Can. J. Chem. 83 (2005) 1812–1825, https://doi.org/10.1139/v05-190.

[22] J.A. González, I. Mozo, I.G.d.l. Fuente, J.C. Cobos, Thermodynamics of organic mixtures containing amines: V. Systems with pyridines, Thermochim. Acta 441 (2006) 53–68, https://doi.org/10.1016/j.tca.2005.11.027.

[23] J.A. González, I. Mozo, I.G. de la Fuente, J.C. Cobos, N. Riesco, Thermodynamics of mixtures containing amines: VII. Systems containing dimethyl or trimethylpyridines, Thermochim. Acta 467 (2008) 30–43, https://doi.org/10.1016/j.tca.2007.10.011.

[24] J.A. González, I.G. de la Fuente, I. Mozo, J.C. Cobos, N. Riesco, Thermodynamics of organic mixtures containing amines. Vii. Study of systems containing pyridines in terms of the Kirkwood–Buff formalism, Ind. Eng. Chem. Res. 47 (2008) 1729–1737, https://doi.org/10.1021/ie071226e.

[25] J.A. González, J.C. Cobos, I. García de la Fuente, I. Mozo, Thermodynamics of mixtures containing amines. IX. Application of the concentration–concentration structure factor to the study of binary mixtures containing pyridines, Thermochim. Acta 494 (2009) 54–64, https://doi.org/10.1016/j.tca.2009.04.017.

[26] J.C.R. Reis, T.P. Iglesias, Kirkwood correlation factors in liquid mixtures from an extended Onsager-Kirkwood-Frohlich equation, Phys. Chem. Chem. Phys. 13 (2011) 10670–10680, https://doi.org/10.1039/C1CP20142E.

[27] H. Fröhlich, Theory of Dielectrics, Clarendon Press, Oxford, 1958.

[28] C. Moreau, G. Douhéret, Thermodynamic and physical behaviour of water + acetonitrile mixtures. Dielectric properties, J. Chem. Thermodyn. 8 (1976) 403–410, https://doi.org/10.1016/0021-9614(76)90060-4.

[29] A. Chelkowski, Dielectric Physics, Elsevier, Amsterdam, 1980.

[30] CIAAW, Atomic Weights of the Elements, 2015 (accessed 2015), ciaaw.org/atomic-weights.htm.

[31] J.A. González, I. Alonso, I. Mozo, I. García de la Fuente, J.C. Cobos, Thermodynamics of (ketone + amine) mixtures. Part VI. Volumetric and speed of sound data at (293.15, 298.15, and 303.15) K for (2-heptanone + dipropylamine, +dibutylamine, or +triethylamine) systems, J. Chem. Thermodyn. 43 (2011) 1506–1514, https://doi.org/10.1016/j.jct.2011.05.003.

[32] K.N. Marsh, Recommended Reference Materials for the Realization of Physicochemical Properties, Blackwell Scientific Publications, Oxford, UK, 1987.

[33] V. Alonso, J.A. González, I. García de la Fuente, J.C. Cobos, Dielectric and refractive index measurements for the systems 1-pentanol + octane, or + dibutyl ether or for dibutyl ether + octane at different temperatures, Thermochim. Acta 543 (2012) 246–253, https://doi.org/10.1016/j.tca.2012.05.036.

[34] J.C.R. Reis, T.P. Iglesias, G. Douhéret, M.I. Davis, The permittivity of thermodynamically ideal liquid mixtures and the excess relative permittivity of binary dielectrics, Phys. Chem. Chem. Phys. 11 (2009) 3977–3986, https://doi.org/10.1039/B820613A.

[35] J.C.R. Reis, I.M.S. Lampreia, Â.F.S. Santos, M.L.C.J. Moita, G. Douhéret, Refractive index of liquid mixtures: theory and experiment, ChemPhysChem 11 (2010) 3722–3733, https://doi.org/10.1002/cphc.201000566.

[36] O. Redlich, A.T. Kister, Algebraic representation of thermodynamic properties and the classification of solutions, Ind. Eng. Chem. 40 (1948) 345–348, https://doi.org/10.1021/ie50458a036.

[37] P.R. Bevington, D.K. Robinson, Data Reduction and Error Analysis for the Physical Sciences, McGraw-Hill, New York, 2000.

[38] N.V. Sastry, M.K. Valand, Densities, speeds of sound, viscosities, and relative permittivities for 1-propanol + and 1-butanol + heptane at 298.15 K and 308.15 K, J. Chem. Eng. Data 41 (1996) 1421–1425, https://doi.org/10.1021/je960135d.

[39] N.V. Sastry, M.K. Valand, Dielectric constants, refractive indexes and polarizations for 1-Alcohol +Heptane mixtures at 298.15 and 308.15 K, Ber. Bunsenges. Phys. Chem. 101 (1997) 243–250, https://doi.org/10.1002/bbpc.19971010212.

[40] J.A. Riddick, W.B. Bunger, T.K. Sakano, Organic Solvents: Physical Properties and Methods of Purification, Wiley, New York, 1986.

[41] A. Skrzecz, Critical evaluation of solubility data in binary systems formed by methanol with n-hydrocarbons, Thermochim. Acta 182 (1991) 123–131, https://doi.org/10.1016/0040-6031(91)87013-M.

[42] V. Alonso, in: Estudio experimental de propiedades termofísicas de mezclas binarias formadas por 1-alcohol + alcano, + éter lineal o + amina aromática primaria, Departamento de Física Aplicada, Facultad de Ciencias, Universidad de Valladolid, 2016, pp. 194–241. Chapter 6.

[43] I.R. Radović, M.L. Kijevčanin, S.P. Šerbanović, B.D. Djordjević, 1-Butanol + hexylamine + *n*-heptane at temperature range (288.15–323.15 K): experimental density data, excess molar volumes determination and modeling with cubic EOS, Fluid Phase Equil. 298 (2010) 117–130, https://doi.org/10.1016/

j.fluid.2010.07.011.
[44] P. Brocos, A. Piñeiro, R. Bravo, A. Amigo, Refractive indices, molar volumes and molar refractions of binary liquid mixtures: concepts and correlations, Phys. Chem. Chem. Phys. 5 (2003) 550–557, https://doi.org/10.1039/B208765K.
[45] Y. Marcus, The structuredness of solvents, J. Solut. Chem. 21 (1992) 1217–1230, https://doi.org/10.1007/bf00667218.
[46] R.D. Bezman, E.F. Casassa, R.L. Kay, The temperature dependence of the dielectric constants of alkanols, J. Mol. Liq. 47-48 (1997) 397–402. https://doi.org/10.1016/S0167-7322(97) 00082–2.
[47] J. Canosa, A. Rodrıguez, J. Tojo, Binary mixture properties of diethyl ether with alcohols and alkanes from 288.15 K to 298.15 K, Fluid Phase Equil. 156 (1999) 57–71, https://doi.org/10.1016/S0378-3812(99)00032-1.
[48] G.J. Janz, R.P.T. Tomkins, Nonaqueus Electrolytes Handbook, vol. 1, Academic Press, New York, 1972.
[49] S.P. Serbanovic, M.L. Kijevcanin, I.R. Radovic, B.D. Djordjevic, Effect of temperature on the excess molar volumes of some alcohol + aromatic mixtures and modelling by cubic EOS mixing rules, Fluid Phase Equil. 239 (2006) 69–82, https://doi.org/10.1016/j.fluid.2005.10.022.
[50] S. Chen, Q. Lei, W. Fang, Density and refractive index at 298.15 K and Vapor–Liquid equilibria at 101.3 kPa for four binary systems of methanol, n-propanol, n-butanol, or isobutanol with N-Methylpiperazine, J. Chem. Eng. Data 47 (2002) 811–815, https://doi.org/10.1021/je010249b.
[51] M.I. Aralaguppi, C.V. Jadar, T.M. Aminabhavi, Density, viscosity, refractive index, and speed of sound in binary mixtures of acrylonitrile with methanol, ethanol, propan-1-ol, butan-1-ol, pentan-1-ol, hexan-1-ol, heptan-1-ol, and butan-2-ol, J. Chem. Eng. Data 44 (1999) 216–221, https://doi.org/10.1021/je9802219.
[52] R. Anwar Naushad, S. Yasmeen, Volumetric, compressibility and viscosity studies of binary mixtures of [EMIM][NTf2] with ethylacetate/methanol at (298.15–323.15) K, J. Mol. Liq. 224 (Part A) (2016) 189–200, https://doi.org/10.1016/j.molliq.2016.09.077.
[53] S.M. Pereira, T.P. Iglesias, J.L. Legido, L. Rodrıguez, J. Vijande, Changes of refractive index on mixing for the binary mixtures {xCH3OH+(1−x) CH3OCH2(CH2OCH2)3CH2OCH3} and {xCH3OH+(1−x)CH3OCH2(CH2OCH2) nCH2OCH3} (n=3–9) at temperatures from 293.15 K to 333.15 K, J. Chem. Thermodyn. 30 (1998) 1279–1287, https://doi.org/10.1006/jcht.1998.0395.
[54] A. Rodríguez, J. Canosa, J. Tojo, Density, refractive index, and speed of sound of binary mixtures (diethyl carbonate + alcohols) at several temperatures, J. Chem. Eng. Data 46 (2001) 1506–1515, https://doi.org/10.1021/je010148d.
[55] A.P. Gregory, R.N. Clarke, Traceable measurements of the static permittivity of dielectric reference liquids over the temperature range 5–50 °C, Meas. Sci. Technol. 16 (2005) 1506, https://doi.org/10.1088/0957-0233/16/7/013.
[56] M.J. Fontao, M. Iglesias, Effect of temperature on the refractive index of aliphatic hydroxilic mixtures (C2–C3), Int. J. Thermophys. 23 (2002) 513–527, https://doi.org/10.1023/A:1015113604024.
[57] J.L. Hales, J.H. Ellender, Liquid densities from 293 to 490 K of nine aliphatic alcohols, J. Chem. Thermodyn. 8 (1976) 1177–1184, https://doi.org/10.1016/0021-9614(76)90126-9.
[58] N.G. Tsierkezos, I.E. Molinou, A.C. Filippou, Thermodynamic properties of binary mixtures of cyclohexanone with n-alkanols (C1–C5) at 293.15 K, J. Solut. Chem. 34 (2005) 1371–1386, https://doi.org/10.1007/s10953-005-8508-9.
[59] C. Yang, H. Lai, Z. Liu, P. Ma, Density and viscosity of binary mixtures of diethyl carbonate with alcohols at (293.15 to 363.15) K and predictive results by UNIFAC-VISCO group contribution method, J. Chem. Eng. Data 51 (2006) 1345–1351, https://doi.org/10.1021/je0600808.
[60] C.P. Smyth, W.N. Stoops, The dielectric polarization of liquids. VI. Ethyl iodide, ethanol, normal-butanol and normal-octanol, J. Am. Chem. Soc. 51 (1929) 3312–3329, https://doi.org/10.1021/ja01386a019.
[61] B. Giner, A. Villares, M.C. López, F.M. Royo, C. Lafuente, Refractive indices and molar refractions for isomeric chlorobutanes with isomeric butanols, Phys. Chem. Liq. 43 (2005) 13–23, https://doi.org/10.1080/00319100420003035l8.
[62] E. Jiménez, M. Cabanas, L. Segade, S. Garcıa-Garabal, H. Casas, Excess volume, changes of refractive index and surface tension of binary 1,2-ethanediol + 1-propanol or 1-butanol mixtures at several temperatures, Fluid Phase Equil. 180 (2001) 151–164, https://doi.org/10.1016/S0378-3812(00)00519-7.
[63] G.A. Iglesias-Silva, A. Guzmán-López, G. Pérez-Durán, M. Ramos-Estrada, Densities and viscosities for binary liquid mixtures of n-undecane + 1-propanol, + 1-butanol, + 1-pentanol, and + 1-hexanol from 283.15 to 363.15 K at 0.1 MPa, J. Chem. Eng. Data 61 (2016) 2682–2699, https://doi.org/10.1021/acs.jced.6b00121.
[64] T.P. Iglesias, J.L. Legido, S.M. Pereira, B. de Cominges, M.I. Paz Andrade, Relative permittivities and refractive indices on mixing for (n-hexane + 1-pentanol, or 1-hexanol, or 1-heptanol) atT = 298.15 K, J. Chem. Thermodyn. 32 (2000) 923–930, https://doi.org/10.1006/jcht.2000.0661.
[65] M.N.M. Al-Hayan, Densities, excess molar volumes, and refractive indices of 1,1,2,2-tetrachloroethane and 1-alkanols binary mixtures, J. Chem. Thermodyn. 38 (2006) 427–433, https://doi.org/10.1016/j.jct.2005.06.015.
[66] S.P. Patil, A.S. Chaudhari, M.P. Lokhande, M.K. Lande, A.G. Shankarwar, S.N. Helambe, B.R. Arbad, S.C. Mehrotra, Dielectric measurements of aniline and alcohol mixtures at 283, 293, 303, and 313 K using the time domain technique, J. Chem. Eng. Data 44 (1999) 875–878, https://doi.org/10.1021/je980250j.
[67] Á. Piñeiro, P. Brocos, A. Amigo, M. Pintos, R. Bravo, Refractive indexes of binary mixtures of tetrahydrofuran with 1-alkanols at 25°C and temperature dependence of n and ρ for the pure liquids, J. Solut. Chem. 31 (2002) 369–380, https://doi.org/10.1023/A:1015807331250.
[68] J.J. Cano-Gómez, G.A. Iglesias-Silva, E.O. Castrejón-González, M. Ramos-Estrada, K.R. Hall, Density and viscosity of binary liquid mixtures of ethanol + 1-hexanol and ethanol + 1-heptanol from (293.15 to 328.15) K at 0.1 MPa, J. Chem. Eng. Data 60 (2015) 1945–1955, https://doi.org/10.1021/je501133u.
[69] U. Domańska, M. Królikowska, Density and viscosity of binary mixtures of {1-Butyl-3-methylimidazolium thiocyanate + 1-heptanol, 1-octanol, 1-nonanol, or 1-decanol}, J. Chem. Eng. Data 55 (2010) 2994–3004, https://doi.org/10.1021/je901043q.
[70] C. Wohlfahrt, Static Dielectric Constants of Pure Liquids and Binary Liquid Mixtures. Landolt-Börnstein - Group IV Physical Chemistry, vol. 6, Springer Berlin Heidelberg, Berlin, 1991.
[71] S. Otín, J. Fernández, J.M. Embid, I. Velasco, C.G. Losa, Thermodynamic, Dielectric Properties, Of binary polar + non-polar mixtures I. Static dielectric constants and excess molar enthalpies of n-alkylamine + n-dodecane systems, Ber. Bunsenges. Phys. Chem. 90 (1986) 1179–1183, https://doi.org/10.1002/bbpc.19860901212.
[72] C. Wohlfahrt, Optical Constants. Refractive Indices of Pure Liquids and Binary Liquid Mixtures. Landolt-Börnstein - Group III Condensed Matter, vol. 47, Springer Berlin Heidelberg, Berlin, 2008.
[73] Y. Miyake, A. Baylaucq, F. Plantier, D. Bessières, H. Ushiki, C. Boned, High-pressure (up to 140 MPa) density and derivative properties of some (pentyl-, hexyl-, and heptyl-) amines between (293.15 and 353.15) K, J. Chem. Thermodyn. 40 (2008) 836–845, https://doi.org/10.1016/j.jct.2008.01.006.
[74] P. Góralski, M. Wasiak, A. Bald, Heat capacities, speeds of sound, and isothermal compressibilities of some n-amines and tri-n-amines at 298.15 K, J. Chem. Eng. Data 47 (2002) 83–86, https://doi.org/10.1021/je010206v.
[75] M. El-Hefnawy, K. Sameshima, T. Matsushita, R. Tanaka, Apparent dipole moments of 1-alkanols in cyclohexane and n-heptane, and excess molar volumes of (1-alkanol + cyclohexane or n-heptane) at 298.15 K, J. Solut. Chem. 34 (2005) 43–69, https://doi.org/10.1007/s10953-005-2072-1.
[76] A.L. McClellan, Tables of Experimental Dipole Moments, Vols. 1,2,3, Rahara Enterprises, El Cerrito, US, 1974.
[77] D.R. Lide, CRC Handbook of Chemistry and Physics, 90th Edition, CRC Press/Taylor and Francis, Boca Raton, FL, 2010.
[78] F. Hevia, J.A. González, A. Cobos, I. García de la Fuente, L.F. Sanz, Thermodynamics of amide + amine mixtures. 4. Relative permittivities of N,N-dimethylacetamide + N-propylpropan-1-amine, + N-butylbutan-1-amine, + butan-1-amine, or + hexan-1-amine systems and of N,N-dimethylformamide + aniline mixture at several temperatures. Characterization of amine + amide systems using ERAS, J. Chem. Thermodyn. 118 (2018) 175–187, https://doi.org/10.1016/j.jct.2017.11.011.

Supplementary material for:

Thermodynamics of mixtures with strongly negative deviations from Raoult's law. XV. Permittivities and refractive indices for 1-alkanol + *n*-hexylamine systems at (293.15-303.15) K. Application of the Kirkwood-Fröhlich model

Fernando Hevia[(1)], Juan Antonio González[(1)]*, Ana Cobos[(1)], Isaías García de la Fuente[(1)], Cristina Alonso-Tristán[(2)]

[(1)] G.E.T.E.F., Departamento de Física Aplicada, Facultad de Ciencias, Universidad de Valladolid, Paseo de Belén, 7, 47011 Valladolid, Spain

[(2)] Unidad de Investigación Consolidada UIC-011, JCyL. Departamento de Ingeniería Electromecánica, Escuela Politécnica Superior, Universidad de Burgos. Avda. Cantabria s/n. 09006, Burgos, Spain.

*e-mail: jagl@termo.uva.es; Tel: +34 983 423757

Reference of the article:

F. Hevia, J.A. González, A. Cobos, I. García de la Fuente, C. Alonso-Tristán. Fluid Phase Equilib. **468** (2018) 18-28. https://doi.org/10.1016/j.fluid.2018.04.007

Table S1. Derivative of the excess relative permittivity of 1-alkanol (1) + *n*-hexylamine (HxA) (2) systems at pressure 0.1 MPa, temperature 298.15 K and frequency 1 MHz [a].

x_1	ϕ_1	$\left(\partial\varepsilon_r^E/\partial T\right)_p$ / K^{-1}	x_1	ϕ_1	$\left(\partial\varepsilon_r^E/\partial T\right)_p$ / K^{-1}
		methanol (1) + HxA (2)			
0.0534	0.0170	0.0008	0.6997	0.4183	–0.0136
0.0942	0.0408	0.0011	0.7995	0.5506	–0.0094
0.1871	0.0672	0.0014	0.8475	0.6314	–0.0077
0.2977	0.1199	0.0014	0.8978	0.7301	–0.0037
0.4039	0.1665	–0.0023	0.9496	0.8521	–0.0012
0.4917	0.2329	–0.0058	0.9834	0.9477	–0.0001
0.5977	0.3177	–0.0127			
		1–propanol (1) + HxA (2)			
0.0520	0.0412	0.0023	0.6040	0.4686	0.0042
0.1015	0.0635	0.0035	0.6965	0.5658	0.0016
0.1475	0.0887	0.0047	0.8013	0.6989	–0.0010
0.2108	0.1193	0.0063	0.8505	0.7486	–0.0020
0.2983	0.2001	0.0083	0.8953	0.8339	–0.0016
0.3967	0.2686	0.0088	0.9486	0.9154	–0.0013
0.4998	0.3660	0.0072			
		1–butanol (1) + HxA (2)			
0.0552	0.0358	0.0022	0.6004	0.5016	0.0132
0.0896	0.0690	0.0048	0.6977	0.6152	0.0106
0.1588	0.1012	0.0064	0.7982	0.7400	0.0062
0.1967	0.1514	0.0096	0.8451	0.7997	0.0041
0.3035	0.2364	0.0127	0.8996	0.8661	0.0024
0.4077	0.3206	0.0149	0.9461	0.9237	0.0010
0.4984	0.4138	0.0150			
		1–pentanol (1) + HxA (2)			
0.0472	0.0429	0.0028	0.6005	0.5519	0.0194
0.1005	0.0899	0.0062	0.7122	0.6468	0.0174
0.1648	0.1347	0.0090	0.7963	0.7602	0.0135
0.2022	0.1708	0.0113	0.8457	0.8104	0.0108
0.3102	0.2684	0.0157	0.8982	0.8809	0.0071
0.3982	0.3508	0.0188	0.9362	0.9312	0.0036
0.5002	0.4526	0.0208			
		1–heptanol (1) + HxA (2)			
0.0560	0.0534	0.0031	0.6020	0.6188	0.0280
0.1018	0.1006	0.0064	0.7029	0.7133	0.0261
0.1463	0.1694	0.0105	0.7979	0.8107	0.0219
0.2047	0.2180	0.0138	0.8534	0.8603	0.0183
0.3044	0.3205	0.0198	0.8986	0.8965	0.014
0.4059	0.4193	0.0239	0.9472	0.9437	0.0087
0.5044	0.5151	0.0266			

[a] The standard uncertainties are: $u(T) = 0.02$ K; $u(p) = 1$ kPa; $u(\nu) = 20$ Hz; $u(x_1) = 0.0010$; $u(\phi_1) = 0.004$; $u\left[\left(\partial\varepsilon_r^E/\partial T\right)_p\right] = 0.0008$ K^{-1}.

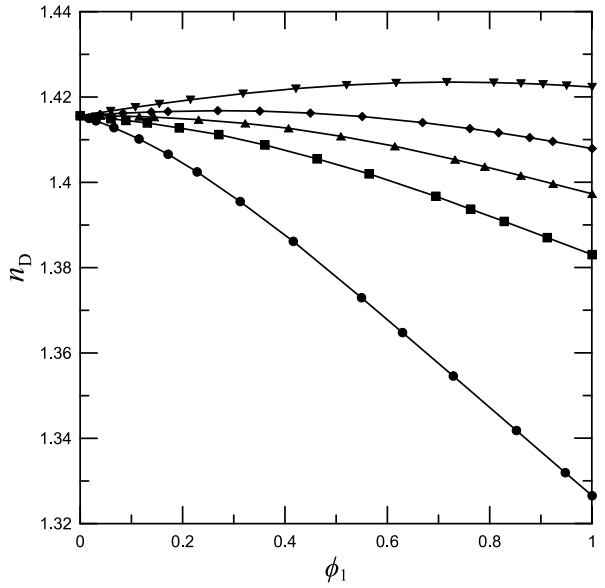

Figure S1: Refractive index at the sodium D line, n_D, of 1-alkanol (1) + HxA (2) systems at pressure 0.1 MPa and temperature 298.15 K. Full symbols, experimental values (this work): (●), methanol; (■), 1-propanol; (▲), 1-butanol; (♦), 1-pentanol; (▼), 1-heptanol.

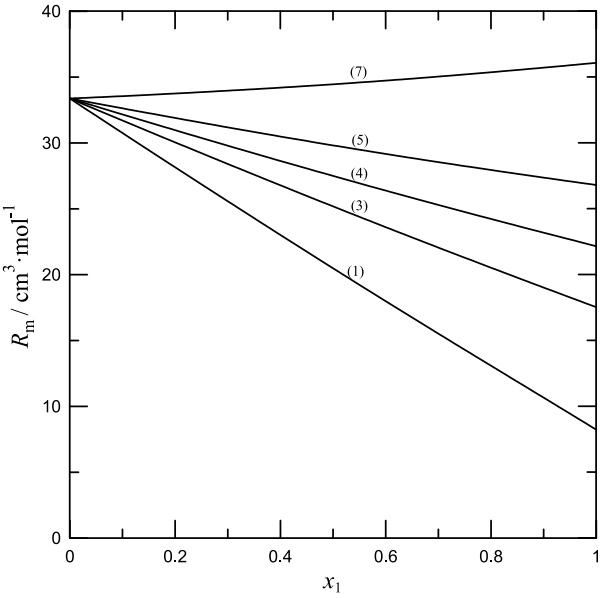

Figure S2: Molar refraction of 1-alkanol (1) + HxA (2) systems at pressure 0.1 MPa and temperature 298.15 K. Numbers in parentheses indicate the number of atoms of the 1-alkanol.

Journal of Molecular Liquids 271 (2018) 704–714

Contents lists available at ScienceDirect

Journal of Molecular Liquids

journal homepage: www.elsevier.com/locate/molliq

Thermodynamics of mixtures with strongly negative deviations from Raoult's law. XVI. Permittivities and refractive indices for 1-alkanol + di-*n*-propylamine systems at (293.15–303.15) K. Application of the Kirkwood-Fröhlich model

Fernando Hevia, Ana Cobos, Juan Antonio González *, Isaías García de la Fuente, Luis Felipe Sanz

G.E.T.E.F., Departamento de Física Aplicada, Facultad de Ciencias, Universidad de Valladolid, Paseo de Belén, 7, 47011 Valladolid, Spain

ARTICLE INFO

Article history:
Received 28 June 2018
Received in revised form 5 September 2018
Accepted 8 September 2018
Available online 13 September 2018

Keywords:
1-alkanol
di-*n*-propylamine
Permittivity
Refractive index
Kirkwood correlation factor

ABSTRACT

Relative permittivities at 1 MHz, ε_r, and refractive indices at the sodium D-line, n_D, are reported at 0.1 MPa and at (293.15–303.15) K for the binary systems 1-alkanol + di-*n*-propylamine (DPA). Their corresponding excess functions are calculated and correlated. For the methanol mixture, positive values of the excess permittivities, ε_r^E, are found. Except at high concentrations of the alcohol in the 1-propanol mixture, the remaining systems show negative values of this property. This fact reveals that the creation of (1-alkanol)-DPA interactions contributes positively to ε_r^E, being this contribution dominant in the methanol mixture. The negative contributions arising from the disruption of interactions between like molecules are prevalent in the other mixtures. At ϕ_1 (volume fraction) = 0.5, ε_r^E changes in the sequence: methanol > 1-propanol > 1-butanol > 1-pentanol < 1-heptanol. An analogous variation with the chain length of the 1-alkanol is observed in mixtures such as 1-alkanol + heptane, +cyclohexylamine or +*n*-hexylamine (HxA). Moreover, for a given 1-alkanol, ε_r^E is larger for DPA than for HxA mixtures, suggesting that in DPA solutions multimers with parallel alignment of the molecular dipoles are favoured and cyclic multimers are disfavoured when compared to HxA mixtures. The $(\partial\varepsilon_r/\partial T)_p$ values are higher for the mixtures than for pure 1-alkanols, because (1-alkanol)-DPA interactions are stronger than those between 1-alkanol molecules. Calculations on molar refractions indicate that dispersive interactions in the systems under study increase with the chain length of the 1-alkanol and are practically identical to those in HxA solutions. The considered mixtures are treated by means of the Kirkwood-Fröhlich model, reporting the Kirkwood correlation factors and their excess values.

1. Introduction

Amines are found in situations of biological interest. For instance, the breaking of amino acids releases amines and proteins that are usually bound to DNA polymers contain several amine groups [1]. Their low vapour pressure makes them useful in green chemistry. Mixtures containing amines are being investigated to be used in CO_2 capture [2]. On the other hand, many of the ions of the technically important ionic liquids are related to amine groups [3]. Linear primary and secondary amines are weakly self-associated compounds [4–8] with rather low dipole moments. Liquid mixtures formed by 1-alkanol and a linear primary or secondary amine are rather interesting from a theoretical point of view, as they show strongly negative deviations from Raoult's law. In fact, the excess molar Gibbs energies, G_m^E, at x_1 (mole fraction) = 0.5 for methanol systems are: −823 J·mol^{-1} (di-*n*-ethylamine; T = 298.15 K [9]) and −799 J·mol^{-1} (*n*-butylamine, T = 348.15 K [10]). Accordingly, the excess molar enthalpies (H_m^E) are large and negative. For instance, at 298.15 K and x_1 = 0.5; H_m^E (methanol)/J·mol^{-1} = −3200 (*n*-hexylamine (HxA)) [11]; −4581 (di-*n*-ethylamine) [12]. This has been explained in terms of two different opposing effects. In the pure liquid state, both 1-alkanols and linear amines are self-associated by means of O-—H—O and N-—H—N bonds, respectively. Such bonds are disrupted along the mixing process, which positively contribute to H_m^E. On the other hand, it is well known that the formation of interactions between unlike molecules upon mixing contributes negatively to H_m^E. Therefore, the large and negative H_m^E values of this type of systems reveal that the new O-—H—N bonds created are stronger than the O-—H—O and N-—H—N bonds. For instance, the values of the enthalpy of the hydrogen bonds between methanol and amine estimated from the application of the ERAS model [13] are: −42.4 kJ·mol^{-1} (*n*-hexylamine) [7]; −45.4 kJ·mol^{-1} (di-*n*-ethylamine) [14]. We remark that such values are much more negative than that used, within this model, for the enthalpy of the H bonds between alkanol molecules,

* Corresponding author.
E-mail address: jagl@termo.uva.es (J.A. González).

https://doi.org/10.1016/j.molliq.2018.09.040
0167-7322/

−25.1 kJ·mol^{-1} [7,13,14]. As a consequence of the strong interactions between unlike molecules, the systems are highly structured. For example, at $T = 298.15$ K and $x_1 = 0.5$, TS_m^E ($=H_m^E - G_m^E$) is −3758 J·mol^{-1} for the methanol + di-*n*-ethylamine mixture (see above). This result is much more negative than the value for the 1-propanol + hexane system, $TS_m^E = (533\ (=H_m^E) - 1295\ (=G_m^E)) = -762$ J·mol^{-1} [15,16]. The large and negative excess molar volumes [7,17–21] and solid-liquid equilibria (SLE) measurements [22] also support the existence of strong interactions between unlike molecules in 1-alkanol + linear amine mixtures. It is to be noted that the SLE phase diagrams show that complex formation is an important feature of these solutions [22]. In addition, ε_r^E values also indicate strong interactions between unlike molecules in 1-alkanol + linear primary amine systems; e.g. for the methanol + HxA mixture [23] $\varepsilon_r^E = 1.480$ at $T = 298.15$ K and ϕ_1 (volume fraction) = 0.5.

We have extended the database of 1-alkanol + amine mixtures reporting excess molar volumes [7,17–21]; dynamic viscosities [19–21]; vapour-liquid equilibria [24]; permittivities (ε_r) and refractive indices (n_D) [19–21,25]. In addition, these systems have been investigated using different models as DISQUAC or ERAS [6,7,14,17,18,20,26–28]; the formalism of the Kirkwood-Buff integrals [29], or the concentration-concentration structure factor ($S_{CC}(0)$) formalism [30]. More recently [23], we have provided ε_r and n_D data for the 1-alkanol + HxA mixtures over the temperature range (293.15–303.15) K, and analysed them using the Kirkwood-Fröhlich model [31–34], which is a useful approach to gain insight into the structure and interactions of mixtures. As a continuation, and in order to investigate the effect of replacing a linear primary amine (HxA) by a linear secondary amine (di-*n*-propylamine, (DPA)), we report similar measurements over the same range of temperature for mixtures formed by the latter amine and methanol, or 1-propanol, or 1-butanol, or 1-pentanol or 1-heptanol. In addition, the systems are also studied by means of Kirkwood-Fröhlich model.

2. Experimental

2.1. Materials

Information about the purity and source of the pure compounds, which were used in the experiments without further purification, is collected in Table 1. Their ε_r values at 1 MHz, densities (ρ) and n_D values at 0.1 MPa and at the working temperatures can be found in Table 2. These results agree well with literature data.

2.2. Apparatus and procedure

Binary mixtures were prepared by mass in small vessels of about 10 cm^3 with the aid of an analytical balance Sartorius MSU125p (weighing accuracy 0.01 mg), taking into account the corresponding corrections on buoyancy effects. The standard uncertainty in the final mole fraction is 0.0010. Molar quantities were calculated using the relative atomic mass Table of 2015 issued by the Commission on Isotopic Abundances and Atomic Weights (IUPAC) [35]. In order to minimize the effects of the interaction of the compounds with air components, they were stored with 4 Å molecular sieves (except methanol, because measurements were affected). In addition, the measurement cell (see below) was completely filled with the samples and appropriately closed. Different density measurements of pure compounds, conducted along experiments, showed that this quantity remained unchanged within the experimental uncertainty.

Temperatures were measured with Pt-100 resistances, calibrated according to the ITS-90 scale of temperature, against the triple point of water and the fusion point of Ga. The standard uncertainty of this quantity is 0.01 K for ρ determinations, and 0.02 K for ε_r and n_D measurements.

The ε_r measurements were performed with the aid of an equipment from Agilent. A 16452A cell, which is a parallel-plate capacitor made of Nickel-plated cobalt (54% Fe, 17% Co, 29% Ni) with a ceramic insulator (alumina, Al_2O_3), is filled with a sample volume of ≈4.8 cm^3. The cell is connected by a 16048G test lead to a precision impedance analyzer 4294A, and immersed in a thermostatic bath LAUDA RE304, with a temperature stability of 0.02 K. Details about the device configuration and calibration are given elsewhere [36]. The relative standard uncertainty of the ε_r measurements (i.e. the repeatability) is 0.0001. The total relative standard uncertainty of ε_r was estimated to be 0.003 from the differences between our data and values available in the literature, in the range of temperature (288.15–333.15) K, for the following pure liquids: water, benzene, cyclohexane, hexane, nonane, decane, dimethyl carbonate, diethyl carbonate, methanol, 1-propanol, 1-pentanol, 1-hexanol, 1-heptanol, 1-octanol, 1-nonanol and 1-decanol.

A Bellingham + Stanley RFM970 refractometer was used for the n_D measurements. The technique is based on the optical detection of the critical angle at the wavelength of the sodium D line (589.3 nm). The temperature is controlled by Peltier modules and its stability is 0.02 K. The refractometer has been calibrated using 2,2,4-trimethylpentane and toluene at (293.15–303.15) K, following the recommendations by Marsh [37]. The standard uncertainty of n_D is 0.00008.

Densities were obtained using a vibrating-tube densimeter and sound analyzer Anton Paar DSA5000, which is automatically thermostated within 0.01 K. The calibration procedure has been described elsewhere [38]. The relative standard uncertainty of the ρ measurements is 0.0012.

Table 1
Sample description.

Chemical name	CAS number	Source	Purification method	Purity[a]
Methanol	67-56-1	Sigma-Aldrich	None	99.99%
1-propanol	71-23-8	Sigma-Aldrich	None	99.84%
1-butanol	71-36-3	Sigma-Aldrich	None	99.86%
1-pentanol	71-41-0	Sigma-Aldrich	None	99.9%
1-heptanol	111-70-6	Sigma-Aldrich	None	99.9%
Di-*n*-propylamine (DPA)	111-26-2	Aldrich	None	99.9%

[a] In mole fraction. By gas chromatography. Provided by the supplier.

3. Results

Let us denote by x_i the mole fraction of component *i*. The corresponding volume fraction, ϕ_i, is given by $\phi_i = x_i V_{mi}^*/(x_1 V_{m1}^* + x_2 V_{m2}^*)$, where V_{mi}^* stands for the molar volume of component *i*. For an ideal mixture at the same temperature and pressure as the mixture under study, the relative permittivity, ε_r^{id}, the derivative $[(\partial\varepsilon_r/\partial T)_p]^{id}$, and the refractive index, n_D^{id}, are given by [39,40]:

$$\varepsilon_r^{id} = \phi_1 \varepsilon_{r1}^* + \phi_2 \varepsilon_{r2}^* \tag{1}$$

$$n_D^{id} = \left[\phi_1 (n_{D1}^*)^2 + \phi_2 (n_{D2}^*)^2\right]^{1/2} \tag{2}$$

$$\left[\left(\frac{\partial \varepsilon_r}{\partial T}\right)_p\right]^{id} = \left(\frac{\partial \varepsilon_r^{id}}{\partial T}\right)_p \tag{3}$$

where ε_{ri}^* and n_{Di}^* denote the relative permittivity and the refractive index of pure species *i*, and $(\partial\varepsilon_r^{id}/\partial T)_p$ is calculated from linear regressions as indicated below. The corresponding excess functions, F^E, are obtained as

$$F^E = F - F^{id} \quad , \quad F = \varepsilon_r, n_D, \left(\frac{\partial \varepsilon_r}{\partial T}\right)_p \tag{4}$$

Table 2
Dipole moment, μ, of the pure compounds, and their relative permittivity at frequency $\nu = 1$ MHz, ε_r^*, refractive index, n_D^* and density, ρ^*, at temperature T and pressure $p = 0.1$ MPa.[a]

Compound	μ/D	T/K	ε_r^*		n_D^*		ρ^*/g · cm^{-3}	
			Exp.	Lit.	Exp.	Lit.	Exp.	Lit.
Methanol	1.664 [57]	293.15	33.569	33.61 [58]	1.32878	1.32859 [59]	0.79163	0.7916 [60] 0.791400 [61]
		298.15	32.619	32.62 [58]	1.32667	1.3267 [62] 1.32652 [63]	0.78695	0.7869 [64] 0.786884 [65]
		303.15	31.652	31.66 [58]	1.32457	1.32457 [66] 1.32410 [67]	0.78222	0.782158 [65]
1-propanol	1.629 [57]	293.15	21.146	21.15 [68]	1.38505	1.38512 [69]	0.80366	0.80361 [70]
		298.15	20.450	20.42 [68]	1.38304	1.38307 [67]	0.79968	0.79960 [70]
		303.15	19.788	19.75 [68]	1.38100	1.38104 [67]	0.79566	0.79561 [70]
1-butanol	1.614 [57]	293.15	18.198	18.19 [68]	1.39925	1.3993 [71]	0.80985	0.80982 [72] 0.8098 [73]
		298.15	17.548	17.53 [68]	1.39732	1.397336 [74]	0.80606	0.80606 [72]
		303.15	16.927	16.89 [68]	1.39536	1.3953 [75]	0.80222	0.8022 [73]
1-pentanol	1.598 [57]	293.15	15.695	15.63 [58]	1.40992	1.40986 [67]	0.81466	0.81468 [76]
		298.15	15.099	15.08 [77]	1.40796	1.40789 [67]	0.81103	0.81103 [76]
		303.15	14.523	14.44 [58]	1.40603	1.40592 [78]	0.80735	0.81737 [76]
1-heptanol	1.583 [57]	293.15	12.016	11.54 [79]	1.42422	1.42433 [80]	0.82237	0.8223 [81]
		298.15	11.506	11.45 [77]	1.42234	1.42240 [80]	0.81890	0.81881 [82]
		303.15	11.021	11.07 [47]	1.42048	1.42047 [78] 1.42048 [80]	0.81537	0.8153 [81]
Di-*n*-propylamine (DPA)	1.1 [83]	293.15	3.130	3.31 [84] 3.068 [45]	1.40417	1.4043 [45]	0.737782	0.7375 [45]
		298.15	3.080	3.24 [84]	1.40154	1.40132 [85]	0.733220	0.73321 [50]
		303.15	3.032	3.18 [84]	1.39890	1.4022 [86]	0.728698	0.729087 [87]

[a] The standard uncertainties are: $u(T) = 0.02$ K (for ρ^* measurements, $u(T) = 0.01$ K); $u(p) = 1$ kPa; $u(\nu) = 20$ Hz; $u(n_D^*) = 0.00008$. The relative standard uncertainties are: $u_r(\rho^*) = 0.0012$, $u_r(\varepsilon_r^*) = 0.003$.

Table 3 lists ϕ_1, ε_r and ε_r^E values of 1-alkanol (1) + DPA (2) systems as functions of x_1, in the temperature range (293.15–303.15) K. Table 4 contains the experimental x_1, ϕ_1, n_D and n_D^E values.

We calculated the derivative $(\partial\varepsilon_r/\partial T)_p$ at 298.15 K as the slope of a linear regression of experimental ε_r values in the range (293.15–303.15) K. The data of $[(\partial\varepsilon_r/\partial T)_p]^E = (\partial\varepsilon_r^E/\partial T)_p$ are collected in Table S1 (supplementary material).

The F^E data were fitted to a Redlich-Kister equation [41] by unweighted linear least-squares regressions:

$$F^E = x_1(1-x_1)\sum_{i=0}^{k-1} A_i(2x_1-1)^i \tag{5}$$

The number, k, of necessary coefficients for this regression has been determined, for each system and temperature, by applying an F-test of additional term [42] at a 99.5% confidence level. Table 5 includes the parameters A_i obtained, and the standard deviations $\sigma(F^E)$, defined by:

$$\sigma\left(F^E\right) = \left[\frac{1}{N-k}\sum_{j=1}^{N}\left(F^E_{cal,j} - F^E_{exp,j}\right)^2\right]^{1/2} \tag{6}$$

where the index j takes one value for each of the N experimental data $F^E_{exp,j}$, and $F^E_{cal,j}$ is the corresponding value of the excess property F^E calculated from Eq. (5).

Values of ε_r^E, n_D^E and $(\partial\varepsilon_r^E/\partial T)_p$ versus ϕ_1 of 1-alkanol + DPA systems at 298.15 K are plotted in Figs. 1, 2 and 3 respectively with their corresponding Redlich-Kister regressions. Data on n_D are plotted in Fig. S1 (supplementary material).

4. Discussion

Unless stated otherwise, the below values of the thermophysical properties and their corresponding excess functions are referred to $T = 298.15$ K and $\phi_1 = 0.5$. We will denote by n the number of C atoms of the 1-alkanol.

4.1. Excess relative permittivities

It is known that the breaking of interactions between like molecules in the mixing process leads to a negative contribution to ε_r^E. On the other hand, the creation of interactions between molecules of different species can lead to either a positive or to a negative contribution to ε_r^E, depending on the capability of the multimers formed to respond to an external electric field and lead to a macroscopic dipole moment. For instance, 1-alkanol + heptane mixtures show rather large and negative values of this quantity, which can be ascribed to the breaking of the 1-alkanol self-association (Fig. 4): $\varepsilon_r^E = -1.075$ ($n = 3$), -2.225 ($n = 4$), -2.525 ($n = 5$), -2.875 ($n = 7$), -1.775 ($n = 10$) [20,43–45]. For methanol, there exists a partial immiscibility region [46]. The corresponding ε_r^E values of 1-alkanol + DPA systems are higher: 2.406 ($n = 1$), -0.246 ($n = 3$), -0.715 ($n = 4$), -0.883 ($n = 5$), -0.747 ($n = 7$) (Fig. 4). This reveals that alkanol-amine interactions contribute positively to the polarization of the mixture. The positive ε_r^E result for the methanol + DPA system strongly confirms this conclusion. 1-Alkanol + cyclohexylamine [21,25], or +HxA [23] mixtures behave similarly and also show higher ε_r^E values than those of 1-alkanol + heptane systems (Fig. 4). On the other hand, the $\varepsilon_r^E(n)$ variation for 1-alkanol + DPA, or +cyclohexylamine, or +HxA mixtures follows the sequence: methanol > 1-propanol > 1-butanol > 1-pentanol < 1-heptanol (Fig. 4), which is similar to that encountered for 1-alkanol + heptane mixtures (see above, Fig. 4). For the latter systems, it has been explained in terms of the lower and weaker self-association of longer 1-alkanols [25]. For amine systems, this statement is still valid, but interactions between unlike molecules must be also considered. Studies on 1-alkanol + amine mixtures using the ERAS model show that solvation effects between unlike molecules decrease when the alkanol size is increased [7,17,18]. This means that the polarization changes, along the mixing process, to a lower extent when longer 1-alkanols are involved, since these alcohols are less self-associated and the corresponding solvation effects are also less important. It is to be noted that ε_r^E changes more sharply when increasing n for mixtures with shorter 1-alkanols than for systems involving longer 1-alkanols, and that the same occurs for the excess molar volumes and for the excess molar enthalpies [17].

Table 3
Volume fractions of 1-alkanol, ϕ_1, relative permittivities, ε_r,and excess relative permittivities, ε_r^E, of 1-alkanol (1) + di-*n*-propylamine (DPA) (2) mixtures as functions of the mole fraction of the 1-alkanol, x_1, at temperature T, pressure $p = 0.1$ MPa and frequency $\nu = 1$ MHz.[a]

x_1	ϕ_1	ε_r	ε_r^E	x_1	ϕ_1	ε_r	ε_r^E
Methanol (1) + DPA (2); T/K = 293.15							
0.0000	0.0000	3.131		0.5940	0.3016	14.249	1.938
0.0664	0.0206	3.698	−0.060	0.6918	0.3985	17.679	2.418
0.1066	0.0340	4.093	−0.073	0.7948	0.5334	21.905	2.538
0.1503	0.0496	4.582	−0.059	0.8492	0.6243	24.438	2.305
0.1990	0.0683	5.201	−0.009	0.9012	0.7291	27.148	1.825
0.3091	0.1166	6.956	0.276	0.9498	0.8481	30.041	1.096
0.4068	0.1683	8.965	0.711	0.9749	0.9198	31.723	0.595
0.5110	0.2357	11.698	1.393	1.0000	1.0000	33.569	
Methanol (1) + DPA (2); T/K = 298.15							
0.0000	0.0000	3.081		0.5940	0.3015	13.735	1.748
0.0664	0.0206	3.620	−0.069	0.6918	0.3984	17.081	2.232
0.1066	0.0340	3.998	−0.087	0.7948	0.5333	21.229	2.395
0.1503	0.0496	4.466	−0.080	0.8492	0.6243	23.704	2.182
0.1990	0.0683	5.054	−0.044	0.9012	0.7291	26.354	1.737
0.3091	0.1166	6.725	0.200	0.9498	0.8481	29.179	1.047
0.4068	0.1683	8.641	0.589	0.9749	0.9197	30.817	0.570
0.5110	0.2357	11.261	1.218	1.0000	1.0000	32.619	
Methanol (1) + DPA (2); T/K = 303.15							
0.0000	0.0000	3.035		0.5940	0.3015	13.252	1.589
0.0664	0.0205	3.552	−0.070	0.6918	0.3984	16.517	2.081
0.1066	0.0340	3.913	−0.095	0.7948	0.5333	20.583	2.287
0.1503	0.0496	4.357	−0.097	0.8492	0.6242	22.980	2.082
0.1990	0.0683	4.920	−0.070	0.9012	0.7290	25.562	1.665
0.3091	0.1166	6.514	0.142	0.9498	0.8481	28.312	1.007
0.4068	0.1683	8.346	0.495	0.9749	0.9197	29.903	0.549
0.5110	0.2356	10.861	1.084	1.0000	1.0000	31.652	
1-propanol (1) + DPA (2); T/K = 293.15							
0.0000	0.0000	3.130		0.5948	0.4445	10.847	−0.291
0.0638	0.0358	3.573	−0.202	0.7018	0.5620	13.243	−0.012
0.0866	0.0492	3.743	−0.273	0.7967	0.6812	15.546	0.144
0.1427	0.0832	4.207	−0.422	0.8431	0.7455	16.741	0.180
0.2045	0.1229	4.789	−0.555	0.8993	0.8296	18.256	0.180
0.2917	0.1834	5.761	−0.673	0.9487	0.9098	19.647	0.126
0.3939	0.2616	7.178	−0.665	1.0000	1.0000	21.146	
0.5012	0.3539	8.988	−0.518				
1-propanol (1) + DPA (2); T/K = 298.15							
0.0000	0.0000	3.080		0.5948	0.4442	10.419	−0.377
0.0638	0.0358	3.501	−0.201	0.7018	0.5617	12.739	−0.098
0.0866	0.0491	3.665	−0.268	0.7967	0.6809	14.969	0.062
0.1427	0.0831	4.108	−0.415	0.8431	0.7453	16.134	0.108
0.2045	0.1228	4.660	−0.553	0.8993	0.8294	17.623	0.136
0.2917	0.1832	5.580	−0.682	0.9487	0.9097	18.987	0.106
0.3939	0.2614	6.929	−0.692	1.0000	1.0000	20.450	
0.5012	0.3536	8.647	−0.575				
1-propanol (1) + DPA (2); T/K = 303.15							
0.0000	0.0000	3.032		0.5948	0.4440	10.029	−0.443
0.0638	0.0357	3.439	−0.191	0.7018	0.5614	12.260	−0.179
0.0866	0.0490	3.593	−0.260	0.7967	0.6807	14.433	−0.005
0.1427	0.0830	4.016	−0.407	0.8431	0.7451	15.567	0.050
0.2045	0.1227	4.540	−0.548	0.8993	0.8293	17.021	0.093
0.2917	0.1830	5.417	−0.681	0.9487	0.9096	18.361	0.088
0.3939	0.2612	6.698	−0.711	1.0000	1.0000	19.788	
0.5012	0.3534	8.331	−0.623				
1-butanol (1) + DPA (2); T/K = 293.15							
0.0000	0.0000	3.132		0.5991	0.4993	9.972	−0.682
0.0484	0.0328	3.455	−0.171	0.6896	0.5972	11.635	−0.494
0.1063	0.0735	3.872	−0.367	0.7484	0.6650	12.765	−0.386
0.1418	0.0993	4.146	−0.482	0.8041	0.7326	13.891	−0.278
0.2157	0.1551	4.788	−0.681	0.8418	0.7803	14.686	−0.202
0.3006	0.2229	5.660	−0.830	0.8890	0.8424	15.681	−0.143
0.4064	0.3136	6.961	−0.896	0.9514	0.9289	17.070	−0.057
0.5030	0.4031	8.373	−0.832	1.0000	1.0000	18.198	
1-butanol (1) + DPA (2); T/K = 298.15							
0.0000	0.0000	3.082		0.5991	0.4989	9.580	−0.719
0.0484	0.0328	3.391	−0.165	0.6896	0.5968	11.179	−0.536
0.1063	0.0734	3.786	−0.358	0.7484	0.6646	12.268	−0.428
0.1418	0.0992	4.049	−0.468	0.8041	0.7323	13.368	−0.307
0.2157	0.1549	4.659	−0.664	0.8418	0.7800	14.125	−0.240
0.3006	0.2226	5.486	−0.816	0.8890	0.8422	15.113	−0.152
0.4064	0.3133	6.718	−0.896	0.9514	0.9288	16.455	−0.063
0.5030	0.4028	8.057	−0.852	1.0000	1.0000	17.548	
1-butanol (1) + DPA (2); T/K = 303.15							
0.0000	0.0000	3.036		0.5991	0.4986	9.223	−0.739
0.0484	0.0327	3.330	−0.160	0.6896	0.5965	10.738	−0.584
0.1063	0.0733	3.710	−0.344	0.7484	0.6643	11.811	−0.453
0.1418	0.0990	3.961	−0.450	0.8041	0.7320	12.869	−0.335
0.2157	0.1547	4.543	−0.642	0.8418	0.7798	13.609	−0.259
0.3006	0.2224	5.329	−0.796	0.8890	0.8420	14.568	−0.164
0.4064	0.3130	6.497	−0.887	0.9514	0.9287	15.872	−0.065
0.5030	0.4024	7.770	−0.856	1.0000	1.0000	16.927	
1-pentanol (1) + DPA (2); T/K = 293.15							
0.0000	0.0000	3.130		0.5985	0.5404	9.078	−0.842
0.0530	0.0423	3.469	−0.192	0.6570	0.6018	9.926	−0.766
0.1086	0.0877	3.850	−0.382	0.6985	0.6464	10.555	−0.697
0.1497	0.1220	4.157	−0.506	0.7450	0.6974	11.282	−0.611
0.2032	0.1675	4.581	−0.654	0.7921	0.7504	12.039	−0.520
0.2597	0.2168	5.076	−0.778	0.8447	0.8110	12.918	−0.402
0.3006	0.2532	5.461	−0.850	0.9027	0.8798	13.918	−0.267
0.4064	0.3507	6.590	−0.947	0.9435	0.9294	14.657	−0.151
0.4882	0.4294	7.589	−0.936	1.0000	1.0000	15.695	
0.5421	0.4829	8.290	−0.908				
1-pentanol (1) + DPA (2); T/K = 298.15							
0.0000	0.0000	3.077		0.5985	0.5400	8.729	−0.840
0.0530	0.0422	3.402	−0.182	0.6570	0.6014	9.540	−0.767
0.1086	0.0875	3.767	−0.362	0.6985	0.6460	10.144	−0.699
0.1497	0.1218	4.062	−0.479	0.7450	0.6970	10.849	−0.607
0.2032	0.1672	4.465	−0.622	0.7921	0.7500	11.574	−0.519
0.2597	0.2165	4.935	−0.745	0.8447	0.8107	12.421	−0.402
0.3006	0.2529	5.303	−0.814	0.9027	0.8796	13.397	−0.255
0.4064	0.3503	6.367	−0.921	0.9435	0.9293	14.100	−0.149
0.4882	0.4290	7.316	−0.918	1.0000	1.0000	15.099	
0.5421	0.4825	7.978	−0.900				
1-pentanol (1) + DPA (2); T/K = 303.15							
0.0000	0.0000	3.031		0.5985	0.5396	8.413	−0.819
0.0530	0.0421	3.342	−0.173	0.6570	0.6010	9.187	−0.751
0.1086	0.0874	3.692	−0.343	0.6985	0.6456	9.765	−0.685
0.1497	0.1216	3.972	−0.456	0.7450	0.6967	10.436	−0.601
0.2032	0.1670	4.357	−0.593	0.7921	0.7497	11.139	−0.508
0.2597	0.2162	4.805	−0.711	0.8447	0.8105	11.962	−0.383
0.3006	0.2526	5.156	−0.778	0.9027	0.8794	12.894	−0.243
0.4064	0.3499	6.167	−0.885	0.9435	0.9292	13.570	−0.139
0.4882	0.4286	7.063	−0.893	1.0000	1.0000	14.523	
0.5421	0.4821	7.695	−0.876				
1-heptanol (1) + DPA (2); T/K = 293.15							
0.0000	0.0000	3.131		0.5883	0.5955	7.677	−0.745
0.0529	0.0544	3.454	−0.160	0.6378	0.6446	8.154	−0.704
0.1003	0.1030	3.745	−0.301	0.6965	0.7028	8.735	−0.640
0.1474	0.1512	4.050	−0.424	0.7424	0.7481	9.197	−0.581
0.1990	0.2038	4.401	−0.541	0.7892	0.7941	9.687	−0.500
0.2471	0.2527	4.748	−0.628	0.8426	0.8465	10.250	−0.402
0.2924	0.2986	5.083	−0.701	0.8913	0.8941	10.777	−0.298
0.3427	0.3494	5.485	−0.750	0.9395	0.9412	11.325	−0.169
0.3943	0.4014	5.915	−0.782	1.0000	1.0000	12.016	
0.4929	0.5003	6.783	−0.793				
1-heptanol (1) + DPA (2); T/K = 298.15							
0.0000	0.0000	3.080		0.5883	0.5950	7.390	−0.703
0.0529	0.0543	3.389	−0.149	0.6378	0.6442	7.847	−0.661
0.1003	0.1028	3.669	−0.277	0.6965	0.7023	8.397	−0.601
0.1474	0.1509	3.957	−0.394	0.7424	0.7477	8.837	−0.543
0.1990	0.2035	4.295	−0.500	0.7892	0.7938	9.307	−0.462
0.2471	0.2523	4.626	−0.580	0.8426	0.8463	9.838	−0.373
0.2924	0.2982	4.941	−0.652	0.8913	0.8940	10.344	−0.269
0.3427	0.3490	5.325	−0.696	0.9395	0.9411	10.854	−0.156
0.3943	0.4010	5.728	−0.731	1.0000	1.0000	11.506	
0.4929	0.4998	6.547	−0.744				
1-heptanol (1) + DPA (2); T/K = 303.15							
0.0000	0.0000	3.033		0.5883	0.5946	7.128	−0.655

Table 3 (*continued*)

x_1	ϕ_1	ε_r	ε_r^E	x_1	ϕ_1	ε_r	ε_r^E
0.0529	0.0542	3.329	−0.137	0.6378	0.6438	7.565	−0.611
0.1003	0.1027	3.597	−0.256	0.6965	0.7020	8.086	−0.555
0.1474	0.1507	3.876	−0.361	0.7424	0.7473	8.497	−0.505
0.1990	0.2032	4.196	−0.460	0.7892	0.7935	8.956	−0.415
0.2471	0.2520	4.512	−0.534	0.8426	0.8460	9.459	−0.332
0.2924	0.2978	4.812	−0.600	0.8913	0.8938	9.923	−0.250
0.3427	0.3486	5.177	−0.641	0.9395	0.9410	10.415	−0.135
0.3943	0.4005	5.558	−0.674	1.0000	1.0000	11.021	
0.4929	0.4994	6.334	−0.688				

[a] The standard uncertainties are: $u(T) = 0.02$ K; $u(p) = 1$ kPa; $u(v) = 20$ Hz; $u(x_1) = 0.0010$; $u(\phi_1) = 0.004$. The relative standard uncertainty is: $u_r(\varepsilon_r) = 0.003$; and the relative combined expanded uncertainty (0.95 level of confidence) is $U_{rc}(\varepsilon_r^E) = 0.03$.

Interestingly, for a given 1-alkanol, say 1-butanol, ε_r^E (DPA) = −0.715 > ε_r^E (HxA) = −1.424 [15] (Fig. 4). This suggests that in DPA solutions multimers with parallel alignment of the molecular dipoles are favoured and cyclic multimers are disfavoured when compared to HxA mixtures. Furthermore, at $\phi_1 = 0.47$, the 1-butanol + di-*n*-ethylamine mixture [47] shows an even higher value (−0.13), which can be explained by the formation of more and stronger H bonds between unlike molecules, because the amine group is less sterically hindered in this amine.

It may be pertinent to compare the dielectric behaviour of mixtures formed by 1-alkanol and DPA or di-*n*-propylether (DPE), as both solvents have similar size and structure. It is well known that the thermodynamic properties of the DPE systems are mainly characterized by the alkanol self-association [48]. Thus, the H_m^E values are moderately positive (H_m^E/J·mol^{-1} = 740 for the 1-propanol system [49]); remain nearly constant for mixtures involving the longer 1-alkanols, and the corresponding H_m^E curves are shifted towards low mole fractions of the 1-alkanol [48]. In contrast, as it has been previously mentioned, solvation, i.e. strong interactions between unlike molecules, is the main feature of 1-alkanol + DPA mixtures [14]. This is clearly demonstrated by the large and negative H_m^E values of these systems (−2432 J·mol^{-1} for the 1-butanol solution [50]). For DPE mixtures, the dependence of ε_r^E with the alcohol size is similar to that encountered for the amine systems examined: −1.03 (ethanol) < −1.24 (1-butanol) < −1.60 (1-hexanol) > −0.80 (1-decanol) [51]. On the other hand, for mixtures with a given 1-alkanol, ε_r^E changes in the order: heptane < DPE < DPA (see above, Fig. 4). This reveals that interactions between unlike molecules contribute more positively to the polarization of the mixture in the case of DPA systems.

4.2. Molar refraction

The refractive index at optical wavelengths is closely related to dispersion forces, since the molar refraction (or molar refractivity), R_m [34,52]:

$$R_m = \frac{n_D^2 - 1}{n_D^2 + 2} V_m = \frac{N_A \alpha_e}{3\varepsilon_0} \quad (7)$$

(where N_A and ε_0 stand for Avogadro's constant and the vacuum permittivity, respectively) is proportional to the mean electronic polarizability, α_e [32,34]. For the investigated systems, the values of R_m/cm^3 · mol^{-1} at $x_1 = 0.5$ are (Fig. S2, supplementary material): 20.5 ($n = 1$), 25.2 ($n = 3$), 27.5 ($n = 4$), 29.8 ($n = 5$), 34.4 ($n = 7$). It is clear that dispersive interactions are more important in longer 1-alkanols. Moreover, the values are practically identical to those of 1-alkanol + HxA mixtures [23]. This is to be expected, as DPA and HxA are isomers and both linear, so dispersive interactions cannot differ appreciably. The excess molar refractions, $R_m^E = R_m - R_m^{id}$, have also been calculated, with R_m^{id} evaluated substituting ideal values in Eq. (7). Values of R_m^E for 1-alkanol + hexane (n = 3, 4, 5, 6, 8 [53,54]) are positive and small (<0.04 cm^3·mol^{-1}). The same occurs for DPA + heptane

Table 4
Volume fractions of 1-alkanol, ϕ_1, refractive indices, n_D, and excess refractive indices, n_D^E, of 1-alkanol (1) + di-*n*-propylamine (DPA) (2) mixtures as functions of the mole fraction of the 1-alkanol, x_1, at temperature T and pressure $p = 0.1$ MPa.[a]

x_1	ϕ_1	n_D	$10^5 n_D^E$	x_1	ϕ_1	n_D	$10^5 n_D^E$
Methanol (1) + DPA (2); T/K = 293.15							
0.0000	0.0000	1.40417		0.5900	0.2981	1.39077	884
0.0374	0.0113	1.40406	72	0.6894	0.3958	1.38332	880
0.1111	0.0356	1.40355	199	0.8067	0.5519	1.36969	715
0.1464	0.0482	1.40324	261	0.8492	0.6243	1.36312	611
0.2203	0.0770	1.40238	387	0.8989	0.7241	1.35397	446
0.3034	0.1139	1.40103	524	0.9498	0.8481	1.34258	234
0.4174	0.1745	1.39825	694	0.9829	0.9443	1.33382	82
0.4937	0.2235	1.39553	785	1.0000	1.0000	1.32878	
Methanol (1) + DPA (2); T/K = 298.15							
0.0000	0.0000	1.40154		0.5900	0.2980	1.38830	864
0.0374	0.0113	1.40142	70	0.6894	0.3957	1.38108	849
0.1111	0.0356	1.40093	199	0.8067	0.5518	1.36764	661
0.1464	0.0482	1.40056	254	0.8492	0.6243	1.36109	552
0.2203	0.0769	1.39974	381	0.8989	0.7240	1.35202	397
0.3034	0.1139	1.39844	522	0.9498	0.8481	1.34058	208
0.4174	0.1745	1.39573	696	0.9829	0.9443	1.33174	73
0.4937	0.2234	1.39316	799	1.0000	1.0000	1.32667	
Methanol (1) + DPA (2); T/K = 303.15							
0.0000	0.0000	1.39890		0.5900	0.2980	1.38601	865
0.0374	0.0113	1.39881	73	0.6894	0.3957	1.37877	868
0.1111	0.0356	1.39834	202	0.8067	0.5518	1.36554	690
0.1464	0.0482	1.39800	259	0.8492	0.6242	1.35909	581
0.2203	0.0769	1.39719	387	0.8989	0.7240	1.34996	427
0.3034	0.1139	1.39590	527	0.9498	0.8481	1.33847	227
0.4174	0.1745	1.39317	695	0.9829	0.9443	1.32964	79
0.4937	0.2234	1.39071	807	1.0000	1.0000	1.32457	
1-propanol (1) + DPA (2); T/K = 293.15							
0.0000	0.0000	1.40417		0.6004	0.4503	1.40172	613
0.0465	0.0259	1.40431	63	0.6962	0.5554	1.39932	574
0.0897	0.0510	1.40448	128	0.7952	0.6792	1.39596	475
0.1524	0.0893	1.40466	219	0.8476	0.7520	1.39367	385
0.2024	0.1215	1.40471	285	0.8965	0.8252	1.39125	284
0.3121	0.1983	1.40456	416	0.9575	0.9247	1.38780	130
0.4059	0.2714	1.40413	512	1.0000	1.0000	1.38505	
0.4936	0.3470	1.40333	577				
1-propanol (1) + DPA (2); T/K = 298.15							
0.0000	0.0000	1.40159		0.6004	0.4500	1.39924	597
0.0465	0.0259	1.40173	62	0.6962	0.5551	1.39697	565
0.0897	0.0509	1.40191	126	0.7952	0.6789	1.39376	474
0.1524	0.0892	1.40207	212	0.8476	0.7518	1.39153	386
0.2024	0.1214	1.40220	285	0.8965	0.8251	1.38914	284
0.3121	0.1981	1.40205	412	0.9575	0.9246	1.38576	131
0.4059	0.2712	1.40163	505	1.0000	1.0000	1.38304	
0.4936	0.3467	1.40092	573				
1-propanol (1) + DPA (2); T/K = 303.15							
0.0000	0.0000	1.39890		0.6004	0.4497	1.39684	596
0.0465	0.0258	1.39904	60	0.6962	0.5548	1.39460	560
0.0897	0.0509	1.39921	122	0.7952	0.6786	1.39143	465
0.1524	0.0891	1.39941	210	0.8476	0.7516	1.38929	382
0.2024	0.1213	1.39951	277	0.8965	0.8249	1.38698	283
0.3121	0.1979	1.39942	404	0.9575	0.9245	1.38362	126
0.4059	0.2709	1.39904	497	1.0000	1.0000	1.38100	
0.4936	0.3465	1.39835	563				
1-butanol (1) + DPA (2); T/K = 293.15							
0.0000	0.0000	1.40409		0.5978	0.4980	1.40746	578
0.0519	0.0352	1.40477	85	0.6903	0.5980	1.40661	541
0.1199	0.0833	1.40556	187	0.7948	0.7210	1.40492	432
0.1581	0.1114	1.40591	236	0.8518	0.7932	1.40366	341
0.2220	0.1600	1.40653	321	0.8875	0.8404	1.40274	272
0.3097	0.2304	1.40713	415	0.9433	0.9174	1.40111	146
0.3936	0.3022	1.40759	496	1.0000	1.0000	1.39925	
0.5007	0.4009	1.40773	558				
1-butanol (1) + DPA (2); T/K = 298.15							
0.0000	0.0000	1.40147		0.5978	0.4976	1.40506	565
0.0519	0.0352	1.40216	84	0.6903	0.5976	1.40427	528
0.1199	0.0832	1.40293	180	0.7948	0.7207	1.40268	420
0.1581	0.1112	1.40325	224	0.8518	0.7929	1.40148	330

Table 4 (*continued*)

x_1	ϕ_1	n_D	$10^5 n_D^E$	x_1	ϕ_1	n_D	$10^5 n_D^E$
0.2220	0.1598	1.40396	315	0.8875	0.8402	1.40059	261
0.3097	0.2301	1.40458	406	0.9433	0.9173	1.39903	137
0.3936	0.3019	1.40504	482	1.0000	1.0000	1.39732	
0.5007	0.4005	1.40529	548				
1-butanol (1) + DPA (2); T/K = 303.15							
0.0000	0.0000	1.39888		0.5978	0.4972	1.40264	551
0.0519	0.0351	1.39950	74	0.6903	0.5973	1.40199	521
0.1199	0.0831	1.40031	172	0.7948	0.7204	1.40048	413
0.1581	0.1111	1.40067	218	0.8518	0.7927	1.39930	321
0.2220	0.1596	1.40138	306	0.8875	0.8400	1.39848	256
0.3097	0.2299	1.40206	399	0.9433	0.9171	1.39698	133
0.3936	0.3016	1.40253	471	1.0000	1.0000	1.39536	
0.5007	0.4002	1.40284	537				
1-pentanol (1) + DPA (2); T/K = 293.15							
0.0000	0.0000	1.40409		0.6080	0.5503	1.41265	535
0.0523	0.0417	1.40515	82	0.7040	0.6523	1.41274	484
0.0950	0.0765	1.40602	148	0.7909	0.7490	1.41238	392
0.1538	0.1254	1.40714	232	0.8562	0.8245	1.41188	298
0.2103	0.1736	1.40815	305	0.8980	0.8741	1.41142	223
0.2984	0.2512	1.40965	409	0.9497	0.9371	1.41074	119
0.4033	0.3478	1.41103	491	1.0000	1.0000	1.40992	
0.5068	0.4477	1.41207	537				
1-pentanol (1) + DPA (2); T/K = 298.15							
0.0000	0.0000	1.40147		0.6080	0.5498	1.41045	541
0.0523	0.0417	1.40255	81	0.7040	0.6519	1.41065	495
0.0950	0.0764	1.40342	145	0.7909	0.7487	1.41035	402
0.1538	0.1252	1.40462	234	0.8562	0.8242	1.40987	305
0.2103	0.1734	1.40562	302	0.8980	0.8740	1.40943	229
0.2984	0.2509	1.40715	405	0.9497	0.9370	1.40875	120
0.4033	0.3474	1.40861	488	1.0000	1.0000	1.40796	
0.5068	0.4473	1.40974	536				
1-pentanol (1) + DPA (2); T/K = 303.15							
0.0000	0.0000	1.39888		0.6080	0.5494	1.40811	530
0.0523	0.0416	1.39999	81	0.7040	0.6516	1.40838	484
0.0950	0.0762	1.40087	144	0.7909	0.7484	1.40813	390
0.1538	0.1250	1.40208	230	0.8562	0.8240	1.40777	300
0.2103	0.1731	1.40316	304	0.8980	0.8738	1.40728	215
0.2984	0.2506	1.40468	400	0.9497	0.9369	1.40671	113
0.4033	0.3470	1.40617	480	1.0000	1.0000	1.40603	
0.5068	0.4469	1.40739	531				
1-heptanol (1) + DPA (2); T/K = 293.15							
0.0000	0.0000	1.40409		0.5988	0.6079	1.42105	469
0.0533	0.0553	1.40617	96	0.6970	0.7050	1.42249	418
0.1009	0.1044	1.40794	173	0.7957	0.8018	1.42346	321
0.1434	0.1482	1.40944	235	0.8458	0.8507	1.42381	258
0.1983	0.2044	1.41129	306	0.8956	0.8991	1.42409	189
0.2939	0.3019	1.41418	398	0.9427	0.9447	1.42420	109
0.3915	0.4006	1.41677	458	1.0000	1.0000	1.42422	
0.4925	0.5021	1.41906	483				
1-heptanol (1) + DPA (2); T/K = 298.15							
0.0000	0.0000	1.40147		0.5988	0.6055	1.41883	469
0.0533	0.0547	1.40355	93	0.6970	0.7028	1.42035	422
0.1009	0.1034	1.40532	168	0.7957	0.8002	1.42142	323
0.1434	0.1468	1.40684	229	0.8458	0.8494	1.42180	258
0.1983	0.2028	1.40873	300	0.8956	0.8982	1.42209	186
0.2939	0.2997	1.41170	394	0.9427	0.9442	1.42226	108
0.3915	0.3981	1.41433	451	1.0000	1.0000	1.42234	
0.4925	0.4994	1.41673	480				
1-heptanol (1) + DPA (2); T/K = 303.15							
0.0000	0.0000	1.39888		0.5988	0.6030	1.41664	470
0.0533	0.0542	1.40101	95	0.6970	0.7007	1.41822	417
0.1009	0.1025	1.40283	172	0.7957	0.7985	1.41935	320
0.1434	0.1456	1.40436	231	0.8458	0.8481	1.41980	258
0.1983	0.2011	1.40628	303	0.8956	0.8972	1.42012	185
0.2939	0.2975	1.40933	399	0.9427	0.9436	1.42034	107
0.3915	0.3957	1.41205	458	1.0000	1.0000	1.42048	
0.4925	0.4969	1.41451	486				

[a] The standard uncertainties are: $u(T) = 0.02$ K; $u(p) = 1$ kPa; $u(x_1) = 0.0010$; $u(\phi_1) = 0.004$, $u(n_D) = 0.00008$. The combined expanded uncertainty (0.95 level of confidence) is $U_{rc}(n_D^E) = 0.0002$.

(<0.07 $cm^3 \cdot mol^{-1}$ [45,55], assuming ideal behaviour of n_D). However, in 1-alkanol + DPA systems the curves are negative; at $x_1 = 0.5$, R_m^E/$cm^3 \cdot mol^{-1}$ –0.45 ($n = 1$), −0.37 ($n = 3$), −0.38 ($n = 4$), −0.39 ($n = 5$), −0.40 ($n = 7$). This loss in dispersive interactions along mixing with respect to the ideal state can then be ascribed to a large number of O-—H-—N bonds formed in the mixing process, being greater for the methanol mixture.

4.3. Temperature dependence of the permittivity

Firstly, we note that, for pure compounds, $(\partial\varepsilon_r^*/\partial T)_p$ values are negative (Table 6), which is the typical behaviour of normal liquids. In the case of 1-alkanols, this quantity increases with n since the alcohol self-association decreases at this condition and a lower number of interactions between alcohol molecules are broken when the temperature is increased. The higher $(\partial\varepsilon_r^*/\partial T)_p$ values of DPA or HxA can be explained similarly. Interestingly, results for $(\partial\varepsilon_r/\partial T)_p$ are larger for the considered systems than for pure 1-alkanols (Table 6), which underlines the existence of (1-alkanol)-amine interactions. It is known that such interactions are stronger than those between alcohol molecules. For example, in the framework of the ERAS model, as already mentioned, the enthalpy of the hydrogen bonds between 1-alkanol molecules is −25 kJ·mol^{-1} [7,11,13,17] while the enthalpies between methanol or 1-heptanol and DPA molecules are, respectively, −42.4 and −34.5 kJ·mol^{-1} [17]. Thus, one can expect that the number of (1-alkanol)-amine interactions broken when the temperature is increased is lower than the number of disrupted interactions between 1-alkanol molecules. This makes ε_r change more smoothly with temperature for the mixtures than for pure 1-alkanols since, as it has been previously indicated, (1-alkanol)-amine interactions contribute positively to the polarization of the system. On the other hand, $(\partial\varepsilon_r/\partial T)_p$ also increases in line with n. The weaker temperature dependence of ε_r for systems containing longer 1-alkanols can be newly explained as above, i.e., in terms of the lower self-association of these 1-alkanols and of the less important solvation effects involved. We also note that $(\partial\varepsilon_r^E/\partial T)_p$ may show either positive or negative values (Table 5). Negative values (systems with $n = 1$–4) mean that ε_r decreases with the increase of temperature more rapidly than ε_r^{id} does. This behaviour is encountered for solutions where the effects related to the alcohol self-association and solvation effects between unlike molecules are more relevant. They become less important in systems with $n = 5,7$, and the temperature dependence of ε_r is weaker than that of ε_r^{id}, leading to positive $(\partial\varepsilon_r^E/\partial T)_p$ values. Finally, the replacement of DPA by HxA in systems with a given 1-alkanol leads to less negative $(\partial\varepsilon_r/\partial T)_p$ values (Table 6). This newly suggests that cyclic multimers formed by unlike molecules also exist in 1-alkanol + HxA systems, as the disruption of such multimers for increased temperature values positively contributes to the mixture polarization.

4.4. Kirkwood-Fröhlich model

In the Kirkwood-Fröhlich model, the fluctuations of the dipole moment in the absence of the electric field are treated as the basis to obtain relations involving the relative permittivity. It is a local-field model in which the molecules are assumed to be in a spherical cavity and the induced contribution to the polarizability is treated macroscopically through its relation to ε_r^∞ (the value of the permittivity at a high frequency at which only the induced polarizability contributes). The local field takes into account long-range dipolar interactions by considering the outside of the cavity as a continuous medium of permittivity ε_r. Short-range interactions are introduced by the so-called Kirkwood correlation factor, g_K, which provides information about the deviations from randomness of the orientation of a dipole with respect to its neighbours. This is an important parameter, as it provides information about specific interactions in the liquid state. For a mixture, g_K can be determined, in the context of a one-fluid model [31], from macroscopic

Table 5
Coefficients A_i and standard deviations, $\sigma(F^E)$ (Eq. (6)), for the representation of F^E at temperature T and pressure $p = 0.1$ MPa for 1-alkanol (1) + di-*n*-propylamine (DPA) (2) systems by Eq. (5).

Property F^E	1-alkanol	T/K	A_0	A_1	A_2	A_3	$\sigma(F^E)$
ε_r^E	Methanol	293.15	5.25	13.23	7.18		0.010
		298.15	4.60	12.65	7.4		0.012
		303.15	4.08	12.16	7.6		0.016
	1-propanol	293.15	−2.03	4.03	2.12	−1.0	0.008
		298.15	−2.27	3.48	2.12	−0.7	0.010
		303.15	−2.46	2.81	2.1		0.011
	1-butanol	293.15	−3.32	2.29	1.15	−1.1	0.006
		298.15	−3.40	1.89	1.23	−0.78	0.005
		303.15	−3.433	1.49	1.29	−0.39	0.003
	1-pentanol	293.15	−3.738	1.02	0.43	−0.71	0.004
		298.15	−3.680	0.77	0.56	−0.45	0.004
		303.15	−3.574	0.59	0.64	−0.20	0.003
	1-heptanol	293.15	−3.178	0.51	−0.05	−0.53	0.004
		298.15	−2.982	0.41	0.06	−0.36	0.004
		303.15	−2.76	0.35	0.14	−0.2	0.006
$10^5 n_D^E$	Methanol	293.15	3200	2053	24	−945	5
		298.15	3218	2133	191	−712	4
		303.15	3247	2236	359	−712	4
	1-propanol	293.15	2328	970			4
		298.15	2301	970			4
		303.15	2269	977			4
	1-butanol	293.15	2240	810	−1	−316	1.7
		298.15	2195	803	−65	−356	3
		303.15	2154	782	−104	−293	4
	1-pentanol	293.15	2126	459			4
		298.15	2138	520			4
		303.15	2102	470			5
	1-heptanol	293.15	1944	59			1.9
		298.15	1931	96			3
		303.15	1942	61			1.3
$(\frac{\partial \varepsilon_r^E}{\partial T})_p$/K^{-1}	Methanol	298.15	−0.117	−0.13	0.04	0.05	0.0011
	1-propanol	298.15	−0.043	−0.104	0.002	0.056	0.0004
	1-butanol	298.15	−0.011	−0.080	0.013	0.08	0.0007
	1-pentanol	298.15	0.0164	−0.043	0.021	0.051	0.0002
	1-heptanol	298.15	0.0415	−0.016	0.019	0.032	0.0004

physical properties according to the expression [31–34]:

$$g_K = \frac{9k_B T V_m \varepsilon_0 (\varepsilon_r - \varepsilon_r^\infty)(2\varepsilon_r + \varepsilon_r^\infty)}{N_A \mu^2 \varepsilon_r (\varepsilon_r^\infty + 2)^2} \quad (8)$$

Here, k_B is Boltzmann's constant; N_A, Avogadro's constant; ε_0, the vacuum permittivity; and V_m, the molar volume of the liquid at the working temperature, T. For polar compounds, ε_r^∞ is estimated from the relation $\varepsilon_r^\infty = 1.1 n_D^2$ [56]. μ represents the dipole moment of the solution,

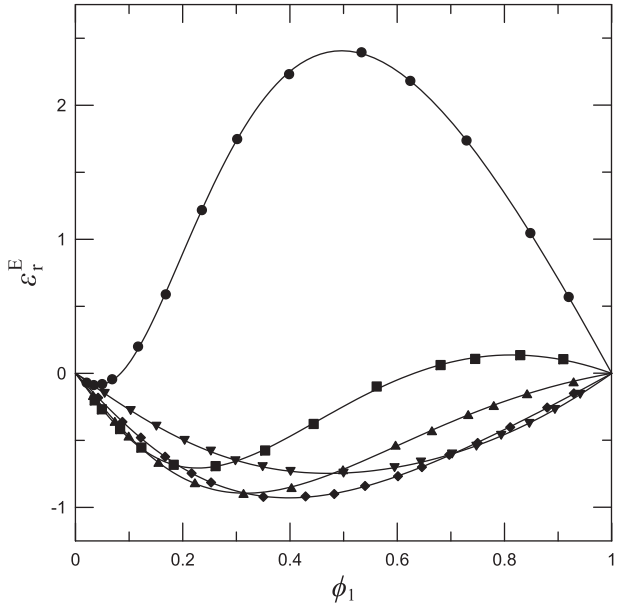

Fig. 1. Excess relative permittivities, ε_r^E, of 1-alkanol (1) + di-*n*-propylamine (2) systems at 0.1 MPa, 298.15 K and 1 MHz. Full symbols, experimental values (this work): (●), methanol; (■), 1-propanol; (▲), 1-butanol; (♦), 1-pentanol; (▼), 1-heptanol. Solid lines, calculations with Eq. (5) using the coefficients from Table 5.

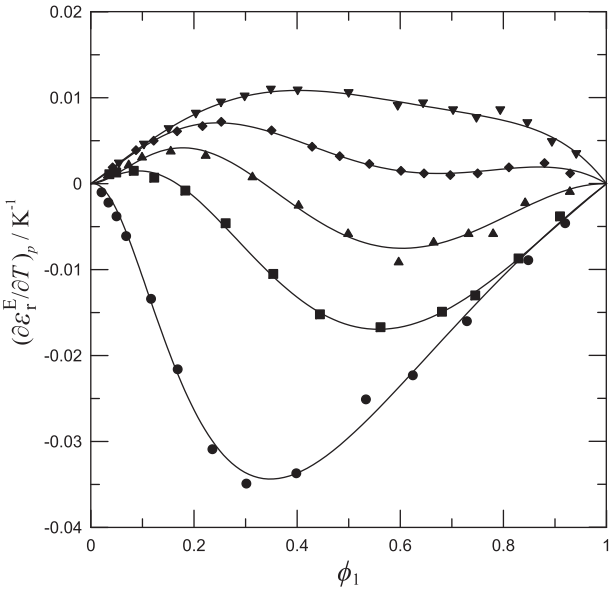

Fig. 2. Derivative of the excess relative permittivity of 1-alkanol (1) + di-*n*-propylamine (2) systems at 0.1 MPa, 298.15 K and 1 MHz. Full symbols, experimental values (this work): (●), methanol; (■), 1-propanol; (▲), 1-butanol; (♦), 1-pentanol; (▼), 1-heptanol. Solid lines, calculations with Eq. (5) using the coefficients from Table 5.

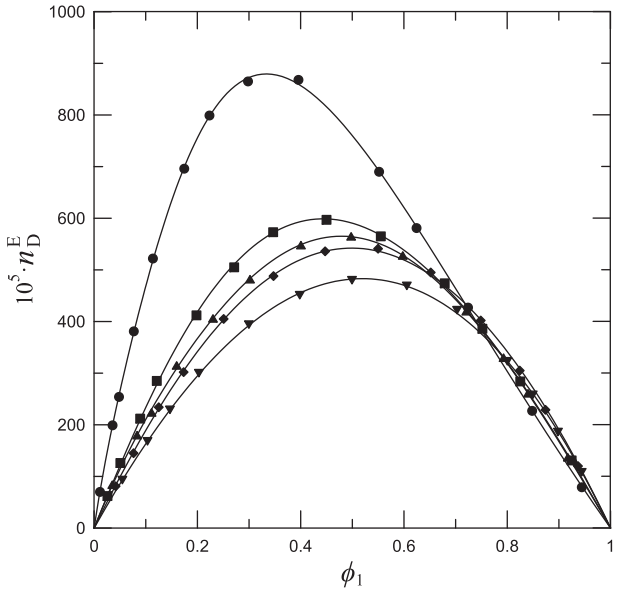

Fig. 3. Excess refractive index, n_D^E, of 1-alkanol (1) + di-*n*-propylamine (2) systems at 0.1 MPa, 298.15 K and 1 MHz. Full symbols, experimental values (this work): (●), methanol; (■), 1-propanol; (▲), 1-butanol; (♦), 1-pentanol; (▼), 1-heptanol. Solid lines, calculations with Eq. (5) using the coefficients from Table 5.

estimated from the equation [31]:

$$\mu^2 = x_1\mu_1^2 + x_2\mu_2^2 \tag{9}$$

where μ_i stands for the dipole moment of component i (=1,2). Calculations have been performed using smoothed values of V_m^E [17], n_D^E (this work) and ε_r^E (this work) at $\Delta x_1 = 0.01$. The source and values of μ_i are collected in Table 2.

Fig. 5 shows our calculations on g_K of 1-alkanol + DPA systems, which takes the values: 2.97 ($n = 1$), 2.72 ($n = 3$), 2.60 ($n = 4$), 2.47 ($n = 5$), 2.25 ($n = 7$). These are greater than the corresponding values for 1-alkanol + HxA mixtures [23]: 2.68 ($n = 1$), 2.32 ($n = 3$), 2.16 ($n = 4$), 2.01 ($n = 5$), 1.77 ($n = 7$). This would mean that parallel alignment of the dipoles is more favoured in DPA mixtures, supporting our previous statement inferred from the analysis of ε_r^E. It is interesting to note that for $\phi_1 > 0.4$ the g_K curve for methanol + DPA is practically constant, suggesting that the structure of the mixture in this concentration range is quite similar to that of the pure methanol because the rupture of the methanol self-association is compensated by the methanol-DPA hydrogen bonds created.

We have calculated as well the excess Kirkwood correlation factors, $g_K^E = g_K - g_K^{id}$, where g_K^{id} is calculated substituting the real quantities by ideal ones in Eq. (8). The values for 1-alkanol + DPA systems are (Figs. 6 and 7): 0.317 ($n = 1$), −0.110 ($n = 3$), −0.270 ($n = 4$), −0.366 ($n = 5$), −0.377 ($n = 7$). The trend is parallel to that of 1-alkanol + HxA mixtures [23], being this, as the corresponding ε_r^E, lower (Fig. 7): 0.170 ($n = 1$), −0.257 ($n = 3$), −0.421 ($n = 4$), −0.505 ($n = 5$), −0.508 ($n = 7$). The interpretation of this fact is thus similar [23]. For the minimum of the curves, the variation is the same as the one encountered for ε_r^E, but it occurs at lower values of ϕ_1. Then, according to the model, the ε_r^E minima are influenced by other factors different from the variation of the correlations in the orientation of the dipoles in the mixing process.

Table 6
Values of the derivative of permittivity with respect to temperature at 298.15 K for pure compounds[a], $(\partial\varepsilon_r^*/\partial T)_p$, and for mixtures, $(\partial\varepsilon_r/\partial T)_p$, at $\phi_1 = 0.5$.

Compound	$(\partial\varepsilon_r^*/\partial T)_p/K^{-1}$		$(\partial\varepsilon_r/\partial T)_p/K^{-1}$	
	Exp.	Lit.	1-alkanol + DPA	1-alkanol + HxA
Methanol	−0.192	−0.195 [68]	−0.131	−0.110
1-propanol	−0.136	−0.130 [88]	−0.094	−0.076
1-butanol	−0.127	−0.122 [88]	−0.077	−0.060
1-pentanol	−0.117	−0.110 [88]	−0.062	−0.044
1-heptanol	−0.099	−0.096 [88]	−0.044	−0.023
DPA	−0.012			
HXA	−0.0098			

[a] *n*-hexylamine (HxA), di-*n*-propylamine (DPA).

5. Conclusions

Measurements of ε_r and n_D have been reported for the 1-alkanol + di-*n*-propylamine systems at (293.15–303.15) K. Interactions

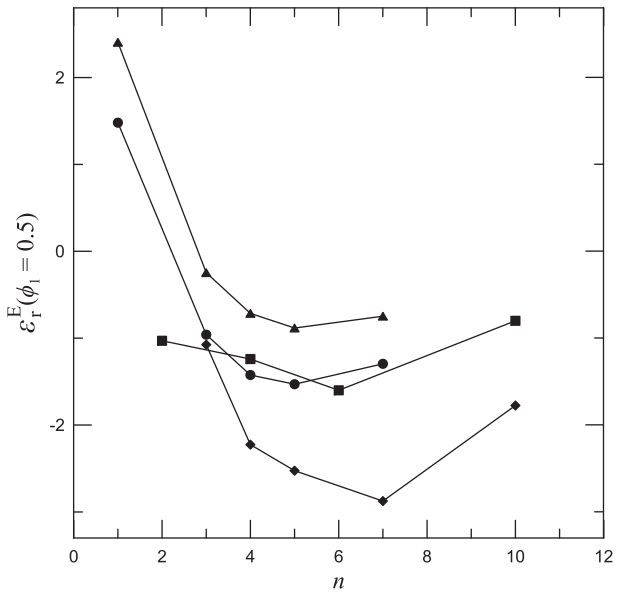

Fig. 4. Excess relative permittivities at $\phi_1 = 0.5$ of 1-alkanol (1) + amine (2) or +heptane (2) systems as functions of the number of carbon atoms of the 1-alkanol, at 0.1 MPa, 298.15 K and 1 MHz: (●), *n*-hexylamine [23]; (▲), di-*n*-propylamine (this work); (♦), heptane [20,43–45]; (■), di-*n*-propylether [51].

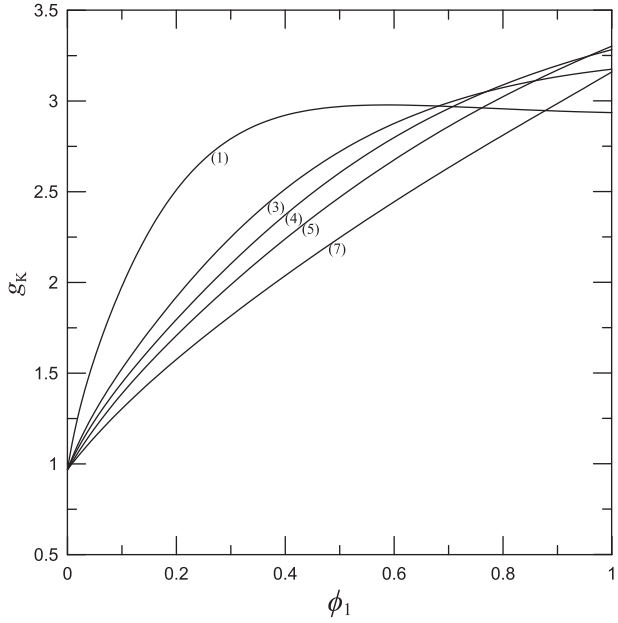

Fig. 5. Kirkwood correlation factor, g_K, of 1-alkanol (1) + di-*n*-propylamine (2) systems at 0.1 MPa, 298.15 K and 1 MHz. Numbers in parentheses indicate the number of atoms of the 1-alkanol.

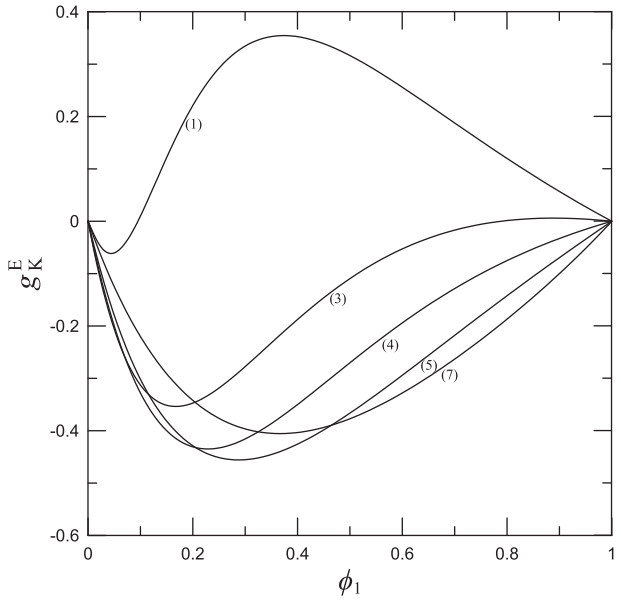

Fig. 6. Excess Kirkwood correlation factor, g_K^E, of 1-alkanol (1) + di-*n*-propylamine (2) systems at 0.1 MPa, 298.15 K and 1 MHz. Numbers in parentheses indicate the number of atoms of the 1-alkanol.

between unlike molecules form multimers that contribute positively to ε_r^E. Such contribution is dominant for the methanol mixture and ε_r^E is positive. For the remaining systems (except for high ϕ_1 values in the 1-propanol mixture) ε_r^E values are negative, indicating that dominant contributions arise from the breaking of interactions between like molecules. For a given 1-alkanol, ε_r^E is larger for di-*n*-propylamine than for *n*-hexylamine mixtures. This suggests that parallel alignment of the dipoles is more favoured and cyclic multimers disfavoured in the former case. The behaviour of $(\partial\varepsilon_r/\partial T)_p$ and the application of the Kirkwood-Fröhlich model support these findings. The values of $(\partial\varepsilon_r/\partial T)_p$ are higher for the mixtures than for pure 1-alkanols, because (1-alkanol)-DPA interactions are stronger than those between 1-alkanol molecules. Calculations on R_m show that dispersive interactions in the studied mixtures

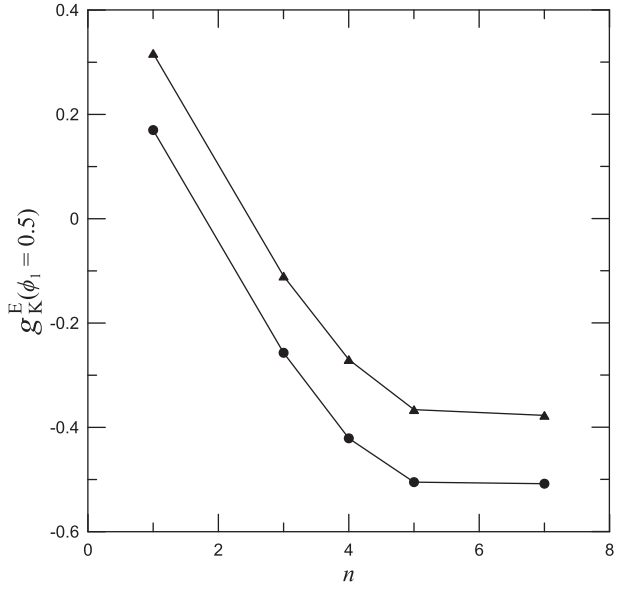

Fig. 7. Excess Kirkwood correlation factors at $\phi_1 = 0.5$ of 1-alkanol (1) + amine (2) systems as functions of the number of carbon atoms of the 1-alkanol, at 0.1 MPa, 298.15 K and 1 MHz: (●), *n*-hexylamine [23]; (▲), di-*n*-propylamine (this work).

increase with the length of the 1-alkanol, and that they have the same importance as in *n*-hexylamine systems.

Acknowledgements

F. Hevia and A. Cobos are grateful to Ministerio de Educación, Cultura y Deporte for the grants FPU14/04104 and FPU15/05456 respectively. The authors gratefully acknowledge the financial support received from the Consejería de Educación, Junta de Castilla y León, under Project BU034U16.

Appendix A. Supplementary data

Supplementary data to this article can be found online at https://doi.org/10.1016/j.molliq.2018.09.040.

References

[1] D.L. Nelson, M.M. Cox, Lehninger Principles of Biochemistry, 3rd ed. Worth Publishing, New York, 2000.
[2] Y. Coulier, A. Lowe, P.R. Tremaine, J.Y. Coxam, K. Ballerat-Busserolles, Absorption of CO_2 in aqueous solutions of 2-methylpiperidine: heats of solution and modeling, Int. J. Greenhouse Gas Control 47 (2016) 322–329, https://doi.org/10.1016/j.ijggc.2016.02.009.
[3] M. Götz, R. Reimert, S. Bajohr, H. Schnetzer, J. Wimberg, T.J.S. Schubert, Long-term thermal stability of selected ionic liquids in nitrogen and hydrogen atmosphere, Thermochim. Acta 600 (2015) 82–88, https://doi.org/10.1016/j.tca.2014.11.005.
[4] H. Funke, M. Wetzel, A. Heintz, New applications of the ERAS model. Thermodynamics of amine + alkane and alcohol + amine mixtures, Pure Appl. Chem. 61 (1989) 1429–1439, https://doi.org/10.1351/pac198961081429.
[5] S. Villa, J.A. González, I.G. De La Fuente, N. Riesco, J.C. Cobos, Thermodynamics of organic mixtures containing amines. II. Excess molar volumes at 25 °C for methylbutylamine + alkane systems and eras characterization of linear secondary amine + alkane mixtures, J. Solut. Chem. 31 (2002) 1019–1038, https://doi.org/10.1023/A:1021881627444.
[6] J.A. González, I. Mozo, I. García de la Fuente, J.C. Cobos, Thermodynamics of organic mixtures containing amines. IV. Systems with aniline, Can. J. Chem. 83 (2005) 1812–1825, https://doi.org/10.1139/v05-190.
[7] S. Villa, N. Riesco, I. Garćia de la Fuente, J.A. González, J.C. Cobos, Thermodynamics of mixtures with strongly negative deviations from Raoult's law. Part 8. Excess molar volumes at 298.15 K for 1-alkanol + isomeric amine (C6H15N) systems: characterization in terms of the ERAS model, Fluid Phase Equilib. 216 (2004) 123–133, https://doi.org/10.1016/j.fluid.2003.10.008.
[8] J.A. González, L.F. Sanz, I. García De La Fuente, J.C. Cobos, Thermodynamics of mixtures containing amines: XIII. Application of the ERAS model to cyclic amine + alkane mixtures, Thermochim. Acta 573 (2013) 229–236, https://doi.org/10.1016/j.tca.2013.09.033.
[9] R. Srivastava, B.D. Smith, Total-pressure vapor-liquid equilibrium data for binary systems of diethylamine with acetone, acetonitrile, and methanol, J. Chem. Eng. Data 30 (1985) 308–313, https://doi.org/10.1021/je00041a022.
[10] K. Nakanishi, H. Shirai, T. Minamiyama, Vapor-liquid equilibrium of binary systems containing alcohols. Methanol with aliphatic amines, J. Chem. Eng. Data 12 (1967) 591–594, https://doi.org/10.1021/je60035a031.
[11] A. Heintz, P.K. Naicker, S.P. Verevkin, R. Pfestorf, Thermodynamics of alkanol + amine mixtures. Experimental results and ERAS model calculations of the heat of mixing, Ber. Bunsenges. Phys. Chem. 102 (1998) 953–959, https://doi.org/10.1002/bbpc.19981020707.
[12] K. Nakanishi, H. Touhara, N. Watanabe, Studies on associated solutions. II. Heat of mixing of methanol with aliphatic amines, Bull. Chem. Soc. Jpn. 43 (1970) 2671–2676, https://doi.org/10.1246/bcsj.43.2671.
[13] A. Heintz, A new theoretical approach for predicting excess properties of alkanol/alkane mixtures, Ber. Bunsenges. Phys. Chem. 89 (1985) 172–181, https://doi.org/10.1002/bbpc.19850890217.
[14] J.A. González, I. García de la Fuente, J.C. Cobos, Thermodynamics of mixtures with strongly negative deviations from Raoult's Law: part 4. Application of the DISQUAC model to mixtures of 1-alkanols with primary or secondary linear amines. Comparison with Dortmund UNIFAC and ERAS results, Fluid Phase Equilib. 168 (2000) 31–58, https://doi.org/10.1016/S0378-3812(99)00326-X.
[15] L. Wang, G.C. Benson, B.C.Y. Lu, Excess enthalpies of 1-propanol + *n*-hexane + *n*-decane or *n*-dodecane at 298.15 K, J. Chem. Eng. Data 37 (1992) 403–406, https://doi.org/10.1021/je00008a007.
[16] S.-c. Hwang, R.L. Robinson, Vapor-liquid equilibria at 25 °C for nine alcohol-hydrocarbon binary systems, J. Chem. Eng. Data 22 (1977) 319–325, https://doi.org/10.1021/je60074a025.
[17] S. Villa, N. Riesco, I. Garćia de la Fuente, J.A. González, J.C. Cobos, Thermodynamics of mixtures with strongly negative deviations from Raoult's law: part 5. Excess molar volumes at 298.15 K for 1-alkanols + dipropylamine systems: characterization in terms of the ERAS model, Fluid Phase Equilib. 190 (2001) 113–125, https://doi.org/10.1016/S0378-3812(01)00595-7.
[18] S. Villa, N. Riesco, I. Garćia de la fuente, J.A. González, J.C. Cobos, Thermodynamics of mixtures with strongly negative deviations from Raoult's law: part 6. Excess molar

volumes at 298.15 K for 1-alkanols + dibutylamine systems. Characterization in terms of the ERAS model, Fluid Phase Equilib. 198 (2002) 313–329, https://doi.org/10.1016/S0378-3812(01)00808-1.
[19] L.F. Sanz, J.A. González, I. García De La Fuente, J.C. Cobos, Thermodynamics of mixtures with strongly negative deviations from Raoult's law. XI. Densities, viscosities and refractives indices at (293.15–303.15) K for cyclohexylamine + 1-propanol, or +1-butanol systems, J. Mol. Liq. 172 (2012) 26–33, https://doi.org/10.1016/j.molliq.2012.05.003.
[20] L.F. Sanz, J.A. González, I. García de la Fuente, J.C. Cobos, Thermodynamics of mixtures with strongly negative deviations from Raoult's law. XII. Densities, viscosities and refractive indices at T = (293.15 to 303.15) K for (1-heptanol, or 1-decanol + cyclohexylamine) systems. Application of the ERAS model to (1-alkanol + cyclohexylamine) mixtures, J. Chem. Thermodyn. 80 (2015) 161–171, https://doi.org/10.1016/j.jct.2014.09.005.
[21] L.F. Sanz, J.A. González, I.G. De La Fuente, J.C. Cobos, Thermodynamics of mixtures with strong negative deviations from Raoult's law. XIV. Density, permittivity, refractive index and viscosity data for the methanol + cyclohexylamine mixture at (293.15–303.15) K, Thermochim. Acta 631 (2016) 18–27, https://doi.org/10.1016/j.tca.2016.03.002.
[22] U. Domańska, M. Głoskowska, Experimental solid + liquid equilibria and excess molar volume of alkanol + octylamine mixtures. Analysis in terms of ERAS, DISQUAC, and modified UNIFAC, J. Chem. Eng. Data 49 (2004) 101–108, https://doi.org/10.1021/je0301895.
[23] F. Hevia, J.A. González, A. Cobos, I. García de la Fuente, C. Alonso-Tristán, Thermodynamics of mixtures with strongly negative deviations from Raoult's law. XV. Permittivities and refractive indices for 1-alkanol + *n*-hexylamine systems at (293.15–303.15) K. Application of the Kirkwood-Fröhlich model, Fluid Phase Equilib. 468 (2018) 18–28, https://doi.org/10.1016/j.fluid.2018.04.007.
[24] S. Villa, R. Garriga, P. Pérez, M. Gracia, J.A. González, I.G. de la Fuente, J.C. Cobos, Thermodynamics of mixtures with strongly negative deviations from Raoult's law: Part 9. Vapor–liquid equilibria for the system 1-propanol + di-*n*-propylamine at six temperatures between 293.15 and 318.15 K, Fluid Phase Equilib. 231 (2005) 211–220, https://doi.org/10.1016/j.fluid.2005.01.013.
[25] J.A. González, L.F. Sanz, I. García de la Fuente, J.C. Cobos, Thermodynamics of mixtures with strong negative deviations from Raoult's law. XIII. Relative permittivities for (1-alkanol + cyclohexylamine) systems, and dielectric study of (1-alkanol + polar) compound (amine, amide or ether) mixtures, J. Chem. Thermodyn. 91 (2015) 267–278, https://doi.org/10.1016/j.jct.2015.07.032.
[26] J.A. González, I.G. de la Fuente, J.C. Cobos, Thermodynamics of mixtures with strongly negative deviations from Raoult's law. Part 3. Application of the DISQUAC model to mixtures of triethylamine with alkanols. Comparison with Dortmund UNIFAC and ERAS results, Can. J. Chem. 78 (2000) 1272–1284, https://doi.org/10.1139/v00-114.
[27] J.A. González, I. Mozo, I.G.d.l. Fuente, J.C. Cobos, Thermodynamics of organic mixtures containing amines: V. Systems with pyridines, Thermochim. Acta 441 (2006) 53–68, https://doi.org/10.1016/j.tca.2005.11.027.
[28] J.A. González, I. Mozo, I.G. de la Fuente, J.C. Cobos, N. Riesco, Thermodynamics of mixtures containing amines: VII. Systems containing dimethyl or trimethylpyridines, Thermochim. Acta 467 (2008) 30–43, https://doi.org/10.1016/j.tca.2007.10.011.
[29] J.A. González, I.G. de la Fuente, I. Mozo, J.C. Cobos, N. Riesco, Thermodynamics of organic mixtures containing amines. VII. Study of systems containing pyridines in terms of the Kirkwood−Buff formalism, Ind. Eng. Chem. Res. 47 (2008) 1729–1737, https://doi.org/10.1021/ie071226e.
[30] J.A. González, J.C. Cobos, I. García de la Fuente, I. Mozo, Thermodynamics of mixtures containing amines. IX. Application of the concentration–concentration structure factor to the study of binary mixtures containing pyridines, Thermochim. Acta 494 (2009) 54–64, https://doi.org/10.1016/j.tca.2009.04.017.
[31] J.C.R. Reis, T.P. Iglesias, Kirkwood correlation factors in liquid mixtures from an extended Onsager-Kirkwood-Frohlich equation, Phys. Chem. Chem. Phys. 13 (2011) 10670–10680, https://doi.org/10.1039/C1CP20142E.
[32] H. Fröhlich, Theory of Dielectrics, Clarendon Press, Oxford, 1958.
[33] C. Moreau, G. Douhéret, Thermodynamic and physical behaviour of water + acetonitrile mixtures. Dielectric properties, J. Chem. Thermodyn. 8 (1976) 403–410, https://doi.org/10.1016/0021-9614(76)90060-4.
[34] A. Chelkowski, Dielectric Physics, Elsevier, Amsterdam, 1980.
[35] CIAAW, Atomic Weights of the Elements, ciaaw.org/atomic-weights.htm 2015 (accessed 2015).
[36] V. Alonso, J.A. González, I. García de la Fuente, J.C. Cobos, Dielectric and refractive index measurements for the systems 1-pentanol + octane, or +ibutyl ether or for dibutyl ether + octane at different temperatures, Thermochim. Acta 543 (2012) 246–253, https://doi.org/10.1016/j.tca.2012.05.036.
[37] K.N. Marsh, Recommended Reference Materials for the Realization of Physicochemical Properties, Blackwell Scientific Publications, Oxford, UK, 1987.
[38] J.A. González, I. Alonso, I. Mozo, I. García de la Fuente, J.C. Cobos, Thermodynamics of (ketone + amine) mixtures. Part VI. Volumetric and speed of sound data at (293.15, 298.15, and 303.15) K for (2-heptanone + dipropylamine, +dibutylamine, or +triethylamine) systems, J. Chem. Thermodyn. 43 (2011) 1506–1514, https://doi.org/10.1016/j.jct.2011.05.003.
[39] J.C. Reis, T.P. Iglesias, G. Douhéret, M.I. Davis, The permittivity of thermodynamically ideal liquid mixtures and the excess relative permittivity of binary dielectrics, Phys. Chem. Chem. Phys. 11 (2009) 3977–3986, https://doi.org/10.1039/B820613A.
[40] J.C.R. Reis, I.M.S. Lampreia, Â.F.S. Santos, M.L.C.J. Moita, G. Douhéret, Refractive index of liquid mixtures: theory and experiment, ChemPhysChem 11 (2010) 3722–3733, https://doi.org/10.1002/cphc.201000566.
[41] O. Redlich, A.T. Kister, Algebraic representation of thermodynamic properties and the classification of solutions, Ind. Eng. Chem. 40 (1948) 345–348, https://doi.org/10.1021/ie50458a036.
[42] P.R. Bevington, D.K. Robinson, Data Reduction and Error Analysis for the Physical Sciences, McGraw-Hill, New York, 2000.
[43] N.V. Sastry, M.K. Valand, Densities, speeds of sound, viscosities, and relative permittivities for 1-propanol+ and 1-butanol + heptane at 298.15 K and 308.15 K, J. Chem. Eng. Data 41 (1996) 1421–1425, https://doi.org/10.1021/je960135d.
[44] N.V. Sastry, M.K. Valand, Dielectric constants, refractive indexes and polarizations for 1-alcohol +heptane mixtures at 298.15 and 308.15 K, Ber. Bunsenges. Phys. Chem. 101 (1997) 243–250, https://doi.org/10.1002/bbpc.19971010212.
[45] J.A. Riddick, W.B. Bunger, T.K. Sakano, Organic Solvents: Physical Properties and Methods of Purification, Wiley, New York, 1986.
[46] A. Skrzecz, Critical evaluation of solubility data in binary systems formed by methanol with *n*-hydrocarbons, Thermochim. Acta 182 (1991) 123–131, https://doi.org/10.1016/0040-6031(91)87013-M.
[47] C. Wohlfahrt, Static dielectric constants of pure liquids and binary liquid mixtures, Landolt-Börnstein - Group IV Physical Chemistry, vol. 6, Springer Berlin Heidelberg, Berlin, 1991.
[48] J.A. González, I. Mozo, I. García de la Fuente, J.C. Cobos, N. Riesco, Thermodynamics of (1-alkanol + linear monoether) systems, J. Chem. Thermodyn. 40 (2008) 1495–1508, https://doi.org/10.1016/j.jct.2008.06.001.
[49] R. Garriga, F. Sánchez, P. Pérez, M. Gracia, Isothermal vapour-liquid equilibrium at eight temperatures and excess functions at 298.15 K of di-*n*-propylether with 1-propanol or 2-propanol, Fluid Phase Equilib. 138 (1997) 131–144, https://doi.org/10.1016/S0378-3812(97)00173-8.
[50] F. Sarmiento, M.I. Paz Andrade, J. Fernandez, R. Bravo, M. Pintos, Excess enthalpies of 1-heptanol + *n*-alkane and di-*n*-propylamine + normal alcohol mixtures at 298.15 K, J. Chem. Eng. Data 30 (1985) 321–323, https://doi.org/10.1021/je00041a025.
[51] M.C. Mateos, P. Pérez, F.M. Royo, M. Gracia, C. Gutiérrez-Losa, Permitividad estática de mezclas de mono-alcoholes + dipropil-éter, +butanona, +butironitrillo (II), Rev. Acad. Cienc. Exact. Fis. Quim. Nat. Zaragoza 41 (1986) 73–82.
[52] P. Brocos, A. Piñeiro, R. Bravo, A. Amigo, Refractive indices, molar volumes and molar refractions of binary liquid mixtures: concepts and correlations, Phys. Chem. Chem. Phys. 5 (2003) 550–557, https://doi.org/10.1039/B208765K.
[53] E. Jiménez, H. Casas, L. Segade, C. Franjo, Surface tensions, refractive indexes and excess molar volumes of hexane + 1-alkanol mixtures at 298.15 K, J. Chem. Eng. Data 45 (2000) 862–866, https://doi.org/10.1021/je000060k.
[54] A. Heintz, B. Schmittecker, D. Wagner, R.N. Lichtenthaler, Excess volumes of binary 1-alkanol/hexane mixtures at temperatures between 283.15 and 323.15 K, J. Chem. Eng. Data 31 (1986) 487–492, https://doi.org/10.1021/je00046a030.
[55] L. Lepori, P. Gianni, A. Spanedda, E. Matteoli, Thermodynamic study of (heptane + amine) mixtures. III: excess and partial molar volumes in mixtures with secondary, tertiary, and cyclic amines at 298.15 K, J. Chem. Thermodyn. 43 (2011) 1453–1462, https://doi.org/10.1016/j.jct.2011.04.017.
[56] Y. Marcus, The structuredness of solvents, J. Solut. Chem. 21 (1992) 1217–1230, https://doi.org/10.1007/bf00667218.
[57] M. El-Hefnawy, K. Sameshima, T. Matsushita, R. Tanaka, Apparent dipole moments of 1-alkanols in cyclohexane and *n*-heptane, and excess molar volumes of (1-alkanol + cyclohexane or *n*-heptane) at 298.15 K, J. Solut. Chem. 34 (2005) 43–69, https://doi.org/10.1007/s10953-005-2072-1.
[58] R.D. Bezman, E.F. Casassa, R.L. Kay, The Temperature Dependence of the Dielectric Constants of Alkanols, 73–74, 1997 397–402, https://doi.org/10.1016/S0167-7322(97)00082-2.
[59] J. Canosa, A. Rodríguez, J. Tojo, Binary mixture properties of diethyl ether with alcohols and alkanes from 288.15 K to 298.15 K, Fluid Phase Equilib. 156 (1999) 57–71, https://doi.org/10.1016/S0378-3812(99)00032-1.
[60] G.J. Janz, R.P.T. Tomkins, Nonaqueus Electrolytes Handbook, vol. 1, Academic Press, New York, 1972.
[61] S.P. Serbanovic, M.L. Kijevcanin, I.R. Radovic, B.D. Djordjevic, Effect of temperature on the excess molar volumes of some alcohol + aromatic mixtures and modelling by cubic EOS mixing rules, Fluid Phase Equilib. 239 (2006) 69–82, https://doi.org/10.1016/j.fluid.2005.10.022.
[62] C. Wohlfahrt, Optical constants, Refractive Indices of Pure Liquids and Binary Liquid Mixtures. Landolt-Börnstein - Group III Condensed Matter, vol. 47, Springer Berlin Heidelberg, Berlin, 2008.
[63] S. Chen, Q. Lei, W. Fang, Density and refractive index at 298.15 K and vapor−liquid equilibria at 101.3 kPa for four binary systems of methanol, *n*-propanol, *n*-butanol, or isobutanol with *n*-methylpiperazine, J. Chem. Eng. Data 47 (2002) 811–815, https://doi.org/10.1021/je010249b.
[64] M.I. Aralaguppi, C.V. Jadar, T.M. Aminabhavi, Density, viscosity, refractive index, and speed of sound in binary mixtures of acrylonitrile with methanol, ethanol, propan-1-ol, butan-1-ol, pentan-1-ol, hexan-1-ol, heptan-1-ol, and butan-2-ol, J. Chem. Eng. Data 44 (1999) 216–221, https://doi.org/10.1021/je9802219.
[65] R. Anwar Naushad, S. Yasmeen, Volumetric, compressibility and viscosity studies of binary mixtures of [EMIM][NTf2] with ethylacetate/methanol at (298.15–323.15) K, J. Mol. Liq. 224 (Part A) (2016) 189–200, https://doi.org/10.1016/j.molliq.2016.09.077.
[66] S.M. Pereira, T.P. Iglesias, J.L. Legido, L. Rodríguez, J. Vijande, Changes of refractive index on mixing for the binary mixtures {xCH3OH + (1−x) CH3OCH2(CH2OCH2)3CH2OCH3} and {xCH3OH + (1−x)CH3OCH2(CH2OCH2)nCH2OCH3} (n = 3–9) at temperatures from 293.15 K to 333.15 K, J. Chem. Thermodyn. 30 (1998) 1279–1287, https://doi.org/10.1006/jcht.1998.0395.
[67] A. Rodríguez, J. Canosa, J. Tojo, Density, refractive index, and speed of sound of binary mixtures (diethyl carbonate + alcohols) at several temperatures, J. Chem. Eng. Data 46 (2001) 1506–1515, https://doi.org/10.1021/je010148d.
[68] A.P. Gregory, R.N. Clarke, Traceable measurements of the static permittivity of dielectric reference liquids over the temperature range 5–50 °C, Meas. Sci. Technol. 16 (2005) 1506, https://doi.org/10.1088/0957-0233/16/7/013.

[69] M.J. Fontao, M. Iglesias, Effect of temperature on the refractive index of aliphatic hydroxilic mixtures (C2–C3), Int. J. Thermophys. 23 (2002) 513–527, https://doi.org/10.1023/A:1015113604024.
[70] J.L. Hales, J.H. Ellender, Liquid densities from 293 to 490 K of nine aliphatic alcohols, J. Chem. Thermodyn. 8 (1976) 1177–1184, https://doi.org/10.1016/0021-9614(76)90126-9.
[71] N.G. Tsierkezos, I.E. Molinou, A.C. Filippou, Thermodynamic properties of binary mixtures of cyclohexanone with *n*-alkanols (C1–C5) at 293.15 K, J. Solut. Chem. 34 (2005) 1371–1386, https://doi.org/10.1007/s10953-005-8508-9.
[72] C. Yang, H. Lai, Z. Liu, P. Ma, Density and viscosity of binary mixtures of diethyl carbonate with alcohols at (293.15 to 363.15) K and predictive results by UNIFAC-VISCO group contribution method, J. Chem. Eng. Data 51 (2006) 1345–1351, https://doi.org/10.1021/je0600808.
[73] C.P. Smyth, W.N. Stoops, The dielectric polarization of liquids. VI. Ethyl iodide, ethanol, normal-butanol and normal-octanol, J. Am. Chem. Soc. 51 (1929) 3312–3329, https://doi.org/10.1021/ja01386a019.
[74] B. Giner, A. Villares, M.C. López, F.M. Royo, C. Lafuente, Refractive indices and molar refractions for isomeric chlorobutanes with isomeric butanols, Phys. Chem. Liq. 43 (2005) 13–23, https://doi.org/10.1080/0031910042000303518.
[75] E. Jiménez, M. Cabanas, L. Segade, S. Garcýa-Garabal, H. Casas, Excess volume, changes of refractive index and surface tension of binary 1,2-ethanediol + 1-propanol or 1-butanol mixtures at several temperatures, Fluid Phase Equilib. 180 (2001) 151–164, https://doi.org/10.1016/S0378-3812(00)00519-7.
[76] G.A. Iglesias-Silva, A. Guzmán-López, G. Pérez-Durán, M. Ramos-Estrada, Densities and viscosities for binary liquid mixtures of *n*-undecane + 1-propanol, +1-butanol, +1-pentanol, and +1-hexanol from 283.15 to 363.15 K at 0.1 MPa, J. Chem. Eng. Data 61 (2016) 2682–2699, https://doi.org/10.1021/acs.jced.6b00121.
[77] T.P. Iglesias, J.L. Legido, S.M. Pereira, B. de Cominges, M.I. Paz Andrade, Relative permittivities and refractive indices on mixing for (*n*-hexane + 1-pentanol, or 1-hexanol, or 1-heptanol) at T = 298.15 K, J. Chem. Thermodyn. 32 (2000) 923–930, https://doi.org/10.1006/jcht.2000.0661.
[78] M.N.M. Al-Hayan, Densities, excess molar volumes, and refractive indices of 1,1,2,2-tetrachloroethane and 1-alkanols binary mixtures, J. Chem. Thermodyn. 38 (2006) 427–433, https://doi.org/10.1016/j.jct.2005.06.015.
[79] S.P. Patil, A.S. Chaudhari, M.P. Lokhande, M.K. Lande, A.G. Shankarwar, S.N. Helambe, B.R. Arbad, S.C. Mehrotra, Dielectric measurements of aniline and alcohol mixtures at 283, 293, 303, and 313 K using the time domain technique, J. Chem. Eng. Data 44 (1999) 875–878, https://doi.org/10.1021/je980250j.
[80] Á. Piñeiro, P. Brocos, A. Amigo, M. Pintos, R. Bravo, Refractive indexes of binary mixtures of tetrahydrofuran with 1-alkanols at 25 °C and temperature dependence of *n* and ρ for the pure liquids, J. Solut. Chem. 31 (2002) 369–380, https://doi.org/10.1023/A:1015807331250.
[81] J.J. Cano-Gómez, G.A. Iglesias-Silva, E.O. Castrejón-González, M. Ramos-Estrada, K.R. Hall, Density and viscosity of binary liquid mixtures of ethanol + 1-hexanol and ethanol + 1-heptanol from (293.15 to 328.15) K at 0.1 MPa, J. Chem. Eng. Data 60 (2015) 1945–1955, https://doi.org/10.1021/je501133u.
[82] U. Domańska, M. Królikowska, Density and viscosity of binary mixtures of {1-butyl-3-methylimidazolium thiocyanate + 1-heptanol, 1-octanol, 1-nonanol, or 1-decanol}, J. Chem. Eng. Data 55 (2010) 2994–3004, https://doi.org/10.1021/je901043q.
[83] R.C. Reid, J.M. Prausnitz, B.E. Poling, The Properties of Gases and Liquids, McGraw-Hill, New York, US, 1987.
[84] C.M. Kinart, A. Ćwiklińska, W.J. Kinart, A. Bald, Density and relative permittivity of 2-methoxyethanol + dipropylamine mixtures at various temperatures, J. Chem. Eng. Data 49 (2004) 1425–1428, https://doi.org/10.1021/je040006u.
[85] J.M. Resa, C. González, S. Ortiz de Landaluce, J. Lanz, Vapor−liquid equilibrium of binary mixtures containing diethylamine + diisopropylamine, diethylamine + dipropylamine, and chloroform + diisopropylamine at 101.3 kPa, and vapor pressures of dipropylamine, J. Chem. Eng. Data 45 (2000) 867–871, https://doi.org/10.1021/je000020g.
[86] S.L. Oswal, P. Oswal, R.L. Gardas, S.G. Patel, R.G. Shinde, Acoustic, volumetric, compressibility and refractivity properties and reduction parameters for the ERAS and Flory models of some homologous series of amines from 298.15 to 328.15 K, Fluid Phase Equilib. 216 (2004) 33–45, https://doi.org/10.1016/j.fluid.2003.09.007.
[87] I. Alonso, I. Mozo, I.G. de la fuente, J.A. González, J.C. Cobos, Thermodynamics of ketone + amine mixtures part IV. Volumetric and speed of sound data at (293.15; 298.15 and 303.15 K) for 2-butanone +dipropylamine, +dibutylamine or +triethylamine systems, Thermochim. Acta 512 (2011) 86–92, https://doi.org/10.1016/j.tca.2010.09.004.
[88] T. Shinomiya, Dielectric dispersion and intermolecular association for 28 pure liquid alcohols. The position dependence of hydroxyl group in the hydrocarbon chain, Bull. Chem. Soc. Jpn. 62 (1989) 908–914, https://doi.org/10.1246/bcsj.62.908.

Supplementary material for:

Thermodynamics of mixtures with strongly negative deviations from Raoult's law. XVI. Permittivities and refractive indices for 1-alkanol + di-*n*-propylamine systems at (293.15-303.15) K. Application of the Kirkwood-Fröhlich model

Fernando Hevia, Ana Cobos, Juan Antonio González*, Isaías García de la Fuente, Luis Felipe Sanz

G.E.T.E.F., Departamento de Física Aplicada, Facultad de Ciencias, Universidad de Valladolid, Paseo de Belén, 7, 47011 Valladolid, Spain

*e-mail: jagl@termo.uva.es; Tel: +34 983 423757

Reference of the article:

F. Hevia, A. Cobos, J.A. González, I. García de la Fuente, L.F. Sanz. J. Mol. Liq. **271** (2018) 704-714. https://doi.org/10.1016/j.molliq.2018.09.040

Table S1. Derivative of the excess relative permittivity of 1-alkanol (1) + di-*n*-propylamine (DPA) (2) systems at pressure 0.1 MPa, temperature 298.15 K and frequency 1 MHz [a].

x_1	ϕ_1	$\left(\partial\varepsilon_r^E/\partial T\right)_p$ / K^{-1}	x_1	ϕ_1	$\left(\partial\varepsilon_r^E/\partial T\right)_p$ / K^{-1}
methanol (1) + DPA (2) ; T/K = 298.15					
0.0664	0.0206	–0.001	0.5940	0.3015	–0.035
0.1066	0.0340	–0.002	0.6918	0.3984	–0.0337
0.1503	0.0496	–0.004	0.7948	0.5333	–0.0251
0.1990	0.0683	–0.006	0.8492	0.6243	–0.0223
0.3091	0.1166	–0.013	0.9012	0.7291	–0.016
0.4068	0.1683	–0.022	0.9498	0.8481	–0.0089
0.5110	0.2357	–0.031	0.9749	0.9197	–0.0046
1-propanol (1) + DPA (2) ; T/K = 298.15					
0.0638	0.0358	0.0011	0.5948	0.4442	–0.0152
0.0866	0.0491	0.0013	0.7018	0.5617	–0.0167
0.1427	0.0831	0.0015	0.7967	0.6809	–0.0149
0.2045	0.1228	0.0007	0.8431	0.7453	–0.0130
0.2917	0.1832	–0.0008	0.8993	0.8294	–0.0087
0.3939	0.2614	–0.0046	0.9487	0.9097	–0.0038
0.5012	0.3536	–0.0105			
1-butanol (1) + DPA (2) ; T/K = 298.15					
0.0484	0.0328	0.0011	0.5991	0.4989	–0.0057
0.1063	0.0734	0.0023	0.6896	0.5968	–0.0090
0.1418	0.0992	0.0032	0.7484	0.6646	–0.0067
0.2157	0.1549	0.0039	0.8041	0.7323	–0.0057
0.3006	0.2226	0.0034	0.8418	0.7800	–0.0057
0.4064	0.3133	0.0009	0.8890	0.8422	–0.0021
0.5030	0.4028	–0.0024	0.9514	0.9288	–0.0008
1-pentanol (1) + DPA (2) ; T/K = 298.15					
0.0530	0.0422	0.0019	0.5985	0.5400	0.0023
0.1086	0.0875	0.0039	0.6570	0.6014	0.0015
0.1497	0.1218	0.0050	0.6985	0.6460	0.0012
0.2032	0.1672	0.0061	0.7450	0.6970	0.0010
0.2597	0.2165	0.0067	0.7921	0.7500	0.0012
0.3006	0.2529	0.0072	0.8447	0.8107	0.0019
0.4064	0.3503	0.0062	0.9027	0.8796	0.0024
0.4882	0.4290	0.0043	0.9435	0.9293	0.0012
0.5421	0.4825	0.0032			
1-heptanol (1) + DPA (2) ; T/K = 298.15					
0.0529	0.0543	0.0023	0.5883	0.5950	0.0090
0.1003	0.1028	0.0045	0.6378	0.6442	0.0093
0.1474	0.1509	0.0063	0.6965	0.7023	0.0085

0.1990	0.2035	0.0081	0.7424	0.7477	0.0076
0.2471	0.2523	0.0094	0.7892	0.7938	0.0085
0.2924	0.2982	0.0101	0.8426	0.8463	0.0070
0.3427	0.3490	0.0109	0.8913	0.8940	0.0048
0.3943	0.4010	0.0108	0.9395	0.9411	0.0034
0.4929	0.4998	0.0105			

[a] The standard uncertainties are: $u(T) = 0.02$ K; $u(p) = 1$ kPa; $u(\nu) = 20$ Hz; $u(x_1) = 0.0010$; $u(\phi_1) = 0.004$; $u\left[\left(\partial\varepsilon_r^E/\partial T\right)_p\right] = 0.0008$ K^{-1}.

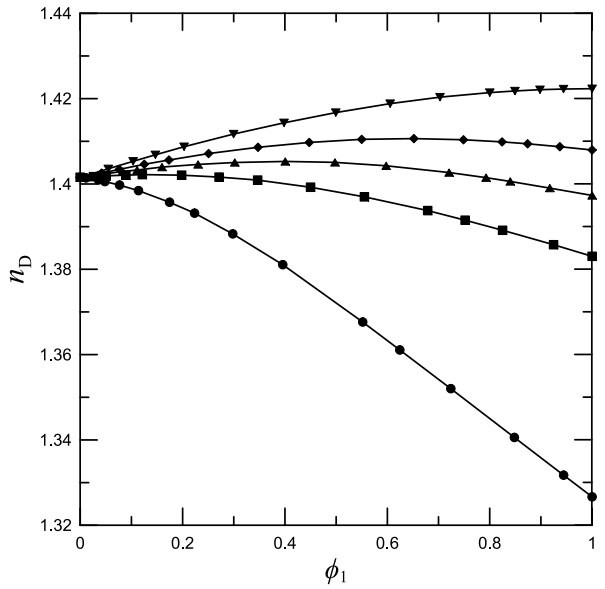

Figure S1: Refractive index at the sodium D line, n_D, of 1-alkanol (1) + DPA (2) systems at pressure 0.1 MPa and temperature 298.15 K. Full symbols, experimental values (this work): (●), methanol; (■), 1-propanol; (▲), 1-butanol; (♦), 1-pentanol; (▼), 1-heptanol.

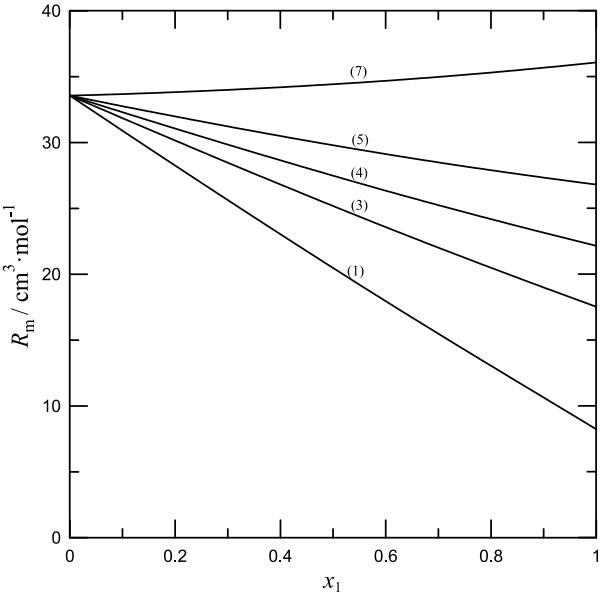

Figure S2: Molar refraction of 1-alkanol (1) + DPA (2) systems at pressure 0.1 MPa and temperature 298.15 K. Numbers in parentheses indicate the number of atoms of the 1-alkanol.

Journal of Molecular Liquids 233 (2017) 517–527

Contents lists available at ScienceDirect

Journal of Molecular Liquids

journal homepage: www.elsevier.com/locate/molliq

Orientational effects in alkanone, alkanal or dialkyl carbonate + alkane mixtures and in alkanone + alkanone or + dialkyl carbonate systems

Fernando Hevia [a], Juan Antonio González [a,*], Cristina Alonso-Tristán [b], Isaías García de la Fuente [a], Luis Felipe Sanz [a]

[a] G.E.T.E.F., Departamento de Física Aplicada, Facultad de Ciencias, Universidad de Valladolid, Paseo de Belén, 7, 47011 Valladolid, Spain
[b] Departamento de Ingeniería Electromecánica, Escuela Politécnica Superior, Universidad de Burgos, Avda. Cantabria s/n, 09006 Burgos, Spain

ARTICLE INFO

Article history:
Received 25 September 2016
Received in revised form 10 February 2017
Accepted 3 March 2017
Available online 07 March 2017

Keywords:
Polar compound
Steric
Cyclization
Aromaticity, Flory
Orientational effects

ABSTRACT

Interactions and structure of alkanone, or alkanal or dialkyl carbonate + alkane mixtures, or of 2-alkanone + 2-alkanone, or of ketone + dialkyl carbonate systems have been investigated by means of a set of thermodynamic properties and by the application of the Flory model. The properties considered are excess molar quantities: enthalpies, H^E_m, volumes, V^E_m, or isobaric heat capacities, C^E_{pm}, and liquid-liquid equilibria. Experimental data show that alkane mixtures are characterized by rather strong dipolar interactions. In the case of systems containing ketones with the same number of C atoms and a given alkane, dipolar interactions become weaker in the sequence: aromatic > cyclic > linear. In addition, the mentioned interactions become also weaker in the order: dialkyl carbonate > linear alkanone > linear alkanal. This is an important result, as carbonates show lower effective dipole moments than the other compounds, and it suggests that the group size may be relevant when evaluating thermodynamic properties of liquid mixtures. Results on H^E_m from the Flory model show that orientational effects (i.e., non-random mixing) are rather similar for systems with linear, cyclic or aromatic ketones or alkanals and alkanes. In contrast, orientational effects become weaker in dialkyl carbonate + alkane mixtures. The behavior of 2-alkanone + 2-alkanone systems and of mixtures of longer 2-alkanones or cyclohexanone with dialkyl carbonate is close to random mixing. Larger orientational effects are encountered in solutions of carbonates and shorter 2-alkanones.

1. Introduction

We are engaged in a systematic investigation on orientational effects (i.e., non-random mixing) in mixtures of organic liquids by means of the application of different models, such as: DISQUAC [1], ERAS [2], Flory [3], Kirkwood-Buff integrals [4,5] or the $S_{CC}(0)$ (concentration-concentration structure factor) formalism [6]. In this framework, along a series of works, we have shown that the Flory model is suitable to gain insight into orientational effects present in systems of the type: 1-alkanol + linear alkanone [7], or + nitrile [8], or + linear or cyclic ether [9,10]; 1-butanol + alkoxyethanol [11], alkoxyethanol + dibutyl ether [11], oxaalkane + alkane [12], or + aromatic compound [13]. Now, we extend these previous studies to alkanone, or alkanal or linear organic carbonate + alkane mixtures. This allows to examine a number of interesting effects in terms of the Flory model: steric effects, cyclization, aromaticity or the group size, which is extremely large in the case of the carbonate group. The latter is rather important, as if the group is too large with respect to the average intermolecular distances, the interaction potential involved could be so complex that no theory would be able to describe it conveniently. This should lead to a poor description of the thermodynamic properties by means of the selected theory. The study is completed with the corresponding treatment of *n*-alkanone + *n*-alkanone, or + linear organic carbonate systems.

Alkane mixtures with linear [14], cyclic [14] or aromatic alkanones [15,16], or with linear [17] or aromatic alkanals [16,18], or including linear organic carbonates [19] have been successfully treated in terms of the DISQUAC model. UNIFAC interaction parameters for the contacts CO/CH_2 [20] CHO/CH_2 [20] or $OCOO/CH_2$ [21] are available in the literature. Interestingly, *n*-alkanone [22,23], or *n*-alkanal [24] + alkane mixtures have also been studied using only the quasi-chemical approximation of DISQUAC with the coordination number equal to 10, obtaining rather good results. This suggests that orientational effects are not very relevant in such systems.

2. The Flory model

In this section, a summary of the Flory model and some results used in this work are presented. More details can be found in the original works [3,25–28].

* Corresponding author.
E-mail address: jagl@termo.uva.es (J.A. González).

http://dx.doi.org/10.1016/j.molliq.2017.03.014
0167-7322/

2.1. Hypotheses

2.1.1. Hypotheses for pure liquids

In the Flory model, a liquid, occupying the volume V, is formed by N molecules (of mean volume $v_m = V/N$). Each of the molecules is divided into r segments. The mean volume of a segment is denoted $v_s = V/rN = v_m/r$. A segment is an arbitrarily chosen isomeric portion of the molecule; its precise definition is left open and may be adapted to circumstances. The core volume of a molecule is defined as $v^*_m = rv^*_s$, where v^*_s is the core volume of a segment. Each segment is endowed with s contacts. The interactions considered are: (i) An attractive intermolecular interaction between pairs of contacts, with a mean potential energy per pair of the form $-\eta/v_s$, where η is a positive constant of the liquid considered. (ii) A repulsive interaction, leading to a free volume term in the partition function [29]. (iii) The effect of the rest of the intramolecular interactions is treated assuming [30] that the $3r$ degrees of freedom of a molecule can be divided into two uncoupled categories, i.e., internal and external. It is also supposed that, for fluids with densities of liquids, the intramolecular potentials associated with the latter degrees of freedom merely restrict the degrees of freedom per molecule from $3r$ to an effective number of $3rc$. The constant $c \leq 1$ would take into account the restrictions on the precise location of a segment by its neighbors in the same chain. Some parameters of the model are better replaced by the reduction parameters p^* and T^*, defined together with the reduced parameters of the liquid, namely, $\overline{T} = T/T^*$, $\overline{p} = p/p^*$ (where p is the pressure and T is the temperature) and $\overline{v} = v_m/v^*_m = v_s/v^*_s = V_m/V^*_m$. In these relations, $V_m = N_A v_m$ denotes the molar volume of the liquid and $V^*_m = N_A v^*_m$ the core molar volume (N_A stands for Avogadro's constant).

2.1.2. Hypotheses for binary mixtures

The components of a binary mixture will be indexed by subscripts $i = 1, 2$. Because the definition of segment is arbitrary, it is convenient to impose that the segments of both components have the same core volume. It is supposed that the number of contacts per molecule of a given component is proportional to the core surface area of the corresponding molecule, assumed spherical. The total number of molecules in the mixture is $N = N_1 + N_2$. The total numbers of segments, contacts and effective number of degrees of freedom (rN, srN and $3rcN$) are taken as additive. It is convenient to define the segment and contact fractions, respectively, by $\varphi_i = r_i N_i/rN$ and $\theta_i = s_i r_i N_i/srN = \varphi_i s_i/s$. Of course, $\sum \varphi_i = \sum \theta_i = 1$. It is also assumed that the mean intensity of the interaction between segments of molecules of the same component is the same in the mixture as in the pure species. The total intermolecular energy of the binary mixtures can be written in the same form as for pure compounds, by defining $v_s = V/rN$, and the η parameter for the mixture by $\eta = \theta_1\eta_1 + \theta_2\eta_2 - A_{12}\Delta\eta/(srN)$. Here, A_{ii} and A_{12} are the numbers of pairs of contacts between equal and different molecules respectively, $\Delta\eta = \eta_1 + \eta_2 - 2\eta_{12}$ and η_{12} characterizes the mean intensity of the interaction between segments of different molecules. Moreover, random mixing is assumed. This hypothesis states that, given a contact, the remaining contacts in the mixture have the same probability of forming an interacting pair with it. It is expressed by the equations $A_{12,\text{random}} = srN\theta_1\theta_2$ and $\eta_{\text{random}} = \theta_1\eta_1 + \theta_2\eta_2 - \theta_1\theta_2\Delta\eta$.

2.1.3. Equations

For both pure compounds and binary mixtures, the intermolecular molar energy, E_m, and the thermal equation of state (in reduced form) are:

$$E_m = -\frac{p^* V^*_m}{\overline{v}} = -TV^*_m \frac{p^*}{T^*}\frac{1}{\overline{v}\overline{T}} \tag{1}$$

$$\frac{\overline{p}\overline{v}}{\overline{T}} = \frac{\overline{v}^{1/3}}{\overline{v}^{1/3}-1} - \frac{1}{\overline{v}\overline{T}} \tag{2}$$

(the last equality of Eq. (1) is useful when treating mixtures; see below). The so-called geometrical parameter of the mixture, $S_{12} = s_1/s_2$, is

$$S_{12} = \left(\frac{V^*_{m1}}{V^*_{m2}}\right)^{-1/3} \tag{3}$$

The relation of the parameters of the mixture with those of the pure compounds is

$$V^*_m = x_1 V^*_{m1} + x_2 V^*_{m2} \tag{4}$$

$$\varphi_i = \frac{x_i V^*_{mi}}{V^*_m} \tag{5}$$

$$\theta_2 = 1 - \theta_1 = \frac{\varphi_2}{\varphi_2 + S_{12}\varphi_1} \tag{6}$$

$$p^* = \varphi_1 p^*_1 + \varphi_2 p^*_2 - \varphi_1\theta_2 X_{12} \tag{7}$$

$$\frac{p^*}{T^*} = \varphi_1 \frac{p^*_1}{T^*_1} + \varphi_2 \frac{p^*_2}{T^*_2} \tag{8}$$

where x_i is the mole fraction of component i and, in Eq. (7), the parameter $\Delta\eta$ has been replaced by the so-called energetic parameter $X_{12} = s_1\Delta\eta/2(v^*_s)^2$. Also, using Eqs. (1) and (2) one can derive [25] simple expressions to obtain V^*_m and p^* of the pure compounds in terms of experimental molar volumes and coefficients of isobaric thermal expansion, α_p, and isothermal compressibility, κ_T:

$$V^*_m = V_m\left[\frac{3T\alpha_p + 3(1-2p\kappa_T)}{4T\alpha_p + 3(1-2p\kappa_T)}\right]^3 \tag{9}$$

$$p^* = \left(\frac{T\alpha_p}{\kappa_T} - p\right)\overline{v}^2 \tag{10}$$

Ignoring the difference between internal energy and enthalpy in condensed systems at low pressure, the molar excess enthalpy, H^E_m, can be calculated from the molar intermolecular energies of the mixture and of the pure compounds, $H^E_m = E_m - x_1E_{m1} - x_2E_{m2}$, or:

$$H^E_m = x_1 p^*_1 V^*_{m1}\left(\frac{1}{\overline{v}_1} - \frac{1}{\overline{v}}\right) + x_2 p^*_2 V^*_{m2}\left(\frac{1}{\overline{v}_2} - \frac{1}{\overline{v}}\right) + \frac{x_1 V^*_{m1}\theta_2 X_{12}}{\overline{v}} \tag{11}$$

The part in Eq. (11) containing X_{12} is named the interactional term, $H^E_{m,\text{int}}$. The rest of the contributions are called the equation of state term, $H^E_{m,\text{eos}}$. The molar volume $V_m = \overline{v}V^*_m$ of the mixture is known from the equation of state, which permits to calculate as well the molar excess volume $V^E_m = V_m - x_1V_{m1} - x_2V_{m2}$.

2.2. Estimation of the Flory energetic parameter

From the composition, pressure, temperature and the reduction parameters of the pure liquids, there are several quantities that can be directly calculated: S_{12}, V^*_m, φ_i, θ_i and the ratios p^*/T^* and $\overline{p}/\overline{T}$ (see Eqs. (3), (4)–(6) and (8)). A procedure to obtain the energetic parameter X_{12} from H^E_m at a given composition without approximations will be now exposed. From H^E_m, the value of E_m follows. Next, use the second equality of Eq. (1) to obtain $(1/\overline{v}\overline{T})$. Then, solve the equation of state for $\overline{v}$, and use the first equality of Eq. (1) to determine p^*. Finally, X_{12} can be calculated from Eq. (7).

2.3. Study of the random mixing hypothesis

If random mixing is not considered but the definition of X_{12} is used, then one can write

$$\eta = \theta_1\eta_1 + \theta_2\eta_2 - X_{12}\frac{A_{12}}{srN}\frac{2\left(v_s^*\right)^2}{s_1} = \theta_1\eta_1 + \theta_2\eta_2 - \theta_1\theta_2 X'_{12}(x_1)\frac{2\left(v_s^*\right)^2}{s_1} \quad (12)$$

where the composition-dependent parameter $X'_{12}(x_1)$ has been defined by

$$X'_{12}(x_1) = X_{12}\frac{A_{12}}{A_{12,\text{random}}} \quad (13)$$

When the random mixing hypothesis is excluded, the equations of the model for binary mixtures have the same form as when including it, by replacing X_{12} by $X'_{12}(x_1)$. Therefore, one can estimate $X'_{12}(x_1)$ from H^E_m at different compositions by exactly the same procedure considered before for X_{12} (see Section 2.2). Furthermore, if X_{12} (the Flory energetic parameter of the mixture) is considered as known, it is possible to study the deviations from the random mixing hypothesis as a function of composition, through the quantity $X'_{12}(x_1)/X_{12} = A_{12}/A_{12,\text{random}}$. In this procedure, the selection of a criterion for the value of X_{12} is implicit. Note that if X_{12} is estimated from H^E_m for some x_1 value, then the value obtained for $X'_{12}(x_1)/X_{12}$ at that composition will be 1, because, in the X_{12} estimation, random mixing is assumed.

3. Results

The physical properties (V_m, molar volume; α_p, isobaric coefficient of thermal expansion; κ_T, coefficient of isothermal compressibility) and Flory reduction parameters (V^*_m, reduction molar volume; and p^*, reduction pressure) of the pure compounds at temperature $T = 298.15$ K and pressure $p = 0.1013$ MPa are listed in Table S1. At $T \neq 298.15$ K, the values of the mentioned properties have been estimated using the well-known equations [31]:

$$V_m = V_{m0}\exp(\alpha_{p0}\Delta T) \quad (14)$$

$$\alpha_p = \alpha_{p0} + {\alpha_{p0}}^2(7 + 4\alpha_{p0}T)\frac{\Delta T}{3} \quad (15)$$

$$\frac{\alpha_p}{\kappa_T} = \frac{\alpha_{p0}}{\kappa_{T0}} - \frac{\alpha_{p0}}{\kappa_{T0}}(1 + 2\alpha_{p0}T)\frac{\Delta T}{T} \quad (16)$$

where the subscript 0 refers to the property at 298.15 K and $\Delta T = T - 298.15$ K.

The Flory energetic parameters X_{12} have been estimated from H^E_m values at equimolar composition (Table 1). Results on H^E_m and V^E_m obtained from the Flory model using them are compared with the experimental values in Table 1 and Table S2 respectively. Table 1 also includes the different contributions to H^E_m and the relative standard deviations for H^E_m, defined as:

$$\sigma_r\left(H^E_m\right) = \left[\frac{1}{N}\sum\left(\frac{H^E_{m,\,\text{exp}} - H^E_{m,\text{calc}}}{H^E_{m,\,\text{exp}}}\right)^2\right]^{1/2} \quad (17)$$

where the sum is taken for $N = 19$ data points, and $H^E_{m,\text{exp}}$ represents smoothed H^E_m values from those reported in the original works calculated at $\Delta x_1 = 0.05$ in the composition range [0.05, 0.95] by means of Redlich-Kister expansions. The mean values of $\sigma_r(H^E_m)$ for some series of compounds are shown graphically in Figs. 1 and 2. They are defined as

$$\left\langle\sigma_r\left(H^E_m\right)\right\rangle = \frac{1}{N_s}\sum\sigma_r\left(H^E_m\right) \quad (18)$$

where N_s is the number of systems considered.

4. Discussion

From now on, unless explicitly stated otherwise, we will refer to values of thermodynamic properties at 298.15 K and, in the case of excess functions, at equimolar composition. Also, n will stand for the number of C atoms in the n-alkane.

The differences between the intermolecular forces of homomorphic compounds may be estimated by the corresponding difference in their standard molar enthalpies of vaporization at 298.15 K, $\Delta H_{m,v}$. To evaluate the weight of non-dispersive interactions in the compounds under study, the quantity $\Delta\Delta H_{m,v}$ [32–34] has been calculated:

$$\Delta\Delta H_{m,v} = \Delta H_{m,v}(\text{compound}) - \Delta H_{m,v}(\text{homomorphic hydrocarbon}) \quad (19)$$

Moreover, the effect of polarity in bulk properties can be examined using the effective dipole moment, $\bar{\mu}$, defined by [35–38]:

$$\bar{\mu} = \mu\left(\frac{N_A}{4\pi\varepsilon_0 V_m k_B T}\right)^{1/2} \quad (20)$$

where N_A is Avogadro's constant, ε_0 the vacuum permittivity, k_B Boltzmann's constant, T is the temperature and μ is the dipole moment. Values of $\Delta\Delta H_{m,v}$ and $\bar{\mu}$ of some pure compounds considered in this work can be found in Table 2.

4.1. Ketone, aldehyde or linear organic carbonate + alkane systems

The excess molar enthalpies, H^E_m, of n-alkanone + n-alkane systems are large and positive, arising from the disruption of strong dipolar interactions between ketone molecules along the mixing process. On the one hand, for mixtures with a given n-alkanone, H^E_m increases with n. For example, H^E_m(2-butanone)/J·mol^{-1}: 1160 ($n = 5$, [39]) < 1254 ($n = 6$, [40]) < 1338 ($n = 7$, [39]) < 1408 ($n = 8$, [39]) < 1545 ($n = 10$, [39]) < 1661 ($n = 12$, [41]) < 1863 ($n = 16$, [41]). These values may be explained in terms of an increase of the number of ketone-ketone interactions broken by longer n-alkanes. On the other hand, H^E_m of systems including a fixed n-alkane decreases when the alkanone size is increased. In fact, $H^E_m(n = 7)$/J·mol^{-1}: 1676 (2-propanone, [42]) > 1338 (2-butanone, [39]) > 1135 (2-pentanone, [39]) > 1055 (2-hexanone, [43]) > 886 (2-heptanone, [44]). This behavior can be ascribed to a weakening of interactions between molecules of longer alkanones, because their CO group is more sterically hindered. Note that the $\Delta\Delta H_{m,v}$ and $\bar{\mu}$ values of 2-alkanones also decrease when the ketone size increases (Table 2).

In addition, H^E_m values of cyclohexane systems are larger than those of mixtures containing hexane (geometrical effect). For example, H^E_m(2-hexanone)/J·mol^{-1} = 949 ($n = 6$, [43]), 1044 (cyclohexane, [45]). The same occurs for many other mixtures, as those involving a linear amine [46] or an oxaalkane [33].

The excess molar volume, V^E_m, values of n-alkanone + n-alkane mixtures are also large and positive and change in line with H^E_m. For instance, $V^E_m(n = 7)$/cm^3·mol^{-1} = 1.130 (2-propanone, [42]) > 0.803 (2-butanone, [47]) > 0.375 (2-hexanone, [48]). Moreover, V^E_m increases with n in mixtures with a given ketone, as it is shown by the following experimental results (in cm^3·mol^{-1}) for 2-butanone systems: 0.803 ($n = 7$) < 0.866 ($n = 8$, [49]) < 0.952 ($n = 10$, [47]) < 0.996 ($n = 12$, [47]). It is clear that the main contribution to V^E_m of the mentioned solutions arises from interactional effects.

The existence of strong dipolar interactions in n-alkanone mixtures is also supported by their relatively high upper critical solution temperatures (UCST). In the case of 2-propanone systems, UCST/K = 286.2 ($n = 12$), 290.6 ($n = 14$); 300.2 ($n = 16$) [50].

n-Alkanone + n-alkane systems show rather low C^E_{pm} values (excess molar isobaric heat capacity), which is a typical feature of mixtures characterized by dipolar interactions. For example, C^E_{pm}/

Table 1
Excess molar enthalpies, H^E_m, at temperature T, pressure $p = 0.1013$ MPa and equimolar composition; X_{12}, Flory energetic parameter calculated from H^E_m at equimolar composition; $H^E_{m,int}$ and $H^E_{m,eos}$ are the interactional and equation of state contributions; $\sigma_r(H^E_m)$ are the relative standard deviations calculated according to Eq. (17).

System	X_{12}/MPa	H^E_m/J·mol^{-1}	$H^E_{m,int}$/J·mol^{-1}	$H^E_{m,eos}$/J·mol^{-1}	$\sigma_r(H^E_m)$	Ref.
Ketone + alkane; T/K = 298.15						
2-Propanone + hexane (243.15 K)	73.26	1256	978	278	0.183	[72]
2-Propanone + hexane (253.15 K)	78.82	1358	1036	322	0.159	[72]
2-Propanone + hexane (273.15 K)	83.75	1462	1066	396	0.153	[72]
2-Propanone + hexane (293.15 K)	87.61	1554	1081	473	0.151	[72]
2-Propanone + heptane	91.85	1676	1176	500	0.132	[42]
2-Propanone + decane	102.54	1968	1456	512	0.249	[50]
2-Propanone + hexadecane [a]	116.57	2377	1866	511	0.179	[50]
2-Butanone + pentane	58.85	1160	805	355	0.149	[39]
2-Butanone + hexane	60.69	1254	881	373	0.144	[40]
2-Butanone + heptane	62.71	1338	955	383	0.148	[39]
2-Butanone + octane	64.32	1408	1021	387	0.144	[39]
2-Butanone + decane	67.93	1545	1150	395	0.139	[39]
2-Butanone + dodecane	71.09	1661	1268	393	0.216	[41]
2-Butanone + hexadecane	76.32	1863	1463	400	0.214	[41]
2-Pentanone + pentane	43.92	966	694	272	0.151	[39]
2-Pentanone + hexane	44.48	1040	748	292	0.149	[40]
2-Pentanone + heptane	46.63	1135	822	313	0.144	[39]
2-Pentanone + octane	47.85	1202	881	321	0.140	[39]
2-Pentanone + decane	50.75	1335	998	337	0.136	[39]
3-Pentanone + pentane	42.14	920	662	258	0.150	[39]
3-Pentanone + hexane	43.06	999	718	281	0.146	[40]
3-Pentanone + heptane	44.60	1078	781	297	0.140	[39]
3-Pentanone + octane	45.76	1141	836	305	0.136	[39]
3-Pentanone + decane	48.35	1262	944	318	0.126	[39]
2-Hexanone + hexane	36.93	949	694	255	0.179	[43]
2-Hexanone + heptane	39.16	1055	773	282	0.158	[43]
2-Hexanone + octane	40.54	1132	835	297	0.151	[43]
2-Hexanone + nonane	41.70	1198	894	304	0.134	[43]
2-Hexanone + decane	43.12	1268	951	317	0.137	[43]
2-Heptanone + heptane	30.26	886	662	224	0.145	[44]
4-Heptanone + heptane	27.78	812	609	203	0.138	[44]
2-Octanone + dodecane	29.06	1068	822	246	0.144	[59]
2-Octanone + tetradecane	30.29	1151	901	250	0.149	[59]
2-Octanone + hexadecane	32.03	1256	984	272	0.133	[59]
2-Decanone + dodecane	22.12	937	725	212	0.157	[73]
2-Decanone + tetradecane	23.16	1020	799	221	0.164	[73]
2-Decanone + hexadecane	24.71	1126	883	243	0.151	[73]
2-Propanone + C_6H_{12}	94.19	1580	1116	464	0.139	[74]
2-Butanone + C_6H_{12}	65.93	1286	923	363	0.163	[75]
2-Pentanone + C_6H_{12}	51.80	1147	834	313	0.156	[45]
3-Pentanone + C_6H_{12}	48.57	1068	777	291	0.121	[45]
2-Hexanone + C_6H_{12}	42.79	1044	767	277	0.126	[45]
c-Pentanone + hexane	56.94	1165	869	296	0.177	[53]
c-Pentanone + heptane	58.64	1256	936	320	0.165	[53]
c-Pentanone + octane	61.01	1353	1012	341	0.176	[53]
c-Pentanone + decane	62.82	1465	1108	357	0.194	[53]
c-Pentanone + dodecane	66.40	1605	1232	373	0.190	[53]
c-Pentanone + hexadecane	85.42	2174	1695	479	0.054	[76]
c-Hexanone + hexane	45.78	1035	794	241	0.118	[53]
c-Hexanone + heptane	47.77	1139	867	272	0.145	[53]
c-Hexanone + octane	51.72	1285	976	309	0.149	[53]
c-Hexanone + decane	52.49	1381	1055	326	0.149	[53]
c-Hexanone + dodecane	54.69	1500	1158	342	0.149	[53]
c-Hexanone + hexadecane	67.49	1962	1534	428	0.107	[76]
c-Pentanone + C_6H_{12}	57.76	1132	847	285	0.153	[76]
c-Hexanone + C_6H_{12}	43.31	939	718	221	0.139	[76]
Acetophenone + pentane	58.69	1339	1056	283	0.132	[58]
Acetophenone + hexane	58.39	1437	1115	322	0.132	[77]
Acetophenone + hexane (328.15 K)	61.31	1515	1131	384	0.139	[78]
Acetophenone + heptane	57.54	1493	1152	341	0.135	[58]
Acetophenone + heptane (328.15 K)	61.88	1619	1197	422	0.129	[78]
Acetophenone + heptane (348.15 K)	63.61	1676	1203	473	0.120	[78]
Acetophenone + octane	57.03	1543	1190	353	0.142	[58]
Acetophenone + decane	56.24	1620	1253	367	0.151	[58]
Acetophenone + C_6H_{12}	56.91	1338	1036	302	0.148	[78]
Acetophenone + C_6H_{12} (328.15 K)	65.24	1550	1148	402	0.131	[78]
Acetophenone + C_6H_{12} (348.15 K)	66.78	1598	1149	449	0.124	[78]
Aldehyde + alkane; T/K = 298.15						
Ethanal + hexane	115.99	1669	1126	543	0.184	[24]
Ethanal + heptane	122.9	1796	1251	545	0.191	[24]
Ethanal + dodecane	144.78	2231	1705	526	0.175	[24]
Ethanal + hexadecane	156.46	2487	1963	524	0.152	[24]
Propanal + hexane	76.09	1343	926	417	0.226	[24]

Table 1 (*continued*)

System	X_{12}/MPa	H^E_m/J·mol^{-1}	$H^E_{m,int}$/J·mol^{-1}	$H^E_{m,eos}$/J·mol^{-1}	$\sigma_r(H^E_m)$	Ref.
Propanal + heptane	80.57	1457	1027	430	0.330	[24]
Propanal + dodecane	96.16	1863	1424	439	0.155	[24]
Propanal + hexadecane	101.92	2045	1615	430	0.182	[24]
Butanal + hexane	54.37	1126	794	332	0.181	[24]
Butanal + heptane	56.87	1218	871	347	0.182	[24]
Butanal + dodecane	67.30	1576	1205	371	0.183	[24]
Butanal + hexadecane	73.25	1792	1409	383	0.163	[24]
Benzaldehyde + hexane	55.88	1241	974	267	0.236	[60]
Benzaldehyde + heptane	57.98	1360	1057	303	0.190	[60]
Linear organic carbonate + *n*-alkane; *T*/K = 298.15						
Dimethyl carbonate + heptane	96.93	1988	1419	569	0.112	[61]
Dimethyl carbonate + decane	100.57	2205	1631	574	0.112	[61]
Diethyl carbonate + heptane	50.26	1328	951	377	0.111	[62]
Diethyl carbonate + decane	54.01	1536	1142	394	0.095	[62]
Ketone + ketone; *T*/K = 303.15						
2-Propanone + 2-butanone	1.95	29	22	7	0.035	[79]
2-Propanone + 2-pentanone	6.65	103	80	23	0.047	[79]
2-Propanone + 2-heptanone	16.27	269	215	54	0.020	[79]
2-Propanone + 2-octanone	21.49	367	292	75	0.033	[79]
2-Propanone + 2-undecanone	30.99	560	458	102	0.047	[79]
2-Butanone + 2-pentanone	0.99	17	14	3	0.061	[79]
2-Butanone + 2-heptanone	5.16	97	81	16	0.043	[79]
2-Butanone + 2-octanone	8.27	163	133	30	0.032	[79]
2-Butanone + 2-undecanone	16.64	354	292	62	0.032	[79]
2-Pentanone + 2-heptanone	1.77	38	31	7	0.054	[79]
2-Pentanone + 2-octanone	3.51	81	66	15	0.031	[79]
2-Pentanone + 2-undecanone	8.82	218	179	39	0.031	[79]
Ketone + linear organic carbonate; *T*/K = 298.15						
2-Propanone + dimethyl carbonate	12.51	187	139	48	0.207	[80]
2-Propanone + diethyl carbonate	13.74	232	169	63	0.378	[80]
2-Butanone + dimethyl carbonate	15.26	274	198	76	0.173	[80]
2-Butanone + diethyl carbonate	7.17	144	103	41	0.512	[80]
2-Pentanone + dimethyl carbonate	18.56	376	275	101	0.200	[80]
2-Pentanone + diethyl carbonate	6.82	154	113	41	0.364	[80]
2-Hexanone + dimethyl carbonate	23.43	519	383	136	0.251	[80]
2-Hexanone + diethyl carbonate	8.67	214	161	53	0.219	[80]
2-Octanone + dimethyl carbonate	29.11	742	562	180	0.120	[80]
2-Octanone + diethyl carbonate	12.43	351	275	76	0.098	[80]
2-Undecanone + dimethyl carbonate	34.58	1028	799	229	0.054	[80]
2-Undecanone + diethyl carbonate	17.15	568	458	110	0.033	[80]
c-Hexanone + dimethyl carbonate	25.81	502	392	110	0.052	[81]
c-Hexanone + diethyl carbonate	11.91	244	203	41	0.050	[81]

[a] There is a partial immiscibility region.

J·mol^{-1}·K^{-1} = 2.9 (2-propanone + *n*-C_7, [51]); 3.7 (2-propanone + *n*-C_{16}, [52]); 1.8 (2-butanone + *n*-C_7, [47]). Their $C^E_{pm}(x_1)$ curves are S-shaped (2-butanone + *n*-C_7, [47]) or W-shaped (2-propanone, or 2-butanone + *n*-C_{12}, [52]). The latter have been interpreted in terms of non-random effects, typically more important when temperature is close to the UCST. The C^E_{pm} function then depends strongly on temperature (it is a decreasing function of *T*) and on the length of the *n*-alkane [52].

H^E_m values of systems containing a cyclic alkanone (1035 J·mol^{-1} for the cyclohexanone + *n*-C_6 mixture [53]) are larger than those of mixtures with homomorphic 2-alkanones (cyclization effect). $\Delta\Delta H_{m,v}$ and $\bar{\mu}$ values of cycloalkanones are also higher. For example, $\Delta\Delta H_{m,v}$/kJ·mol^{-1} and $\bar{\mu}$ values are, respectively, 12.05 [54], 1.337 [55] for cyclohexanone, and 11.41 [56], 0.913 [55] for 2-hexanone. This allows conclude that ketone-ketone interactions are then stronger in the case of cycloalkanones. Interestingly, V^E_m values of mixtures with a given alkane are higher for solutions with 2-alkanones, indicating that structural effects are more relevant in cycloalkanone systems. In this framework, the negative V^E_m value of the cyclohexanone + *n*-C_6 mixture (−0.323 cm^3·mol^{-1} [53]) remarks the existence of strong structural effects in such a solution, as the corresponding H^E_m value is positive [57].

Acetophenone mixtures are characterized by rather high UCST/K values: 277.36 (n = 10), 283.57 (n = 12), 289.90 (n = 14) and 295.16 (n = 16) [15], and, consequently, the corresponding H^E_m values are also large (1620 J·mol^{-1} [58] for the decane solution). The latter value is considerably higher than that of the 2-octanone + *n*-C_{12} mixture (1068 J·mol^{-1} [59]). Therefore, interactions between alkanone molecules are stronger in systems involving aromatic ketones. This has been attributed to the existence of proximity effects between the CO group and the aromatic ring placed in the same molecule, which leads to enhanced dipolar alkanone-alkanone interactions [15,16]. Accordingly, values of $\Delta\Delta H_{m,v}$ and $\bar{\mu}$ of acetophenone are higher than those of 2-octanone (Table 2).

Mixtures of *n*-alkanal or 2-alkanone + *n*-alkane behave similarly. For example, $H^E_m(n = 7)$/J·mol^{-1} = 1796 > 1457 > 1218 > 1066 for ethanal, propanal, butanal and pentanal respectively [24]. It is noteworthy that: (i) systems formed by 2-alkanone and heptane show higher H^E_m values than those of mixtures with homomorphic *n*-alkanals (see above); (ii) values of $\Delta\Delta H_{m,v}$ and $\bar{\mu}$ are also higher for 2-alkanones. For instance, $\Delta\Delta H_{m,v}$/kJ·mol^{-1} = 16.20 (2-propanone) > 14.83 (propanal) [54], and $\bar{\mu}$ = 1.281 (2-propanone) > 1.214 (propanal) [55]. Thus, intermolecular interactions are stronger in *n*-alkanone systems.

Proximity effects are also present in benzaldehyde mixtures, which show the following UCST/K values: 278.54 (n = 10), 284.74 (n = 12), 290.06 (n = 14) and 297.98 (n = 16) [18]. In addition, H_m^E(benzaldehyde + *n*-heptane) = 1360 J·mol^{-1} [60] is larger than the value for the pentanal mixture. This shows again that the interactions

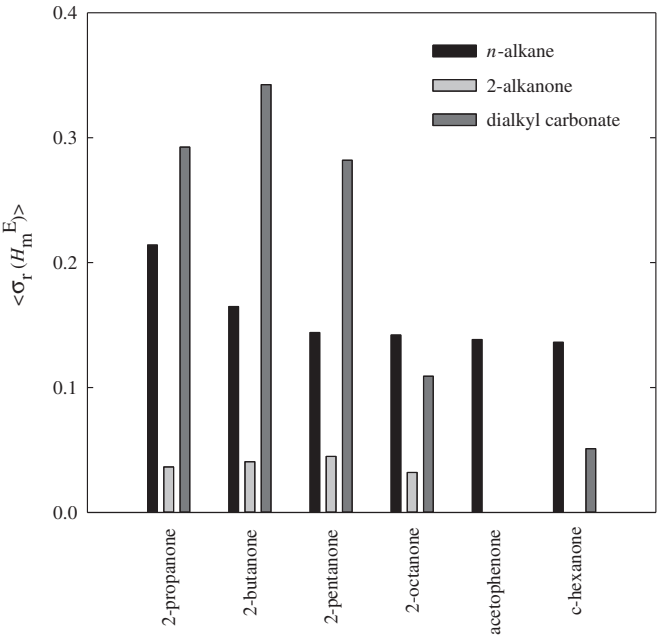

Fig. 1. Mean relative standard deviations of the Flory model, $\langle \sigma_r(H_m^E) \rangle$ (Eq. (18)), of several homologous series of the binary mixtures 2-alkanone + *n*-alkane, or + 2-alkanone, or + dialkyl carbonate.

are stronger when the carbonyl group is attached to an aromatic ring, and it is as well remarked by the corresponding $\Delta\Delta H_{m,v}$ and $\bar{\mu}$ values (Table 2). On the other hand, UCST values are slightly higher for benzaldehyde mixtures than for acetophenone solutions. It seems that dipolar interactions are slightly stronger when the alkanal is involved.

Comments similar to those given above for 2-alkanone + alkane mixtures are valid for the corresponding systems with linear organic carbonates. The large positive values of $H_m^E(n = 7)/J \cdot mol^{-1} = 1988$ (dimethyl carbonate (DMC), [61]); 1328 (diethyl carbonate (DEC), [62]) and of the UCST/K for DMC solutions (297.62, 307.61 and 316.21 for $n = 12, 14, 16$ [63] respectively) point out to the existence of strong interactions between carbonate molecules. The V_m^E values are very large and change in line with H_m^E. For example, $V_m^E(DMC)/cm^3 \cdot mol^{-1} =$ 1.158 ($n = 7$); 1.442 ($n = 10$) [64]. Interestingly, H_m^E of mixtures with the same alkane and homomorphic 2-alkanones (2-propanone, 3-pentanone) are lower. All these considerations reveal that dipolar interactions are weaker in ketone systems. In this framework, the very low $\bar{\mu}$ values of DMC (0.391) and DEC (0.312) [65] are remarkable. They suggest that the size of the group may also play an important role when determining the thermodynamic properties.

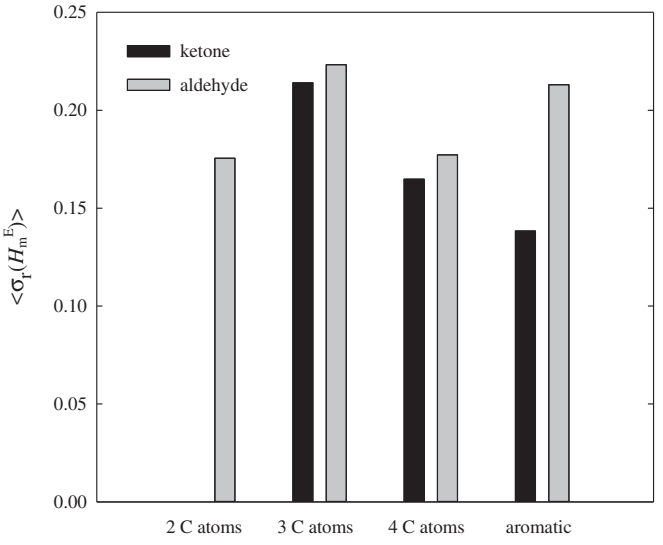

Fig. 2. Mean relative standard deviations of the Flory model, $\langle \sigma_r(H_m^E) \rangle$ (Eq. (18)), of several homologous series of binary systems of the form ketone or alkanal + *n*-alkane (2 C atoms, ethanal; 3 C atoms, 2-propanone or propanal; 4 C atoms, 2-butanone or butanal; aromatic, acetophenone or benzaldehyde).

4.2. Ketone + ketone or organic carbonate systems

In 2-alkanone + alkane mixtures, the replacement of the alkane by a ketone or a linear organic carbonate leads to decreased H_m^E values, which underlines the existence of interactions between unlike molecules. Neglecting structural effects [35,66], it is possible to consider that the H_m^E of A + B mixture (here, A is a ketone and B is either a ketone or a linear organic carbonate) is the result of different contributions. Positive contributions, $\Delta H_m^{A\text{-}A}$ and $\Delta H_m^{B\text{-}B}$, arise from the breaking of interactions between like molecules during the mixing process, which can be evaluated from H_m^E data for A or B + heptane systems, respectively. The negative contribution, $\Delta H_m^{A\text{-}B}$, comes from the creation of interactions between unlike molecules. At equimolar composition, $\Delta H_m^{A\text{-}B}$ may be then determined from the expression:

$$\Delta H_m^{A\text{-}B} = H_m^E(A + B) - H_m^E(A + \text{heptane}) - H_m^E(B + \text{heptane}) \quad (21)$$

The calculated values of $\Delta H_m^{A\text{-}B}$ are listed in Table 3. We note that $|\Delta H_m^{A\text{-}B}|$ diminishes when, for a given solute (e.g., 2-propanone), the solvent size (2-alkanone or carbonate) increases. This clearly indicates that, at such conditions, interactions between unlike molecules are weakened, probably because the polar group of the solvent is more sterically hindered. It explains the observed increase of H_m^E along the homologous series 2-propanone + organic solvent (=2-alkanone, carbonate), as the $\Delta H_m^{A\text{-}B}$ term is less negative. In addition, ketone-carbonate interactions are quite similar to those of ketone-ketone type. For example, $|\Delta H_m^{A\text{-}B}|/J \cdot mol^{-1} = 2985$ (2-propanone + 2-butanone); 3052 (DMC + 2-butanone); 2708 (2-propanone + 2-pentanone); 2747 (DMC + 2-pentanone). Similarly, mixtures with carbonates and 2-hexanone or cyclohexanone show similar $|\Delta H_m^{A\text{-}B}|$ values. The cyclization effect is here of minor importance.

It is remarkable that H_m^E values of 2-alkanone (A) + carbonate (B), systems are higher for solutions with DMC, except for the acetone mixture. This can be analyzed taking into account the relative weight of the different contributions to H_m^E: (i) the positive $\Delta H_m^{B\text{-}B}$ term is higher for DMC systems; (ii) however, the positive $\Delta H_m^{A\text{-}A}$ contribution should be higher for DEC systems, due to the larger aliphatic surface of this carbonate; (iii) the $\Delta H_m^{A\text{-}B}$ term is more negative when DMC is involved (Table 3). For mixtures not including acetone, $H_m^E(DMC) > H_m^E(DEC)$, and this indicates that, in DMC mixtures, the increased $\Delta H_m^{B\text{-}B}$ value compensates the lower $\Delta H_m^{A\text{-}A} + \Delta H_m^{A\text{-}B}$ result. For the acetone mixtures, the opposite behavior is encountered and $H_m^E(DMC) < H_m^E(DEC)$.

4.3. Results from the Flory model

For alkane mixtures, X_{12} values are large and positive, indicating the existence of strong interactions between like polar molecules. We note that $H_{m,int}^E$ is the dominant contribution to H_m^E (Table 1). Nevertheless, the $H_{m,eos}^E$ term, which depends on the reduced volume of the solution compared to those of the pure components, is rather large. This contribution is ranged between 32.5% for ethanal + heptane and 16.5% for 2-butanone + 2-heptanone (Table 1). As a general trend, better results are obtained the lower the $H_{m,eos}^E$ values are. On the other hand, X_{12} and H_m^E change in line (Table 1), which remarks the relevance of interactional effects on H_m^E. Interestingly, in the case of 2-alkanone or *n*-alkanal + heptane mixtures, a linear relationship exists between $\Delta\Delta H_{vap}$ and X_{12}. In fact, $\Delta\Delta H_{vap}(2\text{-alkanone})/kJ \cdot mol^{-1} = 7.86 + 0.089X_{12}/MPa$ (r, correlation coefficient, 0.994); and $\Delta\Delta H_{vap}(n$-

Table 2
Standard molar enthalpies of vaporization, $\Delta H_{m,v}$, differences of standard molar enthalpy of vaporization with respect to the homomorphic hydrocarbon at 298.15 K, $\Delta\Delta H_{m,v}$ (Eq. (19)), dipole moments, μ, and effective dipole moments, $\bar{\mu}$ (Eq. (20)), at $T = 298.15$ K and $p = 0.1013$ MPa of some pure compounds.

Compound	$\Delta H_{m,v}$/kJ·mol^{-1}	$\Delta\Delta H_{m,v}$/kJ·mol^{-1}[a]	μ/D	$\bar{\mu}$
2-Propanone	30.99 [54]	16.20	2.88 [55]	1.281
2-Butanone	34.79 [54]	13.17	2.779 [55]	1.12
2-Pentanone	38.40 [54]	11.97	2.70 [55]	0.996
3-Pentanone	38.52 [54]	12.09	2.82 [55]	1.046
2-Hexanone	42.97 [56]	11.41	2.66 [55]	0.913
2-Heptanone	47.24 [54]	10.67	2.59 [55]	0.835
4-Heptanone	47.8 [82]	11.23		
2-Octanone	51.8 [83]	10.31	2.70 [55]	0.823
c-Pentanone	42.72 [54]	14.20	3.3 [55]	1.337
c-Hexanone	45.06 [54]	12.05	3.246 [55]	1.216
Acetophenone	53.39 [83]	11.15	3.02 [55]	1.066
Ethanal	25.47 [54]	20.31	2.750 [55]	1.392
Propanal	29.62 [54]	14.83	2.72 [55]	1.214
Butanal	33.68 [83]	12.06	2.72 [55]	1.093
Benzaldehyde	50.30 [83]	12.29	3.0 [55]	1.136
Dimethyl carbonate	38.0 [84]	16.38[b]	0.94 [65]	0.391
Diethyl carbonate	43.60 [54]	12.04[b]	0.90 [65]	0.312

[a] Values of $\Delta H_{m,v}$ of the corresponding homomorphic hydrocarbon were taken from the recommended values in ref. [54].
[b] Relative to the *n*-alkane with one more C atom.

alkanal)/kJ·mol^{-1} = 4.84 + 0.0125X_{12}/MPa ($r = 0.999$). This also supports the close relation between X_{12} and interactional effects. We have applied the same approach to dialkyl ether + heptane systems using the values of $\Delta\Delta H_{vap}$ and X_{12} reported previously in our investigation on oxaalkane + alkane systems in terms of the Flory model [12]. The result is: $\Delta\Delta H_{vap}$/kJ·mol^{-1} = −2.243 + 0.1814X_{12}/MPa ($r = 0.982$). We note that for not very large X_{12} values (e.g., 7.10 MPa for the dipropyl ether mixture [12]), $\Delta\Delta H_{vap}$ values become negative, which reveals very weak interactions between dialkyl ether molecules. The replacement of an alkane by an *n*-alkanone or a linear organic carbonate leads to decreased X_{12} values, due to the creation of interactions between unlike molecules during the mixing process (Table 1 and Table 3). For 2-propanone + 2-alkanone mixtures, the linear dependence between $\Delta\Delta H_{vap}$ and X_{12} is somewhat poorer: $\Delta\Delta H_{vap}$/kJ·mol^{-1} = 13.2 − 0.144X_{12}/MPa ($r = 0.958$). Here, the negative slope deserves attention, as it implies that when $\Delta\Delta H_{vap}$ increases X_{12} decreases, which means that interactions between unlike molecules become more relevant.

Table 3
Contribution to the excess molar enthalpy of interactions between unlike molecules, ΔH_m^{A-B} (Eq. (21)), of ketone + ketone or + linear organic carbonate systems at $T = 298.15$ K and $p = 0.1013$ MPa.

System	ΔH_m^{A-B}/J·mol^{-1}[a]
Ketone + ketone	
2-Propanone + 2-butanone	−2985
2-Propanone + 2-pentanone	−2708
2-Propanone + 2-heptanone	−2293
2-Butanone + 2-pentanone	−2456
2-Butanone + 2-heptanone	−2127
2-Pentanone + 2-heptanone	−1983
Ketone + linear organic carbonate	
2-Propanone + dimethyl carbonate	−3477
2-Propanone + diethyl carbonate	−2772
2-Butanone + dimethyl carbonate	−3052
2-Butanone + diethyl carbonate	−2522
2-Pentanone + dimethyl carbonate	−2747
2-Pentanone + diethyl carbonate	−2309
2-Hexanone + dimethyl carbonate	−2524
2-Hexanone + diethyl carbonate	−2169
c-Hexanone + dimethyl carbonate	−2625
c-Hexanone + diethyl carbonate	−2223

[a] For references of H_m^E (ketone + *n*-heptane), see Table 1. The values of H_m^E (linear organic carbonate + *n*-heptane) were taken from refs. [61,62].

Inspection of Table S2 shows that the theoretical V_m^E results are larger than the experimental values, as the interactional contribution from the Flory model to this excess function is overestimated. Nevertheless, the relative variation of V_m^E with the alkane size in mixtures with a given polar component is correctly given by the model. The same trend is also encountered, for example, in oxaalkane + alkane mixtures [12]. The V_m^E results can be better rationalized by means of the Prigogine-Flory-Patterson model [67] (Fig. 5). Here, V_m^E is written as the sum of three contributions: an interactional contribution, a curvature term and the so-called p^* term. The second one depends on $-(\bar{v}_1-\bar{v}_2)^2$ and is always negative. The last one depends on $(p_1^*-p_2^*)(\bar{v}_1-\bar{v}_2)$. For the alkanone + alkane systems considered, $p_1^* > p_2^*$ and the sign of the p^* term depends on that of $(\bar{v}_1-\bar{v}_2)$. For the cyclohexanone + hexane, or + heptane mixtures, the $(\bar{v}_1-\bar{v}_2)$ values are negative and rather large. The contributions from the curvature and p^* terms are then also large and negative and the model predicts low V_m^E values for these systems. Particularly, V_m^E(hexane)/cm^3·mol^{-1} = −0.323 (experimental); −0.194 (calculated). For $(\bar{v}_1-\bar{v}_2) > 0$, the p^* contribution is also positive and may be rather large. The corresponding V_m^E values are then largely overestimated, as the curvature term is usually small in absolute value.

4.3.1. Alkanone + alkane

We note that, in the framework of the Flory model, orientational effects are quite similar in 2-alkanone mixtures (Fig. 6, Table 1). It is noteworthy that the theoretical results are somewhat poorer when temperature is not far from the corresponding UCST. This is the case of the systems 2-propanone + hexane at 243.15 K (UCST = 237.2 K [68]; $\sigma_r(H_m^E) = 0.183$); or + decane at 298.15 K (UCST = 266.8 K [69]; $\sigma_r(H_m^E) = 0.249$); or + hexadecane at 298.15 K (UCST = 300.6 K [41]; $\sigma_r(H_m^E) = 0.179$). The mixtures 2-butanone + dodecane ($\sigma_r(H_m^E) = 0.214$), or + tetradecane ($\sigma_r(H_m^E) = 0.214$) at 298.15 K are also close to the UCST and the C_{pm}^E curves are W-shaped [47], a behavior typically ascribed to non-random effects. Interestingly, the position of the CO group has not a special relevance on orientational effects. In fact, $\langle\sigma_r(H_m^E)\rangle = 0.144$ (2-pentanone) ≈ 0.140 (3-pentanone). In addition, $\langle\sigma_r(H_m^E)\rangle$ values are also rather similar for homologous series including linear or cyclic alkanones. In fact, $\langle\sigma_r(H_m^E)\rangle = 0.144$ (2-pentanone); 0.156 (cyclopentanone); 0.152 (2-hexanone); 0.136 (cyclohexanone). We have applied the UNIFAC model (Dortmund version) [43] to linear or cyclic alkanone + alkane mixtures assuming that these systems differ merely by the presence of the *c*-CH_2 group in cyclic

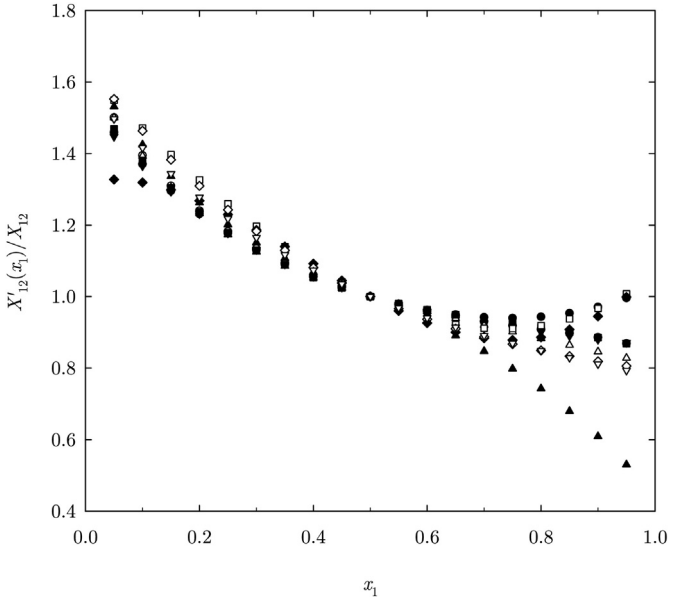

Fig. 3. Representation of $X_{12}(x_1)/X_{12}$ (Eq. (13)) for several systems ketone or aldehyde + heptane as functions of the mole fraction of component 1, x_1. Symbols: 2-propanone (●), 2-butanone (○), 2-pentanone (▼), 2-hexanone (△), 2-heptanone (■), cyclopentanone (□), cyclohexanone (◆), ethanal (◇), propanal (▲), and butanal (▽).

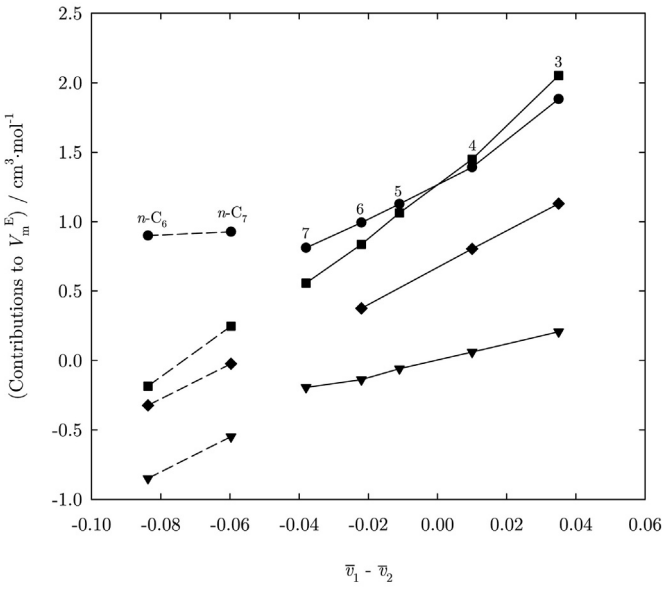

Fig. 5. Contributions to the excess molar volume, V_m^E, according to the Prigogine-Flory-Patterson model, represented in terms of the difference between the reduced volumes of the components 1 and 2, $\overline{v}_1 - \overline{v}_2$. Solid lines, 2-alkanone + heptane systems (the numbers indicate the carbon atoms of the 2-alkanone). Dashed lines, cyclohexanone + *n*-alkane mixtures (*n*-C_6, hexane; *n*-C_7, heptane). Full symbols: interactional contribution (●), p^* term (▼), total V_m^E from the model (■), experimental values (◆).

alkanones –in other words, using the same set of interaction parameters [43] for those contacts where the CO group participates. The results are: $\langle \sigma_r(H_m^E) \rangle = 0.063$ (linear alkanone; $N_S = 42$), and 0.086 (cyclic alkanone; $N_S = 13$). It is remarkable that the largest differences for cycloalkanone mixtures are encountered for the systems with hexadecane ($\sigma_r(H_m^E) = 0.151$ for the cyclopentanone solution). This may be ascribed, at least to some extent, to the existence of the Patterson effect [70,71]. It is known that this effect leads to an extra endothermic contribution to H_m^E, attributed to the destruction of correlations of molecular orientations existing between long *n*-alkanes by a globular or a plate-like molecule [70,71]. The UNIFAC results reveal that: (i) orientational effects are practically independent on the *n*-alkanone under consideration; (ii) the cyclization effect is rather negligible. In the case of acetophenone mixtures, the Flory model provides $\langle \sigma_r(H_m^E) \rangle = 0.135$, a close value to that of 2-octanone systems (0.142). Nevertheless, $\sigma_r(H_m^E)$ is somewhat large for the acetophenone + decane mixture (0.151), whose UCST = 277.4 K [15].

Of course, the rise in temperature is linked in most cases with better theoretical results (Table 1), which agrees with the fact that random mixing effects are more relevant with this increase. For example, for the 2-propanone + *n*-hexane system, $\sigma_r(H_m^E) = 0.183$ (243.15 K) > 0.151 (293.15 K) [72].

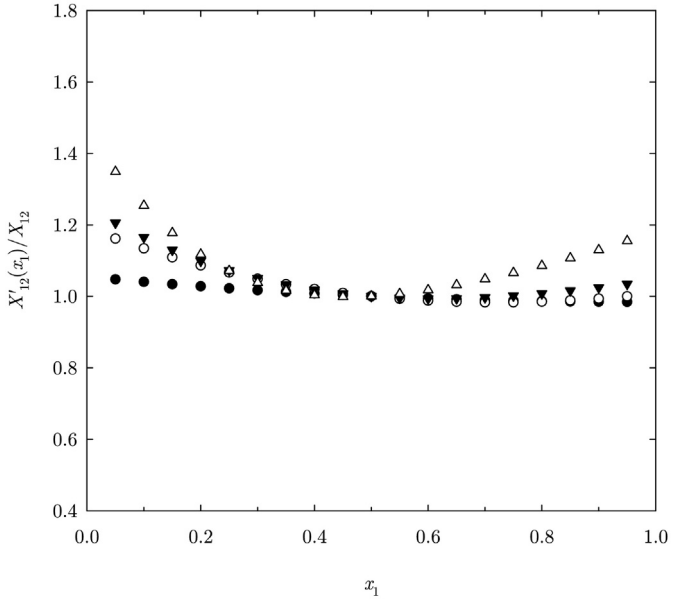

Fig. 4. Representation of $X_{12}(x_1)/X_{12}$ (Eq. (13)) for several systems ether + heptane at 298.15 K as functions of the mole fraction of component 1, x_1. Symbols: dipropyl ether (●), 2,5-dioxahexane (○), 2,5,8-trioxanonane (▼), 2,5,8,11,14-pentaoxapentadecane (△).

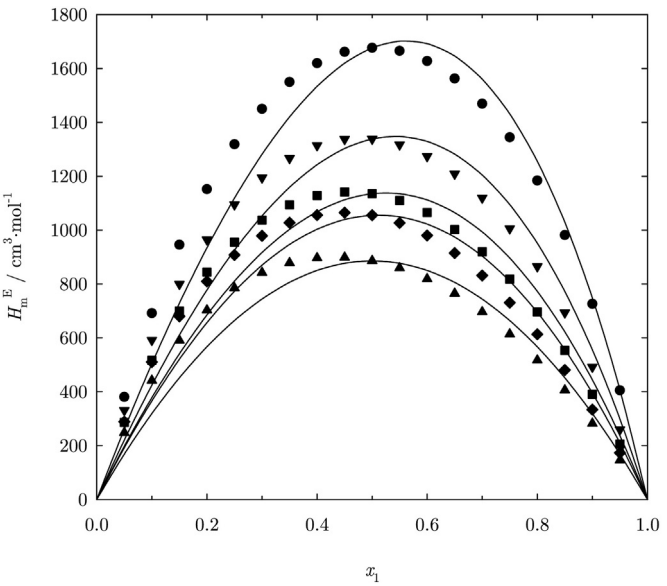

Fig. 6. Excess molar enthalpies, H_m^E, of 2-alkanone + heptane systems as functions of the mole fraction of component 1, x_1. Full symbols, smoothed experimental results: 2-propanone (●), 2-butanone (▼), 2-pentanone (■), 2-hexanone (◆), 2-heptanone (▲). Solid lines, calculations from the Flory model.

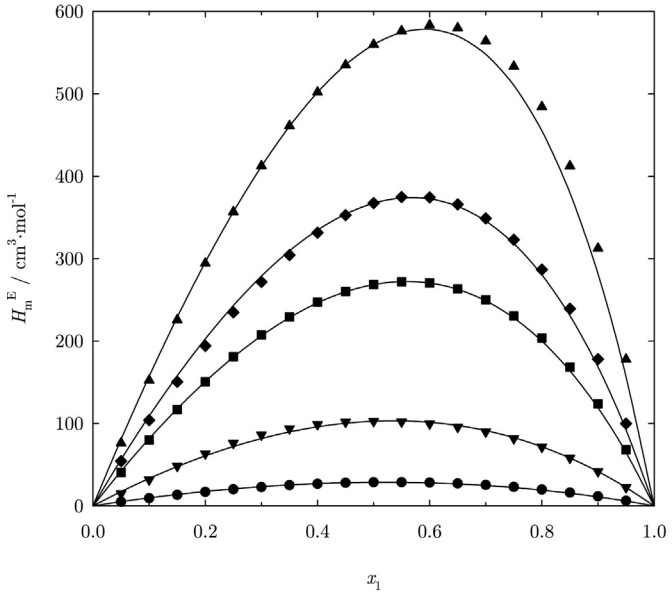

Fig. 7. Excess molar enthalpies, H_m^E, of 2-propanone + *n*-alkanone systems, as functions of the mole fraction of component 1, x_1. Full symbols, smoothed experimental results: 2-butanone (●), 2-pentanone (▼), 2-heptanone (■), 2-octanone (◆), 2-undecanone (▲). Solid lines, calculations from the Flory model.

4.3.2. Alkanal + alkane

The larger $\sigma_r(H_m^E)$ values obtained for the propanal + hexane (0.226), or + heptane (0.333) mixtures are remarkable, as they do not fit into the results for the remaining systems. These large values may be due to experimental inaccuracies. Or they might arise because some of the H_m^E values at low mole fractions of one component are not reliable enough, since they were obtained from Redlich-Kister regressions with coefficients determined from H_m^E measurements at the central range of composition. Similar comments are also valid for benzaldehyde mixtures. Nevertheless, Flory results are very close for butanal or 2-butanone mixtures. Orientational effects do not change when replacing the CO group by the CHO group.

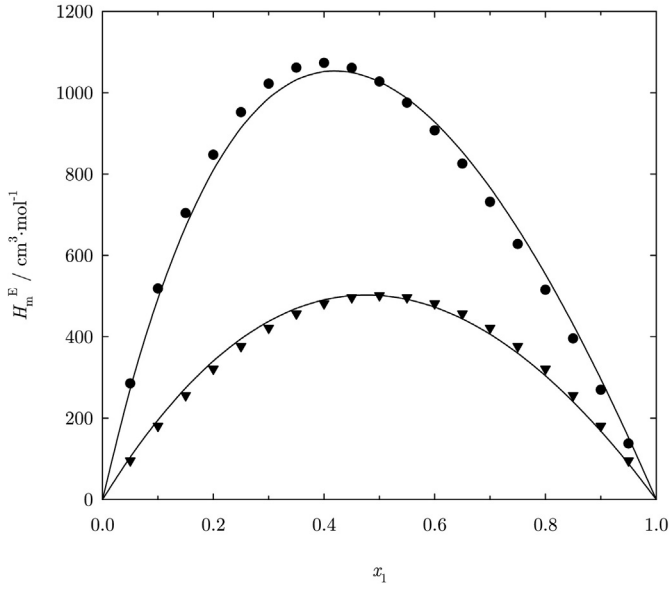

Fig. 8. Excess molar enthalpies, H_m^E, of *n*-alkanone + dimethyl carbotane systems, as functions of the mole fraction of component 1, x_1. Full symbols, smoothed experimental results: 2-undecanone (●), cyclohexanone (▼). Solid lines, calculations from the Flory model.

Fig. 3 shows the plots of $X_{12}^{1/2}(x_1)/X_{12}$ for several systems containing heptane as functions of x_1. It must be remarked that the shape of this function is, to a large extent, not dependent on the 2-alkanone considered, or on if the 2-alkanone is replaced by a cycloalkanone, acetophenone or an *n*-alkanal. This supports that orientational effects are similar for all the systems studied with the CO or the CHO groups. In contrast, such a general behavior is not observed in ether + heptane systems [12], as it is shown in Fig. 4 for various systems of this type realized using data reported earlier [12].

4.3.3. Linear organic carbonate + alkane

Experimental data show that interactions between polar linear molecules become stronger in the sequence: alkanal < alkanone < carbonate. As already pointed out, H_m^E and UCST values are higher for carbonate mixtures. However, theoretical results are slightly better for systems with DMC or DEC than for solutions with 2-propanone or 3-pentanone, indicating that orientational effects are weaker in carbonate systems. This might be explained in terms of higher TS_m^E values ($TS_m^E = H_m^E - G_m^E$; G_m^E, excess molar Gibbs energy) for carbonate mixtures. The application of the DISQUAC model to *n*-alkanone [37] or linear carbonate [19] + heptane mixtures at 298.15 K provides G_m^E/J·mol^{-1} = 1112 (2-propanone); 715 (3-pentanone); 1199 (DMC); 788 (DEC). Using these values, we obtain TS_m^E(heptane)/J·mol^{-1} = 789 (DMC); 564 (2-propanone); 540 (DEC); 363 (3-pentanone).

4.3.4. n-Alkanone + n-alkanone, or + alkanone + linear organic carbonate

For 2-alkanone + 2-alkanone systems (Fig. 7), the random mixing hypothesis is valid to a rather large extent. The replacement of the CO group by the OCOO group has a negative impact on the results from the model. For 2-alkanone + dialkyl carbonate systems, $\langle\sigma_r(H_m^E)\rangle$ = 0.293 (2-propanone), 0.343 (2-butanone), 0.282 (2-pentanone), 0.235 (2-hexanone), 0.109 (2-octanone), and 0.044 (2-undecanone). These results underline that ketone-carbonate interactions are of a more polar nature for the shorter 2-alkanones, as it is seen as well from the $\Delta H_m^{A\text{-}B}$ values (Table 3). In contrast, the behavior of the mixtures cyclohexanone + diakyl carbonate is close to random mixing (Fig. 8).

5. Conclusions

The Flory model has been applied to alkanone, or alkanal or linear organic carbonate + alkane mixtures, and to *n*-alkanone + *n*-alkanone or alkanone + dialkyl carbonate systems. For alkane mixtures, the mean relative standard deviation for the excess molar enthalpies, $\langle\sigma_r(H_m^E)\rangle$, is: 0.152 (*n*-alkanone); 0.134 (cyclic alkanone); 0.135 (acetophenone); 0.192 (*n*-alkanal); 0.213 (benzaldehyde); 0.107 (linear organic carbonate). These results show that orientational effects in alkane mixtures are practically independent of steric effects, or of the position of the polar group in a linear chain, in a ring or in an aromatic ring. In addition, orientational effects are similar in systems containing alkanones or alkanals. Binary systems formed by two *n*-alkanones show a behavior close to random mixing ($\langle\sigma_r(H_m^E)\rangle = 0.039$). In contrast, orientational effects are strong in systems with shorter *n*-alkanones and dialkyl carbonates ($\langle\sigma_r(H_m^E)\rangle = 0.230$). Mixtures with longer alkanones and cyclohexanone are close to random mixing ($\langle\sigma_r(H_m^E)\rangle = 0.047$).

Funding

The authors gratefully acknowledge the financial support received from the Consejería de Educación y Cultura of Junta de Castilla y León, under Project BU034U16. F. Hevia also gratefully acknowledges the grant FPU14/04104 received from the program 'Ayudas para la Formación de Profesorado Universitario (convocatoria 2014)', from Ministerio de Educación, Cultura y Deporte, Gobierno de España.

Appendix A. Supplementary data

This material contains, at temperature $T = 298.15$ K and pressure $p = 0.1013$ MPa: i) the physical properties and Flory reduction parameters of the pure compounds; and ii) the experimental excess molar volumes, together with the corresponding Flory calculations, for ketone or dialkyl carbonate + alkane systems.

References

[1] H.V. Kehiaian, Group contribution methods for liquid mixtures: a critical review, Fluid Phase Equilib. 13 (1983) 243–252, http://dx.doi.org/10.1016/0378-3812(83)80098-3.

[2] A. Heintz, A new theoretical approach for predicting excess properties of alkanol/alkane mixtures, Ber. Bunsenges. Phys. Chem. 89 (1985) 172–181, http://dx.doi.org/10.1002/bbpc.19850890217.

[3] P.J. Flory, Statistical thermodynamics of liquid mixtures, J. Am. Chem. Soc. 87 (1965) 1833–1838, http://dx.doi.org/10.1021/ja01087a002.

[4] J.G. Kirkwood, F.P. Buff, The statistical mechanical theory of solutions. I, J. Chem. Phys. 19 (1951) 774–777, http://dx.doi.org/10.1063/1.1748352.

[5] A. Ben-Naim, Inversion of the Kirkwood–Buff theory of solutions: application to the water–ethanol system, J. Chem. Phys. 67 (1977) 4884–4890, http://dx.doi.org/10.1063/1.434669.

[6] J.C. Cobos, An exact quasi-chemical equation for excess heat capacity with W-shaped concentration dependence, Fluid Phase Equilib. 133 (1997) 105–127, http://dx.doi.org/10.1016/S0378-3812(97)00012-5.

[7] J.A. González, Á. Mediavilla, I. García de la Fuente, J.C. Cobos, C. Alonso Tristán, N. Riesco, Orientational effects and random mixing in 1-alkanol + alkanone mixtures, Ind. Eng. Chem. Res. 52 (2013) 10317–10328, http://dx.doi.org/10.1021/ie4019269.

[8] J.A. González, I. García de la Fuente, J.C. Cobos, C. Alonso Tristán, L.F. Sanz, Orientational effects and random mixing in 1-alkanol + nitrile mixtures, Ind. Eng. Chem. Res. 54 (2015) 550–559, http://dx.doi.org/10.1021/ie504282s.

[9] J.A. González, N. Riesco, I. Mozo, I. García De La Fuente, J.C. Cobos, Application of the Flory theory and of the Kirkwood—Buff formalism to the study of orientational effects in 1-alkanol + linear or cyclic monoether mixtures, Ind. Eng. Chem. Res. 48 (2009) 7417–7429, http://dx.doi.org/10.1021/ie9004354.

[10] J.A. González, Á. Mediavilla, I.G. De la Fuente, J.C. Cobos, Thermodynamics of 1-alkanol + linear polyether mixtures, J. Chem. Thermodyn. 59 (2013) 195–208, http://dx.doi.org/10.1016/j.jct.2012.12.007.

[11] J.A. González, N. Riesco, I. Mozo, I. García De La Fuente, J.C. Cobos, Thermodynamics of mixtures containing alkoxyethanols. XXI. Application of the Flory theory to the study of orientational effects in systems with dibutyl ether or 1-butanol, Ind. Eng. Chem. Res. 46 (2007) 1350–1359, http://dx.doi.org/10.1021/ie0609012.

[12] J.A. González, Thermodynamics of mixtures containing oxaalkanes. 4. Random mixing and orientational effects in ether + alkane systems, Ind. Eng. Chem. Res. 49 (2010) 9511–9524, http://dx.doi.org/10.1021/ie101264p.

[13] J.A. González, I. García De La Fuente, J.C. Cobos, I. Mozo, I. Alonso, Thermodynamics of mixtures containing oxaalkanes. 6. Random mixing in ether + benzene, or + toluene systems, Thermochim. Acta 514 (2011) 1–9, http://dx.doi.org/10.1016/j.tca.2010.11.023.

[14] H.V. Kehiaian, S. Porcedda, B. Marongiu, L. Lepori, E. Matteoli, Thermodynamics of binary mixtures containing linear or cyclic alkanones + *n*-alkanes or + cycloalkanes, Fluid Phase Equilib. 63 (1991) 231–257, http://dx.doi.org/10.1016/0378-3812(91)80035-T.

[15] J.A. González, C. Alonso-Tristán, I.G.D.L. Fuente, J.C. Cobos, Liquid-liquid equilibria for acetophenone + *n*-alkane mixtures and characterization of acetophenone systems using DISQUAC, Fluid Phase Equilib. 391 (2015) 39–48, http://dx.doi.org/10.1016/j.fluid.2015.01.026.

[16] J.A. González, C. Alonso-Tristán, I.G. de la Fuente, J.C. Cobos, Thermodynamics of aromatic polar compound (alkanone, alkanal or alkanoate) + hydrocarbon mixtures, Fluid Phase Equilib. 421 (2016) 49–58, http://dx.doi.org/10.1016/j.fluid.2016.04.004.

[17] M.R. Tiné, B. Marongiu, Application of the DISQUAC group contribution model to binary liquid organic mixtures containing alkanals, Thermochim. Acta 199 (1992) 63–75, http://dx.doi.org/10.1016/0040-6031(92)80251-Q.

[18] J.A. González, C. Alonso-Tristán, I.G. de la Fuente, J.C. Cobos, Liquid-liquid equilibria for benzaldehyde + *n*-alkane mixtures and characterization of benzaldehyde + hydrocarbon systems in terms of DISQUAC, Fluid Phase Equilib. 366 (2014) 61–68, http://dx.doi.org/10.1016/j.fluid.2014.01.013.

[19] J.A. González, I. García de la Fuente, J.C. Cobos, C. Casanova, H.V. Kehiaian, Calorimetric and phase equilibrium data for linear carbonates + hydrocarbons or + CCl_4 mixtures. Comparison with DISQUAC predictions, Thermochim. Acta 217 (1993) 57–69, http://dx.doi.org/10.1016/0040-6031(93)85097-S.

[20] J. Gmehling, J. Li, M. Schiller, A modified UNIFAC model. 2. Present parameter matrix and results for different thermodynamic properties, Ind. Eng. Chem. Res. 32 (1993) 178–193, http://dx.doi.org/10.1021/ie00013a024.

[21] J. Lohmann, J. Gmehling, Modified UNIFAC (Dortmund): reliable model for the development of thermal separation processes, J. Chem. Eng. Jpn 34 (2001) 43–54, http://dx.doi.org/10.1252/jcej.34.43.

[22] H.V. Kehiaian, J.-P.E. Grolier, M.-R. Kechavarz, G.C. Benson, Thermodynamic properties of binary mixtures containing ketones. VI. Analysis of the properties of 2-propanone + *n*-alkane mixtures in terms of a quasi-chemical group contribution model, Fluid Phase Equilib. 5 (1981) 159–189, http://dx.doi.org/10.1016/0378-3812(80)80055-0.

[23] H.V. Kehiaian, J.-P.E. Grolier, M.-R. Kechavarz, G.C. Benson, O. Kiyohara, Y.P. Handa, Thermodynamic properties of binary mixtures containing ketones. VII. Analysis of the properties of *n*-alkanone + *n*-alkane, and *n*-alkanone + *n*-alkanone mixtures in terms of a quasi-chemical group contribution model, Fluid Phase Equilib. 7 (1981) 95–120, http://dx.doi.org/10.1016/0378-3812(81)85016-9.

[24] I. Ferino, B. Marongiu, V. Solinas, S. Torrazza, H.V. Kehiaian, Thermodynamic properties of binary mixtures containing aldehydes. I. Excess enthalpies of some *n*-alkanal + *n*-alkane mixtures: Measurement and analysis in terms of a quasi-chemical group-contribution model and estimation of excess Gibbs energies, Fluid Phase Equilib. 12 (1983) 125–142, http://dx.doi.org/10.1016/0378-3812(83)85016-X.

[25] P.J. Flory, R.A. Orwoll, A. Vrij, Statistical thermodynamics of chain molecule liquids. I. An equation of state for normal paraffin hydrocarbons, J. Am. Chem. Soc. 86 (1964) 3507–3514, http://dx.doi.org/10.1021/ja01071a023.

[26] P.J. Flory, R.A. Orwoll, A. Vrij, Statistical thermodynamics of chain molecule liquids. II. Liquid mixtures of normal paraffin hydrocarbons, J. Am. Chem. Soc. 86 (1964) 3515–3520, http://dx.doi.org/10.1021/ja01071a024.

[27] A. Abe, P.J. Flory, The thermodynamic properties of mixtures of small, nonpolar molecules, J. Am. Chem. Soc. 87 (1965) 1838–1846, http://dx.doi.org/10.1021/ja01087a003.

[28] R.A. Orwoll, P.J. Flory, Thermodynamic properties of binary mixtures of *n*-alkanes, J. Am. Chem. Soc. 89 (1967) 6822–6829, http://dx.doi.org/10.1021/ja01002a003.

[29] L. Tonks, The complete equation of state of one, two and three-dimensional gases of hard elastic spheres, Phys. Rev. 50 (1936) 955–963.

[30] I. Prigogine, The Molecular Theory of Solutions, North-Holland Publishing Company, Amsterdam, 1957.

[31] G. Allen, Z. Chai, C.L. Chong, J.S. Higgins, J. Tripathi, Thermodynamics of oligomeric binary mixtures of polyethylene glycol and polypropylene glycol methylethers, Polymer 25 (1984) 239–244, http://dx.doi.org/10.1016/0032-3861(84)90331-8.

[32] J.A. González, I. Alonso, C. Alonso-Tristán, I.G.D.L. Fuente, J.C. Cobos, Thermodynamics of mixtures containing amines. XI. Liquid + liquid equilibria and molar excess enthalpies at 298.15 K for *N*-methylaniline + hydrocarbon systems. Characterization in terms of DISQUAC and ERAS models, J. Chem. Thermodyn. 56 (2013) 89–98, http://dx.doi.org/10.1016/j.jct.2012.07.006.

[33] H.V. Kehiaian, M.R. Tine, L. Lepori, E. Matteoli, B. Marongiu, Thermodynamics of binary mixtures containing oxaalkanes. Part 3. Monoethers, polyethers, acetals, orthoesters and cyclic monoethers + *n*-alkanes or cyclohexane, Fluid Phase Equilib. 46 (1989) 131–177, http://dx.doi.org/10.1016/0378-3812(89)80033-0.

[34] J.A. González, I. García de la Fuente, J.C. Cobos, Proximity effects and cyclization in oxaalkanes + CCl_4 mixtures DISQUAC characterization of the Cl–O interactions. Comparison with Dortmund UNIFAC results, Fluid Phase Equilib. 154 (1999) 11–31, http://dx.doi.org/10.1016/S0378-3812(98)00421-X.

[35] J.S. Rowlinson, F.L. Swinton, Liquids and Liquid Mixtures, third ed. Butterworths, G. B., 1982

[36] J.A. González, I. García de la Fuente, J.C. Cobos, Thermodynamics of mixtures with strongly negative deviations from Raoult's Law: part 4. Application of the DISQUAC model to mixtures of 1-alkanols with primary or secondary linear amines. Comparison with Dortmund UNIFAC and ERAS results, Fluid Phase Equilib. 168 (2000) 31–58, http://dx.doi.org/10.1016/S0378-3812(99)00326-X.

[37] E. Wilhelm, A. Lainez, J.P.E. Grolier, Thermodynamics of (a halogenated ethane or ethene + an *n*-alkane). VE and CPE of mixtures containing either 1,1,2,2-tetrachloroethane or tetrachloroethene, Fluid Phase Equilib. 49 (1989) 233–250, http://dx.doi.org/10.1016/0378-3812(89)80018-4.

[38] J.A. González, I. Mozo, I. García, D. La Fuente, J.C. Cobos, V.A. Durov, Thermodynamics of 1-alkanol + cyclic ether mixtures, Fluid Phase Equilib. 245 (2006) 168–184, http://dx.doi.org/10.1016/j.fluid.2006.05.003.

[39] O. Kiyohara, Y.P. Handa, G.C. Benson, Thermodynamic properties of binary mixtures containing ketones III. Excess enthalpies of *n*-alkanes + some aliphatic ketones, J. Chem. Thermodyn. 11 (1979) 453–460, http://dx.doi.org/10.1016/0021-9614(79)90123-X.

[40] O. Kiyohara, G.C. Benson, J.-P.E. Grolier, Thermodynamic properties of binary mixtures containing ketones I. Excess enthalpies of some aliphatic ketones + *n*-hexane, + benzene, and + tetrachloromethane, J. Chem. Thermodyn. 9 (1977) 315–323, http://dx.doi.org/10.1016/0021-9614(77)90052-0.

[41] U. Messow, U. Doyé, D. Kuchenbecker, Thermodynamic studies on solvent + *n*-paraffin systems: 9. butanone(1) + *n*-dodecane(2), butanone(1) + *n*-hexadecane(2) and butanone(1) + *n*-octadecane(2) systems, Z. Phys. Chem. (Leipzig) 259 (1978) 664–666.

[42] Y. Akamatsu, H. Ogawa, S. Murakami, Molar excess enthalpies, molar excess volumes and molar isentropic compressions of mixtures of 2-propanone with heptane, benzene and trichloromethane at 298.15 K, Thermochim. Acta 113 (1987) 141–150, http://dx.doi.org/10.1016/0040-6031(87)88317-X.

[43] J.L. Legido, R. Bravo, M.I. Paz Andrade, L. Romani, F. Sarmiento, J. Ortega, Excess enthalpies of five examples of (2-hexanone + an *n*-alkane) and five of (2-hexanone + an *n*-alkanol) at 298.15 K, J. Chem. Thermodyn. 18 (1986) 21–26, http://dx.doi.org/10.1016/0021-9614(86)90038-8.

[44] O. Urdaneta, Y.P. Handa, G.C. Benson, Thermodynamic properties of binary mixtures containing ketones V. Excess enthalpies of an isomeric heptanone + *n*-heptane, J. Chem. Thermodyn. (1979) 857–860, http://dx.doi.org/10.1016/0021-9614(79)90066-1.

[45] B. Marongiu, Excess enthalpies of some normal alkanones (C_3 - C_6) + cyclohexane, Int. DATA Ser., Sel. Data Mixtures, Ser. A 15 (1987) 1–6.

[46] I. Velasco, J. Fernández, S. Otín, H.V. Kehiaian, Estimation of DISQUAC interchange energy parameters for *n*-alkylamine + *n*-alkane mixtures, Fluid Phase Equilib. 69 (1991) 15–32, http://dx.doi.org/10.1016/0378-3812(91)90023-Z.

[47] J.-P.E. Grolier, G.C. Benson, Thermodynamic properties of binary mixtures containing ketones. VIII. Heat capacities and volumes of some *n*-alkanone + *n*-alkane mixtures at 298.15 K, Can. J. Chem. 62 (1984) 949–953, http://dx.doi.org/10.1139/v84-156.
[48] J. Ortega, M.I. Paz-Andrade, E. Rodriguez-Nunez, E. Jimenez, Excess molar volumes of binary mixtures of 2-hexanone with *n*-alkane at 298.15 K, Can. J. Chem. 63 (1985) 3354–3356, http://dx.doi.org/10.1139/v85-552.
[49] G. Rajendra Naidu, P. Ramachandra Naidu, Excess volumes of ternary mixtures containing ethyl ketone, 1-alkanols, and *n*-octane, J. Chem. Eng. Data 27 (1982) 57–59, http://dx.doi.org/10.1021/je00027a018.
[50] U. Messow, U. Doyé, S. Kuntzsch, D. Kuchenbecker, Thermodynamic studies on solvent/*n*-paraffin systems. V. The acetone/*n*- decane, acetone/*n*-dodecane, acetone/*n*-tetradecane and acetone/*n*-hexadecane systems, Z. Phys. Chem. (Leipzig) 258 (1977) 90–96.
[51] K. Yamanaka, H. Ogawa, S. Murakami, Excess molar isobaric heat capacities of mixtures of 2-propanone with heptane, benzene, and trichloromethane at 298.15 K, Thermochim. Acta 169 (1990) 193–201, http://dx.doi.org/10.1016/0040-6031(90)80145-O.
[52] M.-E. Saint-Victor, D. Patterson, The w-shape concentration dependence of C_p^E and solution non-randomness: ketones + normal and branched alkanes, Fluid Phase Equilib. 35 (1987) 237–252, http://dx.doi.org/10.1016/0378-3812(87)80015-8.
[53] B.S. Mahl, H. Kaur, Excess thermodynamic properties of binary mixtures of *n*-alkanes with cycloalkanones, Thermochim. Acta 112 (1987) 351–364, http://dx.doi.org/10.1016/0040-6031(87)88292-8.
[54] V. Majer, V. Svoboda, Enthalpies of Vaporization of Organic Compounds: A Critical Review and Data Compilation, Blackwell Scientific Publications, Oxford, 1985.
[55] D.R. Lide, CRC Handbook of Chemistry and Physics, 90th ed. CRC Press/Taylor and Francis, Boca Raton, FL, 2010.
[56] P.P.S. Saluja, L.A. Peacock, R. Fuchs, Enthalpies of interaction of aliphatic ketones with polar and nonpolar solvents, J. Am. Chem. Soc. 101 (1979) 1958–1962, http://dx.doi.org/10.1021/ja00502a005.
[57] L. Lepori, P. Gianni, E. Matteoli, The effect of the molecular size and shape on the volume behavior of binary liquid mixtures. Branched and cyclic alkanes in heptane at 298.15 K, J. Solut. Chem. 42 (2013) 1263–1304, http://dx.doi.org/10.1007/s10953-013-0023-9.
[58] O. Urdaneta, S. Hamam, Y.P. Handa, G.C. Benson, Thermodynamic properties of binary mixtures containing ketones IV. Excess enthalpies of acetophenone + an *n*-alkane and phenylacetone + an *n*-alkane, J. Chem. Thermodyn. 11 (1979) 851–856, http://dx.doi.org/10.1016/0021-9614(79)90065-X.
[59] W.-C. Liao, H.-m. Lin, M.-J. Lee, Excess molar enthalpies of binary systems of 2-octanone or 3-octanone with dodecane, tetradecane, or hexadecane at 298.15 K, J. Chem. Eng. Data 55 (2010) 217–222, http://dx.doi.org/10.1021/je900311v.
[60] I. Ferino, B. Marongiu, V. Solinas, S. Torrazza, Excess enthalpies of some aromatic aldehydes in *n*-hexane, *n*-heptane and benzene, Thermochim. Acta 57 (1982) 147–154, http://dx.doi.org/10.1016/0040-6031(82)80055-5.
[61] I. Garcia, J.C. Cobos, J.A. Gonzalez, C. Casanova, M.J. Cocero, Thermodynamics of binary mixtures containing organic carbonates. 1. Excess enthalpies of dimethyl carbonate + hydrocarbons or + tetrachloromethane, J. Chem. Eng. Data 33 (1988) 423–426, http://dx.doi.org/10.1021/je00054a010.
[62] I. García, J.C. Cobos, J.A. González, C. Casanova, Excess enthalpies of diethyl carbonate + some normal alkanes (C_6 - C_{14}) + cyclohexane, + methylcyclohexane, + benzene, + toluene, or + tetrachloromethane, Int. DATA Ser., Sel. Data Mixtures, Ser. A 15 (1987) 164–173.
[63] J.A. Gonzalez, I. Garcia, J.C. Cobos, C. Casanova, Thermodynamics of binary mixtures containing organic carbonates. 4. Liquid-liquid equilibria of dimethyl carbonate + selected *n*-alkanes, J. Chem. Eng. Data 36 (1991) 162–164, http://dx.doi.org/10.1021/je00002a009.
[64] I. Garcia de la Fuente, J.A. Gonzalez, J.C. Cobos, C. Casanova, Excess molar volumes for dimethyl carbonate + heptane, decane, 2,2,4-trimethylpentane, cyclohexane, benzene, toluene, or tetrachloromethane, J. Chem. Eng. Data 37 (1992) 535–537, http://dx.doi.org/10.1021/je00008a037.
[65] A.L. McClellan, Tables of Experimental Dipole Moments, Vols. 1, 2, 3, Rahara Enterprises, El Cerrito, US, 1974.
[66] H. Kalali, F. Kohler, P. Svejda, Excess properties of binary mixtures of 2,2,4-trimethylpentane with one polar component, Fluid Phase Equilib. 20 (1985) 75–80, http://dx.doi.org/10.1016/0378-3812(85)90022-6.
[67] H. Van Tra, D. Patterson, Volumes of mixing and the P * effect: part I. Hexane isomers with normal and branched hexadecane, J. Solut. Chem. 11 (1982) 793–805, http://dx.doi.org/10.1007/BF00650519.
[68] G. Spinolo, R. Riccardi, Liquid-liquid equilibrium in acetone + *n*-alkane (C6-C9) binary mixtures, Int. DATA Ser., Sel. Data Mixtures, Ser. A (1977) 91–94.
[69] O. Azócar, J. Edwards, Thermodynamics of the systeme *n*-decane-acetone, 2. Mitt, Monatsh. Chem. 102 (1971) 1867–1872, http://dx.doi.org/10.1007/BF00905662.
[70] M. Costas, D. Patterson, Order destruction and order creation in binary mixtures of non-electrolytes, Thermochim. Acta 120 (1987) 161–181, http://dx.doi.org/10.1016/0040-6031(87)80214-9.
[71] M. Costas, H. Van Tra, D. Patterson, M. Caceres-Alonso, G. Tardajos, E. Aicart, Liquid structure and second-order mixing functions for 1-chloronaphthalene with linear and branched alkanes, J. Chem. Soc. Faraday Trans. 1 (84) (1988) 1603–1616, http://dx.doi.org/10.1039/F19888401603.
[72] K. Schäfer, F.J. Rohr, Excess enthalpies of acetone + *n*-alkane (C_3 - C_6) binary mixtures, Int. DATA Ser., Sel. Data Mixtures, Ser. A (1978) 74–77.
[73] W.-C. Liao, H.-m. Lin, M.-J. Lee, Excess molar enthalpies of binary mixtures containing 2-decanone or dipentyl ether with long-chain *n*-alkanes at T = 298.15 K, J. Chem. Thermodyn. 43 (2011) 515–520, http://dx.doi.org/10.1016/j.jct.2010.11.004.
[74] B. Marongiu, C. Delitala, B. Pittau, S. Porcedda, DISQUAC predictions on excess enthalpies of the ternary mixture: cyclohexane + propanone + tetrahydrofuran, Fluid Phase Equilib. 109 (1995) 67–81, http://dx.doi.org/10.1016/0378-3812(95)96893-2.
[75] K. Tamura, Excess molar enthalpies and excess molar heat capacities of (2-butanone + cyclohexane, or methylcyclohexane, or benzene, or toluene, or chlorobenzene, or cyclohexanone) at T = 298.15 K, J. Chem. Thermodyn. 33 (2001) 1345–1353, http://dx.doi.org/10.1006/jcht.2001.0851.
[76] B. Marongiu, S. Dernini, A.M. Polcaro, Thermodynamics of binary mixtures containing cyclic alkanones. 1. Excess enthalpies of cyclopentanone and cyclohexanone + *n*-alkanes, + cyclohexane, + benzene, and + tetrachloromethane, J. Chem. Eng. Data 31 (1986) 185–189, http://dx.doi.org/10.1021/je00044a017.
[77] J.-P.E. Grolier, O. Kiyohara, G.C. Benson, Thermodynamic properties of binary mixtures containing ketones II. Excess enthalpies of some aromatic ketones + *n*-hexane, + benzene, and + tetrachloromethane, J. Chem. Thermodyn. 9 (1977) 697–703, http://dx.doi.org/10.1016/0021-9614(77)90096-9.
[78] S. Li, H. Gao, W. Yan, Determination and correlation of excess molar enthalpies of eight binary systems containing acetophenone at different temperatures, J. Chem. Eng. Data 53 (2008) 1630–1634, http://dx.doi.org/10.1021/je800193a.
[79] R.S. Ramalho, J.L. Tillie, S. Kaliaguine, Heats of mixing for homologous series of ketones and their prediction from group interaction theory and the congruence principle, Can. J. Chem. Eng. 49 (1971) 830–836, http://dx.doi.org/10.1002/cjce.5450490621.
[80] R. Francesconi, F. Comelli, Excess molar enthalpies of binary mixtures containing dimethyl carbonate or diethyl carbonate and one of six methyl *n*-alkyl ketones application of an extended cell model, Thermochim. Acta 264 (1995) 95–104, http://dx.doi.org/10.1016/0040-6031(95)02395-I.
[81] R. Francesconi, F. Comelli, Excess molar enthalpies of binary mixtures containing dialkylcarbonates + cyclic ketones at 298.15 or 313.15 K, Thermochim. Acta 258 (1995) 49–57, http://dx.doi.org/10.1016/0040-6031(94)02214-9.
[82] J.S. Chickos, S. Hosseini, D.G. Hesse, Determination of vaporization enthalpies of simple organic molecules by correlations of changes in gas chromatographic net retention times, Thermochim. Acta 249 (1995) 41–62, http://dx.doi.org/10.1016/0040-6031(95)90670-3.
[83] J.A. Riddick, W.B. Bunger, T.K. Sakano, Organic Solvents: Physical Properties and Methods of Purification, Wiley, New York, 1986.
[84] S.A. Kozlova, V.N. Emel'yanenko, M. Georgieva, S.P. Verevkin, Y. Chernyak, B. Schäffner, A. Börner, Vapour pressure and enthalpy of vaporization of aliphatic dialkyl carbonates, J. Chem. Thermodyn. 40 (2008) 1136–1140, http://dx.doi.org/10.1016/j.jct.2008.02.012.

Supplementary material for:

Orientational effects in alkanone, alkanal or dialkyl carbonate + alkane mixtures and in alkanone + alkanone or + dialkyl carbonate systems

Fernando Hevia[(1)], Juan Antonio González[(1)]*, Cristina Alonso-Tristán[(2)], Isaías García de la Fuente[(1)], Luis Felipe Sanz[(1)]

[(1)] G.E.T.E.F., Departamento de Física Aplicada, Facultad de Ciencias, Universidad de Valladolid, Paseo de Belén, 7, 47011 Valladolid, Spain

[(2)] Unidad de Investigación Consolidada UIC-011, JCyL. Departamento de Ingeniería Electromecánica, Escuela Politécnica Superior, Universidad de Burgos. Avda. Cantabria s/n. 09006, Burgos, Spain.

*e-mail: jagl@termo.uva.es; Tel: +34 983 423757

Reference of the article:

F. Hevia, J.A. González, C. Alonso-Tristán, I. García de la Fuente, L.F. Sanz. J. Mol. Liq. **233** (2017) 517-527. https://doi.org/10.1016/j.molliq.2017.03.014

Table S1. Physical properties and Flory reduction parameters of the pure compounds at temperature T = 298.15 K and pressure p = 0.1013 MPa. V_m, molar volume; α_p, isobaric coefficient of thermal expansion; κ_T, coefficient of isothermal compressibility; V_m^*, reduction molar volume; and p^*, reduction pressure.

Compound	V_m /cm^3·mol^{-1}	α_p /10^{-3}K^{-1}	κ_T /TPa^{-1}	V_m^* /cm^3·mol^{-1}	p^* /MPa
n-pentane	116.11[1]	1.61[1]	2180[1]	85.33	407.5
n-hexane	131.57[2]	1.387[2]	1794[2]	99.52	402.7
n-heptane	147.45[3]	1.256[3]	1461[3]	113.60	431.7
n-octane	163.52[3]	1.164[3]	1302.4[3]	127.70	436.8
n-nonane	179.69[1]	1.0844[1]	1177[1]	142.07	439.3
n-decane	195.90[3]	1.051[3]	1110[3]	155.71	446.7
n-dodecane	228.47[3]	0.96[3]	988[3]	184.33	444.9
n-tetradecane	261.09[3]	0.886[4]	872[4]	213.33	453.6
n-hexadecane	294.04[3]	0.883[2]	862[2]	240.38	456.8
c-hexane	108.73[1]	1.22[1]	1129.2[1]	84.21	536.9
2-propanone	74.00[5]	1.45[5]	1317.5[5]	55.50	583.2
2-butanone	90.14[6]	1.31[7]	1175.9[7]	68.91	568.2
2-pentanone	107.46[8]	1.198[8]	1098.77[8]	83.50	538.2
3-pentanone	106.41[1]	1.2[9]	1073[9]	82.66	552.4
2-hexanone	124.16[1]	1.14[10]	1012[1]	97.32	546.5
2-heptanone	140.76[11]	1.06[11]	968.9[11]	111.72	517.6
4-heptanone	140.79[1]	1.05[12]	932[12]	111.92	531.4
2-octanone	157.45[1]	1.03[1]	899[1]	125.57	536.9
2-decanone	190.55[13]	0.97 [a]	861.0 [b]	153.48	517.6
2-undecanone	207.12[13]	0.94 [a]	833.4 [b]	167.67	513.0
c-pentanone	89.06[14]	1.023 [c]	725.2 [d]	71.11	659.6
c-hexanone	104.21[1]	0.955 [e]	695 [e]	84.15	628.1
acetophenone	117.35[1]	0.87[1]	710.6 [f]	96.15	543.6
ethanal	57.06[15]	1.69[1]	1400 [g]	41.53	679.2
propanal	73.41[1]	1.472[1]	1067 [g]	54.90	735.3
butanal	90.54[1]	1.306[1]	1056 [g]	69.26	630.0
benzaldehyde	102.03[1]	0.865[1]	585.6 [h]	83.67	654.7
dimethyl carbonate	84.71[16]	1.2541[16]	893.1[16]	65.28	704.8
diethyl carbonate	121.90[16]	1.2971[16]	970[16]	93.36	679.5

[a] Extrapolated from α_p values of smaller 2-alkanones. [b] Estimated using α_p/κ_T values obtained by the Manzini-Crescenzi group contribution method [17]. [c] Calculated from data of ref. [14]. [d] Calculated from data of refs. [14, 18]. [e] Calculated from data of ref. [19]. [f] Calculated from data of refs. [1, 20]. [g] Calculated from data of ref. [21]. [h] Calculated from data of ref. [22].

Table S2. Experimental excess molar volumes, $V^{E}_{m,exp}$, and Flory calculations, $V^{E}_{m,Flory}$, at temperature T = 298.15 K, pressure p = 0.1013 MPa and equimolar composition for ketone or dialkyl carbonate + alkane systems.

System	$V^{E}_{m,exp}$ /cm³·mol⁻¹	$V^{E}_{m,Flory}$ /cm³·mol⁻¹	Ref.
2-propanone + heptane	1.130	2.060	[23]
2-propanone + decane	1.333	2.137	[24]
2-propanone + hexadecane [a]	1.422	2.101	[24]
2-butanone + heptane	0.803	1.419	[25]
2-butanone + octane	0.866	1.505	[26]
2-butanone + decane	0.952	1.590	[25]
2-butanone + dodecane	0.996	1.657	[25]
2-pentanone + octane	0.695	1.153	[27]
2-pentanone + decane	0.812	1.272	[28]
3-pentanone + heptane	0.512	0.970	[29]
2-hexanone + hexane	0.154	0.525	[30]
2-hexanone + heptane	0.375	0.822	[30]
2-hexanone + octane	0.516	0.977	[30]
2-hexanone + nonane	0.595	1.091	[30]
2-hexanone + decane	0.643	1.154	[30]
2-butanone + C_6H_{12}	0.912	1.140	[29]
3-pentanone + C_6H_{12}	0.763	0.893	[29]
c-pentanone[b] + hexane	–0.172	0.159	[31]
c-pentanone + heptane	0.082	0.536	[31]
c-pentanone + octane	0.252	0.777	[31]
c-pentanone + decane	0.482	1.046	[31]
c-pentanone + dodecane	0.634	1.291	[31]
c-hexanone[c] + hexane	–0.323	–0.194	[31]
c-hexanone + heptane	–0.023	0.235	[31]
c-hexanone + octane	0.173	0.526	[31]
c-hexanone + decane	0.442	0.803	[31]
c-hexanone + dodecane	0.622	1.040	[31]
dimethyl carbonate + heptane	1.158	1.830	[32]
dimethyl carbonate + decane	1.442	2.218	[32]
diethyl carbonate + heptane	0.736	1.275	[33]
diethyl carbonate + decane	1.063	1.771	[33]

[a] There is a partial immiscibility region; [b]cyclopentanone; [c]cyclohexanone.

References

[1] J.A. Riddick, W.B. Bunger, T.K. Sakano, Organic solvents: physical properties and methods of purification, Wiley, New York, 1986.

[2] L. Wang, G.C. Benson, B.C.Y. Lu, Excess enthalpies for (di-*n*-propyl ether + *n*-alkane) at 298.15 K, J. Chem. Thermodyn., 20 (1988) 975-979. DOI: 10.1016/0021-9614(88)90226-1.

[3] N. Riesco, J.A. González, S. Villa, I. García de La Fuente, J.C. Cobos, Thermodynamics of organic mixtures containing amines - III: Molar excess volumes at

298.15 K for tripropylamine + *n*-alkane systems. Application of the Flory theory to *N,N,N*-trialkylamine + *n*-alkane mixtures, Phys. Chem. Liq., 41 (2003) 309-321. DOI: 10.1080/0031910031000097079.

[4] S. Zhu, S. Shen, G.C. Benson, B.C.Y. Lu, Excess enthalpies of (methyl 1,1-dimethylpropyl ether + an *n*-alkane) at the temperature 298.15 K, J. Chem. Thermodyn., 26 (1994) 35-39. DOI: 10.1006/jcht.1994.1017.

[5] I. Alonso, V. Alonso, I. Mozo, I. García de la Fuente, J.A. González, J.C. Cobos, Thermodynamics of ketone + amine mixtures: Part II. Volumetric and speed of sound data at (293.15, 298.15 and 303.15) K for 2-propanone + dipropylamine, + dibutylamine or + triethylamine systems, J. Mol. Liq., 155 (2010) 109-114. DOI: 10.1016/j.molliq.2010.05.022.

[6] J.A. González, I. Alonso, I.G. De La Fuente, J.C. Cobos, Thermodynamics of ketone + amine mixtures. Part X. Excess molar enthalpies at 298.15 K for *N,N,N*-triethylamine + 2-alkanone systems. Characterization of tertiary amine + 2-alkanone, and of amino-ketone + *n*-alkane mixtures in terms of DISQUAC, Fluid Phase Equilib., 356 (2013) 117-125. DOI: 10.1016/j.fluid.2013.07.037.

[7] I. Alonso, I. Mozo, I.G. de la fuente, J.A. González, J.C. Cobos, Thermodynamics of ketone + amine mixtures Part IV. Volumetric and speed of sound data at (293.15; 298.15 and 303.15 K) for 2-butanone +dipropylamine, +dibutylamine or +triethylamine systems, Thermochim. Acta, 512 (2011) 86-92. DOI: 10.1016/j.tca.2010.09.004.

[8] I. Alonso, I. Mozo, I.G. De La Fuente, J.A. González, J.C. Cobos, Thermodynamics of ketone + amine mixtures 7. Volumetric and speed of sound data at (293.15, 298.15 and 303.15) K for 2-pentanone + aniline, + *N*-methylaniline, or + pyridine systems, J. Mol. Liq., 160 (2011) 180-186. DOI: 10.1016/j.molliq.2011.03.015.

[9] R. Malhotra, W.E. Price, L.A. Woolf, Thermodynamic properties of pentan-3-one at temperatures from 278 K to 338 K and pressures from 0.1 MPa to 380 MPa, J. Chem. Thermodyn., 25 (1993) 361-366. DOI: 10.1006/jcht.1993.1037.

[10] R. Malhotra, L.A. Woolf, Volumetric measurements of liquid pentan-2-one, hexan-2-one, and 4-methylpentan-2-one at temperatures from 278.15 K to 338.13 K and pressures in the range from 0.1 MPa to 386 MPa, J. Chem. Thermodyn., 28 (1996) 1411-1421. DOI: 10.1006/jcht.1996.0124.

[11] I. Alonso, I. Mozo, I.G. La Fuente, J.A. González, J.C. Cobos, Thermodynamics of ketone + amine mixtures Part V. Volumetric and speed of sound data at (293.15, 298.15

and 303.15) K for mixtures of 2-heptanone with aniline, *N*-methylaniline or pyridine, J. Solution Chem., 40 (2011) 2057-2071. DOI: 10.1007/s10953-011-9774-3.

[12] U. Domanska, J. Lachwa, T.M. Letcher, Densities, excess molar volumes, and excess molar enthalpies of (*N*-methyl-2-pyrrolidinone + ketone) at T = 298.15 K, J. Chem. Eng. Data, 47 (2002) 1446-1452. DOI: 10.1021/je020068p.

[13] F. Comelli, R. Francesconi, Densities and excess molar volumes of propylene carbonate + linear and cyclic ketones at 298.15 K, J. Chem. Eng. Data, 40 (1995) 808-810. DOI: 10.1021/je00020a015.

[14] V.K. Sharma, J. Kataria, S. Solanki, Molecular interactions in binary mixtures of lactams with cyclic alkanones, J. Solution Chem., 43 (2014) 486-524. DOI: 10.1007/s10953-014-0152-9.

[15] C.F. Coleman, T.D. Vries, The heat capacity of organic vapors. V. Acetaldehyde, J. Am. Chem. Soc., 71 (1949) 2839-2841. DOI: 10.1021/ja01176a072.

[16] J.A. González, I. Mozo, S. Villa, N. Riesco, I.G. Fuente, J.C. Cobos, Thermodynamics of mixtures containing organic carbonates. Part XV. Application of the Kirkwood-Buff theory to the study of interactions in liquid mixtures containing dialkyl carbonates and alkanes, benzene, CCl_4 or 1-alkanols, J. Solution Chem., 35 (2006) 787-801. DOI: 10.1007/s10953-006-9030-4.

[17] G. Manzini, V. Crescenzi, Simple, accurate method of calculation of the thermal pressure coefficient of non-polar liquids and a possible estimate of their excess volumes of mixing, Gazz. Chim. Ital., 104 (1974) 51-61.

[18] V.K. Sharma, J. Kataria, Topological investigations of excess heat capacities of binary liquid mixtures containing lactams and cycloalkanone, J. Mol. Liq., 188 (2013) 210-221. DOI: 10.1016/j.molliq.2013.10.010.

[19] K. Ohomuro, K. Tamura, S. Murakami, Excess volumes and isentropic compressibilities of the binary mixtures of cyclohexanone with globular species at T=298.15 K, J. Chem. Thermodyn., 29 (1997) 287-294. DOI: 10.1006/jcht.1996.0152.

[20] M.N. Roy, B.K. Sarkar, R. Chanda, Viscosity, density, and speed of sound for the binary mixtures of formamide with 2-methoxyethanol, acetophenone, acetonitrile, 1,2-dimethoxyethane, and dimethylsulfoxide at different temperatures, J. Chem. Eng. Data, 52 (2007) 1630-1637. DOI: 10.1021/je700026d.

[21] P.M. Chaudhuri, R.A. Stager, G.P. Mathur, Properties of aliphatic and aromatic aldehydes under high pressure. Compressibility and viscosity determination, J. Chem. Eng. Data, 13 (1968) 9-11. DOI: 10.1021/je60036a003.

[22] I. Cibulka, L. Hnedkovsky, T. Takagi, P−ρ−T data of liquids: Summarization and evaluation. 3. Ethers, ketones, aldehydes, carboxylic acids, and esters, J. Chem. Eng. Data, 42 (1997) 2-26. DOI: 10.1021/je960199o.

[23] Y. Akamatsu, H. Ogawa, S. Murakami, Molar excess enthalpies, molar excess volumes and molar isentropic compressions of mixtures of 2-propanone with heptane, benzene and trichloromethane at 298.15 K, Thermochim. Acta, 113 (1987) 141-150. DOI: 10.1016/0040-6031(87)88317-X.

[24] U. Messow, U. Doyé, S. Kuntzsch, D. Kuchenbecker, Thermodynamic studies on solvent/*n*-paraffin systems. V. The acetone/*n*- decane, acetone/*n*-dodecane, acetone/*n*-tetradecane and acetone/*n*-hexadecane systems, Z. Phys. Chem. (Leipzig), 258 (1977) 90-96.

[25] J.-P.E. Grolier, G.C. Benson, Thermodynamic properties of binary mixtures containing ketones. VIII. Heat capacities and volumes of some *n*-alkanone + *n*-alkane mixtures at 298.15K, Can. J. Chem., 62 (1984) 949-953. DOI: 10.1139/v84-156.

[26] G. Rajendra Naidu, P. Ramachandra Naidu, Excess volumes of ternary mixtures containing ethyl ketone, 1-alkanols, and *n*-octane, J. Chem. Eng. Data, 27 (1982) 57-59. DOI: 10.1021/je00027a018.

[27] C.P. Menaut, J.M. Pico, C. Franjo, E. Jimenez, L. Segade, M.I. Paz Andrade, Excess molar volumes of ternary mixtures of 2-butanone or 2-pentanone with 1-chloroctane + *n*-Octane at 25°C, J. Solution. Chem., 27 (1998) 1139-1148. DOI: 10.1023/A:1022614101952.

[28] C.P. Menaut, J.M. Pico, C. Franjo, E. Jiménez, J.L. Legido, M.I.P. Andrade, Excess molar volumes of $\{x_1CH_3CO(CH_2)_2CH_3 + x_2CH_3(CH_2)_3CH_2Cl + (1-x_1-x_2)CH_3(CH_2)_{\nu-2}CH_3\}$ (ν=10, 12) at the temperature of 298.15 K, J. Chem. Thermodyn., 29 (1997) 337-343. DOI: 10.1006/jcht.1996.0157.

[29] K. Ohomuro, K. Tamura, S. Murakami, Speeds of sound, excess molar volumes, and isentropic compressibilities of "$xCH_3COC_2H_5 + (1-x)C_7H_{16}$', "$xCH_3COC_2H_5 + (1-x)c$-$C_6H_{12}$', "$xCH_3COC_2H_5 + (1-x)c$-$C_6H_{11}CH_3$, "$xC_2H_5COC_2H_5 + (1-x)C_7H_{16}$', and "$xC_2H_5COC_2H_5 + (1-x)c$-$C_6H_{12}$' at 298.15 K, J. Chem. Thermodyn., 19 (1987) 163-169. DOI: 10.1016/0021-9614(87)90107-8.

[30] J. Ortega, M.I. Paz-Andrade, E. Rodriguez-Nunez, E. Jimenez, Excess molar volumes of binary mixtures of 2-hexanone with *n*-alkane at 298.15K, Can. J. Chem., 63 (1985) 3354-3356. DOI: 10.1139/v85-552.

[31] B.S. Mahl, H. Kaur, Excess thermodynamic properties of binary mixtures of *n*-alkanes with cycloalkanones, Thermochim. Acta, 112 (1987) 351-364. DOI: 10.1016/0040-6031(87)88292-8.

[32] I. Garcia de la Fuente, J.A. Gonzalez, J.C. Cobos, C. Casanova, Excess molar volumes for dimethyl carbonate + heptane, decane, 2,2,4-trimethylpentane, cyclohexane, benzene, toluene, or tetrachloromethane, J. Chem. Eng. Data, 37 (1992) 535-537. DOI: 10.1021/je00008a037.

[33] I. García de la Fuente, J.A. González, J.C. Cobos, C. Casanova, Excess molar volumes of diethyl carbonate with hydrocarbons or tetrachloromethane at 25°C, J. Solution Chem., 24 (1995) 827-835. DOI: 10.1007/BF01131047.

Fluid Phase Equilibria 449 (2017) 91–103

Contents lists available at ScienceDirect

Fluid Phase Equilibria

journal homepage: www.elsevier.com/locate/fluid

Orientational effects in mixtures of organic carbonates with alkanes or 1-alkanols

Juan Antonio González [a, *], Fernando Hevia [a], Cristina Alonso-Tristán [b], Isaías García de la Fuente [a], José Carlos Cobos [a]

[a] G.E.T.E.F., Departamento de Física Aplicada, Facultad de Ciencias, Universidad de Valladolid, Paseo de Belén, 7, 47011 Valladolid, Spain
[b] Dpto. Ingeniería Electromecánica, Escuela Politécnica Superior, Avda. Cantabria s/n, 09006, Burgos, Spain

ARTICLE INFO

Article history:
Received 13 November 2016
Received in revised form
15 June 2017
Accepted 15 June 2017
Available online 17 June 2017

Keywords:
Carbonates
Thermodynamic properties
Flory
$S_{CC}(0)$
Orientational effects
Homocoordination

ABSTRACT

Interactions and structure of organic carbonate + alkane, and 1-alkanol + organic carbonate mixtures have been investigated by means of a set of molar excess functions, enthalpies (H_m^E), volumes (V_m^E), isobaric heat capacities, (C_{pm}^E) or entropies; and considering internal pressure (P_{int}); liquid-liquid equilibria or permittivity data. In addition, the mentioned systems have been studied using the Flory model and the concentration-concentration structure factor$S_{CC}(0)$, formalism. The mixtures under consideration are characterized by dipolar interactions and by homocoordination (that is, by interactions between like molecules). In systems with a given solvent, dipolar interactions are weakened in the order: propylene carbonate (PC) > dimethyl carbonate (DMC) > diethyl carbonate (DEC). Comparison of mixtures containing DMC or DEC with those involving 2-propanone or 3-pentanone shows that dipolar interactions are not determined merely by values of the dipole moment, but they also depend on the size group. The enthalpies of the alkanol-carbonate interactions have been evaluated from calorimetric data. They are stronger in DMC solutions, and become weaker when the alcohol size increases in mixtures with a given carbonate. Application of the Flory model to 43 systems of the type 1-alkanol + carbonate provides a mean relative standard deviation for H_m^E equal to 0.107. Results reveal that orientational effects decrease in the order DEC > PC > DMC. Orientational effects are particularly relevant in methanol or ethanol + DEC mixtures. Interestingly, the mentioned effects are weaker in 1-alkanol + DMC mixtures than in DMC + alkane systems. A similar trend is observed in DEC solutions when the considered alcohol is longer than ethanol.

1. Introduction

We are engaged in a systematic study on orientational effects in liquid mixtures by means of the Flory model [1–5]. Using this approach, we have investigated systems such as 1-alkanol + linear or cyclic monoether [6], or + linear polyether [7], or + alkanone [8], or + nitrile [9] or 1-butanol + alkoxyethanol [10], or ether + alkane [11], + benzene, or + toluene [12], or + CCl_4 [13] and now extend these studies to dimethyl (DMC), diethyl (DEC) or propylene (PC) carbonate + alkane, or + 1-alkanol mixtures. Solutions including DMC or DEC have been previously treated [14–16] in terms of the DISQUAC [17] and ERAS [18] models, or using the Kirkwood-Buff integrals [19,20]. Similarly, in the framework of the UNIFAC (Dortmund version) [21] and Nitta-Chao [22] models, interaction parameters for the carbonate/alkane contacts, when dialkyl carbonates are involved, have been reported [23,24]. In the present work, systems with DMC or DEC are also investigated using the concentration-concentration structure factor formalism [25]. In fact, it is of high interest to link thermodynamic properties of liquid mixtures with local deviations from the bulk composition. At least, two procedures exist to investigate fluctuations in a binary mixture [25–27]. In the Kirkwood-Buff integrals formalism [19,20], fluctuations in the number of molecules of each component and the cross fluctuations are considered. A different alternative, based on the Bhatia-Thorton partial structure factors [28], is concerned with the study of fluctuations in the number of molecules regardless of the components, the fluctuations in the mole fraction and the cross fluctuations. This approach was generalized to link the asymptotic behaviour of the ordering potential to the interchange energy

* Corresponding author.
E-mail address: jagl@termo.uva.es (J.A. González).

http://dx.doi.org/10.1016/j.fluid.2017.06.012
0378-3812/

parameters in the semi-phenomenological theories of thermodynamic properties of liquid solutions [29–32]. We have applied this approach to mixtures involving pyridines [33] or to 1-alkanol + cyclic ether [34], or + alkanone [8] systems.

From a theoretical point of view, the study of mixtures including carbonates is interesting for different reasons. Firstly, the investigation of solutions with linear organic carbonates is a previous step to the analysis of cyclic carbonates, ethylene or propylene carbonate, and of aromatic carbonates, methyl phenylcarbonate, e.g. The latter is particularly important when systems including aromatic heteroatoms are considered as then proximity effects between the phenyl and the polar groups may change considerably the molecular properties, and hence the interaction parameters when mixtures of these compounds are treated theoretically [35]. On the other hand, propylene carbonate is an aprotic solvent of very high dipole moment (5.36 D [36]) which is interesting to be studied in view of its local structure [37,38]. Secondly, carbonates are characterized by possessing the large functional group OCOO and it is important to investigate if the group size is relevant when describing the thermodynamic properties of liquid mixtures including the mentioned group. In fact, if the group is too large with respect to the average intermolecular distances, the interaction potential involved could be so complex that no theory can describe it conveniently, in such way that the thermodynamic properties are poorly described by means of the selected theory. From a practical point of view, it must be remarked that linear, cyclic or aromatic carbonates are widely employed in the industry. For example, they are used in the synthesis of organic compounds [39], as pharmaceuticals and agricultural chemicals, and as solvents for many synthetic and natural resins [40]. They are also very important in the Li battery technology [41,42]. DMC is used in the replacement of hazardous chemicals [43,44], as fuel additive or in the design of new refrigerants [24,45]. DMC and methyl phenyl carbonate are important intermediates obtained in the production of polycarbonates from diphenyl carbonate and bisphenol following green procedures which do not involve the highly toxic phosgene process [46]. All this supports that we have largely contributed to the development of databases of carbonate mixtures reporting experimental data on vapor-liquid [47–50], liquid-liquid and solid-liquid equilibria [15,51–53], excess molar volumes (V_m^E) [54,55] and excess molar enthalpies (H_m^E) [56,57] for such type of systems.

2. Theories

2.1. Flory model

We present here a brief summary of the main equations and hypotheses of the theory [1–5]. (i) Molecules are divided into segments (arbitrarily chosen isomeric portions of a molecule). (ii) The mean intermolecular energy per contact is assumed to be proportional to $-\eta/v_s$(where η is a positive constant which characterizes the energy of interaction for a pair of neighbouring sites and v_s is the segment volume). (iii) The configurational partition function is obtained assuming that the number of external degrees of freedom of the segments is lower than 3. In this way, restrictions on the precise location of a given segment by its neighbours in the same chain are taken into account. (iv) Random mixing is assumed. The probability of having species of kind i neighbours to any given site is equal to the site fraction (θ_i). In the case of very large total number of contact sites, the probability of formation of an interaction between contacts sites belonging to different liquids is$\theta_1\theta_2$. Under these hypotheses, the Flory equation of state is:

$$\frac{\overline{PV}}{\overline{T}} = \frac{\overline{V}^{1/3}}{\overline{V}^{1/3}-1} - \frac{1}{\overline{VT}} \tag{1}$$

where $\overline{V} = V/V^*$;$\overline{P} = P/P^*$ and $\overline{T} = T/T^*$ are the reduced volume, pressure and temperature, respectively. Equation (1) is valid for pure liquids and liquid mixtures. For pure liquids, the reduction parameters, V_i^*, P_i^* and T_i^* are obtained from densities, ρ_i, isobaric expansion coefficients, α_{Pi}, and isothermal compressibilities, κ_{Ti}, data. The corresponding expressions for reduction parameters for mixtures are given elsewhere [6]. $H_m^E$is determined from

$$H_m^E = \frac{x_1V_1^*\theta_2X_{12}}{\overline{V}} + x_1V_1^*P_1^*\left(\frac{1}{\overline{V}_1}-\frac{1}{\overline{V}}\right) + x_2V_2^*P_2^*\left(\frac{1}{\overline{V}_2}-\frac{1}{\overline{V}}\right) \tag{2}$$

All the symbols have their usual meaning [6]. In this expression, the part which depends directly on X_{12} is termed the interaction contribution toH_m^E. The remaining terms are the so-called equation of state contribution toH_m^E. The reduced volume of the mixture$\overline{V}$, in equation (2) is obtained from the equation of state. Therefore, the molar excess volume can be also calculated:

$$V_m^E = \left(x_1V_1^* + x_2V_2^*\right)\left(\overline{V} - \varphi_1\overline{V}_1 - \varphi_2\overline{V}_2\right) \tag{3}$$

2.2. Estimation of the Flory interaction parameter

X_{12} is determined from a H_m^E measurement at given composition from Refs. [6–8]:

$$X_{12} = \frac{x_1P_1^*V_1^*\left(1-\frac{\overline{T}_1}{\overline{T}}\right) + x_2P_2^*V_2^*\left(1-\frac{\overline{T}_2}{\overline{T}}\right)}{x_1V_1^*\theta_2} \tag{4}$$

For the application of this expression, we note that $\overline{VT}$ is a function ofH_m^E:

$$H_m^E = \frac{x_1P_1^*V_1^*}{\overline{V}_1} + \frac{x_2P_2^*V_2^*}{\overline{V}_2} + \frac{1}{\overline{VT}}\left(x_1P_1^*V_1^*\overline{T}_1 + x_2P_2^*V_2^*\overline{T}_2\right) \tag{5}$$

and that from the equation of state, $\overline{V} = \overline{V}(\overline{T})$. More details have been given elsewhere [6–8]. Equation (5) is a generalization of that previously given to calculate X_{12} from H_m^E at $x_1 = 0.5$ [58]. Properties of organic carbonates at 298.15 K, molar volumesV_i, $\alpha_{Pi}\kappa_{Ti}$, and the corresponding reduction parameters, P_i^* and V_i^*, needed for calculations are listed in Table 1. For 1-alkanols and alkanes, values have been taken from the literature [7,11]. At $T \neq$ 298.15 K, the mentioned properties were estimated using the same equations as in previous applications for the temperature dependence of density, α_p and γ ($= \alpha_p/\kappa_T$) [7,11]. X_{12} values determined from experimental H_m^E data at $x_1 = 0.5$ are collected in Table 2.

2.3. The concentration-concentration structure factor

Mixture structure can be investigated by means of the $S_{CC}(0)$ function [25,27,29,30,59]:

$$S_{CC}(0) = \frac{RT}{\left(\partial^2G^M/\partial x_1^2\right)_{P,T}} = \frac{x_1x_2}{D} \tag{6}$$

with

Table 1
Physical properties and Flory reduction parameters of organic carbonates at 298.15 K at pressure 0.1 MPa: V_m, molar volume; α_p, isobaric coefficient of thermal expansion; κ_T, isothermal compressibility; V_m^*, reduction molar volume; and P^*, reduction pressure.

Carbonate	V_m/cm^3·mol^{-1}	α_p/10^{-3}K^{-1}	κ_T/TPa^{-1}	V_m^*/cm^3·mol^{-1}	P^*/MPa
dimethyl carbonate (DMC) [16]	84.71	1.2541	893.1	65.28	704.8
Diethyl carbonate (DEC) [16]	121.90	1.2971	970	93.36	679.5
Propylene carbonate (PC) [123]	85.25	0.84	509	70.22	725

$$D = \frac{x_1 x_2}{RT}\left(\partial^2 G^M \Big/ \partial x_1^2\right)_{P,T} = 1 + \frac{x_1 x_2}{RT}\left(\frac{\partial^2 G_m^E}{\partial x_1^2}\right)_{P,T} \quad (7)$$

In equations (6) and (7), G^M, G_m^E stand for the molar Gibbs energy of mixing and the molar excess Gibbs energy, respectively. D is a function closely related to thermodynamic stability [60–62]. For ideal mixtures, $G_m^{E,id} = 0$ (excess Gibbs energy of the ideal mixture); $D^{id} = 1$ and $S_{CC}(0) = x_1x_2$. From stability conditions, $S_{CC}(0) > 0$. If a system is close to phase separation, $S_{CC}(0)$ must be large and positive (∞, if the mixture presents a miscibility gap). In the case of compound formation between components, $S_{CC}(0)$ must be very low (0, in the limit). Therefore, $S_{CC}(0) > x_1x_2$ ($D < 1$) indicates that the dominant trend in the system is the homocoordination (separation of the components), and the mixture is then less stable than the ideal. If $0 < S_{CC}(0) < x_1x_2 = S_{CC}(0)^{id}$, ($D > 1$), the fluctuations in the system have been removed, and the dominant trend in the solution is heterocoordination (compound formation). In such a case, the system is more stable than ideal. Therefore, $S_{CC}(0)$ is an useful magnitude to evaluate the non-randomness in the mixture [27,59].

3. Results

Results on H_m^E obtained from the Flory model using X_{12} values at $x_1 = 0.5$ are listed in Table 2, which also contains the interactional contribution to H_m^E at equimolar composition. Experimental and theoretical values for H_m^E are compared graphically in Figs. 1–5. For clarity, Table 2 also includes the relative standard deviations for H_m^E defined as:

$$\sigma_r\left(H_m^E\right) = \left[\frac{1}{N}\sum\left(\frac{H_{m,exp}^E - H_{m,calc}^E}{H_{m,exp}^E}\right)^2\right]^{1/2} \quad (8)$$

where N (=19) is the number of data points, and $H_{m,exp}^E$ stands for the smoothed H_m^E values calculated at $\Delta x_1 = 0.05$ in the composition range [0.05,0.95] from polynomial expansions, previously checked, given in the original works. Table 3 lists the results obtained for the $S_{CC}(0)$ function (Figs. 6 and 7), with D values calculated from G_m^E functions obtained using DISQUAC and the needed parameters previously reported [14,15].

4. Discussion

Below, we are referring to thermodynamic properties at equimolar composition and 298.15 K. On the other hand, n and n_{OH} stand for the number of C atoms in the n-alkane or 1-alkanol, respectively.

4.1. Organic carbonate + alkane

4.1.1. Mixtures with dialkyl carbonates

These systems are characterized by rather strong dipolar interactions. The following features support such statement. (i) Large and positive values of $H_m^E(n = 7)$/J·mol^{-1} = 1988 (DMC) [56]; 1328 (DEC) [57]. For $n = 10$, H_m^E/J·mol^{-1} = 2205 (DMC) [56]; 1536 (DEC) [57] (Fig. 1). (ii) Relatively high upper critical solutions temperatures (UCST) in the case of DMC mixtures [51]: 297.62 K ($n = 12$); 307.61 K ($n = 14$); 316.21 K ($n = 16$). (iii) Low values of excess heat capacities at constant pressure, $C_{pm}^E(n = 7)$/J·mol^{-1}·K^{-1} = 2.83 (DMC); 0.056 (DEC) [63]. The C_{pm}^E curves are W-shaped [63,64]. This seems to be a typical feature of systems where non-random effects exist, which become more important when the mixture temperature is close to its UCST [65]. Consequently, the maximum of the C_{pm}^E curves of DMC systems increases rapidly with n [63,64]. (iv) Large and positive TS_m^E(= $H_m^E - G_m^E$) values (Table 3; Fig. 8). The curves shown in Fig. 8 were calculated using the DISQUAC model with interaction parameters for the carbonate/aliphatic contacts determined previously [14]. (v) The Kirkwood-Buff integrals G_{ii}(i = 1,2) are also large and positive, while the G_{12} integrals are negative [16]. In addition, the G_{11} curves show a maximum [16], a trend usually encountered in systems where strong interactions occur between molecules of the same species. These features also reveal that dipolar interactions are stronger in DMC systems. Accordingly with the H_m^E data, the corresponding V_m^E values are also very large and change in line with H_m^E when n increases. Thus, V_m^E(DMC)/cm^3·mol^{-1} = 1.158 ($n = 7$); 1.442 ($n = 10$) (Table 4) [54]. One can conclude that the main contribution to V_m^E arises from interactional effects. This is also supported by the strong positive dependence of V_m^E with T. For the DEC + hexane mixture [66], $\frac{\partial V_m^E}{\partial T}$ = 0.014 cm^3·mol^{-1}·K^{-1}. Systems where structural effects are very important, hexane + hexadecane, e.g., are characterized by large negative $\frac{\partial V_m^E}{\partial T}$ values (− 0.013 cm^3·mol^{-1}·K^{-1} for the mentioned solution) [67].

4.1.2. Propylene carbonate systems

There is a rather large database including LLE measurements for multicomponent mixtures including PC due, e.g., to its applications to extract aromatic hydrocarbons from napththa reformate [68–70]. In contrast, the corresponding data for binary systems with alkanes is scarce. For the PC + methylcyclohexane system, the liquid-liquid equilibrium temperature is, at x_1(PC) = 0.0431, 348.15 K [69], the decane mixture shows a miscibility gap at 403.15 K between [0.033, 0.953] in mole fraction of PC [71]; and the upper critical solution temperature for the 1-octene mixture is 423.15 K [72]. On the other hand, activity coefficients of alkanes in solvent PC are extremely large: 81.7 for the octane system at 303.15 K [73]. These results are consistent with the very large dipole moment of PC (see above) and, together with those shown in the previous subsection for DMC or

Table 2
Molar excess enthalpies, H^E_m, at equimolar composition and at temperature T for dialkyl carbonate(1) + alkane(2) or 1-alkanol (1) + organic carbonate(2) systems. The interaction parameters, X_{12}, calculated from H^E_m values at equimolar composition and the interactional contribution to H^E_m, $H^E_{m,int}$, are also included.

Compound	T/K	H^E_m /J·mol^{-1}	$H^E_{m,int}$ /J·mol^{-1}	X_{12}/J·cm^{-3}	$\sigma_r(H^E_m)$[a]	Ref.
Dimethyl carbonate(1) + Alkane (2)						
Heptane	298.15	1988	1418	96.93	0.112	[56]
	363.15	1972[b]	1219	90.82	0.088	[124]
	413.15	1988[c]	1079	85.87	0.065	[124]
Octane	298.15	2053	1485	97.47	0.117	[56]
Decane	298.15	2205	1631	100.57	0.112	[56]
cyclohexane	298.15	1947	1395	103.61	0.113	[56]
Diethyl carbonate (1) + Alkane (2)						
Hexane	298.15	1264	895	49.74	0.137	[57]
Heptane	298.15	1328	951	50.26	0.111	[57]
Octane	298.15	1399	1015	51.40	0.098	[57]
Decane	298.15	1536	1142	54.01	0.095	[57]
Tetradecane	298.15	1798	1406	59.96	0.094	[57]
Cyclohexane	298.15	1320	949	55.19	0.142	[57]
1-Alkanol (1) + Dimethyl carbonate (2)						
Methanol	298.15	1308[d]	936	125.84	0.086	[120]
	313.15	1542	1067	146.79	0.270	[125]
		1457[d]	1009	138.66	0.049	[120]
	328.15	1626[d]	1086	152.76	0.046	[120]
Ethanol	298.15	1688[d]	1220	124.08	0.076	[120]
	303.15	1805	1268	131.80	0.155	[126]
	313.15	1972	1374	142.95	0.163	[125]
		1863[d]	1300	135.11	0.047	[120]
	328.15	2069[d]	1394	148.26	0.051	[120]
1-propanol	298.15	1955[d]	1428	120.34	0.073	[120]
	303.15	2156	1556	132.23	0.088	[126]
	313.15	2321	1638	141.39	0.092	[125]
		2181[d]	1543	132.95	0.046	[120]
	328.15	2372[d]	1625	143.08	0.049	[120]
1-butanol	288.15	2126	1599	114.95	0.087	[90]
	298.15	2356	1737	126.63	0.082	[90]
	313.15	2570	1839	136.92	0.058	[90]
1-pentanol	303.15	2469	1826	119.0	0.075	[126]
1-octanol	303.15	2772	2110	106.6	0.050	[126]
1-Alkanol (1) + Diethyl carbonate (2)						
Methanol	298.15	1257	898	110.73	0.319	[87]
Ethanol	298.15	1523	1096	101.11	0.230	[87]
	303.15	1645	1171	108.81	0.217	[127]
1-propanol	298.15	1794	1308	99.09	0.166	[87]
	303.15	1880	1357	103.54	0.147	[127]
1-butanol	293.15	1858	1385	89.29	0.116	[91]
	298.15	1944	1435	93.19	0.134	[87]
	303.15	2076	1517	99.21	0.108	[91]
	313.15	2206	1581	104.83	0.091	[91]
1-pentanol	298.15	1984	1485	85.10	0.070	[128]
	303.15	2036	1508	86.97	0.088	[127]
1-hexanol	298.15	2016	1524	78.89	0.096	[87]
1-octanol	298.15	2159	1666	73.08	0.072	[87]
	303.15	2277	1740	76.77	0.056	[127]
1-decanol	298.15	2248	1757	67.93	0.063	[87]
1-Alkanol (1) + Propylene carbonate (2)						
Methanol	298.15	1362	1067	133.03	0.123	[129]
	323.15	1595	1205	154.38	0.196	[129]
Ethanol	298.15	1876	1457	137.96	0.103	[130]
		1783	1387	131.17	0.091	[129]
	323.15	2102	1575	153.15	0.079	[129]
1-propanol	298.15	2138	1662	130.69	0.126	[130]
		2115	1644	129.29	0.084	[129]
	323.15	2455	1839	148.57	0.031	[129]
1-butanol	298.15	2200	1715	116.66	0.153	[130]

[a] Relative standard deviation (eq. (8)).
[b] $p = 1.584$ MPa.
[c] $p = 1.686$ MPa.
[d] $p = 1$ MPa.

DEC mixtures, allow conclude that dipolar interactions between carbonate molecules become stronger in the sequence: DEC < DMC < PC.

4.2. 1-alkanol + organic carbonate

4.2.1. Enthalpies of the hydroxyl-carbonate interactions

Neglecting structural effects [60,74], H^E_m can be considered as the result of three contributions. The positive ones,

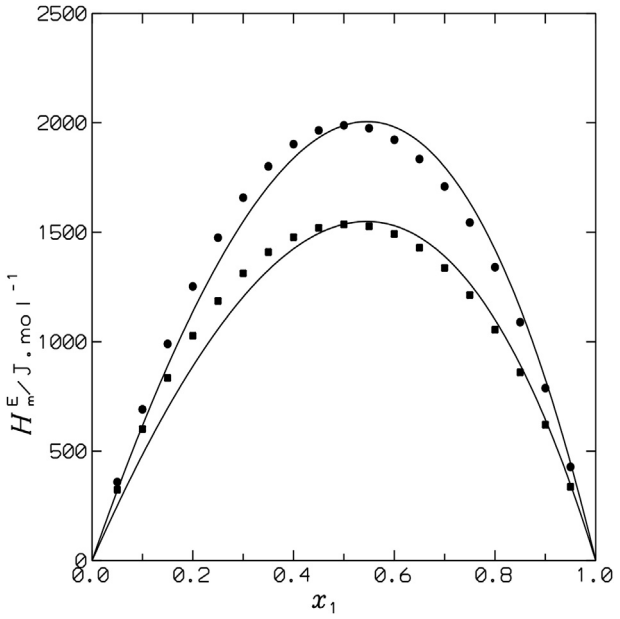

Fig. 1. H^E_m of dialkyl carbonate(1) + alkane(2) mixtures. Symbols, experimental results: (●), DMC(1) + heptane(2) (T = 413.15 K; P = 1.686 MPa) [124]; (■), DEC(1) + decane(2) (T = 298.15 K) [57]. Solid lines, Flory calculations using interaction parameters listed in Table 2.

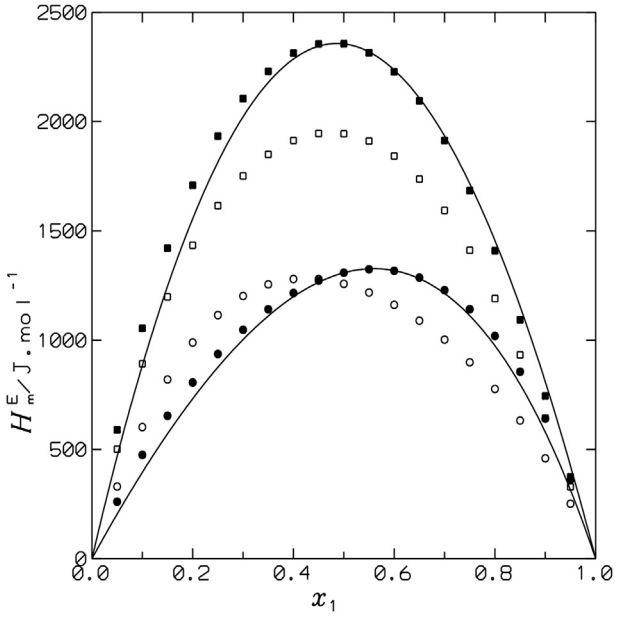

Fig. 2. H^E_m of 1-alkanol(1) + dialkyl carbonate(2) mixtures at 298.15 K. Symbols, experimental results. Full symbols, DMC mixtures [120] (P = 1 MPa): (●), methanol; (■), 1-butanol. Open symbols, DEC systems [87] (P = 0.1 MPa): (○), methanol; (□), 1-butanol. Solid lines, Flory calculations using interaction parameters listed in Table 2.

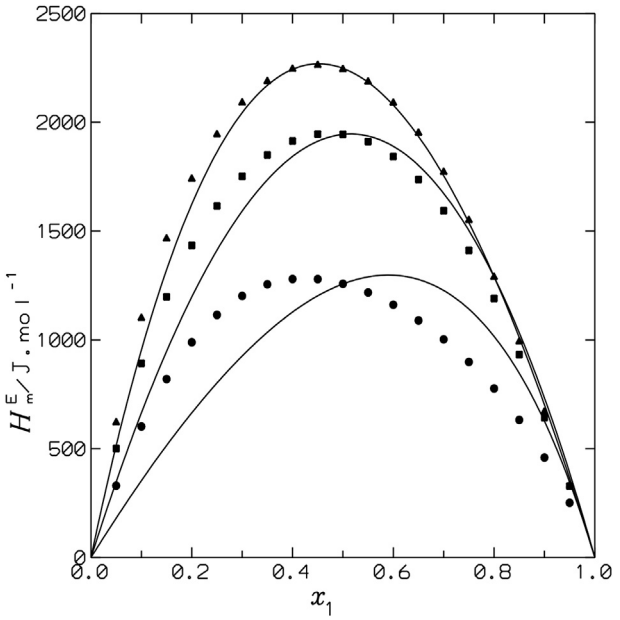

Fig. 3. H^E_m of 1-alkanol(1) + DEC(2) mixtures at 298.15 K and 0.1 MPa. Symbols, experimental results [87]: (●), methanol; (■), 1-butanol; (▲), 1-decanol. Solid lines, Flory calculations using interaction parameters listed in Table 2.

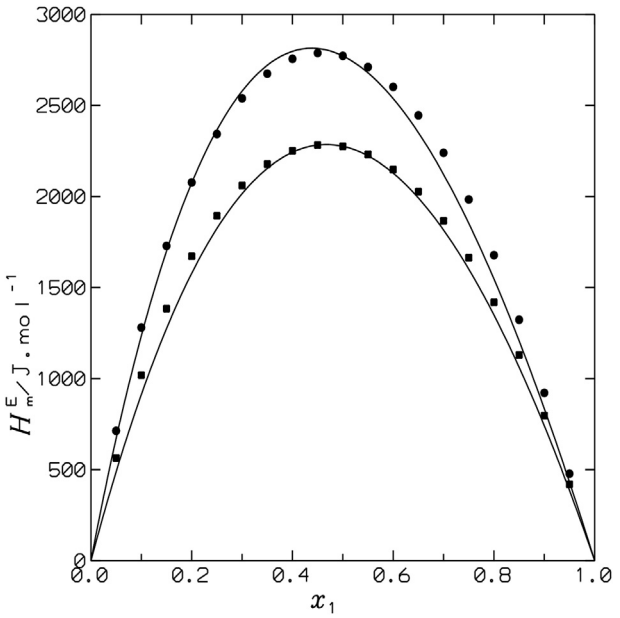

Fig. 4. H^E_m of 1-octanol(1) + DMC(2), or + DEC(2) mixtures at 303.15 K and 0.1 MPa. Symbols, experimental results: (●), DMC [126]; (■), DEC [127]. Solid lines, Flory calculations using interaction parameters listed in Table 2.

ΔH_{OH-OH}, $\Delta H_{CO3-CO3}$, come, respectively, from the breaking of alkanol-alkanol and carbonate-carbonate interactions upon mixing. The negative contribution, ΔH_{OH-CO3}, is due to the new OH—OCOO interactions created along the mixing process. That is [75–78]:

$$H^E_m = \Delta H_{OH-OH} + \Delta H_{CO3-CO3} + \Delta H_{OH-CO3} \quad (9)$$

The ΔH_{OH-CO3} term represents the enthalpy of the H-bonds between 1-alkanols and organic carbonates. An estimation of this magnitude can be conducted extending equation (9) to $x_1 \rightarrow 0$ [78–80]. In such a case, ΔH_{OH-OH} and $\Delta H_{CO3-CO3}$ can be replaced by $H^{E,\infty}_{m1}$ (partial excess molar enthalpy at infinite dilution of the first component) of 1-alkanol or carbonate + heptane systems. Thus,

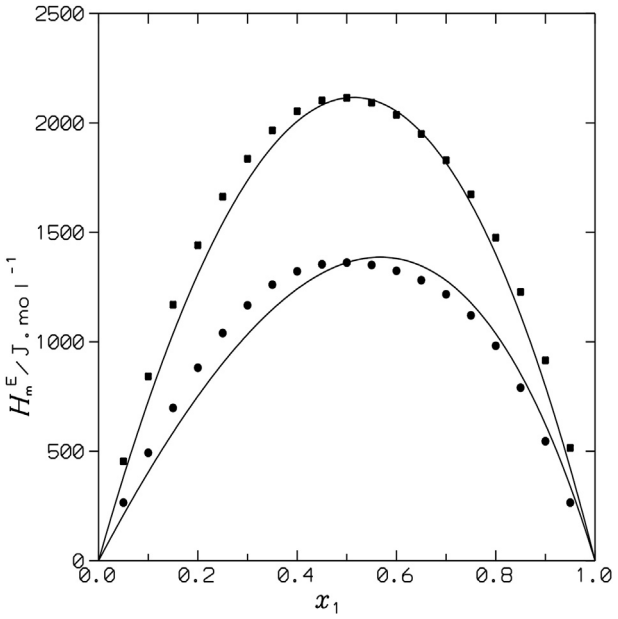

Fig. 5. H_m^E of methanol(1) or 1-propanol(1) + PC(2) mixtures at 298.15 K and 0.1 MPa. Symbols, experimental results [129]: (●), methanol; (■), 1-propanol Solid lines, Flory calculations using interaction parameters listed in Table 2.

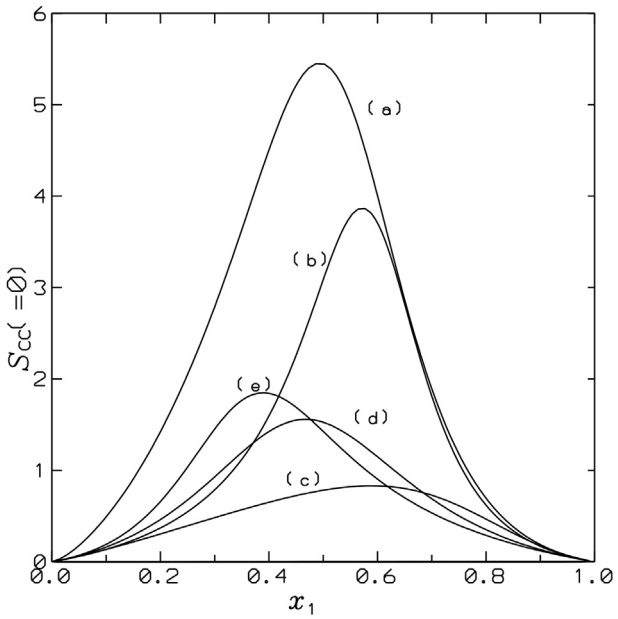

Fig. 6. $S_{CC}(0)$ curves, obtained from the DISQUAC model, for systems at 298.15 K and 0.1 MPa: (a), ethanol(1) + heptane(2); (b), DMC(1) + heptane(2); (c), methanol(1) + DMC(2); (d), 1-butanol(1) + DMC(2); (e), 1-hexanol(1) + DMC(2).

Table 3
Values of $TS_m^E(=H_m^E - G_m^E)$ and of concentration-concentration structure factor, $S_{CC}(0)$, calculated according the DISQUAC model for dialkyl carbonate (1) + *n*-alkane(2), or 1-alkanol(1) + dialkyl carbonate(2) mixtures at composition x_1, 298.15 K and 0.1 MPa.

System	$TS_m^E(x_1 = 0.5)$/J·mol^{-1}	x_1	$S_{CC}(0)_{max}(x_1)$[a]
DMC + heptane	832	0.57	3.87
DEC + heptane	556	0.48	0.66
Methanol + DMC	176	0.59	0.83
ethanol + DMC	578	0.55	0.98
1-propanol + DMC	937	0.51	1.17
1-butanol + DMC	1211	0.47	1.56
1-hexanol + DMC	1493	0.39	1.85
Methanol + DEC	303	0.59	0.72
ethanol + DEC	559	0.56	0.77
1-propanol + DEC	622	052	0.89
1-butanol + DEC	1002	0.50	0.74
1-hexanol + DEC	1277	0.46	0.60
1-octanol + DEC	1408	0.43	0.55

[a] maximum $S_{CC}(0)$ value.

$$\Delta H_{OH-CO3} = H_{m1}^{E,\infty}(1-\text{alkanol} + \text{carbonate}) - H_{m1}^{E,\infty}(1-\text{alkanol} + \text{heptane}) - H_{m1}^{E,\infty}(\text{carbonate} + \text{heptane}) \quad (10)$$

Certainly, this is a rough estimation of ΔH_{OH-CO3} values due to: i) $H_{m1}^{E,\infty}$ data used were calculated from H_m^E measurements over the entire mole fraction range. ii) For 1-alkanol + *n*-alkane systems, it was assumed that $H_{m1}^{E,\infty}$ is independent of the alcohol, a common approach when applying association theories [18,81–83]. We have used in this work, as in previous applications [7,78], $H_{m1}^{E,\infty} = 23.2$ kJ mol^{-1} [84–86]. Nevertheless, it should be remarked that the values of ΔH_{OH-CO3} collected in Table 5, for systems with DMC or DEC, are still meaningful as they were obtained following the same procedure that in other previous investigations, which allows to compare enthalpies of interaction between 1-alkanols

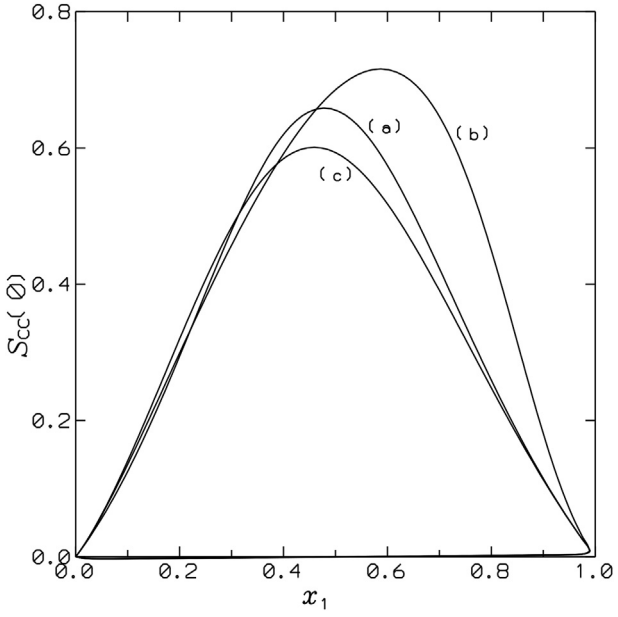

Fig. 7. $S_{CC}(0)$ curves, obtained from the DISQUAC model, for systems at 298.15 K and 0.1 MPa: (a), DEC(1) + heptane(2); (b), methanol(1) + DEC(2); (c), 1-hexanol(1) + DEC(2).

and different organic solvents. Inspection of Table 5 shows: (i) For a given carbonate, ΔH_{OH-CO3} increases more or less smoothly with n_{OH}. (ii) For a given 1-alkanol, ΔH_{OH-CO3} is lower for mixtures with DMC. That is, the OH and OCOO groups are more sterically hindered in longer 1-akanols and DEC, respectively, and this leads to weaker interactions between unlike molecules in systems with such compounds. No data on $H_{m1}^{E,\infty}$ for PC + alkane mixtures have been encountered in the literature, and, consequently, ΔH_{OH-CO3} values for 1-alkanol + PC systems remain unknown. Nevertheless, it is expected that their variation with n_{OH} is similar to that

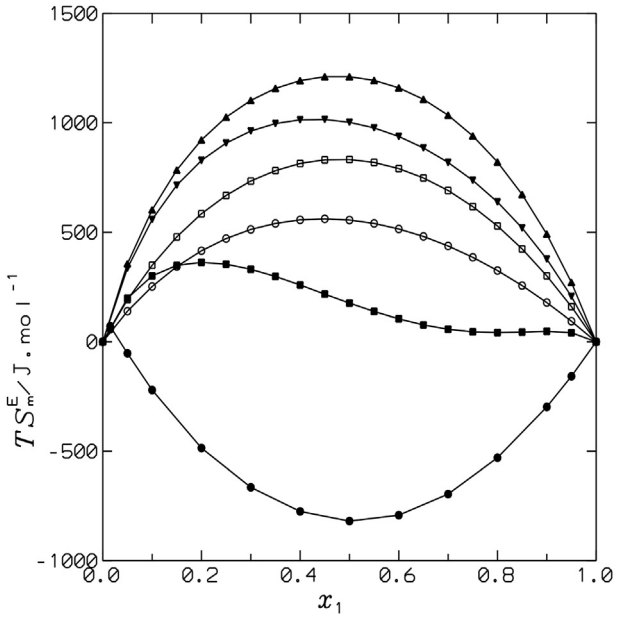

Fig. 8. TS^E_m curves for systems at 298.15 K and 0.1 MPa: (●), ethanol(1) + hexane(2) [85]; (■), methanol(1) + DMC(2); (▲), 1-butanol(1) + DMC(2); (▼), 1-butanol(1) + DEC(2); (□) DMC(1) + heptane(2); (O), DEC(1) + heptane(2). Lines are only for the aid of the eye.

Table 4
Molar excess volumes, V^E_m, at 0.1 MPa, 298.15 K and equimolar composition for dialkyl carbonate(1) + *n*-alkane(2) and for 1-alkanol(1) + organic carbonate(2) systems. Comparison of experimental (exp.) results with Flory calculations using interaction parameters listed in Table 2. Also included are the equation of state contribution ($\frac{\alpha_p}{\kappa_T}TV^E_m$) to H^E_m and the excess molar internal energy at constant volume, U^E_{Vm}.

Compound	V^E_m/cm^3·mol^{-1}		$\frac{\alpha_p}{\kappa_T}TV^E_m$/J·mol^{-1}	U^E_{Vm}/J·mol^{-1}	Ref.
	Exp.	Flory			
Dimethyl carbonate(1) + alkane (2)					
Heptane	1.158	1.825	346	1642	[54]
Decane	1.4425	2.217	458	1747	[54]
Diethyl carbonate(1) + alkane (2)					
Heptane	0.7362	1.266	226	1102	[55]
Octane	0.8755	1.493	275	1124	[55]
Decane	1.0629	1.769	344	1192	[55]
Tetradecane	1.2403	2.147	416	1382	[55]
1-alkanol (1) + dimethyl carbonate (2)					
Methanol	− 0.0628	1.048	− 23	1331	[96]
Ethanol	0.1505	1.492	53	1630	[98]
1-propanol	0.3693	1.802	135	1823	[98]
1-butanol	0.4771	2.192	191	2187	[90]
1-alkanol (1) + diethyl carbonate (2)					
Methanol	− 0.048	1.054	− 23	1274	[87]
Ethanol	0.1143	1.405	39	1481	[87]
1-propanol	0.2225	1.736	81	1714	[87]
1-butanol	0.2815	1.931	98	1844	[87]
1-hexanol	0.3940	2.032	141	1875	[87]
1-octanol	0.5200	2.124	187	1973	[87]
1-decanol	0.6386	2.120	232	2016	[87]
1-alkanol (1) + propylene carbonate (2)					
Methanol	− 0.3362	0.352	− 128	1490	[130]
Ethanol	− 0.2021	0.631	− 85	1961	[130]
1-propanol	− 0.037	0.931	− 14	2152	[130]
1-butanol	0.067	1.057	25	2175	[130]

observed for ΔH_{OH-CO3} in systems with DMC or DEC.

4.2.2. Excess molar enthalpies

The large and positive H^E_m values of these systems (Table 2; Figs. 2–5) indicate that the positive ΔH_{OH-OH}, $\Delta H_{CO3-CO3}$ contributions are predominant over the negative ΔH_{OH-CO3} term. Except for methanol systems, H^E_m(1-alkanol + carbonate) > H^E_m (1-alkanol + isomeric alkane). Thus, $H^E_m(n_{OH}= 3)$/J·mol^{-1} = 1794 (DEC) [87] > 459 (pentane) [88]. Clearly, organic carbonates are good breakers of the alcohol self-association. A similar trend is also encountered for 1-alkanol + linear polyether [7], or + *n*-alkanone mixtures [8]. This result suggests that in the studied mixtures, dipolar interactions play an essential role. Consequently, the shape of the H^E_m curves for 1-alkanol + *n*-alkane, or + organic carbonate mixtures greatly differ. Systems with *n*-alkanes are characterized by H^E_m curves skewed towards lower mole fractions of 1-alkanol (x_1), as the self-association of this compound is more easily broken at such condition. Carbonate mixtures show much more symmetrical H^E_m curves (Figs. 2–5). Interestingly, the H^E_m curve of methanol + DMC is skewed towards higher x_1 values, while that of the methanol + DEC is much more symmetrical (Fig. 2). One can conclude then that dipolar interactions are more relevant in DMC mixtures. It should be mentioned the very strong dipolar interactions existing in 1-alkanol + ethylene carbonate (dipole moment 4.81 D [36]) systems as it is shown by the upper critical solution temperatures of these mixtures: 312 K (1-propanol); 345.5 (1-hexanol) [89].

Table 5
Partial molar excess enthalpies,[a] $H^{E,\infty}_1$, at 298.15 K at 0.1 MPa for dialkyl carbonate(1) + oheptane(2) mixtures, and hydrogen bond enthalpies, ΔH_{OH-CO3}, for 1-alkanol(1) + dialkyl carbonate(2) systems.

System	$H^{E,\infty}_1$/kJ·mol^{-1}	ΔH_{OH-CO3}/kJ·mol^{-1}
DMC(1) + heptane(2)	9.54 [56]	
DEC(1)+ heptane(2)	7.07 [57]	
Methanol(1) + DMC(2)	5.78 [120]	− 27.0
ethanol(1) + DMC(2)	6.98 [120]	− 25.8
1-propanol(1) + DMC(2)	7.38 [120]	− 25.4
1-butanol(1) + DMC(2)	13.22 [90]	− 25.3
Methanol(1) + DEC(2)	8.04 [87]	− 22.2
ethanol(1) + DEC(2)	9.53 [87]	− 20.7
1-propanol(1) + DEC(2)	10.35 [87]	− 19.9
1-butanol(1) + DEC(2)	11.28 [87]	− 19.0
1-pentanol(1) + DEC(2)	10.66 [128]	− 19.6
1-hexanol(1) + DEC(2)	12.24 [87]	− 18.0
1-octanol(1) + DEC(2)	12.42 [87]	− 18.7
1-decanol(1) + DEC(2)	14.19 [87]	− 16.1

[a] values obtained from H^E_m data over the whole concentration range.

Comparison of H^E_m values of systems formed by a given dialkyl carbonate and 1-alkanol or alkane of similar size shows that H^E_m is higher for the solution including 1-alkanol. Thus, H^E_m(DEC)/J·mol^{-1} = 2159 (1-octanol) [87] > 1399 (octane) [57]. This indicates that interactions between unlike molecules are of low relevance in systems with longer 1-alkanols and that such compounds are good breakers of the dipolar interactions between carbonate molecules.

On the other hand, H^E_m data available in the literature [90,91] for 1-butanol + DMC or + DEC mixtures reveal that H^E_m is a function strongly dependent on temperature. For the mentioned systems, $\Delta H^E_m/\Delta T \approx$ 17 J mol^{-1} K^{-1}. Large positive C^E_{pm}/J·mol^{-1}·K^{-1} values are typically encountered in mixtures characterized by alcohol self-association (12.6 for 1-propanol + heptane) [92]. In contrast, mixtures where dipolar interactions are relevant show low C^E_{pm}/J·mol^{-1}·K^{-1} values (0.96 for ethanol + DMF) [93]. The large $\Delta H^E_m/\Delta T$ values of these solutions may indicate that any type of interactions, including those between unlike molecules, is largely broken when *T* is increased. Interestingly, for the methanol + PC mixture, C^E_{pm}/J·mol^{-1}·K^{-1} = 6.6 [94], and this newly remarks the relevance of dipolar interactions in PC systems.

4.2.2.1. The effect of increasing n_{OH} in systems with a given dialkyl carbonate. At this condition, H^E_m values increase (Table 2). This may be explained taking into account that both $\Delta H_{CO3-CO3}$ and ΔH_{OH-CO3} terms also increase with n_{OH} (Table 5). The former is due to the larger aliphatic surface of longer 1-alkanols break a higher number of carbonate-carbonate interactions, as H^E_m of linear organic carbonate + *n*-alkane increases with *n* (Table 2). The latter is related to the weaker interactions which exist between long 1-alkanols and carbonates. The increased $\Delta H_{CO3-CO3}$ and ΔH_{OH-CO3} values are predominant over the expected decrease of the contribution from the breaking of alkanol-alkanol interactions. It should be remembered that H^E_m of heptane systems increases from ethanol to 1-butanol and then slowly decreases [95]. Thus, 1-alkanol + *n*-alkane or + carbonate mixtures show a different variation of H^E_m with n_{OH}, and this also supports the relevance of dipolar interactions in carbonate systems.

4.2.2.2. The effect of replacing DMC by DEC in systems with a given 1-alkanol. DMC mixtures are characterized by larger H^E_m values than those containing DEC (see above, Table 2). This means that the positive difference ($\Delta H_{CO3-CO3}$(DMC) $-\Delta H_{CO3-CO3}$(DEC)) is predominant over the negative value of (ΔH_{OH-CO3}(DMC) $-\Delta H_{OH-CO3}$(DEC)) and over the higher contribution from the breaking of alkanol-alkanol interactions by the larger aliphatic surface of DEC. Note that H^E_m of mixtures formed by a given 1-alkanol and *n*-alkane, increases with *n* [95].

4.2.2.3. The effect of replacing DMC by PC in systems with a given 1-alkanol. The H^E_m dependence with n_{OH} for PC systems is similar to those observed for mixtures containing DMC or DEC, and may be explained in similar terms. The larger H^E_m(PC) values compared to those including DMC can be ascribed to theH^E_m contribution from the breaking of the carbonate-carbonate interactions is higher in the case of PC solutions due to the large dipole moment of this carbonate; and reveal that dipolar interactions are more important in PC mixtures. The lowerH^E_m value of the 1-butanol + PC system (Table 2) does not fit within this picture, and should be taken with caution.

4.2.3. Excess entropies

An interesting study can be conducted in terms of the TS^E_m magnitude (Table 3; Fig. 8). As previously, the TS^E_m curves of 1-alkanol + dialkyl carbonate mixtures were calculated using DISQUAC with interaction parameters available in the literature [14,15]. TS^E_m values of 1-alkanol + *n*-alkane mixtures are negative over almost the entire composition range, which is related to the alcohol self-association [85]. Only at low mole fractions of alcohol, positive TS^E_m values are encountered (Fig. 8) [85], as interactions between alkanol molecules are then more easily broken by alkanes. In addition, TS^E_m and n_{OH} values increase in line, as the weaker self-association of longer 1-alkanols leads to increased values ofTS^E_m. 1-Alkanol + DMC or + DEC mixtures show positive TS^E_m values at anyx_1 value (Table 3; Fig. 8). This clearly underlines that association/solvation effects are of minor importance. Such effects become even weakened for longer 1-alkanols, as TS^E_m increases with-n_{OH}(Table 3). Accordingly with the H^E_m results, TS^E_m values of mixtures with a given carbonate and 1-alkanol are higher than those of the corresponding system with an alkane of similar size. This is also supported by the G_{ii} values determined for these solutions [16]. In fact, the G_{ii} curves show maxima on both sides of the concentration range, which is characteristic of mixtures where interactions between like molecules exist. The observed decrease of TS^E_m when DMC is replaced by DEC may be ascribed to the less polar nature of DEC and to a lower enthalpic contribution toTS^E_m.

4.2.4. Excess molar volumes

For many of the systems considered, V^E_m values are positive (Table 4). Therefore, the main contribution to this excess function comes from interactional effects. Interestingly, for DEC mixtures, H^E_m/J mol^{-1} = 2248 (1-decanol) [87] > 1536 (decane) [57], while V^E_m/cm^3 mol^{-1} = 0.6386 (decanol) [96] < 1.0629 (decane) [55]. This clearly indicates that structural effects are also present in systems with 1-alkanols. The different sign of H^E_m andV^E_m for methanol + DMC (V^E_m=− 0.0628 cm^3 mol^{-1}) [96] or + DEC (V^E_m=− 0.048 cm^3 mol^{-1}) [87] mixtures, or for methanol (− 0.336 cm^3 mol^{-1} [97]), or + 1-propanol − 0.037 cm^3 mol^{-1} [97]) + PC mixtures supports our conclusion. On the other hand, bothH^E_m and V^E_m magnitudes increase withn_{OH}, and the V^E_m variation is closely related to that of the corresponding interactional contribution to this excess function.

4.3. Excess molar internal energies at constant volume

The large H^E_m values are not entirely due to interactional effects, but also to structural effects. The former are more properly considered usingU^E_{Vm}, the excess internal energy at constant volume. Neglecting terms of higher order inV^E_m, U^E_{Vm} can be written as [60,74]:

$$U^E_{Vm} = H^E_m - \frac{\alpha_p}{\kappa_T} TV^E_m \quad (11)$$

where $\frac{\alpha_p}{\kappa_T} TV^E_m$ is the so-called equation of state (eos) contribution toH^E_m, and α_p is the isobaric thermal expansion coefficient of the mixture. Calculations of α_p and κ_T were conducted on the basis of experimental data available in the literature on densities and adiabatic compressibilities of the involved mixtures [63,64,66,96,98–100], or assuming ideal behaviour ($F = \Phi_1 F_1 + \Phi_2 F_2$;$F_i$ is the property of the pure compound *i*) when such data are not available. The latter is a reasonable approximation in view of the rather low values of the excess values of α_p and κ_T available in the literature [63,64,66,96,98–100]. Values of $\frac{\alpha_p}{\kappa_T} TV^E_m$ and U^E_{Vm} are listed in Table 4. The eos contribution is very large for alkane mixtures and U^E_{Vm} changes more smoothly with *n* than H^E_m does. A similar trend is observed for mixtures with 1-alkanols, although the eos contribution is lower. It is to be noted that, for a given 1-alkanol, the difference U^E_{Vm} (PC) $-U^E_{Vm}$(DMC) is larger than that between the corresponding H^E_m values, which underlines that dipolar interactions are stronger in PC mixtures.

4.4. Internal pressures

Internal pressures, P_{int}, have been determined using the expression [101–104]:

$$P_{int} = \frac{\alpha_p T}{\kappa_T} - p \quad (12)$$

Values obtained in this work for some systems, using α_p and κ_T data available in the literature [63,64,66,96,98–100], are collected in Table 6. From these results, some general trends can be stated. (i) P_{int} values for carbonate + alkane mixtures are lower than those of 1-alkanol + carbonate mixtures. This may be due to the existence of interactions between unlike molecules and of structural effects in

Table 6
Internal pressures of pure compounds, $P_{int,i}$, and for the mixtures dialkyl carbonate + *n*-alkane or 1-alkanol + carbonate, P_{int}(eq. (12)), at equimolar composition, 298.15 K and 0.1 MPa. Comparison with results obtained from the Van der Waals model, P_{int}^{VDW}(eq. (13)).

System	$P_{int,1}$/MPa	$P_{int,2}$/MPa	P_{int}/MPa	P_{int}^{VDW}/MPa	Ref.
DMC(1) + *n*-C_8(2)	418.6	264.5	302.3	276.5	[64,131]
DMC(1) + *n*-C_9(2)	418.6	273.9	308.6	279.0	[64,132]
DEC(1) + *n*-C_{10}(2)	398.6	267.2	306.8	289.7	[133]
Methanol(1) + DMC(2)	285.6	411.2	366.0	342.5	[96,98]
Ethanol(1) + DMC(2)	283.2	411.2	345.6	332.7	[98]
1-propanol(1) + DMC(2)	291.7	411.2	363.4	321.7	[98]
1-butanol(1) + DMC(2)	298.1	411.2	359.7	324.5	[98]
Methanol(1) + DEC(2)	285.6	356.4	335.8	335.8	[99]
Ethanol(1) + DEC(2)	283.2	356.4	340.0	326.2	[99]
1-propanol(1) + DEC(2)	291.7	356.4	342.2	326.5	[99]
1-butanol(1) + DEC(2)	298.1	356.4	335.1	328.0	[99]
Ethanol(1) + PC(2)	283.2	492	421.5	367.6	[100,130]
1-propanol(1) + PC(2)	291.7	492	390.1	368.2	[100,130]
1-butanol(1) + PC(2)	298.1	492	372.2	367.6	[100,130]

the latter systems; (ii) It is known that the main contributions to P_{int} arise from dispersion forces and weak dipole-dipole interactions [103]; therefore, it seems that such type of interactions in 1-alkanol + carbonate mixtures become weaker in the order: PC > DMC > DEC. On the other hand, P_{int} values can be also obtained from the equation [102]:

$$P_{int}^{VDW} = \frac{RT}{x_1 v_{f1} + x_1 v_{f2} + V_m^E} - P \tag{13}$$

In this expression, $v_{fi}(=RT/(`p + P_{int,i}))$ is the free volume of component i [102]. Experimental P_{int} results are compared with those of P_{int}^{VDW} in Table 6. The average difference between these magnitudes is 6.1% and this demonstrates that the Van der Waals equation is hold in large extent for the current mixtures, as eq. (13) is derived from this equation of state [102].

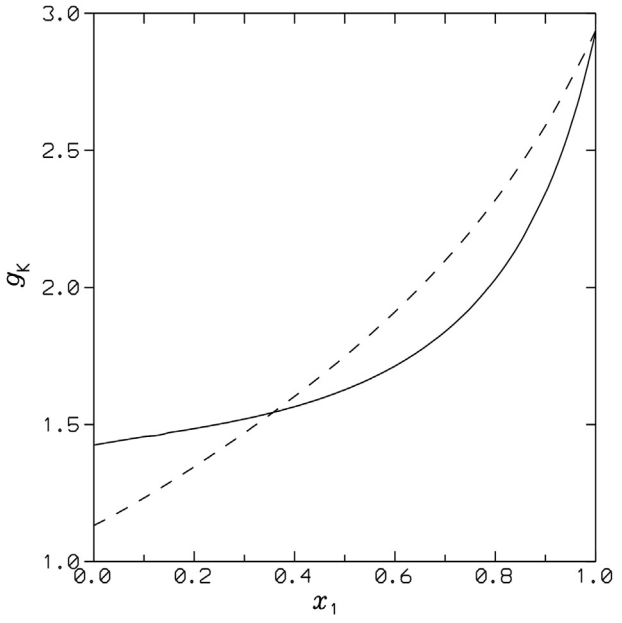

Fig. 9. Kirkwood correlation factor, g_K, for the methanol(1) + ethylene carbonate(2) (solid line) [105], or + *N,N*-dimethylformamide (dashed line) [106,107] mixtures at 298.15 K and 0.1 MPa.

4.5. Dielectric constants and Kirkwood's correlation factor

We pay attention here to the permittivity dataε_r, of the methanol + ethylene carbonate (EC) system which, as far as we know, are the only available in the literature for this type of mixtures [105]. Interestingly, the excess permittivity ($\varepsilon_r^E = \varepsilon_r - \phi_1\varepsilon_{r1} - \phi_2\varepsilon_{r2}$) of the solution is − 3.1, much lower than the results for methanol + *N,N*-dimethylformamide (2.57 [106,107]), or + *N,N*-dimethylacetamide (0.52 [107,108]) systems. These very different results are remarkable as the considered amides have large dipole moments (3.7 D, *N,N*-dimethylformamide; 3.68 D, *N,N*-dimethylacetamide [109]). The large negative ε_r^E value of the EC mixture reveals that the predominant trend in the solution is the breaking of the alcohol network and of the dipolar interactions between EC molecules in such way that a decrease of the dipolar polarization is produced [108]. The opposite behaviour is encountered in the mentioned systems with amides, characterized by an increase of the total effective dipole moment of the mixtures. This is supported by the calculation of the Kirkwood's correlation factorg_K, of methanol + EC system according to the equation [110–112]:

$$g_K = \frac{9k_B T V_m \varepsilon_0 (\varepsilon_r - \varepsilon_r^\infty)(2\varepsilon_r + \varepsilon_r^\infty)}{N_A \mu_r \varepsilon_2 (\varepsilon_r^\infty + 2)^2} \tag{14}$$

where the symbols have the usual meaning [107]. Details of the calculation procedure are given elsewhere [107]. In absence of experimental measurements on density and refractive indices, molar, these magnitude were considered as ideal [113]. Results (Fig. 9) show that the mixture structure slowly changes in a wide concentration range as the addition of methanol to EC does not lead to cooperative effects which increase the total effective dipole moment of the mixture. The methanol + DMF mixture behave differently (Fig. 9). Experimental work on this matter is currently undertaken.

4.6. The role of the size group in dialkyl carbonates

Finally, it is pertinent to conduct a comparison between experimental results for systems with *n*-alkanones (particularly, 2-propanone, 3-pentanone) or with DMC or DEC. Firstly, it is necessary to remark that both the dipolar moment (μ) and the effective dipolar moment ($\bar{\mu}$) are higher for *n*-alkanones. The dipole moments of the mentioned ketones are [114]: 2.88 D (2-propanone) and 2.82 D (3-pentanone); for the carbonates [109], μ/D = 0.94

(DMC); 0.90 (DEC). The effective dipole moment is a useful magnitude to evaluate the impact of polarity on bulk properties and is defined by Refs. [60,115,116].

$$\overline{\mu} = \left(\frac{\mu^2 N_A}{4\pi\varepsilon_0 k_B V_m T}\right)^{1/2} \quad (15)$$

Results for $\overline{\mu}$ are: 1.28 (2-propanone); 1.05 (3-pentanone); 0.39 (DMC); 0.31 (DEC). However for systems with a given alkane, say dodecane, UCST/K = 286.2 (2-propanone) [117] < 307.61 (DMC) [51]. Similarly, H^E_m and U^E_{Vm} values are also lower for alkanone mixtures including alkanes (Table S1; supplementary material). All this allows conclude that dipolar interactions are stronger in mixtures involving dialkyl carbonates and that the size group plays an important role when evaluating such interactions which are not merely determined by μ values. The high UCST value of the acetic anhydride + heptane system (342.52 K) [118] is consistent with this picture as, for acetic anhydride [109],μ/D = 3.10 and $\overline{\mu}$ = 1.22. Regarding mixtures with a given 1-alkanol and 2-propanone, or 3-pentanone, they show lower H^E_m values than those of the corresponding systems with DMC or DEC (Table S1, supplementary material). Thus, $H^E_m(n_{OH}=1)$/J·mol^{-1} = 686 (2-propanone) [119]; 1308 (DMC) [120]; 725 (3-pentanone) [121]; 1257 (DEC) [87]. This can be explained taking into account that the contribution to H^E_m from the breaking of interactions between carbonate molecules is larger than that corresponding to the disruption of the ketone-ketone interactions. Moreover, interactions between unlike molecules are stronger in systems involving alkanones [8]. For example, the values $\Delta H_{OH-CO}(n_{OH}=1)$/kJ·mol^{-1} = − 28.6 (2-propanone); − 24.2 (3-pentanone) are lower than those listed in Table 5 for methanol + DMC, or + DEC systems.

4.7. Results from the Flory model

The large and positive X_{12} values obtained for the studied mixtures (Table 2) reveal that the main contribution to H^E_m arises from interactions between like molecules. In the case of dialkyl carbonate mixtures, for enough large n and n_{OH} values, we note that $X_{12}(n) < X_{12}(n_{OH})$ (n=n_{OH}), in agreement with the trend encountered for the correspondingH^E_m values. Thus, X_{12}(DEC)/J·cm^{-3} = 73.08 (1-octanol) > 51.40 (octane) and H^E_m/J·mol^{-1} = 2159 (1-octanol) [87] > 1399 (octane) [57]. That is, interactions between unlike molecules are of minor importance for systems with longer 1-alkanols. On the other hand, X_{12} of DEC + n-alkane mixtures increases linearly with$n$: X_{12} = 41.22 + 1.317n (r = 0.989). DMC systems behave somewhat differently as at 298.15 K, the temperatures of solutions with the longer n-alkanes are close to the UCST and the H^E_m curves become flattened. Interestingly, X_{12} and H^E_m do not change in line withn_{OH}, as the former magnitude decreases when n_{OH} is increased. This is due to the $H^E_{m,int}$ depends on $\theta_2 V^*_1$(eq. (2)), a magnitude which is ranged for DEC solutions between 21.31 (n_{OH}= 1) and 65.33 (n_{OH} = 10) cm^3 mol^{-1}.

Let's define the mean standard relative deviation ofH^E_m as:

$$\overline{\sigma}_r\left(H^E_m\right) = \frac{1}{N_S}\sum \sigma_r\left(H^E_m\right) \quad (16)$$

where N_S represents the number of systems considered. From the theoretical results using the Flory model, we can provide the following statements. (i) Orientational effects in 1-alkanol mixtures become stronger in the order: DMC < PC < DEC, as $\overline{\sigma}_r(H^E_m)$ = 0.086 (DMC) < 0.109 (PC) < 0.132 (DEC). Orientational effects become weakened when n_{OH} is increased, and are particularly relevant in DEC solutions with n_{OH} = 1,2 ($\overline{\sigma}_r(H^E_m)$ = 0.255). (iii) For systems with DMC, orientational effects are weaker in solutions with 1-alkanols than in those with alkanes ($\overline{\sigma}_r(H^E_m)$ = 0.101). This supports our previous statement about the ability of DMC as a breaker of the alcohol self-association. In addition, note that alkane systems are close to the UCST. (iv) The poor results obtained for methanol or ethanol + DEC mixtures remark that the alcohol self-association and/or interactions between unlike molecules are relatively more important in these mixtures. Orientational effects are also weaker in DEC systems with n_{OH} > 3 ($\overline{\sigma}_r(H^E_m)$ = 0.088) than in those containing alkanes ($\overline{\sigma}_r(H^E_m)$ = 0.113). (v) As usually, the increase of temperature leads to improve Flory results. It is interesting to compare experimental H^E_m results at $T \neq$ 298.15 K with results provided by the model using X_{12} values determined from H^E_m data at 298.15 K. Of course, theoretical results become then poorer as it is indicated by the following H^E_m/J mol^{-1} values for DMC systems: 1321 (methanol, T = 313.15 K); 1728 (ethanol, T = 313.15 K); 1990 (1-propanol, T = 313.15 K); 2104 (heptane, T = 413.15 K). The differences with experimental results (see Table 2), in the same order, are: − 14%; − 13.2%; − 15% and 5.8%. We note that these differences are larger (and negative) for 1-alkanol systems, which clearly indicates that non-random effects are more relevant in such solutions. In fact, orientational effects show a stronger temperature dependence than effects related to dispersive interactions. It should be kept in mind that dipole-dipole interactions, or molecular anisotropy, are usually approximated by a spherical pair interaction inversely proportional to temperature [60,74]. (vi). The model provides very largeV^E_m values (Table 3) as the interactional contribution to this excess function is overestimated. Nevertheless, the variation of V^E_m with n orn_{OH} is correctly represented. The V^E_m results can be better examined by means of the Prigogine-Flory-Patterson model (PFP) [122], where V^E_m is written as the sum of three contributions: an interactional contribution, a curvature term and the so-called P^* term. The second one depends on $-(\overline{V}_1 - \overline{V}_2)^2$

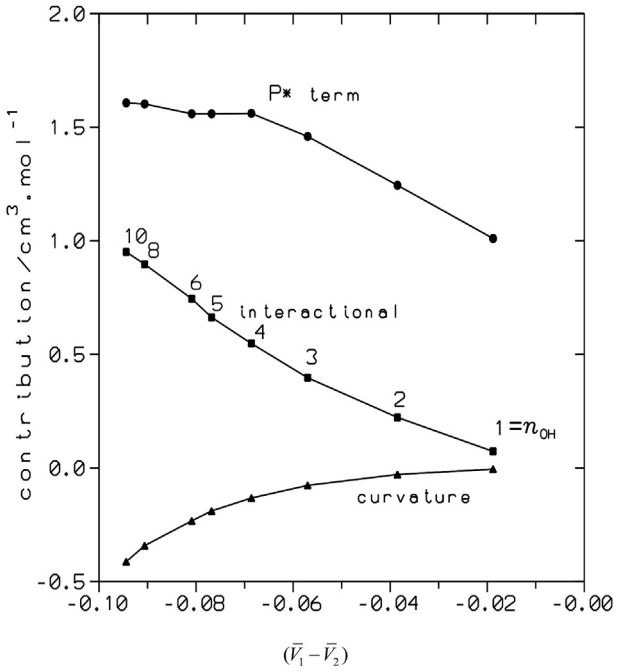

Fig. 10. Interactional, curvature and P^* contributions to V^E_m, calculated using the PFP model, for 1-alkanol(1) + DEC(2) mixtures at 298.15 K and equimolar composition vs. $(\overline{V}_1 - \overline{V}_2)$ the difference between the reduced volumes. n_{OH} stands for the number of C atoms in the 1-alkanol. Lines are only for the aid of the eye.

and is always negative. The latter depends on $(P_1^* - P_2^*)(\overline{V}_1 - \overline{V}_2)$. For the 1-alkanol + DEC systems considered, $P_1^* < P_2^*$; $\overline{V}_1 < \overline{V}_2$ and the P^* term is always positive and increases rapidly with n_{OH}. This leads to large positive V_m^E values as the curvature term is much lower than the P^* contribution and the interactional contribution is also very large (Fig. 10; Table S2, supplementary material). Similar trends are also valid for 1-alkanol + DMC, or + PC systems, although in the case of PC solutions, $P_1^* < P_2^*$; $\overline{V}_1 > \overline{V}_2$ and the P^* contribution is negative.

We have investigated previously, using the Flory model, orientational effects in systems of the type: 1-alkanol + liner mono- [6] or polyether [7], + alkanone [8], or + alkanenitrile [9]. The $\overline{\sigma}(H_m^E)$ values change in the sequence: 0.323 (linear monoether) > 0.137 (linear polyether) > 0.114 (alkanenitrile) ≈ 0.107 (carbonate) ≈ 0.099 (*n*-alkanone). Clearly, orientational effects are stronger in systems with linear monoethers, where the alcohol self-association plays the main role. Results for linear polyether mixtures are improved when systems with methanol or ethanol are discarded ($\overline{\sigma}(H_m^E)$= 0.054). Mixtures with alkanenitriles, *n*-alkanone or carbonates behave similarly.

4.8. $S_{CC}(0)$ results

Firstly, we note the very large $S_{CC}(0)$ values of ethanol or DMC + heptane mixtures, indicating that interactions between like molecules are predominant (Table 3; Figs. 6–7). In the case of the ethanol system, it is due to the strong alcohol self-association. For all the examined systems, $S_{CC}(0) > 0.25$, and they are characterized by homocoordination. The large $S_{CC}(0)$ values of the DMC + heptane mixture can be ascribed to the proximity of the UCST at 298.15 K. Accordingly, the$S_{CC}(0)$ and LLE curves are skewed to higher carbonate concentrations. On the other hand, $S_{CC}(0)$ values of DMC systems are higher than those of DEC mixtures. That is, interactions between like molecules are more relevant in DMC solutions. When comparing $S_{CC}(0)$ results for 1-alkanol + DMC or DMC + heptane systems (Fig. 6), we note that 1-alkanol systems show lower $S_{CC}(0)$ values, which can be ascribed to the new interactions between unlike molecules created upon mixing. In addition, $S_{CC}(0)$ increases with the alkanol size. One can conclude that alkanol-DMC interactions become then less relevant. This is supported by the variation of the symmetry of the $S_{CC}(0)$ curves. In fact, the mentioned symmetry is similar for the systems 1-hexanol + DMC and DMC + heptane as the curves are skewed to higher carbonate mole fractions. In contrast, the $S_{CC}(0)$ curve of the methanol solution is skewed to higher alkanol concentrations, which suggests that the self-association of this compound could be here more important (Fig. 6). 1-Alkanol + DEC mixture behave differently (Fig. 7). Thus, it is remarkable that $S_{CC}(0)$(methanol + DEC) > $S_{CC}(0)$(DEC + heptane), which may be ascribed to alkanol-alkanol interactions are relatively more relevant than those between unlike molecules. In constrast, for mixtures with enough long 1-alkanols, say 1-hexanol, $S_{CC}(0)$(1-hexanol + DEC) <$S_{CC}(0)$ (DEC + heptane), which points out that interactions between unlike molecules play now a more important role. On the other hand, $S_{CC}(0)$ increases up to 1-butanol and then decreases. This variation together with the change of the symmetry of the $S_{CC}(0)$ curves (Fig. 7) might indicate that the role of the alkanol self-association becomes less relevant.

5. Conclusions

Organic carbonate + alkane, and 1-alkanol + organic carbonate mixtures have been investigated on the basis of different thermophysical properties and using the Flory model and the $S_{CC}(0)$ formalism. The studied systems are characterized by dipolar interactions and show homocoordination. For a given solvent, dipolar interactions become more relevant in the sequence: DEC < DMC < PC. It has been shown that dipolar interactions in systems with DMC or DEC are not determined merely by μ values, but they also depend on the size group. In mixtures with 1-alkanols, hydroxyl-carbonate mixtures are stronger in solutions with DMC, and become weaker when the alcohol size increases in systems with a given carbonate. Results from the Flory model show that orientational effects decrease in the order: DEC > PC > DEC. These effects seem to be particularly important in mixtures with methanol or ethanol. In systems containing DMC, orientational effects are weaker in 1-alkanol mixtures than in those containing alkanes. A similar trend is encountered in DEC systems for n_{OH}> 2.

Funding

The authors gratefully acknowledge the financial support received from the Consejería de Educación y Cultura of Junta de Castilla y León, under Project BU034U16. F. Hevia gratefully acknowledges the grant received from the program 'Ayudas para la Formación de Profesorado Universitario (convocatoria 2014), de los subprogramas de Formación y de Movilidad incluidos en el Programa Estatal de Promoción del Talento y su Empleabilidad, en el marco del Plan Estatal de Investigación Científica y Técnica y de Innovación 2013-2016, de la Secretaría de Estado de Educación, Formación Profesional y Universidades, Ministerio de Educación, Cultura y Deporte, Gobierno de España'.

List of symbols

C_p	heat capacity at constant pressure
ΔH	enthalpy of interaction
g_K	Kirkwood's correlation factor (eq. (14))
G	Gibbs energy
H	enthalpy
n	number of C atoms in *n*-alkane
n_{OH}	number of C atoms in 1-alkanol
P_{int}	internal pressure (eq. (12))
P^*	reduction parameter for pressure in the Flory model
S	entropy
$S_{CC}(0)$	concentration-concentration structure factor (eq. (6))
T	temperature
U_V	internal energy at constant volume
V	molar volume
V^*	reduction parameter for volume in the Flory model
x	mole fraction in liquid phase

Greek letters

α_P	isobaric themal expansion coefficient
ε_r	relative permittivity
κ_T	isothermal compressibility
μ	dipole moment
$\overline{\mu}$	effective dipole momento (eq. (15))
σ_r	relative standard deviation (eq. (8))
X_{12}	interaction parameter in the Flory model

Superscripts

E	excess property

Subscripts

i,j	compound in the mixture, (i, j = 1,2)
m	molar property

Appendix A. Supplementary data

Supplementary data related to this article can be found at http://dx.doi.org/10.1016/j.fluid.2017.06.012.

References

[1] P.J. Flory, J. Am. Chem. Soc. 87 (1965) 1833–1838.
[2] A. Abe, P.J. Flory, J. Am. Chem. Soc. 87 (1965) 1838–1846.
[3] P.J. Flory, R.A. Orwoll, A. Vrij, J. Am. Chem. Soc. 86 (1964) 3507–3514.
[4] P.J. Flory, R.A. Orwoll, A. Vrij, J. Am. Chem. Soc. 86 (1964) 3515–3520.
[5] R.A. Orwoll, P.J. Flory, J. Am. Chem. Soc. 89 (1967) 6822–6829.
[6] J.A. González, N. Riesco, I. Mozo, I. García de la Fuente, J.C. Cobos, Ind. Eng. Chem. Res. 48 (2009) 7417–7429.
[7] J.A. González, A. Mediavilla, I. García de la Fuente, J.C. Cobos, J. Chem. Thermodyn. 59 (2013) 195–208.
[8] J.A. González, A. Mediavilla, I. García de la Fuente, J.C. Cobos, C. Alonso-Tristán, N. Riesco, Ind. Eng. Chem. Res. 52 (2013) 10317–10328.
[9] J.A. González, I. García de la Fuente, J.C. Cobos, C. Alonso-Tristán, L.F. Sanz, Ind. Eng. Chem. Res. 54 (2015) 550–559.
[10] J.A. González, N. Riesco, I. Mozo, I. García de la Fuente, J.C. Cobos, Ind. Eng. Chem. Res. 46 (2007) 1350–1359.
[11] J.A. González, Ind. Eng. Chem. Res. 49 (2010) 9511–9524.
[12] J.A. González, I. García de la Fuente, J.C. Cobos, I. Mozo, I. Alonso, Thermochim. Acta 514 (2011) 1–9.
[13] J.A. González, I. García de la Fuente, J.C. Cobos, N. Riesco, Ind. Eng. Chem. Res. 51 (2012) 5108–5116.
[14] J.A. González, I. García de la Fuente, J.C. Cobos, C. Casanova, H.V. Kehiaian, Thermochim. Acta 217 (1993) 57–69.
[15] J.A. González, M. Szurgocinska, U. Domanska, Fluid Phase Equilib. 200 (2002) 349–374.
[16] J.A. González, I. Mozo, S. Villa, N. Riesco, I. García de la Fuente, J.C. Cobos, J. Solut. Chem. 35 (2006) 787–801.
[17] H.V. Kehiaian, Fluid Phase Equilib. 13 (1983) 243–252.
[18] A. Heintz, Ber. Bunsenges. Phys. Chem. 89 (1985) 172–181.
[19] J.G. Kirkwood, F.P, J. Chem. Phys. 19 (1951) 774–777.
[20] A. Ben-Naim, J. Chem. Phys. 67 (1977) 4884–4889.
[21] J. Gmehling, J. Li, M. Schiller, Ind. Eng. Chem. Res. 32 (1993) 178–193.
[22] T. Nitta, E.A. Turek, R.A. Greenkorn, K.C. Chao, K.C, AIChE J. 23 (1977) 144–160.
[23] J. Lohman, J. Gmehling, J. Chem. Eng. Jpn. 34 (2001) 43–54.
[24] J. García, L. Lugo, M.J. Comuñas, E.R. López, J. Fernández, J. Chem. Soc. Faraday Trans. 94 (1998) 1707–1712.
[25] J.C. Cobos, Fluid Phase Equilib. 133 (1997) 105–127.
[26] L.D. Landau, E.M. Lifshitz, Física Estadística, Reverté, Barcelona, 1969.
[27] R.G. Rubio, M. Cáceres, R.M. Masegosa, L. Andreoli-Ball, M. Costas, D. Patterson, Ber. Bunsenges. Phys. Chem. 93 (1989) 48–56.
[28] A.B. Bhatia, D.E. Thornton, Phys. Rev. B 2 (1970) 3004–3012.
[29] W.H. Young, Rep. Prog. Phys. 55 (1992) 1769–1853.
[30] B. Karaoglu, W.H. Young, Phys. Chem. Liq. 30 (1995) 187–193.
[31] L.J. Gallego, J.A. Somoza, J.A. Alonso, Phys. Chem. Liq. 16 (1987) 249–258.
[32] L.J. Gallego, J.A. Somoza, J.A. Alonso, Chem. Phys. 99 (1985) 35–41.
[33] J.A. González, J.C. Cobos, I. García de la Fuente, I. Mozo, Thermochim. Acta 494 (2009) 54–64.
[34] J.A. González, I. Mozo, I. García de la Fuente, J.C. Cobos, V.A. Durov, Fluid Phase Equilib. 245 (2006) 168–184.
[35] J.A. González, C. Alonso-Tristán, I. García de la Fuente, J.C. Cobos, Fluid Phase Equilib. 421 (2016) 49–58.
[36] Y. Cherniak, J. Chem. Eng. Data 51 (2006) 416–418.
[37] L. Simeral, R.L. Amey, J. Phys. Chem. 74 (1970) 1443–1446.
[38] R. Payne, I.E. Theodorou, J. Phys. Chem. 76 (1972) 2892–2900.
[39] J.P. Parrish, R.N. Salvatore, K.W. Jung, Tetrahedron 56 (2000) 8207–8237.
[40] M.C. Annesini, R. De Santis, I. Kikic, R. Marrelli, J. Chem. Eng. Data 29 (1984) 39–41.
[41] R. Naejus, D. Lemordant, R. Coudert, P. Willmann, J. Chem. Thermodyn. 29 (1997) 1503–1515.
[42] S. Tobishima, A. Yamaji, Electrochim. Acta 28 (1983) 1067–1072.
[43] F. Rivetti, Comptes Rendus, Acad. Sci. Ser. IIc, Chim. 3 (2000) 497–503.
[44] T.J. Wallington, M.D. Hurley, J.C. Ball, A.M. Straccia, J. Platz, L.N. Christensen, J. Sehested, O.J. Nielsen, J. Phys. Chem. A 101 (1997) 5302–5308.
[45] M.A. Pacheco, C.L. Marshall, Energy & Fuel 11 (1997) 2–29.
[46] I.-Y. Jeong, S.-H. You, S.-J. Park, Fluid Phase Equilib. 278 (2014) 93–101.
[47] M.J. Cocero, I. García, J.A. González, J.C. Cobos, Fluid Phase Equilib. 68 (1991) 151–161.
[48] M.J. Cocero, J.A. González, I. García, J.C. Cobos, F. Mato, Int. Data Ser. Sel. Data Mix. Ser. A 2 (1991) 130–138.
[49] M.J. Cocero, J.A. González, I. García, J.C. Cobos, F. Mato, Int. Data Ser. Sel. Data Mix. Ser. A 2 (1991) 112–129.
[50] A. Sporzynski, M. Szurgocinska, U. Domanska, J.A. González, Ind. Eng. Chem. Res. 42 (2003) 4382–4388.
[51] J.A. González, I. García, J.C. Cobos, C. Casanova, J. Chem. Eng. Data 36 (1991) 162–164.
[52] U. Domanska, M. Szurgocinska, J.A. González, Fluid Phase Equilib. 190 (2001) 15–31.
[53] U. Domanska, M. Szurgocinska, J.A. González, Ind. Eng. Chem. Res. 41 (2002) 3253–3259.
[54] I. García de la Fuente, J.A. González, J.C. Cobos, C. Casanova, J. Chem. Eng. Data 37 (1992) 535–537.
[55] I. García de la Fuente, J.A. González, J.C. Cobos, C. Casanova, J. Solut. Chem. 24 (1995) 827–835.
[56] I. García, J.C. Cobos, J.A. González, C. Casanova, M.J. Cocero, J. Chem. Eng. Data 33 (1988) 423–426.
[57] I. García, J.C. Cobos, J.A. González, C. Casanova, Int. Data Ser. Sel. Data Mix. Ser. A 3 (1987) 164–173.
[58] P.J. Howell, B.J. Skillerne de Bristowe, D. Stubley, J. Chem. Soc. A (1971) 397–400.
[59] L.M. Trejo, M. Costas, D. Patterson, J. Chem. Soc. Faraday Trans. 87 (1991) 3001–3008.
[60] J.S. Rowlinson, F.L. Swinton, Liquids and Liquid Mixtures, 3th Ed., Butterworths, London, 1982.
[61] H.V. Kehiaian, Bull. Acad. Pol. Sci. Ser. Sci. Chim. 10 (1962) 569.
[62] B. Karaoglu, W.H. Young, Phys. Chem. Liq. 24 (1991) 43–53.
[63] J.M. Pardo, C.A. Tovar, C.A. Cerdeiriña, E. Carballo, L. Romaní, J. Chem. Thermodyn. 31 (1999) 787–796.
[64] J.M. Pardo, C.A. Tovar, J. Troncoso, E. Carballo, L. Romaní, Thermochim. Acta 433 (2005) 128–133.
[65] M.-E. Saint-Victor, D. Patterson, Fluid Phase Equilib. 35 (1987) 237–252.
[66] A. Rodríguez, J. Canosa, J. Tojo, J. Chem. Thermodyn. 35 (2003) 1321–1333.
[67] M.F. Bolotnikov, Y.A. Neruchev, Y.F. Melikhov, V.N. Verveyko, M.V. Verveyko, J. Chem. Eng. Data 50 (2005) 1095–1098.
[68] S.H. Ali, H.M.S. Lababidi, S.Q. Merchant, M.A. Fahim, Fluid Phase Equilib. 214 (2003) 25–38.
[69] M.A. Fahim, S.Q. Merchant, J. Chem. Eng. Data 43 (1998) 884–888.
[70] A. Bakr, S.H. Salem, E.Z. Hamad, M.A. Al-Naafa, Ind. Chem. Eng. Res. 33 (1994) 689–692.
[71] E. Schafer, G. Sadowski, Ind. Eng. Chem. Res. 51 (2012) 14525–14534.
[72] A.W. Francis, Critical Solution Temperatures, Advances in Chemitry Series, Washington (, 1961.
[73] M. Topphoff, D. Gruber, J. Gmehling, J. Chem. Eng. Data 44 (1999) 1355–1359.
[74] H. Kalali, F. Kohler, P. Svejda, Fluid Phase Equilib. 20 (1985) 75–80.
[75] H.P. Diogo, M.E. Minas de Piedade, J. Moura Ramos, J. Simoni, J.A. Martinho Simoes, J. Chem. Educ. 70 (1993) A227.
[76] T.M. Letcher, U.P. Govender, J. Chem. Eng. Data 40 (1995) 1097–1100.
[77] E. Calvo, P. Brocos, A. Piñeiro, M. Pintos, A. Amigo, R. Bravo, A.H. Roux, G. Roux-Desgranges, J. Chem. Eng. Data 44 (1999) 948–954.
[78] J.A. González, I. Mozo, I. García de la Fuente, J.C. Cobos, N. Riesco, J. Chem. Thermodyn. 40 (2008) 1495–1508.
[79] T.M. Letcher, B.C. Bricknell, J. Chem. Eng. Data 41 (1996) 166–169.
[80] J.A. González, I. García de la Fuente, J.C. Cobos, Fluid Phase Equilib. 301 (2011) 145–155.
[81] V. Brandani, J.M. Prausnitz, Fluid Phase Equilib. 7 (1981) 233–257.
[82] A. Liu, F. Kohler, L. Karrer, J. Gaube, P.A. Spelluci, Pure Appl. Chem. 61 (1989) 1441–1452.
[83] H. Renon, J.M. Prausnitz, Chem. Eng. Sci. 22 (1967) 299–307.
[84] R.H. Stokes, C. Burfitt, J. Chem. Thermodyn.. 5(9173) 623–631.
[85] S.J. O'Shea, R.H. Stokes, J. Chem. Thermodyn. 18 (1986) 691–696.
[86] H.C. Van Ness, J. Van Winkle, H.H. Richtol, H.B. Hollinger, J. Phys. Chem. 71 (1967) 1483–1494.
[87] R. Francesconi, F. Comelli, J. Chem. Eng. Data 42 (1997) 45–48.
[88] S.G. Collins, J.J. Christensen, R.M. Izatt, R.W. Hanks, J. Chem. Thermodyn. 12 (1980) 609–614.
[89] M. Iwahashi, T. Nozaki, K. Kamaya, K. Taguchi, M. Fujita, Y. Kasahara, H. Minami, H. Matsuzawa, Sh Nakamura, K. Harada, Y. Ozaki, T. Inoue, J. Chem. Thermodyn. 43 (2011) 80–87.
[90] R. Francesconi, F. Comelli, J. Chem. Eng. Data 44 (1999) 44–47.
[91] F. Comelli, R. Francesconi, C. Castellari, J. Chem. Eng. Data 44 (1999) 739–743.
[92] R. Tanaka, S. Toyama, S. Murakami, J. Chem. Thermodyn. 18 (1986) 63–73.
[93] G. Conti, P. Giani, L. Lepori, E. Matteoli, Fluid Phase Equilib. 105 (1995) 93–107.
[94] H. Piekarski, A. Pietrzak, D. Waliszewski, J. Mol. Liq. 121 (2001) 41–45.
[95] J.A. González, I. García de la Fuente, J.C. Cobos, C. Casanova, Ber. Bunsenges. Phys. Chem. 95 (1991) 1658–1668.
[96] A. Rodríguez, J. Canosa, J. Tojo, J. Chem. Eng. Data 44 (1999) 1298–1303.
[97] R. Francesconi, F. Comelli, J. Chem. Eng. Data 41 (1996) 1397–1400.
[98] A. Rodríguez, J. Canosa, J. Tojo, J. Chem. Eng. Data 46 (2001) 1476–1486.
[99] A. Rodríguez, J. Canosa, J. Tojo, J. Chem. Eng. Data 46 (2001) 1506–1515.
[100] D.S. Whankhede, N.N. Whankhede, M.K. Lande, B.R. Arbad, Ind. J. Pure Appl. Phys. 44 (2006) 909–916.
[101] E.B. Bagley, T.P. Nelson, J.W. Barlow, S.-A. Chen, I&EC Fund. 9 (1970) 93–97.
[102] E.B. Bagley, T.P. Nelson, J.M. Scigliano, J. Phys. Chem. 77 (1973) 2794–2798.
[103] M.R.J. Dack, Aust. J. Chem. 28 (1975) 1643–1648.
[104] E. Zorebski, Mol. Quantum. Acoust. 26 (2005) 317–326.
[105] R.P. Seward, E.C. Vieira, J. Phys. Chem., 62(1058) 127–128.
[106] M.S. Bakshi, G. Kaur, J. Chem. Eng. Data 42 (1997) 298–300.
[107] J.A. González, L.F. Sanz, I. García de la Fuente, J.C. Cobos, J. Chem. Thermodyn. 91 (2015) 267–278.

[108] G. Ritzoulis, A. Fidantsi, J. Chem. Eng. Data 45 (2000) 207–209.
[109] A.L. McClellan, Tables of Experimental Dipole Moments. Vols. 1,2,3, Rahara Enterprises, El Cerrito, US, 1974.
[110] A. Chelkowski, Dielectric Physics, Elsevier, Warsaw (, 1980.
[111] C. Moreau, G. Douhéret, J. Chem. Thermodyn. 8 (1978) 403–410.
[112] J.C.R. Reis, T.P. Iglesias, Phys. Chem. Chem. Phys. 13 (2011) 10670–10680.
[113] G. Douheret, H. Degeilh, Adv. Mol. Relax. Int. Process 12 (1978) 107–121.
[114] D.R. Lide, CRC Handbook of Chemistry and Physics, 90th Edition, CRC Press/Taylor and Francis, Boca Raton, FL, 2010.
[115] J.A. González, I. García de la Fuente, J.C. Cobos, Fluid Phase Equilib. 168 (2000) 31–58.
[116] E. Wilhelm, A. Laínez, J.-P.E. Grolier, Fluid Phase Equilib. 49 (1989) 233–250.
[117] U. Messow, U. Doyé, S. Kuntzsch, D. Kuchenbecker, Z. Phys. Chem. (Leipzig) 258 (1977) 90–96.
[118] M. Aboy, S. Villa, N. Riesco, J.A. González, I. García de la Fuente, J.C. Cobos, J. Chem. Eng. Data 47 (2002) 950–953.
[119] I. Nagata, K. Tamura, Fluid Phase Equilib. 15 (1983) 67–79.
[120] S. Li, H. Dong, W. Tan, B. Peng, J. Chem. Eng. Data 50 (2005) 1087–1090.
[121] T.M. Letcher, J.A. Nevines, J. Chem. Eng. Data 40 (1995) 995–996.
[122] H.V. Tra, D. Patterson, J. Solut. Chem. 11 (1982) 793–805.
[123] H. Piekarski, K. Kubalcyk, M. Wasiak, J. Chem.Eng.Data 55 (2010) 5435–5440.
[124] J. Lohmann, R. Bölts, J. Gmehling, J. Chem. Eng. Data 46 (2001) 208–211.
[125] F. Comelli, R. Francesconi, J. Chem. Eng. Data 42 (1997) 705–709.
[126] E. Romano, J.L. Trenzado, E. González, J.S. Matos, L. Segade, E. Jiménez, Fluid Phase Equilib. 211 (2003) 219–240.
[127] J.L. Trenzado, E. Romano, L. Segade, M.N. Caro, E. González, S. Galván, J. Chem. Eng. Data 56 (2011) 2841–2848.
[128] R. Francesconi, F. Comelli, C. Castellari, Thermochim. Acta 327 (1999) 145–149.
[129] S.B. Park, J.S. Kim, H. Lee, J. Chem. Thermodyn. 31 (1999) 1265–1271.
[130] R. Francesconi, F. Comelli, J.Chem Data 41 (1996) 1397–1400.
[131] L. Mosteiro, A.B. Mariano, L.M. Casás, M.N. Piñeiro, J.L. Legido, J. Chem. Data 54 (2009) 1056–1062.
[132] J. Tojo, J. Canosa, A. Rodríguez, J. Ortega, R. Dieppa, J. Chem. Eng. Data 49 (2004) 86–93.
[133] L. Mosteiro, E. Mascato, B.E. de Cominges, T.P. Iglesias, J.L. Legido, J. Chem. Thermodyn. 33 (2001) 787–801.

Supplementary material for:

Orientational effects in mixtures of organic carbonates with alkanes or 1-alkanols

Juan Antonio González[(1)]*, Fernando Hevia[(1)], Cristina Alonso-Tristán[(2)], Isaías García de la Fuente[(1)], José Carlos Cobos[(1)]

[(1)] G.E.T.E.F., Departamento de Física Aplicada, Facultad de Ciencias, Universidad de Valladolid, Paseo de Belén, 7, 47011 Valladolid, Spain

[(2)] Unidad de Investigación Consolidada UIC-011, JCyL. Departamento de Ingeniería Electromecánica, Escuela Politécnica Superior, Universidad de Burgos. Avda. Cantabria s/n. 09006, Burgos, Spain.

*e-mail: jagl@termo.uva.es; Tel: +34 983 423757

Reference of the article:

J.A. González, F. Hevia, C. Alonso-Tristán, I. García de la Fuente, J.C. Cobos. Fluid Phase Equilib. **449** (2017) 91-103. https://doi.org/10.1016/j.fluid.2017.06.012

Table S1. Molar excess enthalpies, H_m^E, volumes, V_m^E, at pressure 0.1 MPa, temperature 298.15 K and equimolar composition for *n*-alkanone (1) + alkane (2) and for 1-alkanol (1) + *n*-alkanone (2) systems. Also included are the equation of state contribution ($\frac{\alpha_p}{\kappa_T} T V_m^E$) to the excess molar enthalpy and the excess molar internal energy at constant volume , U_{Vm}^E.

Compound	H_m^E /J·mol^{-1}	V_m^E /cm^3·mol^{-1}	$\frac{\alpha_p}{\kappa_T} T V_m^E$ /J·mol^{-1}	U_{Vm}^E /J·mol^{-1}
		2-propanone (1) + *n*-alkane (2)		
Heptane	1676 [S1]	1.130 [S1]	315	1361
Decane	1968 [S2]	1.333 [S2]	395	1573
		3-pentanone (1) + *n*-alkane (2)		
Heptane	1078 [S3]	0.520 [S4]	145	933
		1-alkanol (1) + 2-propanone (2)		
Methanol	686 [S5]	–0.339 [S6]	–106	792
Ethanol	1150 [S7]	–0.071[S6]	–22	1172
1-butanol	1537 [S8]	0.050 [S9]	16	1521
		1-alkanol (1) + 3-pentanone (2)		
Methanol	725 [S10]	–0.199 [S11]	–63	788
Ethanol	987 [S10]	–0.063 [S11]	–20	1007
1-propanol	1160 [S10]	–0.036 [S11]	–11	1171

Table S2. Contributions to V_m^E according to the Prigogine-Flory-Patterson model for dialkyl carbonate + *n*-alkane, or 1-alkanol + organic carbonate systems at temperature 298.15 K, pressure 0.1 MPa and equimolar composition.

System	$V_{m,int}^E$ / cm^3·mol^{-1}	P^* term / cm^3·mol^{-1}	Curvature term / cm^3·mol^{-1}	V_m^E / cm^3·mol^{-1}	Ref.
DMC + *n*-C_7	1.894	−0.013	0	1.158	[S12]
DMC + *n*-C_{10}	1.876	0.448	−0.061	1.442	[S12]
DEC + *n*-C_7	1.209	0.078	−0.002	0.7362	[S13]
DEC + *n*-C_{10}	1.288	0.604	−0.103	1.0629	[S13]
Methanol + DMC	1.038	0.043	−0.002	−0.0628	[S14]
Ethanol + DMC	1.385	0.172	−0.016	0.1635	[S15]
1-propanol + DMC	1.583	0.329	−0.052	0.3693	[S15]
1-butanol + DMC	1.900	0.459	−0.093	0.4771	[S16]
Methanol + DEC	1.010	0.0723	−0.005	−0.048	[S17]
Ethanol + DEC	1.244	0.222	−0.028	0.1143	[S17]
1-propanol + DEC	1.459	0.397	−0.078	0.2225	[S17]
1-butanol + DEC	1.561	0.548	−0.132	0.2815	[S17]
1-hexanol + DEC	1.559	0.745	−0.233	0.3940	[S17]
1-octanol + DEC	1.602	0.897	−0.342	0.5200	[S17]
1-decanol + DEC	1.607	0.951	−0.413	0.6386	[S17]
Methanol + PC	0.745	−0.309	−0.071	−0.3362	[S18]
Ethanol + PC	1.030	−0.323	−0.051	−0.2021	[S18]
1-propanol + PC	1.243	−0.251	−0.026	−0.037	[S18]

References

[S1] Y. Akamatsu, H. Ogawa, S. Murakami, Thermochim. Acta 113 (1987) 141-150.

[S2] U. Messow, U. Doyé, S. Kuntzsch, D. Kuchenbecker, D. Z. Phys. Chem. (Leipzig) 258 (1977) 90-96.

[S3] O. Kiyohara, Y.P. Handa, G.C. Benson, J. Chem. Thermodyn. 11 (1979) 453-460.

[S4] J.-P.E. Grolier, G.C. Benson, Can. J. Chem. 62 (1984) 949-953.

[S5] I. Nagata, K. Tamura, Fluid Phase Equilib. 15 (1983) 67-79.

[S6] M. Iglesias, B. Orge, M. Domínguez, J. Tojo, Phys. Chem. Liq. 37 (1998) 9-29.

[S7] A. Lietzmann, B. Loewen, S. Schulz, J. Chem. Eng. Data 39 (1994) 785-788.

[S8] I. Nagata, K. Tamura, H. Kataoka, A. Ksiazczak, J. Chem. Eng. Data 41 (1996) 593-597.

[S9] M. Iglesias, B. Orge, J. Tojo, Fluid Phase Equilib. 126 (1996) 203-223

[S10] T.M. Letcher, J.A. Nevines, J. Chem. Eng. Data 40 (1995) 995-996.

[S11] T.M. Letcher, J.A. Nevines, J. Chem. Eng. Data 40 (1995) 293-295.

[S12] I. García de la Fuente, J.A. González, J.C. Cobos, C. Casanova, J. Chem. Eng. Data 37 (1992) 535-537.

[S13] I. García de la Fuente, J.A. González, J.C. Cobos, C. Casanova, J. Solution Chem. 24 (1995) 827-835.

[S14] A. Rodríguez, J. Canosa, J. Tojo, J. Chem. Eng. Data 44 (1999) 1298-1303.

[S15] A. Rodríguez, J. Canosa, J. Tojo, J. Chem. Eng. Data 46 (2001) 1476-1486.

[S16] R. Francesconi, F. Comelli, J. Chem. Eng. Data 44 (1999) 44-47.

[S17] R. Francesconi, F. Comelli, J. Chem. Eng. Data 42 (1997) 45-48.

[S18] R. Francesconi, F. Comelli, J.Chem Data 41 (1996) 1397-1400

Part III
Discussion and conclusions

Chapter 5.

Discussion of the results

5.1. Introduction

5.1.1. Amide + amine liquid mixtures

It is well-known that a suitable approach for the investigation of the highly complex chemical environment of proteins is the study of small organic molecules whose functional groups are similar to those present in the biomolecule [1]. The systematic physical and chemical characterization of such molecules and of their mixtures in terms of thermodynamic, transport and dielectric properties is necessary in this framework. The study of amide + amine systems is relevant, as it allows to gain insight into the behavior of the amide group when it is surrounded by different environments. In fact, the hydrogen-bonded structures where the amide group is involved can show very different biological activities depending on the mentioned environments [2]. On the other hand, the strong polarity of amides, which in the case of tertiary amides leads to the creation of a certain local order [3, 4], together with their high solvating capability and liquid state range –due to their ability to form hydrogen bonds– [5], makes them a very important kind of organic solvents. Similarly, amines are also a relevant class of substances, since many biologically crucial molecules contain the amine group [6-8]. In addition, the low vapor pressure of amines makes them useful in green chemistry. Thus, mixtures containing amines are being investigated to be used in CO_2 capture [9] and, interestingly, many of the ions of the technically important ionic liquids are related to amine groups [10].

In this Thesis, measurements of thermophysical properties of amide + amine mixtures have been performed. The amides considered are tertiary amides: *N,N*-dimethylformamide (DMF) and *N,N*-dimethylacetamide (DMA). They are mixed with linear primary or secondary amines: butan-1-amine (BA), hexan-1-amine (HxA), *N*-propylpropan-1-amine (DPA) or *N*-butylbutan-1-amine (DBA). A literature survey shows that there are no other similar data for the systems under study to use for comparison. Nevertheless, DMF, or DMA + aniline or pyridine mixtures have been investigated rather extensively, reporting calorimetric, volumetric, vapor-liquid equilibria, c, or n_D data [11-16]. Data on excess molar enthalpy (H_m^E) are also available for the *N*-methylacetamide + HxA system at 363.15 K [17].

5.1.2. 1-Alkanol + amine liquid mixtures

Mixtures formed by 1-alkanol and amine are a very interesting class of systems, as they show a variety of different behaviors. For example, 1-alkanol + linear primary or secondary amine

systems are characterized by strongly negative excess molar enthalpies (H_m^E). For instance, at 298.15 K and equimolar composition, H_m^E /J·mol^{-1} = –3200 (methanol + HxA) [18]; –4581 (methanol + *N*-ethylethan-1-amine (DEA)) [19]. This has been interpreted as the result of two different opposing effects. In the pure liquid state, both 1-alkanols and amines are self-associated by means of O-H---O and N-H---N bonds, respectively. When the mixing process takes place, such bonds are broken, and this process leads to a positive contribution to H_m^E. However, new interactions between unlike molecules are simultaneously created upon mixing, which contribute negatively to H_m^E. Therefore, the large and negative H_m^E values reveal that the new O-H---N bonds created are stronger than the O-H---O and N-H---N bonds. Thus, the values of the enthalpy of the hydrogen bonds between methanol and amine estimated from the application of the ERAS model [20] are: –42.4 kJ·mol^{-1} (HxA) [21]; –45.4 kJ·mol^{-1} (DEA) [22]. The value used, within this model, for the enthalpy of the H bonds between 1-alkanol molecules is higher: –25.1 kJ·mol^{-1} [20-22]. As a consequence of the strong interactions between unlike molecules, the systems are highly structured. For example, at 298.15 K and x_1 = 0.5, TS_m^E (= H_m^E – G_m^E ; G_m^E molar excess Gibbs energy) is –3758 J·mol^{-1} for the methanol + DEA mixture (value determined using G_m^E = –823 J·mol^{-1} [23]). For comparison, we provide similar results for the 1-propanol + hexane system, TS_m^E = (533 (= H_m^E) – 1295 (= G_m^E)) = –762 J·mol^{-1} [24, 25]. The existence of strong interactions between unlike molecules in this type of solutions is also supported by large and negative excess molar volumes [21, 26-30] and by solid-liquid equilibria measurements, as the corresponding phase diagrams show that complex formation is an important feature of the systems [31]. Interestingly, the replacement of a linear primary amine by aniline leads to very different H_m^E /J·mol^{-1} values: –170 (methanol) [32]; 1020 (1-butanol) [33]. This can be explained in terms of a large contribution to H_m^E from the breaking of the strong dipolar interactions between aniline molecules along the mixing process. Note that the upper critical solution temperature of the aniline + heptane system is 343.11 K [34].

GETEF has extended the database of 1-alkanol + amine mixtures reporting excess molar volumes [21, 26-30]; dynamic viscosities [28-30]; vapor-liquid equilibria [35]; permittivities (ε_r) and refractive indices (n_D) [28-30, 36]. In addition, these systems have been studied by using different models as DISQUAC or ERAS [21, 22, 26, 27, 29, 37-40], the formalism of the Kirkwood-Buff integrals [41], or the concentration-concentration structure factor ($S_{CC}(0)$) formalism [42]. As a continuation, we have made now ε_r and n_D measurements over the temperature range (293.15-303.15) K for the systems 1-alkanol + HxA, + DPA or + *N,N,N*-triethylamine (TEA).

5.1.3. Experimental data

Volumetric, refractive and dielectric properties of amide + amine mixtures are published in references [43-46] (**Articles 1 to 4**). For H_m^E data and ERAS results of amide + amine mixtures, see Appendix A. The dielectric of refractive data and Kirkwood-Fröhlich results of 1-alkanol + HxA or + DPA mixtures are already published in references [46, 47] (**Articles 5 to 6**). The corresponding results for 1-alkanol + TEA mixtures are shown in Appendix B.

We recall that results from **Articles 7 and 8** will not be discussed in this chapter.

5.2. Discussion of amide + amine liquid mixtures

Throughout the rest of the discussion we will refer, unless pointed otherwise, to values of the thermophysical properties at temperature 298.15 K; non-dielectric properties will be given at $x_1 = 0.5$ and dielectric properties at volume fraction $\phi_1 = 0.5$.

5.2.1. Excess molar enthalpies and volumes

DMF and DMA are very polar substances, with a dipole moment of 3.7 D [48, 49]. Consequently, their alkane mixtures show immiscibility gaps up to rather high temperatures. Thus, systems formed by DMF and heptane or hexadecane have upper critical solution temperatures (UCST) of 342.55 K [50] and 385.15 K [51] respectively, and the UCST of the DMA + heptane mixture is 309.40 K [52].

Linear primary and secondary amines are weakly self-associated compounds [21, 38, 53-55] with lower dipole moments than tertiary amides: 1.3 D (BA) [56], 1.3 D (HxA) [48], 1.0 D (DPA) [56], and 1.1 D (DBA) [56]. For mixtures of these linear amines and heptane, H_m^E values [57, 58] are positive (Figure 5.1). We note that H_m^E results are larger for systems with primary amines, and that they decrease with the chain length of the amine. Therefore, these values can be interpreted as arising from the rupture of interactions between like molecules in the mixing process. On the other hand, it is well stated that positive V_m^E values are related to the breaking of interactions between like molecules, while negative values come from the creation of solute-solvent interactions and/or structural effects (geometrical factors including differences in size and shape between the mixture compounds [59-61] or interstitial accommodation [62]). The V_m^E (linear amine + heptane) values [63, 64] (Figure 5.2) are positive and change in line with H_m^E, which reveals that the most important contribution to V_m^E comes from the disruption of amine-amine interactions upon mixing. However, structural effects may also be present. The low V_m^E value of DBA + heptane system, and the negative value of the DBA + hexane mixture (–0.185 $cm^3 \cdot mol^{-1}$) [65] support this statement, as positive H_m^E values and those negative of V_m^E for a given solution suggest that the most relevant contribution to the latter excess function arises from structural effects [61].

Our H_m^E /J·mol^{-1} values obtained for amide + amine systems are also positive (Figure 5.1 and Figure 5.3, Appendix A). They can be ascribed to the dominance of contributions from the breaking of amide-amide and amine-amine interactions over that related to the formation of interactions between unlike molecules. Note that H_m^E values of the DMA + cyclohexane mixture are much higher than those of DMA + linear amine systems [66] (Figure A.S2 of Appendix A). The same trend is observed, e.g., when H_m^E results of BA + heptane are compared with *N,N*-dialkylamide systems (Figure A.S1). For a fixed amide and along both series (of primary or secondary linear amines), H_m^E becomes larger when the chain length of the amine is longer. This suggests that the lower contribution from the breaking of amine-amine interactions in longer amines is overcompensated by the higher contributions which arise from: i) the larger number of amide-amide interactions broken by longer amines; and ii) the lower number and weaker amide-amine interactions created when longer amines are involved, since then the amine group is more sterically hindered.

For a fixed amine, the replacement of DMF by DMA leads to decreased H_m^E values (Figure 5.1). The difference in size between both amides suggests that the contribution from the disruption of amine-amine interactions should be higher for DMA mixtures. However, the amide group is less sterically hindered in DMF, and we recognize that, in pure state, DMF-DMF interactions are stronger than those between DMA molecules. In fact (see above), UCST(DMF + heptane) > UCST(DMA + heptane). This is also supported by calculations on entropy changes under the action of an electrostatic field and by the application of the Kirkwood-Fröhlich model [46]. Therefore, we can conclude that the breaking of DMF-DMF interactions contributes more positively to H_m^E than the disruption of DMA-DMA interactions, and that the formation of interactions between unlike molecules should contribute more negatively to H_m^E in the case of DMF systems. The mentioned trend suggests that the variation of the contribution of amide-amide interactions is predominant over the other two. The same phenomenon is encountered in 2-alkanone + amine mixtures when the chain length of the 2-alkanone is increased (Figure 5.3) [67].

Interestingly, the replacement of HxA by DPA in systems involving a given amide leads to slightly higher H_m^E values (Figure 5.1). This can be explained taking into account that, since the amine group is less sterically hindered in HxA, a higher number of interactions between unlike molecules is formed in solutions with this amine and that such interactions are also stronger. It should be noted that the opposite trend is encountered for HxA or DPA + heptane mixtures, and that the difference H_m^E(HxA)– H_m^E(DPA) for these systems is remarkably higher than that for the corresponding amide solutions: 438 (heptane); –90 (DMF) and –85 (DMA) (all values in J·mol^{-1}). This underlines the relevance of amide-amine interactions in the studied solutions. The difference between amide + HxA or + DPA solutions is rather low in terms of H_m^E values, but it increases when considering $U_{m,V}^E$, reinforcing our statement (Appendix A). Eventually, let us mention the large and negative value of the H_m^E of the system *N*-methylacetamide + HxA (–1000 J·mol^{-1}, T = 363.15 K) [17], for which the contribution from the formation of amide-amine interactions is dominant by far.

The excess molar volumes, V_m^E, of the considered mixtures are either negative or small and positive [43, 44] (Figure 5.2 and Figure 5.4), and can be ascribed to important contributions from amide-amine interactions and structural effects. The latter are clearly seen because the corresponding H_m^E values are positive, showing in this aspect a similar behavior to amine + *n*-alkane systems (see above).

It is also to be noted that H_m^E and V_m^E change in line, which reveals that the interactional contribution to V_m^E is relevant. For a fixed amide, the increase of the amine size along a homologous series leads to increased V_m^E values. This means that the contributions that increase V_m^E (larger number of DMF-DMF interactions broken by the longer amines and the weakening of the amide-amine interactions related to the fact that the amine group is more sterically hindered in such amines) are predominant over those decreasing V_m^E (structural effects, lower positive contribution from the disruption of the amine-amine interactions). The replacement of a linear primary amine (HxA) by a linear secondary amine (DPA) leads to lower V_m^E values (Figure 5.2). It is remarkable that the same behavior is encountered for HxA or DPA + heptane

mixtures (see above). Therefore, the observed variation in DMF solutions can be ascribed to a lower positive contribution to V_m^E from the breaking of the amine-amine interactions. A similar trend is encountered in 1-alkanol + HxA, or + DPA systems (Figure 5.4) [21, 26]. Finally, the replacement of DMF by DMA for a fixed amine leads to a higher V_m^E, due to the stronger amide-amine interactions in mixtures with DMF (Figure 5.2).

Mixtures of DMF or DMA with aniline contrast drastically with those of linear primary or secondary amines. The dipole moment of aniline (1.51 D [49]) is higher than that of linear primary and secondary amines, and proximity effects between the phenyl ring and the amine group lead to strong dipolar interactions between aniline molecules. As a consequence, aniline + *n*-alkane mixtures are characterized by relatively high UCST (see introduction). When aniline molecules are mixed with DMF or DMA molecules, very strong interactions between unlike molecules are created, and we have $H_m^E/\text{J·mol}^{-1} = -2946$ (DMF + aniline) [14]; -352 (DMA + aniline) [16] (Figure 5.3). Similarly, large differences are also encountered between values of the excess relative permittivity for the DMF + linear primary or secondary amine or + aniline mixtures [45, 46] (see below). It must be observed that H_m^E values are very different for DMF and DMA + aniline systems, newly remarking that interactions between unlike molecules are much more relevant in DMF systems. The rather large and negative $V_m^E / \text{cm}^3\text{·mol}^{-1}$ results for the mentioned aniline solutions (–0.6615 (DMF + aniline) [11] and –0.6092 (DMA + aniline, T = 303.15 K) [15]) (Figure 5.3) are in agreement with the H_m^E values and underline the importance of the interactional contribution to V_m^E. The same trends are encountered for 2-alkanone + DPA or + aniline systems [67-74] (Figure 5.3 and Figure 5.4).

It is here pertinent to examine the effect of replacing the *N,N*-dialkylamide (DMF or DMA) by a 2-alkanone of similar size (propanone or butanone). For a fixed linear secondary amine (DPA or DBA), H_m^E values of DMF or DMA systems are higher than those of propanone or butanone solutions respectively (Figure 5.3), pointing out a contribution from the breaking of amide-amide interactions that is larger than the contribution from alkanone-alkanone interactions. In contrast, V_m^E values of propanone or butanone + DPA, or + DBA (Figure 5.4) mixtures are higher than those of the corresponding systems with DMF or DMA, thus suggesting that structural effects in V_m^E are more relevant in *N,N*-dialkylamide mixtures. The behavior of these two types of mixtures is parallel when: (i) for a given amine (DPA or DBA), we increase the size of the amide or alkanone (lower H_m^E and V_m^E values are obtained); and (ii) for a fixed amide (DMF or DMA) or alkanone (propanone or butanone), DPA is replaced by DBA (it gives higher H_m^E and V_m^E values). Both effects can be explained in similar terms (see above). Interestingly, aniline mixtures show a rather different behavior (Figure 5.3 and Figure 5.4). The lower V_m^E and the higher H_m^E values of the propanone mixture compared to those of the DMF system indicate that interactions between unlike molecules are stronger in the latter solution and that structural effects are more relevant in the propanone system. Surprisingly, DMA-aniline interactions seem to be weaker than butanone-aniline interactions (see the corresponding H_m^E values of these systems). This matter deserves a careful investigation.

The results are very different when replacing the *N,N*-dialkylamide (strongly polar compound) by a 1-alkanol (self-associated compound) of similar size (1-propanol or 1-butanol)

(Figure 5.3 and Figure 5.4). Both H_m^E and V_m^E of 1-alkanol + HxA, DPA or DBA mixtures are large and negative. This can be explained by the (1-alkanol)-amine cross-association, which is stronger than the self-association of the 1-alkanol (see introduction). Replacing the aliphatic amine by aniline in the case of 1-alkanol mixtures has the opposite effect to *N,N*-dialkylamide or 2-alkanone systems. In fact, H_m^E turn positive or small and negative, and V_m^E values become much higher. Their V_m^E are still negative, though, due to strong structural effects. Actually, the differences $H_m^E - U_{m,V}^E$ are significant not only for (1-alkanol) + aniline systems but also for (1-alkanol) + aliphatic amine solutions [21].

5.2.2. ERAS model results

Both excess functions, H_m^E and V_m^E, are reasonably well represented by the model (Figure 5.5 to Figure 5.8, Appendix A). Larger differences for V_m^E results are encountered for mixtures characterized by low V_m^E values, as then the overall result is obtained from the difference of two large magnitudes of different sign: the positive physical contribution and the negative chemical contribution.

ERAS parameters of amide + amine mixtures (Table A.4, [46]) are represented from Figure 5.9 to Figure 5.12, together with the corresponding parameters of 1-alkanol + HxA, + DPA and + TEA solutions [21, 26]. The low $\left|\Delta h_{AB}^*\right|$ and K_{AB} and values for *N,N*-dialkylamide + linear primary or secondary amine systems (2 to 9 kJ·mol^{-1} and 1 to 1.3 respectively) indicate that solvation effects are not relevant and that the enthalpy of the H bonds between unlike molecules is weak. The large X_{AB} values reveal that the physical contribution is important, particularly with regards to H_m^E. These ERAS parameters largely differ from those determined for 1-alkanol + linear primary or secondary amine systems, which are characterized by strong solvation effects and, in consequence, by large K_{AB} and Δh_{AB}^* values and low X_{AB} values.

For *N,N*-dialkylamide + linear primary or secondary amine systems, we note that ERAS results on H_m^E are, as an average, better for DMA systems (Table A.5). This suggests that, in such a case, physical interactions are more properly described by the model, that is, dipolar interactions are more relevant in DMF mixtures, particularly in the BA solution.

5.2.3. Excess relative permittivities

It is known that the disruption of interactions between like molecules, in the present case amide-amide and amine-amine interactions, contributes negatively to ε_r^E. The creation of new interactions between unlike molecules along this process leads to the formation of multimers whose molecular structure is determinant to provide a more or less effective impact on the macroscopic response to an electric field [36]. If the mentioned multimers are linear chains, the contribution to ε_r^E is positive. In contrast, if cyclic species are created, the contribution to ε_r^E is negative.

n-Alkylamine + dodecane systems at 293.15 K show negative ε_r^E values that increase with the chain length of the amine [75] (Figure 5.13). The negative contribution from the rupture of amine-amine interactions diminishes when increasing the chain length of the amine, as the

amine group is then more sterically hindered, in such a way that the effective polarity of longer amines becomes weaker.

The ε_r^E values of *N,N*-dialkylamide (DMF or DMA) + linear amine (BA, HxA, DPA or DBA) are large and negative (Figure 5.13), revealing that the negative contributions from the breaking of interactions between molecules of the same species are dominant. They are much lower than those of *n*-alkylamine + dodecane mixtures, suggesting that amide-amide interactions are dominant. On the other hand, one can expect that interactions between unlike molecules contribute positively to ε_r^E. In fact, the ε_r^E value of the DMF + heptane mixture at $\phi_1 = 0.0171$ and 293.15 K is lower (–0.24, calculated from data of the literature [76]) than the values of the corresponding systems with amines at the same conditions: –0.129 (DPA), –0.146 (DBA), –0.104 (BA), and –0.137 (HxA) [75].

We note that, for a fixed amide, $\varepsilon_r^E(\text{DBA}) < \varepsilon_r^E(\text{DPA})$ and $\varepsilon_r^E(\text{HxA}) < \varepsilon_r^E(\text{BA})$. This can be explained as follows: (i) longer amines are better breakers of the amide-amide interactions due to their large aliphatic surface; (ii) the formation of interactions between unlike molecules becomes easier when shorter amines are involved, as the amine group is then less sterically hindered. This also explains why $\varepsilon_r^E(\text{HxA}) > \varepsilon_r^E(\text{DPA})$ in mixtures with a given amide. Comparison between ε_r^E values of mixtures with a given linear amine shows that $\varepsilon_r^E(\text{DMF}) > \varepsilon_r^E(\text{DMA})$. In addition, ε_r^E curves of the DMA systems are more skewed towards larger ϕ_1 values (Table 7 of reference [46]). This suggests that linear amines can disrupt more easily DMA-DMA interactions and that the creation of amide-amine interactions is favored when DMF molecules participate.

Finally, we must remark that the replacement of HxA by aniline in DMF solutions has a large impact on the ε_r^E values of these mixtures, which show opposite signs. Therefore, the aromaticity effect leads here to an increase of the number of effective dipole moments in the aniline system. The fact that ε_r^E is positive for the DMF + aniline mixture clearly indicates that ε_r^E is now mainly determined by the positive contribution related to the aniline-DMF interactions created upon mixing. Other systems like methanol + DMF ($\varepsilon_r^E = 2.57$ [77]); + DMA (0.52 [78]); + pyridine (2.85 [77]), or + cyclohexylamine (1.13 [30]) also show positive ε_r^E values.

5.2.4. Kirkwood-Fröhlich model results

From ε_r and n_D (refractive index) data, we can calculate the Kirkwood correlation factor (g_K) in the framework of a one-fluid model (see section 4.3.6). However, g_K values of pure *N,N*-dialkylamides and linear amines are very similar. For such systems, the shape of the g_K curves is very sensitive to the μ values of the pure compounds. Since the uncertainty in the dipole moments of linear amines is not low enough to ensure a unique shape of the curves, it is better to evaluate the Balankina relative excess Kirkwood correlation factors of the mixtures, $g_{K,rel}^E$, defined by [79]:

$$g_{K,rel}^E = \frac{g_K - g_K^{id}}{g_K^{id}} = \frac{V_m(\varepsilon_r - \varepsilon_r^\infty)(2\varepsilon_r + \varepsilon_r^\infty)\varepsilon_r^{id}(\varepsilon_r^{\infty,id} + 2)^2}{V_m^{id}(\varepsilon_r^{id} - \varepsilon_r^{\infty,id})(2\varepsilon_r^{id} + \varepsilon_r^{\infty,id})\varepsilon_r(\varepsilon_r^\infty + 2)^2} - 1 \qquad (5.1)$$

where g_K^{id} is obtained substituting ideal values in the definition of g_K. The quantity $g_{K,rel}^E$ does not depend on the dipole moments of the pure compounds and is a useful tool to probe into the structure of the mixtures, as it gives a measure of the balance of structure creation and destruction during the mixing process in comparison to the ideal mixture. The $g_{K,rel}^E$ curves are very skewed to low ϕ_1 values [46], which means that according to the model the change in the relative orientation of neighboring permanent dipoles is not the only responsible for the shape of ε_r^E curves of such systems. However, their contribution is relevant, as the curves are negative and the relative variation of the minimum of the $g_{K,rel}^E$ curves (Figure 5.14) is parallel to the ε_r^E change (Figure 5.13). This is consistent with the conclusions extracted from the analysis of ε_r^E.

It is interesting to see the effect of replacing the *N,N*-dialkylamide by a 1-alkanol of similar size. The dielectric and refractive properties of such systems were measured experimentally, and are interpreted in the following section.

5.3. Discussion of 1-alkanol + amine liquid mixtures

Along the discussion, *n*OH will denote the 1-alkanol with *n* carbon atoms.

5.3.1. Excess relative permittivities

1-Alkanols are self-associated compounds with moderate dipole moments [80]: 1.666 (1OH), 1.650 (2OH), 1.627 (3OH), 1.612 (4OH), 1.597 (5OH), 1.586 (6OH), 1.581 (7OH), 1.568 (8OH), 1.566 (9OH), 1.564 (10OH). Accordingly, *n*OH + heptane mixtures show large and negative values of ε_r^E (Figure 5.15), which can be ascribed to the rupture of the 1-alkanol self-association. For the system 1OH + heptane, a partial immiscibility region appears [81].

The comparison of these results with *n*OH + HxA (for $n \geq 3$), + DPA (for $n \geq 3$) or + TEA (for $n \geq 4$), which show higher ε_r^E values (Figure 5.15), reveals that (1-alkanol)-amine interactions contribute positively to ε_r^E in these type of mixtures. The positive values for the 1OH systems confirm this statement. An important result is that ε_r^E(3OH + TEA) < ε_r^E(3OH + heptane). This suggests that TEA is an effective breaker of the alkanol self-association, and that the interactions between unlike molecules do not sufficiently compensate the large negative contribution to ε_r^E from the disruption of 3OH-3OH interactions.

For systems with heptane or a given amine (HxA, DPA or TEA) and increasing n, ε_r^E decreases to a minimum ($n = 7$ for the available data in heptane mixtures, $n = 5$ for HxA and DPA, and $n = 4$ for TEA) and then increases again. A similar trend is encountered for systems with cyclohexylamine (c-HxA) (Figure 5.16). For heptane systems, it has been explained in terms of the lower and weaker self-association of longer 1-alkanols [36]. For amine systems, this statement is still valid, but interactions between unlike molecules must also be considered. Studies on 1-alkanol + amine mixtures using the ERAS model show that solvation effects between unlike molecules decrease when the 1-alkanol size is increased [21, 26, 27]. This means that, along the mixing process, the polarization changes to a lower extent when longer 1-alkanols are involved, since these alcohols are less self-associated and the corresponding solvation effects are also less important. It is to be noted that ε_r^E changes more sharply when

increasing n for mixtures with shorter 1-alkanols than for systems involving longer 1-alkanols and that the same occurs for the excess molar volumes and for the excess molar enthalpies [26].

For a given 1-alkanol, ε_r^E varies in the following manner: TEA < HxA < DPA. The fact that ε_r^E(HxA) < ε_r^E(DPA) suggests that in DPA solutions multimers with parallel alignment of the molecular dipoles are favored and cyclic multimers are disfavored when compared to HxA mixtures. Furthermore, at $\phi_1 = 0.47$, the 4OH + *N*-ethylethan-1-amine mixture [76] shows an even higher value (–0.13), which can be explained by the formation of more and stronger H bonds between unlike molecules, because the amine group is less sterically hindered in this amine. ε_r^E(TEA) is lower due to the effectivity of this amine in breaking the self-association of the 1-alkanol (see above).

For a better understanding of systems containing TEA, we start examining 1-alkanol + linear primary or secondary amine systems. A literature survey shows that ε_r^E(3OH + DPA) = –0.246 [82] > ε_r^E(3OH + HxA) = –0.96 [47] > ε_r^E(3OH + propan-1-amine) = –1.99 [83] and that ε_r^E (4OH + DPA) = –0.715 [82] > ε_r^E (4OH + HxA) = –1.424 [47] > ε_r^E(4OH + butan-1-amine) = –2.87 [83]. Since solvation effects are expected to be more relevant in systems involving amines where the amine group is less sterically hindered (propan-1-amine, butan-1-amine), one can conclude that characteristic mixtures where larger solvation effects are present show more negative ε_r^E values. The same trend is observed when comparing, at 303.15 K, ε_r^E results for 3OH + primary aromatic amine, aniline, (–2.07) [84] or + secondary aromatic amine, *N*-methylaniline, (–1.27) [85]. This behavior can be explained taking into account that larger solvation effects imply a decreased number of interactions between like molecules and, therefore, a more negative contribution to ε_r^E from the disruption of interactions between like molecules, particularly between alkanol molecules. In the case of amine mixtures, cyclic species may be more probable in mixtures containing amines with the functional group less sterically hindered. We must now remark that systems with TEA deviate from this picture. This can be ascribed to the globular shape of TEA molecules, which makes them better breakers of the 1-alkanol self-association (see above). In fact, the volume fraction at which minimum ε_r^E values are measured changes in the sequence DPA < HxA < TEA for mixtures with shorter 1-alkanols. Thus, ϕ_1 (4OH) = 0.3183 (DPA; ε_r^E = –0.896) [82] < 0.4138 (HxA; ε_r^E = –1.428) [47] < 0.4969 (TEA; ε_r^E = –1.964). For 7OH, the alcohol self-association becomes less relevant, and the minimum ε_r^E values are encountered at similar volume fractions for HxA or TEA mixtures, although these concentrations are still higher than for the DPA solution, e.g. ϕ_1(7OH) = 0.5003 (DPA; ε_r^E = –0.793) [82] < 0.5982 (TEA; ε_r^E = –1.455). The fact that the ε_r^E curves of HxA systems are skewed to higher ϕ_1 values than those of mixtures with DPA supports our previous statement about that higher solvation effects lead to a more important breaking of the alcohol network upon mixing. We complete the present analysis as follows. (i) According to the ERAS model, the equilibrium constants, K_{AB}, change in the order HxA > DPA > TEA in systems with a given 1-alkanol [21, 26, 37]. For example, K_{AB}(1OH) = 2500 (HxA) > 2450 (DPA) > 620 (TEA). That is, solvation effects are less important in mixtures with TEA, in agreement with the fact that the amine group becomes more sterically hindered in the same sequence [86]. (ii) The $S_{CC}(0)$ function is a quantity which allows to study the fluctuations in the number of

molecules of a binary mixture regardless of the components, the fluctuations in the mole fraction and the cross fluctuations. It is defined by [87, 88]:

$$S_{CC}(0) = \frac{x_1 x_2}{D} \tag{5.2}$$

where, denoting by ΔG_m the molar Gibbs energy of mixing:

$$D = \frac{x_1 x_2}{RT}\left(\frac{\partial^2 \Delta G_m}{\partial x_1^2}\right)_{T,p} = 1 + \frac{x_1 x_2}{RT}\left(\frac{\partial^2 G_m^E}{\partial x_1^2}\right)_{T,p} \tag{5.3}$$

For ideal mixtures, $G_m^{E,id} = 0$ (excess Gibbs energy of the ideal mixture); $D^{id} = 1$ and $S_{CC}(0) = x_1 x_2$. From stability conditions, $S_{CC}(0) > 0$. If a system is close to phase separation, $S_{CC}(0)$ must be large and positive (∞, if the mixture presents a miscibility gap). In the case of compound formation between components, $S_{CC}(0)$ must be very low (0, in the limit). Therefore, $S_{CC}(0) > x_1 x_2$ ($D < 1$) indicates that the dominant trend in the system is homocoordination (separation of the components), and the mixture is then less stable than the ideal. If $0 < S_{CC}(0) < x_1 x_2 = S_{CC}(0)^{id}$, ($D > 1$), the fluctuations in the system have been removed, and the dominant trend in the solution is heterocoordination (compound formation). In such a case, the system is more stable than ideal. We have shortly applied this formalism to methanol + HxA, or + DPA, or + TEA systems at 298.15 K, calculating G_m^E by means of the DISQUAC [89] model with interaction parameters for the OH/amine contacts previously determined [22, 37]. At equimolar composition, we have obtained: $S_{CC}(0) = 0.165$ (HxA) < 0.201 (DPA) < 0.341 (TEA). This means that heterocoordination is dominant in the systems with HxA or DPA, while homocoordination is prevalent in the TEA mixture. It is in full agreement with the variation of the K_{AB} constants given above, and with available G_m^E data for methanol + amine mixtures. Thus, G_m^E (methanol)/J·mol^{-1}= –799 (BA, 348.15 K) [90], 284 (TEA, 303.15 K) [91].

Cyclohexylamine (c-HxA, $\varepsilon_r^* = 4.53$ [36]) is a cyclic primary amine with a slightly higher permittivity than HxA ($\varepsilon_r^* = 3.904$ [47]). Cyclization of the amine leads to increased ε_r^E values compared to those of systems with HxA [30, 36] (Figure 5.16); i.e., multimers formed by unlike molecules contribute more positively to ε_r^E in cyclohexylamine solutions. The effect of aromaticity is more dramatic than that of cyclization. In fact, aniline ($\varepsilon_r^* = 7.004$ [92]) shows a greater value of the relative permittivity, underlining the importance of aniline-aniline interactions and the polarizability of the aromatic ring. The values of the corresponding excess property are of course negative [92] (Figure 5.16). In addition, they are lower than those of the mixtures with HxA or c-HxA. This may be explained taking into account that the breaking of the dipolar interactions between aniline molecules contributes more negatively to ε_r^E.

It may be pertinent to compare the dielectric behavior of mixtures formed by 1-alkanol and DPA or di-*n*-propylether (DPE), as both solvents have similar size and structure (Figure 5.17). It is well known that the thermodynamic properties of the DPE systems are mainly characterized by the 1-alkanol self-association [93]. Thus, the H_m^E values are moderately positive (H_m^E/J·mol^{-1} = 740 for the 3OH system [94]); remain nearly constant for mixtures involving the longer 1-alkanols, and the corresponding H_m^E curves are shifted towards low mole fractions of the 1-alkanol [93]. In contrast, as it has been previously mentioned, solvation, i.e. strong

interactions between unlike molecules, is the main feature of 1-alkanol + DPA mixtures [22]. This is clearly demonstrated by the large and negative H_m^E values of these systems (Figure 5.3). For DPE mixtures, the dependence of ε_r^E with the alcohol size is similar to that encountered for the amine systems examined (Figure 5.17): –1.03 (2OH) < –1.24 (4OH) < –1.60 (6OH) > –0.80 (10OH) [95]. On the other hand, for mixtures with a given 1-alkanol, as a general trend it is observed that ε_r^E changes in the order: heptane < DPE < DPA (see above, Figure 5.17). This reveals that interactions between unlike molecules contribute more positively to the polarization of the mixture in the case of DPA systems.

5.3.2. Temperature dependence of the permittivity

Firstly, we note that, for pure compounds, $(\partial\varepsilon_r^*/\partial T)_p$ values are negative (see below and Figure 5.18), which is the typical behavior of normal liquids. In the case of 1-alkanols, this quantity increases with n, because then the alcohol self-association decreases and a lower number of interactions between alcohol molecules are broken when the temperature is increased. The higher $(\partial\varepsilon_r^*/\partial T)_p$ values of HxA (–0.0098 K^{-1}), DPA (–0.012 K^{-1}) or TEA (–0.004 K^{-1}) can be explained similarly. Pure TEA shows a very low absolute value of $(\partial\varepsilon_r^*/\partial T)_p$, since TEA is not self-associated and has a low ε_r^* value (= 2.419). Thus, the increase of thermal agitation hardly modifies the liquid structure.

Values of $(\partial\varepsilon_r/\partial T)_p$ of 1-alkanol + HxA, DPA or TEA systems are higher than for pure alkanols (Figure 5.18), which underlines the existence of (1-alkanol)-amine interactions. This can be explained as follows. (i) The contribution to $(\partial\varepsilon_r/\partial T)_p$ related to the breaking of amine-amine interactions when T is increased is very low, especially for TEA (see above); (ii) The enthalpy of hydrogen bonds between 1-alkanol molecules is larger than that corresponding to 1-alkanol-amine interactions (see introduction). Therefore, one can expect that the number of (1-alkanol)-TEA interactions broken when the temperature is increased is lower than the number of disrupted (1-alkanol)-(1-alkanol) interactions. This leads to a lower ε_r decrease when T is increased in comparison to that produced in pure 1-alkanols. The variation of $(\partial\varepsilon_r/\partial T)_p$ with n can be explained in similar terms, i.e., in terms of the lower self-association of longer 1-alkanols and of the less important solvation effects involved.

For mixtures with a given 1-alkanol, $(\partial\varepsilon_r/\partial T)_p$ changes in the order TEA > HxA > DPA (Figure 5.18). The ε_r values vary in the opposite sequence; for example, for 1OH mixtures we have ε_r = 17.597 (TEA) < 19.739 (HxA) < 20.256 (DPA). That is, the structure of mixtures characterized by a higher dielectric polarization is more sensitive to temperature changes. In addition, $(\partial\varepsilon_r^*/\partial T)_p$ of pure amines varies in the same order as $(\partial\varepsilon_r/\partial T)_p$. We remark that the replacement of DPA by HxA in systems with a given 1-alkanol leads to less negative $(\partial\varepsilon_r/\partial T)_p$ values, newly suggesting that cyclic multimers formed by unlike molecules exist in 1-alkanol + HxA systems, as the disruption of such multimers for increased temperature values should contribute positively to the polarization of the mixture.

Finally, we note that $(\partial\varepsilon_r^E/\partial T)_p$ can show negative or positive values (Figure 5.19). Lower results are encountered for mixtures for which the effects from 1-alkanol self-association and solvation between unlike molecules are more relevant, leading to a network that is more difficult to break with the increase of temperature when compared with the ideal mixture. Thus, for a fixed amine (HxA, DPA or TEA) it increases with n, whereas for a given 1-alkanol it varies as HxA < DPA < TEA.

5.3.3. Kirkwood-Fröhlich model results

We compare the g_K curves obtained from 1OH or 7OH + isomeric amine in Figure 5.20. Except for values of ϕ_1 very close to zero, where the structure of the mixture is basically that of the pure amine, it is found that g_K (DPA) > g_K (TEA) > g_K (HxA). DPA mixtures show higher values of g_K than HxA systems, which would mean that parallel alignment of the dipoles is more favored in DPA mixtures, supporting our previous statement inferred from the analysis of ε_r^E and $(\partial\varepsilon_r/\partial T)_p$. The g_K results for the 1OH + DPA mixture deserve a comment. We note that g_K rapidly increases with ϕ_1, and that it is nearly constant from $\phi_1 = 0.5$ and very close to the value of the neat alcohol. This might occur because the contribution to the mixture polarization arising from interactions between alcohol molecules also increases rapidly with ϕ_1 in such a way that interactions between unlike molecules contribute to g_K to a lower extent. It is remarkable that g_K changes more smoothly with ϕ_1 for the 1OH + HxA system, in agreement with our analysis of ε_r^E results. It is quite clear that 1-alkanol + TEA mixtures show an intermediate behavior, which could be due to the existence of a higher proportion of shorter linear-like multimers of 1-alkanol molecules which are less present in the systems with HxA.

In order to examine these results with more detail, we provide some g_K values for 1-alkanol + amine mixtures: g_K (3OH) = 2.72 (DPA) > 2.32 (HxA) > 1.87 (propan-1-amine), and g_K (4OH) = 2.60 (DPA) > 2.16 (HxA) > 1.72 (BA). In addition, g_K (3OH, 303.15 K) = 1.54 (aniline) < 1.71 (*N*-methylaniline). This points out that parallel alignment of molecular dipoles has a lower weight in those systems characterized by larger solvation effects and, according to our previous description of ε_r^E, these cooperative effects will lead to a lower polarization of the mixture. This underlines the lower contribution to the structure of the mixture from alkanol-alkanol interactions in systems with larger solvation effects, and suggests the presence of cyclic species in such systems.

We have also evaluated the excess Kirkwood correlation factors (Figure 5.21), $g_K^E = g_K - g_K^{id}$, where g_K^{id} is calculated as already explained. Positive values are encountered for 1OH + HxA or + DPA mixtures, which can be justified by the strong solvation effects present in these solutions. The minima of the g_K^E curves occurs at lower ϕ_1 than in the ε_r^E curves. Moreover, for a fixed amine, in general it does not change with n in the same order as ε_r^E. Thus, according to the Kirkwood-Fröhlich model, the destruction of the correlations of the dipoles is not the only responsible for the ε_r^E minima, but there are other effects involved. The trend of g_K^E (TEA) is slightly deviated from the parallel behavior of g_K^E (HxA) and g_K^E (DPA), and this reflects the stronger structural effects already mentioned in the former mixtures.

We now examine the effect of cyclization and aromaticity in 1-alkanol + primary amine systems (Figure 5.22). For c-HxA systems, $g_{\mathrm{K}}^{\mathrm{E}}$ values are higher, indicating that in these mixtures the balance of destruction and creation of correlations is more inclined to the latter than in the case 1-alkanol + HxA. Aniline systems are quite interesting, as $g_{\mathrm{K}}^{\mathrm{E}}$(HxA) $< g_{\mathrm{K}}^{\mathrm{E}}$ (aniline) for the 1-pentanol mixtures. This phenomenon may be related to the higher importance of the rupture of interactions between like molecules in 1-alkanol + aniline solutions, as showed by $\varepsilon_{\mathrm{r}}^{\mathrm{E}}$ values and also by $H_{\mathrm{m}}^{\mathrm{E}}$.

It is interesting to compare these g_{K} results with those for nOH + strongly polar compounds (work included in reference [96]), such as nitromethane (NM), ethanenitrile (EtN), dimethyl sulfoxide (DMSO), sulfolane (SULF), nitrobenzene (NTBz) or benzonitrile (BzCN). In fact, the g_{K} of these mixtures are slightly higher than 1 or very close to 1. For example, g_{K}(3OH) = 1.04 (NM, T = 293.15 K [76, 97]), 1.13 (EtN [98, 99]), 1.55 (DMSO [100, 101]). 1.20 (NTBz, T = 293.15 K [102, 103]), 1.13 (BzCN, T = 303.15 K [104, 105]); and g_{K}(1OH + SULF [106, 107]) = 1.33. When n increases along a homologous series, the $g_{\mathrm{K}}(\phi_1)$ have progressively a wider region where g_{K} values remain close to 1 (see, for example, ethanenitrile systems, Figure 5.23). For low ϕ_1, interactions between unlike molecules do not contribute to g_{K} as much as in nOH + amine mixtures (Figure 5.20 and Figure 5.23).

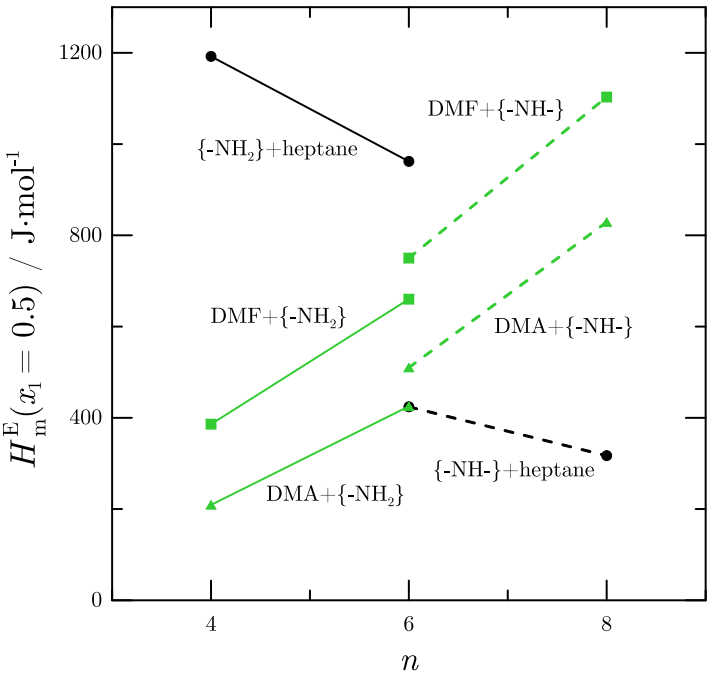

Figure 5.1: H^E_m at $x_1 = 0.5$, $T = 298.15$ K and $p = 0.1$ MPa of *N,N*-dialkylamide + amine (Appendix A) or amine + heptane [57, 58] liquid mixtures as functions of n, the number of C atoms of the amine. Solid lines, primary amines (-NH$_2$); dashed lines, secondary amines (-NH-). Full symbols: (●), heptane; (■), DMF; (▲), DMA.

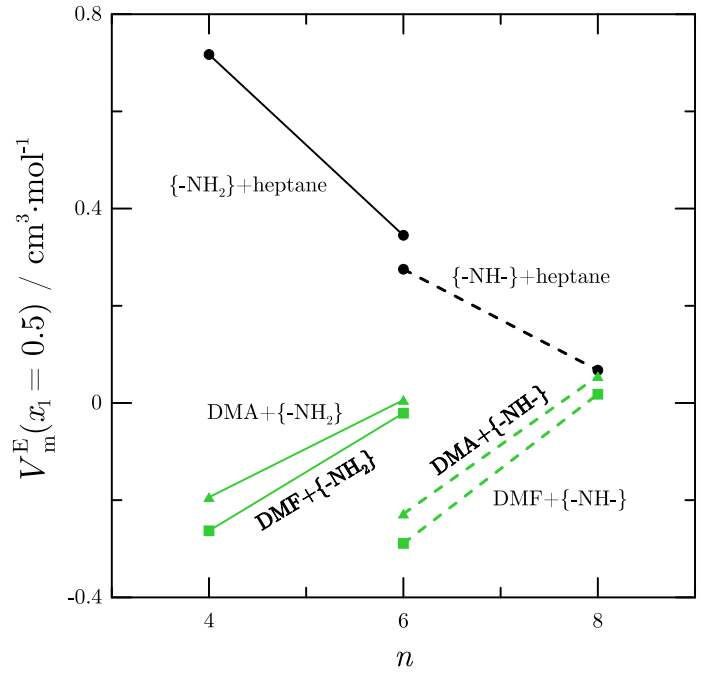

Figure 5.2: V^E_m at $x_1 = 0.5$, $T = 298.15$ K and $p = 0.1$ MPa of *N,N*-dialkylamide + amine [43, 44] or amine + heptane [63, 64] liquid mixtures as functions of n, the number of C atoms of the amine. Solid lines, primary amines (-NH$_2$); dashed lines, secondary amines (-NH-). Full symbols: (●), heptane; (■), DMF; (▲), DMA.

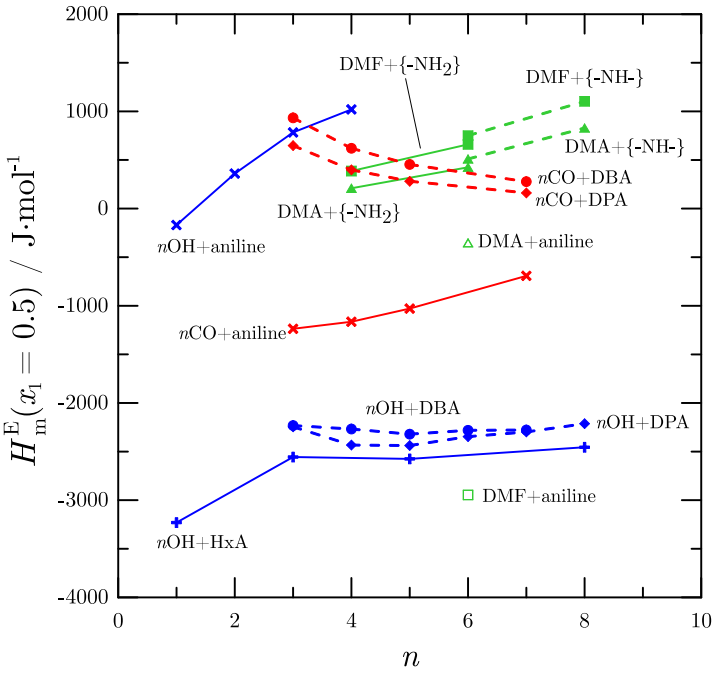

Figure 5.3: H^E_m at $x_1 = 0.5$, $T = 298.15$ K and $p = 0.1$ MPa of *N,N*-dialkylamide + amine (Appendix A, [14, 16]), 1-alkanol(*n*OH) + amine [18, 32, 33, 108-111] or 2-alkanone(*n*CO) + amine [67, 73] mixtures as functions of *n*, the number of C atoms of the amine, *n*OH or *n*CO. Solid lines, primary amines (-NH$_2$); dashed lines, secondary amines (-NH-). Full symbols: (■), DMF; (▲), DMA; (◆), DPA; (●), DBA;.(✚), HxA; (✖), aniline. Hollow symbols: (□), DMF + aniline; (△), DMA + aniline. H^E_m (3OH + DPA) was estimated using Gibbs-Helmholtz equation and vapor-liquid equilibrium data [112].

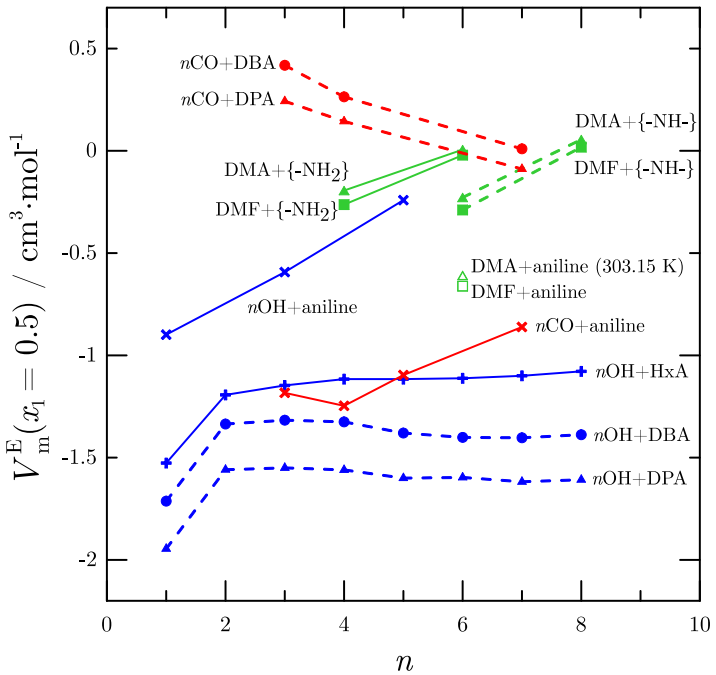

Figure 5.4: V^E_m at $x_1 = 0.5$, $T = 298.15$ K and $p = 0.1$ MPa of *N,N*-dialkylamide + amine [11, 15, 43, 44], 1-alkanol(*n*OH) + amine [21, 26, 27, 92] or 2-alkanone(*n*CO) + amine [68-72, 74, 113] mixtures as functions of *n*, the number of C atoms of the amine, *n*OH or *n*CO. Solid lines, primary amines (-NH$_2$); dashed lines, secondary amines (-NH-). Full symbols: (■), DMF; (▲), DMA; (◆), DPA; (●), DBA;.(✚), HxA; (✖), aniline. Hollow symbols: (□), DMF + aniline; (△), DMA + aniline (303.15 K).

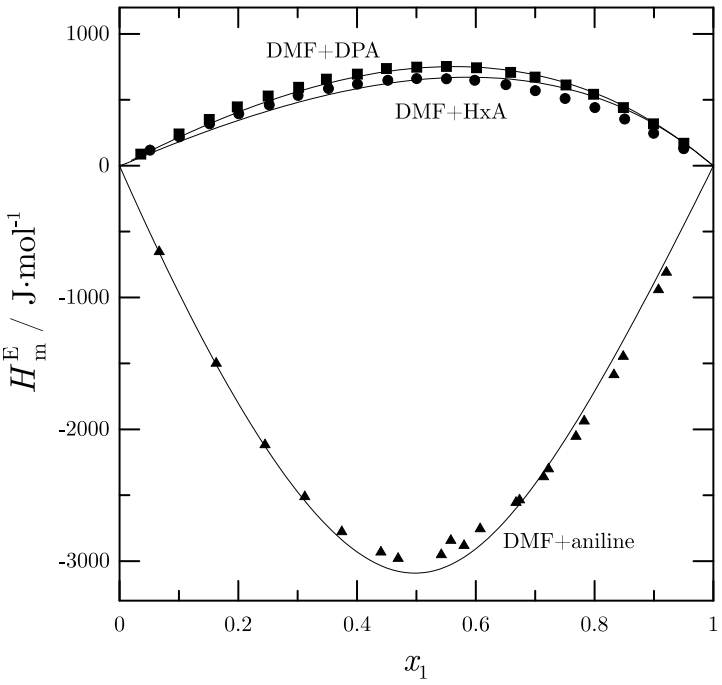

Figure 5.5: H^E_m at $T = 298.15$ K and $p = 0.1$ MPa of DMF + amine liquid mixtures as functions of x_1. Full symbols: (●), HxA (Appendix A); (■), DPA (Appendix A); (▲), aniline [14]. Solid lines, ERAS results (Appendix A, [46]).

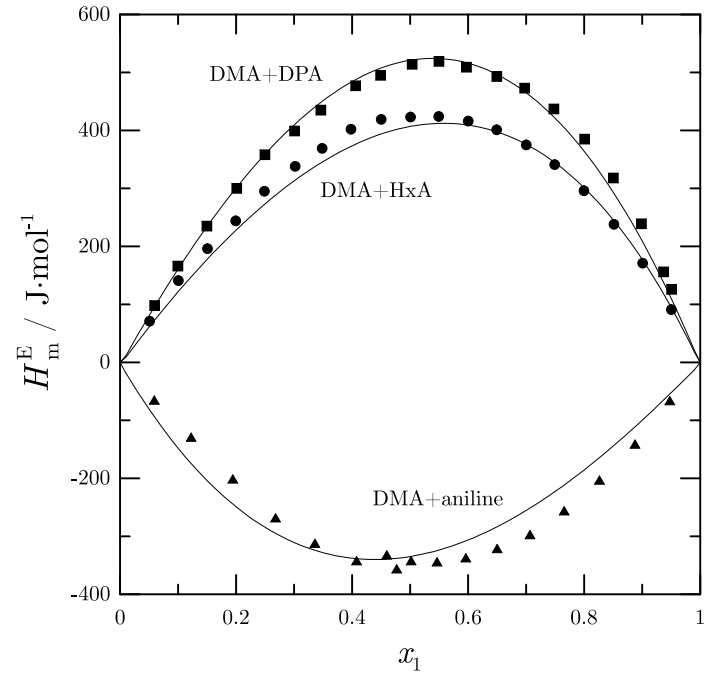

Figure 5.6: H^E_m at $T = 298.15$ K and $p = 0.1$ MPa of DMA + amine liquid mixtures as functions of x_1. Full symbols: (●), HxA (Appendix A); (■), DPA (Appendix A); (▲), aniline [16]. Solid lines, ERAS results (Appendix A, [46]).

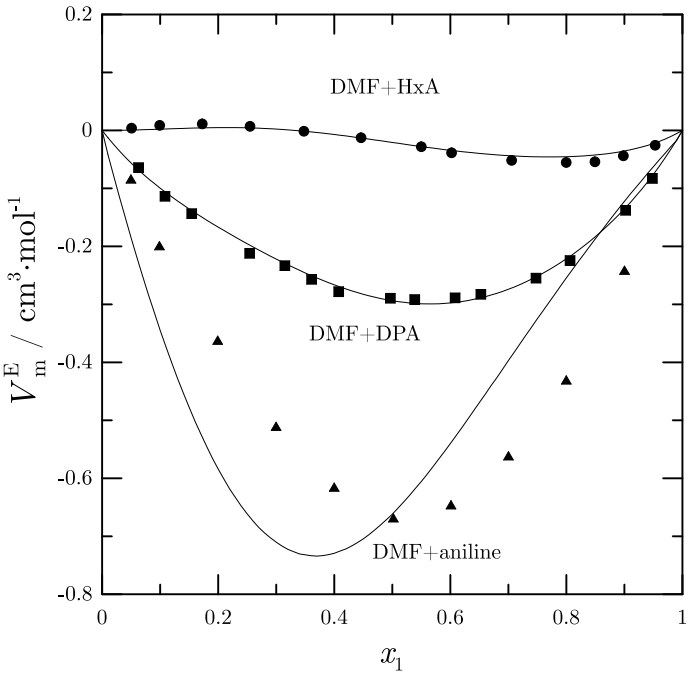

Figure 5.7: V^E_m at $T = 298.15$ K and $p = 0.1$ MPa of DMF + amine liquid mixtures as functions of x_1. Full symbols: (●), HxA [43], (■), DPA [43]; (▲), aniline [11]. Solid lines, ERAS results (Appendix A, [46]).

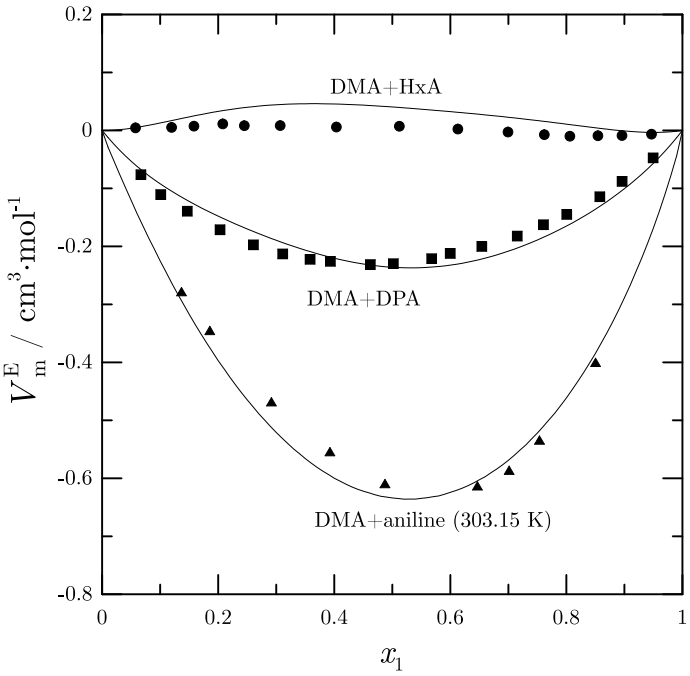

Figure 5.8: V^E_m at $T = 298.15$ K and $p = 0.1$ MPa of DMA + amine liquid mixtures as functions of x_1. Full symbols: (●), HxA [44], (■), DPA [44]; (▲), aniline (303.15 K [15]). Solid lines, ERAS results (Appendix A, [46]).

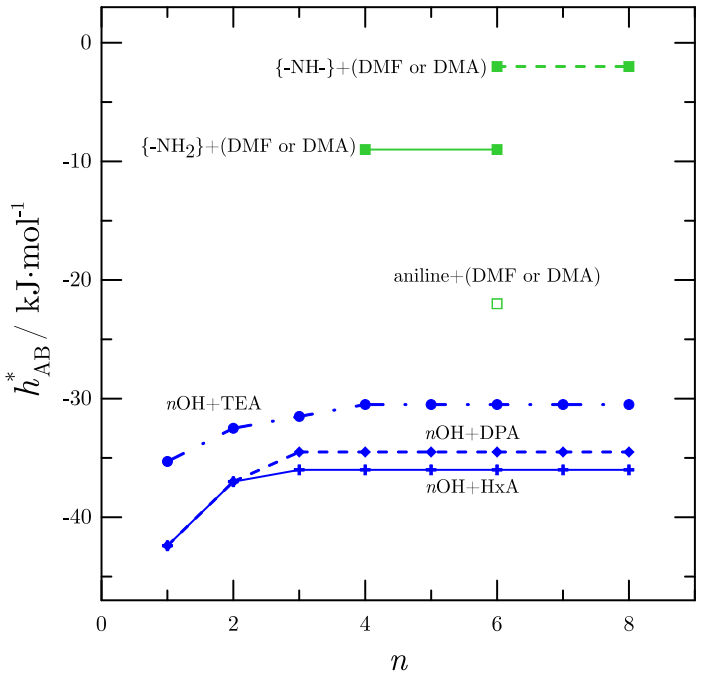

Figure 5.9: Cross-association molar enthalpy of the ERAS model, h^*_{AB}, of amine + *N,N*-dialkylamide (Appendix A, [46]) or 1-alkanol(*n*OH) + amine [21, 26] liquid mixtures as functions of n, the number of C atoms of the amine or 1-alkanol. Solid lines, primary amines (-NH_2); dashed lines, secondary amines (-NH-); dashed-dotted lines, tertiary amines. Full symbols: (■), DMF or DMA;.(✚), HxA; (◆), DPA; (●), TEA. Hollow symbols: (□), aniline + DMF or DMA.

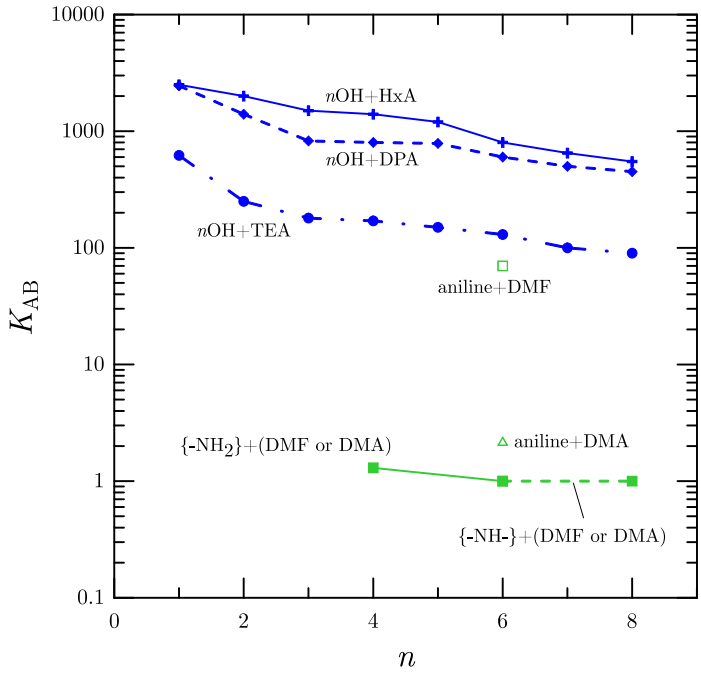

Figure 5.10: Cross-association equilibrium constant of the ERAS model, K_{AB}, of amine + *N,N*-dialkylamide (Appendix A, [46]) or 1-alkanol(*n*OH) + amine [21, 26] liquid mixtures as functions of n, the number of C atoms of the amine or 1-alkanol. Solid lines, primary amines (-NH_2); dashed lines, secondary amines (-NH-); dashed-dotted lines, tertiary amines. Full symbols: (■), DMF or DMA;.(✚), HxA; (◆), DPA; (●), TEA. Hollow symbols: (□), aniline + DMF; (△), aniline + DMA.

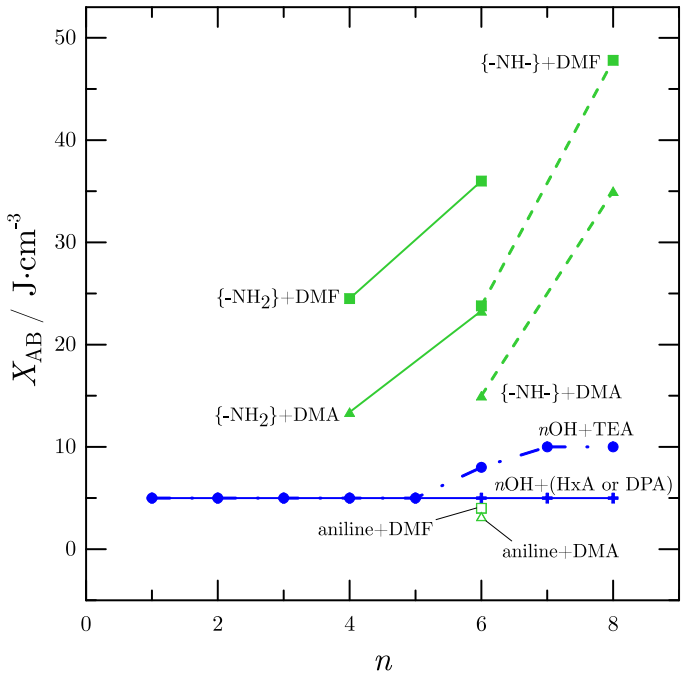

Figure 5.11: Physical parameter of the ERAS model, X_{AB}, of amine + *N,N*-dialkylamide (Appendix A, [46]) or 1-alkanol(nOH) + amine [21, 26] liquid mixtures as functions of n, the number of C atoms of the amine or 1-alkanol. Solid lines, primary amines (-NH$_2$); dashed lines, secondary amines (-NH-); dashed-dotted lines, tertiary amines. Full symbols: (■), DMF or DMA;.(✚), HxA or DPA; (●), TEA. Hollow symbols: (□), DMF + aniline; (△), DMA + aniline.

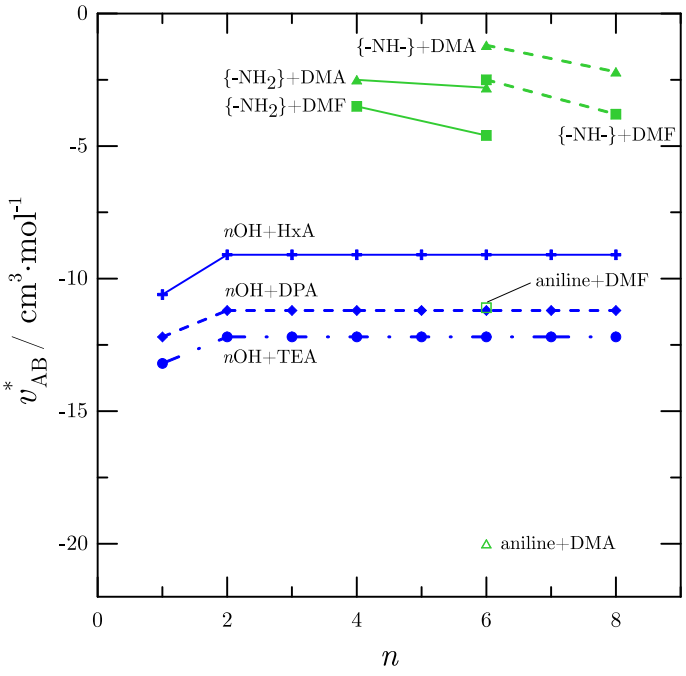

Figure 5.12: Cross-association molar volume of the ERAS model, v^*_{AB}, of amine + *N,N*-dialkylamide (Appendix A, [46]) or 1-alkanol(nOH) + amine [21, 26] liquid mixtures as functions of n, the number of C atoms of the amine or 1-alkanol. Solid lines, primary amines (-NH$_2$); dashed lines, secondary amines (-NH-); dashed-dotted lines, tertiary amines. Full symbols: (■), DMF or DMA;.(✚), HxA; (◆), DPA; (●), TEA. Hollow symbols: (□), DMF + aniline; (△), DMA + aniline.

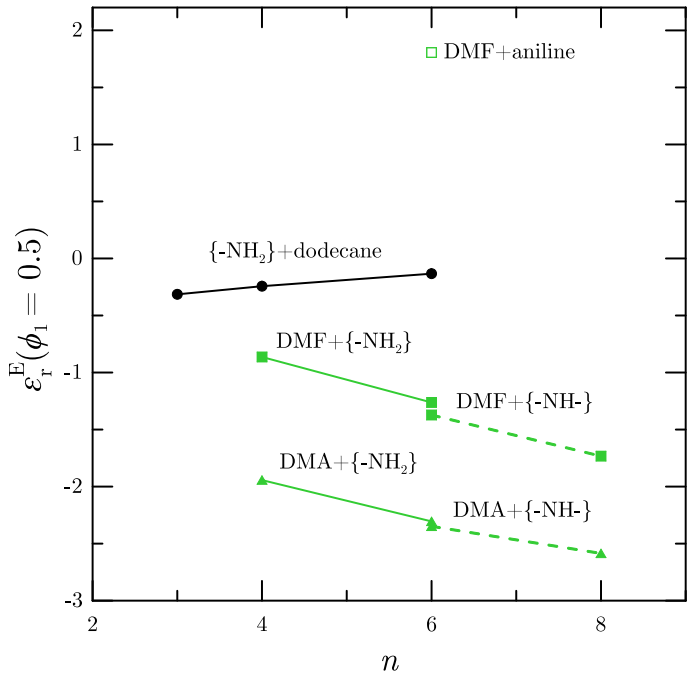

Figure 5.13: ε_r^E at $\phi_1 = 0.5$, $T = 298.15$ K and $p = 0.1$ MPa of *N,N*-dialkylamide + amine [45, 46] or primary amine + dodecane ([75], [76]) liquid mixtures as functions of n, the number of C atoms of the amine. Solid lines, primary amines (-NH_2); dashed lines, secondary amines (-NH-). Symbols: (●), dodecane; (■), DMF; (▲), DMA.

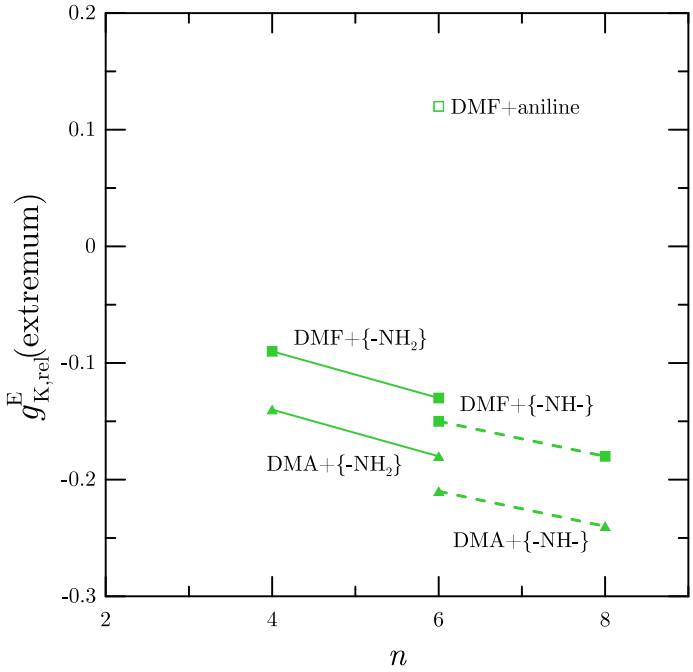

Figure 5.14: Minimum (primary or secondary amine) or maximum (aniline) of $g^E_{K,rel}$ (equation (5.1)) at $T = 298.15$ K and $p = 0.1$ MPa of *N,N*-dialkylamide + amine [45, 46] liquid mixtures as functions of n, the number of C atoms of the amine. Solid lines, primary amines (-NH_2); dashed lines, secondary amines (-NH-). Full symbols: (■), DMF; (▲), DMA. Hollow symbols: (□), DMF + aniline.

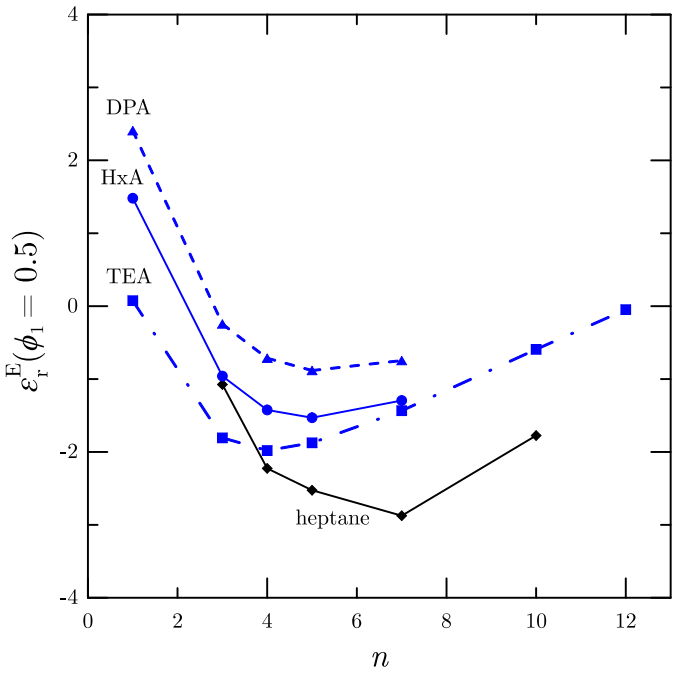

Figure 5.15: ε_r^E at $\phi_1 = 0.5$, $T = 298.15$ K and $p = 0.1$ MPa of 1-alkanol + amine or + heptane liquid mixtures as functions of n, the number of C atoms of the 1-alkanol. Full symbols: (●), HxA [47]; (▲), DPA [82]; (■), TEA (Appendix B); (◆), heptane [114, 115].

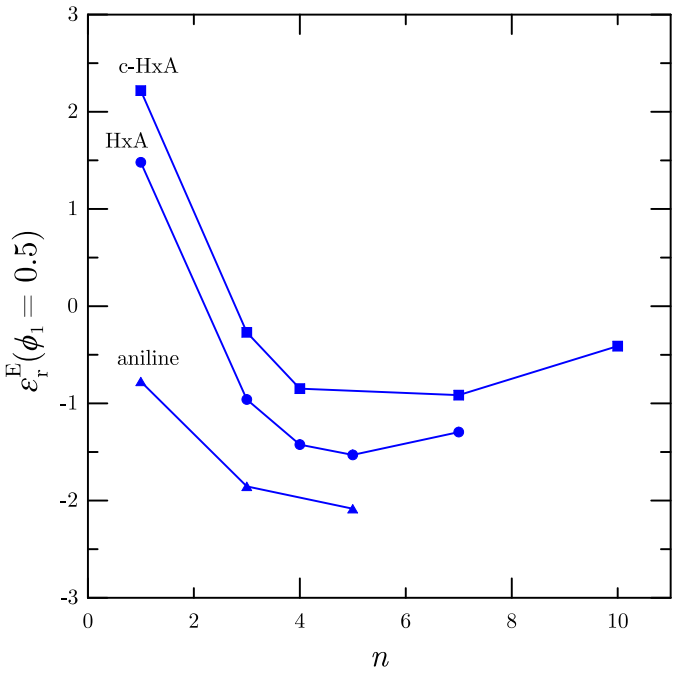

Figure 5.16: ε_r^E at $\phi_1 = 0.5$, $T = 298.15$ K and $p = 0.1$ MPa of 1-alkanol + primary amine liquid mixtures as functions of n, the number of C atoms of the 1-alkanol. Symbols: (●), HxA [47]; (■), c-HxA [30, 36]; (▲), aniline [92].

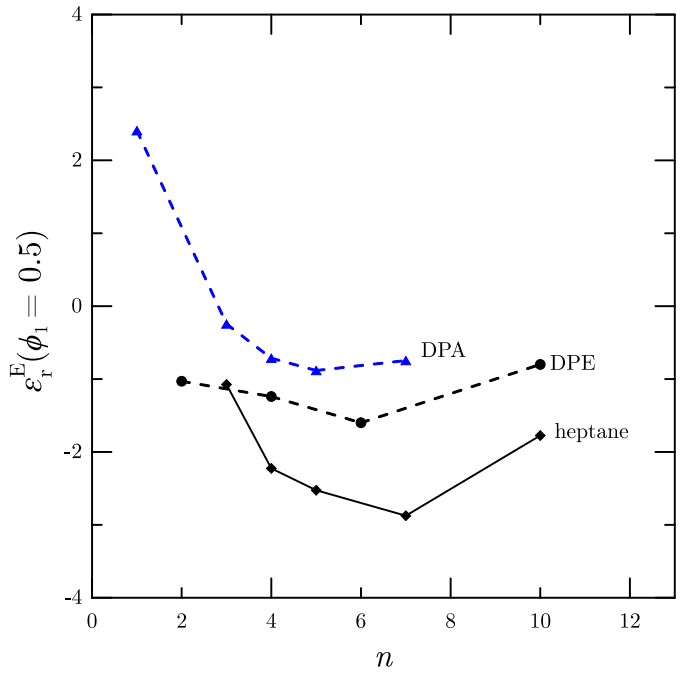

Figure 5.17: ε_r^E at $\phi_1 = 0.5$, $T = 298.15$ K and $p = 0.1$ MPa of 1-alkanol + DPA, + DPE or + heptane liquid mixtures as functions of n, the number of C atoms of the 1-alkanol. Symbols: (▲), DPA [82]; (●), DPE [95]; (◆), heptane [114, 115].

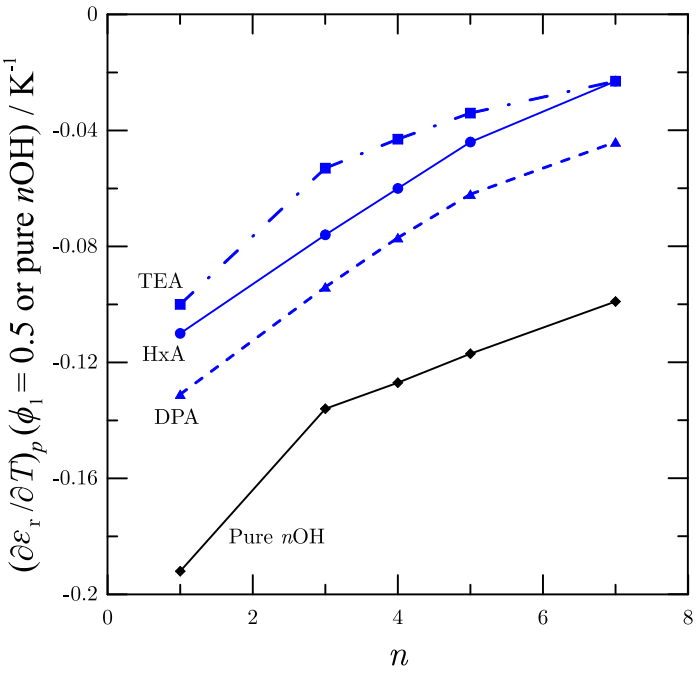

Figure 5.18: $(\partial\varepsilon_r/\partial T)_p$ at $T = 298.15$ K and $p = 0.1$ MPa of pure 1-alkanols and of 1-alkanol(nOH) + amine liquid mixtures at $\phi_1 = 0.5$ as functions of n, the number of C atoms of the 1-alkanol. Full symbols: (●), HxA [47]; (▲), DPA [82]; (■), TEA (Appendix B); (◆), pure 1-alkanols ([47, 82], Appendix B).

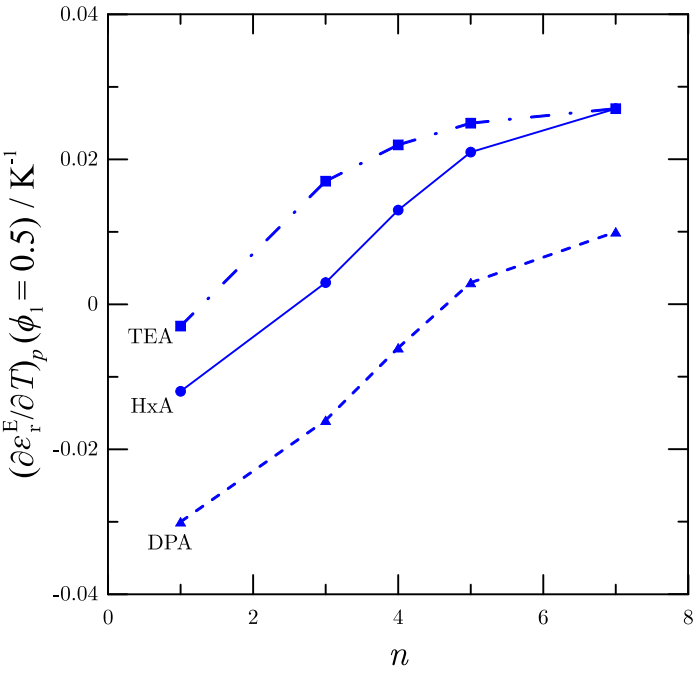

Figure 5.19: $(\partial\varepsilon_r^E/\partial T)_p$ at $\phi_1 = 0.5$, $T = 298.15$ K and $p = 0.1$ MPa of 1-alkanol + amine liquid mixtures as functions of n, the number of C atoms of the 1-alkanol. Full symbols: (●), HxA [47]; (▲), DPA [82]; (■), TEA (Appendix B).

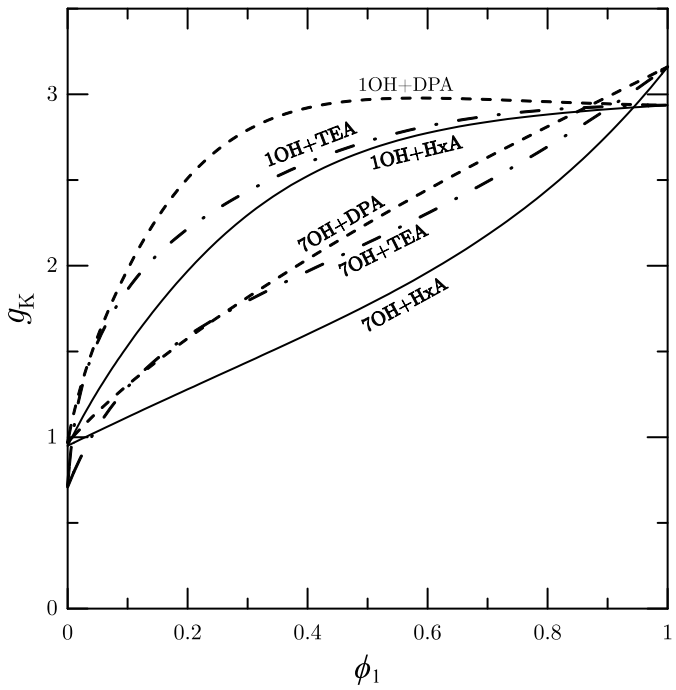

Figure 5.20: g_K at $T = 298.15$ K and $p = 0.1$ MPa of 1OH or 7OH + amine liquid mixtures as functions of ϕ_1. Solid lines, HxA [47]; dashed lines, DPA [82]; dashed-dotted lines, TEA (Appendix B).

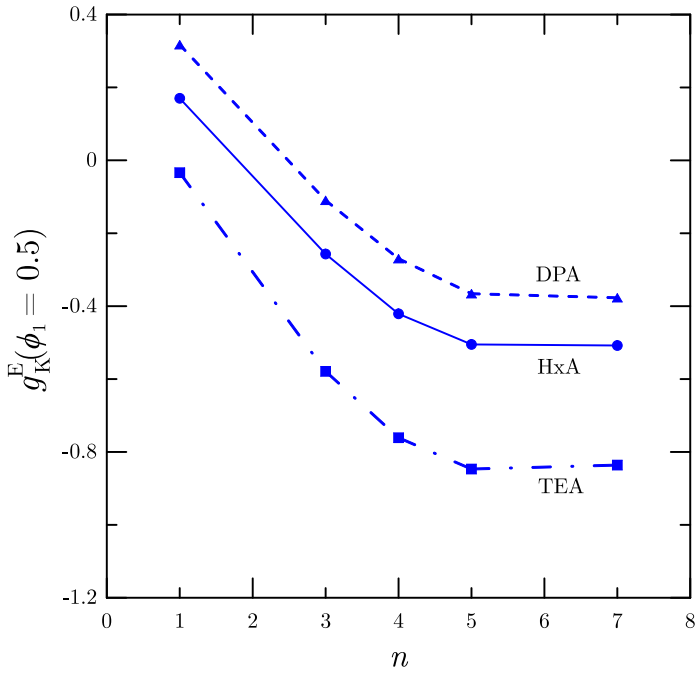

Figure 5.21: g^{E}_{K} at $\phi_1 = 0.5$, $T = 298.15$ K and $p = 0.1$ MPa of 1-alkanol + amine liquid mixtures as functions of n, the number of C atoms of the 1-alkanol. Full symbols: (●), HxA [47]; (▲), DPA [82]; (■), TEA (Appendix B).

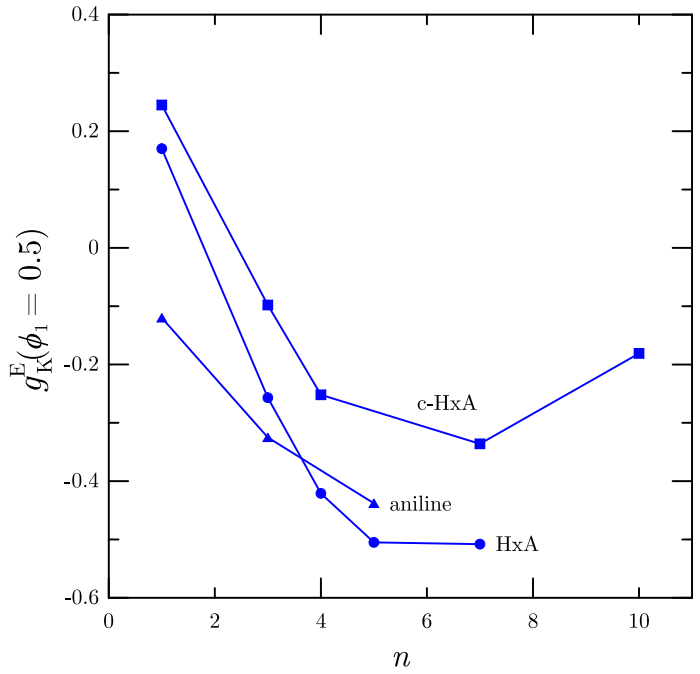

Figure 5.22: g^{E}_{K} at $\phi_1 = 0.5$, $T = 298.15$ K and $p = 0.1$ MPa of 1-alkanol + primary amine liquid mixtures as functions of n, the number of C atoms of the 1-alkanol. Symbols: (●), HxA [47]; (■), c-HxA [30, 36]; (▲), aniline [92].

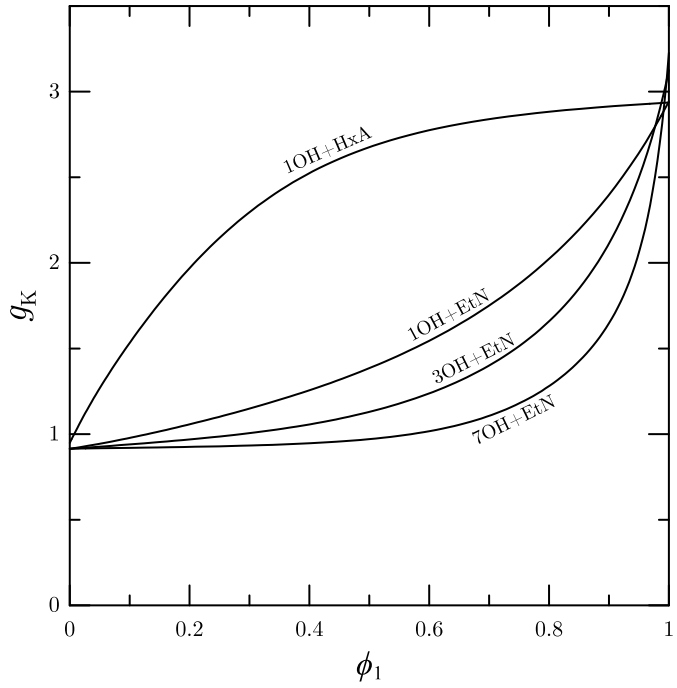

Figure 5.23: g_K at $T = 298.15$ K and $p = 0.1$ MPa of 1-alkanol(nOH) + EtN [98, 99] or + HxA [47] liquid mixtures as functions of ϕ_1.

5.4. References

[1] E.S. Eberhardt, R.T. Raines, *Amide-Amide and Amide-Water Hydrogen Bonds: Implications for Protein Folding and Stability.* J. Am. Chem. Soc. **116** (1994) 2149-2150. https://doi.org/10.1021/ja00084a067

[2] T.W. Whitfield, G.J. Martyna, S. Allison, S.P. Bates, H. Vass, J. Crain, *Structure and Hydrogen Bonding in Neat N-Methylacetamide: Classical Molecular Dynamics and Raman Spectroscopy Studies of a Liquid of Peptidic Fragments.* J. Phys. Chem. B **110** (2006) 3624-3637. https://doi.org/10.1021/jp053140+

[3] J.A. Gonzalez, J.C. Cobos, I. García de la Fuente, *Thermodynamics of liquid mixtures containing a very strongly polar compound: Part 6. DISQUAC characterization of N,N-dialkylamides.* Fluid Phase Equilib. **224** (2004) 169-183. https://doi.org/10.1016/j.fluid.2004.02.007

[4] J. Barthel, R. Buchner, B. Wurm, *The dynamics of liquid formamide, N-methylformamide, N,N-dimethylformamide, and N,N-dimethylacetamide. A dielectric relaxation study.* J. Mol. Liq. **98** (2002) 51-69. https://doi.org/10.1016/S0167-7322(01)00309-9

[5] W.L. Jorgensen, C.J. Swenson, *Optimized intermolecular potential functions for amides and peptides. Structure and properties of liquid amides.* J. Am. Chem. Soc. **107** (1985) 569-578. https://doi.org/10.1021/ja00289a008

[6] F.F. Liew, T. Hasegawa, M. Fukuda, E. Nakata, T. Morii, *Construction of dopamine sensors by using fluorescent ribonucleopeptide complexes.* Bioorg. Med. Chem. **19** (2011) 4473-4481. https://doi.org/10.1016/j.bmc.2011.06.031

[7] J.M. Sonner, R.S. Cantor, *Molecular Mechanisms of Drug Action: An Emerging View.* Annu. Rev. Biophys. **42** (2013) 143-167. https://doi.org/10.1146/annurev-biophys-083012-130341

[8] D.L. Nelson, M.M. Cox, *Lehninger Principles of Biochemistry.* 3rd ed., Worth Publishing, New York, 2000.

[9] Y. Coulier, A. Lowe, P.R. Tremaine, J.Y. Coxam, K. Ballerat-Busserolles, *Absorption of CO2 in aqueous solutions of 2-methylpiperidine: Heats of solution and modeling.* Int. J. Greenh. Gas Control **47** (2016) 322-329. https://doi.org/10.1016/j.ijggc.2016.02.009

[10] M. Götz, R. Reimert, S. Bajohr, H. Schnetzer, J. Wimberg, T.J.S. Schubert, *Long-term thermal stability of selected ionic liquids in nitrogen and hydrogen atmosphere.* Thermochim. Acta **600** (2015) 82-88. https://doi.org/10.1016/j.tca.2014.11.005

[11] H.J. Noh, S.J. Park, S.J. In, *Excess molar volumes and deviations of refractive indices at 298.15 K for binary and ternary mixtures with pyridine or aniline or quinoline.* J. Ind. Eng. Chem. **16** (2010) 200-206. https://doi.org/10.1016/j.jiec.2010.01.038

[12] P.S. Nikam, S.J. Kharat, *Excess Molar Volumes and Deviations in Viscosity of Binary Mixtures of N,N-Dimethylformamide with Aniline and Benzonitrile at (298.15, 303.15, 308.15, and 313.15) K.* J. Chem. Eng. Data **48** (2003) 972-976. https://doi.org/10.1021/je030101n

[13] T.E. Vittal Prasad, A. Adi Sankara Reddy, S. Kailash, D.H.L. Prasad, *Activity coefficients and excess Gibbs energy of binary mixtures of N,N-dimethyl formamide with selected compounds at 95.5 kPa.* Fluid Phase Equilib. **273** (2008) 52-58. https://doi.org/10.1016/j.fluid.2008.07.018

[14] R.S. Ramadevi, P. Venkatesu, M.V. Prabhakara Rao, M.R. Krishna, *Excess enthalpies of binary mixtures of N,N-dimethylformamide with substituted benzenes at 298.15 K.* Fluid Phase Equilib. **114** (1996) 189-197. https://doi.org/10.1016/0378-3812(95)02816-1

[15] G. Chandrasekhar, P. Venkatesu, M.V. Prabhakara Rao, *Excess Volumes and Ultrasonic Studies of n,n-Dimethyl Acetamide with Substituted Benzenes at 303.15 k.* Phys. Chem. Liq. **40** (2002) 181-189. https://doi.org/10.1080/00319100208086661

[16] G. Chandra Sekhar, M.V. Prabhakara Rao, D.H.L. Prasad, Y.V.L. Ravi Kumar, *Excess molar enthalpies of N,N-dimethylacetamide with substituted benzenes at 298.15 K.* Thermochim. Acta **402** (2003) 99-103. https://doi.org/10.1016/S0040-6031(02)00542-7

[17] A.B. de Haan, J. Gmehling, *Excess Enthalpies for Various Binary Mixtures with N-Methylacetamide or Acetic Anhydride.* J. Chem. Eng. Data **41** (1996) 474-478. https://doi.org/10.1021/je950294h

[18] A. Heintz, P.K. Naicker, S.P. Verevkin, R. Pfestorf, *Thermodynamics of alkanol + amine mixtures. Experimental results and ERAS model calculations of the heat of mixing.* Ber. Bunsenges. Phys. Chem. **102** (1998) 953-959. https://doi.org/10.1002/bbpc.19981020707

[19] K. Nakanishi, H. Touhara, N. Watanabe, *Studies on Associated Solutions. II. Heat of Mixing of Methanol with Aliphatic Amines.* Bull. Chem. Soc. Jpn. **43** (1970) 2671-2676. https://doi.org/10.1246/bcsj.43.2671

[20] A. Heintz, *A New Theoretical Approach for Predicting Excess Properties of Alkanol/Alkane Mixtures.* Ber. Bunsenges. Phys. Chem. **89** (1985) 172-181. https://doi.org/10.1002/bbpc.19850890217

[21] S. Villa, N. Riesco, I. García de la Fuente, J.A. González, J.C. Cobos, *Thermodynamics of mixtures with strongly negative deviations from Raoult's law. Part 8. Excess molar volumes at 298.15 K for 1-alkanol + isomeric amine (C6H15N) systems:*

Characterization in terms of the ERAS model. Fluid Phase Equilib. **216** (2004) 123-133. https://doi.org/10.1016/j.fluid.2003.10.008

[22] J.A. González, I. García de la Fuente, J.C. Cobos, *Thermodynamics of mixtures with strongly negative deviations from Raoult's Law: Part 4. Application of the DISQUAC model to mixtures of 1-alkanols with primary or secondary linear amines. Comparison with Dortmund UNIFAC and ERAS results.* Fluid Phase Equilib. **168** (2000) 31-58. https://doi.org/10.1016/S0378-3812(99)00326-X

[23] R. Srivastava, B.D. Smith, *Total-pressure vapor-liquid equilibrium data for binary systems of diethylamine with acetone, acetonitrile, and methanol.* J. Chem. Eng. Data **30** (1985) 308-313. https://doi.org/10.1021/je00041a022

[24] L. Wang, G.C. Benson, B.C.Y. Lu, *Excess enthalpies of 1-propanol + n-hexane + n-decane or n-dodecane at 298.15 K.* J. Chem. Eng. Data **37** (1992) 403-406. https://doi.org/10.1021/je00008a007

[25] S.-c. Hwang, R.L. Robinson, *Vapor-liquid equilibria at 25 ^{o}C for nine alcohol-hydrocarbon binary systems.* J. Chem. Eng. Data **22** (1977) 319-325. https://doi.org/10.1021/je60074a025

[26] S. Villa, N. Riesco, I. García de la Fuente, J.A. González, J.C. Cobos, *Thermodynamics of mixtures with strongly negative deviations from Raoult's law: Part 5. Excess molar volumes at 298.15 K for 1-alkanols+dipropylamine systems: characterization in terms of the ERAS model.* Fluid Phase Equilib. **190** (2001) 113-125. https://doi.org/10.1016/S0378-3812(01)00595-7

[27] S. Villa, N. Riesco, I. García de la fuente, J.A. González, J.C. Cobos, *Thermodynamics of mixtures with strongly negative deviations from Raoult's law: Part 6. Excess molar volumes at 298.15 K for 1-alkanols + dibutylamine systems. Characterization in terms of the ERAS model.* Fluid Phase Equilib. **198** (2002) 313-329. https://doi.org/10.1016/S0378-3812(01)00808-1

[28] L.F. Sanz, J.A. González, I. García De La Fuente, J.C. Cobos, *Thermodynamics of mixtures with strongly negative deviations from Raoult's law. XI. Densities, viscosities and refractives indices at (293.15–303.15) K for cyclohexylamine + 1-propanol, or +1-butanol systems.* J. Mol. Liq. **172** (2012) 26-33. https://doi.org/10.1016/j.molliq.2012.05.003

[29] L.F. Sanz, J.A. González, I. García de la Fuente, J.C. Cobos, *Thermodynamics of mixtures with strongly negative deviations from Raoult's law. XII. Densities, viscosities and refractive indices at T = (293.15 to 303.15) K for (1-heptanol, or 1-decanol + cyclohexylamine) systems. Application of the ERAS model to (1-alkanol + cyclohexylamine) mixtures.* J. Chem. Thermodyn. **80** (2015) 161-171. https://doi.org/10.1016/j.jct.2014.09.005

[30] L.F. Sanz, J.A. González, I.G. De La Fuente, J.C. Cobos, *Thermodynamics of mixtures with strong negative deviations from raoult's law. XIV. density, permittivity, refractive index and viscosity data for the methanol + cyclohexylamine mixture at (293.15–303.15) K.* Thermochim. Acta **631** (2016) 18-27. https://doi.org/10.1016/j.tca.2016.03.002

[31] U. Domańska, M. Głoskowska, *Experimental Solid + Liquid Equilibria and Excess Molar Volume of Alkanol + Octylamine Mixtures. Analysis in Terms of ERAS, DISQUAC, and Modified UNIFAC.* J. Chem. Eng. Data **49** (2004) 101-108. https://doi.org/10.1021/je0301895

[32] K. Nakanishi, H. Touhara, *Excess molar enthalpies of (methanol + aniline), (methanol + N-methylaniline), and (methanol + N,N-dimethylaniline).* J. Chem. Thermodyn. **18** (1986) 657-660. https://doi.org/10.1016/0021-9614(86)90067-4

[33] I. Nagata, *Excess enthalpies of (aniline + butan-1-ol) and of (aniline + butan-1-ol + benzene) at the temperature 298.15 K.* J. Chem. Thermodyn. **25** (1993) 1281-1285. https://doi.org/10.1006/jcht.1993.1127

[34] H. Matsuda, K. Ochi, K. Kojima, *Determination and Correlation of LLE and SLE Data for the Methanol + Cyclohexane, Aniline + Heptane, and Phenol + Hexane System.* J. Chem. Eng. Data **48** (2003) 184-189. https://doi.org/10.1021/je020156+

[35] S. Villa, R. Garriga, P. Pérez, M. Gracia, J.A. González, I.G. de la Fuente, J.C. Cobos, *Thermodynamics of mixtures with strongly negative deviations from Raoult's law: Part 9. Vapor–liquid equilibria for the system 1-propanol + di-n-propylamine at six temperatures between 293.15 and 318.15 K.* Fluid Phase Equilib. **231** (2005) 211-220. https://doi.org/10.1016/j.fluid.2005.01.013

[36] J.A. González, L.F. Sanz, I. García de la Fuente, J.C. Cobos, *Thermodynamics of mixtures with strong negative deviations from Raoult's law. XIII. Relative permittivities for (1-alkanol + cyclohexylamine) systems, and dielectric study of (1-alkanol + polar) compound (amine, amide or ether) mixtures.* J. Chem. Thermodyn. **91** (2015) 267-278. https://doi.org/10.1016/j.jct.2015.07.032

[37] J.A. González, I.G. de la Fuente, J.C. Cobos, *Thermodynamics of mixtures with strongly negative deviations from Raoult's law. Part 3. Application of the DISQUAC model to mixtures of triethylamine with alkanols. Comparison with Dortmund UNIFAC and ERAS results.* Can. J. Chem. **78** (2000) 1272-1284. https://doi.org/10.1139/v00-114

[38] J.A. González, I. Mozo, I. García de la Fuente, J.C. Cobos, *Thermodynamics of organic mixtures containing amines. IV. Systems with aniline.* Can. J. Chem. **83** (2005) 1812-1825. https://doi.org/10.1139/v05-190

[39] J.A. González, I. Mozo, I.G.d.l. Fuente, J.C. Cobos, *Thermodynamics of organic mixtures containing amines: V. Systems with pyridines.* Thermochim. Acta **441** (2006) 53-68. https://doi.org/10.1016/j.tca.2005.11.027

[40] J.A. González, I. Mozo, I.G. de la Fuente, J.C. Cobos, N. Riesco, *Thermodynamics of mixtures containing amines: VII. Systems containing dimethyl or trimethylpyridines.* Thermochim. Acta **467** (2008) 30-43. https://doi.org/10.1016/j.tca.2007.10.011

[41] J.A. González, I.G. de la Fuente, I. Mozo, J.C. Cobos, N. Riesco, *Thermodynamics of Organic Mixtures Containing Amines. VII. Study of Systems Containing Pyridines in Terms of the Kirkwood−Buff Formalism.* Ind. Eng. Chem. Res. **47** (2008) 1729-1737. https://doi.org/10.1021/ie071226e

[42] J.A. González, J.C. Cobos, I. García de la Fuente, I. Mozo, *Thermodynamics of mixtures containing amines. IX. Application of the concentration–concentration structure factor to the study of binary mixtures containing pyridines.* Thermochim. Acta **494** (2009) 54-64. https://doi.org/10.1016/j.tca.2009.04.017

[43] F. Hevia, A. Cobos, J.A. González, I. García de la Fuente, L.F. Sanz, *Thermodynamics of Amide + Amine Mixtures. 1. Volumetric, Speed of Sound, and Refractive Index Data for N,N-Dimethylformamide + N-Propylpropan-1-amine, + N-Butylbutan-1-amine, + Butan-1-amine, or + Hexan-1-amine Systems at Several Temperatures.* J. Chem. Eng. Data **61** (2016) 1468-1478. https://doi.org/10.1021/acs.jced.5b00802

[44] F. Hevia, A. Cobos, J.A. González, I.G. de la Fuente, V. Alonso, *Thermodynamics of Amide + Amine Mixtures. 2. Volumetric, Speed of Sound and Refractive Index Data for*

N,N-Dimethylacetamide + N-Propylpropan-1-Amine, + N-Butylbutan-1-Amine, + Butan-1-Amine, or + Hexan-1-Amine Systems at Several Temperatures. J. Solution Chem. **46** (2017) 150-174. https://doi.org/10.1007/s10953-016-0560-0

[45] F. Hevia, J.A. González, I. García de la Fuente, L.F. Sanz, J.C. Cobos, *Thermodynamics of amide + amine mixtures. 3. Relative permittivities of N,N-dimethylformamide + N-propylpropan-1-amine, + N-butylbutan-1-amine, + butan-1-amine, or + hexan-1-amine systems at several temperatures.* J. Mol. Liq. **238** (2017) 440-446. https://doi.org/10.1016/j.molliq.2017.05.025

[46] F. Hevia, J.A. González, A. Cobos, I. García de la Fuente, L.F. Sanz, *Thermodynamics of amide + amine mixtures. 4. Relative permittivities of N,N-dimethylacetamide + N-propylpropan-1-amine, + N-butylbutan-1-amine, + butan-1-amine, or + hexan-1-amine systems and of N,N-dimethylformamide + aniline mixture at several temperatures. Characterization of amine + amide systems using ERAS.* J. Chem. Thermodyn. **118** (2018) 175-187. https://doi.org/10.1016/j.jct.2017.11.011

[47] F. Hevia, J.A. González, A. Cobos, I. García de la Fuente, C. Alonso-Tristán, *Thermodynamics of mixtures with strongly negative deviations from Raoult's law. XV. Permittivities and refractive indices for 1-alkanol + n-hexylamine systems at (293.15–303.15) K. Application of the Kirkwood-Fröhlich model.* Fluid Phase Equilib. **468** (2018) 18-28. https://doi.org/10.1016/j.fluid.2018.04.007

[48] A.L. McClellan, *Tables of Experimental Dipole Moments*. Vols. 1,2,3, Rahara Enterprises, El Cerrito, US, 1974.

[49] J.A. Riddick, W.B. Bunger, T.K. Sakano, *Organic solvents: physical properties and methods of purification*. Wiley, New York, 1986.

[50] J. Lobos, I. Mozo, M. Fernández Regúlez, J.A. González, I. García de la Fuente, J.C. Cobos, *Thermodynamics of Mixtures Containing a Strongly Polar Compound. 8. Liquid−Liquid Equilibria for N,N-Dialkylamide + Selected N-Alkanes.* J. Chem. Eng. Data **51** (2006) 623-627. https://doi.org/10.1021/je050428j

[51] M. Rogalski, R. Stryjek, *Mutual solubility of binary n-hexadecane and polar compound systems.* Bull. Acad. Pol. Sci., Ser. Sci. Chim. **28** (1980) 139-147.

[52] X. An, H. Zhao, F. Jiang, W. Shen, *The (liquid + liquid) critical phenomena of (a polar liquid + an n-alkane) V. Coexistence curves of (N,N-dimethylacetamide + heptane).* J. Chem. Thermodyn. **28** (1996) 1221-1232. https://doi.org/10.1006/jcht.1996.0109

[53] H. Funke, M. Wetzel, A. Heintz, *New applications of the ERAS model. Thermodynamics of amine + alkane and alcohol + amine mixtures.* Pure Appl. Chem. **61** (1989) 1429-1439. https://doi.org/10.1351/pac198961081429

[54] S. Villa, J.A. González, I.G. De La Fuente, N. Riesco, J.C. Cobos, *Thermodynamics of Organic Mixtures Containing Amines. II. Excess Molar Volumes at 25°C for Methylbutylamine + Alkane Systems and Eras Characterization of Linear Secondary Amine + Alkane Mixtures.* J. Solution Chem. **31** (2002) 1019-1038. https://doi.org/10.1023/A:1021881627444

[55] J.A. González, L.F. Sanz, I. García De La Fuente, J.C. Cobos, *Thermodynamics of mixtures containing amines: XIII. Application of the ERAS model to cyclic amine + alkane mixtures.* Thermochim. Acta **573** (2013) 229-236. https://doi.org/10.1016/j.tca.2013.09.033

[56] R.C. Reid, J.M. Prausnitz, B.E. Poling, *The Properties of Gases and Liquids*. McGraw-Hill, New York, US, 1987.

[57] E. Matteoli, L. Lepori, A. Spanedda, *Thermodynamic study of heptane + amine mixtures: I. Excess and solvation enthalpies at 298.15 K.* Fluid Phase Equilib. **212** (2003) 41-52. https://doi.org/10.1016/S0378-3812(03)00260-7

[58] E. Matteoli, P. Gianni, L. Lepori, *Thermodynamic study of heptane + secondary, tertiary and cyclic amines mixtures. Part IV. Excess and solvation enthalpies at 298.15 K.* Fluid Phase Equilib. **306** (2011) 234-241. https://doi.org/10.1016/j.fluid.2011.04.013

[59] D. Patterson, *Free Volume and Polymer Solubility. A Qualitative View.* Macromolecules **2** (1969) 672-677. https://doi.org/10.1021/ma60012a021

[60] S.N. Bhattacharyya, M. Costas, D. Patterson, H.V. Tra, *Thermodynamics of mixtures containing alkanes.* Fluid Phase Equilib. **20** (1985) 27-45. https://doi.org/10.1016/0378-3812(85)90019-6

[61] L. Lepori, P. Gianni, E. Matteoli, *The Effect of the Molecular Size and Shape on the Volume Behavior of Binary Liquid Mixtures. Branched and Cyclic Alkanes in Heptane at 298.15 K.* J. Solution Chem. **42** (2013) 1263-1304. https://doi.org/10.1007/s10953-013-0023-9

[62] A.J. Treszczanowicz, G.C. Benson, *Excess volumes for n-alkanols + n-alkanes II. Binary mixtures of n-pentanol, n-hexanol, n-octanol, and n-decanol + n-heptane.* J. Chem. Thermodyn. **10** (1978) 967-974. https://doi.org/10.1016/0021-9614(78)90058-7

[63] L. Lepori, P. Gianni, A. Spanedda, E. Matteoli, *Thermodynamic study of (heptane + amine) mixtures. II. Excess and partial molar volumes at 298.15 K.* J. Chem. Thermodyn. **43** (2011) 805-813. https://doi.org/10.1016/j.jct.2010.12.025

[64] L. Lepori, P. Gianni, A. Spanedda, E. Matteoli, *Thermodynamic study of (heptane + amine) mixtures. III: Excess and partial molar volumes in mixtures with secondary, tertiary, and cyclic amines at 298.15 K.* J. Chem. Thermodyn. **43** (2011) 1453-1462. https://doi.org/10.1016/j.jct.2011.04.017

[65] T.M. Letcher, *Thermodynamics of aliphatic amine mixtures I. The excess volumes of mixing for primary, secondary, and tertiary aliphatic amines with benzene and substituted benzene compounds.* J. Chem. Thermodyn. **4** (1972) 159-173. https://doi.org/10.1016/S0021-9614(72)80021-1

[66] H. Ukibe, R. Tanaka, S. Murakami, R. Fujishiro, *Excess enthalpies of N,N-dialkyl amides + cyclohexane, + benzene, and + toluene at 298.15 K.* J. Chem. Thermodyn. **6** (1974) 201-206. https://doi.org/10.1016/0021-9614(74)90263-8

[67] J.A. González, I. Alonso, I. García De La Fuente, J.C. Cobos, *Thermodynamics of ketone + amine mixtures. Part IX. Excess molar enthalpies at 298.15 K for dipropylamine, or dibutylamine + 2-alkanone systems and modeling of linear or aromatic amine + 2-alkanone mixtures in terms of DISQUAC and ERAS.* Fluid Phase Equilib. **343** (2013) 1-12. https://doi.org/10.1016/j.fluid.2013.01.011

[68] I. Alonso, V. Alonso, I. Mozo, I. García de la Fuente, J.A. González, J.C. Cobos, *Thermodynamics of ketone + amine mixtures: Part II. Volumetric and speed of sound data at (293.15, 298.15 and 303.15) K for 2-propanone + dipropylamine, + dibutylamine or + triethylamine systems.* J. Mol. Liq. **155** (2010) 109-114. https://doi.org/10.1016/j.molliq.2010.05.022

[69] I. Alonso, I. Mozo, I.G. de la Fuente, J.A. González, J.C. Cobos, *Thermodynamics of Ketone + Amine Mixtures. Part III. Volumetric and Speed of Sound Data at (293.15, 298.15, and 303.15) K for 2-Butanone + Aniline, + N-Methylaniline, or + Pyridine Systems.* J. Chem. Eng. Data **55** (2010) 5400-5405. https://doi.org/10.1021/je100472t

[70] J.A. González, I. Alonso, I. Mozo, I. García de la Fuente, J.C. Cobos, *Thermodynamics of (ketone + amine) mixtures. Part VI. Volumetric and speed of sound data at (293.15, 298.15, and 303.15) K for (2-heptanone + dipropylamine, +dibutylamine, or +triethylamine) systems.* J. Chem. Thermodyn. **43** (2011) 1506-1514. https://doi.org/10.1016/j.jct.2011.05.003

[71] I. Alonso, I. Mozo, I.G. De La Fuente, J.A. González, J.C. Cobos, *Thermodynamics of ketone + amine mixtures 7. Volumetric and speed of sound data at (293.15, 298.15 and 303.15) K for 2-pentanone + aniline, + N-methylaniline, or + pyridine systems.* J. Mol. Liq. **160** (2011) 180-186. https://doi.org/10.1016/j.molliq.2011.03.015

[72] I. Alonso, I. Mozo, I.G. de la fuente, J.A. González, J.C. Cobos, *Thermodynamics of ketone + amine mixtures Part IV. Volumetric and speed of sound data at (293.15; 298.15 and 303.15 K) for 2-butanone +dipropylamine, +dibutylamine or +triethylamine systems.* Thermochim. Acta **512** (2011) 86-92. https://doi.org/10.1016/j.tca.2010.09.004

[73] I. Alonso, I. Mozo, I. García de la Fuente, J.A. González, J.C. Cobos, *Thermodynamics of Ketone + Amine Mixtures. Part VIII. Molar Excess Enthalpies at 298.15 K for n-Alkanone + Aniline or + N-Methylaniline Systems.* J. Chem. Eng. Data **56** (2011) 3236-3241. https://doi.org/10.1021/je200333p

[74] I. Alonso, V. Alonso, I. Mozo, I. García de la Fuente, J.A. González, J.C. Cobos, *Thermodynamics of Ketone + Amine Mixtures. I. Volumetric and Speed of Sound Data at (293.15, 298.15, and 303.15) K for 2-Propanone + Aniline, + N-Methylaniline, or + Pyridine Systems.* J. Chem. Eng. Data **55** (2010) 2505-2511. https://doi.org/10.1021/je900874z

[75] S. Otín, J. Fernández, J.M. Embid, I. Velasco, C.G. Losa, *Thermodynamic and Dielectric Properties of Binary Polar + Non-Polar Mixtures I. Static Dielectric Constants and Excess Molar Enthalpies of n-Alkylamine + n-Dodecane Systems.* Ber. Bunsenges. Phys. Chem. **90** (1986) 1179-1183. https://doi.org/10.1002/bbpc.19860901212

[76] C. Wohlfahrt, *Static Dielectric Constants of Pure Liquids and Binary Liquid Mixtures. Landolt-Börnstein - Group IV Physical Chemistry Vol. 6.* Springer Berlin Heidelberg, Berlin, 1991.

[77] M.S. Bakshi, G. Kaur, *Thermodynamic Behavior of Mixtures. 4. Mixtures of Methanol with Pyridine and N,N-Dimethylformamide at 25 °C.* J. Chem. Eng. Data **42** (1997) 298-300. https://doi.org/10.1021/je960300p

[78] G. Ritzoulis, A. Fidantsi, *Relative Permittivities, Refractive Indices, and Densities for the Binary Mixtures N,N'-Dimethylacetamide with Methanol, Ethanol, 1-Butanol, and 2-Propanol at 298.15 K.* J. Chem. Eng. Data **45** (2000) 207-209. https://doi.org/10.1021/je990116e

[79] J.C.R. Reis, T.P. Iglesias, *Kirkwood correlation factors in liquid mixtures from an extended Onsager-Kirkwood-Frohlich equation.* Phys. Chem. Chem. Phys. **13** (2011) 10670-10680. https://doi.org/10.1039/C1CP20142E

[80] M. El-Hefnawy, K. Sameshima, T. Matsushita, R. Tanaka, *Apparent Dipole Moments of 1-Alkanols in Cyclohexane and n-Heptane, and Excess Molar Volumes of (1-Alkanol + Cyclohexane or n-Heptane) at 298.15 K.* J. Solution Chem. **34** (2005) 43-69. https://doi.org/10.1007/s10953-005-2072-1

[81] A. Skrzecz, *Critical evaluation of solubility data in binary systems formed by methanol with n-hydrocarbons.* Thermochim. Acta **182** (1991) 123-131. https://doi.org/10.1016/0040-6031(91)87013-M

[82] F. Hevia, A. Cobos, J.A. González, I. García de la Fuente, L.F. Sanz, *Thermodynamics of mixtures with strongly negative deviations from Raoult's law. XVI. Permittivities and refractive indices for 1-alkanol + di-n-propylamine systems at (293.15–303.15) K. Application of the Kirkwood-Fröhlich model.* J. Mol. Liq. **271** (2018) 704-714. https://doi.org/10.1016/j.molliq.2018.09.040

[83] J. Liszi, T. Salomon, F. Ratkovics, *Properties of alcohol-amine mixtures. II. Static dielectric properties of the binary mixtures propylamine-propanol and butylamine-butanol.* Acta Chim. Acad. Sci. Hung. **81** (1974) 467-474.

[84] V.A. Rana, A.D. Vyas, S.C. Mehrotra, *Dielectric relaxation study of mixtures of 1-propanol with aniline, 2-chloroaniline and 3-chloroaniline at different temperatures using time domain reflectometry.* J. Mol. Liq. **102** (2003) 379-391. https://doi.org/10.1016/S0167-7322(02)00162-9

[85] T.V. Krishna, S.S. Sastry, V.R.K. Murthy, *Correlation studies on dielectric and thermodynamic parameters in the binary mixtures of N-methyl aniline and alcohols.* Indian J. Phys. **85** (2011) 1495-1511. https://doi.org/10.1007/s12648-011-0168-6

[86] K.V. Zaitseva, M.A. Varfolomeev, B.N. Solomonov, *Thermodynamic functions of hydrogen bonding of amines in methanol derived from solution calorimetry data and headspace analysis.* Thermochim. Acta **535** (2012) 8-16. https://doi.org/10.1016/j.tca.2012.02.005

[87] J.C. Cobos, *An exact quasi-chemical equation for excess heat capacity with W-shaped concentration dependence.* Fluid Phase Equilib. **133** (1997) 105-127. https://doi.org/10.1016/S0378-3812(97)00012-5

[88] R.G. Rubio, M. Cáceres, R.M. Masegosa, L. Andreolli-Ball, M. Costas, D. Patterson, *Mixtures with "w-Shape" CEp curves. A light scattering study.* Ber. Bunsenges. Phys. Chem. **93** (1989) 48-56. https://doi.org/10.1002/bbpc.19890930110

[89] J.A. González, I. García de la Fuente, J.C. Cobos, *Correlation and prediction of excess molar enthalpies using DISQUAC*, in *Enthalpy and Internal Energy: Liquids, Solutions and Vapours*, E. Wilhelm and T.M. Letcher, Editors. 2017, Royal Society of Chemistry: Croydon. p. 543-568.

[90] K. Nakanishi, H. Shirai, T. Minamiyama, *Vapor-liquid equilibrium of binary systems containing alcohols. Methanol with aliphatic amines.* J. Chem. Eng. Data **12** (1967) 591-594. https://doi.org/10.1021/je60035a031

[91] K.W. Chun, R.R. Davison, *Thermodynamic properties of binary mixtures of triethylamine with methyl and ethyl alcohol.* J. Chem. Eng. Data **17** (1972) 307-310. https://doi.org/10.1021/je60054a039

[92] V. Alonso, *Estudio experimental de propiedades termofísicas de mezclas binarias formadas por 1-alcohol + alcano, + éter lineal o + amina aromática primaria.* Tesis Doctoral, 2016. Departamento de Física Aplicada, Facultad de Ciencias, Universidad de Valladolid.

[93] J.A. González, I. Mozo, I. García de la Fuente, J.C. Cobos, N. Riesco, *Thermodynamics of (1-alkanol+linear monoether) systems.* J. Chem. Thermodyn. **40** (2008) 1495-1508. https://doi.org/10.1016/j.jct.2008.06.001

[94] R. Garriga, F. Sánchez, P. Pérez, M. Gracia, *Isothermal vapour-liquid equilibrium at eight temperatures and excess functions at 298.15 K of di-n-propylether with 1-propanol or 2-propanol.* Fluid Phase Equilib. **138** (1997) 131-144. https://doi.org/10.1016/S0378-3812(97)00173-8

[95] M.C. Mateos, P. Pérez, F.M. Royo, M. Gracia, C. Gutiérrez-Losa, *Permitividad estática de mezclas de mono-alcoholes + dipropil-éter, + butanona. + butironitrillo (II).* Rev. Acad. Cienc. Exact. Fis. Quim. Nat. Zaragoza **41** (1986) 73-82.

[96] J.A. González, F. Hevia, L.F. Sanz, I.G. De La Fuente, J.C. Cobos, *Characterization of 1-alkanol + strongly polar compound mixtures from thermophysical data and the application of the Kirkwood-Buff integrals and Kirkwood-Fröhlich formalisms.* Fluid Phase Equilib. **492** (2019) 41-54. https://doi.org/10.1016/j.fluid.2019.03.012

[97] M. Almasi, L. Mousavi, *Excess molar volumes of binary mixtures of aliphatic alcohols (C1–C5) with Nitromethane over the temperature range 293.15 to 308.15K: Application of the ERAS model and cubic EOS.* J. Mol. Liq. **163** (2011) 46-52. https://doi.org/10.1016/j.molliq.2011.07.011

[98] F. Mato, F. Fernández-Polanco, An. Quim. **71** (1975) 815.

[99] I. Cibulka, V.D. Nguyen, R. Holub, *Excess molar volumes of (an alkanol + acetonitrile) at 298.15 and 308.15 K.* J. Chem. Thermodyn. **16** (1984) 159-164. https://doi.org/10.1016/0021-9614(84)90149-6

[100] C.M. Kinart, W.J. Kinart, *Physicochemical Properties and Internal Structures of Dimethyl Sulfoxide-1-Propanol Liquid Mixtures.* Phys. Chem. Liq. **33** (1996) 151-158. https://doi.org/10.1080/00319109608039816

[101] H. Iloukhani, H.A. Zarei, *Volumetric properties of dimethyl sulfoxide with some alcohols at 298.15 K.* Phys. Chem. Liq. **46** (2008) 154-161. https://doi.org/10.1080/00319100601124203

[102] A. Mohan, M. Malathi, A.C. Kumbharkhane, *Microwave dielectric relaxation spectroscopy studies on associative polar binary mixtures of nitrobenzene with primary alcohols.* J. Mol. Liq. **222** (2016) 640-647. https://doi.org/10.1016/j.molliq.2016.07.024

[103] P.S. Nikam, M.C. Jadhav, M. Hasan, *Density and Viscosity of Mixtures of Nitrobenzene with Methanol, Ethanol, Propan-1-ol, Propan-2-ol, Butan-1-ol, 2-Methylpropan-1-ol, and 2-Methylpropan-2-ol at 298.15 and 303.15 K.* J. Chem. Eng. Data **40** (1995) 931-934. https://doi.org/10.1021/je00020a044

[104] A.N. Prajapati, A.D. Vyas, V.A. Rana, S.P. Bhatnagar, *Dielectric relaxation and dispersion studies of mixtures of 1-propanol and benzonitrile in pure liquid state at radio and microwave frequencies.* J. Mol. Liq. **151** (2010) 12-16. https://doi.org/10.1016/j.molliq.2009.10.010

[105] T.M. Letcher, P.K. Naicker, *Excess molar enthalpies and excess molar volumes of (an alkanol + a nitrile compound) at T= 298.15 K and p= 0.1 MPa.* J. Chem. Thermodyn. **33** (2001) 1035-1047. https://doi.org/10.1006/jcht.2000.0799

[106] A. D'Aprano, I.D. Donato, *Solvent–solute interactions in moderate and high dielectric constant solvents.* J. Chem. Soc. Faraday. Trans. 1 **69** (1973) 1685-1693. https://doi.org/10.1039/F19736901685

[107] A. Sacco, A.K. Rakshit, *Thermodynamic and physical properties of binary mixtures involving sulfolane III. Excess volumes of sulfolane with each of nine alcohols.* J. Chem. Thermodyn. **7** (1975) 257-261. https://doi.org/10.1016/0021-9614(75)90063-4

[108] F. Sarmiento, M.I. Paz Andrade, J. Fernandez, R. Bravo, M. Pintos, *Excess enthalpies of 1-heptanol + n-alkane and di-n-propylamine + normal alcohol mixtures at 298.15 K.* J. Chem. Eng. Data **30** (1985) 321-323. https://doi.org/10.1021/je00041a025

[109] J. Fernandez, M.I. Paz Andrade, M. Pintos, F. Sarmiento, R. Bravo, *Excess enthalpies of (secondary amine + alcohol) at 298.15 K.* J. Chem. Thermodyn. **15** (1983) 581-584. https://doi.org/10.1016/0021-9614(83)90057-5

[110] I. Nagata, M. Sano, *Thermodynamics of associated solutions involving aniline and ethanol.* Thermochim. Acta **200** (1992) 475-488. https://doi.org/10.1016/0040-6031(92)85139-M

[111] I. Nagata, *Excess molar enthalpies of binary and ternary mixtures containing aniline and 1-propanol.* Thermochim. Acta **208** (1992) 73-82. https://doi.org/10.1016/0040-6031(92)80153-N

[112] S. Villa, *Contribución experimental y teórica al estudio de las propiedades termodinámicas de mezclas líquidas formdas por aminas y alcanos o 1-alcoholes.* Tesis Doctoral, 2003. Departamento de Física Aplicada, Facultad de Ciencias, Universidad de Valladolid.

[113] I. Alonso, I. Mozo, I.G. La Fuente, J.A. González, J.C. Cobos, *Thermodynamics of Ketone + Amine Mixtures Part V. Volumetric and Speed of Sound Data at (293.15, 298.15 and 303.15) K for Mixtures of 2-Heptanone with Aniline, N-Methylaniline or Pyridine.* J. Solution Chem. **40** (2011) 2057-2071. https://doi.org/10.1007/s10953-011-9774-3

[114] N.V. Sastry, M.K. Valand, *Densities, Speeds of Sound, Viscosities, and Relative Permittivities for 1-Propanol + and 1-Butanol + Heptane at 298.15 K and 308.15 K.* J. Chem. Eng. Data **41** (1996) 1421-1425. https://doi.org/10.1021/je960135d

[115] N.V. Sastry, M.K. Valand, *Dielectric constants, refractive indexes and polarizations for 1 - Alcohol +Heptane mixtures at 298.15 and 308.15 K.* Ber. Bunsenges. Phys. Chem. **101** (1997) 243-250. https://doi.org/10.1002/bbpc.19971010212

Chapter 6.

Conclusions

In this chapter, a brief summary of the results obtained along the Thesis is presented.

a) Amide + amine mixtures

- H_m^E, V_m^E and ε_r^E of *N,N*-dimethylformamide (DMF) or *N,N*-dimethylacetamide (DMA) + butan-1-amine (BA), + hexan-1-amine (HxA), + *N*-propylpropan-1-amine (DPA), + *N*-butylbutan-1-amine (DBA) or + aniline are fundamentally determined by dipolar interactions.
- Dipolar interactions are stronger in DMF than in DMA mixtures.
- In mixtures with linear primary or secondary amines:
  - Interactions between like molecules (especially amide-amide interactions) are dominant for H_m^E (positive values) and ε_r^E (negative values). Longer linear amines are better breakers of amide-amide interactions.
  - Amide-amine interactions are relevant, and they are stronger in HxA than in DPA mixtures. They are also more important if DMF, or shorter linear amines, are involved.
  - Structural effects are important for V_m^E (negative or small positive values).
- In mixtures with aniline, interactions between unlike molecules are dominant, especially for DMF, giving negative H_m^E and V_m^E, and positive ε_r^E for the mixture DMF + aniline.
- H_m^E and V_m^E are correctly described by the ERAS model. The theory shows that solvation is not relevant.
- The application of Kirkwood-Fröhlich model shows that parallel alignment of dipoles is diminished along mixing in relation to the ideal mixture.

b) 1-Alkanol + amine mixtures

- For mixtures with HxA, DPA, *N,N,N*-triethylamine (TEA) or cyclohexylamine (c-HxA), (1-alkanol)-amine interactions contribute positively to ε_r^E.
- For mixtures with a given amine (HxA, DPA, TEA or c-HxA) and increasing the length of the 1-alkanol, ε_r^E decreases to a minimum and then increases again. This is explained by the lower and weaker self-association of longer 1-alkanols.

- In HxA mixtures, cyclic multimers are favored and linear multimers disfavored when compared with DPA systems.
- As a general trend in mixtures with primary or secondary amines, higher solvation effects appear together with lower ε_r^E and g_K values.
- 1-alkanol + TEA mixtures behave in a different way from systems with primary or secondary amines, due to structural effects and to the effectiveness of TEA to break the 1-alkanol self-association.
- Solvation determines to a great extent the structure of the HxA, DPA, TEA or c-HxA mixtures. For methanol mixtures, $g_K(\phi_1)$ curves increase sharply for low ϕ_1 values and remain practically constant in the high ϕ_1 region.
- Cyclization (c-HxA) of a primary amine (HxA) leads to increased ε_r^E values. The effect of aromaticity (aniline) of the primary amine leads to decreased ε_r^E, due to the rupture of strong aniline-aniline interactions.

c) Orientational effects in alkanone, alkanal or dialkyl carbonate + alkane mixtures and in alkanone + alkanone or + dialkyl carbonate systems

- In systems containing ketones with the same number of C atoms and a given alkane, dipolar interactions become weaker in the sequence: aromatic > cyclic > linear.
- For a given alkane, they are also weaker in the order: dialkyl carbonate > linear alkanone > linear alkanal. The size and shape of the OCOO group has a large impact on the thermodynamic properties.
- According to the Flory model, in alkanone, alkanal or linear organic carbonate + alkane mixtures, orientational (i.e. non-random) effects are similar for linear, cyclic or aromatic polar compounds. They are also similar in alkanone or alkanal + alkane mixtures. In contrast, orientational effects become weaker in dialkyl carbonate + alkane mixtures.
- Mixtures of two alkanones show a behavior close to random mixing, and so do systems of long 2-alkanones or cyclohexanone and a dialkyl carbonate.
- Larger orientational effects are encountered in solutions of carbonates and short 2-alkanones.

d) Orientational effects in mixtures of organic carbonates and alkanes or 1-alkanols

- The considered mixtures are characterized by dipolar interactions and by interactions between like molecules.
- In systems with a given solvent, dipolar interactions become weaker in the sequence: propylene carbonate (PC) > dimethyl carbonate (DMC)> diethyl carbonate (DEC).
- (1-alkanol)-carbonate interactions are stronger in solutions with DMC, and become weaker when the alcohol size increases in systems with a given carbonate.
- Results from the Flory model show that orientational effects decrease in the order: DEC > PC > DMC. They are particularly important for mixtures with methanol or ethanol.
- In systems with DMC, orientational effects are weaker in 1-alkanol mixtures than in those containing alkanes. A similar trend appears in DEC systems for 1-alkanols longer than ethanol.

Part IV
Appendices

Appendix A.

Excess molar enthalpies of amide + amine mixtures and ERAS model results

Although at the time of writing this manuscript the experimental data and the results of the application of the model to amide + amine mixtures have not yet been published, they have been sent for publication. We will provide this part of the work in the form of the submitted manuscript.

Thermodynamics of amide + amine mixtures. 5. Excess molar enthalpies of *N,N*-dimethylformamide or *N,N*-dimethylacetamide + *N*-propylpropan-1-amine, + *N*-butylbutan-1-amine, + butan-1-amine, or + hexan-1-amine systems at 298.15 K. Application of the ERAS model

Fernando Hevia[(1)], Karine Ballerat-Busserolles[(2)], Yohann Coulier[(2)], Jean-Yves Coxam[(2)], Juan Antonio González[(1)], Isaías García de la Fuente[(1)], José Carlos Cobos[(1)]

[(1)] G.E.T.E.F., Departamento de Física Aplicada, Facultad de Ciencias, Universidad de Valladolid, Paseo de Belén, 7, 47011 Valladolid, Spain. [(2)] Institut de Chimie de Clermont Ferrand, University Clermont Auvergne, CNRS UMR 6296, SIGMA Clermont, F-63000 Clermont-Ferrand, France.

Abstract

Excess molar enthalpies, H_m^E, over the whole composition range have been determined for the liquid mixtures *N,N*-dimethylformamide (DMF) or *N,N*-dimethylacetamide (DMA) + butan-1-amine (BA), or + hexan-1-amine (HxA), or + *N*-propylpropan-1-amine (DPA), or *N*-butylbutan-1-amine (DBA) at 298.15 K and at 0.1 MPa using a BT2.15 calorimeter from Setaram adapted to work in dynamic mode at constant temperature and pressure. All the H_m^E values are positive, indicating that interactions between like molecules are predominant. The replacement of DMF by DMA in systems with a given amine leads to lower H_m^E results, which have been ascribed to stronger amide-amide interactions in DMF mixtures. The replacement of HxA by DPA in systems with a given amide leads to slightly higher H_m^E values, as interactions between unlike molecules are weaker for the latter. Structural effects in the investigated solutions are also present, since the corresponding excess molar volumes (V_m^E), previously determined, are negative or slightly positive. The systems have been characterized in terms of the ERAS model reporting the interaction parameters. The model correctly describes both H_m^E and V_m^E. The application of the model suggests that, in the systems under study, solvation effects are of minor importance and that physical interactions are dominant.

A.1. Introduction

It is well-known that a suitable approach for the investigation of the highly complex chemical environment of proteins is to study small organic molecules whose functional groups are similar to those present in the biomolecule [1]. The systematic physical and chemical characterization of such molecules and of their mixtures in terms of thermodynamic, transport and dielectric properties is necessary in this framework. The study of amide + amine systems is relevant, as it allows to gain insight into the behavior of the amide group when it is surrounded by different environments. In fact, the hydrogen-bonded structures where the amide group is involved can show very different biological activities depending on the mentioned environments [2]. On the other hand, the strong polarity of amides, which in the case of tertiary amides leads to the creation of a certain local order [3, 4], together with their high solvating capability and liquid state range –due to their ability to form hydrogen bonds– [5], makes them a very important kind of organic solvents. Similarly, amines are also an important class of substances since many biological relevant molecules contain the amine group [6-8]. In addition, the low vapor pressure of amines makes them useful in green chemistry. Thus, mixtures containing amines are being investigated to be used in CO_2 capture [9] and, interestingly, many of the ions of the technically important ionic liquids are related to amine groups [10].

In previous works, we have measured densities, speeds of sound and refractive indices of *N,N*-dimethylformamide (DMF) [11], or *N,N*-dimethylacetamide (DMA) [12] + *N*-propylpropan-1-amine (DPA) or + butan-1-amine (BA) at (293.15-303.15) K, and + *N*-butylbutan-1-amine (DBA) or + hexan-1-amine (HxA) at 298.15 K. In addition, we have reported low-frequency permittivity measurements of the mentioned systems and of the DMF + aniline mixture at (293.15-303.15) K [13, 14]. This database has been interpreted in terms of solute-solvent interactions and structural effects. We have also applied the ERAS [15] and the Kirkwood-Fröhlich models [16-19] to the study of amine + amide mixtures. The latter is useful for the calculation of the Balankina relative excess Kirkwood correlation factors [20], which provide information on the dipole correlations present in the considered systems. Calorimetric data are essential for the study of the type and strength of interactions present in liquid mixtures. As the data available in the literature on excess molar enthalpies, H_m^E, for amine + amide mixtures is scarce [21-23], we continue this series of works reporting H_m^E values for DMF or DMA + DPA, or + DBA, or + BA or + HxA systems at 298.15 K. Finally, the systems are characterized in terms of the ERAS model, revisiting the previously reported parameters which were determined using volumetric data only [14].

A.2. Experimental

A.2.1. Materials

Information about the purity and source of the pure compounds used along the experiments is collected in Table A.1. They were used without further purification. It also shows their densities (ρ) at 0.1 MPa and at 298.15 K. These results agree well with literature data.

A.2.2. Apparatus and procedure

Molar quantities were calculated using the relative atomic mass Table of 2015 issued by the Commission on Isotopic Abundances and Atomic Weights (IUPAC) [24].

Table A.1. Description, source and purity of the pure liquids and their density, ρ, at temperature $T = 298.15$ K and pressure $p = 0.1$ MPa. [b]

Chemical name	CAS number	Source	Purity[a]	ρ / g·cm^{-3}	
				Exp.	Lit.
N,*N*-dimethylformamide (DMF)	68-12-2	Sigma-Aldrich	0.9996	0.94378	0.944163 [25]
N,*N*-dimethylacetamide (DMA)	127-19-5	Honeywell	>0.999	0.93614	0.936233 [26]
N-propylpropan-1-amine (DPA)	142-84-7	Aldrich	0.999	0.73337	0.73321 [27]
N-butylbutan-1-amine (DBA)	111-92-2	Aldrich	0.997	0.75570	0.755457 [28]
butan-1-amine (BA)	109-73-9	Sigma-Aldrich	0.9978	0.73218	0.73233 [29]
hexan-1-amine (HxA)	111-26-2	Aldrich	0.999	0.76016	0.76013 [30]

[a] In mole fraction. By gas chromatography. Provided by the supplier. [b] The standard uncertainties are: $u(T) = 0.01$ K, $u(p) = 1$ kPa. The relative standard uncertainty is: $u_r(\rho) = 0.0012$.

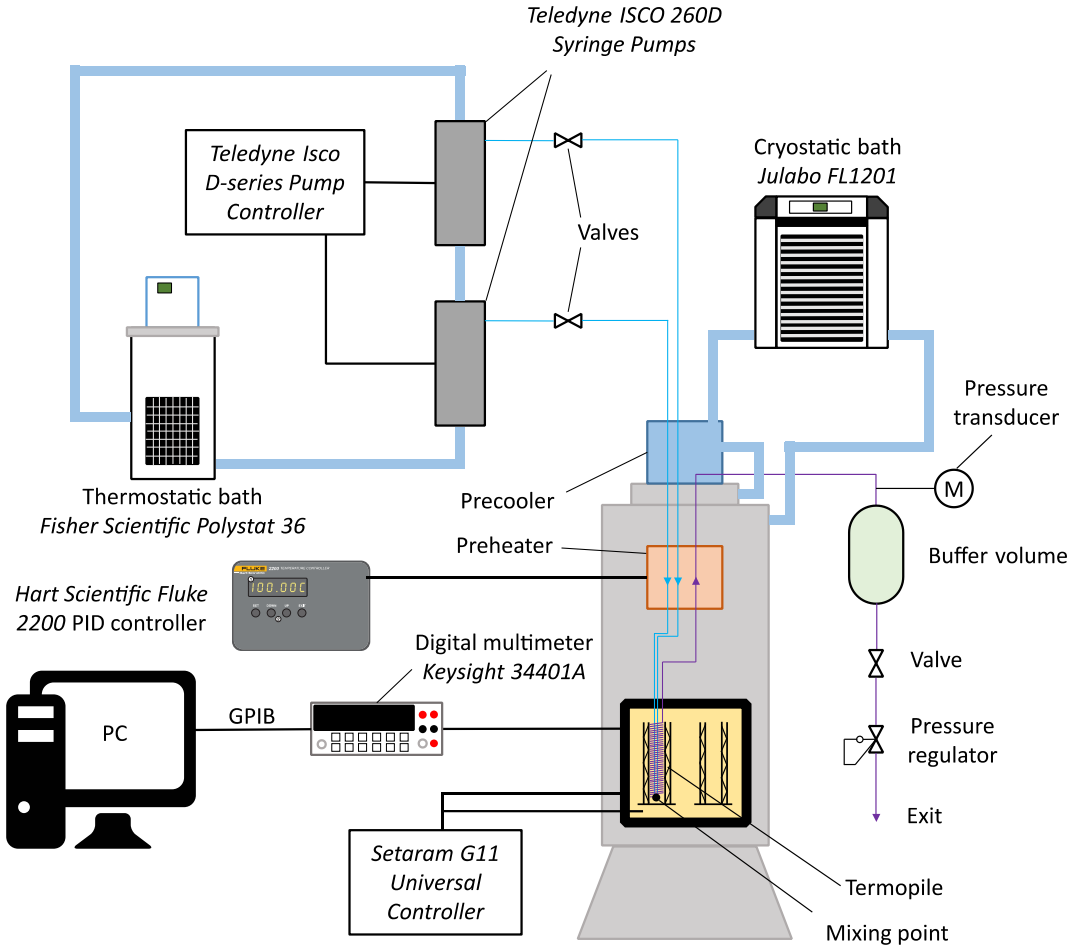

Figure A.1: Schematic view of the experimental setup used to determine excess molar enthalpies.

Densities were obtained using a vibrating-tube densimeter DMA HPM from Anton Paar. The temperature regulation of the densimetric block is insured by the use of a thermostatic bath from Julabo. The standard uncertainty in the temperature is 0.01 K. Experiments were performed at atmospheric pressure, in a static mode. The calibration was carried out using pure octane, dodecane and tridistilled water, and comparing with literature values.

The excess molar enthalpies were determined from heat of mixing measurements performed with a BT2.15 calorimeter from Setaram adapted to work in dynamic mode at constant temperature and pressure. The arrangement is depicted in Figure A.1. The fluids flow in stainless steel tubes with an external diameter of 1.6 mm and an internal diameter of 1.0 mm and mix in a custom-made cell. They are injected into the system by means of two syringe pumps model Teledyne ISCO 260 D, which are controlled by a Teledyne ISCO D-Series Pump Controller. Mixtures of different concentrations are obtained varying the volumetric flow rates given by the pumps. These flow rates can be chosen from 1 $\mu L \cdot min^{-1}$ to 25 $mL \cdot min^{-1}$ with a relative standard uncertainty of 0.5%. The capacity of the pumps is 266.05 mL, and they can be regulated up to a pressure of 52 MPa with a 2% relative standard uncertainty. To ensure the stability of the molar flow rates, the fluids are kept inside the pumps at a constant temperature of 298.15 K by means of a thermostatic bath Fisher Scientific Polystat 36, with a stability of 0.03 K. The relative standard uncertainty in the mole fraction is estimated to be 0.004. The pressure in the system is maintained constant with the help of a pressure regulator located at the end of the flow line, and the pressure relative to the atmospheric pressure is determined by a Keller transducer with a relative standard uncertainty of 0.25% of full scale (40 MPa). For the measurements in this work, the pressure regulator was open to the atmospheric pressure. The temperature of the calorimetric block is regulated by heating a cold can by means of a Setaram G11 Universal Controller. The temperature of the can is maintained constant using a circulating fluid at 10 K below the expected temperature of the experiment, using an external ultra-cryostat Julabo FL1201. The temperature of the block is then regulated using the G11 Universal Controller with a stability of 0.01 K. The temperature of the injected fluids is adjusted to the working temperature with the help of an external precooler and an internal preheater. The external precooler is situated on top of the calorimetric block and is connected in series to the cooler can of the calorimeter and to the ultra-cryostatic bath. The internal preheater is inside the calorimetric block; it supplies the necessary power to reach the exact temperature of the experiment using a heating cartridge, and its temperature is controlled by means of a platinum resistance connected to a Fluke Hart Scientific 2200 PID controller with a stability of 0.01 K. The heat flow is detected by a thermopile, generating an electromotive force (EMF) that is collected by a 6 ½ digit multimeter from Keysight model 34401A and sent to a computer through a GPIB connection. The thermopile EMF, S, is converted into the mixing enthalpy through the steady-state relation:

$$H_{\mathrm{m}}^{\mathrm{E}} = \frac{S - S_{\mathrm{BL}}}{K\left(\dot{n}_1 + \dot{n}_2\right)} \tag{A.1}$$

where K is a temperature-dependent calibration constant, $\dot{n}_i$ is the molar flow rate of component i and S_{BL} is the baseline signal, recorded when only one of the fluids is flowing. The constant K is obtained by measuring the $H_{\mathrm{m}}^{\mathrm{E}}$ of the system ethanol + water and comparing the results with reference values from Ott *et al.* [31, 32]. Taking into account uncertainties on fluid flow rates, thermopile calibration K, and calorimetric signal noises, the estimated maximum relative standard uncertainty on $H_{\mathrm{m}}^{\mathrm{E}}$ for the set of experimental points in this work is 0.03.

A.3. Results

Data on $H_{\mathrm{m}}^{\mathrm{E}}$ are listed in Table A.2. They were fitted to a Redlich-Kister equation [33] by an unweighted linear least-squares regression. The Redlich-Kister equation for the excess property F^{E} is given by:

$$F^{\mathrm{E}} = x_1 (1 - x_1) \sum_{i=0}^{k-1} A_i (2x_1 - 1)^i \tag{A.2}$$

The number, k, of necessary coefficients for this regression has been determined, for each system, by applying an F-test of additional term [34] at 99.5% confidence level. The standard deviations, $\sigma\left(F^{\mathrm{E}}\right)$, are defined by:

$$\sigma\left(F^{\mathrm{E}}\right) = \left[\frac{1}{N-k} \sum_{j=1}^{N} \left(F_{\mathrm{cal},j}^{\mathrm{E}} - F_{\mathrm{exp},j}^{\mathrm{E}} \right)^2 \right]^{1/2} \tag{A.3}$$

where the index j takes one value for each of the N data points $F_{\mathrm{exp},j}^{\mathrm{E}}$, and $F_{\mathrm{cal},j}^{\mathrm{E}}$ is the corresponding value of the excess property calculated from equation (A.2).

Excess molar energies of constant volume, $U_{\mathrm{m},V}^{\mathrm{E}}$, are given by [35]:

$$U_{\mathrm{m},V}^{\mathrm{E}} = H_{\mathrm{m}}^{\mathrm{E}} - T \frac{\alpha_p}{\kappa_T} V_{\mathrm{m}}^{\mathrm{E}} \tag{A.4}$$

where α_p is the isobaric thermal expansion coefficient, κ_T is the coefficient of isothermal compressibility and $V_{\mathrm{m}}^{\mathrm{E}}$ is the excess molar volume. The $U_{\mathrm{m},V}^{\mathrm{E}}$ curves of amide + amine systems were obtained at $\Delta x_1 = 0.05$ using smoothed values of $H_{\mathrm{m}}^{\mathrm{E}}$ and of volumetric properties previously measured [11, 12]. Let us denote by $V_{\mathrm{m},i}$, $\alpha_{p,i}$ and $C_{p,\mathrm{m},i}$ the molar volume, isobaric thermal expansion coefficient and molar isobaric heat capacity of component i respectively, and by $\phi_i = x_i V_{\mathrm{m},i} / (x_1 V_{\mathrm{m},1} + x_2 V_{\mathrm{m},2})$ the volume fraction of component i. In the application of equation (A.4), α_p was assumed ideal ($\alpha_p^{\mathrm{id}} = \phi_1 \alpha_{p,1} + \phi_2 \alpha_{p,2}$) for HxA and DBA mixtures; the error in using this assumption is negligible due to the smallness of $V_{\mathrm{m}}^{\mathrm{E}}$ for these systems and, actually, the difference $U_{\mathrm{m},V}^{\mathrm{E}} - H_{\mathrm{m}}^{\mathrm{E}}$ is not relevant. κ_T was obtained from the equation:

$$\kappa_T = \kappa_S + \frac{T V_{\mathrm{m}} \alpha_p^2}{C_{p,\mathrm{m}}} \tag{A.5}$$

with the molar isobaric heat capacity of the mixture, $C_{p,\mathrm{m}}$, taken as ideal ($C_{p,\mathrm{m}}^{\mathrm{id}} = x_1 C_{p,\mathrm{m},1} + x_2 C_{p,\mathrm{m},2}$). The $U_{\mathrm{m},V}^{\mathrm{E}}$ curves have also been adjusted to Redlich-Kister polynomials using the same procedure given above.

Table A.3 includes the parameters A_i obtained for F^{E} ($= H_{\mathrm{m}}^{\mathrm{E}}, U_{\mathrm{m},V}^{\mathrm{E}}$), together with the standard deviations $\sigma\left(F^{\mathrm{E}}\right)$. Values of $H_{\mathrm{m}}^{\mathrm{E}}$ at temperature 298.15 K are plotted in Figure A.2 Figure A.3, and their corresponding Redlich-Kister regressions in Figures A.S1 and A.S2. The corresponding $U_{\mathrm{m},V}^{\mathrm{E}}$ curves are depicted in Figures A.S3 and A.S4.

Table A.2. Excess molar enthalpies, H_m^E, of amide (1) + amine (2) liquid mixtures as functions of the mole fraction of the amide, x_1, at temperature $T = 298.15$ K and pressure $p = 0.1$ MPa. [a]

x_1	H_m^E / J·mol^{-1}	x_1	H_m^E / J·mol^{-1}	x_1	H_m^E / J·mol^{-1}	x_1	H_m^E / J·mol^{-1}
			DMF (1) + DPA (2)				
0.0358	88	0.3016	595	0.5505	753	0.7983	542
0.1002	241	0.3483	657	0.6012	743	0.8485	441
0.1512	351	0.4005	695	0.6587	708	0.8991	318
0.1984	446	0.4495	737	0.6997	673	0.9504	170
0.2504	529	0.5005	748	0.7518	613		
			DMF (1) + DBA (2)				
0.0491	188	0.3006	877	0.5505	1118	0.7994	815
0.1014	386	0.3510	956	0.5990	1098	0.8503	669
0.1488	543	0.4021	1032	0.6500	1060	0.9000	488
0.2006	680	0.4497	1082	0.6997	1001	0.9501	270
0.2482	782	0.4982	1113	0.7506	921		
			DMF (1) + BA (2)				
0.0510	89	0.2498	320	0.5008	384	0.7559	245
0.1009	166	0.3007	352	0.5463	374	0.8005	208
0.1496	226	0.3496	373	0.6008	355	0.8495	158
0.1703	247	0.4008	391	0.6463	326	0.9003	106
0.2005	279	0.4508	393	0.7011	289	0.9519	55
			DMF (1) + HxA (2)				
0.0514	118	0.3006	533	0.5505	659	0.8005	441
0.1007	219	0.3519	586	0.5982	648	0.8506	354
0.1516	318	0.4007	619	0.6507	615	0.8995	246
0.2009	394	0.4518	648	0.7002	569	0.9502	129
0.2522	461	0.5003	661	0.7503	510		
			DMA (1) + DPA (2)				
0.0597	98	0.3009	399	0.5497	519	0.8009	385
0.0996	166	0.3462	435	0.5972	509	0.8504	318
0.1496	235	0.4062	477	0.6495	493	0.8989	239
0.2011	300	0.4491	495	0.6975	473	0.9368	156
0.2497	358	0.5035	514	0.7478	437	0.9507	126
			DMA (1) + DBA (2)				
0.0499	150	0.3002	673	0.5507	832	0.8004	618
0.0976	276	0.3526	732	0.6007	825	0.8512	508
0.1510	405	0.3983	774	0.6477	803	0.9019	371
0.1969	503	0.4472	807	0.6968	756	0.9507	203
0.2472	590	0.5007	833	0.7481	698		

			DMA (1) + BA (2)				
0.0498	48	0.3004	189	0.5509	201	0.9002	64
0.0992	89	0.3493	202	0.6005	195	0.9594	27
0.1518	123	0.4015	207	0.7008	160		
0.1985	152	0.4508	209	0.7995	120		
0.2512	165	0.5005	208	0.8502	94		
			DMA (1) + HxA (2)				
0.0509	71	0.3018	338	0.5493	424	0.7996	296
0.1005	141	0.3484	369	0.6002	416	0.8513	238
0.1507	196	0.3980	402	0.6492	401	0.9008	171
0.1994	244	0.4502	419	0.7001	375	0.9503	91
0.2488	295	0.5006	423	0.7491	341		

[a] The standard uncertainties are: $u(T) = 0.01$ K, $u(p) = 1$ kPa. The relative standard uncertainty is: $u_r(x_1) = 0.004$. The relative combined expanded uncertainty (0.95 level of confidence) is $U_{rc}\left(H_m^E\right) = 0.06$.

Table A.3. Coefficients A_i and standard deviations, $\sigma\left(F^E\right)$ (equation (A.3)), for the representation of F^E at temperature $T = 298.15$ K and pressure $p = 0.1$ MPa for amide + amine liquid mixtures by equation (A.2).

Property F^E	System	A_0	A_1	A_2	A_3	$\sigma\left(F^E\right)$
H_m^E / J·mol^{-1}	DMF + DPA	2999	476	178		4
	DMF + DBA	4410	731	634		7
	DMF + BA	1545	–374	–75		1.9
	DMF + HxA	2639	238	–93		4
	DMA + DPA	2038	444	274		4
	DMA + DBA	3314	476	544	255	2
	DMA + BA	834	–158			3
	DMA + HxA	1699	234			3
$U_{m,V}^E$ / J·mol^{-1}	DMF + DPA	3408	657	338		0.7
	DMF + DBA	4385.4	841	758		0.5
	DMF + BA	1954.3	–193	45		0.4
	DMF + HxA	2669.7	376			0.7
	DMA + DPA	2359.7	457	368		0.4
	DMA + DBA	3237.3	436	532	250	0.3
	DMA + BA	1131	–59	93		0.3
	DMA + HxA	1690	269	31		0.6

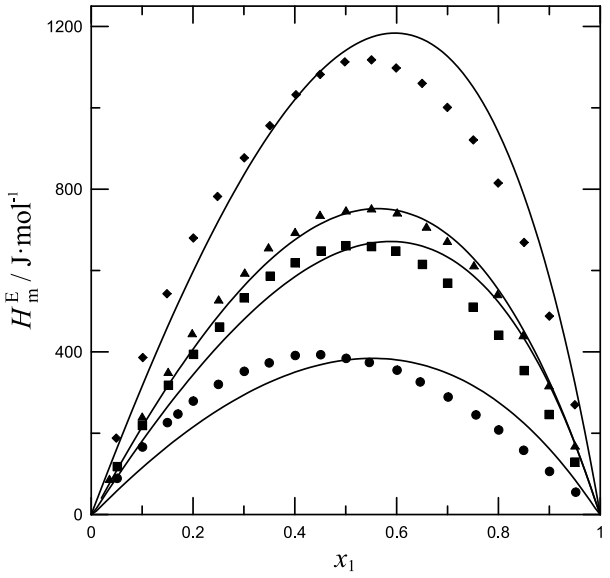

Figure A.2: Excess molar enthalpies, H^E_m, of DMF (1) + amine (2) liquid mixtures at 0.1 MPa and 298.15 K. Full symbols, experimental values (this work): (●), BA; (■), HxA; (▲), DPA; (♦), DBA. Solid lines, ERAS results using interaction parameters listed in Table A.4.

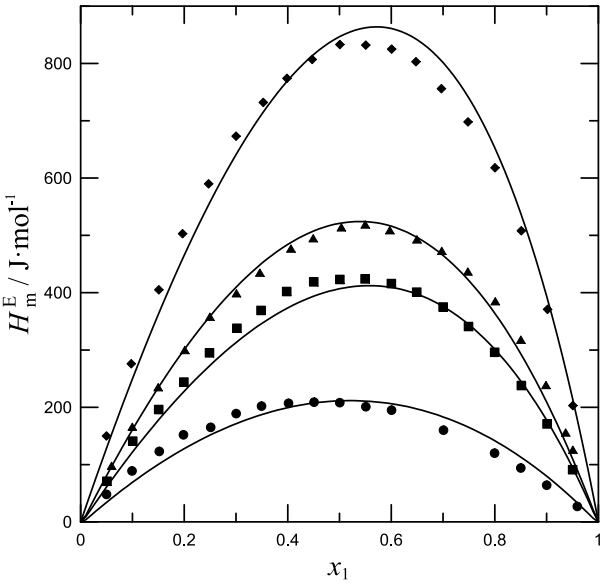

Figure A.3: Excess molar enthalpies, H^E_m, of DMA (1) + amine (2) liquid mixtures at 0.1 MPa and 298.15 K. Full symbols, experimental values (this work): (●), BA; (■), HxA; (▲), DPA; (♦), DBA. Solid lines, ERAS results using interaction parameters listed in Table A.4.

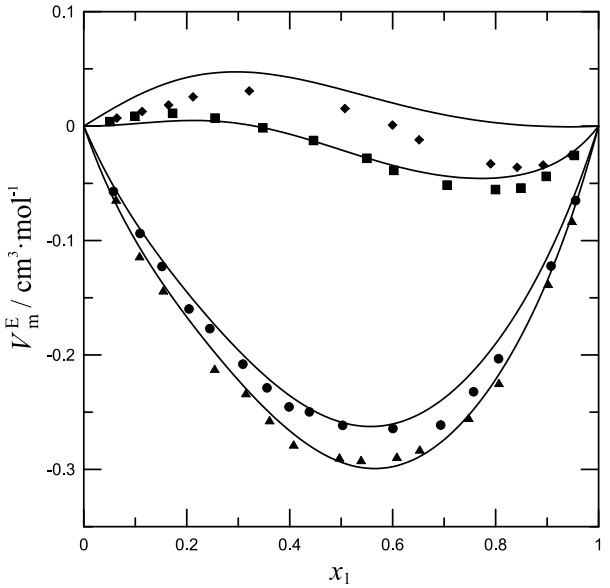

Figure A.4: Excess molar volumes, V^E_m, of DMF (1) + amine (2) liquid mixtures at 0.1 MPa and 298.15 K. Full symbols, experimental values [11]: (●), BA; (■), HxA; (▲), DPA; (♦), DBA. Solid lines, ERAS results using interaction parameters listed in Table A.4.

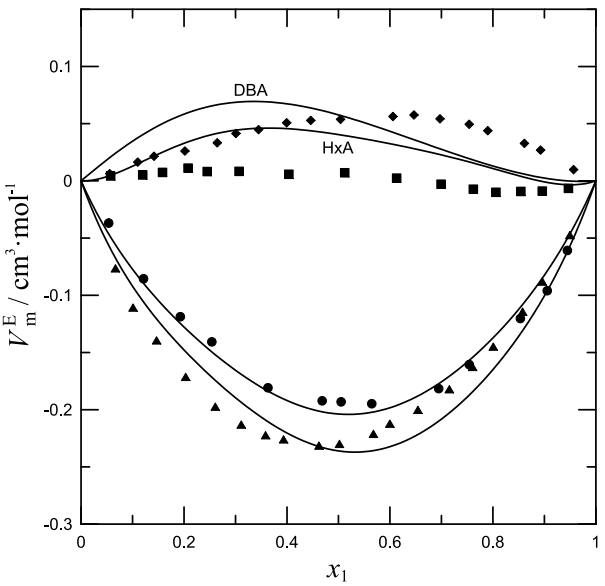

Figure A.5: Excess molar volumes, V^E_m, of DMA (1) + amine (2) liquid mixtures at 0.1 MPa and 298.15 K. Full symbols, experimental values [12]: (●), BA; (■), HxA; (▲), DPA; (♦), DBA. Solid lines, ERAS results using interaction parameters listed in Table A.4.

A.4. ERAS model

The Extended Real Associated Solution (ERAS) model [15, 36] combines the Real Association Solution Model [37-40] with Flory's thermal equation of state [41-45]. Some important features of this model are now given. (i) The excess molar functions of enthalpy and volume ($F_{\mathrm{m}}^{\mathrm{E}} = H_{\mathrm{m}}^{\mathrm{E}}$, $V_{\mathrm{m}}^{\mathrm{E}}$) are calculated as the sum of two contributions. The chemical contribution, $F_{\mathrm{m,chem}}^{\mathrm{E}}$, arises from hydrogen bonding; the physical contribution, $F_{\mathrm{m,phys}}^{\mathrm{E}}$, is related to nonpolar Van der Waals interactions and free volume effects. Expressions for the molar excess functions $H_{\mathrm{m}}^{\mathrm{E}}$ and $V_{\mathrm{m}}^{\mathrm{E}}$ can be found elsewhere [46, 47]. (ii) It is assumed that only consecutive linear association occurs. Accordingly, self-association is described by a chemical equilibrium constant (K_{A}) independent of the chain length of the self-associated species A (in this case, amines), according to the equation:

$$\mathrm{A}_m + \mathrm{A} \xleftrightarrow{K_{\mathrm{A}}} \mathrm{A}_{m+1} \tag{A.6}$$

with m ranging from 1 to ∞. The cross-association between a self-associated species A_m and a non self-associated compound B (in this study, tertiary amides) is represented by

$$\mathrm{A}_m + \mathrm{B} \xleftrightarrow{K_{\mathrm{AB}}} \mathrm{A}_m\mathrm{B} \tag{A.7}$$

where cross-association constants, K_{AB}, are also considered to be independent of the chain length. The molar enthalpies of intermolecular hydrogen-bonding for these two kinds of reactions, $\Delta h_{\mathrm{A}}^{*}$ and $\Delta h_{\mathrm{AB}}^{*}$, are introduced, and the corresponding equilibrium constants depend on temperature according to them and the Van't Hoff equation. Moreover, negative molar hydrogen-bonding volumes, $\Delta v_{\mathrm{A}}^{*}$ and $\Delta v_{\mathrm{AB}}^{*}$, are defined in order to take into account the decrease of the core volume of the molecules upon multimer formation. (iii) The $F_{\mathrm{m,phys}}^{\mathrm{E}}$ term is derived from the Flory's equation of state [41-45], which is assumed to be valid not only for pure compounds but also for the mixture [48, 49]:

$$\frac{\overline{p}_i \overline{V}_i}{\overline{T}_i} = \frac{\overline{V}_i^{1/3}}{\overline{V}_i^{1/3} - 1} - \frac{1}{\overline{V}_i \overline{T}_i} \tag{A.8}$$

where i = A, B or M (mixture). In equation (A.8), $\overline{V}_i = V_{\mathrm{m},i} \big/ V_{\mathrm{m},i}^{*}$; $\overline{p}_i = p \big/ p_i^{*}$; $\overline{T}_i = T \big/ T_i^{*}$ are the reduced properties for volume, pressure and temperature, respectively. The pure component reduction parameters ($V_{\mathrm{m},i}^{*}, p_i^{*}, T_i^{*}$) are obtained from p-V-T data (density, isobaric thermal expansion coefficient, and coefficient of isothermal compressibility) and association parameters [48, 49]. The reduction parameters for the mixture p_{M}^{*} and T_{M}^{*} are calculated from mixing rules [48, 49]. The total relative molecular volumes and surfaces of the compounds were calculated additively on the basis of the group volumes and surfaces recommended by Bondi [50].

A.4.1. Adjustment of ERAS parameters

Values of $V_{\mathrm{m},i}$, $V_{\mathrm{m},i}^{*}$ and p_i^{*} of pure compounds [51-53] at T = 298.15 K, needed for calculations, are listed in Table A.S1 of supplementary material. K_{A}, $\Delta h_{\mathrm{A}}^{*}$, and $\Delta v_{\mathrm{A}}^{*}$ of the self-associated amines are known from $H_{\mathrm{m}}^{\mathrm{E}}$ and $V_{\mathrm{m}}^{\mathrm{E}}$ data for the corresponding mixtures with

alkanes [51-53], and are also collected in Table A.S1. The binary parameters to be fitted against H_m^E and V_m^E [11, 12] data of amine + amide systems are then K_{AB}, Δh_{AB}^*, Δv_{AB}^* and X_{AB}. They are collected in Table A.4.

Table A.4. ERAS parameters for amine (A) + DMF (B) or + DMA (B) liquid mixtures at temperature 298.15 K and pressure 0.1 MPa. K_{AB}, association constant of component A with component B; Δh_{AB}^*, association enthalpy of component A with component B; Δv_{AB}^*, association volume of component A with component B; X_{AB}, physical parameter.

System	K_{AB}	Δh_{AB}^* / kJ·mol^{-1}	Δv_{AB}^* / cm^3·mol^{-1}	X_{AB} / J·cm^{-3}
BA + DMF	1.3	–9	–3.5	24.5
HxA + DMF	1	–9	–4.6	36.0
BA + DMA	1.3	–9	–2.5	13.4
HxA + DMA	1	–9	–2.8	23.3
DPA + DMF	1	–2	–2.5	23.8
DBA + DMF	1	–2	–3.8	47.8
DPA + DMA	1	–2	–1.2	15.0
DBA + DMA	1	–2	–2.2	35.1

Table A.5. Excess molar enthalpies (H_m^E) and volumes (V_m^E) at equimolar composition, temperature 298.15 K and pressure 0.1 MPa, of amine (A) + DMF (B) or DMA (B) liquid mixtures, and standard deviations $\sigma\left(H_m^E\right)$.

System	N	H_m^E / J·mol^{-1}		$\sigma\left(H_m^E\right)$ / J·mol^{-1}		V_m^E / cm^3·mol^{-1}	
		Exp.	ERAS	Exp.[a]	ERAS[b]	Exp.[c]	ERAS
BA + DMF	20	386	380	1.9	50	–0.263	–0.258
HxA + DMF	19	660	651	4	51	–0.021	–0.021
BA + DMA	17	744	740	4	22	–0.289	–0.293
HxA + DMA	19	1102	1137	7	79	0.018	0.020
DPA + DMF	19	208	211	3	16	–0.194	–0.203
DBA + DMF	19	425	407	3	16	0.006	0.040
DPA + DMA	20	509	521	4	13	–0.228	–0.235
DBA + DMA	19	828	842	2	32	0.055	0.046

[a] Obtained from equation (A.3). [b] Defined as: $\sigma\left(H_m^E\right)=\left[\frac{1}{N}\sum_{j=1}^{N}\left(F_{ERAS,j}^E-F_{exp,j}^E\right)^2\right]^{1/2}$, with notation similar to equation (A.3). [c] References: [11] for DMF mixtures, [12] for DMA systems.

A.5. Discussion

We are referring throughout this section to values of the excess functions and of the thermophysical properties at 298.15 K and at $x_1 = 0.5$, except otherwise specified.

As previously mentioned, DMF and DMA are very polar substances since their dipole moment is 3.7 D [54, 55]. Consequently, their alkane mixtures show immiscibility gaps up to rather high temperatures. Thus, systems formed by DMF and heptane or hexadecane have upper critical solution temperatures (UCST) of 342.55 K [56] and 385.15 K [57] respectively, and the UCST of the DMA + heptane mixture is 309.40 K [58].

Primary and secondary amines are self-associated compounds [36, 51, 52, 59, 60] with lower dipole moments than tertiary amides: 1.3 D (BA) [61], 1.3 D (HxA) [54], 1.0 D (DPA) [61], and 1.1 D (DBA) [61]. For heptane solutions, H_m^E/J·mol^{-1} = 1192 (BA) [62], 962 (HxA) [62], 424 (DPA) [63], and 317 (DBA) [63]. We note that H_m^E results are larger for systems with primary amines, and that they decrease with the chain length of the amine. Therefore, these values can be interpreted as arising from the rupture of interactions between like molecules in the mixing process.

Our H_m^E/J·mol^{-1} values obtained for amide + amine systems are also positive. We have H_m^E(DMF)/J·mol^{-1} = 386 (BA), 660 (HxA), 750 (DPA), 1103 (DBA); and H_m^E(DMA)/J·mol^{-1} = 209 (BA), 425 (HxA), 510 (DPA), and 829 (DBA). They can be ascribed to the dominance of contributions from the breaking of amide-amide and amine-amine interactions over that related to the formation of interactions between unlike molecules. Note that H_m^E values of the DMA + cyclohexane mixture are much higher than those of DMA + linear amine systems (Figure A.S2). The same trend is observed, e.g., when H_m^E results are compared for BA + heptane and *N,N*-dialkylamide systems (Figures A.S1 and A.S2). For a fixed amide and along both series of primary or secondary linear amines, H_m^E becomes larger when the chain length of the amine is longer. This suggests that the lower contribution from the breaking of amine-amine interactions in longer amines is overcompensated by the higher contributions which arise from: i) the larger number of amide-amide interactions broken by longer amines; and ii) the lower number and weaker amide-amine interactions created when longer amines are involved, since then the amine group is more sterically hindered.

For a fixed amine, the replacement of DMF by DMA leads to decreased H_m^E values. The difference in size between both amides suggests that the contribution from the disruption of amine-amine interactions should be higher for DMA mixtures. However, the amide group is less sterically hindered in DMF, and we recognize that, in pure state, DMF-DMF interactions are stronger than those between DMA molecules. In fact (see above), UCST(DMF + heptane) > UCST(DMA + heptane). This is also supported by calculations on entropy changes under the action of an electrostatic field and by the application of the Kirkwood-Fröhlich model [14]. Therefore, we can conclude that the breaking of DMF-DMF interactions contributes more positively to H_m^E than the disruption of DMA-DMA interactions, and that the formation of interactions between unlike molecules should contribute more negatively to H_m^E in the case of DMF systems. The mentioned trend suggests that the variation of the contribution of amide-amide interactions is predominant over the other two. The same phenomenon is encountered in

2-alkanone + amine mixtures when the chain length of the 2-alkanone is increased. For example, H_m^E(DPA) / J·mol^{-1} = 648 (propanone), 398 (butanone), 281 (2-pentanone) and 161 (2-heptanone) [64].

Interestingly, the replacement of HxA by DPA in systems involving a given amide leads to slightly higher H_m^E values. This can be explained taking into account that, since the amine group is less sterically hindered in HxA, a higher number of interactions between unlike molecules is formed in solutions with this amine and that such interactions are also stronger. It should be noted that the opposite trend is encountered for HxA or DPA + heptane mixtures, and that the difference H_m^E(HxA)– H_m^E(DPA) for these systems is remarkably higher than that for the corresponding amide solutions: 438 (*n*-heptane); –90 (DMF) and –85 (DMA) (all values in J·mol^{-1}). This underlines the relevance of amide-amine interactions in the studied solutions, which had already been mentioned [11, 12]. The previous statement could seem somewhat hasty, since the difference between H_m^E values for amide + HxA or + DPA solutions is rather low. In order to reinforce it, let us remove equation-of-state effects from H_m^E by the calculation of $U_{m,V}^E$ (equation (A.4)), retaining only interactional contributions. For our mixtures, $U_{m,V}^E$ /J·mol^{-1} = 489 (DMF + BA), 667 (DMF + HxA), 852 (DMF + DPA), and 1096 (DMF + DBA); 283 (DMA + BA), 423 (DMA + HxA), 590 (DMA + DPA), and 809 (DMA + DBA). The difference between $U_{m,V}^E$ values of amide + HxA or + DPA solutions is approximately twice the corresponding difference between their H_m^E results. This supports our previous discussion on the importance of amide-amine interactions. Eventually, let us point out the large and negative value of the H_m^E of the system *N*-methylacetamide + HxA (–1000 J·mol^{-1}, T = 363.15 K) [23], for which the formation of amide-amine interactions is dominant by far.

The excess molar volumes, V_m^E/cm^3·mol^{-1}, of the considered mixtures are either negative or small and positive [11, 12]: –0.263 (DMF + BA), –0.021 (DMF + HxA), –0.289 (DMF + DPA), and 0.018 (DMF+DBA); –0.194 (DMA + BA), 0.006 (DMA + HxA), –0.228 (DMA + DPA), and 0.055 (DMA + DBA). It is to be noted that H_m^E and V_m^E change in line, which reveals that the interactional contribution to V_m^E is relevant. However, positive H_m^E values together with negative V_m^E results are indicative of the existence of structural effects [65]. Similar structural effects are also encountered in amine + *n*-alkane systems; for example, see the low value of V_m^E / cm^3·mol^{-1} in DBA + heptane, 0.0675 (DBA) [66], and the negative one of the DBA + hexane system, –0.1854 cm^3·mol^{-1} [67].

Mixtures of DMF or DMA with aniline contrast drastically with those of linear primary or secondary amines. The dipole moment of aniline (1.51 D [55]) is higher than that of linear primary and secondary amines, and proximity effects between the phenyl ring and the amine group lead to strong dipolar interactions between aniline molecules. As a consequence, aniline + *n*-alkane mixtures are characterized by relatively high UCST (343.11 K for the heptane solution [68]). When aniline molecules are mixed with DMF or DMA molecules, very strong interactions between unlike molecules are created, and we have H_m^E /J·mol^{-1} = − 2946 (DMF + aniline) [21]; − 352 (DMA + aniline) [22]. Similarly, large differences are also encountered between values of the excess relative permittivity for the DMF + linear primary or secondary amine or + aniline mixtures [13, 14]: –0.864 (DMF + BA), –1.262 (DMF + HxA), –1.372 (DMF + DPA), –1.733

(DMF + DBA), 1.806 (DMF + aniline). It must be observed that H_m^E values are very different for DMF and DMA + aniline systems, newly remarking that interactions between unlike molecules are much more relevant in DMF systems. The rather large and negative V_m^E / cm^3·mol^{-1} results for the mentioned aniline solutions (–0.6615 (DMF + aniline) [69] and –0.6092 (DMA + aniline, T = 303.15 K) [70]) are in agreement with the H_m^E values and underline the importance of the interactional contribution to V_m^E.

A.5.1. ERAS results

Results from ERAS are collected in Table A.5 and are shown graphically in Figure A.2–Figure A.5. Both excess functions, H_m^E and V_m^E, are reasonably well represented by the model. Larger differences for V_m^E results are encountered for mixtures characterized by low V_m^E values, as then the overall result is obtained from the difference of two large magnitudes of different sign: the positive physical contribution and the negative chemical contribution.

The low K_{AB} and $\left|\Delta h_{AB}^*\right|$ values (Table A.4) indicate that solvation effects are not relevant and that the enthalpy of the H bonds between unlike molecules is weak. The large X_{AB} values (Table A.4) reveal that the physical contribution is important, particularly with regards to H_m^E. The present ERAS parameters largely differ from those determined for 1-alkanol + linear primary or secondary amine systems, which are characterized by strong solvation effects and, in consequence, by large K_{AB} and Δh_{AB}^* values and low X_{AB} values. For example, for the 1-hexanol + HxA mixture at 298.15 K: K_{AB} = 800; Δh_{AB}^* = –36 kJ·mol^{-1}; X_{AB} = 5 J·cm^{-3} [47]. As we have pointed out (see above), aniline-amide interactions are rather strong and, accordingly, the corresponding ERAS parameters are also very different. We have: K_{AB} = 70 (DMF); 2.2 (DMA); Δh_{AB}^* /kJ·mol^{-1} = –22 (DMF; DMA); Δv_{AB}^* /cm^3·mol^{-1} = –11.1 (DMF); –20 (DMA); X_{AB} /J·cm^{-3} = 4 (DMF); 3.2 (DMA) [14]. On the other hand, we note that ERAS results on H_m^E are, as an average, better for DMA systems (Table A.5). This suggests that, in such a case, physical interactions are more properly described by the model, that is, dipolar interactions are more relevant in DMF mixtures, particularly in the BA solution.

A.6. Conclusions

Excess molar enthalpies of amide (DMF or DMA) + linear primary or secondary amine (BA, HxA, DPA or DBA) have been reported at T = 298.15 K and p = 0.1 MPa. The positive H_m^E values arise from the dominant contribution from the rupture of amide-amide and amine-amine interactions along mixing. Dipolar interactions are stronger in DMF systems. DMA mixtures show lower H_m^E values for a fixed amine, suggesting that the variation of the rupture of amide-amide interactions is the predominant effect. Results on H_m^E and $U_{m,V}^E$ reveal that interactions between unlike molecules are stronger in mixtures containing HxA compared to those with DPA for a given amide. Negative or small positive V_m^E values point to the existence of important structural effects in the investigated solutions. The binary interaction parameters of the ERAS model have been adjusted to fit H_m^E and V_m^E curves simultaneously, and these properties are

represented with a rather good degree of approximation. The results from the model suggest that physical interactions are important when calculating the excess functions of the mixtures under study.

A.7. Supplementary material

Table A.S1. ERAS parameters[a] for pure liquids at temperature 298.15 K and pressure 0.1 MPa.

Compound	$V_{m,i}$ /cm^3·mol^{-1}	K_i	Δh_i^* /kJ·mol^{-1}	Δv_i^* /cm^3·mol^{-1}	$V_{m,i}^*$ /cm^3 ·mol^{-1}	p_i^* /J·cm^{-3}
BA[b]	99.89	0.96	–13.2	–2.8	77.59	565.7
HxA[b]	133.11	0.78	–13.2	–2.8	106.87	495.0
DPA[c]	138.07	0.55	–7.5	–2.8	106.50	526.0
DBA[c]	171.03	0.16	–4.5	–2.8	135.86	466.2
DMF[d]	77.44	0	0	0	62.07	714.1
DMA[d]	93.04	0	0	0	75.56	649.5

[a] $V_{m,i}$, molar volume; K_i, equilibrium constant; $V_{m,i}^*$ and p_i^*, reduction parameters for volume and pressure, respectively; Δh_i^*, hydrogen-bonding enthalpy; Δv_i^*, self-association volume; [b] Ref. [51]; [c] Ref. [52]; [d] [53].

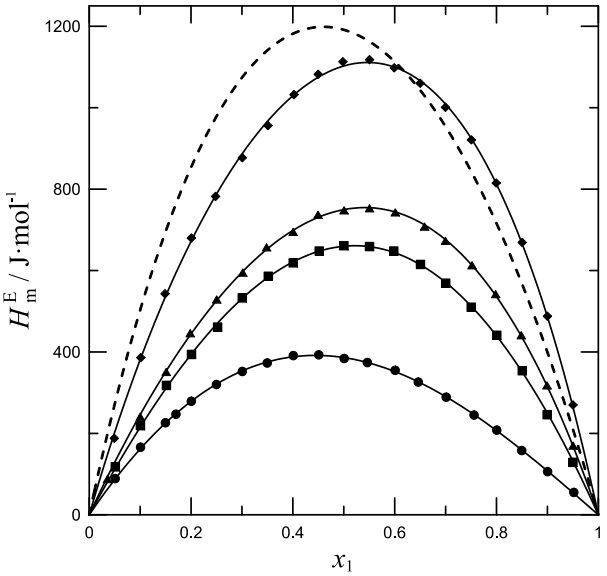

Figure A.S1: Excess molar enthalpies, H_m^E, of DMF (1) + amine (2), or BA (1) + heptane (2) liquid mixtures at 0.1 MPa and 298.15 K. Full symbols, DMF (1) + amine (2) experimental values (this work): (●), BA; (■), HxA; (▲), DPA; (♦), DBA. Solid lines, calculations with equation (A.2) using the coefficients from Table A.3. Dashed line, BA (1) + heptane (2) [62].

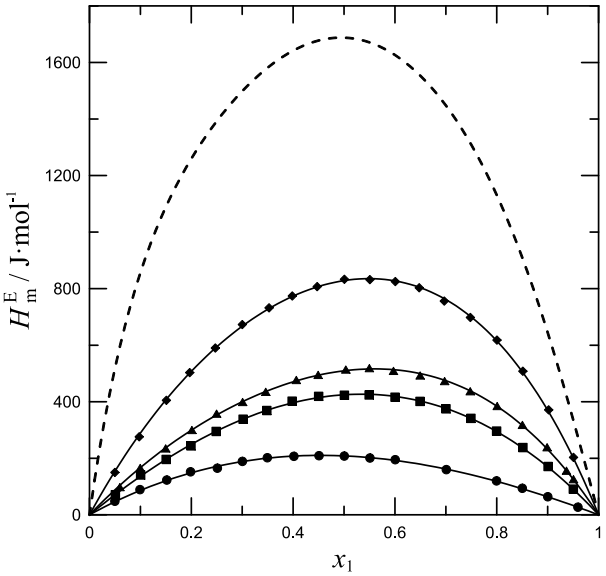

Figure A.S2: Excess molar enthalpies, H_m^E, of DMA (1) + amine (2), or + cyclohexane (2) liquid mixtures at 0.1 MPa and 298.15 K. Full symbols, DMA (1) + amine (2) experimental values (this work): (●), BA; (■), HxA; (▲), DPA; (♦), DBA. Solid lines, calculations with equation (A.2) using the coefficients from Table A.3. Dashed line, DMA (1) + cyclohexane (2) [71].

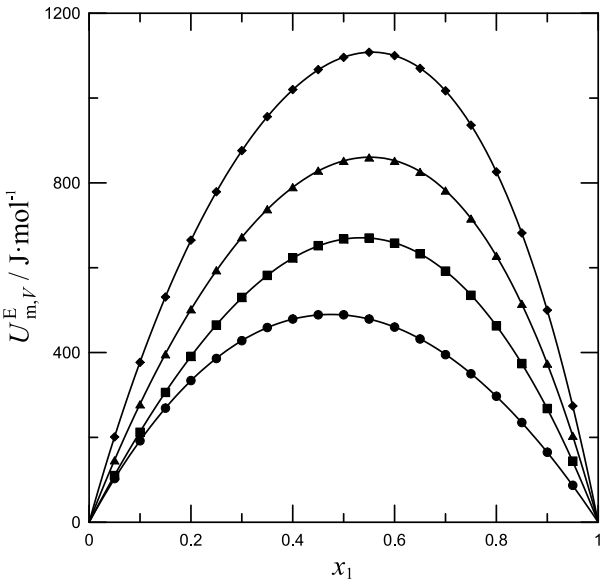

Figure A.S3: Excess molar energies at constant volume, $U^{E}_{m,V}$, of DMF (1) + amine (2) liquid mixtures at 0.1 MPa and 298.15 K. Full symbols, calculations at $\Delta x_1 = 0.05$ from smoothed experimental values: (●), BA; (■), HxA; (▲), DPA; (♦), DBA. Solid lines, calculations with equation (A.2) using the coefficients from Table A.3.

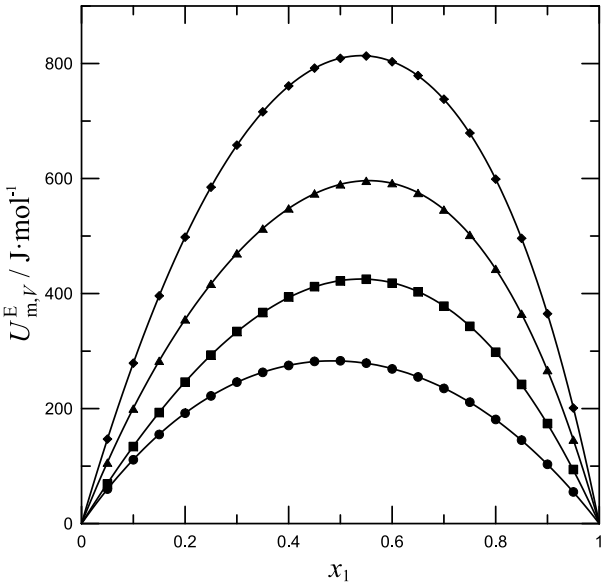

Figure A.S4: Excess molar energies at constant volume, $U^{E}_{m,V}$, of DMA (1) + amine (2) liquid mixtures at 0.1 MPa and 298.15 K. Full symbols, calculations at $\Delta x_1 = 0.05$ from smoothed experimental values: (●), BA; (■), HxA; (▲), DPA; (♦), DBA. Solid lines, calculations with equation (A.2) using the coefficients from Table A.3.

A.8. Acknowledgements

F. Hevia is grateful to J.-Y. Coxam and K. Ballerat-Busserolles for the opportunity to do the experimental part of this work at their laboratory at *Institut de Chimie de Clermont-Ferrand*, and also acknowledges *Ministerio de Educación, Cultura y Deporte* for the grant FPU14/04104 and for the complementary grants EST16/00824 and EST17/00292.

A.9. References

[1] E.S. Eberhardt, R.T. Raines, *Amide-Amide and Amide-Water Hydrogen Bonds: Implications for Protein Folding and Stability.* J. Am. Chem. Soc. **116** (1994) 2149-2150. https://doi.org/10.1021/ja00084a067

[2] T.W. Whitfield, G.J. Martyna, S. Allison, S.P. Bates, H. Vass, J. Crain, *Structure and Hydrogen Bonding in Neat N-Methylacetamide: Classical Molecular Dynamics and Raman Spectroscopy Studies of a Liquid of Peptidic Fragments.* J. Phys. Chem. B **110** (2006) 3624-3637. https://doi.org/10.1021/jp053140+

[3] J.A. Gonzalez, J.C. Cobos, I. García de la Fuente, *Thermodynamics of liquid mixtures containing a very strongly polar compound: Part 6. DISQUAC characterization of N,N-dialkylamides.* Fluid Phase Equilib. **224** (2004) 169-183. https://doi.org/10.1016/j.fluid.2004.02.007

[4] J. Barthel, R. Buchner, B. Wurm, *The dynamics of liquid formamide, N-methylformamide, N,N-dimethylformamide, and N,N-dimethylacetamide. A dielectric relaxation study.* J. Mol. Liq. **98** (2002) 51-69. https://doi.org/10.1016/S0167-7322(01)00309-9

[5] W.L. Jorgensen, C.J. Swenson, *Optimized intermolecular potential functions for amides and peptides. Structure and properties of liquid amides.* J. Am. Chem. Soc. **107** (1985) 569-578. https://doi.org/10.1021/ja00289a008

[6] F.F. Liew, T. Hasegawa, M. Fukuda, E. Nakata, T. Morii, *Construction of dopamine sensors by using fluorescent ribonucleopeptide complexes.* Bioorg. Med. Chem. **19** (2011) 4473-4481. https://doi.org/10.1016/j.bmc.2011.06.031

[7] J.M. Sonner, R.S. Cantor, *Molecular Mechanisms of Drug Action: An Emerging View.* Annu. Rev. Biophys. **42** (2013) 143-167. https://doi.org/10.1146/annurev-biophys-083012-130341

[8] D.L. Nelson, M.M. Cox, *Lehninger Principles of Biochemistry.* 3rd ed., Worth Publishing, New York, 2000.

[9] Y. Coulier, A. Lowe, P.R. Tremaine, J.Y. Coxam, K. Ballerat-Busserolles, *Absorption of CO2 in aqueous solutions of 2-methylpiperidine: Heats of solution and modeling.* Int. J. Greenh. Gas Control **47** (2016) 322-329. https://doi.org/10.1016/j.ijggc.2016.02.009

[10] M. Götz, R. Reimert, S. Bajohr, H. Schnetzer, J. Wimberg, T.J.S. Schubert, *Long-term thermal stability of selected ionic liquids in nitrogen and hydrogen atmosphere.* Thermochim. Acta **600** (2015) 82-88. https://doi.org/10.1016/j.tca.2014.11.005

[11] F. Hevia, A. Cobos, J.A. González, I. García de la Fuente, L.F. Sanz, *Thermodynamics of Amide + Amine Mixtures. 1. Volumetric, Speed of Sound, and Refractive Index Data for N,N-Dimethylformamide + N-Propylpropan-1-amine, + N-Butylbutan-1-amine, + Butan-1-amine, or + Hexan-1-amine Systems at Several Temperatures.* J. Chem. Eng. Data **61** (2016) 1468-1478. https://doi.org/10.1021/acs.jced.5b00802

[12] F. Hevia, A. Cobos, J.A. González, I.G. de la Fuente, V. Alonso, *Thermodynamics of Amide + Amine Mixtures. 2. Volumetric, Speed of Sound and Refractive Index Data for N,N-Dimethylacetamide + N-Propylpropan-1-Amine, + N-Butylbutan-1-Amine, + Butan-1-Amine, or + Hexan-1-Amine Systems at Several Temperatures.* J. Solution Chem. **46** (2017) 150-174. https://doi.org/10.1007/s10953-016-0560-0

[13] F. Hevia, J.A. González, I. García de la Fuente, L.F. Sanz, J.C. Cobos, *Thermodynamics of amide + amine mixtures. 3. Relative permittivities of N,N-dimethylformamide + N-propylpropan-1-amine, + N-butylbutan-1-amine, + butan-1-amine, or + hexan-1-amine systems at several temperatures.* J. Mol. Liq. **238** (2017) 440-446. https://doi.org/10.1016/j.molliq.2017.05.025

[14] F. Hevia, J.A. González, A. Cobos, I. García de la Fuente, L.F. Sanz, *Thermodynamics of amide + amine mixtures. 4. Relative permittivities of N,N-dimethylacetamide + N-propylpropan-1-amine, + N-butylbutan-1-amine, + butan-1-amine, or + hexan-1-amine systems and of N,N-dimethylformamide + aniline mixture at several temperatures. Characterization of amine + amide systems using ERAS.* J. Chem. Thermodyn. **118** (2018) 175-187. https://doi.org/10.1016/j.jct.2017.11.011

[15] A. Heintz, *A New Theoretical Approach for Predicting Excess Properties of Alkanol/Alkane Mixtures.* Ber. Bunsenges. Phys. Chem. **89** (1985) 172-181. https://doi.org/10.1002/bbpc.19850890217

[16] H. Fröhlich, *Theory of Dielectrics.* Clarendon Press, Oxford, 1958.

[17] C. Moreau, G. Douhéret, *Thermodynamic and physical behaviour of water + acetonitrile mixtures. Dielectric properties.* J. Chem. Thermodyn. **8** (1976) 403-410. https://doi.org/10.1016/0021-9614(76)90060-4

[18] P. Bordewijk, *On the derivation of the Kirkwood-Fröhlich equation.* Physica **69** (1973) 422-432.

[19] A. Chelkowski, *Dielectric Physics.* Elsevier, Amsterdam, 1980.

[20] J.C.R. Reis, T.P. Iglesias, *Kirkwood correlation factors in liquid mixtures from an extended Onsager-Kirkwood-Frohlich equation.* Phys. Chem. Chem. Phys. **13** (2011) 10670-10680. https://doi.org/10.1039/C1CP20142E

[21] R.S. Ramadevi, P. Venkatesu, M.V. Prabhakara Rao, M.R. Krishna, *Excess enthalpies of binary mixtures of N,N-dimethylformamide with substituted benzenes at 298.15 K.* Fluid Phase Equilib. **114** (1996) 189-197. https://doi.org/10.1016/0378-3812(95)02816-1

[22] G. Chandra Sekhar, M.V. Prabhakara Rao, D.H.L. Prasad, Y.V.L. Ravi Kumar, *Excess molar enthalpies of N,N-dimethylacetamide with substituted benzenes at 298.15 K.* Thermochim. Acta **402** (2003) 99-103. https://doi.org/10.1016/S0040-6031(02)00542-7

[23] A.B. de Haan, J. Gmehling, *Excess Enthalpies for Various Binary Mixtures with N-Methylacetamide or Acetic Anhydride.* J. Chem. Eng. Data **41** (1996) 474-478. https://doi.org/10.1021/je950294h

[24] CIAAW, *Atomic weights of the elements 2015.* ciaaw.org/atomic-weights.htm (accessed 2015)

[25] D. Keshapolla, V. Singh, R.L. Gardas, *Volumetric, acoustic and transport properties of binary mixtures of benzyldimethylammonium based ionic liquids with N,N-dimethylformamide at temperature from 293.15 to 328.15 K.* J. Mol. Liq. **199** (2014) 330-338. https://doi.org/10.1016/j.molliq.2014.09.030

[26] J. Krakowiak, H. Koziel, W. Grzybkowski, *Apparent molar volumes of divalent transition metal perchlorates and chlorides in N,N-dimethylacetamide.* J. Mol. Liq. **118** (2005) 57-65. https://doi.org/10.1016/j.molliq.2004.07.013

[27] F. Sarmiento, M.I. Paz Andrade, J. Fernandez, R. Bravo, M. Pintos, *Excess enthalpies of 1-heptanol + n-alkane and di-n-propylamine + normal alcohol mixtures at 298.15 K.* J. Chem. Eng. Data **30** (1985) 321-323. https://doi.org/10.1021/je00041a025

[28] I. Alonso, I. Mozo, I.G. de la fuente, J.A. González, J.C. Cobos, *Thermodynamics of ketone + amine mixtures Part IV. Volumetric and speed of sound data at (293.15; 298.15 and 303.15 K) for 2-butanone +dipropylamine, +dibutylamine or +triethylamine systems.* Thermochim. Acta **512** (2011) 86-92. https://doi.org/10.1016/j.tca.2010.09.004

[29] S.S. Bittencourt, R.B. Torres, *Volumetric properties of binary mixtures of (acetonitrile + amines) at several temperatures with application of the ERAS model.* J. Chem. Thermodyn. **93** (2016) 222-241. https://doi.org/10.1016/j.jct.2015.09.002

[30] P. Góralski, M. Wasiak, A. Bald, *Heat Capacities, Speeds of Sound, and Isothermal Compressibilities of Some n-Amines and Tri-n-amines at 298.15 K.* J. Chem. Eng. Data **47** (2002) 83-86. https://doi.org/10.1021/je010206v

[31] J.B. Ott, C.E. Stouffer, G.V. Cornett, B.F. Woodfield, R.C. Wirthlin, J.J. Christensen, U.K. Deiters, *Excess enthalpies for (ethanol + water) at 298.15 K and pressures of 0.4, 5, 10, and 15 MPa.* J. Chem. Thermodyn. **18** (1986) 1-12. https://doi.org/10.1016/0021-9614(86)90036-4

[32] J.B. Ott, G.V. Cornett, C.E. Stouffer, B.F. Woodfield, C. Guanquan, J.J. Christensen, *Excess enthalpies of (ethanol+water) at 323.15, 333.15, 348.15, and 373.15 K and from*

0.4 to 15 MPa. J. Chem. Thermodyn. **18** (1986) 867-875. https://doi.org/10.1016/0021-9614(86)90121-7

[33] O. Redlich, A.T. Kister, *Algebraic Representation of Thermodynamic Properties and the Classification of Solutions.* Ind. & Eng. Chem. **40** (1948) 345-348. https://doi.org/10.1021/ie50458a036

[34] P.R. Bevington, D.K. Robinson, *Data Reduction and Error Analysis for the Physical Sciences.* McGraw-Hill, New York, 2000.

[35] J.S. Rowlinson, F.L. Swinton, *Liquids and Liquid Mixtures.* 3rd Edition, Butterworths, G. B., 1982.

[36] H. Funke, M. Wetzel, A. Heintz, *New applications of the ERAS model. Thermodynamics of amine + alkane and alcohol + amine mixtures.* Pure Appl. Chem. **61** (1989) 1429-1439. https://doi.org/10.1351/pac198961081429

[37] C.B. Kretschmer, R. Wiebe, *Thermodynamics of Alcohol - Hydrocarbon Mixtures.* J. Chem. Phys. **22** (1954) 1697-1701. https://doi.org/10.1063/1.1739878

[38] H. Renon, J.M. Prausnitz, *On the thermodynamics of alcohol-hydrocarbon solutions.* Chem. Eng. Sci. **22** (1967) 299-307. https://doi.org/10.1016/0009-2509(67)80116-7

[39] H.V. Kehiaian, Bull. Acad. Pol. Sci. **16** (1968) 165.

[40] H.V. Kehiaian, A. Treszczanowicz, Bull. Acad. Pol. Sci. **16** (1968) 171.

[41] P.J. Flory, R.A. Orwoll, A. Vrij, *Statistical Thermodynamics of Chain Molecule Liquids. I. An Equation of State for Normal Paraffin Hydrocarbons.* J. Am. Chem. Soc. **86** (1964) 3507-3514. https://doi.org/10.1021/ja01071a023

[42] P.J. Flory, R.A. Orwoll, A. Vrij, *Statistical Thermodynamics of Chain Molecule Liquids. II. Liquid Mixtures of Normal Paraffin Hydrocarbons.* J. Am. Chem. Soc. **86** (1964) 3515-3520. https://doi.org/10.1021/ja01071a024

[43] P.J. Flory, *Statistical Thermodynamics of Liquid Mixtures.* J. Am. Chem. Soc. **87** (1965) 1833-1838. https://doi.org/10.1021/ja01087a002

[44] A. Abe, P.J. Flory, *The Thermodynamic Properties of Mixtures of Small, Nonpolar Molecules.* J. Am. Chem. Soc. **87** (1965) 1838-1846. https://doi.org/10.1021/ja01087a003

[45] R.A. Orwoll, P.J. Flory, *Thermodynamic properties of binary mixtures of n-alkanes.* J. Am. Chem. Soc. **89** (1967) 6822-6829. https://doi.org/10.1021/ja01002a003

[46] J.A. González, S. Villa, N. Riesco, I. García de la Fuente, J.C. Cobos, *Thermodynamics of mixtures containing alkoxyethanols: Part XVII — ERAS characterization of alkoxyethanol + alkane systems.* Can. J. Chem. **81** (2003) 319-329. https://doi.org/10.1139/v03-063

[47] J.A. González, I. García de la Fuente, J.C. Cobos, *Thermodynamics of mixtures with strongly negative deviations from Raoult's Law: Part 4. Application of the DISQUAC model to mixtures of 1-alkanols with primary or secondary linear amines. Comparison with Dortmund UNIFAC and ERAS results.* Fluid Phase Equilib. **168** (2000) 31-58. https://doi.org/10.1016/S0378-3812(99)00326-X

[48] A. Heintz, P.K. Naicker, S.P. Verevkin, R. Pfestorf, *Thermodynamics of alkanol + amine mixtures. Experimental results and ERAS model calculations of the heat of mixing.* Ber. Bunsenges. Phys. Chem. **102** (1998) 953-959. https://doi.org/10.1002/bbpc.19981020707

[49] A. Heintz, D. Papaioannou, *Excess enthalpies of alcohol+amine mixtures. Experimental results and theoretical description using the ERAS-model.* Thermochim. Acta **310** (1998) 69-76. https://doi.org/10.1016/S0040-6031(97)00224-4

[50] A. Bondi, *Physical Properties of Molecular Crystals, Liquids and Glasses.* Wiley, New York, 1968.

[51] S. Villa, N. Riesco, I. García de la Fuente, J.A. González, J.C. Cobos, *Thermodynamics of mixtures with strongly negative deviations from Raoult's law. Part 8. Excess molar volumes at 298.15 K for 1-alkanol + isomeric amine (C6H15N) systems: Characterization in terms of the ERAS model.* Fluid Phase Equilib. **216** (2004) 123-133. https://doi.org/10.1016/j.fluid.2003.10.008

[52] S. Villa, J.A. González, I.G. De La Fuente, N. Riesco, J.C. Cobos, *Thermodynamics of Organic Mixtures Containing Amines. II. Excess Molar Volumes at 25°C for Methylbutylamine + Alkane Systems and Eras Characterization of Linear Secondary Amine + Alkane Mixtures.* J. Solution Chem. **31** (2002) 1019-1038. https://doi.org/10.1023/A:1021881627444

[53] J.A. Gonzalez, U. Domanska, J. Lachwa, *Thermodynamics of Binary Mixtures Containing a Very Strongly Polar Compound. 7. Isothermal VLE Measurements for NMP + 2-Propanol or + 2-Butanol Systems. DISQUAC and ERAS Characterization of NMP or N,N-Dialkylamide + 2-Alkanol Mixtures. Comparison with Results from Dortmund UNIFAC.* Ind. Eng. Chem. Res. **44** (2005) 5795-5804. https://doi.org/10.1021/ie0580046

[54] A.L. McClellan, *Tables of Experimental Dipole Moments.* Vols. 1,2,3, Rahara Enterprises, El Cerrito, US, 1974.

[55] J.A. Riddick, W.B. Bunger, T.K. Sakano, *Organic solvents: physical properties and methods of purification.* Wiley, New York, 1986.

[56] J. Lobos, I. Mozo, M. Fernández Regúlez, J.A. González, I. García de la Fuente, J.C. Cobos, *Thermodynamics of Mixtures Containing a Strongly Polar Compound. 8. Liquid−Liquid Equilibria for N,N-Dialkylamide + Selected N-Alkanes.* J. Chem. Eng. Data **51** (2006) 623-627. https://doi.org/10.1021/je050428j

[57] M. Rogalski, R. Stryjek, *Mutual solubility of binary n-hexadecane and polar compound systems.* Bull. Acad. Pol. Sci., Ser. Sci. Chim. **28** (1980) 139-147.

[58] X. An, H. Zhao, F. Jiang, W. Shen, *The (liquid + liquid) critical phenomena of (a polar liquid + an n-alkane) V. Coexistence curves of (N,N-dimethylacetamide + heptane).* J. Chem. Thermodyn. **28** (1996) 1221-1232. https://doi.org/10.1006/jcht.1996.0109

[59] J.A. González, I. Mozo, I. García de la Fuente, J.C. Cobos, *Thermodynamics of organic mixtures containing amines. IV. Systems with aniline.* Can. J. Chem. **83** (2005) 1812-1825. https://doi.org/10.1139/v05-190

[60] J.A. González, L.F. Sanz, I. García De La Fuente, J.C. Cobos, *Thermodynamics of mixtures containing amines: XIII. Application of the ERAS model to cyclic amine + alkane mixtures.* Thermochim. Acta **573** (2013) 229-236. https://doi.org/10.1016/j.tca.2013.09.033

[61] R.C. Reid, J.M. Prausnitz, B.E. Poling, *The Properties of Gases and Liquids.* McGraw-Hill, New York, US, 1987.

[62] E. Matteoli, L. Lepori, A. Spanedda, *Thermodynamic study of heptane + amine mixtures: I. Excess and solvation enthalpies at 298.15 K.* Fluid Phase Equilib. **212** (2003) 41-52. https://doi.org/10.1016/S0378-3812(03)00260-7

[63] E. Matteoli, P. Gianni, L. Lepori, *Thermodynamic study of heptane + secondary, tertiary and cyclic amines mixtures. Part IV. Excess and solvation enthalpies at 298.15 K.* Fluid Phase Equilib. **306** (2011) 234-241. https://doi.org/10.1016/j.fluid.2011.04.013

[64] J.A. González, I. Alonso, I. García De La Fuente, J.C. Cobos, *Thermodynamics of ketone + amine mixtures. Part IX. Excess molar enthalpies at 298.15 K for dipropylamine, or dibutylamine + 2-alkanone systems and modeling of linear or aromatic amine + 2-alkanone mixtures in terms of DISQUAC and ERAS.* Fluid Phase Equilib. **343** (2013) 1-12. https://doi.org/10.1016/j.fluid.2013.01.011

[65] L. Lepori, P. Gianni, E. Matteoli, *The Effect of the Molecular Size and Shape on the Volume Behavior of Binary Liquid Mixtures. Branched and Cyclic Alkanes in Heptane at 298.15 K.* J. Solution Chem. **42** (2013) 1263-1304. https://doi.org/10.1007/s10953-013-0023-9

[66] L. Lepori, P. Gianni, A. Spanedda, E. Matteoli, *Thermodynamic study of (heptane + amine) mixtures. III: Excess and partial molar volumes in mixtures with secondary, tertiary, and cyclic amines at 298.15 K.* J. Chem. Thermodyn. **43** (2011) 1453-1462. https://doi.org/10.1016/j.jct.2011.04.017

[67] T.M. Letcher, *Thermodynamics of aliphatic amine mixtures I. The excess volumes of mixing for primary, secondary, and tertiary aliphatic amines with benzene and substituted benzene compounds.* J. Chem. Thermodyn. **4** (1972) 159-173. https://doi.org/10.1016/S0021-9614(72)80021-1

[68] H. Matsuda, K. Ochi, K. Kojima, *Determination and Correlation of LLE and SLE Data for the Methanol + Cyclohexane, Aniline + Heptane, and Phenol + Hexane System.* J. Chem. Eng. Data **48** (2003) 184-189. https://doi.org/10.1021/je020156+

[69] H.J. Noh, S.J. Park, S.J. In, *Excess molar volumes and deviations of refractive indices at 298.15 K for binary and ternary mixtures with pyridine or aniline or quinoline.* J. Ind. Eng. Chem. **16** (2010) 200-206. https://doi.org/10.1016/j.jiec.2010.01.038

[70] G. Chandrasekhar, P. Venkatesu, M.V. Prabhakara Rao, *Excess Volumes and Ultrasonic Studies of n,n-Dimethyl Acetamide with Substituted Benzenes at 303.15 k.* Phys. Chem. Liq. **40** (2002) 181-189. https://doi.org/10.1080/00319100208086661

[71] H. Ukibe, R. Tanaka, S. Murakami, R. Fujishiro, *Excess enthalpies of N,N-dialkyl amides + cyclohexane, + benzene, and + toluene at 298.15 K.* J. Chem. Thermodyn. **6** (1974) 201-206. https://doi.org/10.1016/0021-9614(74)90263-8

Appendix B.

Dielectric and refractive properties of 1-alkanol + *N,N,N*-triethylamine mixtures and Kirkwood-Fröhlich results

As in Appendix A, this appendix will be dedicated to a manuscript already submitted for publication. In this case, it is related to the dielectric and refractive properties of 1-alkanol + *N,N,N*-triethylamine liquid mixtures and the results of applying the Kirkwood-Fröhlich model for their interpretation.

Thermodynamics of mixtures with strongly negative deviations from Raoult's law. XVII. Permittivities and refractive indices for 1-alkanol + *N,N,N*-triethylamine systems at (293.15-303.15) K. Application of the Kirkwood-Fröhlich model

Fernando Hevia, Juan Antonio González, Ana Cobos, Isaías García de la Fuente, Luis Felipe Sanz

G.E.T.E.F., Departamento de Física Aplicada, Facultad de Ciencias, Universidad de Valladolid, Paseo de Belén, 7, 47011 Valladolid, Spain.

Abstract

Relative permittivities at 1 MHz, ε_r, at 0.1 MPa and (293.15-303.15) K and refractive indices, n_D, at similar conditions have been measured for the 1-alkanol (methanol, 1-propanol, 1-butanol, 1-pentanol or 1-heptanol)+ *N,N,N*-triethylamine (TEA) systems. Positive values of the excess permittivities, ε_r^E, are encountered for the methanol system at high alcohol concentrations. The remaining mixtures are characterized by negative ε_r^E values over the whole composition range. At ϕ_l (volume fraction) = 0.5, ε_r^E changes in the order: methanol > 1-propanol > 1-butanol < 1-pentanol < 1-heptanol. Mixtures formed by 1-alkanol and an isomeric amine, hexan-1-amine (HxA) or *N*-propylpropan-1-amine (DPA) or cyclohexylamine, behave similarly. This has been explained in terms of the lower and weaker self-association of longer 1-alkanols. From the permittivity data, it is shown that: (i) (1-alkanol)-TEA interactions contribute positively to ε_r^E; (ii) TEA is an effective breaker of the network of the 1-alkanols; (iii) structural effects, which are very important for the volumetric and calorimetric data of 1-alkanol + TEA systems, are also relevant when evaluating dielectric data. This is confirmed by the comparison of ε_r^E measurements for 1-alkanol + aliphatic amine mixtures; (iv) the aromaticity effect (i.e., the replacement of TEA by pyridine in systems with a given 1-alkanol) leads to an increase of the mixture polarization. Calculations conducted in the framework of the Kirkwood-Fröhlich model are consistent with the previous statements.

B.1. Introduction

1-Alkanol + linear primary or secondary amine mixtures are characterized by showing strongly negative deviations from Raoult's law [1]. As a consequence, their excess molar Gibbs energies, G_m^E, and enthalpies, H_m^E, are both negative, the former even at rather high temperatures. For example, for the methanol + butan-1-amine mixture at equimolar composition, G_m^E = –799 J·mol^{-1} (T = 348.15 K) [2] and H_m^E = –3767 J.mol^{-1} (T = 298.15 K) [3]. On the other hand, this type of solutions is characterized by large solvation effects. In fact, the equilibrium constants, K_{AB}, related to the formation of linear chains of the type $A_n(1-\text{alkanol}) + B_m(\text{linear amine}) \rightleftarrows A_nB_m$, calculated by means of the ERAS model [1, 4], are rather large and the corresponding enthalpies of hydrogen bonds between 1-alkanol and amine, Δh_{AB}^*, are large and negative [1, 5-8], and the same occurs for Δv_{AB}^*, the association volume of component A with B. Thus, for the methanol + hexan-1-amine (HxA) system, K_{AB} = 2500 (T = 298.15 K); Δh_{AB}^* = –42.4 kJ·mol^{-1}; Δv_{AB}^* = 9.1 cm^3·mol^{-1} [5]. Interestingly, Δh_{AB}^* values are lower than those related to the H-bonds between 1-alkanol molecules (–25.1 kJ·mol^{-1} [1, 3, 4]). That is, (1-alkanol)-amine interactions are stronger than those between molecules of 1-alkanol, which explains the large and negative H_m^E values observed for these systems. Hereafter, we are referring, except when indicated, to excess molar functions at equimolar composition and 298.15 K.

1-Alkanol + *N,N,N*-triethylamine (TEA) mixtures are somewhat different. Some of their most relevant features are the following. (i) G_m^E values are usually positive: 284 J·mol^{-1} for the methanol-containing mixture (T = 303.2 K) [9]; (ii) H_m^E values are negative but lower in absolute value than for 1-alkanol + linear primary or secondary amine systems: –1871 J·mol^{-1} [10], and –1520 J·mol^{-1} [11] for the solutions with methanol, or ethanol, respectively; (iii) Results on V_m^E, excess molar volume, are much more negative than for the systems with the isomeric amines HxA or *N*-propylpropan-1-amine (DPA). For example, V_m^E(1-propanol)/cm^3·mol^{-1} = –1.147 (HxA) [5]; –1.550 (DPA) [7]; –1.997 (TEA) [5]. This has been explained in terms of strong structural effects in systems with TEA, which lead to excess molar internal energies at constant volume (–846 J·mol^{-1} for the 1-propanol + TEA mixture [5]) which largely differ from the corresponding H_m^E results (–1413 J·mol^{-1} [12]).

We have investigated in detail 1-alkanol + amine systems by means of different models [1, 5-8, 13-16]: DISQUAC [17, 18], ERAS [1, 3], the concentration-concentration structure factor, $S_{CC}(0)$ [19, 20], or the Kirkwood-Buff formalism [21]. In addition, we have reported data on V_m^E [5, 7, 8], vapor-liquid equilibria [22] or viscosity [23-25]. More recently, we have determined permittivities, ε_r, and refractive indices, n_D, for 1-alkanol + cyclohexylamine [26], or + HxA [27], or + DPA [28] mixtures. As a continuation, and in order to investigate the influence of the shape of TEA molecules on dielectric properties, here we provide ε_r and n_D measurements for methanol, or 1-propanol, or 1-butanol, or 1-pentanol, or 1-heptanol + TEA systems at (293.15-303.15) K. In addition, and as in previous applications [26-28], the ε_r and n_D results are used to investigate the systems using the Kirkwood-Fröhlich theory [29-32].

This type of studies is relevant for a better understanding of non-covalent interactions, i.e. hydrogen bonding. Hydrogen bonding leads to cooperative effects which are crucial in

supramolecular chemistry and biochemistry [33, 34]. Thus, such effects are essential for the characterization of association of molecules in the condensed phase [35, 36] or of the DNA molecule [37]. Mixtures with amines are of particular interest, since the disruption of amino acids releases amines and proteins that are usually bound to DNA polymers contain several amine groups [38]. They are also used for CO_2 capture [39]. Finally, we remark that many of the ions of the technically important ionic liquids include amine groups [40].

B.2. Experimental

B.2.1. Materials

Pure compounds were used in the experiments without further purification. Information about their source and purity is shown in Table B.1. Their ε_r at 1 MHz, density (ρ) and n_D at the working temperatures and their dipole moments (μ) are collected in Table B.2. Comparison with literature values reveals a good agreement.

Table B.1. Sample description.

Chemical name	CAS Number	Source	Purification method	Purity[a]
methanol	67-56-1	Sigma-Aldrich	none	0.9999
1-propanol	71-23-8	Sigma-Aldrich	none	0.9984
1-butanol	71-36-3	Sigma-Aldrich	none	0.9986
1-pentanol	71-41-0	Sigma-Aldrich	none	0.999
1-heptanol	111-70-6	Sigma-Aldrich	none	0.998
N,N,N-triethylamine (TEA)	121-44-8	Sigma-Aldrich	none	0.9999

[a] In mole fraction. By gas chromatography. Provided by the supplier.

B.2.2. Apparatus and procedure

Binary mixtures were prepared by mass in small vessels of about 10 cm^3 using an analytical balance Sartorius MSU125p (weighing accuracy 0.01 mg), correcting the weighings for buoyancy effects. The standard uncertainty in the mole fraction is 0.0010. Molar quantities were calculated using the relative atomic mass Table of 2015 issued by the Commission on Isotopic Abundances and Atomic Weights (IUPAC) [41]. Pure liquids were stored with 4 Å molecular sieves (except methanol, because measurements were affected) in order to minimize the effects of the interaction with air components. The measurement cell (see below) was completely filled with the samples and appropriately closed to avoid their evaporation. The density of the pure compounds was measured along the experiments, remaining constant within the experimental uncertainty.

Temperatures were measured with Pt-100 resistances calibrated according to the ITS-90 scale of temperature, using the triple point of water and the melting point of Ga as reference points. The standard uncertainty of this quantity is 0.01 K for ρ measurements, and 0.02 K for ε_r and n_D measurements.

Table B.2. Dipole moment, μ, of the pure liquids, and their relative permittivity at frequency $\nu = 1$ MHz, ε_r^*, refractive index at the sodium D-line, n_D^*, and density, ρ^*, at temperature T and pressure p = 0.1 MPa. [a]

Compound	μ / D	T/K	ε_r^*		n_D^*		ρ^* / g·cm^{-3}	
			Exp.	Lit.	Exp.	Lit.	Exp.	Lit.
methanol	1.664 [42]	293.15	33.576	33.61 [43]	1.32863	1.32859 [44]	0.79163	0.7916 [45]
								0.791400 [46]
		298.15	32.624	32.62 [43]	1.32649	1.32652 [47]	0.78695	0.7869 [48]
								0.786884 [49]
		303.15	31.684	31.66 [43]	1.32435	1.32457 [50]	0.78222	0.782158 [49]
						1.32410 [51]		
1-propanol	1.629 [42]	293.15	21.150	21.15 [52]	1.38511	1.38512 [53]	0.80366	0.80361 [54]
		298.15	20.469	20.42 [52]	1.38306	1.38307 [51]	0.79968	0.79960 [54]
		303.15	19.799	19.75 [52]	1.38099	1.38104 [51]	0.79566	0.79561 [54]
1-butanol	1.614 [42]	293.15	18.201	18.19 [52]	1.39929	1.3993 [55]	0.80985	0.80982 [56]
								0.8098 [57]
		298.15	17.566	17.53 [52]	1.39730	1.397336 [58]	0.80606	0.80606 [56]
		303.15	16.942	16.89 [52]	1.39529	1.3953 [59]	0.80222	0.8022 [57]
1-pentanol	1.598 [42]	293.15	15.689	15.63 [43]	1.40993	1.40986 [51]	0.81466	0.81468 [60]
		298.15	15.110	15.08 [61]	1.40794	1.40789 [51]	0.81103	0.81103 [60]
		303.15	14.537	14.44 [43]	1.40592	1.40592 [62]	0.80735	0.81737 [60]
1-heptanol	1.583 [42]	293.15	12.005	11.54 [63]	1.42433	1.42433 [64]	0.82237	0.8223 [65]
		298.15	11.504	11.45 [61]	1.42236	1.42240 [64]	0.81890	0.81881 [66]
		303.15	11.013	11.07 [67]	1.42041	1.42047 [62]	0.81537	0.8153 [65]
						1.42048 [64]		
TEA	0.66 [68]	293.15	2.440	2.43 [69]	1.40044	1.40040 [72]	0.72738	0.7266 [69]
				2.450 [70]		1.1004 [69]		0.7276 [74]
				2.46 [71]		1.400333 [73]		
		298.15	2.419	2.42 [71]	1.39775	1.39825 [72]	0.72276	0.72306 [74]
				2.404 [75]		1.3983 [76]		
		303.15	2.398	2.387 [75]	1.39503	1.39555 [72]	0.71811	0.7179 [77]
				2.41 [71]		1.3955 [76]		

[a] The standard uncertainties are: $u(T) = 0.02$ K (for ρ^* measurements, $u(T) = 0.02$ K); $u(p) = 1$ kPa; $u(\nu) = 20$ Hz; $u(n_D^*) = 0.00008$. The relative standard uncertainties are: $u_r(\rho^*) = 0.0012$, $u_r(\varepsilon_r^*) = 0.003$.

A RFM970 refractometer from Bellingham + Stanley was used for the experimental n_D determination. This device exploits the optical detection of the critical angle at the wavelength of the sodium D line (589.3 nm). A temperature stability of 0.02 K is guaranteed by Peltier modules. The calibration of the refractometer was performed using 2,2,4-trimethylpentane and

toluene at (293.15 – 303.15) K, following the recommendations by Marsh [78]. The standard uncertainty of n_D is 0.00008.

Densities were obtained using a vibrating-tube densimeter and sound analyzer Anton Paar DSA 5000, which is automatically thermostated within 0.01 K. The calibration procedure has been described elsewhere [79]. The relative standard uncertainty of the ρ measurements is 0.0012.

The experimental device to determine ε_r consists of a 16452A cell –parallel-plate capacitor made of Nickel-plated cobalt (54% Fe, 17% Co, 29% Ni) with a ceramic insulator (alumina, Al_2O_3)–, which is filled with a sample volume of ≈ 4.8 cm^3 and connected by a 16048G test lead to a precision impedance analyzer 4294A, all of them from Agilent. The cell is immersed in a thermostatic bath LAUDA RE304, with a temperature stability of 0.02 K. Details about the equipment configuration and calibration are given elsewhere [80]. The relative standard uncertainty of the ε_r measurements (i.e. the repeatability) is 0.0001. The total relative standard uncertainty of ε_r was estimated to be 0.003 from the differences between our data and values available in the literature, in the range of temperature (288.15 – 333.15) K, for the following pure liquids: water, benzene, cyclohexane, hexane, nonane, decane, dimethyl carbonate, diethyl carbonate, methanol, 1-propanol, 1-pentanol, 1-hexanol, 1-heptanol, 1-octanol, 1-nonanol and 1-decanol.

B.3. Results

The volume fraction of component i, ϕ_i, is calculated as $\phi_i = x_i V_{mi}^* / \left(x_1 V_{m1}^* + x_2 V_{m2}^*\right)$, where x_i is the mole fraction of component i and V_{mi}^* is its molar volume. The derivative $\left(\partial\varepsilon_r / \partial T\right)_p$ was calculated at 298.15 K as the slope of a linear regression of experimental ε_r values in the range (293.15 – 303.15) K. For an ideal mixture at the same temperature and pressure as the mixture under study, the relative permittivity, ε_r^{id}, the derivative $\left[\left(\partial\varepsilon_r / \partial T\right)_p\right]^{id}$, and the refractive index, n_D^{id}, are given by [81, 82]:

$$\varepsilon_r^{id} = \phi_1 \varepsilon_{r1}^* + \phi_2 \varepsilon_{r2}^* \tag{B.1}$$

$$n_D^{id} = \left[\phi_1 \left(n_{D1}^*\right)^2 + \phi_2 \left(n_{D2}^*\right)^2\right]^{1/2} \tag{B.2}$$

$$\left[\left(\frac{\partial\varepsilon_r}{\partial T}\right)_p\right]^{id} = \left(\frac{\partial\varepsilon_r^{id}}{\partial T}\right)_p \tag{B.3}$$

where ε_{ri}^* and n_{Di}^* denote the relative permittivity and the refractive index of pure species i, and $\left(\partial\varepsilon_r^{id} / \partial T\right)_p$ is calculated from linear regressions as already mentioned. The corresponding excess functions, F^E, are calculated from these according to the equation:

$$F^E = F - F^{id} \qquad , \qquad F = \varepsilon_r,\ n_D,\ \left(\frac{\partial\varepsilon_r}{\partial T}\right)_p \tag{B.4}$$

Table B.3 collects ϕ_1, ε_r and ε_r^E values of 1-alkanol (1) + TEA (2) systems as functions of x_1, in the temperature range (293.15 – 303.15) K. Table B.4 contains the experimental x_1, ϕ_1, n_D and n_D^E values at the same conditions. The data of $\left[\left(\partial\varepsilon_r/\partial T\right)_p\right]^E = \left(\partial\varepsilon_r^E/\partial T\right)_p$ at 298.15 K are collected in Table B.S1 (supplementary material).

The F^E data were fitted to a Redlich-Kister equation [83] by unweighted linear least-squares regressions:

$$F^E = x_1(1-x_1)\sum_{i=0}^{k-1} A_i (2x_1-1)^i \tag{B.5}$$

The number, k, of appropriate coefficients for each system, property and temperature has been determined by the application of an F-test of additional term [84] at a 99.5% confidence level. Table B.5 includes the parameters A_i obtained, and the standard deviations, $\sigma\left(F^E\right)$, defined by:

$$\sigma\left(F^E\right) = \left[\frac{1}{N-k}\sum_{j=1}^{N}\left(F_{cal,j}^E - F_{exp,j}^E\right)^2\right]^{1/2} \tag{B.6}$$

where the index j takes values for each of the N experimental data $F_{exp,j}^E$, and $F_{cal,j}^E$ is the corresponding value of the excess property F^E calculated from equation (B.5).

Values of ε_r^E, $\left(\partial\varepsilon_r^E/\partial T\right)_p$ and n_D^E versus ϕ_1 of 1-alkanol + TEA systems at 298.15 K are plotted in Figures B.1, B.2 and B.3 respectively with their corresponding Redlich-Kister regressions. Data on n_D are plotted in Figure B.S1 (supplementary material).

Table B.3. Volume fractions of 1-alkanol, ϕ_1, relative permittivities at frequency ν = 1 MHz, ε_r, and excess relative permittivities at ν = 1 MHz, ε_r^E, of 1-alkanol (1) + TEA (2) liquid mixtures as functions of the mole fraction of the 1-alkanol, x_1, at temperature T and pressure p = 0.1 MPa. [a]

x_1	ϕ_1	ε_r	ε_r^E	x_1	ϕ_1	ε_r	ε_r^E
methanol (1) + TEA (2) ; T/K = 293.15							
0.0000	0.0000	2.442		0.5979	0.3020	11.168	–0.676
0.0580	0.0176	2.801	–0.189	0.7096	0.4155	15.117	–0.261
0.0878	0.0272	3.038	–0.251	0.7992	0.5366	19.374	0.225
0.1593	0.0523	3.575	–0.495	0.8445	0.6124	21.941	0.433
0.1981	0.0671	3.939	–0.592	0.8997	0.7230	25.536	0.584
0.2880	0.1053	4.938	–0.782	0.9515	0.8509	29.454	0.520
0.3971	0.1608	6.538	–0.910	0.9856	0.9522	32.327	0.239

0.4959	0.2225	8.475	–0.894	1.0000	1.0000	33.576	
		methanol (1) + TEA (2) ; T/K = 298.15					
0.0000	0.0000	2.422		0.5979	0.3019	10.874	–0.666
0.0580	0.0176	2.769	–0.185	0.7096	0.4154	14.708	–0.260
0.0878	0.0272	2.998	–0.245	0.7992	0.5365	18.829	0.204
0.1593	0.0522	3.518	–0.481	0.8445	0.6123	21.315	0.400
0.1981	0.0670	3.868	–0.578	0.8997	0.7229	24.811	0.556
0.2880	0.1053	4.834	–0.768	0.9515	0.8509	28.615	0.494
0.3971	0.1608	6.387	–0.891	0.9856	0.9522	31.414	0.234
0.4959	0.2224	8.263	–0.876	1.0000	1.0000	32.624	
		methanol (1) + TEA (2) ; T/K = 303.15					
0.0000	0.0000	2.402		0.5979	0.3018	10.582	–0.657
0.0580	0.0176	2.736	–0.181	0.7096	0.4153	14.302	–0.261
0.0878	0.0272	2.958	–0.240	0.7992	0.5364	18.293	0.184
0.1593	0.0522	3.461	–0.470	0.8445	0.6122	20.705	0.377
0.1981	0.0670	3.799	–0.565	0.8997	0.7228	24.096	0.529
0.2880	0.1052	4.732	–0.750	0.9515	0.8508	27.792	0.477
0.3971	0.1607	6.236	–0.872	0.9856	0.9521	30.513	0.232
0.4959	0.2224	8.054	–0.860	1.0000	1.0000	31.684	
		1–propanol (1) + TEA (2) ; T/K = 293.15					
0.0000	0.0000	2.440		0.6027	0.4492	8.889	–1.956
0.0476	0.0262	2.686	–0.244	0.6997	0.5560	11.070	–1.773
0.0932	0.0524	2.954	–0.466	0.7966	0.6780	13.743	–1.382
0.1394	0.0801	3.248	–0.691	0.8455	0.7463	15.298	–1.105
0.2032	0.1206	3.718	–0.978	0.9014	0.8309	17.310	–0.676
0.2896	0.1797	4.459	–1.343	0.9484	0.9081	19.076	–0.355
0.4084	0.2706	5.770	–1.733	1.0000	1.0000	21.150	
0.5043	0.3535	7.131	–1.923				
		1–propanol (1) + TEA (2) ; T/K = 298.15					
0.0000	0.0000	2.419		0.6027	0.4488	8.651	–1.869
0.0476	0.0261	2.660	–0.230	0.6997	0.5557	10.757	–1.692
0.0932	0.0523	2.916	–0.447	0.7966	0.6776	13.343	–1.307
0.1394	0.0800	3.200	–0.663	0.8455	0.7460	14.842	–1.042
0.2032	0.1204	3.654	–0.938	0.9014	0.8307	16.775	–0.638
0.2896	0.1795	4.368	–1.291	0.9484	0.9080	18.481	–0.327
0.4084	0.2704	5.640	–1.660	1.0000	1.0000	20.469	
0.5043	0.3532	6.954	–1.840				
		1–propanol (1) + TEA (2) ; T/K = 303.15					
0.0000	0.0000	2.398		0.6027	0.4485	8.417	–1.785
0.0476	0.0261	2.631	–0.221	0.6997	0.5553	10.450	–1.611
0.0932	0.0522	2.878	–0.428	0.7966	0.6773	12.945	–1.239
0.1394	0.0799	3.153	–0.635	0.8455	0.7458	14.392	–0.984
0.2032	0.1203	3.592	–0.899	0.9014	0.8305	16.243	–0.607
0.2896	0.1793	4.281	–1.237	0.9484	0.9078	17.887	–0.308

0.4084	0.2701	5.510	–1.588	1.0000	1.0000	19.799	
0.5043	0.3529	6.781	–1.758				
		1–butanol (1) + TEA (2) ; T/K = 293.15					
0.0000	0.0000	2.444		0.6006	0.4973	8.204	–2.076
0.0536	0.0359	2.727	–0.283	0.6985	0.6038	10.001	–1.957
0.1102	0.0753	3.052	–0.579	0.8023	0.7275	12.371	–1.536
0.1536	0.1067	3.335	–0.790	0.8438	0.7804	13.458	–1.283
0.2025	0.1431	3.670	–1.029	0.8910	0.8432	14.801	–0.929
0.2941	0.2151	4.453	–1.380	0.9475	0.9223	16.509	–0.468
0.3957	0.3011	5.409	–1.779	1.0000	1.0000	18.201	
0.5082	0.4047	6.786	–2.035				
		1–butanol (1) + TEA (2) ; T/K = 298.15					
0.0000	0.0000	2.424		0.6006	0.4969	7.984	–1.964
0.0536	0.0359	2.696	–0.272	0.6985	0.6034	9.718	–1.843
0.1102	0.0752	3.010	–0.553	0.8023	0.7272	11.994	–1.441
0.1536	0.1065	3.285	–0.752	0.8438	0.7801	13.032	–1.204
0.2025	0.1429	3.608	–0.980	0.8910	0.8430	14.322	–0.867
0.2941	0.2148	4.365	–1.312	0.9475	0.9222	15.961	–0.427
0.3957	0.3007	5.288	–1.689	1.0000	1.0000	17.566	
0.5082	0.4043	6.618	–1.928				
		1–butanol (1) + TEA (2) ; T/K = 303.15					
0.0000	0.0000	2.403		0.6006	0.4965	7.768	–1.854
0.0536	0.0358	2.666	–0.257	0.6985	0.6030	9.438	–1.732
0.1102	0.0751	2.970	–0.525	0.8023	0.7268	11.621	–1.349
0.1536	0.1063	3.235	–0.713	0.8438	0.7798	12.614	–1.127
0.2025	0.1427	3.547	–0.931	0.8910	0.8428	13.847	–0.809
0.2941	0.2146	4.278	–1.245	0.9475	0.9221	15.415	–0.394
0.3957	0.3004	5.169	–1.602	1.0000	1.0000	16.942	
0.5082	0.4039	6.449	–1.826				
		1–pentanol (1) + TEA (2) ; T/K = 293.15					
0.0000	0.0000	2.437		0.5968	0.5352	7.514	–2.015
0.0588	0.0463	2.743	–0.308	0.7072	0.6526	9.204	–1.881
0.1062	0.0846	3.009	–0.549	0.7960	0.7522	10.867	–1.538
0.1482	0.1192	3.260	–0.757	0.8517	0.8171	12.041	–1.224
0.2159	0.1764	3.708	–1.067	0.8939	0.8676	13.011	–0.923
0.3011	0.2510	4.361	–1.402	0.9465	0.9323	14.330	–0.462
0.4089	0.3498	5.319	–1.754	1.0000	1.0000	15.689	
0.5014	0.4389	6.314	–1.939				
		1–pentanol (1) + TEA (2) ; T/K = 298.15					
0.0000	0.0000	2.417		0.5968	0.5347	7.316	–1.888
0.0588	0.0463	2.716	–0.289	0.7072	0.6522	8.943	–1.752
0.1062	0.0844	2.969	–0.519	0.7960	0.7518	10.533	–1.427
0.1482	0.1190	3.212	–0.715	0.8517	0.8168	11.652	–1.133
0.2159	0.1761	3.644	–1.008	0.8939	0.8674	12.576	–0.851

0.3011	0.2506	4.276	–1.322	0.9465	0.9321	13.822	–0.426
0.4089	0.3494	5.202	–1.650	1.0000	1.0000	15.110	
0.5014	0.4384	6.162	–1.820				
		1–pentanol (1) + TEA (2) ; T/K = 303.15					
0.0000	0.0000	2.397		0.5968	0.5342	7.123	–1.759
0.0588	0.0462	2.685	–0.273	0.7072	0.6517	8.683	–1.626
0.1062	0.0843	2.928	–0.492	0.7960	0.7514	10.201	–1.318
0.1482	0.1188	3.164	–0.675	0.8517	0.8165	11.265	–1.044
0.2159	0.1758	3.583	–0.948	0.8939	0.8672	12.144	–0.781
0.3011	0.2503	4.193	–1.243	0.9465	0.9320	13.320	–0.391
0.4089	0.3490	5.087	–1.547	1.0000	1.0000	14.537	
0.5014	0.4379	6.010	–1.703				
		1–heptanol (1) + TEA (2) ; T/K = 293.15					
0.0000	0.0000	2.438		0.5950	0.5987	6.560	–1.606
0.0451	0.0458	2.663	–0.213	0.6948	0.6981	7.608	–1.509
0.1029	0.1043	2.973	–0.463	0.7925	0.7950	8.806	–1.238
0.1466	0.1486	3.212	–0.648	0.8478	0.8498	9.584	–0.984
0.1997	0.2022	3.527	–0.845	0.8982	0.8996	10.352	–0.692
0.2979	0.3012	4.163	–1.157	0.9465	0.9473	11.135	–0.366
0.3963	0.4000	4.855	–1.410	1.0000	1.0000	12.005	
0.4950	0.4989	5.647	–1.564				
		1–heptanol (1) + TEA (2) ; T/K = 298.15					
0.0000	0.0000	2.418		0.5950	0.5982	6.398	–1.455
0.0451	0.0457	2.635	–0.198	0.6948	0.6976	7.398	–1.358
0.1029	0.1041	2.933	–0.431	0.7925	0.7947	8.532	–1.107
0.1466	0.1483	3.167	–0.598	0.8478	0.8495	9.268	–0.869
0.1997	0.2019	3.470	–0.782	0.8982	0.8994	9.979	–0.611
0.2979	0.3007	4.086	–1.064	0.9465	0.9472	10.706	–0.318
0.3963	0.3995	4.752	–1.296	1.0000	1.0000	11.504	
0.4950	0.4984	5.518	–1.428				
		1–heptanol (1) + TEA (2) ; T/K = 303.15					
0.0000	0.0000	2.397		0.5950	0.5977	6.233	–1.314
0.0451	0.0456	2.607	–0.183	0.6948	0.6972	7.187	–1.217
0.1029	0.1039	2.896	–0.396	0.7925	0.7944	8.262	–0.980
0.1466	0.1480	3.122	–0.550	0.8478	0.8493	8.954	–0.761
0.1997	0.2015	3.414	–0.719	0.8982	0.8992	9.611	–0.534
0.2979	0.3003	4.010	–0.974	0.9465	0.9471	10.282	–0.275
0.3963	0.3990	4.652	–1.183	1.0000	1.0000	11.013	
0.4950	0.4978	5.389	–1.297				

[a] The standard uncertainties are: $u(T) = 0.02$ K; $u(p) = 1$ kPa; $u(\nu) = 20$ Hz; $u(x_1) = 0.0010$; $u(\phi_1) = 0.004$. The relative standard uncertainty is: $u_r(\varepsilon_r) = 0.003$; and the relative combined expanded uncertainty (0.95 level of confidence) is $U_{rc}\left(\varepsilon_r^E\right) = 0.03$.

Table B.4. Volume fractions of 1-alkanol, ϕ_1, refractive indices at the sodium D-line, n_D, and excess refractive indices at the sodium D-line, n_D^E, of 1-alkanol (1) + TEA (2) liquid mixtures as functions of the mole fraction of the 1-alkanol, x_1, at temperature T and pressure $p = 0.1$ MPa. [a]

x_1	ϕ_1	n_D	$10^5 n_D^E$	x_1	ϕ_1	n_D	$10^5 n_D^E$
methanol (1) + TEA (2) ; T/K = 293.15							
0.0000	0.0000	1.40044		0.6002	0.3040	1.38753	852
0.0588	0.0179	1.40013	94	0.6953	0.3990	1.38081	857
0.1072	0.0338	1.39980	173	0.7943	0.5291	1.37056	764
0.1765	0.0587	1.39918	285	0.8504	0.6232	1.36254	641
0.2036	0.0692	1.39890	331	0.9003	0.7243	1.35360	479
0.2989	0.1104	1.39750	481	0.9510	0.8496	1.34215	247
0.4053	0.1655	1.39510	629	0.9851	0.9506	1.33303	76
0.5193	0.2391	1.39143	782	1.0000	1.0000	1.32863	
methanol (1) + TEA (2) ; T/K = 298.15							
0.0000	0.0000	1.39775		0.6002	0.3039	1.38506	858
0.0588	0.0178	1.39752	101	0.6953	0.3989	1.37844	867
0.1072	0.0337	1.39719	178	0.7943	0.5290	1.36825	773
0.1765	0.0587	1.39661	294	0.8504	0.6231	1.36028	649
0.2036	0.0692	1.39635	341	0.9003	0.7242	1.35146	494
0.2989	0.1103	1.39493	486	0.9510	0.8495	1.34008	262
0.4053	0.1654	1.39271	649	0.9851	0.9506	1.33092	82
0.5193	0.2391	1.38891	786	1.0000	1.0000	1.32649	
methanol (1) + TEA (2) ; T/K = 303.15							
0.0000	0.0000	1.39503		0.6002	0.3038	1.38258	864
0.0588	0.0178	1.39482	102	0.6953	0.3988	1.37601	873
0.1072	0.0337	1.39452	181	0.7943	0.5289	1.36595	784
0.1765	0.0586	1.39396	297	0.8504	0.6230	1.35795	652
0.2036	0.0692	1.39371	346	0.9003	0.7241	1.34908	486
0.2989	0.1103	1.39236	495	0.9510	0.8494	1.33782	259
0.4053	0.1654	1.39003	644	0.9851	0.9505	1.32875	81
0.5193	0.2390	1.38631	784	1.0000	1.0000	1.32435	
1-propanol (1) + TEA (2) ; T/K = 293.15							
0.0000	0.0000	1.40044		0.6011	0.4475	1.40027	667
0.0476	0.0262	1.40088	84	0.6989	0.5551	1.39836	641
0.0989	0.0557	1.40121	162	0.7959	0.6770	1.39548	540
0.1620	0.0941	1.40154	254	0.8455	0.7463	1.39359	457
0.1967	0.1163	1.40171	304	0.9017	0.8314	1.39090	319
0.2936	0.1826	1.40195	430	0.9484	0.9081	1.38836	183
0.4005	0.2642	1.40203	562	1.0000	1.0000	1.38511	
0.4973	0.3471	1.40153	639				
1-propanol (1) + TEA (2) ; T/K = 298.15							
0.0000	0.0000	1.39775		0.6011	0.4472	1.39795	675
0.0476	0.0261	1.39822	85	0.6989	0.5547	1.39615	653
0.0989	0.0556	1.39864	170	0.7959	0.6767	1.39338	555
0.1620	0.0940	1.39904	266	0.8455	0.7460	1.39142	461
0.1967	0.1162	1.39921	316	0.9017	0.8312	1.38887	332

0.2936	0.1824	1.39954	446	0.9484	0.9080	1.38629	187
0.4005	0.2639	1.39949	560	1.0000	1.0000	1.38306	
0.4973	0.3468	1.39902	635				
		1-propanol (1) + TEA (2) ; T/K = 303.15					
0.0000	0.0000	1.39503		0.6011	0.4468	1.39556	679
0.0476	0.0261	1.39553	86	0.6989	0.5544	1.39378	652
0.0989	0.0556	1.39595	170	0.7959	0.6764	1.39103	548
0.1620	0.0939	1.39642	270	0.8455	0.7458	1.38916	459
0.1967	0.1160	1.39665	324	0.9017	0.8310	1.38667	330
0.2936	0.1822	1.39700	452	0.9484	0.9078	1.38419	190
0.4005	0.2637	1.39705	571	1.0000	1.0000	1.38099	
0.4973	0.3465	1.39662	644				
		1-butanol (1) + TEA (2) ; T/K = 293.15					
0.0000	0.0000	1.40044		0.6063	0.5033	1.40628	642
0.0556	0.0373	1.40139	99	0.7054	0.6117	1.40572	598
0.1033	0.0705	1.40215	179	0.8013	0.7263	1.40448	488
0.1482	0.1027	1.40284	252	0.8498	0.7882	1.40353	400
0.1992	0.1406	1.40356	328	0.8978	0.8525	1.40241	295
0.2974	0.2178	1.40473	454	0.9530	0.9303	1.40085	148
0.3982	0.3033	1.40566	557	1.0000	1.0000	1.39929	
0.5027	0.3994	1.40624	626				
		1-butanol (1) + TEA (2) ; T/K = 298.15					
0.0000	0.0000	1.39775		0.6063	0.5029	1.40397	645
0.0556	0.0372	1.39877	104	0.7054	0.6113	1.40352	605
0.1033	0.0703	1.39958	186	0.8013	0.7259	1.40234	492
0.1482	0.1026	1.40029	259	0.8498	0.7880	1.40148	408
0.1992	0.1404	1.40107	338	0.8978	0.8523	1.40036	299
0.2974	0.2175	1.40228	463	0.9530	0.9302	1.39884	151
0.3982	0.3029	1.40324	563	1.0000	1.0000	1.39730	
0.5027	0.3990	1.40385	628				
		1-butanol (1) + TEA (2) ; T/K = 303.15					
0.0000	0.0000	1.39503		0.6063	0.5024	1.40168	652
0.0556	0.0372	1.39616	112	0.7054	0.6109	1.40125	606
0.1033	0.0702	1.39701	196	0.8013	0.7256	1.40015	493
0.1482	0.1024	1.39776	270	0.8498	0.7877	1.39932	409
0.1992	0.1402	1.39852	345	0.8978	0.8521	1.39827	302
0.2974	0.2172	1.39982	473	0.9530	0.9300	1.39680	153
0.3982	0.3026	1.40078	567	1.0000	1.0000	1.39529	
0.5027	0.3986	1.40150	637				
		1-pentanol (1) + TEA (2) ; T/K = 293.15					
0.0000	0.0000	1.40044		0.5966	0.5349	1.41188	636
0.0473	0.0372	1.40173	94	0.6985	0.6431	1.41225	570
0.1017	0.0809	1.40321	200	0.8018	0.7588	1.41214	449
0.1483	0.1193	1.40432	274	0.8501	0.8152	1.41197	379
0.2080	0.1696	1.40566	361	0.8985	0.8732	1.41156	283
0.2989	0.2490	1.40765	484	0.9499	0.9365	1.41079	146
0.4002	0.3417	1.40941	572	1.0000	1.0000	1.40993	
0.4963	0.4339	1.41092	635				

		1-pentanol (1) + TEA (2) ; T/K = 298.15					
0.0000	0.0000	1.39775		0.5966	0.5345	1.40966	645
0.0473	0.0371	1.39912	99	0.6985	0.6427	1.41021	590
0.1017	0.0808	1.40057	199	0.8018	0.7585	1.41012	463
0.1483	0.1191	1.40176	279	0.8501	0.8149	1.40986	380
0.2080	0.1693	1.40332	384	0.8985	0.8730	1.40944	279
0.2989	0.2487	1.40516	487	0.9499	0.9364	1.40873	144
0.4002	0.3412	1.40707	583	1.0000	1.0000	1.40794	
0.4963	0.4334	1.40855	637				
		1-pentanol (1) + TEA (2) ; T/K = 303.15					
0.0000	0.0000	1.39503		0.5966	0.5340	1.40737	651
0.0473	0.0370	1.39653	110	0.6985	0.6422	1.40796	593
0.1017	0.0806	1.39806	215	0.8018	0.7581	1.40796	467
0.1483	0.1189	1.39927	294	0.8501	0.8146	1.40777	386
0.2080	0.1691	1.40089	401	0.8985	0.8728	1.40733	279
0.2989	0.2483	1.40272	498	0.9499	0.9363	1.40669	146
0.4002	0.3408	1.40473	598	1.0000	1.0000	1.40592	
0.4963	0.4329	1.40620	645				
		1-heptanol (1) + TEA (2) ; T/K = 293.15					
0.0000	0.0000	1.40044		0.5968	0.6005	1.42052	569
0.0521	0.0529	1.40283	112	0.6945	0.6978	1.42217	502
0.0980	0.0994	1.40484	201	0.7957	0.7982	1.42340	386
0.1540	0.1560	1.40719	300	0.8465	0.8485	1.42384	310
0.2017	0.2042	1.40913	378	0.8935	0.8950	1.42413	229
0.2992	0.3025	1.41266	495	0.9479	0.9487	1.42431	120
0.3958	0.3995	1.41568	565	1.0000	1.0000	1.42433	
0.4951	0.4990	1.41832	591				
		1-heptanol (1) + TEA (2) ; T/K = 298.15					
0.0000	0.0000	1.39775		0.5968	0.6000	1.41831	574
0.0521	0.0528	1.40021	115	0.6945	0.6973	1.42004	508
0.0980	0.0992	1.40230	209	0.7957	0.7979	1.42135	393
0.1540	0.1558	1.40469	308	0.8465	0.8482	1.42183	318
0.2017	0.2039	1.40664	384	0.8935	0.8948	1.42213	234
0.2992	0.3020	1.41026	503	0.9479	0.9486	1.42234	123
0.3958	0.3990	1.41334	572	1.0000	1.0000	1.42236	
0.4951	0.4985	1.41607	600				
		1-heptanol (1) + TEA (2) ; T/K = 303.15					
0.0000	0.0000	1.39503		0.5968	0.5995	1.41611	581
0.0521	0.0527	1.39757	119	0.6945	0.6969	1.41794	517
0.0980	0.0990	1.39971	215	0.7957	0.7975	1.41930	399
0.1540	0.1555	1.40218	317	0.8465	0.8480	1.41980	322
0.2017	0.2035	1.40415	392	0.8935	0.8946	1.42014	238
0.2992	0.3016	1.40783	510	0.9479	0.9485	1.42036	125
0.3958	0.3985	1.41100	580	1.0000	1.0000	1.42041	
0.4951	0.4979	1.41379	607				

[a] The standard uncertainties are: $u(T) = 0.02$ K; $u(p) = 1$ kPa; $u(x_1) = 0.0010$; $u(\phi_1) = 0.004$, $u(n_D) = 0.00008$. The combined expanded uncertainty (0.95 level of confidence) is $U_c\left(n_D^E\right) = 0.0002$.

Table B.5. Coefficients A_i and standard deviations, $\sigma\left(F^E\right)$ (equation (B.6)), for the representation of F^E at temperature T and pressure p = 0.1 MPa for 1-alkanol (1) + TEA liquid mixtures by equation (B.5).

Property F^E	1-alkanol	T/K	A_0	A_1	A_2	A_3	A_3	$\sigma\left(F^E\right)$
ε_r^E	methanol	293.15	–3.50	1.8	4.4	7.0	5.7	0.02
		298.15	–3.43	1.8	4.2	6.6	5.5	0.02
		303.15	–3.37	1.7	4.0	6.4	5.4	0.02
	1-propanol	293.15	–7.71	–2.7	1.4	2.0		0.018
		298.15	–7.39	–2.5	1.5	2.0		0.017
		303.15	–7.06	–2.4	1.5	1.9		0.014
	1-butanol	293.15	–8.09	–3.4	0.4	1.6		0.015
		298.15	–7.67	–3.1	0.5	1.6		0.014
		303.15	–7.26	–2.9	0.6	1.5		0.014
	1-pentanol	293.15	–7.81	–2.70				0.019
		298.15	–7.31	–2.43				0.018
		303.15	–6.82	–2.15				0.018
	1-heptanol	293.15	–6.33	–1.80				0.018
		298.15	–5.75	–1.46				0.017
		303.15	–5.19	–1.15				0.018
$10^5 n_D^E$	methanol	293.15	3050	2224	809			8
		298.15	3080	2236	918			5
		303.15	3090	2233	945			8
	1-propanol	293.15	2547	1161	251			4
		298.15	2557	1164	412			3
		303.15	2587	1120	356			1.4
	1-butanol	293.15	2500	832	136			2
		298.15	2515	816	221			3
		303.15	2538	774	269			3
	1-pentanol	293.15	2528	551				7
		298.15	2573	545				6
		303.15	2585	475	205			6
	1-heptanol	293.15	2366	–16	–30	144		1.1
		298.15	2392	–23	28	148		1.1
		303.15	2422	–16	69	101		0.9
$\left(\partial\varepsilon_r^E/\partial T\right)_p$ / K^{-1}	methanol	298.15	0.014	–0.014	–0.04	–0.06	–0.03	0.0005
	1-propanol	298.15	0.0661	0.030				0.0005
	1-butanol	298.15	0.0832	0.047	0.014			0.0004
	1-pentanol	298.15	0.0953	0.056	0.017			0.0004
	1-heptanol	298.15	0.1079	0.065	0.029			0.0004

B.4. Discussion

Unless stated otherwise, the below values of the dielectric properties and their corresponding excess functions are referred to T = 298.15 K and $\phi_1 = 0.5$. On the other hand, n will stand for the number of C atoms of the 1-alkanol.

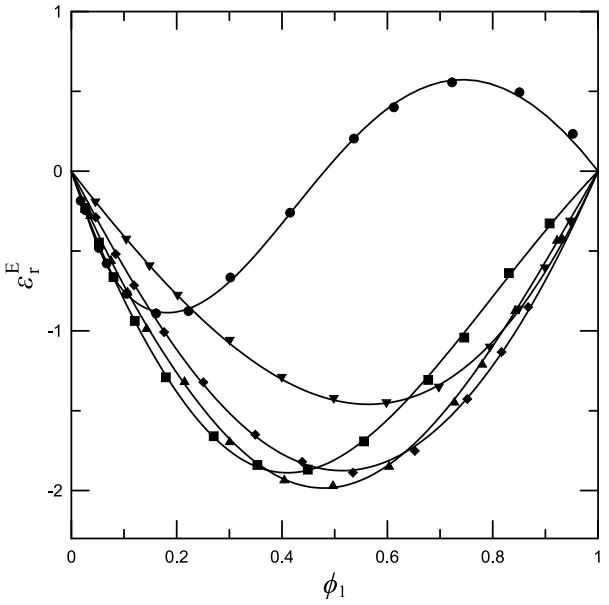

Figure B.1: Excess relative permittivity, ε_r^E, of 1-alkanol (1) + TEA (2) liquid mixtures as a function of the 1-alkanol volume fraction, ϕ_1, at 0.1 MPa, 298.15 K and 1 MHz. Full symbols, experimental values (this work): (●), methanol; (■), 1-propanol; (▲), 1-butanol; (♦), 1-pentanol; (▼), 1-heptanol. Solid lines, calculations with equation (B.5) using the coefficients from Table B.5.

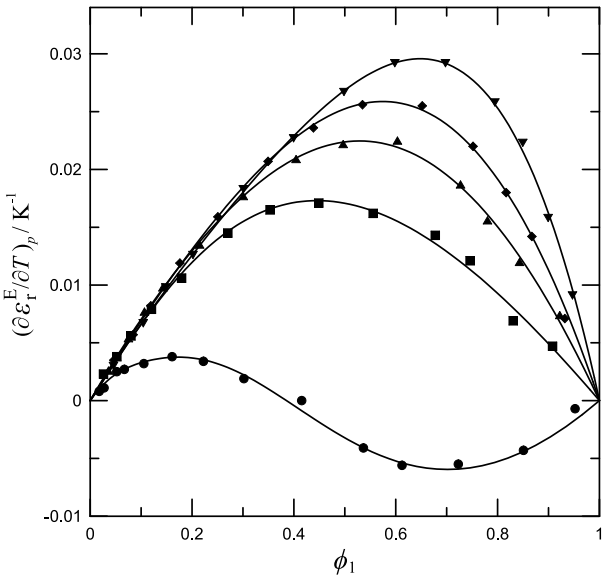

Figure B.2: Temperature derivative of the excess relative permittivity, $(\partial\varepsilon_r^E / \partial T)_p$, of 1-alkanol (1) + TEA (2) liquid mixtures as a function of the 1-alkanol volume fraction, ϕ_1, at 0.1 MPa, 298.15 K and 1 MHz. Full symbols, experimental values (this work): (●), methanol; (■), 1-propanol; (▲), 1-butanol; (♦), 1-pentanol; (▼), 1-heptanol. Solid lines, calculations with equation (B.5) using the coefficients from Table B.5.

B.4.1. Relative permittivities

The magnitude of ε_r for a liquid system is determined by a number of factors, such as the permanent dipole moments and polarizabilities of its molecules, the nature of the liquid structure and collective dynamics. Figure B.4 shows our $\varepsilon_r(\phi_1)$ results for systems with methanol or 1-heptanol and an isomeric amine TEA, HxA [27], or DPA [28]. We note that, at any composition, $\varepsilon_r(\phi_1)$ values for the mixtures with TEA are lower, which indicates that a weakening of the dielectric polarization of the system is produced with regards to that of solutions with linear isomeric amines. This may be ascribed to the dipole moment of TEA (0.66 D [68]), which is lower than the dipole moments of HxA (1.3 D [85]) or DPA (1.1 D [86]). Interestingly, there is a range of concentrations, which depends on the system components, where small negative differences $\varepsilon_r(\phi_1)$(HxA) − $\varepsilon_r(\phi_1)$(DPA) (for a fixed 1-alkanol) are encountered (Figure B.4). Therefore, in those regions, the effective dipole moments of the multimers formed by unlike molecules upon mixing are lower in the case of HxA-containing systems, probably due to the existence of cyclic species. Outside of the mentioned range of compositions $\varepsilon_r(\phi_1)$(DPA) < $\varepsilon_r(\phi_1)$(HxA), in agreement with the lower dipole moment of DPA. This can be better visualized in Figure B.5, where we have eliminated volume effects present in the permittivity by representing the molar susceptibility, $\chi_m = (\varepsilon_r - 1)V_m$ (V_m, molar volume of the mixture), of these mixtures vs ϕ_1. The quantity χ_m is useful to compare the response of different liquids given a value of the equilibrium electric field, because it is proportional to the

macroscopic dipole moment resulting from a fixed amount (1 mol) of molecules. The ϕ_1 dependence of χ_m and ε_r are very different for the methanol + DPA or + HxA systems (Figures B.4 and B.5). In fact, there is a more or less large concentration range where χ_m slowly increases, i.e., where the molar macroscopic dipole moment remains nearly unchanged.

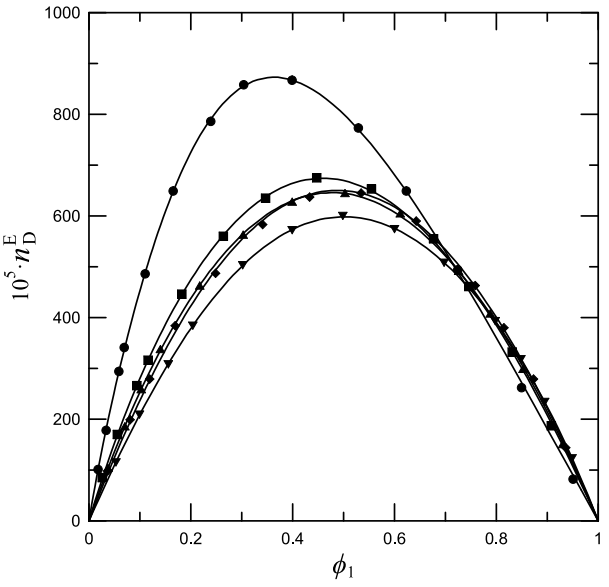

Figure B.3: Excess refractive index at the sodium D-line, n_D^E, of 1-alkanol (1) + TEA (2) liquid mixtures as a function of the 1-alkanol volume fraction, ϕ_1, at 0.1 MPa and 298.15 K. Full symbols, experimental values (this work): (●), methanol; (■), 1-propanol; (▲), 1-butanol; (♦), 1-pentanol; (▼), 1-heptanol. Solid lines, calculations with equation (B.5) using the coefficients from Table B.5.

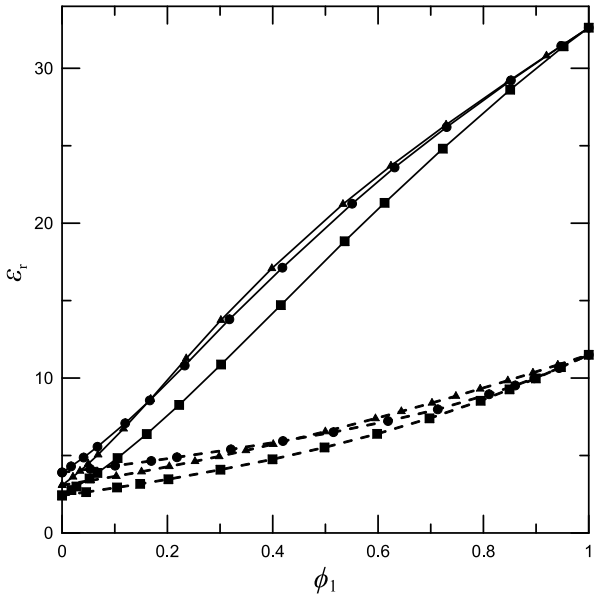

Figure B.4: Relative permittivity, ε_r, of 1-alkanol (1) + amine (2) liquid mixtures as a function of the 1-alkanol volume fraction, ϕ_1, at 0.1 MPa, 298.15 K and 1 MHz: (●), HxA [27]; (▲), DPA [28]; (■), TEA (this work). Solid lines, methanol; dashed lines, 1-heptanol.

B.4.2. Excess relative permittivities

It is known that the rupture of interactions between molecules of the same species upon mixing provides a negative contribution to ε_r^E. For example, ε_r^E(heptane) = –1.075 (n = 3), –2.225 (n = 4), –2.525 (n = 5), –2.875 (n = 7), –1.775 (n = 10) [24, 87, 88] (Figure B.6). For the system methanol + heptane, a partial immiscibility region appears [89]. These rather large and negative values can be ascribed to the disruption of the alcohol network along the mixing process. The creation of new interactions between unlike molecules along this process leads to the formation of multimers whose molecular structure is determinant to provide a more or less effective impact on the macroscopic response to an electric field. If the mentioned multimers are linear chains, the contribution to ε_r^E is positive. In contrast, if cyclic species are created, the contribution to ε_r^E is negative. The ε_r^E values of 1-alkanol + TEA mixtures are: 0.074 (n = 1), –1.807 (n = 3), –1.980 (n = 4), –1.874 (n = 5), –1.435 (n = 7) (this work), –0.593 (T = 293.15 K) (n = 10); –0.048 (T = 293.15 K) (n = 12); [90] (Figure B.6). The comparison of these results for $n \geq 4$ with the lower values given above for 1-alkanol + heptane systems reveals that the

creation of the new (1-alkanol)-TEA interactions contributes positively to the ε_r^E of the mixture. In addition, positive ε_r^E values are encountered for the methanol-containing system. An important result is that, for systems with $n = 3$, ε_r^E(TEA) < ε_r^E(heptane). This suggests that TEA is an effective breaker of the alkanol self-association, and that the interactions between unlike molecules do not compensate enough the large negative contribution to ε_r^E from the disruption of (1-propanol)-(1-propanol) interactions. The variation of ε_r^E with the chain length of the 1-alkanol follows the order: methanol > 1-propanol > 1-butanol < 1-pentanol < 1-heptanol < 1-decanol < 1-dodecanol. In other words, ε_r^E decreases to a minimum and then increases again. Such a trend is similar to those encountered for 1-alkanol + heptane (see above), + HxA [27], + DPA [28] or + cyclohexylamine [25, 26] systems. The observed ε_r^E dependence on n has been explained in terms of a weaker and lower self-association of longer alkanols. In the case of 1-alkanol + amine systems, one must also take into account that the solvation between molecules of different species decreases when n is increased [1, 5, 7, 8, 91]. Thus, the mixture polarization shows a weaker variation with n when longer 1-alkanols are involved, since they are characterized by a lower self-association and the related solvation effects are also less relevant. Consequently, and as in previous studies, ε_r^E shows a sharper dependence for low n values [27, 28]. Other available data on ε_r^E for the 1-dodecanol + TEA system at different temperatures [92] should be taken with caution, as they are rather scattered and the corresponding curves are S-shaped, with positive values at higher concentrations of the 1-alkanol which increase in line with the temperature [92]. This needs further experimental confirmation.

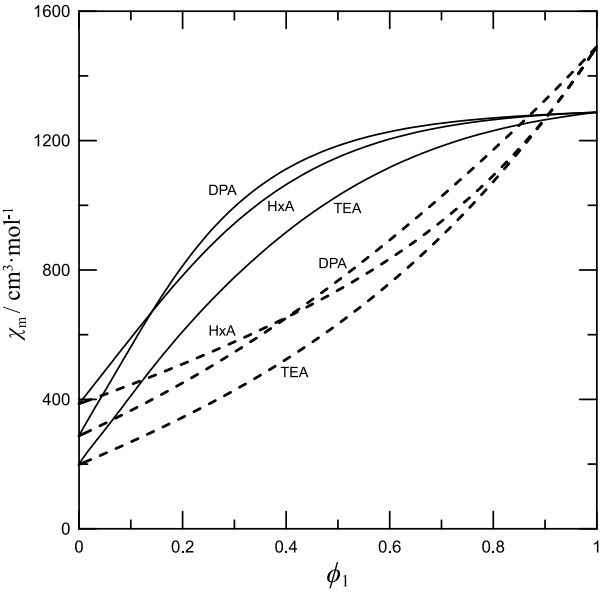

Figure B.5: Molar susceptibility, χ_m, of 1-alkanol (1) + amine (2) liquid mixtures as a function of the 1-alkanol volume fraction, ϕ_1, at 0.1 MPa, 298.15 K and 1 MHz: HxA [27]; DPA [28]; TEA (this work). Solid lines, methanol; dashed lines, 1-heptanol.

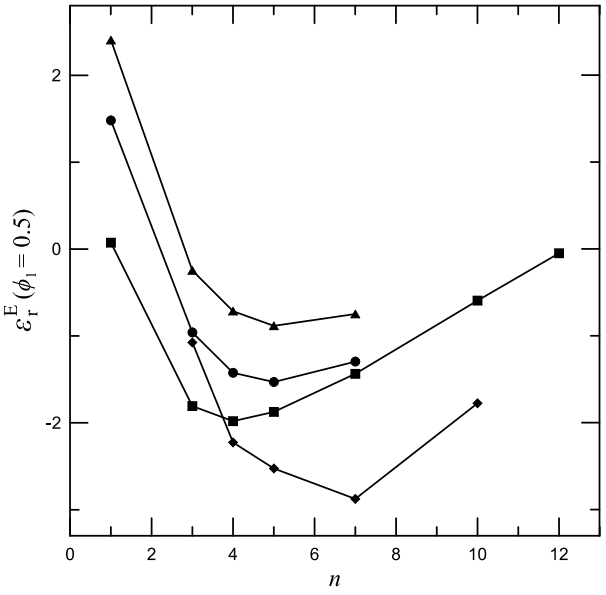

Figure B.6: Excess relative permittivity at $\phi_1 = 0.5$ (ϕ_1, 1-alkanol volume fraction) of 1-alkanol (1) + amine (2) or + heptane (2) liquid mixtures as a function of the number of carbon atoms of the 1-alkanol, n, at 0.1 MPa, 298.15 K and 1 MHz: (●), HxA [27]; (▲), DPA [28]; (■), TEA (n = 1 to 7, this work; n = 10,12 are literature values [90] at 293.15 K); (♦), heptane [24, 87, 88].

For a given 1-alkanol, ε_r^E(DPA) [28] > ε_r^E(HxA) [27] > ε_r^E(TEA) (Figure B.6). This variation is similar to, although stronger than, the observed change for ε_r. For a better understanding of systems containing TEA, we start examining 1-alkanol + linear primary or secondary amine systems. A literature survey shows that ε_r^E(1-propanol + DPA) = –0.246 [28] > ε_r^E(1-propanol + HxA) = –0.96 [27] > ε_r^E(1-propanol + propan-1-amine) = –1.99 [93] and that ε_r^E(1-butanol + DPA) = –0.715 [28] > ε_r^E (1-butanol + HxA) = –1.424 [27] > ε_r^E(1-butanol + butan-1-amine) = –2.87 [93]. Since solvation effects are expected to be more relevant in systems involving amines where the amine group is less sterically hindered (propan-1-amine, butan-1-amine), one can conclude that mixtures characterized by larger solvation effects show more negative ε_r^E values. The same trend is observed when comparing, at 303.15 K, ε_r^E results for 1-propanol + primary aromatic amine, aniline, (–2.07) [94] or + secondary aromatic amine, *N*-methylaniline, (–1.27) [95]. This behavior can be explained taking into account that larger solvation effects imply a decreased number of interactions between like molecules and, therefore, a more negative contribution to ε_r^E from the disruption of interactions between like molecules, particularly between alkanol molecules. In the case of amine mixtures, cyclic species may be more probable in mixtures containing amines with the characteristic group less sterically hindered. We must now remark that systems with TEA deviate from this picture. This can be ascribed to the globular shape of TEA molecules, which makes them better breakers of the 1-alkanol self-association (see above). In fact, the volume fraction at which minimum ε_r^E values are measured changes in the sequence DPA < HxA < TEA for mixtures with shorter 1-alkanols. Thus, ϕ_1 (n = 4) = 0.3183 (DPA; ε_r^E = –0.896) [28] < 0.4138 (HxA; ε_r^E = –1.428) [27] < 0.4969 (TEA; ε_r^E = –1.964). For n = 7, the alcohol self-association becomes less relevant, and the minimum ε_r^E values are encountered at similar volume fractions for HxA or TEA mixtures, although these concentrations are still higher than for the DPA solution, e.g. ϕ_1 (n = 7) = 0.5003 (DPA; ε_r^E = –0.793) [28] < 0.5982 (TEA; ε_r^E = –1.455). The fact that the ε_r^E curves of HxA systems are skewed to higher ϕ_1 values than those of mixtures with DPA supports our previous statement about that higher solvation effects lead to a more important breaking of the alcohol network upon mixing. We complete the present analysis as follows. (i) According to the ERAS model, the equilibrium constants, K_{AB}, change in the order HxA > DPA > TEA in systems with a given 1-alkanol [5-7]. For example, K_{AB}(methanol) = 2500 (HxA) > 2450 (DPA) > 620 (TEA). That is, solvation effects are less important in mixtures with TEA, in agreement with the fact that the amine group becomes more sterically hindered in the same sequence [91]. (ii) The $S_{CC}(0)$ function is a quantity which allows to study the fluctuations in the number of molecules of a binary mixture regardless of the components, the fluctuations in the mole fraction and the cross fluctuations. It is defined by [19, 20]:

$$S_{CC}(0) = \frac{x_1 x_2}{1 + \frac{x_1 x_2}{RT}\left(\frac{\partial^2 G_m^E}{\partial x_1^2}\right)_{T,p}} = \frac{x_1 x_2}{D} \tag{B.7}$$

where $D = 1 + \left(x_1 x_2 / RT\right)\left(\partial^2 G_m^E / \partial x_1^2\right)_{T,p}$. For ideal mixtures, $G_m^{E,id}$ = 0 (excess Gibbs energy of the ideal mixture); D^{id} = 1 and $S_{CC}(0) = x_1 x_2$. From stability conditions, $S_{CC}(0) > 0$. If a system is close to phase separation, $S_{CC}(0)$ must be large and positive (∞, if the mixture

presents a miscibility gap). In the case of compound formation between components, $S_{CC}(0)$ must be very low (0, in the limit). Therefore, $S_{CC}(0) > x_1x_2$ ($D < 1$) indicates that the dominant trend in the system is homocoordination (separation of the components), and the mixture is then less stable than the ideal. If $0 < S_{CC}(0) < x_1x_2 = S_{CC}(0)^{id}$, ($D > 1$), the fluctuations in the system have been removed, and the dominant trend in the solution is heterocoordination (compound formation). In such a case, the system is more stable than ideal. We have shortly applied this formalism to methanol + HxA, or + DPA, or + TEA systems at 298.15 K calculating G_m^E by means of the DISQUAC model with interaction parameters for the OH/amine contacts previously determined [1, 6]. At equimolar composition, we have obtained: $S_{CC}(0)$ = 0.165 (HxA) < 0.201 (DPA) < 0.341 (TEA). This means that heterocoordination is dominant in the systems with HxA or DPA, while homocoordination is prevalent in the TEA mixture. It is in full agreement with the variation of the K_{AB} constants given above, and with available G_m^E data for methanol + amine mixtures. Thus, G_m^E (methanol)/J·mol^{-1}= –799 (butan-1-amine, 348.15 K) [2], 284 (TEA, 303.15 K) [9]. (iii) Interestingly, viscosity data show that values of $\Delta\eta$ ($=\eta - x_1\eta_1 + x_2\eta_2$; where η is the mixture viscosity and η_i is the viscosity of component i) become more negative in 1-alkanol mixtures when DPA is replaced by TEA. For example, at 303.15 K and equimolar composition, $\Delta\eta$ (DPA)/mPa·s = –0.142 (1-propanol) < –0.259 (1-butanol) [96] and $\Delta\eta$ (TEA)/mPa·s = –0.328 (1-propanol) [97] < –0.612 (1-butanol) [98]. Therefore, the mixture fluidization becomes more relevant in solutions with TEA. This is not only explained by the lower solvation effects present in such systems, but also because a larger number of interactions between 1-alkanol molecules are broken along the mixing process. Interestingly, at 298.15 K and equimolar composition, $\Delta\eta$ (1-propanol)/mPa·s = –0.305 (propan-1-amine) [99] < –0.253 (butan-1-amine) [100] and $\Delta\eta$ (1-butanol)/mPa·s = –0.460 (propan-1-amine) [99] < –0.280 (butan-1-amine) [100]. It seems that for 1-alkanol + linear primary amine systems including compounds of similar size and shape, $\Delta\eta$ is lower for the solutions with larger solvation effects. This trend is still valid for mixtures including short chain 1-alkanols and DPA. For instance, at 303.15 K and x_1 = 0.5, the values $\Delta\eta$ (propan-1-amine)/mPa·s = –0.252 (1-propanol); –0.320 (1-butanol) [101] are lower than the results given above for 1-alkanol + DPA systems.

B.4.3. Temperature dependence of the permittivity

Values of $(\partial\varepsilon_r^*/\partial T)_p$ of pure compounds used in this work are negative, as it is usual for normal liquids. Pure TEA shows a very low absolute value of this derivative, $(\partial\varepsilon_r^*/\partial T)_p$ = –0.004 K^{-1}, since TEA is not self-associated and has a low ε_r^* value (= 2.419). Thus, the increase of thermal agitation hardly modifies the liquid structure. On the other hand, values of $(\partial\varepsilon_r/\partial T)_p$ of TEA systems are higher than for pure alkanols (e.g., for 1-pentanol $(\partial\varepsilon_r^*/\partial T)_p$ = –0.117 K^{-1} < $(\partial\varepsilon_r/\partial T)_p$ = –0.034; Figure B.7, Table B.S2). This can be explained as follows. (i) The contribution to $(\partial\varepsilon_r/\partial T)_p$ related to the breaking of TEA-TEA interactions when T is increased is practically negligible (see above); (ii) The enthalpy of hydrogen bonds between 1-alkanol molecules is larger than that corresponding to 1-alkanol-TEA interactions. Thus, in the framework of the ERAS model, Δh_{AB}^* (TEA)/ kJ·mol^{-1} = –35.3 (methanol); –30.5 (1-heptanol) [5], while the enthalpies between 1-alkanol molecules are –25 kJ·mol^{-1} [4, 5, 7, 102]. Therefore, one can expect that the number of (1-alkanol)-TEA interactions broken when the temperature is

increased is lower than the number of disrupted alkanol-alkanol interactions. This leads to a lower ε_r decrease when T is increased in comparison to that produced in pure 1-alkanols. The variation of $(\partial\varepsilon_r/\partial T)_p$ with n can be explained in similar terms. On the other hand, for mixtures with a given 1-alkanol, $(\partial\varepsilon_r/\partial T)_p$ changes in the order TEA > HxA > DPA (Figure B.7). The ε_r values vary in the opposite sequence (Figure B.4). That is, the structure of mixtures characterized by a higher dielectric polarization is more sensitive to temperature changes. In addition, $(\partial\varepsilon_r^*/\partial T)_p$ / K^{-1} = –0.004 (TEA) > –0.0098 (HxA) > –0.012 (DPA). Finally, we note that $(\partial\varepsilon_r^E/\partial T)_p$ / K^{-1} can show negative or positive values (Figures B.2 and B.S2): –0.003 (n = 1), 0.017 (n = 3), 0.022 (n = 4), 0.025 (n = 5), 0.027 (n = 7). The negative value is encountered only for the methanol solution, for which the effects from 1-alkanol self-association and solvation between unlike molecules are more relevant, leading to a network that is more difficult to break with the increasing of temperature when compared with the ideal mixture. DPA and HxA systems behave similarly [27, 28] but, since association/solvation effects are stronger, the corresponding values are more negative.

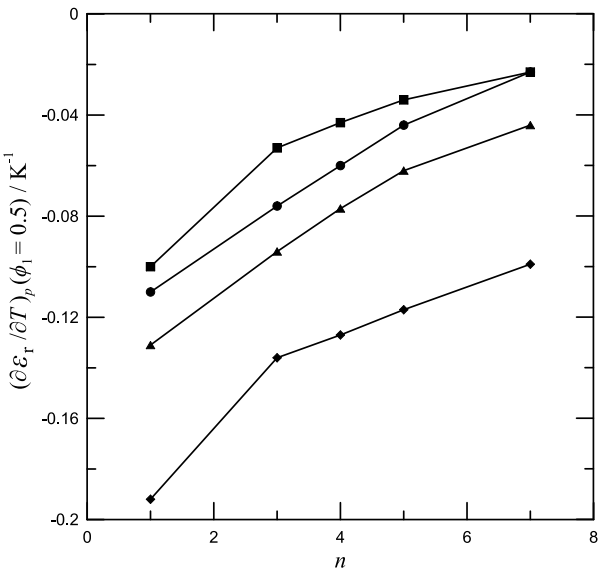

Figure B.7: Temperature derivative of the relative permittivity, $(\partial\varepsilon_r/\partial T)_p$, at $\phi_1 = 0.5$ (ϕ_1, 1-alkanol volume fraction) of 1-alkanol (1) + amine (2) liquid mixtures or pure 1-alkanols as a function of the number of carbon atoms of the 1-alkanol, n, at 0.1 MPa, 298.15 K and 1 MHz: (●), HxA [27]; (▲), DPA [28]; (■), TEA (this work); (♦), pure 1-alkanols (this work).

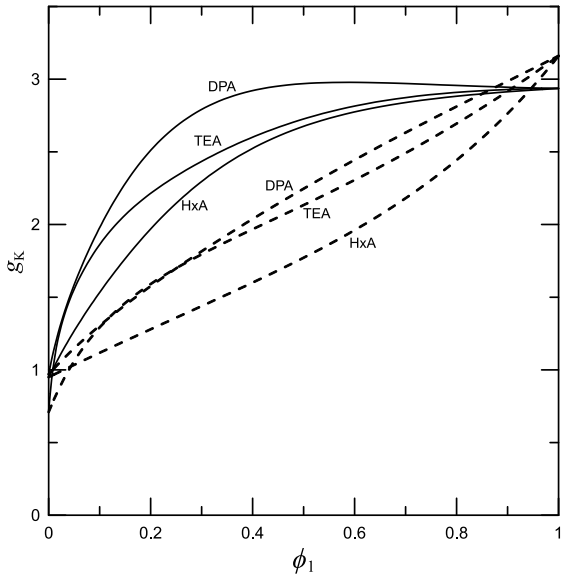

Figure B.8: Kirkwood correlation factor, g_K, of 1-alkanol (1) +amine (2) liquid mixtures as a function of the 1-alkanol volume fraction, ϕ_1, at 0.1 MPa, 298.15 K: HxA [27]; DPA [28]; TEA (this work). Solid lines, methanol; dashed lines, 1-heptanol.

B.4.4. Molar refraction

The molar refraction or molar refractivity is defined by the Lorentz-Lorenz equation [30, 32]:

$$R_m = \frac{n_D^2 - 1}{n_D^2 + 2} V_m = \frac{N_A \alpha_e}{3\varepsilon_0} \tag{B.8}$$

where N_A is Avogadro's constant and ε_0 denotes the vacuum permittivity. R_m is related to dispersive interactions [32, 103], since it is proportional to the average electronic contribution to the polarizability, α_e, from one molecule in a macroscopic sphere of liquid [30, 32]. The R_m / cm^3·mol^{-1} values for 1-alkanol + TEA mixtures are (at equimolar composition): 20.7 (n = 1), 25.4 (n = 3), 27.7 (n = 4), 30.0 (n = 5), 34.7 (n = 7). That is, dispersive interactions are more relevant in mixtures with longer 1-alkanols. Interestingly, the R_m values are very similar to those of 1-alkanol + HxA or + DPA systems [27, 28], and one can conclude that these mixtures differ essentially by solvation effects. The application of the ERAS model [5, 7] to 1-alkanol + HxA, or + DPA, or + TEA systems shows that these mixtures are characterized by the same small physical parameter and that they differ in the parameters K_{AB}, Δh^*_{AB} and Δv^*_{AB}.

B.4.5. Aromaticity effect

The available ε_r^E data in the literature for 1-alkanol + pyridine systems [104, 105] indicate that they are higher than those of the TEA solutions. Thus, ε_r^E(methanol) = 2.85 (pyridine) [104] > 0.074 (TEA, this work); and, at 303.15 K, ε_r^E(1-propanol) = 0.10 [105] (pyridine) > –1.807 (TEA, this work). Therefore, cooperative effects which lead to an increase of the dielectric polarization of the mixture are more relevant in the systems with pyridine, probably because the amine group is less sterically hindered in the aromatic amine and the creation of multimers, formed by unlike molecules, with larger effective dipole moments is favored. This effect predominates over the larger negative contribution to ε_r^E from the breaking of dipolar interactions between pyridine molecules. Note that the dipole moment of pyridine (2.37 D, [74]) is much higher than the dipole moment of TEA. It is remarkable that the behavior of 1-alkanol + HxA, or + aniline systems is the opposite, and ε_r^E values are more negative for the solutions involving aniline [27]. That is, the large negative contribution to ε_r^E from the disruption of aniline-aniline interactions predominates. The mentioned interactions are much stronger than those between pyridine molecules, as it is shown by the upper critical solution temperatures (UCST) of their mixtures with *n*-alkanes. For example. UCST/K= 268.7 (pyridine + dodecane) [106] < 343.1 (aniline + heptane) [107].

B.4.6. Kirkwood-Fröhlich model

In the Kirkwood-Fröhlich model, the fluctuations of the dipole moment in the absence of electric field are treated as the basis to obtain relations involving the relative permittivity. It is a local-field model in which the molecules are assumed to be in a spherical cavity of an infinitely large piece of dielectric and the induced contribution to the polarizability is treated macroscopically through its relation to ε_r^∞ (the value of the permittivity at a high frequency at which only the induced polarizability contributes). The local field takes into account long-range dipolar interactions by considering the outside of the cavity as a continuous medium of permittivity ε_r. Short-range interactions are introduced by the so-called Kirkwood correlation factor, g_K, which provides information about the deviations from randomness of the orientation of a dipole with respect to its neighbors. This is an important parameter, as it provides information about specific interactions in the liquid state. For a mixture of polar liquids, g_K can

be determined, in a one-fluid model approach [29], from macroscopic physical properties according to the expression [29-32]:

$$g_K = \frac{9k_B T V_m \varepsilon_0 (\varepsilon_r - \varepsilon_r^\infty)(2\varepsilon_r + \varepsilon_r^\infty)}{N_A \mu^2 \varepsilon_r (\varepsilon_r^\infty + 2)^2} \quad \text{(B.9)}$$

Here, k_B is Boltzmann's constant; N_A, Avogadro's constant; ε_0, the vacuum permittivity; and V_m, the molar volume of the liquid at the working temperature, T. For polar compounds, ε_r^∞ is estimated from the relation $\varepsilon_r^\infty = 1.1 n_D^2$ [108]. μ represents the dipole moment of the solution, estimated from the equation [29]:

$$\mu^2 = x_1 \mu_1^2 + x_2 \mu_2^2 \quad \text{(B.10)}$$

where μ_i stands for the dipole moment of component i (= 1,2). Calculations have been performed using smoothed values of V_m^E [5], n_D^E (this work) and ε_r^E (this work) at $\Delta x_1 = 0.01$. The source and values of μ_i are collected in Table B.2.

We compare the g_K curves obtained from methanol or 1-heptanol + isomeric amine in Figure B.8. Except for values of ϕ_1 very close to zero, where the structure of the mixture is basically that of the pure amine, it is found that g_K (DPA) > g_K (TEA) > g_K (HxA). In order to examine these results, we provide some g_K values for 1-alkanol + amine mixtures. Thus, g_K (1-propanol) = 2.72 (DPA) > 2.32 (HxA) > 1.87 (propan-1-amine), and g_K (1-butanol) = 2.60 (DPA) > 2.16 (HxA) > 1.72 (butan-1-amine). In addition, g_K (1-propanol, 303.15 K) = 1.54 (aniline) < 1.71 (*N*-methylaniline). This points out that parallel alignment of molecular dipoles has a lower weight in those systems characterized by larger solvation effects and, according to our previous description of ε_r^E, these cooperative effects will lead to a lower polarization of the mixture. This underlines the lower contribution to the mixture structure from alkanol-alkanol interactions in systems with larger solvation effects, and suggests the presence of cyclic species in such systems. The g_K results for the methanol + DPA mixture deserve a comment. We note that g_K rapidly increases with ϕ_1, and that it is nearly constant from $\phi_1 = 0.5$ and very close to the value of the neat alcohol. This might occur because the contribution to the mixture polarization arising from interactions between alcohol molecules also increases rapidly with ϕ_1 in such a way that interactions between unlike molecules contribute to g_K to a lower extent. It is remarkable that g_K changes more smoothly with ϕ_1 for the methanol + HxA system, in agreement with our analysis of ε_r^E results. For 1-alkanol + TEA systems, g_K = 2.73 (n = 1), 2.47 (n = 3), 2.38 (n = 4), 2.30 (n = 5), 2.13 (n = 7) (see Figure B.S3). For n = 1, the g_K curve remains nearly constant from $\phi_1 > 0.7$. It is quite clear that TEA mixtures show an intermediate behavior, which could be due to the existence of a higher proportion of shorter linear-like multimers of 1-alkanol molecules which are less present in the systems with HxA.

The excess Kirkwood correlation factors ($g_K^E = g_K - g_K^{id}$, where g_K^{id} is obtained replacing real by ideal quantities in equation (B.9)) of 1-alkanol + TEA mixtures are: –0.03 (n = 1), –0.58 (n = 3), –0.76 (n = 4), –0.85 (n = 5), –0.84 (n = 7). Their curves are plotted in Figure B.S4. The variation of the minimum of the curves as n increases is not the same as the one encountered for ε_r^E, and it occurs at lower values of ϕ_1. The model consequently indicates that the variation of the structure of the dipoles in the mixing process is only one of the factors that determine the

ε_r^E minima. The g_K^E values are compared with the corresponding ones of 1-alkanol + HxA or DPA systems in Figure B.S5. The trend of g_K^E(TEA) is slightly deviated from the parallel behavior of g_K^E(HxA) and g_K^E(DPA). This underlines the stronger structural effects already mentioned in the former mixtures.

B.5. Conclusions

Measurements of ε_r and n_D have been reported for the 1-alkanol + TEA mixtures at (293.15-303.15) K. Positive ε_r^E results are encountered only for the methanol system at high ϕ_1 values. ε_r^E changes in the sequence: methanol > 1-propanol > 1-butanol < 1-pentanol < 1-heptanol. This variation is similar to 1-alkanol + HxA, or + DPA or + cyclohexylamine. It has been shown that: (i) (1-alkanol)-TEA interactions contribute positively to ε_r^E; (ii) TEA is a good breaker of the 1-alkanol self-association; (iii) structural effects are relevant for ε_r data. (iv) the aromaticity effect leads to an increase of the mixture polarization, and it is opposite to the effect encountered when considering 1-alkanol + HxA, or + aniline mixtures. The application of the Kirkwood-Fröhlich model supports these statements.

B.6. Supplementary material

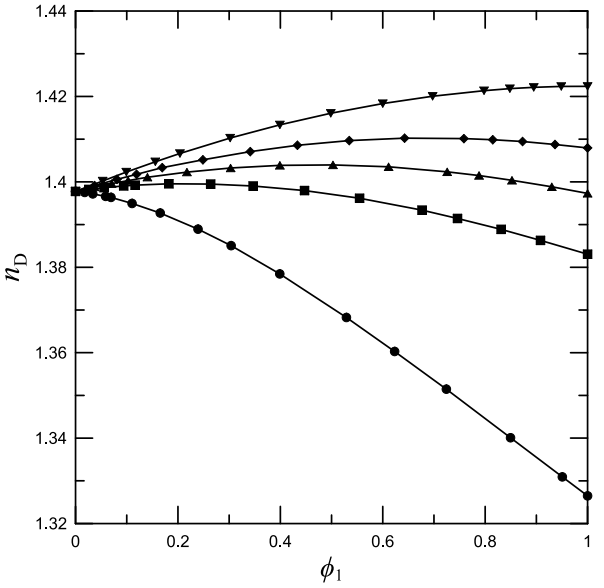

Figure B.S1: Refractive index at the sodium D-line, n_D, of 1-alkanol (1) + TEA (2) liquid mixtures as a function of the 1-alkanol volume fraction, ϕ_1, at 0.1 MPa, 298.15 K. Full symbols, experimental values (this work): (●), methanol; (■), 1-propanol; (▲), 1-butanol; (♦), 1-pentanol; (▼), 1-heptanol.

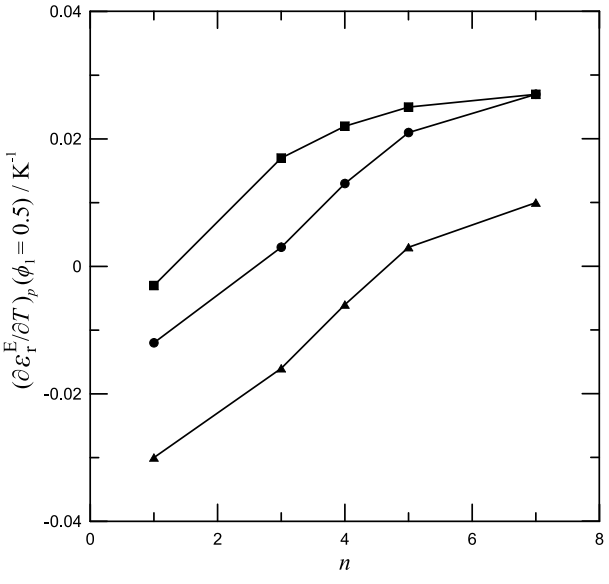

Figure B.S2: Temperature derivative of the excess relative permittivity, $\left(\partial\varepsilon_r^E / \partial T\right)_p$, at $\phi_1 = 0.5$ of 1-alkanol (1) + amine (2) liquid mixtures as a function of the number of carbon atoms of the 1-alkanol, n, at 0.1 MPa, 298.15 K and 1 MHz: (●), HxA [27]; (▲), DPA [28]; (■), TEA (this work).

Table B.S1. Volume fraction of 1-alkanol, ϕ_1, and derivative of the excess relative permittivity at frequency ν = 1 MHz, $\left(\partial\varepsilon_r^E/\partial T\right)_p$, of 1-alkanol (1) + *N,N,N*-triethylamine (TEA) (2) liquid mixtures as functions of the mole fraction of the 1-alkanol, x_1, at temperature T and pressure p = 0.1 MPa. [a]

x_1	ϕ_1	$(\partial\varepsilon_r^E/\partial T)_p$ / K^{-1}	x_1	ϕ_1	$(\partial\varepsilon_r^E/\partial T)_p$ / K^{-1}
		methanol (1) + TEA (2) ; T/K = 298.15			
0.0580	0.0176	0.0008	0.5979	0.3019	0.0019
0.0878	0.0272	0.0011	0.7096	0.4154	0.0000
0.1593	0.0522	0.0025	0.7992	0.5365	–0.0041
0.1981	0.0670	0.0027	0.8445	0.6123	–0.0056
0.2880	0.1053	0.0032	0.8997	0.7229	–0.0055
0.3971	0.1608	0.0038	0.9515	0.8509	–0.0043
0.4959	0.2224	0.0034	0.9856	0.9522	–0.0007
		1-propanol (1) + TEA (2) ; T/K = 298.15			
0.0476	0.0261	0.0023	0.6027	0.4488	0.0171
0.0932	0.0523	0.0038	0.6997	0.5557	0.0162
0.1394	0.0800	0.0056	0.7966	0.6776	0.0143
0.2032	0.1204	0.0079	0.8455	0.7460	0.0121
0.2896	0.1795	0.0106	0.9014	0.8307	0.0069
0.4084	0.2704	0.0145	0.9484	0.9080	0.0047
0.5043	0.3532	0.0165			
		1-butanol (1) + TEA (2) ; T/K = 298.15			
0.0536	0.0359	0.0026	0.6006	0.4969	0.0222
0.1102	0.0752	0.0054	0.6985	0.6034	0.0225
0.1536	0.1065	0.0077	0.8023	0.7272	0.0187
0.2025	0.1429	0.0098	0.8438	0.7801	0.0156
0.2941	0.2148	0.0135	0.8910	0.8430	0.0120
0.3957	0.3007	0.0177	0.9475	0.9222	0.0074
0.5082	0.4043	0.0209			
		1-pentanol (1) + TEA (2) ; T/K = 298.15			
0.0588	0.0463	0.0035	0.5968	0.5347	0.0256
0.1062	0.0844	0.0057	0.7072	0.6522	0.0255
0.1482	0.1190	0.0082	0.7960	0.7518	0.0220
0.2159	0.1761	0.0119	0.8517	0.8168	0.0180
0.3011	0.2506	0.0159	0.8939	0.8674	0.0142
0.4089	0.3494	0.0207	0.9465	0.9321	0.0071
0.5014	0.4384	0.0236			
		1-heptanol (1) + TEA (2) ; T/K = 298.15			
0.0451	0.0457	0.0030	0.5950	0.5982	0.0292
0.1029	0.1041	0.0067	0.6948	0.6976	0.0292
0.1466	0.1483	0.0098	0.7925	0.7947	0.0258
0.1997	0.2019	0.0126	0.8478	0.8495	0.0223
0.2979	0.3007	0.0183	0.8982	0.8994	0.0158

0.3963	0.3995	0.0227	0.9465	0.9472	0.0091
0.4950	0.4984	0.0267			

[a] The standard uncertainties are: $u(T) = 0.02$ K; $u(p) = 1$ kPa; $u(\nu) = 20$ Hz; $u(x_1) = 0.0010$; $u(\phi_1) = 0.004$; $u\left[(\partial\varepsilon_r^E/\partial T)_p\right] = 0.0008$ K^{-1}.

Table B.S2. Values of the derivative of permittivity with respect to temperature for pure compounds, $\left(\partial\varepsilon_r^*/\partial T\right)_p$, and for mixtures, $\left(\partial\varepsilon_r/\partial T\right)_p$, at $\phi_1 = 0.5$ (ϕ_1, volume fraction of the 1-alkanol), temperature $T = 298.15$ K and pressure $p = 0.1$ MPa. [a]

Compound	$\left(\partial\varepsilon_r^*/\partial T\right)_p$ /K^{-1}		$\left(\partial\varepsilon_r/\partial T\right)_p$ /K^{-1}		
	Exp.	Lit.	1-alkanol + HxA [27]	1-alkanol + DPA [28]	1-alkanol + TEA
Methanol	–0.192	–0.195 [52]	–0.110	–0.131	–0.100
1-propanol	–0.136	–0.130 [109]	–0.076	–0.094	–0.053
1-butanol	–0.127	–0.122 [109]	–0.060	–0.077	–0.043
1-pentanol	–0.117	–0.110 [109]	–0.044	–0.062	–0.034
1-heptanol	–0.099	–0.096 [109]	–0.023	–0.044	–0.023

[a] hexan-1-amine (HxA), *N*-propylpropan-1-amine (DPA), *N,N,N*-triethylamine (TEA).

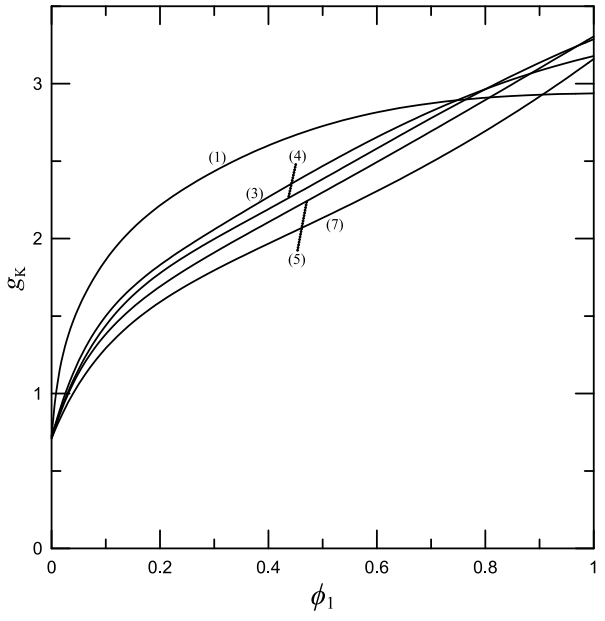

Figure B.S3: Kirkwood correlation factor, g_K, of 1-alkanol (1) + TEA (2) liquid mixtures as a function of the 1-alkanol volume fraction, ϕ_1, at 0.1 MPa, 298.15 K. Numbers in parentheses indicate the number of carbon atoms of the 1-alkanol.

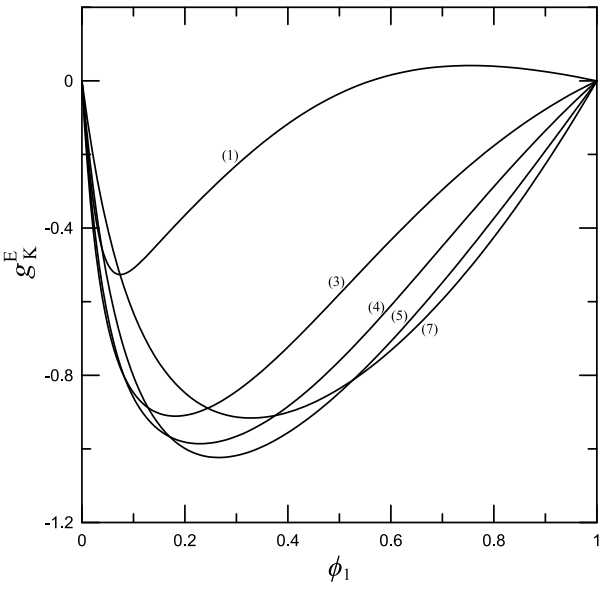

Figure B.S4: Excess Kirkwood correlation factor, g_K^E, of 1-alkanol (1) + TEA (2) liquid mixtures as a function of the 1-alkanol volume fraction, ϕ_1, at 0.1 MPa, 298.15 K. Numbers in parentheses indicate the number of carbon atoms of the 1-alkanol.

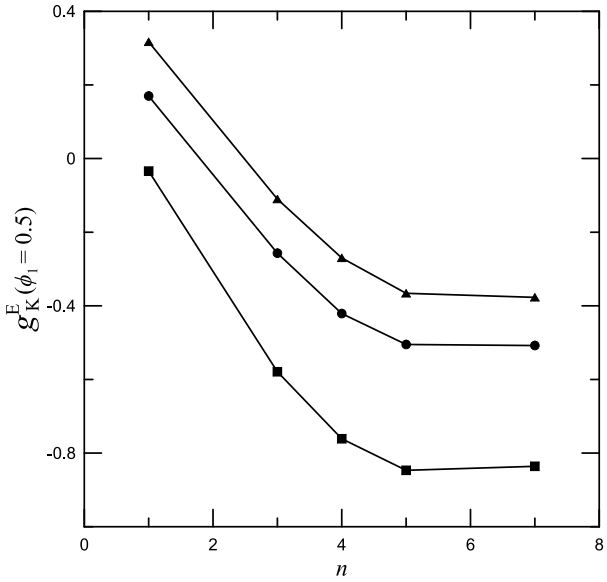

Figure B.S5: Excess Kirkwood correlation factor at $\phi_1 = 0.5$ (ϕ_1 , 1-alkanol volume fraction) of 1-alkanol (1) + amine (2) liquid mixtures as a function of the number of carbon atoms of the 1-alkanol, at 0.1 MPa, 298.15 K: (●), HxA [27]; (▲), DPA [28]; (■), TEA (this work).

B.7. Acknowledgements

F. Hevia and A. Cobos are grateful to Ministerio de Educación, Cultura y Deporte for the grants FPU14/04104 and FPU15/05456 respectively.

B.8. References

[1] J.A. González, I. García de la Fuente, J.C. Cobos, *Thermodynamics of mixtures with strongly negative deviations from Raoult's Law: Part 4. Application of the DISQUAC model to mixtures of 1-alkanols with primary or secondary linear amines. Comparison with Dortmund UNIFAC and ERAS results.* Fluid Phase Equilib. **168** (2000) 31-58. https://doi.org/10.1016/S0378-3812(99)00326-X

[2] K. Nakanishi, H. Shirai, T. Minamiyama, *Vapor-liquid equilibrium of binary systems containing alcohols. Methanol with aliphatic amines.* J. Chem. Eng. Data **12** (1967) 591-594. https://doi.org/10.1021/je60035a031

[3] A. Heintz, D. Papaioannou, *Excess enthalpies of alcohol+amine mixtures. Experimental results and theoretical description using the ERAS-model.* Thermochim. Acta **310** (1998) 69-76. https://doi.org/10.1016/S0040-6031(97)00224-4

[4] A. Heintz, *A New Theoretical Approach for Predicting Excess Properties of Alkanol/Alkane Mixtures.* Ber. Bunsenges. Phys. Chem. **89** (1985) 172-181. https://doi.org/10.1002/bbpc.19850890217

[5] S. Villa, N. Riesco, I. García de la Fuente, J.A. González, J.C. Cobos, *Thermodynamics of mixtures with strongly negative deviations from Raoult's law. Part 8. Excess molar volumes at 298.15 K for 1-alkanol + isomeric amine (C6H15N) systems:*

Characterization in terms of the ERAS model. Fluid Phase Equilib. **216** (2004) 123-133. https://doi.org/10.1016/j.fluid.2003.10.008

[6] J.A. González, I.G. de la Fuente, J.C. Cobos, *Thermodynamics of mixtures with strongly negative deviations from Raoult's law. Part 3. Application of the DISQUAC model to mixtures of triethylamine with alkanols. Comparison with Dortmund UNIFAC and ERAS results.* Can. J. Chem. **78** (2000) 1272-1284. https://doi.org/10.1139/v00-114

[7] S. Villa, N. Riesco, I. García de la Fuente, J.A. González, J.C. Cobos, *Thermodynamics of mixtures with strongly negative deviations from Raoult's law: Part 5. Excess molar volumes at 298.15 K for 1-alkanols+dipropylamine systems: characterization in terms of the ERAS model.* Fluid Phase Equilib. **190** (2001) 113-125. https://doi.org/10.1016/S0378-3812(01)00595-7

[8] S. Villa, N. Riesco, I. García de la fuente, J.A. González, J.C. Cobos, *Thermodynamics of mixtures with strongly negative deviations from Raoult's law: Part 6. Excess molar volumes at 298.15 K for 1-alkanols + dibutylamine systems. Characterization in terms of the ERAS model.* Fluid Phase Equilib. **198** (2002) 313-329. https://doi.org/10.1016/S0378-3812(01)00808-1

[9] K.W. Chun, R.R. Davison, *Thermodynamic properties of binary mixtures of triethylamine with methyl and ethyl alcohol.* J. Chem. Eng. Data **17** (1972) 307-310. https://doi.org/10.1021/je60054a039

[10] A. Chand, D.V. Fenby, *Thermodynamic properties of alcohol-amine mixtures: excess enthalpies of methanol-triethylamine and ethanol-triethylamine.* J. Chem. Eng. Data **22** (1977) 289-290. https://doi.org/10.1021/je60074a016

[11] T.J.V. Findlay, *The Heat of Mixing for Binary Mixtures of Triethylamine with Alcohols.* Aust. J. Chem. **14** (1961) 520-526. https://doi.org/10.1071/CH9610520

[12] M. Bender, J. Hauser, A. Heintz, *Thermodynamics of the Ternary Mixture Propan-1-ol + Triethylamine + n-Heptane. Experimental Results and ERAS-Model Calculations of HE and VE.* Ber. Bunsenges. Phys. Chem. **95** (1991) 801-811. https://doi.org/10.1002/bbpc.19910950708

[13] J.A. González, I. Mozo, I. García de la Fuente, J.C. Cobos, *Thermodynamics of organic mixtures containing amines. IV. Systems with aniline.* Can. J. Chem. **83** (2005) 1812-1825. https://doi.org/10.1139/v05-190

[14] J.A. González, I. Mozo, I.G.d.l. Fuente, J.C. Cobos, *Thermodynamics of organic mixtures containing amines: V. Systems with pyridines.* Thermochim. Acta **441** (2006) 53-68. https://doi.org/10.1016/j.tca.2005.11.027

[15] J.A. González, I.G. de la Fuente, I. Mozo, J.C. Cobos, N. Riesco, *Thermodynamics of Organic Mixtures Containing Amines. VII. Study of Systems Containing Pyridines in Terms of the Kirkwood−Buff Formalism.* Ind. Eng. Chem. Res. **47** (2008) 1729-1737. https://doi.org/10.1021/ie071226e

[16] J.A. González, J.C. Cobos, I. García de la Fuente, I. Mozo, *Thermodynamics of mixtures containing amines. IX. Application of the concentration–concentration structure factor to the study of binary mixtures containing pyridines.* Thermochim. Acta **494** (2009) 54-64. https://doi.org/10.1016/j.tca.2009.04.017

[17] H.V. Kehiaian, *Group contribution methods for liquid mixtures: A critical review.* Fluid Phase Equilib. **13** (1983) 243-252. https://doi.org/10.1016/0378-3812(83)80098-3

[18] J.A. González, I. García de la Fuente, J.C. Cobos, *Correlation and prediction of excess molar enthalpies using DISQUAC*, in *Enthalpy and Internal Energy: Liquids, Solutions*

and Vapours, E. Wilhelm and T.M. Letcher, Editors. 2017, Royal Society of Chemistry: Croydon. p. 543-568.

[19] J.C. Cobos, *An exact quasi-chemical equation for excess heat capacity with W-shaped concentration dependence.* Fluid Phase Equilib. **133** (1997) 105-127. https://doi.org/10.1016/S0378-3812(97)00012-5

[20] R.G. Rubio, M. Cáceres, R.M. Masegosa, L. Andreolli-Ball, M. Costas, D. Patterson, *Mixtures with "w-Shape" CEp curves. A light scattering study.* Ber. Bunsenges. Phys. Chem. **93** (1989) 48-56. https://doi.org/10.1002/bbpc.19890930110

[21] J.G. Kirkwood, F.P. Buff, *The Statistical Mechanical Theory of Solutions. I.* J. Chem. Phys. **19** (1951) 774-777. https://doi.org/10.1063/1.1748352

[22] S. Villa, R. Garriga, P. Pérez, M. Gracia, J.A. González, I.G. de la Fuente, J.C. Cobos, *Thermodynamics of mixtures with strongly negative deviations from Raoult's law: Part 9. Vapor–liquid equilibria for the system 1-propanol + di-n-propylamine at six temperatures between 293.15 and 318.15 K.* Fluid Phase Equilib. **231** (2005) 211-220. https://doi.org/10.1016/j.fluid.2005.01.013

[23] L.F. Sanz, J.A. González, I. García De La Fuente, J.C. Cobos, *Thermodynamics of mixtures with strongly negative deviations from Raoult's law. XI. Densities, viscosities and refractives indices at (293.15–303.15) K for cyclohexylamine + 1-propanol, or +1-butanol systems.* J. Mol. Liq. **172** (2012) 26-33. https://doi.org/10.1016/j.molliq.2012.05.003

[24] L.F. Sanz, J.A. González, I. García de la Fuente, J.C. Cobos, *Thermodynamics of mixtures with strongly negative deviations from Raoult's law. XII. Densities, viscosities and refractive indices at T = (293.15 to 303.15) K for (1-heptanol, or 1-decanol + cyclohexylamine) systems. Application of the ERAS model to (1-alkanol + cyclohexylamine) mixtures.* J. Chem. Thermodyn. **80** (2015) 161-171. https://doi.org/10.1016/j.jct.2014.09.005

[25] L.F. Sanz, J.A. González, I.G. De La Fuente, J.C. Cobos, *Thermodynamics of mixtures with strong negative deviations from raoult's law. XIV. density, permittivity, refractive index and viscosity data for the methanol + cyclohexylamine mixture at (293.15–303.15) K.* Thermochim. Acta **631** (2016) 18-27. https://doi.org/10.1016/j.tca.2016.03.002

[26] J.A. González, L.F. Sanz, I. García de la Fuente, J.C. Cobos, *Thermodynamics of mixtures with strong negative deviations from Raoult's law. XIII. Relative permittivities for (1-alkanol + cyclohexylamine) systems, and dielectric study of (1-alkanol + polar) compound (amine, amide or ether) mixtures.* J. Chem. Thermodyn. **91** (2015) 267-278. https://doi.org/10.1016/j.jct.2015.07.032

[27] F. Hevia, J.A. González, A. Cobos, I. García de la Fuente, C. Alonso-Tristán, *Thermodynamics of mixtures with strongly negative deviations from Raoult's law. XV. Permittivities and refractive indices for 1-alkanol + n-hexylamine systems at (293.15–303.15) K. Application of the Kirkwood-Fröhlich model.* Fluid Phase Equilib. **468** (2018) 18-28. https://doi.org/10.1016/j.fluid.2018.04.007

[28] F. Hevia, A. Cobos, J.A. González, I. García de la Fuente, L.F. Sanz, *Thermodynamics of mixtures with strongly negative deviations from Raoult's law. XVI. Permittivities and refractive indices for 1-alkanol + di-n-propylamine systems at (293.15–303.15) K. Application of the Kirkwood-Fröhlich model.* J. Mol. Liq. **271** (2018) 704-714. https://doi.org/10.1016/j.molliq.2018.09.040

[29] J.C.R. Reis, T.P. Iglesias, *Kirkwood correlation factors in liquid mixtures from an extended Onsager-Kirkwood-Frohlich equation.* Phys. Chem. Chem. Phys. **13** (2011) 10670-10680. https://doi.org/10.1039/C1CP20142E

[30] H. Fröhlich, *Theory of Dielectrics.* Clarendon Press, Oxford, 1958.

[31] C. Moreau, G. Douhéret, *Thermodynamic and physical behaviour of water + acetonitrile mixtures. Dielectric properties.* J. Chem. Thermodyn. **8** (1976) 403-410. https://doi.org/10.1016/0021-9614(76)90060-4

[32] A. Chelkowski, *Dielectric Physics.* Elsevier, Amsterdam, 1980.

[33] C.A. Hunter, S. Tomas, *Cooperativity, Partially Bound States, and Enthalpy-Entropy Compensation.* Chem. Biol. **10** (2003) 1023-1032. https://doi.org/10.1016/j.chembiol.2003.10.009

[34] S.K. Silverman, T.R. Cech, *Energetics and Cooperativity of Tertiary Hydrogen Bonds in RNA Structure.* Biochemistry **38** (1999) 8691-8702. https://doi.org/10.1021/bi9906118

[35] T. Steiner, *The Hydrogen Bond in the Solid State.* Angew. Chem. Int. Ed. **41** (2002) 48-76. https://doi.org/10.1002/1521-3773(20020104)41:1<48::AID-ANIE48>3.0.CO;2-U

[36] A. Karpfen, *Cooperative Effects in Hydrogen Bonding*, in *Advances in Chemical Physics*, I. Prigogine and S.A. Rice, Editors. 2002. p. 569-510.

[37] N.M. Luscombe, R.A. Laskowski, J.M. Thornton, *Amino acid–base interactions: a three-dimensional analysis of protein–DNA interactions at an atomic level.* Nucleic Acids Res. **29** (2001) 2860-2874. https://doi.org/10.1093/nar/29.13.2860

[38] D.L. Nelson, M.M. Cox, *Lehninger Principles of Biochemistry.* 3rd ed., Worth Publishing, New York, 2000.

[39] Y. Coulier, A. Lowe, P.R. Tremaine, J.Y. Coxam, K. Ballerat-Busserolles, *Absorption of CO2 in aqueous solutions of 2-methylpiperidine: Heats of solution and modeling.* Int. J. Greenh. Gas Control **47** (2016) 322-329. https://doi.org/10.1016/j.ijggc.2016.02.009

[40] M. Götz, R. Reimert, S. Bajohr, H. Schnetzer, J. Wimberg, T.J.S. Schubert, *Long-term thermal stability of selected ionic liquids in nitrogen and hydrogen atmosphere.* Thermochim. Acta **600** (2015) 82-88. https://doi.org/10.1016/j.tca.2014.11.005

[41] CIAAW, *Atomic weights of the elements 2015.* ciaaw.org/atomic-weights.htm (accessed 2015)

[42] M. El-Hefnawy, K. Sameshima, T. Matsushita, R. Tanaka, *Apparent Dipole Moments of 1-Alkanols in Cyclohexane and n-Heptane, and Excess Molar Volumes of (1-Alkanol + Cyclohexane or n-Heptane) at 298.15 K.* J. Solution Chem. **34** (2005) 43-69. https://doi.org/10.1007/s10953-005-2072-1

[43] R.D. Bezman, E.F. Casassa, R.L. Kay, *The temperature dependence of the dielectric constants of alkanols.* **73–74** (1997) 397-402. https://doi.org/10.1016/S0167-7322(97)00082-2

[44] J. Canosa, A. Rodríguez, J. Tojo, *Binary mixture properties of diethyl ether with alcohols and alkanes from 288.15 K to 298.15 K.* Fluid Phase Equilib. **156** (1999) 57-71. https://doi.org/10.1016/S0378-3812(99)00032-1

[45] G.J. Janz, R.P.T. Tomkins, *Nonaqueus Electrolytes Handbook, Vol. 1.* Academic Press, New York, 1972.

[46] S.P. Serbanovic, M.L. Kijevcanin, I.R. Radovic, B.D. Djordjevic, *Effect of temperature on the excess molar volumes of some alcohol + aromatic mixtures and modelling by cubic EOS mixing rules.* Fluid Phase Equilib. **239** (2006) 69-82. https://doi.org/10.1016/j.fluid.2005.10.022

[47] S. Chen, Q. Lei, W. Fang, *Density and Refractive Index at 298.15 K and Vapor−Liquid Equilibria at 101.3 kPa for Four Binary Systems of Methanol, n-Propanol, n-Butanol, or Isobutanol with N-Methylpiperazine.* J. Chem. Eng. Data **47** (2002) 811-815. https://doi.org/10.1021/je010249b

[48] M.I. Aralaguppi, C.V. Jadar, T.M. Aminabhavi, *Density, Viscosity, Refractive Index, and Speed of Sound in Binary Mixtures of Acrylonitrile with Methanol, Ethanol, Propan-1-ol, Butan-1-ol, Pentan-1-ol, Hexan-1-ol, Heptan-1-ol, and Butan-2-ol.* J. Chem. Eng. Data **44** (1999) 216-221. https://doi.org/10.1021/je9802219

[49] R. Anwar Naushad, S. Yasmeen, *Volumetric, compressibility and viscosity studies of binary mixtures of [EMIM][NTf2] with ethylacetate/methanol at (298.15–323.15) K.* J. Mol. Liq. **224, Part A** (2016) 189-200. https://doi.org/10.1016/j.molliq.2016.09.077

[50] S.M. Pereira, T.P. Iglesias, J.L. Legido, L. Rodríguez, J. Vijande, *Changes of refractive index on mixing for the binary mixtures {xCH3OH+(1−x) CH3OCH2(CH2OCH2)3CH2OCH3} and {xCH3OH+(1−x)CH3OCH2(CH2OCH2)nCH2OCH3} (n=3–9) at temperatures from 293.15 K to 333.15 K.* J. Chem. Thermodyn. **30** (1998) 1279-1287. https://doi.org/10.1006/jcht.1998.0395

[51] A. Rodríguez, J. Canosa, J. Tojo, *Density, Refractive Index, and Speed of Sound of Binary Mixtures (Diethyl Carbonate + Alcohols) at Several Temperatures.* J. Chem. Eng. Data **46** (2001) 1506-1515. https://doi.org/10.1021/je010148d

[52] A.P. Gregory, R.N. Clarke, *Traceable measurements of the static permittivity of dielectric reference liquids over the temperature range 5–50 °C.* Meas. Sci. Technol. **16** (2005) 1506-1516. https://doi.org/10.1088/0957-0233/16/7/013

[53] M.J. Fontao, M. Iglesias, *Effect of Temperature on the Refractive Index of Aliphatic Hydroxilic Mixtures (C2–C3).* Int. J. Thermophys. **23** (2002) 513-527. https://doi.org/10.1023/A:1015113604024

[54] J.L. Hales, J.H. Ellender, *Liquid densities from 293 to 490 K of nine aliphatic alcohols.* J. Chem. Thermodyn. **8** (1976) 1177-1184. https://doi.org/10.1016/0021-9614(76)90126-9

[55] N.G. Tsierkezos, I.E. Molinou, A.C. Filippou, *Thermodynamic Properties of Binary Mixtures of Cyclohexanone with n-Alkanols (C1–C5) at 293.15 K.* J. Solution Chem. **34** (2005) 1371-1386. https://doi.org/10.1007/s10953-005-8508-9

[56] C. Yang, H. Lai, Z. Liu, P. Ma, *Density and Viscosity of Binary Mixtures of Diethyl Carbonate with Alcohols at (293.15 to 363.15) K and Predictive Results by UNIFAC-VISCO Group Contribution Method.* J. Chem. Eng. Data **51** (2006) 1345-1351. https://doi.org/10.1021/je0600808

[57] C.P. Smyth, W.N. Stoops, *The dielectric polarization of liquids. VI. Ethyl iodide, ethanol, normal-butanol and normal-octanol.* J. Am. Chem. Soc. **51** (1929) 3312-3329. https://doi.org/10.1021/ja01386a019

[58] B. Giner, A. Villares, M.C. López, F.M. Royo, C. Lafuente, *Refractive indices and molar refractions for isomeric chlorobutanes with isomeric butanols.* Phys. Chem. Liq. **43** (2005) 13-23. https://doi.org/10.1080/00319100420003035l8

[59] E. Jiménez, M. Cabanas, L. Segade, S. García-Garabal, H. Casas, *Excess volume, changes of refractive index and surface tension of binary 1,2-ethanediol + 1-propanol or 1-butanol mixtures at several temperatures.* Fluid Phase Equilib. **180** (2001) 151-164. https://doi.org/10.1016/S0378-3812(00)00519-7

[60] G.A. Iglesias-Silva, A. Guzmán-López, G. Pérez-Durán, M. Ramos-Estrada, *Densities and Viscosities for Binary Liquid Mixtures of n-Undecane + 1-Propanol, + 1-Butanol,*

+ 1-Pentanol, and + 1-Hexanol from 283.15 to 363.15 K at 0.1 MPa. J. Chem. Eng. Data **61** (2016) 2682-2699. https://doi.org/10.1021/acs.jced.6b00121

[61] T.P. Iglesias, J.L. Legido, S.M. Pereira, B. de Cominges, M.I. Paz Andrade, *Relative permittivities and refractive indices on mixing for (n-hexane + 1-pentanol, or 1-hexanol, or 1-heptanol) atT = 298.15 K.* J. Chem. Thermodyn. **32** (2000) 923-930. https://doi.org/10.1006/jcht.2000.0661

[62] M.N.M. Al-Hayan, *Densities, excess molar volumes, and refractive indices of 1,1,2,2-tetrachloroethane and 1-alkanols binary mixtures.* J. Chem. Thermodyn. **38** (2006) 427-433. https://doi.org/10.1016/j.jct.2005.06.015

[63] S.P. Patil, A.S. Chaudhari, M.P. Lokhande, M.K. Lande, A.G. Shankarwar, S.N. Helambe, B.R. Arbad, S.C. Mehrotra, *Dielectric Measurements of Aniline and Alcohol Mixtures at 283, 293, 303, and 313 K Using the Time Domain Technique.* J. Chem. Eng. Data **44** (1999) 875-878. https://doi.org/10.1021/je980250j

[64] Á. Piñeiro, P. Brocos, A. Amigo, M. Pintos, R. Bravo, *Refractive Indexes of Binary Mixtures of Tetrahydrofuran with 1-Alkanols at 25°C and Temperature Dependence of n and ϱ for the Pure Liquids.* J. Solution Chem. **31** (2002) 369-380. https://doi.org/10.1023/A:1015807331250

[65] J.J. Cano-Gómez, G.A. Iglesias-Silva, E.O. Castrejón-González, M. Ramos-Estrada, K.R. Hall, *Density and Viscosity of Binary Liquid Mixtures of Ethanol + 1-Hexanol and Ethanol + 1-Heptanol from (293.15 to 328.15) K at 0.1 MPa.* J. Chem. Eng. Data **60** (2015) 1945-1955. https://doi.org/10.1021/je501133u

[66] U. Domańska, M. Królikowska, *Density and Viscosity of Binary Mixtures of {1-Butyl-3-methylimidazolium Thiocyanate + 1-Heptanol, 1-Octanol, 1-Nonanol, or 1-Decanol}.* J. Chem. Eng. Data **55** (2010) 2994-3004. https://doi.org/10.1021/je901043q

[67] S.C. Srivastava, A. Khare, Natl. Acad. Sci. Lett. **14** (1991) 183 (cf. C. Wohlfahrt, Static Dielectric Constants of Pure Liquids and Binary Liquid Mixtures. Landolt-Börnstein - Group IV Physical Chemistry Vol. 17 (Supplement to IV/6), Springer Berlin Heidelberg, Berlin, 2008).

[68] D.R. Lide, *CRC Handbook of Chemistry and Physics, 90th Edition.* CRC Press/Taylor and Francis, Boca Raton, FL, 2010.

[69] F. Ratkovics, M. László-Parragi, *Measurements of vapour-liquid equilibria, densities, viscosities and dielectric properties of cyclohexanone + triethylamine mixtures with respect to keto-enol tautomerism.* Fluid Phase Equilib. **17** (1984) 97-113. https://doi.org/10.1016/0378-3812(84)80014-X

[70] E. Nowak, Acta Phys. Pol. A **41** (1972) 617 (cf. C. Wohlfahrt, Static Dielectric Constants of Pure Liquids and Binary Liquid Mixtures. Landolt-Börnstein - Group IV Physical Chemistry Vol. 6, Springer Berlin Heidelberg, Berlin, 1991).

[71] C.M. Kinart, W.J. Kinart, D. Checinska-Majak, A. Bald, *Densities and relative permittivities for mixtures of 2-methoxyethanol with DEA and TEA, at various temperatures.* J. Therm. Anal. Calorim. **75** (2004) 347-354. https://doi.org/10.1023/B:JTAN.0000017355.26845.a4

[72] W.J. Kinart, D. Chęcińska-Majak, D. Szychowski, *Refractive properties of binary mixtures containing 2-methoxyethanol and diethylamine, triethylamine, and propylamine AU - Kinart, Cezary M.* Phys. Chem. Liq. **42** (2004) 367-374. https://doi.org/10.1080/00319100420002093 42

[73] N. Tekin, C. Tarimci, *Study of the structure and refractive parameters of diethylamine and triethylamine.* Opt. Laser Technol. **38** (2006) 498-505. https://doi.org/10.1016/j.optlastec.2004.12.006

[74] J.A. Riddick, W.B. Bunger, T.K. Sakano, *Organic solvents: physical properties and methods of purification.* Wiley, New York, 1986.

[75] H.-J. Hörig, W. W. Michel, H.-J. Bittrich, Wiss. Z. Tech. Hochsch. Carl Schorlemmer, Leuna-Merseburg **8** (1966) 298 (cf. C. Wohlfahrt, Static Dielectric Constants of Pure Liquids and Binary Liquid Mixtures. Landolt-Börnstein - Group IV Physical Chemistry Vol. 6, Springer Berlin Heidelberg, Berlin, 1991).

[76] J.N. Nayak, M.I. Aralaguppi, T.M. Aminabhavi, *Density, Viscosity, Refractive Index, and Speed of Sound in the Binary Mixtures of 1,4-Dioxane + Ethanediol, + Hexane, + Tributylamine, or + Triethylamine at (298.15, 303.15, and 308.15) K.* J. Chem. Eng. Data **48** (2003) 1152-1156. https://doi.org/10.1021/je030107c

[77] A. Ali, D. Chand, A.K. Nain, R. Ahmad, *Densities and Refractive Indices of Binary Mixtures of Benzene with Triethylamine and Tributylamine at Different Temperatures.* Int. J. Thermophys. **27** (2006) 1482. https://doi.org/10.1007/s10765-006-0095-5

[78] K.N. Marsh, *Recommended reference materials for the realization of physicochemical properties.* Blackwell Scientific Publications, Oxford, UK, 1987.

[79] J.A. González, I. Alonso, I. Mozo, I. García de la Fuente, J.C. Cobos, *Thermodynamics of (ketone + amine) mixtures. Part VI. Volumetric and speed of sound data at (293.15, 298.15, and 303.15) K for (2-heptanone + dipropylamine, +dibutylamine, or +triethylamine) systems.* J. Chem. Thermodyn. **43** (2011) 1506-1514. https://doi.org/10.1016/j.jct.2011.05.003

[80] V. Alonso, J.A. González, I. García de la Fuente, J.C. Cobos, *Dielectric and refractive index measurements for the systems 1-pentanol + octane, or + dibutyl ether or for dibutyl ether + octane at different temperatures.* Thermochim. Acta **543** (2012) 246-253. https://doi.org/10.1016/j.tca.2012.05.036

[81] J.C.R. Reis, T.P. Iglesias, G. Douhéret, M.I. Davis, *The permittivity of thermodynamically ideal liquid mixtures and the excess relative permittivity of binary dielectrics.* Phys. Chem. Chem. Phys. **11** (2009) 3977-3986. https://doi.org/10.1039/B820613A

[82] J.C.R. Reis, I.M.S. Lampreia, Â.F.S. Santos, M.L.C.J. Moita, G. Douhéret, *Refractive Index of Liquid Mixtures: Theory and Experiment.* ChemPhysChem **11** (2010) 3722-3733. https://doi.org/10.1002/cphc.201000566

[83] O. Redlich, A.T. Kister, *Algebraic Representation of Thermodynamic Properties and the Classification of Solutions.* Ind. & Eng. Chem. **40** (1948) 345-348. https://doi.org/10.1021/ie50458a036

[84] P.R. Bevington, D.K. Robinson, *Data Reduction and Error Analysis for the Physical Sciences.* McGraw-Hill, New York, 2000.

[85] A.L. McClellan, *Tables of Experimental Dipole Moments.* Vols. 1,2,3, Rahara Enterprises, El Cerrito, US, 1974.

[86] R.C. Reid, J.M. Prausnitz, B.E. Poling, *The Properties of Gases and Liquids.* McGraw-Hill, New York, US, 1987.

[87] N.V. Sastry, M.K. Valand, *Densities, Speeds of Sound, Viscosities, and Relative Permittivities for 1-Propanol + and 1-Butanol + Heptane at 298.15 K and 308.15 K.* J. Chem. Eng. Data **41** (1996) 1421-1425. https://doi.org/10.1021/je960135d

[88] N.V. Sastry, M.K. Valand, *Dielectric constants, refractive indexes and polarizations for 1-Alcohol +Heptane mixtures at 298.15 and 308.15 K.* Ber. Bunsenges. Phys. Chem. **101** (1997) 243-250. https://doi.org/10.1002/bbpc.19971010212

[89] A. Skrzecz, *Critical evaluation of solubility data in binary systems formed by methanol with n-hydrocarbons.* Thermochim. Acta **182** (1991) 123-131. https://doi.org/10.1016/0040-6031(91)87013-M

[90] T. Krupkowski, Poznan Tow. Przyj. Nauk. Pr. Kom. Mat. Przyr. Fiz. Dielektr. Radiospektrosk. **5** (1971) 233 (cf. C. Wohlfahrt, Static Dielectric Constants of Pure Liquids and Binary Liquid Mixtures. Landolt-Börnstein - Group IV Physical Chemistry Vol. 6, Springer Berlin Heidelberg, Berlin, 1991).

[91] K.V. Zaitseva, M.A. Varfolomeev, B.N. Solomonov, *Thermodynamic functions of hydrogen bonding of amines in methanol derived from solution calorimetry data and headspace analysis.* Thermochim. Acta **535** (2012) 8-16. https://doi.org/10.1016/j.tca.2012.02.005

[92] A.K.S. Jeevaraj, U. Sankar, *Molecular interactions of triethylamine and 1-dodecanol binary liquid mixtures.* Main Group Chemistry **12** (2013) 251-256. https://doi.org/10.3233/MGC-130105

[93] J. Liszi, T. Salomon, F. Ratkovics, *Properties of alcohol-amine mixtures. II. Static dielectric properties of the binary mixtures propylamine-propanol and butylamine-butanol.* Acta Chim. Acad. Sci. Hung. **81** (1974) 467-474.

[94] V.A. Rana, A.D. Vyas, S.C. Mehrotra, *Dielectric relaxation study of mixtures of 1-propanol with aniline, 2-chloroaniline and 3-chloroaniline at different temperatures using time domain reflectometry.* J. Mol. Liq. **102** (2003) 379-391. https://doi.org/10.1016/S0167-7322(02)00162-9

[95] T.V. Krishna, S.S. Sastry, V.R.K. Murthy, *Correlation studies on dielectric and thermodynamic parameters in the binary mixtures of N-methyl aniline and alcohols.* Indian J. Phys. **85** (2011) 1495-1511. https://doi.org/10.1007/s12648-011-0168-6

[96] S.L. Oswal, H.S. Desai, *Studies of viscosity and excess molar volume of binary mixtures: 3. 1-Alkanol+di-n-propylamine, and+di-n-butylamine mixtures at 303.15 and 313.15 K.* Fluid Phase Equilib. **186** (2001) 81-102. https://doi.org/10.1016/S0378-3812(01)00504-0

[97] R.L. Gardas, S. Oswal, *Volumetric and transport properties of ternary mixtures containing 1-propanol, triethylamine or tri-n-butylamine and cyclohexane at 303.15K: Experimental data, correlation and prediction by ERAS model.* Thermochim. Acta **479** (2008) 17-27. https://doi.org/10.1016/j.tca.2008.09.006

[98] R.L. Gardas, S.L. Oswal, *Volumetric and Transport Properties of Ternary Mixtures Containing 1-Butanol or 1-Pentanol, Triethylamine and Cyclohexane at 303.15 K: Experimental Data, Correlation and Prediction by the ERAS Model.* J. Solution Chem. **37** (2008) 1449. https://doi.org/10.1007/s10953-008-9316-9

[99] D. Papaioannou, C. Panayiotou, *Viscosity of Binary Mixtures of Propylamine with Alkanols at Moderately High Pressures.* J. Chem. Eng. Data **40** (1995) 202-209. https://doi.org/10.1021/je00017a042

[100] D. Papaioannou, M. Bridakis, C.G. Panayiotou, *Excess dynamic viscosity and excess volume of N-butylamine + 1-alkanol mixtures at moderately high pressures.* J. Chem. Eng. Data **38** (1993) 370-378. https://doi.org/10.1021/je00011a010

[101] S.L. Oswal, H.S. Desai, *Studies of viscosity and excess molar volume of binary mixtures.: 1. Propylamine+1-alkanol mixtures at 303.15 and 313.15 K.* Fluid Phase Equilib. **149** (1998) 359-376. https://doi.org/10.1016/S0378-3812(98)00318-5

[102] A. Heintz, P.K. Naicker, S.P. Verevkin, R. Pfestorf, *Thermodynamics of alkanol + amine mixtures. Experimental results and ERAS model calculations of the heat of mixing.* Ber. Bunsenges. Phys. Chem. **102** (1998) 953-959. https://doi.org/10.1002/bbpc.19981020707

[103] P. Brocos, A. Piñeiro, R. Bravo, A. Amigo, *Refractive indices, molar volumes and molar refractions of binary liquid mixtures: concepts and correlations.* Phys. Chem. Chem. Phys. **5** (2003) 550-557. https://doi.org/10.1039/B208765K

[104] M.S. Bakshi, G. Kaur, *Thermodynamic Behavior of Mixtures. 4. Mixtures of Methanol with Pyridine and N,N-Dimethylformamide at 25 °C.* J. Chem. Eng. Data **42** (1997) 298-300. https://doi.org/10.1021/je960300p

[105] F.M. Trivedi, V.A. Rana, *Static permittivity, refractive index, density and related properties of binary mixtures of pyridine and 1-propanol at different temperatures.* Indian J. Pure. Appl. Phys. **52** (2014) 183-191.

[106] O. Dahmani, A. Ait-Kaci, *Diagramme d'equilibre liquide-liquide de systemes binaires pyridine+n-alcanes.* J. Thermal Anal. **44** (1995) 385-393. https://doi.org/10.1007/BF02636129

[107] H. Matsuda, K. Ochi, K. Kojima, *Determination and Correlation of LLE and SLE Data for the Methanol + Cyclohexane, Aniline + Heptane, and Phenol + Hexane System.* J. Chem. Eng. Data **48** (2003) 184-189. https://doi.org/10.1021/je020156+

[108] Y. Marcus, *The structuredness of solvents.* J. Solution Chem. **21** (1992) 1217-1230. https://doi.org/10.1007/bf00667218

[109] T. Shinomiya, *Dielectric Dispersion and Intermolecular Association for 28 Pure Liquid Alcohols. The Position Dependence of Hydroxyl Group in the Hydrocarbon Chain.* Bull. Chem. Soc. Jpn. **62** (1989) 908-914. https://doi.org/10.1246/bcsj.62.908

Appendix C.

Measurement and modeling of enthalpies of solution of SO_2 and NO in water

C.1. Introduction

Carbon dioxide (CO_2) removal from post-combustion industrial effluents will contribute substantially to the reduction of anthropogenic emission of carbon [1]. Indeed, separation of multicomponent gases using CO_2 capture processes is developed to mitigate CO_2 emissions and tackle climate change issues. The recovered carbon dioxide must then be stored in a secure site, such as deep saline aquifers. However, depending on the effluent origin [2] and the selected capture process, the injected CO_2 stream may contain small amounts of associated gaseous components such as O_2, N_2, SO_x, NO_x. These impurities will impact the thermo-physical properties (density, viscosity) and phase diagram behavior of the gas mixture [3] and then, co-injection of such gas impurities with CO_2 will have to be taken into consideration for the development of geological storage processes [4].

Before looking at the effects of the co-injection of multiple gas impurities with CO_2 in geological fluids, we first focus here on the dissolution of SO_2 in water and NO in water. The objective is to select a model capable of predicting solubility and enthalpy of solution as functions of temperature and pressure of the SO_2 + H_2O and NO + H_2O systems. This model will represent the vapor-liquid and chemical equilibria taking into account the non-ideality in liquid and gas phases. Because these are the most available experimental data, the thermodynamic models are generally adjusted with solubility data. Then the enthalpies are essentially derived from solubility data using Van't Hoff relations. Direct measurements of solution enthalpies will make it possible to test the robustness and consistency of the models.

Literature data for enthalpy of solution of SO_2 in water are scarce. The enthalpy of solution was experimentally determined at 298.15 K as a function of loading charge (ratio of the overall amount of substance of SO_2 to that of H_2O) by Stiles and Felsing [5]. Johnstone and Leppla [6] determined ionization constants of sulfurous acid and Henry's law coefficients at temperatures from 273.15 K to 323.15 K. The authors report enthalpies of ionization and enthalpies of solution, derived from the temperature dependence of the ionization constant and Henry's law constant, respectively. No enthalpy data were found for dissolution of NO in water.

In this work, the enthalpies of solution of SO_2 in water have been measured at temperatures 323.15 K and 373.15 K, and around an average pressure of 0.31 MPa. For NO in water, they

have been experimentally determined at temperature 323.15 K and average pressures 2.27 MPa, 2.56 MPa and 2.80 MPa. The measurements were carried out using a flow calorimetry technique previously developed to study hydrogen sulfide (H_2S) dissolution in aqueous solutions [7].

We also represent the vapor-liquid equilibrium of the SO_2 + H_2O system using the thermodynamic model developed by Rumpf and Maurer [8]. The model was assessed using available experimental solubility data [6, 8-21]. A calculation of the enthalpies of solution, based on a derivation of Gibbs energy of solution, has been added to this model to test its ability to represent both solubility and enthalpy data.

On the other hand, the NO + H_2O system was considered to be ideal because of a very low solubility of NO, and vapor-liquid equilibrium was represented by Henry's law. Experimental vapor-liquid equilibrium data of NO in water [22, 23] was used to calculate Henry's law constant, from which the enthalpy of solution can be derived.

C.2. Experimental

C.2.1. Material

Details about the source and purity of the pure compounds are listed in Table C.1. They were used without further purification.

Table C.1. Sample description.

Chemical name	CAS	Source	Purification method	Mole fraction purity
Sulfur dioxide (SO_2)	7446-09-5	Linde (France)	None	≥ 0.998
Nitrogen monoxide (NO)	10102-43-9	Linde (France)	None	≥ 0.998
Water	7732-18-5	Triple distilled and degassed		

C.2.2. Apparatus and procedure

The flow calorimetric technique (Fig. 1) is similar to the one used by Koschel *et al.* [7] for the measurement of the enthalpies of solution of hydrogen sulfide (H_2S) in water. The principle consists of flowing gas and water from two high pressure syringe pumps into a mixing cell, located inside a Calvet-type calorimeter (Setaram C80). The heat power effect during dissolution is detected by a thermopile surrounding the mixing cell. The temperature of the calorimetric block is kept constant by a Setaram G11 Universal Controller with a standard uncertainty of 0.03 K. The pressure is read along the flow line by pressure gauges located at the input and output of the mixing cell (Fig. 1), and its standard uncertainty is 0.02 MPa.

The detected heat power ($\dot{q}$) is proportional to the electromotive force of the thermopile (S), $\dot{q} = K \cdot S$. The temperature-dependent calibration constant (K) is determined by chemical calibration using the reference system ethanol + water [24, 25].

The enthalpy of solution per mol of substance i (i = w for water, and i = SO_2 or NO) is calculated from the equation (C.1), by dividing the heat power by the gas or water molar flow rate, $\dot{n}_i$, which are obtained from the volume flow rates ($\dot{V}_i$) and fluid molar volumes (V_i).

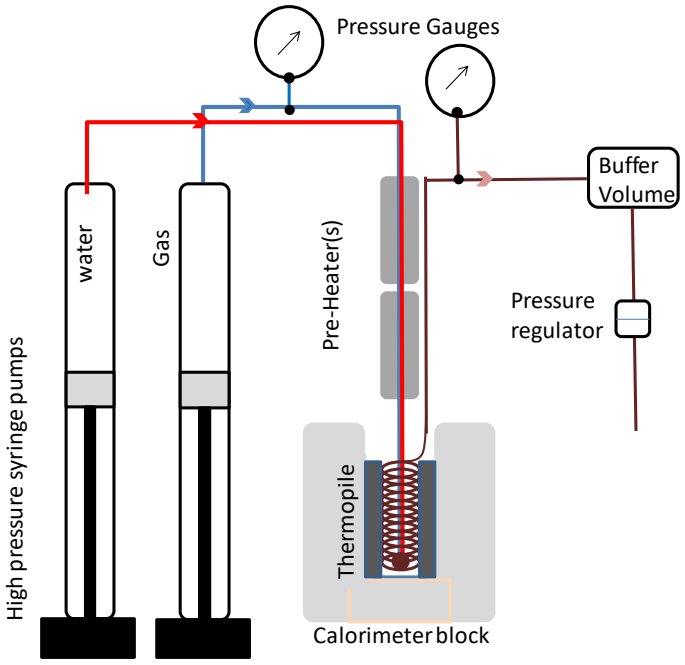

Figure C.1: Schematic representation of the flow calorimetric technique.

$$\Delta_{\mathrm{sol}}H_i = \frac{\dot{q}}{\dot{n}_i} = \frac{\dot{q}\cdot V_i}{\dot{V}_i} \qquad (i = \mathrm{w},\ \mathrm{SO_2}\ \text{or NO}) \tag{C.1}$$

The molar volumes of SO_2 and water were taken from the equations of state recommended by NIST [26, 27]. The molar volume of NO was calculated using the translated-consistent-Peng-Robinson equation of state as described by Le Guennec *et al.* [28].

The enthalpies of solution of SO_2 and NO in water are determined as functions of gas loading charge $\alpha = \dot{n}_{\mathrm{gas}}/\dot{n}_{\mathrm{w}}$, which is the ratio of gas (=SO_2 or NO) molar flow rate ($\dot{n}_{\mathrm{gas}}$) and water molar flow rate ($\dot{n}_{\mathrm{w}}$). The loading charge is related to the overall molality of the gas, $\bar{m}_{\mathrm{gas}} = \alpha/M_{\mathrm{w}}$, where M_{w} is the molar mass of water.

The enthalpy of solution is expressed either per mole of water ($\Delta_{\mathrm{sol}}H_{\mathrm{w}}$) or per mole of gas ($\Delta_{\mathrm{sol}}H_{\mathrm{gas}}$). The representation of the enthalpy of solution per mole of water as a function of the gas loading charge is used for graphical estimation of the gas solubility. Indeed, $\Delta_{\mathrm{sol}}H_{\mathrm{w}}$ increases up to reach a plateau when the solution is gas-saturated. The limit of gas solubility corresponds to the intersection between the part of the curve where the enthalpy increases and the plateau. For a correct determination, the measurements must be carried out below and above the limit of gas solubility. For small gas solubility, the measurements below saturation are restricted by the difficulties to control gas dissolution with small gas volume flow rates. In addition, small gas absorptions are associated to small heat effects, and then high relative uncertainties on the calorimetric signal. In contrast, for systems with high gas solubility, the experimental difficulties are encountered for the measurements in the saturated domain. For a gas loading charge above the limit of solubility, only a part of the gas is absorbed and gas bubbles appear in the mixing cell. It increases the total volume flow rate and the residence time inside the mixing cell may be too short to fully detect the heat effect.

C.3. Dissolution of sulfur dioxide in water

C.3.1. Thermodynamic equations for chemical equilibria and phase equilibria

The non-ideality of the liquid phase is described by means of activity coefficients (γ_i for species i). For liquid water (solvent), γ_w is mole-fraction based and normalized to one for pure water. The γ_i of the rest of the species in the liquid phase (solutes) are based on molalities (m_i), and are normalized to one at infinite dilution in the solvent.

The representation of the dissolution of SO_2 in water implies accounting for the presence of chemical reactions in the liquid phase. The chemical reactions of SO_2 in water [8, 17, 29] are given in equation (I) for first SO_2 dissociation, equation (II) for second SO_2 dissociation; water dissociation is represented by equation (W).

$$SO_2 + H_2O \rightleftarrows HSO_3^- + H^+ \quad \text{(I)}$$

$$HSO_3^- \rightleftarrows SO_3^{2-} + H^+ \quad \text{(II)}$$

$$H_2O \rightleftarrows H^+ + OH^- \quad \text{(W)}$$

The equations for chemical equilibria are given by the law of mass action (equation (C.2)) where a_i and ν_i are the activity and the algebraic stoichiometric coefficient of species i in reaction N, respectively. The equilibrium constants K_N, defined according to the standard states described above, are represented as functions of temperature following equation (C.3); values of coefficients A_N, B_N, C_N and D_N are summarized in Table C.2.

$$K_N = \prod_i a_i^{\nu_i} \qquad \text{with } N = \text{I, II or W} \quad \text{(C.2)}$$

$$\ln K_N = \frac{A_N}{(T/\text{K})} + B_N \cdot \ln(T/\text{K}) + C_N \cdot (T/\text{K}) + D_N \quad \text{(C.3)}$$

Table C.2. Parameters used in equation (C.3) to represent the temperature dependence of equilibrium constants K_N.

Reaction N	A_N	B_N	C_N	D_N	Reference
I	26404.29	160.3981	–0.2752224	–924.6255	[30]
II	–5421.930	4.689868	–0.04987690	43.13158	[30]
W	–13445.9	–22.4773	0	140.932	[29]

The balance equations for the overall amounts $\overline{n}_i$ of sulfur dioxide and water are represented by equations (C.4)-(C.5), where n_i is the amount of component i in the liquid phase at equilibrium.

$$\overline{n}_{SO_2} = n_{SO_2} + n_{HSO_3^-} + n_{SO_3^{2-}} \quad \text{(C.4)}$$

$$\overline{n}_w = n_w + n_{HSO_3^-} + n_{SO_3^{2-}} + n_{OH^-} \quad \text{(C.5)}$$

The charge balance is represented by equation (C.6).

$$n_{H^+} = n_{HSO_3^-} + 2n_{SO_3^{2-}} + n_{OH^-} \tag{C.6}$$

The vapor-liquid equilibria are defined by equations (C.7)-(C.8). All ionic species have been considered as non-volatile.

$$H_2O^{(l)} \rightleftarrows H_2O^{(v)} \tag{C.7}$$

$$SO_2{}^{(l)} \rightleftarrows SO_2{}^{(v)} \tag{C.8}$$

The conservation equation in the vapor phase is expressed by equation (C.9), where y_i is the mole fraction of component i in the vapor.

$$y_{SO_2} + y_w = 1 \tag{C.9}$$

The equations representative of the vapor-liquid equilibrium at temperature T and pressure p are stated using extended Raoult's law (equation (C.10)) for water and extended Henry's law for SO_2 (equation (C.11)).

$$\phi_w y_w p = p_w^s \phi_w^s \exp\left[\frac{V_w\left(p - p_w^s\right)}{RT}\right] a_w \tag{C.10}$$

$$\phi_{SO_2} y_{SO_2} p = H_{SO_2,w} \exp\left[\frac{\bar{V}_{SO_2}^{\infty}\left(p - p_w^s\right)}{RT}\right] m_{SO_2} \gamma_{SO_2} \tag{C.11}$$

The saturation pressure (p_w^s) and molar volume (V_w) of water were taken from recommended equations given by Saul and Wagner [31]. The partial molar volume of SO_2 at infinite dilution in water ($\bar{V}_{SO_2}^{\infty}$) was calculated as a function of temperature (equation (C.12)) using a simple second-order polynomial equation adjusted on values obtained from Brelvi and O'Connell [32] and given in reference [8].

$$\bar{V}_{SO_2}^{\infty} \Big/ \mathrm{cm^3 \cdot mol^{-1}} = 84.2113 - 0.334941 \cdot \left(T/\mathrm{K}\right) + 6.35086 \cdot 10^{-4} \left(T/\mathrm{K}\right)^2 \tag{C.12}$$

The molality-based Henry's law constant of SO_2 in water at the saturation pressure of water ($H_{SO_2,w}$, equation (C.13)) is calculated using the correlation developed by Rumpf and Maurer [8].

$$\begin{aligned} \ln\left[H_{SO_2,w} \Big/ \left(\mathrm{MPa \cdot kg \cdot mol^{-1}}\right)\right] = -154.827 + \frac{321.17}{\left(T/\mathrm{K}\right)} \\ -0.0634 \cdot \left(T/\mathrm{K}\right) + 29.872 \cdot \ln\left(T/\mathrm{K}\right) \end{aligned} \tag{C.13}$$

The vapor phase is represented by a virial equation of state (equation (C.14)), truncated after the second virial coefficient (B).

$$\frac{pV}{RT} = 1 + \frac{Bp}{RT} \tag{C.14}$$

The second virial coefficient of the mixture (B), is calculated (equation (C.15)) from the virial coefficients of the pure components, B_{ii} (i = w, SO_2), and the symmetric cross coefficients B_{ij} (i,j = w, SO_2; and $i \neq j$). The second virial coefficient of pure water was calculated (equation (C.16)) from the correlation of Bieling *et al.* [33].

$$B = \sum_i \sum_j y_i y_j B_{ij} \tag{C.15}$$

$$B_{\mathrm{w,w}} \big/ \mathrm{cm}^3 \cdot \mathrm{mol}^{-1} = -53.53 - 39.29 \cdot \left[\frac{647.3}{(T/\mathrm{K})} \right]^{4.3} \tag{C.16}$$

Mixed second virial coefficients B_{ij} are calculated with the method proposed by Hayden and O'Connell [34]. Pseudocritical temperatures and pressures ($T_{c,i}$, $p_{c,i}$), molecular dipole moments (μ_i), and mean radii of gyration ($R_{\mathrm{D},i}$) of the pure components as well as association parameters (η_{ij}) were taken from reference [34] (Table C.3).

The fugacity coefficients of the components are calculated using equation (C.17).

$$\ln \phi_i = \frac{p}{RT} \left(2 \sum_j y_j B_{ij} - B \right) \tag{C.17}$$

The activity coefficients (γ_i) of the solutes in the liquid phase are calculated (equation (C.18)) using the Pitzer model as modified by Edwards *et al.* [29], where α = 2.0 $\mathrm{kg}^{1/2}\cdot\mathrm{mol}^{-1/2}$, b = 1.2 $\mathrm{kg}^{1/2}\cdot\mathrm{mol}^{-1/2}$, z_i is the charge number of species i, A_ϕ is the Debye-Hückel limiting slope for the osmotic coefficient, and I is the ionic strength (equation (C.19)).

$$\begin{aligned} \ln \gamma_i = & -A_\phi z_i^2 \left[\frac{\sqrt{I}}{1 + b\sqrt{I}} + \frac{2}{b} \ln\left(1 + b\sqrt{I}\right) \right] \\ & + 2 \sum_{j \neq \mathrm{w}} m_j \left\{ \beta_{ij}^{(0)} + \beta_{ij}^{(1)} \frac{2}{\alpha^2 I} \left[1 - \left(1 + \alpha\sqrt{I}\right) \exp\left(-\alpha\sqrt{I}\right) \right] \right\} \\ & - z_i^2 \sum_{j \neq \mathrm{w}} \sum_{k \neq \mathrm{w}} m_j m_k \beta_{jk}^{(1)} \frac{1}{\alpha^2 I^2} \left[1 - \left(1 + \alpha\sqrt{I} + \frac{\alpha^2 I}{2} \right) \exp\left(\alpha\sqrt{I}\right) \right] \\ & + 3 \sum_{j \neq \mathrm{w}} \sum_{k \neq \mathrm{w}} m_j m_k \tau_{ijk} \end{aligned} \tag{C.18}$$

$$I = \frac{1}{2} \sum_{i \neq \mathrm{w}} m_i z_i^2 \tag{C.19}$$

Table C.3. Parameters for the Hayden and O'Connell equation for estimating pure and mixed second virial coefficients.

(a) Pure component parameters: critical temperature ($T_{c,i}$), critical pressure ($p_{c,i}$), dipole moment (μ_i) and radius of gyration ($R_{\mathrm{D},i}$).

Compound	$T_{c,i}$ / K	$p_{c,i}$ / MPa	μ_i / D	$R_{\mathrm{D},i}$ / 10^{-10} m
H_2O	647.3	22.13	1.83	0.615
SO_2	430.7	7.78	1.51	1.674

(b) Parameter η_{ij} for association between molecules i and j

η_{ij}	$j = H_2O$	$j = SO_2$
$i = H_2O$	1.7	0
$i = SO_2$	0	0

A_ϕ /kg$^{1/2}$·mol$^{-1/2}$ is calculated as a function of the temperature using the equation given by Chen *et al.* [35]. $\beta_{ij}^{(0)}$, $\beta_{ij}^{(1)}$ and τ_{ijk} are binary zeroth-order, binary first-order and ternary interaction parameters among the solute species respectively. The activity of water is given by equation (C.20).

$$\ln a_{\mathrm{w}} = M_{\mathrm{w}} \left\{ 2A_\phi \frac{I^{3/2}}{1+b\sqrt{I}} - \sum_{i\neq \mathrm{w}} \sum_{j\neq \mathrm{w}} m_i m_j \left[\beta_{ij}^{(0)} + \beta_{ij}^{(1)} \exp\left(-\alpha\sqrt{I}\right) \right] \right. \\ \left. -2\sum_{i\neq \mathrm{w}} \sum_{j\neq \mathrm{w}} \sum_{k\neq \mathrm{w}} m_i m_j m_k \tau_{ijk} - \sum_{i\neq \mathrm{w}} m_i \right\} \tag{C.20}$$

Following Rumpf and Maurer's approach [8], parameters for interactions between molecular and ionic species and those between ionic species themselves were neglected, because the majority of dissolved SO_2 is molecular. For molecular SO_2-SO_2 interactions, only the binary zeroth order parameter $\beta_{\mathrm{SO_2,SO_2}}^{(0)}$ (equation (C.21)) was retained.

$$\beta_{\mathrm{SO_2,SO_2}}^{(0)} \Big/ \left(\mathrm{kg\cdot mol^{-1}}\right) = 0.0934 - \frac{137.92}{\left(T/\mathrm{K}\right)} + \frac{3.127\cdot 10^4}{\left(T/\mathrm{K}\right)^2} \tag{C.21}$$

In order to calculate the equilibrium concentrations given two of the variables of the set $(T, p, \bar{m}_{\mathrm{SO_2}})$, where $\bar{m}_{\mathrm{SO_2}}$ is the overall molality of SO_2, the 9 following equations were solved simultaneously using the iterative Newton-Raphson technique: material balance in the solution (equations (C.4)-(C.5)) and in the gas phase (equation (C.9)), charge balance (equation (C.6)), chemical equilibria (equation (C.2)) for all the reactions involved in SO_2 dissolution (I, II and W) and vapor-liquid equilibria (equations (C.10)-(C.11)).

C.3.2. Thermodynamic calculation of the enthalpy of the process

All the quantities of the processes in this paragraph will refer to one mole of dissolved SO_2. The enthalpy of solution ($\Delta_{\mathrm{sol}}H_{\mathrm{SO_2}}$) is the sum of the enthalpy of physical dissolution ($\Delta_{\mathrm{r},8}H$) and the enthalpies $\Delta_{\mathrm{r},N}H$ of all the chemical reactions (equation (C.22)).

$$\Delta_{\mathrm{sol}}H_{\mathrm{SO_2}} = \Delta_{\mathrm{r},8}H + \sum_N \Delta_{\mathrm{r},N}H \tag{C.22}$$

To calculate the enthalpy of physical dissolution $\Delta_{\mathrm{r},8}H$, we consider the Gibbs energy change of the vapor-liquid equilibrium of SO_2 (equation (C.23)) and use the Gibbs-Helmholtz relation (equation (C.24)).

$$\frac{\Delta_{\mathrm{r},8}G}{RT} = \ln H_{\mathrm{SO_2,w}} + \ln\gamma_{\mathrm{SO_2}} + \frac{\bar{V}_{\mathrm{SO_2}}^{\infty}\left(p - p_{\mathrm{w}}^{\mathrm{s}}\right)}{RT} + \ln m_{\mathrm{SO_2}} - \ln\phi_{\mathrm{SO_2}} - \ln\left(y_{\mathrm{SO_2}} p\right) \tag{C.23}$$

$$\Delta_{\mathrm{r},8}H = -RT^2 \left(\frac{\partial}{\partial T} \left\{ \frac{\Delta_{\mathrm{r},8}G}{RT} \right\} \right)_{p,\{m_i\}} \\ = -RT^2 \left(\frac{\partial}{\partial T} \left\{ \ln H_{\mathrm{SO_2,w}} + \ln\gamma_{\mathrm{SO_2}} + \frac{\bar{V}_{\mathrm{SO_2}}^{\infty}\left(p - p_{\mathrm{w}}^{\mathrm{s}}\right)}{RT} - \ln\phi_{\mathrm{SO_2}} \right\} \right)_{p,\{m_i\}} \tag{C.24}$$

The enthalpy of reaction N (N = I, II, W) per mole of SO_2 (equation (C.25)) is calculated from the standard enthalpy of reaction ($\Delta_{r,N}H^\circ$) (equation (C.26)), the excess partial molar enthalpy of every compound i ($\bar{H}_i^E$) (equation (C.27)), and the extent of reaction (ξ_N) when one mole of gas is absorbed.

$$\Delta_{r,N}H = \frac{\xi_N}{\bar{n}_{SO_2}}\left(\Delta_{r,N}H^\circ + \sum_i \nu_{i,N}\bar{H}_i^E\right) \tag{C.25}$$

$$\Delta_{r,N}H^\circ = RT^2\left(\frac{\partial \ln K_N}{\partial T}\right)_p \tag{C.26}$$

$$\bar{H}_i^E = -RT^2\left(\frac{\partial \ln \gamma_i}{\partial T}\right)_{p,\{m_i\}} = -RT^2\left(\frac{\partial \ln a_i}{\partial T}\right)_{p,\{m_i\}} \tag{C.27}$$

Table C.4. Experimental solubility data of SO_2 in water, with their temperature (T) and pressure (p) ranges, used to test the validity of the model [8]. $\sigma_r\left(\bar{m}_{SO_2}\right)$ are the relative standard deviations from the model[a].

Reference	Data points	T/K range	p/MPa range	$100\,\sigma_r\left(\bar{m}_{SO_2}\right)$
Beuschlein and Simenson [9]	53	296.35 to 386.15	0.0653 to 1.925 [b]	6.7
Byerley *et al.* [10]	2	298.15 to 323.15	0.101325 [c]	5.0
Douabul and Riley [11]	6	278.97 to 303.25	0.101325 [c]	7.8 [d]
Hudson [12]	42	283.15 to 363.15	0.1008 to 0.1272 [c]	3.9
Johnstone and Leppla [6]	16	298.15 to 323.15	0.000027 to 0.001370 [b]	4.3
Maass and Maass [13]	29	283.15 to 300.15	0.0324 to 0.3408 [c]	18.3
Mondal [14]	20	293 to 333	0.000447 to 0.000963 [b]	4.7 [d]
Otuka [15]	22	373 to 423	0.174 to 0.354 [c]	29.7 [d]
Rabe and Harris [16]	43	303.15 to 353.15	0.00523 to 0.101 [b]	3.8
Rumpf and Maurer [8]	66	293.14 to 393.33	0.0356 to 2.509 [c]	2.5
Shaw *et al.* [17]	3	297.75 to 312.25	0.0252 to 0.196 [c]	43.6
Sherwood [18]	109	273.15 to 323.15	0.000033 to 0.0968 [b]	30.4
Siddiqi *et al.* [19]	50 [e]	290.15 to 294.65	0.0000011 to 0.000534 [b]	5.4
Smith and Parkhurst [20]	8	278.15 to 333.15	0.02342 to 0.14769 [b]	3.3
Tokunaga [21]	4	283.15 to 313.15	0.1025 to 0.1087 [c]	4.6

[a] $\sigma_r\left(\bar{m}_{SO_2}\right) = \sqrt{\frac{1}{N_p - 1}\sum_i\left(\frac{\bar{m}_{SO_2,i}^{calc} - \bar{m}_{SO_2,i}^{exp}}{\bar{m}_{SO_2,i}^{exp}}\right)^2}$; N_p , number of experimental data points; $\bar{m}_{SO_2,i}^{exp}$, experimental solubility; $\bar{m}_{SO_2,i}^{calc}$, calculated solubility. [b] Partial pressure of SO_2. [c] Total pressure. [d] Molality estimated from molarity using density of water. [e] Excluded two points reported with zero partial pressure of SO_2.

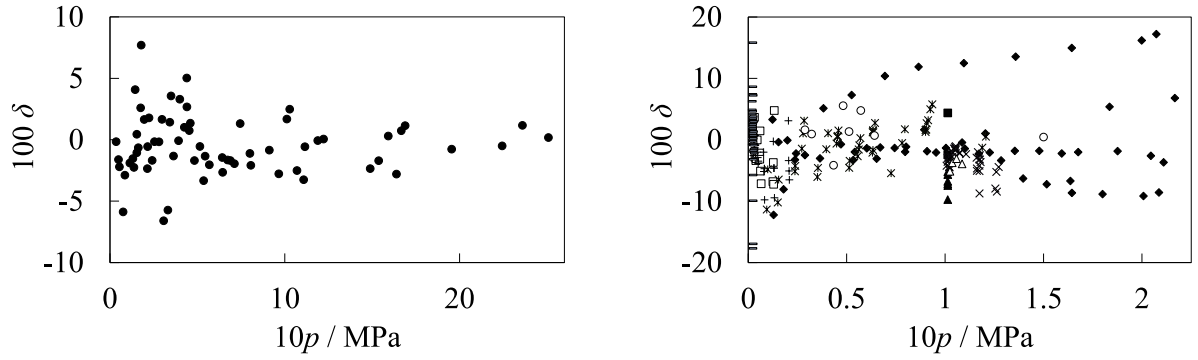

(a) (b)

Figure C.2. Relative deviation, δ, of the predicted from the experimental solubility (molality) of gaseous sulfur dioxide in liquid water as a function of experimental pressure, p. (a) Data from Rumpf and Maurer [8]. (b) Data from other references. (♦): Beuschlein and Simenson [9]; (■): Byerley *et al.* [10]; (▲): Douabul and Riley [11]; (×): Hudson [12]; (□): Johnstone and Leppla [6]; (+): Mondal [14]; (∗): Rabe and Harris [16]; (▬): Siddiqi *et al.* [19]; (○): Smith and Parkhurst [20]; (△): Tokunaga [21].

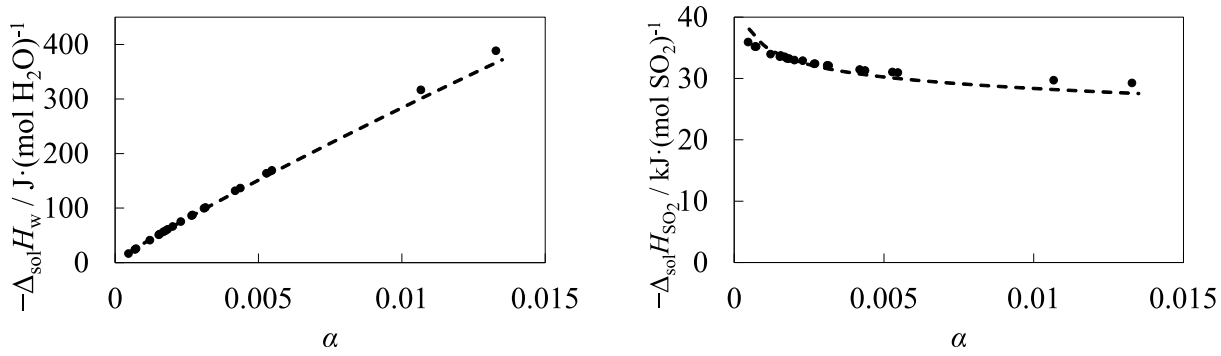

(a) (b)

Figure C.3. Enthalpy of solution of gaseous sulfur dioxide in liquid water per mole of water (a), $\Delta_{sol}H_w$, and per mole of sulfur dioxide (b), $\Delta_{sol}H_{SO_2}$, at temperature T = 298.15 K. (●): experimental values (Stiles and Felsing [5]); (- - -): calculated values.

C.3.3. Results and discussion

C.3.3.1. Model validation

The thermodynamic model, taken into account the non-ideality, was assessed using gas solubility data from literature [6, 8-21]. The relative standard deviations, $\sigma_r\left(\overline{m}_{SO_2}\right)$, between calculated and experimental solubility (molality) data have been determined for each reference and are given in Table C.4. The model provides a satisfactory representation of most of the experimental solubility data with a relative standard deviation around 5%. A significant scattering is observed between some of the oldest references, published before 1939 [13, 15, 18], and the rest of the data. The high relative standard deviation observed with Shaw *et al.* [17]

data concerns only 3 data points for which the authors reported possible experimental imprecision. The relative deviation, $\delta = \left(\bar{m}_{SO_2}^{calc} - \bar{m}_{SO_2}^{exp}\right) \Big/ \bar{m}_{SO_2}^{exp}$, of the predicted solubility ($\bar{m}_{SO_2}^{calc}$) from the experimental data ($\bar{m}_{SO_2}^{exp}$) issued from the rest of the mentioned references, is plotted against experimental pressure in Figure C.2. The graphs show that the relative deviations are symmetrically distributed around $\delta = 0$. The results of Figure 2a concern only the data from Rumpf and Maurer [8] and we have checked that our computations, determined with the set of parameters from this reference, are compatible with the calculations of the authors.

The enthalpies of solution derived from the vapor-liquid equilibrium model were compared to the experimental data at 298.15 K of Stiles and Felsing [5]. As illustrated in Figure 3, the model adequately represents the experimental enthalpies.

C.3.3.2. Results

The calorimetric measurements with SO_2 were carried out at temperatures $T = 323.15$ K and $T = 373.15$ K and pressure around an average value of 0.31 MPa. Experimental values are reported in Table C.5. The experimental and calculated enthalpies of solution are plotted as functions of gas loading charge in Figure C.4.

Table C.5. Enthalpy of solution of gaseous sulfur dioxide in liquid water per mole of water, $\Delta_{sol}H_w$, and per mole of sulfur dioxide, $\Delta_{sol}H_{SO_2}$, at temperatures $T = 323.15$ K and $T = 373.15$ K and pressure p, as functions of the loading charge of the gas, a. The corresponding standard uncertainties are $u(\Delta_{sol}H_w)$, $u(\Delta_{sol}H_{SO_2})$ and $u(\alpha)$.[a]

$\frac{p}{MPa}$	a	$u(a)$	$\frac{-\Delta_{sol}H_w}{J\cdot(mol\ H_2O)^{-1}}$	$\frac{u(\Delta_{sol}H_w)}{J\cdot(mol\ H_2O)^{-1}}$	$\frac{-\Delta_{sol}H_{SO_2}}{kJ\cdot(mol\ SO_2)^{-1}}$	$\frac{u(\Delta_{sol}H_{SO_2})}{kJ\cdot(mol\ SO_2)^{-1}}$
			$T = 323.15$ K			
0.29	0.0022	0.0003	50.1	4.3	22.8	2.0
0.36	0.0028	0.0002	64.7	12.0	23.1	4.3
0.30	0.0036	0.0004	85.3	12.0	23.7	3.3
0.28	0.0043	0.0002	106.7	7.9	24.9	1.8
0.29	0.0043	0.0002	130.0	7.8	30.2	1.8
0.28	0.0043	0.0006	106.7	6.4	24.8	1.5
0.31	0.0047	0.0006	109.5	3.2	23.3	0.7
0.30	0.0047	0.0006	120.6	12.0	25.7	2.6
0.32	0.0048	0.0006	137.3	3.5	28.6	0.7
0.32	0.0048	0.0002	137.3	8.4	28.4	1.7
0.31	0.0060	0.0007	147.2	3.3	24.5	0.6
0.29	0.0061	0.0003	170.2	10.2	27.7	1.7
0.29	0.0064	0.0003	185.1	11.9	28.8	1.8
0.28	0.0065	0.0003	168.8	10.9	26.0	1.7
0.28	0.0065	0.0008	168.8	6.5	26.0	1.0
0.29	0.0086	0.0004	245.2	14.8	28.6	1.7
0.28	0.0092	0.0004	232.1	13.6	25.1	1.5
0.28	0.0103	0.0004	304.8	17.9	29.5	1.7
0.30	0.0112	0.0005	315.4	18.4	28.2	1.6

0.29	0.0123	0.0005	335.5	20.0	27.2	1.6
0.28	0.0124	0.0005	340.2	20.4	27.5	1.7
0.30	0.0135	0.0006	342.0	20.0	25.4	1.5
0.30	0.0136	0.0006	391.2	24.9	28.8	1.8
0.28	0.0145	0.0006	391.3	23.0	27.0	1.6
0.28	0.0166	0.0007	450.4	26.7	27.1	1.6
0.31	0.0168	0.0001	377.0	6.7	22.4	0.4
0.30	0.0183	0.0020	496.2	13.1	27.1	0.7
0.30	0.0183	0.0008	496.2	30.5	27.1	1.7
0.29	0.0185	0.0008	501.5	29.3	27.1	1.6
0.29	0.0216	0.0009	552.1	32.5	25.6	1.5
0.28	0.0239	0.0010	589.2	34.4	24.7	1.4
0.29	0.0259	0.0011	667.6	39.0	25.8	1.5
0.29	0.0281	0.0012	693.2	40.5	24.6	1.4
0.28	0.0314	0.0013	709.4	41.4	22.6	1.3
0.28	0.0335	0.0014	725.2	42.3	21.6	1.3
0.28	0.0358	0.0015	735.0	42.9	20.6	1.2
				$T = 373.15$ K		
0.28	0.0011	0.0001	21.9	0.6	20.8	0.6
0.28	0.0021	0.0003	40.6	0.6	19.3	0.3
0.28	0.0024	0.0003	45.7	0.5	18.8	0.2
0.28	0.0026	0.0004	48.4	0.6	18.4	0.2
0.36	0.0027	0.0003	46.7	2.3	17.1	0.8
0.28	0.0032	0.0004	56.6	0.6	17.9	0.2
0.28	0.0032	0.0004	56.6	0.6	17.9	0.2
0.28	0.0037	0.0005	64.6	0.7	17.5	0.2
0.37	0.0042	0.0004	70.0	4.5	16.8	1.1
0.28	0.0042	0.0006	71.7	0.7	17.0	0.2
0.29	0.0042	0.0006	72.1	0.5	17.1	0.1
0.37	0.0050	0.0005	80.7	4.5	16.1	0.9
0.37	0.0057	0.0006	88.9	4.5	15.7	0.8
0.28	0.0063	0.0008	95.1	1.3	15.1	0.2
0.37	0.0065	0.0006	99.5	4.5	15.4	0.7
0.36	0.0074	0.0008	103.3	4.5	13.9	0.6
0.37	0.0075	0.0008	103.6	4.5	13.7	0.6
0.37	0.0084	0.0008	98.4	4.5	11.7	0.5
0.37	0.0085	0.0008	95.5	3.7	11.2	0.4
0.36	0.0088	0.0009	102.5	4.5	11.7	0.5
0.37	0.0098	0.0010	102.5	4.5	10.4	0.5
0.37	0.0112	0.0011	108.5	4.5	9.7	0.4
0.37	0.0114	0.0011	101.7	2.1	8.9	0.2
0.37	0.0126	0.0013	103.6	4.5	8.2	0.4
0.37	0.0127	0.0013	107.4	4.5	8.5	0.4
0.37	0.0142	0.0014	101.3	4.5	7.2	0.3

[a] Standard uncertainties: $u(T) = 0.03$ K; $u(p) = 0.02$ MPa.

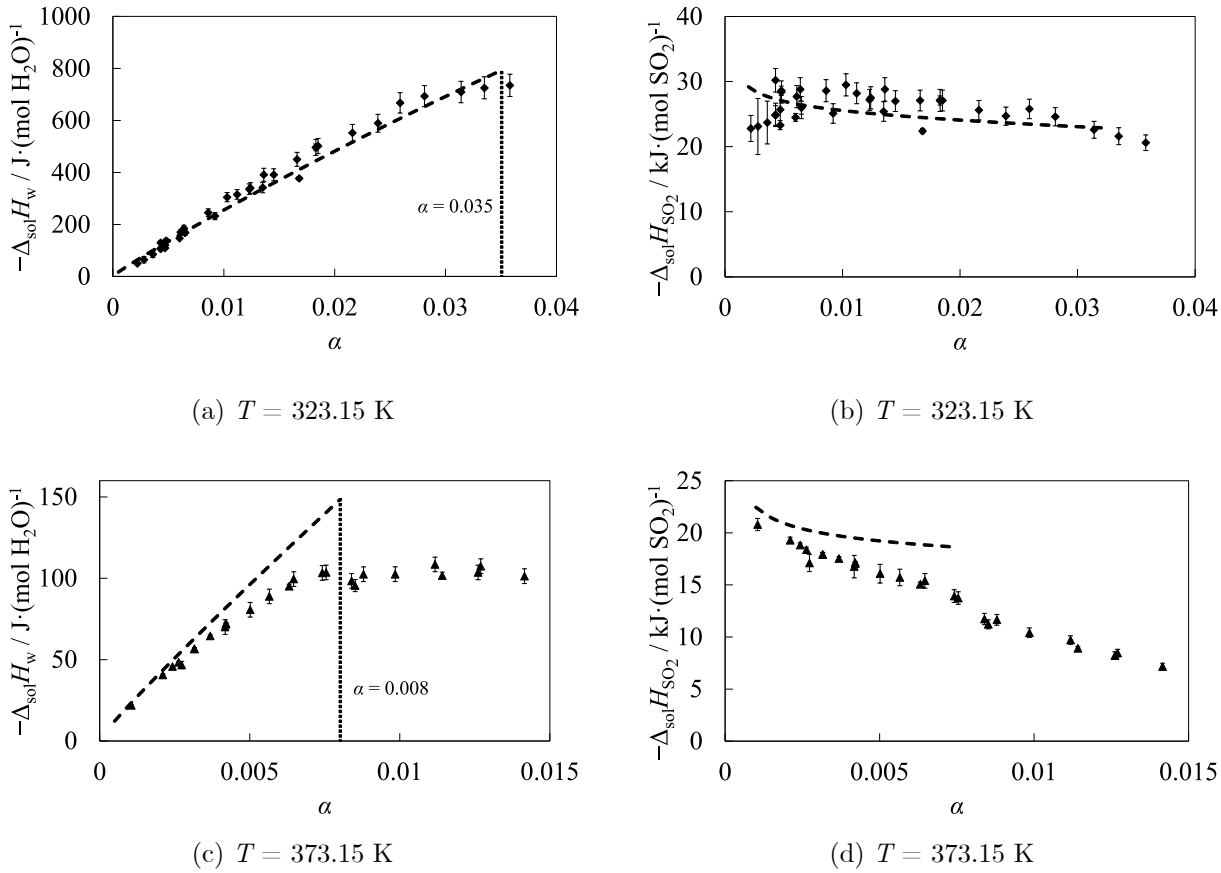

(a) T = 323.15 K (b) T = 323.15 K

(c) T = 373.15 K (d) T = 373.15 K

Figure C.4. Enthalpy of solution of gaseous sulfur dioxide in liquid water per mole of water (a, c), $\Delta_{sol}H_w$, and per mole of sulfur dioxide (b, d), $\Delta_{sol}H_{SO_2}$, at average pressure $<p>$ = 0.31 MPa and temperature T. ♦ and ▲: experimental values at 323.15 K and 373.15 K (this work); - - -: calculated values. Vertical dotted line: solubility limit calculated by the model.

At 323.15 K, $\Delta_{sol}H_w$ increases with gas loading charge (a) up to the limit of solubility. Above the calculated solubility limit (a_{calc} = 0.035 at p = 0.31 MPa), the enthalpy remains constant. However, the number of experimental points in the saturated domain (Figure C.4a) is not sufficient to make possible an accurate experimental estimation of the solubility limit. The highest gas loading charge a corresponds to sulfur dioxide and water volume flow rates of 0.85 mL/min and 0.05 mL/min, respectively. These experimental flow rates correspond to the upper and lower limits for the gas and the liquid, respectively. Concerning the thermodynamic model, the enthalpies of solution calculated are in good agreement with the experimental data (Figures C.4a and C.4b).

At 373.15 K, the gas solubility is low enough to allow measurements in the saturated domain (Figure C.4c). The calculated solubility limit of SO_2 in water (a_{calc} = 0.008 at p =0.31 MPa), is consistent with the value which can be determined from the experimental enthalpy of solution $\Delta_{sol}H_w$ (see Figure C.4c). A correct representation of the enthalpy of solution (Figures C.4c and C.4d) is obtained from the model for the lowest gas loading but enthalpies are overestimated when approaching the gas solubility limit.

The speciation is calculated by the model as function of gas loading charge. It shows that only SO_2 and HSO_3^- are significantly present in solution (Figure C.5); the molalities of SO_3^{2-}

and OH^- species at equilibrium are comparable and negligible. The enthalpy of solution $\Delta_{sol}H_{SO_2}$ is calculated as a combination of four contributions: $\Delta_{r,I}H$ for HSO_3^- formation, $\Delta_{r,II}H$ for SO_3^{2-} formation, $\Delta_{r,W}H$ for water dissociation and $\Delta_{r,8}H$ for physical dissolution. In agreement with the speciation calculations, the only non-negligible enthalpy contributions are issued from HSO_3^- formation and physical dissolution (Figure C.6), the latter being the dominant contribution. Basically, the mechanism of SO_2 dissolution in water is depicted by the model as a physical dissolution in water followed by a chemical dissociation yielding HSO_3^- formation. At 373.15 K, the overestimated enthalpy of solution could indicate that the chemical dissociation is less significant than the one estimated by the model. Indeed, chemical dissolution being more energetic than physical dissolution, this mechanism will increase the calculated total enthalpy of solution.

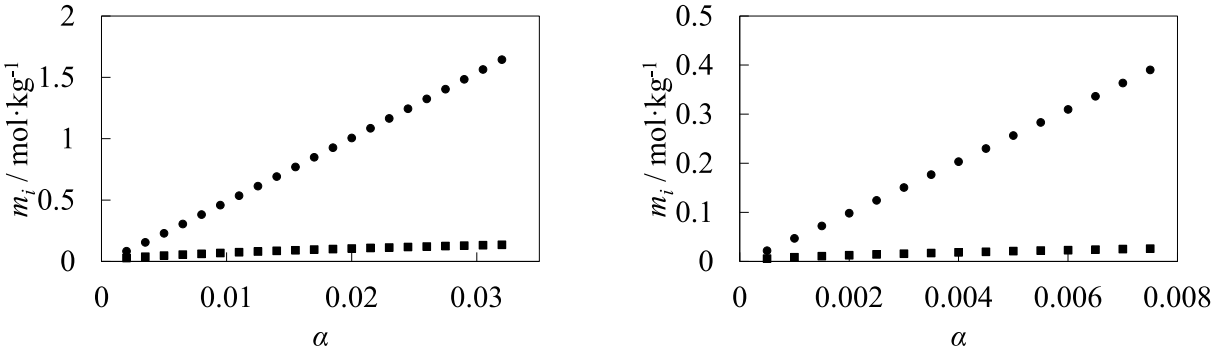

(a) $T = 323.15$ K (b) $T = 373.15$ K

Figure C.5. Equilibrium molality, m_i , of species i present in the liquid phase after the dissolution of gaseous sulfur dioxide in liquid water at temperature T as functions of the loading charge, α . (●): SO_2; (■): HSO_3^- and H^+.

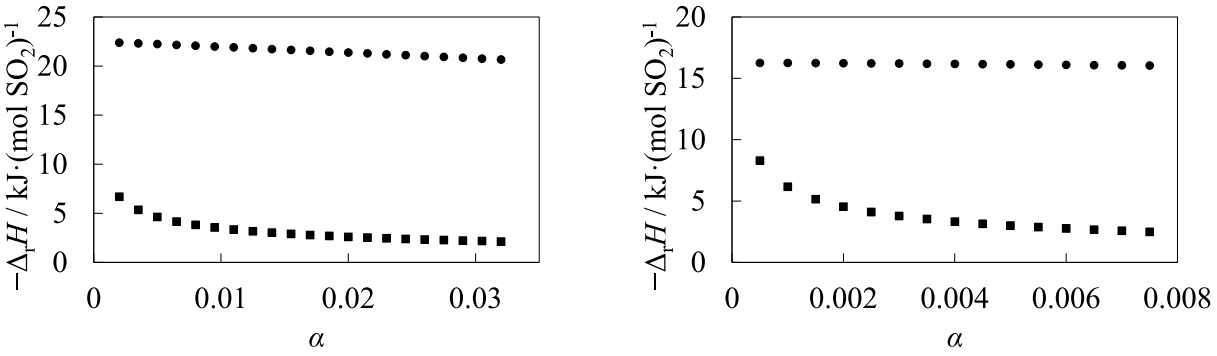

(a) $T = 323.15$ K (b) $T = 373.15$ K

Figure C.6: Model contributions to the enthalpy of solution of gaseous sulfur dioxide in liquid water per mol of SO_2, $\Delta_{sol}H_{SO_2}$, at temperature T as functions of the loading charge, α . (●): physical dissolution ($\Delta_{r,8}H$); (■): HSO_3^- formation ($\Delta_{r,I}H$).

C.4. Dissolution of nitrogen monoxide in water

C.4.1. Thermodynamic representation

Considering the low solubility of NO in water, the liquid solution was assumed to be ideal and the vapor-liquid equilibrium was represented by Henry's law. Experimental data on the dissolution of NO in aqueous solution is scarce. The solubility of NO in water has been investigated by Winkler [22] at a partial pressure of NO (p_{NO}) of 101325 Pa and temperatures from 273 to 353 K, and Armor [23] has studied the influence of pH and ionic strength on the solubility of NO in aqueous solutions. These data were used by Shaw and Vosper [36] to calculate Henry's law constants. Several reviews have been published later [37-40] based on the experimental data from Winkler [22] and Armor [23]. These reviews propose different equations for solubility and Henry's constant as functions of temperature. The mole-fraction based Henry's law constants at p_{NO} = 101325 Pa ($H_{NO,w}$) were here obtained from the equation reported by Gevantman [39] for solubility as a function of temperature and the same partial pressure of NO, and are represented by eq. 28, where A = 179.418, B = –8234.20 K, and C = –22.8155.

$$\ln\left(H_{NO,w}/\mathrm{Pa}\right) = A + \frac{B}{T} + C \cdot \ln\left(T/\mathrm{K}\right) \tag{C.28}$$

The enthalpy of solution was estimated from Henry's law constant, neglecting its pressure dependence and using Van't Hoff equation (eq. 29).

$$\Delta_{sol}H = R\left(B - C \cdot T\right) \tag{C.29}$$

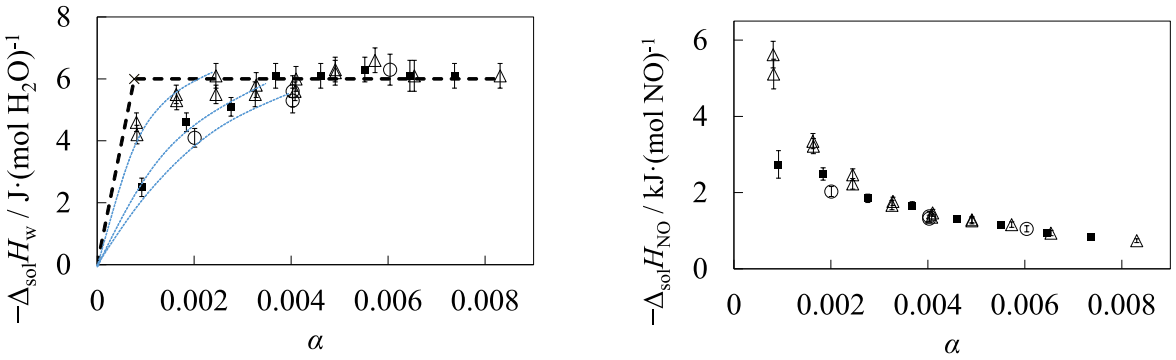

(a) (b)

Figure C.7. Enthalpy of solution of gaseous nitrogen monoxide in liquid water per mole of water (a), $\Delta_{sol}H_w$, and per mole of nitric oxide (b), $\Delta_{sol}H_{NO}$, at temperature T = 323.15 K and average pressure $<p>$. (△): $<p>$ = 2.27 MPa; (■): $<p>$ = 2.56 MPa; (○): $<p>$ = 2.80 MPa; (x): estimated solubility limit; - - - : hypothetic enthalpy behavior; dotted lines: curves connecting the points at constant $<p>$ = 2.27 MPa, 2.50 MPa or 2.80 MPa.

C.4.2. Results

The calorimetric measurements for NO dissolution in water were carried out at temperatures T = 323.15 K and pressures around the average values 2.27 MPa, 2.56 MPa and 2.80 MPa. The enthalpies of solution of NO in water were measured at 323.15 K. Due to the low solubility of

NO in water at 373.15 K, it was not possible to perform reliable enthalpy of solution experiments at this temperature. The experimental values are reported in Table C.6. The experimental and calculated enthalpies of solution are illustrated in Figure C.7.

Table C.6. Enthalpy of solution of gaseous nitrogen monoxide in liquid water per mole of water, $\Delta_{sol}H_w$, and per mole of nitric oxide, $\Delta_{sol}H_{NO}$, at temperature T = 323.15 K and pressure p, as functions of the loading charge of the gas, a. The corresponding standard uncertainties are $u(\Delta_{sol}H_w)$, $u(\Delta_{sol}H_{NO})$ and $u(\alpha)$. Measurements are carried out around an average pressure $<p>$. [a]

$\frac{p}{\text{MPa}}$	a	$u(a)$	$\frac{-\Delta_{sol}H_w}{\text{J}\cdot(\text{mol } H_2O)^{-1}}$	$\frac{u(\Delta_{sol}H_w)}{\text{J}\cdot(\text{mol } H_2O)^{-1}}$	$\frac{-\Delta_{sol}H_{NO}}{\text{kJ}\cdot(\text{mol NO})^{-1}}$	$\frac{u(\Delta_{sol}H_{NO})}{\text{kJ}\cdot(\text{mol NO})^{-1}}$
			$<p>$ = 2.80 MPa			
2.80	0.00201	0.00009	4.1	0.3	2.03	0.13
2.80	0.00403	0.00017	5.6	0.5	1.38	0.13
2.80	0.00403	0.00017	5.3	0.4	1.32	0.09
2.80	0.00604	0.00026	6.3	0.5	1.05	0.08
			$<p>$ = 2.56 MPa			
2.55	0.00092	0.00004	2.5	0.3	2.74	0.36
2.56	0.00184	0.00008	4.6	0.3	2.49	0.16
2.56	0.00276	0.00012	5.1	0.3	1.85	0.11
2.56	0.00368	0.00016	6.1	0.4	1.66	0.10
2.56	0.00461	0.00020	6.1	0.4	1.32	0.08
2.56	0.00552	0.00023	6.3	0.4	1.15	0.07
2.56	0.00645	0.00027	6.1	0.5	0.95	0.07
2.57	0.00737	0.00031	6.1	0.4	0.83	0.05
			$<p>$ = 2.27 MPa			
2.27	0.00081	0.00003	4.6	0.3	5.62	0.35
2.28	0.00082	0.00003	4.2	0.3	5.11	0.39
2.27	0.00163	0.00007	5.5	0.3	3.35	0.20
2.27	0.00164	0.00007	5.3	0.3	3.22	0.20
2.28	0.00245	0.00010	6.1	0.4	2.47	0.15
2.27	0.00245	0.00010	5.5	0.3	2.23	0.14
2.27	0.00326	0.00014	5.5	0.4	1.67	0.12
2.28	0.00328	0.00014	5.8	0.4	1.77	0.11
2.27	0.00408	0.00017	5.6	0.3	1.36	0.08
2.28	0.00410	0.00017	6.0	0.4	1.47	0.09
2.28	0.00491	0.00021	6.2	0.4	1.26	0.08
2.29	0.00491	0.00021	6.3	0.4	1.29	0.08
2.28	0.00573	0.00024	6.6	0.4	1.16	0.07
2.28	0.00654	0.00028	6.1	0.5	0.94	0.07
2.27	0.00831	0.00035	6.1	0.4	0.74	0.05

[a] Standard uncertainties: $u(T)$ = 0.03 K; $u(p)$ = 0.02 MPa.

The plot in Figure C.7a shows that the enthalpy of solution $\Delta_{sol}H_w$ increases with the gas loading charge a up to solution saturation and remains constant within experimental uncertainty when no more gas can be absorbed. The intersection between the two parts of the curve should correspond to the limit of gas solubility.

A theoretical gas solubility limit ($a_{calc} = 6.45 \cdot 10^{-4}$) at 323.15 K and 2.5 MPa was estimated using the value at atmospheric pressure ($a = 2.58 \cdot 10^{-5}$) reported by Gevantman [39] and Henry's law constant (equation (C.28)). This calculated solubility is represented in Figure C.7a, together with the plot of a hypothetical enthalpy behavior, i.e. a linear increase up to reach a plateau. This limit of solubility is lower than those which can be estimated experimentally. For gas loading charge below 0.00245, the enthalpy of solution is lower than expected. However, decreasing slightly the pressure from 2.27 to 2.80 MPa the enthalpy values get closer to the hypothetical plateau. The gap between experimental values and the plateau around the limit of solubility could be due to mixing problems when running experiments at very low gas flow rates (i.e. below 0.05 mL/min)

Because of the lack of reliable experimental data points in the unsaturated domain (Figure C.7), the enthalpy of solution per mole of gas, $\Delta_{sol}H_{NO}$ can only be estimated using the average enthalpy value of the plateau ($\Delta_{sol}H_w = (-6.0 \pm 0.5)$ J·(mol H_2O)$^{-1}$) and the theoretically estimated limit of gas solubility ($a_{calc} = 6.45 \cdot 10^{-4}$). Assuming a linear increase of the enthalpy up to the plateau, the enthalpy of solution ($\Delta_{sol}H_{NO}$) is estimated to be (-9.5 ± 0.8) kJ·(mol NO)$^{-1}$. The calculated $\Delta_{sol}H_{NO}$ value at 323.15 K and atmospheric pressure using literature Henry's constants (equations (C.28)-(C.29)) is (-7.2 ± 0.2) kJ·(mol NO)$^{-1}$. More experimental measurements at low gas loading charges will be necessary to conclude on the consistency between solubility and enthalpy data.

C.5. Conclusion

Dissolution of SO_2 and NO in water was investigated using a thermodynamic approach. Experimental enthalpies of solution were determined as a function of temperature and pressure, and their consistency with literature solubility data was tested. The dissolution of SO_2 in water was described using a thermodynamic model representative of vapor-liquid equilibrium and gas chemical dissociations. The enthalpies of solution were derived from the model as a combination of terms related to physical dissolution and gas dissociation. The main contribution to the enthalpy of solution has been found to be the physical dissolution. At 373.15 K. the model predicts accurately the solubility limits but slightly overestimates the enthalpy of solution. For dissolution of NO in water, the system exhibits very low gas solubility. It was difficult to measure enthalpies of solution for a gas loading charge below the limit of solubility. Combining our result with literature values of solubility and Henry's constants, the experimental enthalpy data at 323.15 K seem consistent. However, the calorimetric technique used in this work will require some improvement to investigate the domain where the solution is unsaturated and make it possible to develop a rigorous model representative of vapor-liquid equilibrium and enthalpy of solution.

C.6. References

[1] G.T. Rochelle, *Amine Scrubbing for CO2 Capture.* Science **325** (2009) 1652-1654. https://doi.org/10.1126/science.1176731

[2] N. Meunier, S. Laribi, L. Dubois, D. Thomas, G. De Weireld, *CO2 Capture in Cement Production and Re-use: First Step for the Optimization of the Overall Process.* Energy Procedia **63** (2014) 6492-6503. https://doi.org/10.1016/j.egypro.2014.11.685

[3] B. Creton, T. de Bruin, D. Le Roux, P. Duchet-Suchaux, V. Lachet, *Impact of Associated Gases on Equilibrium and Transport Properties of a CO2 Stream: Molecular Simulation and Experimental Studies.* Int. J. Thermophys. **35** (2014) 256-276. https://doi.org/10.1007/s10765-014-1592-6

[4] J. Corvisier, E.E. Ahmar, C. Coquelet, J. Sterpenich, R. Privat, J.N. Jaubert, K. Ballerat-Busserolles, J.Y. Coxam, P. Cézac, F. Contamine, J.P. Serin, V. Lachet, B. Creton, M. Parmentier, P. Blanc, L. André, L. de Lary, E.C. Gaucher, *Simulations of the Impact of Co-injected Gases on CO2 Storage, the SIGARRR Project: First Results on Water-gas Interactions Modeling.* Energy Procedia **63** (2014) 3160-3171. https://doi.org/10.1016/j.egypro.2014.11.341

[5] A.G. Stiles, W.A. Felsing, *The heat of solution of sulfur dioxide.* J. Am. Chem. Soc. **48** (1926) 1543-1547. https://doi.org/10.1021/ja01417a014

[6] H.F. Johnstone, P.W. Leppla, *The Solubility of Sulfur Dioxide at Low Partial Pressures. The Ionization Constant and Heat of Ionization of Sulfurous Acid.* J. Am. Chem. Soc. **56** (1934) 2233-2238. https://doi.org/10.1021/ja01326a009

[7] D. Koschel, J.-Y. Coxam, V. Majer, *Enthalpy and Solubility Data of H2S in Water at Conditions of Interest for Geological Sequestration.* Ind. Eng. Chem. Res. **46** (2007) 1421-1430. https://doi.org/10.1021/ie061180+

[8] B. Rumpf, G. Maurer, *Solubilities of hydrogen cyanide and sulfur dioxide in water at temperatures from 293.15 to 413.15 K and pressures up to 2.5 MPa.* Fluid Phase Equilib. **81** (1992) 241-260. https://doi.org/10.1016/0378-3812(92)85155-2

[9] W.L. Beuschlein, L.O. Simenson, *Solubility of Sulfur Dioxide in Water.* J. Am. Chem. Soc. **62** (1940) 610-612. https://doi.org/10.1021/ja01860a053

[10] J.J. Byerley, G.L. Rempel, V.T. Le, *Solubility of sulfur dioxide in water-acetonitrile solutions.* J. Chem. Eng. Data **25** (1980) 55-56. https://doi.org/10.1021/je60084a017

[11] A. Douabul, J. Riley, *Solubility of sulfur dioxide in distilled water and decarbonated sea water.* J. Chem. Eng. Data **24** (1979) 274-276. https://doi.org/10.1021/je60083a014

[12] J.C. Hudson, *The solubility of sulphur dioxide in water and in aqueous solutions of potassium chloride and sodium sulphate.* J. Chem. Soc., Trans. **127** (1925) 1332-1347. https://doi.org/10.1039/CT9252701332

[13] C.E. Maass, O. Maass, *Sulfur dioxide and its aqueous solutions. I. Analytical methods, vapor density and vapor pressure of sulfur dioxide. Vapor pressure and concentrations of the solutions.* J. Am. Chem. Soc. **50** (1928) 1352-1368. https://doi.org/10.1021/ja01392a016

[14] M.K. Mondal, *Experimental determination of dissociation constant, Henry's constant, heat of reactions, SO2 absorbed and gas bubble–liquid interfacial area for dilute sulphur dioxide absorption into water.* Fluid Phase Equilib. **253** (2007) 98-107. https://doi.org/10.1016/j.fluid.2007.01.015

[15] Y. Otuka, J. Soc. Chem. Ind. Japan. Suppl. **42** (1939) 205B-209B.

[16] A.E. Rabe, J.F. Harris, *Vapor Liquid Equilibrium Data for the Binary System Sulfur Dioxide and Water.* J. Chem. Eng. Data **8** (1963) 333-336. https://doi.org/10.1021/je60018a017

[17] A.C. Shaw, M.A. Romero, R.H. Elder, B.C.R. Ewan, R.W.K. Allen, *Measurements of the solubility of sulphur dioxide in water for the sulphur family of thermochemical cycles.*

Int. J. Hydrog. Energy **36** (2011) 4749-4756. https://doi.org/10.1016/j.ijhydene.2011.01.105

[18] T.K. Sherwood, *Solubilities of Sulfur Dioxide and Ammonia in Water.* Ind. Eng. Chem. **17** (1925) 745-747. https://doi.org/10.1021/ie50187a043

[19] M.A. Siddiqi, J. Krissmann, P. Peters-Gerth, M. Luckas, K. Lucas, *Spectrophotometric measurement of the vapour-liquid equilibria of (sulphur dioxide + water).* J. Chem. Thermodyn. **28** (1996) 685-700. https://doi.org/10.1006/jcht.1996.0064

[20] W.T. Smith, R.B. Parkhurst, *The solubility of sulfur dioxide in suspensions of calcium and magnesium hydroxides.* J. Am. Chem. Soc. **44** (1922) 1918-1927. https://doi.org/10.1021/ja01430a010

[21] J. Tokunaga, *Solubilities of sulfur dioxide in aqueous alcohol solutions.* J. Chem. Eng. Data **19** (1974) 162-165. https://doi.org/10.1021/je60061a009

[22] L.W. Winkler, Ber. **34** (1901) 1408-1422.

[23] J.N. Armor, *Influence of pH and ionic strength upon solubility of nitric oxide in aqueous solution.* J. Chem. Eng. Data **19** (1974) 82-84. https://doi.org/10.1021/je60060a013

[24] J.B. Ott, G.V. Cornett, C.E. Stouffer, B.F. Woodfield, C. Guanquan, J.J. Christensen, *Excess enthalpies of (ethanol+water) at 323.15, 333.15, 348.15, and 373.15 K and from 0.4 to 15 MPa.* J. Chem. Thermodyn. **18** (1986) 867-875. https://doi.org/10.1016/0021-9614(86)90121-7

[25] J.B. Ott, C.E. Stouffer, G.V. Cornett, B.F. Woodfield, C. Guanquan, J.J. Christensen, *Excess enthalpies for (ethanol + water) at 398.15, 423.15, 448.15, and 473.15 K and at pressures of 5 and 15 MPa. Recommendations for choosing (ethanol + water) as an HmE reference mixture.* J. Chem. Thermodyn. **19** (1987) 337-348. https://doi.org/10.1016/0021-9614(87)90115-7

[26] E.C. Ihmels, E.W. Lemmon, J. Gmehling, *An equation of state and compressed liquid and supercritical densities for sulfur dioxide.* Fluid Phase Equilib. **207** (2003) 111-130. https://doi.org/10.1016/S0378-3812(03)00004-9

[27] W. Wagner, A. Pruß, *The IAPWS Formulation 1995 for the Thermodynamic Properties of Ordinary Water Substance for General and Scientific Use.* J. Phys. Chem. Ref. Data **31** (2002) 387-535. https://doi.org/10.1063/1.1461829

[28] Y. Le Guennec, R. Privat, J.-N. Jaubert, *Development of the translated-consistent tc-PR and tc-RK cubic equations of state for a safe and accurate prediction of volumetric, energetic and saturation properties of pure compounds in the sub- and super-critical domains.* Fluid Phase Equilib. **429** (2016) 301-312. https://doi.org/10.1016/j.fluid.2016.09.003

[29] T.J. Edwards, G. Maurer, J. Newman, J.M. Prausnitz, *Vapor-liquid equilibria in multicomponent aqueous solutions of volatile weak electrolytes.* AIChE J. **24** (1978) 966-976. https://doi.org/10.1002/aic.690240605

[30] K. Kawazuishi, J.M. Prausnitz, *Correlation of vapor-liquid equilibria for the system ammonia-carbon dioxide-water.* Ind. Eng. Chem. Res. **26** (1987) 1482-1485. https://doi.org/10.1021/ie00067a036

[31] A. Saul, W. Wagner, *International Equations for the Saturation Properties of Ordinary Water Substance.* J. Phys. Chem. Ref. Data **16** (1987) 893-901. https://doi.org/10.1063/1.555787

[32] S.W. Brelvi, J.P. O'Connell, *Correspondling states correlations for liquid compressibility and partial molal volumes of gases at infinite dilution in liquids.* AIChE J. **18** (1972) 1239-1243. https://doi.org/10.1002/aic.690180622

[33] V. Bieling, F. Kurz, B. Rumpf, G. Maurer, *Simultaneous Solubility of Ammonia and Carbon Dioxide in Aqueous Solutions of Sodium Sulfate in the Temperature Range 313-393 K and Pressures up to 3 MPa.* Ind. Eng. Chem. Res. **34** (1995) 1449-1460. https://doi.org/10.1021/ie00043a054

[34] J.G. Hayden, J.P. O'Connell, *A Generalized Method for Predicting Second Virial Coefficients.* Ind. Eng. Chem. Process. Des. Dev. **14** (1975) 209-216. https://doi.org/10.1021/i260055a003

[35] C.-C. Chen, H.I. Britt, J.F. Boston, L.B. Evans, *Local composition model for excess Gibbs energy of electrolyte systems. Part I: Single solvent, single completely dissociated electrolyte systems.* AIChE J. **28** (1982) 588-596. https://doi.org/10.1002/aic.690280410

[36] A.W. Shaw, A.J. Vosper, *Solubility of nitric oxide in aqueous and nonaqueous solvents.* J. Chem. Soc. Faraday. Trans. 1 **73** (1977) 1239-1244. https://doi.org/10.1039/F19777301239

[37] W.F. Linke, *Solubilities of Inorganic and Metal Organic Compounds.* American Chemical Society, Washington D.C., 1965.

[38] R. Battino, *IUPAC Solubility Data Series, Vol. 10, Nitrogen and Air.* Pergamon Press, Oxford, England, 1982.

[39] L.H. Gevantman, *Solubility of Selected Gases in Water*, in *CRC Handbook of Chemistry and Physics, 90th Edition*, D.R. Lide, Editor. 2010, CRC Press/Taylor and Francis, pp. (8-81)-(8-82). Boca Raton, FL.

[40] E. Wilhelm, R. Battino, R.J. Wilcock, *Low-pressure solubility of gases in liquid water.* Chem. Rev. **77** (1977) 219-262. https://doi.org/10.1021/cr60306a003